Heads or tails? An insight into the nature of antibacterial structures of an entomopathogenic bacterium *Brevibacillus laterosporus*

A thesis

submitted in partial fulfilment

of the requirements for the Degree of

Doctor of Philosophy

at

Lincoln University

by

Tauseef Khan Babar

Lincoln University

2021

Abstract of a thesis submitted in partial fulfilment of the requirements for the Degree of Doctor of Philosophy

Heads or tails? An insight into the nature of antibacterial structures of an entomopathogenic bacterium *Brevibacillus laterosporus*

by

Tauseef Khan Babar

"Bacterium eating viruses" (phages) are one of the biotic factors that can disrupt the mass production of bacteria through the lysis of the cells during growth. *Brevibacillus laterosporus* (Laubach) is an entomopathogenic, gram-positive, and spore-forming bacterium found around the world, but individual strains can differ greatly in their virulence and hosts. Since 2012, three *B. laterosporus* strains (*Bl* 1821L, *Bl* 1951, *Bl* Rsp) have been discovered and characterised in New Zealand. All the strains exhibited pathogenicity against diamondback moth larvae and mosquitoes. However, during culturing, the cultures often lost virulence, which was perceived to be due to growth issues and the presence of potential bacteriophages. Though isolates *Bl* 1821L and *Bl* 1951 are under development as a biopesticide, the lack of consistent production has hindered their development. Based on these issues this research project commenced to isolate and characterise the suspected bacteriophages, cure the bacteria of the invading phage particles, compare the virulence of phage cured and uncured strains against diamondback moth, and finally develop a production protocol that would allow a biopesticide to be developed from this insect pathogenic bacterium free of phages. However, initial work involving classical phage isolation and enumeration assays (plaque and serial dilutions) and an electron microscopic examination could not substantiate the presence of putative phage particles, despite bioinformatic predictions indicating the presence of intact phages in *Bl* 1821L, *Bl* 1951, and *Bl* Rsp genomes.

Assessment of electron micrographs of mitomycin C induced cultures (*Bl* 1821L & *Bl* 1951) and bioactivity tests of polyethylene glycol precipitated cultures validated the presence of incomplete phage particles with hexagonal or phage head (encapsulating) and contractile tail-sheath like structures. Subsequent N-terminal sequencing of a prominent ~48 kD protein of SDS-PAGE after mitomycin C induction led to the discovery of putative antibacterial phage tail-like bacteriocins (PTLBs) in the *Bl* 1821L genome. The putative *Bl* 1821L PTLB displayed a broader spectrum of activity than the *Bl* 1951 PTLB. N-terminal sequencing of purified ~48 kD protein of *Bl* 1821L identified a phage-like

element PBSX protein XkdK in the *Bl* 1821L genome. BLASTp analysis of *Bl* 1821L 48 kD identified protein accessions with >90% amino acid similarity to the phage tail-sheath protein of *Bl* LMG 15441. Using the same methodology an XkdK homolog was identified in the *Bl* 1951 genome. Although the translated product of the *Bl* 1821L *xkdK* gene encoding region exhibited amino acid identity to the analogous region of *Bl* 1951, the bioinformatic analysis revealed some differences in the operon surrounding the gene, a region which corresponded to the PBSX region in *Bacillus subtilis*. Bioinformatically, the PBSX-like region in *Bl* 1951 encodes imperfect repeats of glycine rich proteins (1700 bp long) while a putative phage region resides in the analogous *Bl* 1821L region.

A second putative antibacterial protein (bacteriocin) of ~30 kD was also found in SDS PAGE analysis of purified *Bl* 1821L and *Bl* 1951 putative antibacterial protein. N-terminal sequencing of purified ~30 kD protein identified matches to both a 25 kD hypothetical and a 30 kD putative encapsulating protein homologs residing in each of the genomes.

Various purification methods employed in this study enabled the purification of one putative antibacterial protein (~30 kD) of *Bl* 1951 and two putative antibacterial proteins (~30 kD & ~48 kD) of *Bl* 1821L. Subsequent TEM examination of purified antibacterial *Bl* 1821L proteins revealed the presence of phage head-like encapsulin (~30 kD) and polysheath-like (~48 kD) structures. Although only the ~30 kD protein was purified from *Bl* 1951, both the phage head-like encapsulin and polysheath-like structures were observed under an electron microscope. SDS-PAGE analysis of spontaneously produced putative antibacterial proteins of *Bl* 1821L and *Bl* 1951 upon purification also yielded two prominent bands of ~30 kD and ~48 kD. Assaying size exclusion chromatographic fractions of *Bl* 1951 harbouring the 30 kD against *Bl* 1821L resulted in the presence of small *Bl* 1821L cells that may be indicative of persister cell formation in the population of *Bl* 1821L.

BLASTp analysis of the homologs *Bl* 1821L and *Bl* 1951 30 kD amino acid sequences identified >97% amino acid identity to the Linocin M18 bacteriocin family protein of *Bl* LMG 15441 and *Bl* GI-9 which are known as encapsulating proteins. Using the bioinformatic tools AMPA and CellPPD motifs relating to the bactericidal activity and cell penetrating peptides were identified. Antibacterial activity of the identified 25 kD hypothetical and 30 kD putative encapsulating proteins of *Bl* 1821L was further validated through gene expression in a gram-positive bacterium *Bacillus subtilis* WB800N and the subsequent assay tests and SDS-PAGE analysis of purified proteins from the recombinants. A preliminary assessment of the expressed 25 kD hypothetical gene (pHT01-*hypo*) exhibited an increased effect against *Bl* 1821L and *Bl* 1951 compared to the 30 kD putative encapsulating gene (pHT01-*encap*).

The putative antibacterial proteins (bacteriocins) of *Bl* 1821L and *Bl* 1951 sustained the antagonistic activity against *B. laterosporus* over a wide range of pHs and temperatures. A loss in the antagonistic activity of putative bacteriocins of *Bl* 1821L and *Bl* 1951 after treatment with proteolytic enzymes

authenticated their proteinaceous nature. However, catalase treatment could not abrogate the inhibitory action of the putative antibacterial proteins of *Bl* 1821L and *Bl* 1951, which showed that growth inhibition was not due to hydrogen peroxide production. This study describes the first examples of the spontaneous induction of high molecular weight (HMW) bacteriocins of *Bl* 1821L and *Bl* 1951 from the genus *Brevibacillus*. Spontaneously induced HMW bacteriocins of *Bl* 1951 affected the growth of bacterium by causing a significant decline in the number of viable cells after 18 hours of culture inoculation that corresponded to the highest antagonistic activity against *Bl* 1951 and *Bl* 1821L. Likewise, though not at a significant level spontaneously induced HMW bacteriocins of *Bl* 1821L decreased the number of viable cells of *Bl* 1821L after 18 hours of growth.

Antagonistic activity of putative antibacterial proteins in growth assays not only varied between the different proteins but also with the state of the proteins (crude or purified). Crude lysate of *Bl* 1821L and *Bl* 1951 harbouring both the putative encapsulating (30 kD) and phage tail-like (48 kD) proteins prominently caused autocidal activity with a decrease of 30.1% and 48.4% in the number of viable cells. The purified ~30 kD putative encapsulating protein of *Bl* 1821L and *Bl* 1951 exhibited bactericidal activity against both strains. Numerous plausible killing mechanisms of 30 kD putative encapsulating protein of *Bl* 1821L and *Bl* 1951 are proposed. These include the activation of stress relevant transcriptional regulator family proteins (PadR & MarR) or YtxJ protein under some unknown stresses, iron malnutrition, failure of ferritin protein to detoxify iron, and cell penetrating peptides activity. The purified ~48 kD putative phage tail-sheath protein of the PBSX-like region of *Bl* 1821L was active against *Bl* 1951. Bactericidal activity of ~48 kD purified phage tail-sheath protein of *Bl* 1821L was likely due to the contractile injection system by forming pores in susceptible cells.

Overall, this research identified and characterised two bactericidal proteins of ~30 kD (encapsulating) and ~48 kD (phage tail-sheath) in *Bl* 1821L and one ~30 kD encapsulating protein in *Bl* 1951 that were found to be implicated in the growth issues of the insect pathogenic strains *Bl* 1821L and *Bl* 1951. A hypothetical protein (25 kD) with more potent putative antibacterial activity in *Bl* 1821L and *Bl* 1951 was also identified and expressed late in the project but requires further investigation. The findings provided a wealth of knowledge that will be useful in the future development of a biopesticide from this beneficial bacterium.

Keywords: antibacterial, autocidal, bactericidal proteins, bacteriophages, biopesticides, *Brevibacillus laterosporus*, cell lysis, cell penetrating peptides, contractile phage tail-sheath protein, defective phages, diamondback moth, encapsulating protein, entomopathogenic bacterium, ferritin-proteins, PBSX, phage tail-like bacteriocins.

Dedication

"All I am, or hope to be, I owe to my parents"

This thesis is dedicated to my beloved parents

For their love, endless support, and encouragement.

Tauseef Khan Babar

Acknowledgements

All the praise belongs to Almighty Allah for His countless blessings and granting me the good health, wellbeing, wisdom, and perseverance that were necessary to complete this project. Undertaking PhD has been a truly life-changing experience for me and it would not have been possible to do without the support and guidance that I received from many people.

First of all, I would like to thank my chief supervisor, Professor Travis Glare who has always supported me and has never given up on me during difficult times. I am highly obliged and indebted to you for your unwavering support, motivation, and patience as I completed this dissertation. My sincere thanks to my associate supervisor, Professor John Hampton for his guidance, supervision, and constructive criticism during the studies and writing of the dissertation, which paved to boost my critical thinking and writing skills. I would like to take this opportunity to offer my sincere thanks to the associate co-supervisor, Dr. Mark Hurst, Senior Scientist at AgResearch, Lincoln for his versatile and valuable support, which assisted me to design the experimental protocols. It was due to his kind support and trust that he allowed me to use some of the equipment in his laboratory. The research work could not have been accomplished without learning numerous laboratory skills and the advisor, Dr. Josefina Narciso, stood with me to achieve the goals. I am thankful to you for all the love and support that you have given me as an advisor. I would like to express my gratitude to Dave Saville, for all the statistical analysis guidance and to Dr. Andrew Holyoake for lending precious advice at various phases of my PhD research project. My sincere thanks also go to lab manager, Karl Gately, of Replacement for Hilgendorf (RFH) building, Lincoln University, New Zealand for not only imparting technical training of proper usage of ultracentrifugation machines but also providing lab space for the uninterrupted scientific work.

A massive thanks to the AgResearch scientists for extending technical facilities for the successful completion of the project. I am pleased to thank Amy Beattie for her help in using size exclusion chromatography equipment to purify the putative antibacterial proteins. I offer my gratitude to senior scientist, Dr. Evelyne Maes, and research associate, Ancy Thomas of Proteomics Platform, AgResearch, Lincoln for the N-terminal sequencing facility. Enormous thanks to Dr. Marina Richena for her persistent support in TEM analysis and patience in taking worthwhile images.

The most crucial part of the research was the transformation of putative antibacterial proteins in a gram-positive bacterium *Bacillus subtilis* and I was fortunate to have the collaboration of Callaghan Innovation's Protein Science & Engineering Team based at the University of Canterbury, New Zealand for this purpose. Thank you very much, Dr. Campbell Sheen and Dr. Barbara Koch for lending me your expertise and intuition in achieving the goal.

I am supremely grateful for the opportunities that were granted to me during my studies at the Bio-Protection Research Centre, Lincoln University, to develop my scientific faculties and acquire diversified skills. I would like to express my greatest appreciation to our lab managers Brian Kwan and Fariba Nourozi, who were always ready to help when needed. I thank Norma Merrick for her expeditious assistance in autoclaving the experimental materials. I am indebted to the whole operations team, Dr. Andrew Holyoake, Sandy Wilson, Claire Tee, Ashley Campbell, Michelle Boyle, Lorien Tarjomi, and Jenny Brookes for their efforts to make my PhD journey incredibly amazing and memorable.

PhD journey would not have been a success without the friendly support of my research group fellows. I earnestly thank postdoc fellows, Dr. Marsha Ormskirk, for her help in providing an insight into various aspects of the entomopathogenic bacterium *Brevibacillus laterosporus*, Dr. Amber Paulson and Dr. Lesley Sitter for bioinformatic guidance, and Dr. Marion Schoof in LIVE/DEAD staining of bacterial cultures. Special thanks to Dr. Hossein Alizadeh and Dr. Artemio Mendoza for their company in the lab and scientific discussions. I am also extremely grateful to my office mates, Jaesung Lee and Sereyboth Soth for cheering me up and all the happy moments we shared combined with professionalism and assistance. I am indeed obliged and thankful to my friends Dr. Maria Elena Duter, Sayed Ahmed, Sundar Tiwari, and Sunita Sanjyal for their cooperation and support in the completion of my studies.

I also thank for heart-warming kindness and great hospitality from the families of my dear friends Dr. Farhat Ali Shah, Dr. Raheel Khan, and Nadeem Khan during my stay in New Zealand. I owe a massive thanks to my flatmates Muhammad Arif and Maisam Ali for your great cooperation and enjoyable environment.

This wonderful period of learning and expansion of knowledge horizons would not have been possible without the provision of a scholarship. I would like to say a heartfelt thank you to the Bahauddin Zakariya University, Multan, and the Higher Education Commission, Pakistan for providing me with an opportunity under the “Faculty Development Programme” to pursue PhD at the Bio-Protection Research Centre, Lincoln University, New Zealand.

I will forever be indebted to my former M.Sc. (Hons.) research supervisor and eminent scientist, Dr. Muhammad Afzal, currently working as Vice Chancellor Baba Guru Nanak University, Nankana Sahib, Pakistan for his eternal support and encouragement in my life. I take this opportunity to express gratitude to Dr. Sajid Nadeem, Senior Scientist Entomology Division, Nuclear Institute of Agriculture & Biology (NIAB), Faisalabad, Pakistan for his motivation and guidance in my career journey.

I can’t forget my friends from Pakistan who went through hard times together, cheered me on, and celebrated each accomplishment: Ayesha Kashif, Muhammad Awais Malik, Abdul Rauf, Khalid Saeed, Dr. Azam Khan, Dr. Anjum Aqeel, Dr. Dilber Hussain, Muhammad Akram, Muhammad Hasnain, Mussadiq Khan, Ikram Ahmad, Zahid Aslam, Junaid Khan, Iftikhar Ahmad, and Abrar Ahmad.

I wish to acknowledge the support and great love of my family. Words cannot express how grateful I am to my beloved parents for all of the sacrifices that you have made on my behalf. Your prayers for me was what sustained me thus far. I would like to recognise the invaluable support of my dear uncle Ayub Nasir, brothers Tauqeer Khan Babar and Hammad Khan Babar, and sisters during the study. Immense love and thanks for the beautiful messages and gifts from my cute nephews and nieces from overseas. Thank you very much for your love.

Tauseef Khan Babar

Table of Contents

List of Tables

List of Figures

List of Abbreviations

Abbreviation	Definition
ABPs	Antibacterial proteins
Afp	Antifeeding prophage
AI	Antimicrobial index
AMPs	Antimicrobial peptides
ANOVA	Analysis of variance
AOI	Areas of interest
APS	Ammonium per sulphate
ASP	Ammonium sulphate precipitation
ATP	Adenosine triphosphate
Bfr	Bacterioferritin
Bin	Binary
Bl	*Brevibacillus laterosporus*
BLAST	Basic local alignment search tool
BLASTp	Protein BLAST search against a protein sequence
BOA	Bacteriocin operon and gene block associator
Bp	*Bacillus pumilus*
BPRC	Bio-protection research centre
Bt	*Bacillus thuringiensis*
CBB	Coomassie brilliant blue
CDI	Contact dependent inhibition
CDS	Coding sequence
CFS	Cell free supernatant
CFU	Colony forming unit
CPPs	Cell penetrating peptides
CRISPR	Clustered regulatory interspaced short palindromic repeats
Cry	Crystal
Cyto	Cytolic
DNA	Deoxyribonucleic acid
Dps	DNA-binding protein from the starved cells
ds	Double stranded
eCIS	Extracellular contractile injection system
EDTA	Ethylenediaminetetraacetic acid
EM	Electron microscope
EP	Encapsulating protein
FB	Phosphate buffer
FS	Full strength
Ftn	Ferritin
gDNA	Genomic DNA
GTAs	Gene transfer agents
HGT	Horizontal gene transfer
HMW	High molecular weight
HPI	Hours post incubation
HTH	Helix-turn-helix
ICTV	International committee on taxonomy of viruses
IdeR	Iron dependent regulator
Ig	Immunoglobulin
IRAC	Insecticide resistance action committee
kbp	Kilo base pair

kD	Kilo dalton
LAPs	Latency associated peptides
LB	Luria-Bertani
LMW	Low molecular weight
LPS	Lipo polysaccharides
LSD	Least significant difference
MACs	Metamorphosis associated contractile structures
Mauve	Multiple alignment of conserved genomic sequence with rearrangements
mLB	Modified Luria Bertani
MMC	Mitomycin C
MQW	Milli Q water
mRNA	Messenger RNA
Mtx	Mosquitocidal toxin
MWCO	Molecular weight cut off
NCBI	National centre for biotechnology information
NRSPs	Non ribosomally synthesised peptides
NYSM	Nutrient yeast extract salt medium
O/N	Overnight
OD	Optical density
ORFs	Open reading frames
pADAP	Amber disease associated plasmid
PCD	Programmed cell death
PCR	Polymerase chain reaction
PEG	Polyethylene glycol
pfu	Phage forming unit
PHASTER	PHAge search tool enhanced release
PI	Propidium iodide
PTLBs	Phage tail-like bacteriocins
PTLP	Phage tail-like protein
PVS	Photorhabdus virulence cassettes
RAST	Rapid annotation using subsystems technology
RBP	Receptor binding protein
RBPs	Receptor binding proteins
RFH	Replacement for hilgendorf
RiPPs	Ribosomally synthesized and post translationally modified peptides
RNA	Ribonucleic acid
rpm	Rotations per minute
RSPs	Ribosomally synthesised peptides
SDG	Sucrose density gradient
SDS	Sodium dodecyl sulphate
SDS-PAGE	Sodium dodecyl sulphate polyacrylamide gel electrophoresis
SEC	Size exclusion chromatography
SOS	Save our souls
SPI	Spontaneous prophage induction
ss	Single stranded
SVM	Support vector machine
T6SSs	Type 6 secretion systems
TA	Toxin-antitoxin
TBS	Tris phosphate saline
TEM	Transmission electron microscope
TEMED	Tetramethylethylenediamine
UA	Uranyl acetate

UV	Ultraviolet
VIP	Vegetative insecticidal protein
16S rDNA	16S ribosomal DNA
16S rRNA	16S ribosomal RNA

Chapter 1

Introduction

1.1 Entomopathogenic bacteria as microbial pesticides

Nature has bequeathed us with enormous microbial diversity and one such treasure are bacteria. Bacteria are the most ubiquitous microorganisms on the earth (Soumia et al., 2021) with an estimated population of 4-6 x 10^{30} (Whitman et al., 1998) but only a fraction have been identified (Dykhuizen, 2005; Louca et al., 2019). These unicellular prokaryotic microorganisms lacking a nuclear membrane and other defined intracellular membrane-enclosed organelles exist in diverse shapes including spherical (cocci), rod (bacilli), and spiral (spirochaetes) (Glare et al., 2017; Jurat-Fuentes & Jackson, 2012). Bacteria proliferate through binary fission, a process resulting in daughter cells that are essentially identical copies of the mother cell (Couch & Jurat-Fuentes, 2014). Based on cell wall structure bacteria can be categorised into two groups, gram-positive and gram-negative, through a staining procedure first defined by Hans Christian Gram (Beveridge, 2001; Gram, 1884). Gram-positive bacterial cells have a thick peptidoglycan layer (90% of the cell wall) and stain blue to purple, while gram-negative cells have a thin peptidoglycan layer (10% of the cell wall) and stain red to pink (O'Toole, 2016; Popescu & Doyle, 1996).

Prokaryotic organisms are known to establish diverse interactions with many eukaryotic taxa, including insects (Jackson, 2017; Sanchez-Contreras & Vlisidou, 2008). Insects are the most diverse group of macroorganisms with over a million different species found in almost every habitat except the sea (Vilmos & Kurucz, 1998; Wernegreen, 2012). Due to their widespread distribution, all insect life stages are inevitably associated with bacteria in various forms (Aronson et al., 1986; Glare et al., 2017; Jurat-Fuentes & Jackson, 2012). The insect-bacteria relationship is either obligate or facultative with their hosts or produces toxins that can be used for insect control (Blow et al., 2020; Ferrari & Vavre, 2011). Entomopathogenic bacteria are pathogens that infect insects (Dimopoulos, 2003). The obligate bacterial entomopathogens like some *Paenibacillus* spp. complete their life cycles within the insect host (Koppenhöfer et al., 2012), while facultative pathogens such as *Serratia* spp. grow in an environment outside the host (Jackson, 2017). *Bacillus thuringiensis* (*Bt*) and *Chromobacterium subtsugae* are well known examples of bacteria that produce toxins that can be used without live bacteria against insect pest (Martin et al., 2007; Schnepf et al., 1998).

For infective bacteria, the insect pathogenic bacterium first enters the host hemocoel and hijacks the insect defence system to proliferate and produce virulence factors that aid infection, which ultimately kills the host (Raymond et al., 2010; Vallet-Gely et al., 2008). The virulence factors in most bacteria

are encoded by genes typically organised in operons, enabling the co-expressions of functionally related genes. Pathogenicity islands acquired through horizontal gene transfer and containing virulence genes have been identified in commercially relevant entomopathogenic bacteria, such as *Photorhabdus luminescens* (Vlisidou et al., 2019) and *Xenorhabdus nematophila* (Brown et al., 2004). However, in other cases, virulence factors are localised on plasmids that may be transferred through conjugation as in the case of many crystal toxin genes from *B. thuringiensis* (Held et al., 1982). The bacteria, upon killing the host, use their cadaver as a nutrient resource until the formation of dormant life stages, such as spores in the case of *Bacillus* spp., or cells that can infect a new host (Glare et al., 2017).

Entomopathogenic bacteria are classified within *Eubacteria* (Jackson, 2017). This group contains three major divisions based on the presence or structure of the cell walls: bacteria with a gram-positive type cell wall (*Firmicutes*), a gram-negative type cell wall (*Gracilicutes*), and those lacking a cell wall (*Tenericutes*) (Fisher & Garczynski, 2012; Jackson, 2017; Jurat-Fuentes & Jackson, 2012). Numerous bacteria have been defined for their entomopathogenic potential but only a few groups have been considered for commercialisation (Jurat-Fuentes & Jackson, 2012). Microbial pesticides derived from entomopathogenic bacteria dominate the biopesticide market worldwide due to their cost-effective mass production, specificity, persistence in the environment, and safety (Kabaluk & Gazdik, 2005). This is not surprising, as bacteria are often intricately associated with insects in diverse forms such as natural symbionts, disease-causing agents, and those encoding insecticidal toxins. The massive diversity of bacteria with natural and manipulated recombinants, and transferrable plasmids, provides an excellent resource for those seeking to develop unique biopesticides. Since the early 1930s, a wide range of spore-forming and non-spore forming bacterial strains have been developed as biopesticides (Lacey et al., 2015).

1.2 Entomopathogenic gram-negative bacteria as microbial pesticides

Insect pathogenic non-spore forming gram-negative bacteria are not preferred for use as biopesticides due to their instability during storage. However, improvements in formulation resulting in expanded shelf life under ambient conditions have allowed a strain of *Serratia entomophila* to be commercialised to manage the New Zealand grass grub, *Costelytra giveni* (Jackson et al., 1992; Johnson et al., 2001). Some other gram-negative bacteria developed into biopesticides include *Burkholderia* spp. (Cordova-Kreylos et al., 2013), *Chromobacterium subtsugae* (Koivunen et al., 2009; Stamm et al., 2013), *Pseudomonas entomophila* (Dieppois et al., 2015), *Yersinia entomophaga* (Hurst et al., 2019; Marshall et al., 2012) and *Wolbachia* spp. (Mateos et al., 2020; Moretti et al., 2018).

Entomopathogenic bacteria of Class *Mollicutes* are characterised by a lack of a cell wall, the low G+C content of genomic DNA, and the small size of genomes. They include organisms in the genera *Phytoplasma* (=*Mycoplasma*-like organisms) and *Spiroplasma* that are associated with insects but are principally known as plant pathogens which must be vectored by an insect host (Garnier et al., 2001). However, due to difficulties in their propagation, there are no examples of commercially developed entomopathogenic bacteria of this category (Jurat-Fuentes & Jackson, 2012).

1.3 Entomopathogenic gram-positive bacteria as microbial pesticides

The most commercially successful bacterial entomopathogens are gram-positive bacteria in the order Bacillales, more specifically the genera *Paenibacillus, Bacillus*, and *Lysinibacillus*. The vast majority of these are capable of producing an endospore- a dispersal form of the organism that is viable for extended time periods under adverse conditions. Endospore production greatly facilitates the commercial development and application of these bacteria for pest control (Couch & Jurat-Fuentes, 2014).

1.3.1 *Paenibacillus popilliae*

One of the first insect pathogens used for the control of insect pests was *Paenibacillus popilliae* (=*Bacillus popilliae*), the causative agent for milky disease in Japanese beetle (*Popillia japonica*) (Klein, 1988; White & Dutky, 1940). However, despite successful use, problems related to the mass production of viable *P. popilliae* spores (Stahly & Klein, 1992) stymied its commercial development. Commercial products based on *P. popilliae* are still available but their use is limited to control the Japanese beetle (grubs), specifically in areas of organic agriculture (Johnson et al., 2001).

1.3.2 *Bacillus thuringiensis*

The spore-forming bacilli bacteria of the family Bacillaceae are by far the most widely used in biopesticides, as the family contains a wide range of toxin-producing isolates, mostly belonging to *B. thuringiensis* (Bravo et al., 2011a; Crickmore, 2006). The insecticidal potential of *B. thuringiensis* has been reviewed in detail (Jallouli et al., 2020; Raymond & Federici, 2017; Sanchis, 2011). Since its discovery, isolation and screening efforts have demonstrated insecticidal activity against a range of insect pests from six taxonomic orders (Frankenhuyzen, 2009; Milner, 1994) and some of the species have been developed as commercial biopesticides for the management of coleopteran, dipterous, and

lepidopterous insect pests (Glare et al., 2017; Jurat-Fuentes & Jackson, 2012). *B. thuringiensis* produces numerous virulence factors and the specificity is mostly determined by the production of toxins, with the main toxins synthesised and packaged during sporulation into a parasporal crystal. Phenotypically, it is distinguished from other spore-forming *Bacilli* due to the presence of this crystal. The parasporal bodies may produce two main types of toxins, Cry (crystal) and Cyt (cytolytic) while Vip (vegetative insecticidal protein) toxins are produced and secreted by the vegetative cells. These toxins are named and classified according to protein sequence similarity (Crickmore et al., 1998); >300 Cry, 11 Cyt, and 32 Vip toxin holotypes have been described (Crickmore et al., 2016). All these *B. thuringiensis* toxins target midgut epithelial cells in the host to compromise epithelial integrity and facilitate the bacterial invasion of the haemocoel. Once *B. thuringiensis* cells invade the haemocoel, they grow and multiply until nutritional resources are exhausted, then enter the sporulation phase (Raymond et al., 2010).

1.3.3 *Lysinibacillus sphaericus*

Lysinibacillus sphaericus, a gram-positive bacterium was previously named *Bacillus sphaericus* (White & Lotay, 1980) due to the production of a spherical spore located in a terminal position within a swollen sporangium (Ahmed et al., 2007). This insect-pathogenic bacteria has been largely employed to control *Culex* and other mosquito species (Riaz et al., 2020; Su, 2017) and its mosquitocidal activity depends on the production of Bin (Binary) and Mtx (Mosquitocidal) toxins that target midgut cells in the host larvae (Silva Filha et al., 2014). Insecticidal activity is highly variable among the mosquito species (Silva Filha et al., 2014), with *Culex* mosquitoes being the most sensitive followed by *Anopheles*, *Mansoni*a, and some *Aedes* spp. (Berry, 2012; Lacey, 2007).

1.3.4 *Clostridium bifermentans*

Clostridium bifermentans is an anaerobic, spore-forming, gram-positive bacterium and its toxin have exhibited insecticidal activity against mosquitoes and blackflies (Chawla, 2015; Juárez-Pérez & Delécluse, 2001).

1.3.5 *Streptomyces* spp.

Streptomyces is a genus of gram-positive bacteria that grows in various environments, with a filamentous form similar to fungi (Bubici, 2018). Members of the genus can produce several compounds which are toxic to insects, whether their metabolites are used or viable cells are applied directly (Ruiu, 2013). The morphological differentiation of *Streptomyces* involves the formation of a layer of hyphae that can differentiate into a chain of spores. This process is unique among gram-positive bacteria, requiring specialised and coordinated metabolism (Ohnishi et al., 2008; Vetsigian et al., 2011). Vijayabharathi et al. (2014) reported that fifteen isolates of *Streptomyces* were consistently pathogenic to *Helicoverpa armigera*, *Spodoptera litura*, and *Chilo partellus*. *Streptomyces albus*, an endophyte of grass, showed high toxicity to the cotton aphid, *Aphis gossypii* (Shi et al., 2013). Avermectin (*Streptomyces avermitilis*) and Spinosad (*Saccharopolyspora spinosa)* are some of the microbial pesticides developed from this genus or the closely related *Saccharopolyspora* (Cai et al., 2011; Sparks et al., 2001).

1.3.6 *Brevibacillus laterosporus*

Brevibacillus laterosporus (*Bl*) is a gram-positive and spore-forming bacterium belonging to the *Brevibacillus brevis* phylogenetic cluster in the family Paenibacillaceae (Shida et al., 1996). The bacterial strains are known to exhibit broad-spectrum pathogenicity against insect pests (Glare et al., 2020; Ruiu, 2018). Several potential invertebrate toxin-encoding genes in *B. laterosporus* have been identified through genome sequencing, including *cry* (crystal) genes, although their role in toxicity in some cases has yet to be demonstrated (Djukic et al., 2011; Glare et al., 2020; Sharma et al., 2012).

1.4 Critical issues affecting the development of bacterial biopesticides

1.4.1 Abiotic factors influencing the effectiveness of bacterial biopesticides

The successful use of entomopathogenic bacteria for the control of insect pests is dependent upon several abiotic factors like temperature and sunlight (Baur & Fuxa, 2007; Koul, 2011). For example, during the application of the bacterium, a suspension of minute particles is deposited on the plant foliage and from the time the bacterium leaves the application equipment until it is consumed by the target species, it is exposed to fluctuations in environmental conditions. The period of exposure will vary depending on the feeding habits and activities of the target insect pest (Borges & Hussey, 1971; Legwaila et al., 2015). Often ultraviolet (UV) light limits the use of *Bt*-based biopesticides due to the inactivation of its crystals toxins against insect pests (Cohen et al., 1991).

1.4.2 Persistence of bacterial biopesticides

Insect pathogenic microorganisms that are being used in agriculture as biopesticides need to be repeatedly applied to the pest-infested areas because their populations are not self-sustaining for more than one or a few growing seasons, and they are not capable of spreading beyond the area of application. Typically, they have been delivered inundatively as a spray, drench, seed coating, or granules (except for endophytes that are delivered in seed or other propagation material). Post application of live organism-based biopesticides and/or their bioactives, their persistence and therefore activity on the plant or in the soil is not more than a few days. In this context, the persistence of activity for 14 days is a realistic target for most foliar-applied biopesticides (Glare et al., 2012). However limited persistence of the applied biopesticide/bioactive alleviates possible environmental and non-target concerns.

1.4.3 Narrow spectrum of bacterial biopesticides

Microbial pesticides, or biopesticides, represent a range of bio-based substances acting against invertebrate pests with different mechanisms of action (Ruiu, 2018). However, many commercially available biopesticides have a narrow spectrum of activity, which generally limits their potential market. For example, the bacterial biopesticide based on *P. popilliae* has a single susceptible host, the Japanese beetle (*P. japonica*), (Jurat-Fuentes & Jackson, 2012). Bioshield™, a product based on *S. entomophila*, is only effective against a single insect pest (*C. giveni*) (Grimont et al., 1979; Jackson et al., 1992). There is no doubt that the limited spectrum of activity contributes to environmental and non-target safety, but it has confined biopesticides to niche markets, making their development and commercialisation more difficult (Glare et al., 2012).

1.4.4 Evolution of resistance against bacterial biopesticides

Globally, microbial pesticides based on gram-positive bacteria, especially *B. thuringiensis*, are the most extensively used biopesticides (Glare & O'Callaghan, 2000) but several insect pests have developed resistance to *B. thuringiensis* based pesticides or transgenic crops that express usually single *B. thuringiensis* toxin (Bernardi et al., 2015; Dara, 2017; Peralta & Palma, 2017; Tabashnik, 1994). There are reports that at least 27 pest species have evolved resistance to the most widely used *B. thuringiensis* based biopesticide in the world (Berling et al., 2009; Bravo et al., 2011b; Siegwart et al., 2015).

Biopesticides synthesised from another gram-positive bacteria, *L. sphaericus*, have been extensively used against dipterous insect pests. However, since 1994, both laboratory and field populations of *Culex pipiens* complex have developed resistance to these microbial pesticides (Sinègre et al., 1994; Su et al., 2019; Wirth et al., 2015).

1.4.5 Biotic factors affecting the development of bacterial biopesticides

Bacteria seldom exist in isolation and generally reside within diverse microbial communities (Klein et al., 2020). Within these, microbial communities they are vulnerable to certain competitors or enemies for their survival (Hibbing et al., 2010). The role of these microbial antagonists is significant for the use of entomopathogenic bacteria in the development of microbial pesticides (Liao et al., 2008; Wilson et al., 1993). Based on this context an outline of the microbial antagonists is presented the next section.

1.5 Microbial antagonists

Like many other organisms, bacterial growth can be inhibited by a range of viruses or non-replicating virus-like particles, which fall naturally into two physiologically separate groups, bacteriophages, and bacteriocins. The bacteriocins differ in that they do not multiply in the cell after infecting it, but only kill it (Bradley, 1967b; Hockett & Baltrus, 2017).

1.5.1 Bacteriophages

Bacteriophages are “bacterium eating viruses” that kill bacteria through lysis of their cells (Paczesny et al., 2020). Phages were discovered independently by Frederick Twort and Felix d’Herelle in 1915 and 1917 respectively (Grabow, 2001; Nelson, 2004) and are known to play an important role in driving the global geochemical cycles (Suttle, 2005). Over a century of phage research has revealed the extreme diversity and ubiquitous nature of these viruses preying on eubacteria and archaea in a wide range of biological niches. Bacteriophages are considered the most abundant ‘‘organisms” on earth with an estimated population of 10^{31} virions in the earth's biosphere (Brüssow & Hendrix, 2002; Hambly & Suttle, 2005; Wommack & Colwell, 2000). This number is 10 times greater than the bacterial population (Canchaya et al., 2004; Hendrix, 2002).

Bacteriophages play many roles in the ecology and genomic evolution of bacteria. For example, they can mediate lateral gene transfer (Wommack & Colwell, 2000) and in some cases provide their hosts with beneficial genes (Abedon & LeJeune, 2005; Brüssow et al., 2004). Bacteriophages can also

regulate the numbers of their host bacteria by inhibiting their replication or inducing cell lysis (Bordenstein et al., 2006). An estimate of the number of extant bacterial species suggests it to be ten million upwards and multiple types of tailed phages have been found to infect each bacterial species which suggests the number of types could be extremely large (Dykhuizen, 1998; Rohwer, 2003). Rohwer (2003) calculated that over two billion novel phage genotypes likely remain to be discovered. The extensive genetic diversity of these viruses is due to their very ancient origin, large population size, and high ability to evolve. Despite more than 10^5 genes already described in phage genomes (Kristensen et al., 2013), a recent study suggests that the function of the majority of phage genes has yet to be elucidated (Turner et al., 2021).

A. Bacteriophage life cycle

A bacteriophage particle or virion consists of a single (ss) or double-stranded (ds) DNA or RNA molecule, encapsulated inside a protein or lipoprotein coat. After infection, a phage can follow two alternative cycles of replication, lytic or lysogenic (Figure 1.1) (Olszak et al., 2017; Young et al., 2000). Most phages undergo lytic phage infection cycles whereby daughter progeny are produced and released at the expense of host cell lysis and death (Bordenstein et al., 2006). These are considered "productive infections" where infections quickly lead to the release of viral progeny. Once the viral genome enters the host cell, phage-encoded genes are expressed in the bacterial cytoplasm, the function of which is to take over the host bacterial metabolism (Young, 2014). The phage replicates its genome and assembles hundreds of new progeny, which are then released after cell lysis (Abedon, 2012; Young, 2014).

In the lysogenic cycle, the temperate phage genome interacts reversibly with the host genetic apparatus in such a way that does not lead to multiplication but allows the viral genome to replicate in synchrony with the host DNA replication and cell division. The phage genome either remains in the host as a plasmid or integrated into the host chromosome as a "prophage" and bacterium incorporating a prophage are called "lysogens". Lysogeny comes at a cost to the bacterial host due to the extra burden of replication of prophage DNA and the threat of lysogen induction, which is lethal to the host cell. On the other hand, there are many well-documented examples of lysogenic conversion, where prophage encoded products confer new and advantageous characteristics on the host (Brüssow et al., 2004; Fortier, 2017). These intact prophages are molecular time bombs that can kill their hosts upon activation of the lytic cycle (Casjens, 2003; Harrison & Brockhurst, 2017b; Ptashne, 1992). The prophage, under certain conditions, is induced into the lytic cycle of phage replication in response to host and/or other external danger signals (typically the host SOS response) (Grabow, 2001; Mardanov & Ravin, 2007). Lysogeny is widespread in bacteria (Howard-Varona et al., 2017;

Weinbauer, 2004) and most prophage genomes share the same genetic organisation: they are organised in two clusters of genes each controlling related functions, which are transcribed divergently. One of these clusters comprises genes participating in the integration and maintenance of lysogeny; the other includes genes involved in the lytic life cycle. These genomes have a mosaic structure of conserved sequences interspersed by non-homologous regions (Botstein, 1980; Brüssow et al., 2004) which suggests that prophages evolve by horizontal DNA transfer through the exchange of modules via homologous recombination (Brüssow et al., 2004; Casjens, 2003).

B. Bacteriophage classification

Historically, the International Committee on the Taxonomy of Viruses (ICTV) used virion morphology, nucleic acid composition, and the presence or absence of an envelope or lipid as a basis for the classification of phages into 13 families. Over 95% of all phages described in the literature belong to the order 'Caudovirales' or tailed dsDNA phages (Ackermann, 2001). The three main families that constitute the Caudovirales are distinguished by their distinctive tail morphologies: 60% of the characterised phages are *Siphoviridae*, with long, flexible tails; 25% are *Myoviridae*, with double-layered, contractile tails; and 15% are *Podoviridae* with short, stubby tails. Polyhedral, filamentous, and pleomorphic phages represent only 3% to 4% of the studied phages, some of which are very small and belong to 10 families (Ackermann, 2007). The ICTV classification approach described above is currently being re-evaluated since it ignores the vast amount of available genome sequences data, which occasionally causes contradictions (Turner et al., 2021). For example, despite an absence of DNA sequence relatedness, the current taxonomic system lists both the *Salmonella* P22 phage and the Coliphage T7 as belonging to the *Podoviridae* family based on the shared presence of short tails. However, it has been known for more than 35 years that P22 is genetically related to the long-tailed phage lambda and that recombination between genomes of the two groups forms functional hybrids (Botstein & Herskowitz, 1974). There have been efforts to use alternative (molecular) classification methods, but this has been proven to be difficult because no universal gene, analogous to the 16S rRNA gene used for bacteria, exists throughout all phage families (Paul et al., 2002). Comparative approaches based on terminase sequences (Serwer et al., 2004), structural genes (Chibani-Chennoufi et al., 2004), and whole proteomes (Dion et al., 2020; Rohwer & Edwards, 2002) were proposed as novel taxonomic tools. Lavigne et al. (2008) delineated new phage subfamilies and genera using a method that integrated BLASTp-based tools with a careful review of the available literature, which laid the basis for systematic and genome-based classification of sequenced phages.

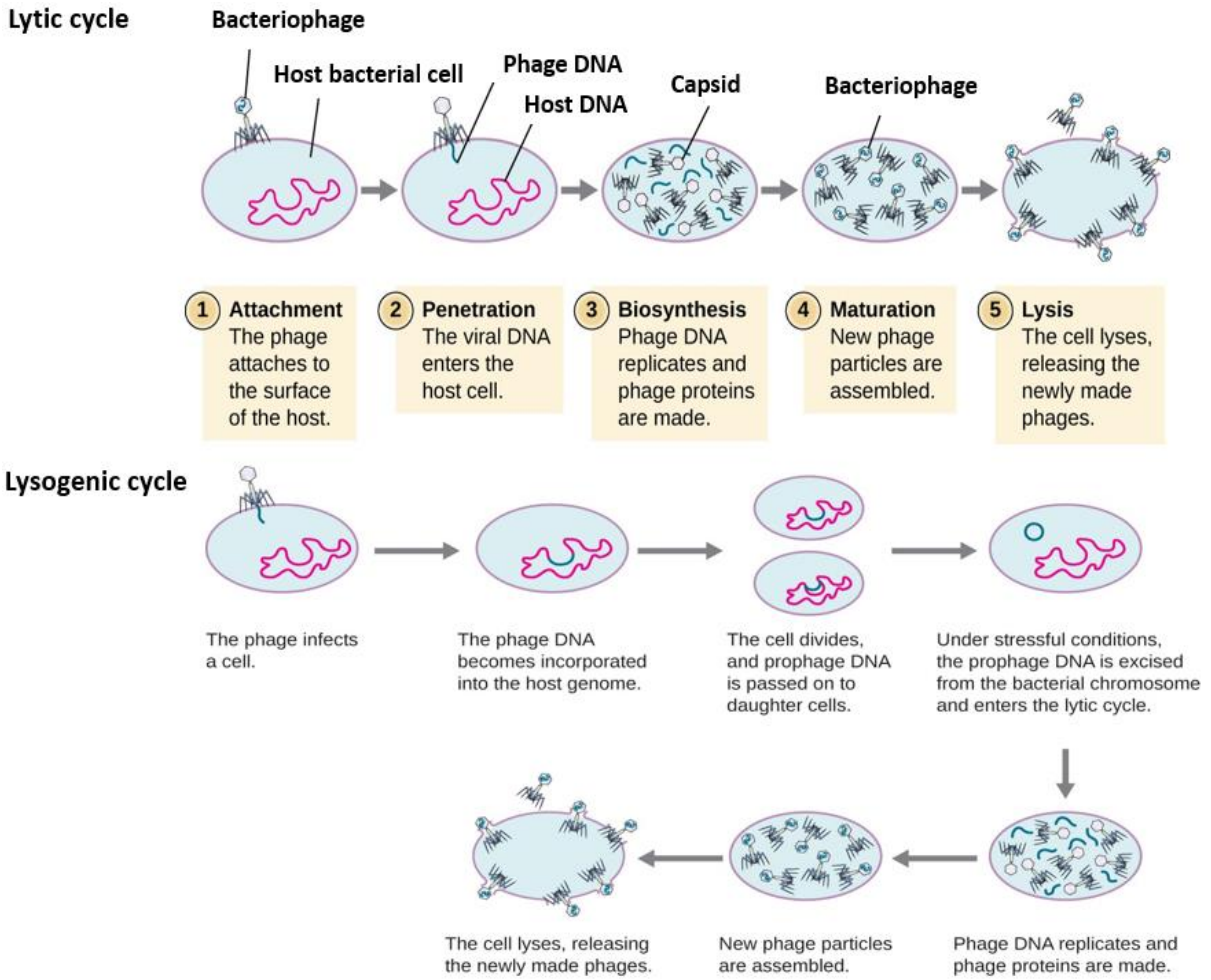

Figure 1.1 Life cycle of a bacteriophage. A temperate bacteriophage has both lytic and lysogenic cycles. The phage replicates and lyses the host cell in the lytic cycle, whereas in the lysogenic cycle, phage DNA is incorporated into the host genome, where it is passed on to subsequent generations. Environmental stressors such as starvation or exposure to toxic chemicals may cause the prophage to excise and enter the lytic cycle (Sourced from: www.lumenlearning.com)

C. Bacteriophages contribution towards the pathogenicity of host bacteria

A significant threat to the large-scale production of bacteria is an infection by bacteriophages which can cause a collapse of the culture through lysis of the cells (Beegle, 1991). About 83% of *B. thuringiensis* strains contain lysogenic phages, which are highly detrimental during fermentation and can cause 15% to 30% failure of production batches (Liao et al., 2008). Wu et al. (2014), using proteomics, have shown how bacteriophages infection of *B. thuringiensis* depressed host metabolism

and hijacked the host translational machinery to damage the cells and suppress the growth of the culture.

Similarly, Wilson et al. (1993) described the isolation of bacteriophages specific to an insect pathogenic and the gram-negative bacterium *S. entomophila* from macerated grass grub larvae. These phages caused problems in biomass production of *S. entomophila* before its field application (O'Callaghan et al., 1992).

1.5.2 Bacteriocins

Bacteriocins are ribosomally synthesised cationic and hydrophobic toxic peptides or proteins, produced by all major lineages of bacteria, generally inhibit the growth of bacterial strains closely related to the producer and often encode immunity proteins that protect producer strains from their lethal action (Cotter et al., 2005; Riley, 2011). The bactericidal effect of bacteriocins against other bacterial strains has been investigated for many years (Bastos et al., 2009; Cleveland et al., 2001; Gratia, 1925). The bacteriocin effects may be just bacteriostatic halting growth without causing lethality to host cells. For example, some *B. thuringiensis* bacteriocins play a bacteriostatic role against *Salmonella* spp. (de la Fuente-Salcido et al., 2012). However, certain bacteriocinogenic strains are sensitive to their own bacteriocin, like hyicin 3682 (Fagundes et al., 2011).

The vast majority of bacteria are known to produce at least one bacteriocin as part of their defence mechanism (Lucas et al., 2006; Riley & Wertz, 2002a). Gratia (1925) was the first to introduce a description of bacteriocins while describing the antagonism of *Escherichia coli* V*,* against *E. coli* Ø however, Jacob and Wollman (1953) coined the term “bacteriocin”. The bactericidal spectrum of bacteriocins is relatively narrow because the bacteriocins produced by gram-positive bacteria cannot kill gram-negative strains under normal growth conditions (Jack et al., 1995). Nevertheless, several bacteriocins of gram-positive bacteria display a fairly broad inhibitory spectrum of activity (Hata et al., 2010; Riley & Wertz, 2002a). Genes encoding bacteriocin production and immunity are often located on plasmids, although they can be found on the bacterial chromosome as well (Heng et al., 2007).

A. Bacteriocins of gram-positive bacteria

Bacteriocins of gram-positive bacteria are more abundant and even more diverse than those from gram-negative bacteria (Jack et al., 1995). Most members of this category display bactericidal activity with fairly broad inhibitory activities (Hata et al., 2010). The major classifications of gram-positive bacteriocins are:

Class I bacteriocins

Class I bacteriocins are characterised by small peptides/lantibiotics (<5 kD, 19–37 amino acids) having the unusual amino acids lanthionine and methyllanthionine in their primary structure. These bacteriocins are post-translationally modified, heat-stable peptides, and generally target the cell wall of pathogens particularly gram-positive bacteria (Arnison et al., 2013).

Subclass Ia bacteriocins: Positively charged elongated bacteriocins that kill bacteria by pore formation. Nisin, is an example of this group (Deegan et al., 2006; McAuliffe et al., 2001).

Subclass Ib bacteriocins: Negatively charged or with no net charge with globular and inflexible structures. These bacteriocins inhibit various catalytic enzymes required to complete the life-supporting processes of susceptible bacteria. Lacticin 481, cytolysin, and salivaricin are typical examples of this category (Deegan et al., 2006).

Class II bacteriocins

Class II bacteriocins are heat-stable, small, 30-60 amino acids (<10 kD) peptides that are not post-translationally modified, and positively charged with isoelectric points (pIs) varying from 8.3 to 10.0 (Ennahar et al., 2000; Heng et al., 2007).

Subclass IIa bacteriocins: The antilisterial bacteriocins are grouped in this class. The representative bacteriocins of this group are leucocin A, acidocin A, mesentericin, pediocin PA-1, and sakacin P (Ennahar et al., 2000; Venema et al., 1997).

Subclass IIb bacteriocins: Bacteriocins of this class require at least two different peptides for activity and thus generally act synergistically. These peptides have little or no activity when tested individually, e.g. lactococcin G and plantaricins (Gong et al., 2010).

Subclass IIc bacteriocins: These are small and heat-stable peptides that are carried by leader peptides. The members of this subclass are further divided into two groups, the thiolbiotics, and cystibiotics. Thiolbiotics are bacteriocins with two cysteine residues, whilst bacteriocins with one cysteine residue are cystibiotics. Lactococcin A, divergicin A, and acidocin B are typical members of this class (Joerger & Klaenhammer, 1986).

Class III bacteriocins

These are large (>30 kD) peptides which may be heat-labile lytic bacteriocins lysing the cell wall of bacteria in an enzymatic manner or heat-labile, high-molecular weight bacteriocins without a lytic mode of action such as helveticin J from *Lactobacillus helveticus* 481, dysgalacticin from *Streptococcus dysgalactiae* subsp. *equisimilis* W2580, and s*treptococcin* A-M57 (Joerger & Klaenhammer, 1986; Vaughan et al., 1992).

Class IV or complex bacteriocins or cyclic bacteriocins

These complex bacteriocins containing lipid or carbohydrate moieties are sensitive to glycolytic or lipolytic enzymes, e.g. plantaricin S, leuconocin S, and uberolysin (Lewus & Montville, 1991; Wirawan et al., 2007).

B. Bacteriocins of gram-negative bacteria

Gram-negative bacteria bacteriocins are typically larger in comparison to bacteriocins of gram-positive bacteria, and range in size from < 10 kD to > 20 kD. Gram-negative bacteria bacteriocins differ from bacteriocins of gram-positive bacteria in two fundamental ways: First, they are usually released through cell lysis, and second, they are often dependent on host regulatory pathways, like SOS regulation (Chavan & Riley, 2007). Furthermore, this group contains colicins and microcins categories.

Colicins

Colicins are protease-sensitive, heat-sensitive, high-molecular weight (HMW) (30-80 kD), and narrow-spectrum antibacterial proteins of gram-negative bacteria, *E. coli*, that have a single colicinogenic plasmid (Gordon et al., 2007; Zimina et al., 2020). Colicin synthesis is carried out under stress and is fatal for producing cells, due to co-expression with lysis protein (Braun et al., 1994) that kills target cells through a variety of mechanisms (Riley & Wertz, 2002b). Colicins can inhibit macromolecular synthesis without the arrest of respiration (Colicins A, E1, K), cause DNA breakdown (Colicins E2, E7, E8, E9), and stop protein synthesis (Colicins E3, E4, E6) (Cascales et al., 2007; Chavan & Riley, 2007).

Microcins

Microcins are low-molecular weight (LMW) (<10 kD), highly stable peptides, and are resistant to proteases, extreme pH, and temperature values (Baquero & Moreno, 1984; Gillor et al., 2004). The classic example is microcin V, of *Escherichia coli* (Jeziorowski & Gordon, 2007) . Gene clusters encoding microcins are located in plasmids, and less often, in genomic DNA. Microcins express a powerful

antibacterial activity and typically have a broader killing spectrum as compared to colicins. The killing mechanism involves the formation of pores or disrupting the cell membrane potential of sensitive cells (Destoumieux-Garzón et al., 2003; Morin et al., 2011).

C. Mode of action of bacteriocins

Bacteriocins can kill the target cells in a variety of ways, through their effect on the cytoplasmic membrane (Riley & Chavan, 2007). Bacteriocins of both gram-positive and gram-negative bacteria exert their bactericidal activity through their adsorption to specific receptors (Tagg et al., 1976) located on the surface of the susceptible bacteria. The attachment of the bacteriocins alters the metabolic activities and morphological features of the cells due to lysis (Oscáriz & Pisabarro, 2001). However, various other modes of action, including inhibition of cell wall peptidoglycan synthesis (Bierbaum & Sahl, 2009), production of bacteriolytic enzymes (Kumar, 2008), interference with quorum sensing (Kleerebezem, 2004), and the secondary action of bacteriocins are also observed (Martínez-Cuesta et al., 2000). Sometimes, the autolytic system of the bacteriocin sensitive cells causes the lysis due to degradation of cell wall instead of disruption of the membrane potential. Therefore, it is often called the secondary action of bacteriocins (Jack et al., 1995)

1.5.3 Phage tail-like bacteriocins (PTLBs)

High-molecular weight (HWM) proteinaceous structures resembling phage tails which are functional without an associated phage head are known as “Phage tail-like bacteriocins” (Ghequire & De Mot, 2015). Occasionally these are also referred to as defective prophages (Bobay et al., 2014; Krogh et al., 1998) or phage remnants (Canchaya et al., 2002; Ventura et al., 2003). These multi-protein antibacterials consist of eight to fourteen different polypeptide subunits that are encoded in the genomes of bacteria by a cluster of genes >40 kbp (Zimina et al., 2020). The locus includes genes encoding structural proteins, assembly enzymes, chaperones, regulatory genes, and lysis cassettes, whose function is to release bacteriocins into the environment (Alvarez-Sieiro et al., 2016; Young, 2013).

Phage tail-like bacteriocins have been extensively isolated and characterised in various gram-negative bacteria (Fischer et al., 2012; Hockett et al., 2015; Yao et al., 2017). The most well studied phage tail-like bacteriocins are R-type and F-type pyocins of *Pseudomonas aeruginosa*. The induction of synthesis of these compounds is associated with the SOS response of the producer cell to DNA damage (Scholl, 2017). Diffocins of *Clostridium difficile* are the only gram-positive contractile R-type PTLBs that have been studied in any detail (Gebhart et al., 2012).

A. R-type pyocins

Kageyama and Egami (1962) described a pyocin produced by *P. aeruginosa* strain R which appears as a rod-like particle resembling a *Myoviridae* phage tail (Nakayama et al., 2000) (Figure 1.2). R-type pyocins are categorised into five subgroups based on their target spectrum *i.e.*, R1-R5 (Kageyama, 1975; Michel-Briand & Baysse, 2002; Takeda & Kageyama, 1975). Some additional R-type pyocins, not assigned to one of these groups, include C9 (Higerd et al., 1967), pyocin 21, and 430c (Govan, 1974).
The killing mechanism of R-type bacteriocins is related to the mechanism in which *Myoviridae* phages translocate DNA into the cell after binding but instead of DNA entering the cell, a pore is created (Ge et al., 2020; Scholl, 2017). This mechanism is also similar to that described for the bactericidal activity of phage T4 ghosts, which are phages that lack DNA (Duckworth, 1970).

B. F-type pyocins

F-type pyocins are the non-contractile and rod-shaped structures of *P. aeruginosa* which are similar in form to the *Siphoviridae p*hages (Lee et al., 2016; Saha et al., 2021) (Figure 1.2). Numerous F-type pyocins have been reported: pyocin 28 (Takeya et al., 1967), 430f (Govan, 1974), F1 and F2 (Kuroda & Kageyama, 1979), and F3 (Kuroda & Kageyama, 1981). These antibacterials are often produced and co-expressed with R-type pyocins or bacteriophages (Kuroda & Kageyama, 1979; Saha et al., 2021).
F-type pyocins do not have a contractile mechanism; they possess a simple tube that presumably does not penetrate the inner membrane (Saha et al., 2021). Little work has been done to understand the mechanism of action of F-type pyocins. However, as with R-type pyocins, a single particle can kill a cell, particularly with F-type monocins, suggesting that a similar channel is formed in the inner membrane, resulting in disruption of respiration, but this is still only a speculation (Lee et al., 2016; Scholl, 2017).

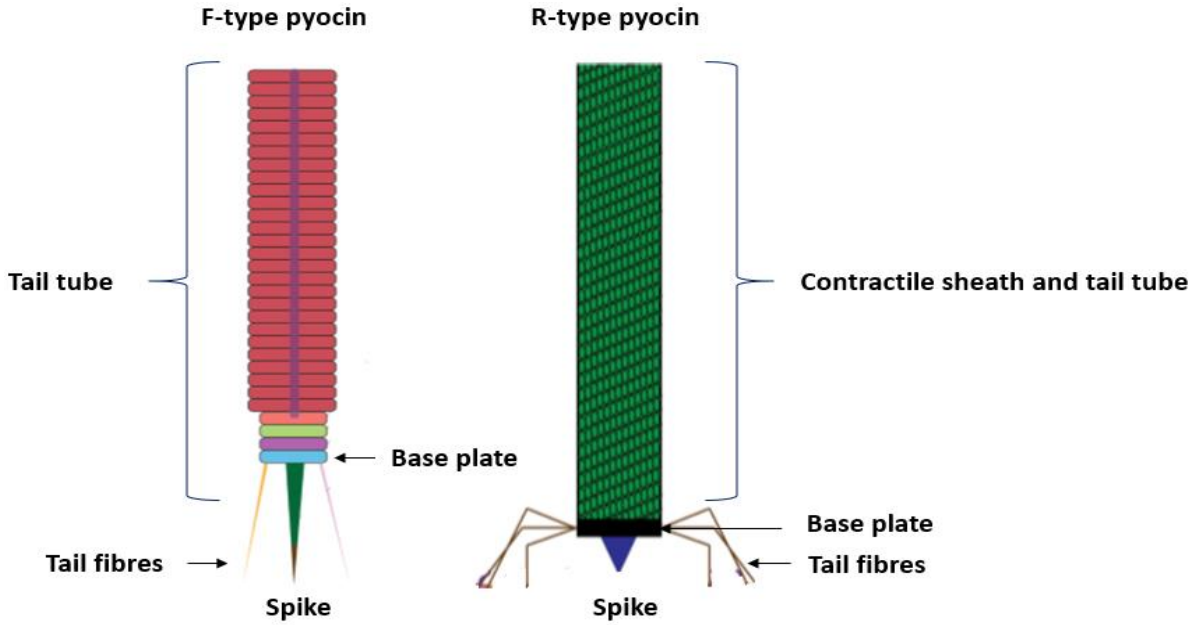

Figure 1.2 Typical structures of phage tail-like bacteriocins (Saha, 2016)

1.6 Phage tail-like homologous structures

1.6.1 *Photorhabdus* virulence cassettes (PVC)

Photorhabdus luminescens is an insect pathogenic, gram-negative, bioluminescent bacterium formerly known as *Xenorhabdus luminescens* (Clarke, 2020). The bacterium dwells in the gut of a free-living form known as the infective juvenile (IJ) of the entomopathogenic nematode, *Heterorhabditis bacteriophora* (Ehlers, 2001). The particular combination holds great potential to control agricultural pests due to its toxicity to a wide range of insect pests belonging to families like Pyralidae, Sphingidae, and Aleyrodidae (Kooliyottil et al., 2013). It should be noted that PVC-like elements are not restricted to *Photorhabdus* as a well-characterised homologous operon can also be found on the pADAP plasmid of the insect pathogenic bacterium *S. entomophila* (Hurst et al., 2004). This system has been named "Antifeeding prophage" (Afp), as it is responsible for the cessation of feeding in the New Zealand grass grub host (*C. giveni*). Cryo-electron microscopy of Afp particles has revealed morphological similarities to the contractile sheathed T4 bacteriophages (Hurst et al., 2004).

PVCs constituent proteins exhibit structural similarities with other contractile phage tail derived systems, including the Type VI secretion system (T6SS) (Desfosses et al., 2019; Kapitein & Mogk, 2013) and to a lesser extent R-type pyocins (Taylor et al., 2018). However, PVC-like elements are distinct in two important ways. Firstly, unlike the T6SS, they require no membrane complex for anchoring and

synthesis and are freely released from the producing bacterial cell (Durand et al., 2015). Therefore, in common with R-type pyocins, they can act at a distance. Secondly, like T6SSs but unlike R-type pyocins, they have evolved to inject bioactive protein effectors into other cells (Vlisidou et al., 2019).

1.6.2 Metamorphosis associated contractile structures (MACs)

Metamorphosis associated contractile structures are the first extracellular contractile injection system (eCIS) discovered to puncture membranes and deliver an array of phage tail-like structures (proteinaceous effectors) into target cells (Brackmann et al., 2017). The interaction of the marine tubeworm *Hydroides elegans* and the bacterium *Pseudoalteromonas luteoviolacea* presents a typical model for the study of invertebrate metamorphosis (Ericson et al., 2019; Hadfield, 2011). Like other contractile injection systems, MACs are also evolutionarily related to the contractile tails of bacteriophages (Rocchi et al., 2019; Shikuma et al., 2014).

1.6.3 Type VI Secretion System (T6SS)

Gram-negative bacteria over time have developed sophisticated nanomachines resembling phage tail-like structures that span both membranes to guide the exoproteins from the interior to the exterior of the cell (Bingle et al., 2008; Filloux, 2011). Mekalanos and co-workers in 2006 identified the novel Type VI secretion system (T6SS) (Mougous et al., 2006), which has since been predicted to be present in 25% of all the sequenced gram-negative bacteria (Basler et al., 2013). T6SS has the potential to act as “antibacterial T6SS” (Russell et al., 2014) or “anti-eukaryotic T6SS” (Basler, 2015) by translocating bacterial effector proteins. T6SSs can serve as effective weapons against gram-negative bacteria both of the same or different species (Kapitein & Mogk, 2013). To protect against the potentially lethal effect of effectors, bacteria that encode T6SS most often produce a set of corresponding “anti-effectors” (immunity proteins) that confer “immunity” to effectors of their own or from other bacteria (Journet & Cascales, 2016).

Morphologically, the T6SS machine resembles an “inverted” bacteriophage tail and shares a common origin with contractile tail phages (Leiman et al., 2009). However, in T6SS, the tail-like structures are built inside the cytoplasm and inversely oriented, with their spike pointing outwards (Galán & Waksman, 2018). T6SS tail is composed of an external layer, a contractile sheath, and a hollow inner tube that stores small protein effectors before their secretion. Similar to an armed crossbow, the assembled T6SS remains inactive and ready to fire until it somehow senses a prey cell within the firing range (Ho et al., 2014). This activates sheath contraction, which exposes the spike, then penetrates

the prey cell envelope and delivers its deadly cargo into target cells using a dynamic 'firing' mechanism related to the action of contractile bacteriophage tails (Cianfanelli et al., 2016).

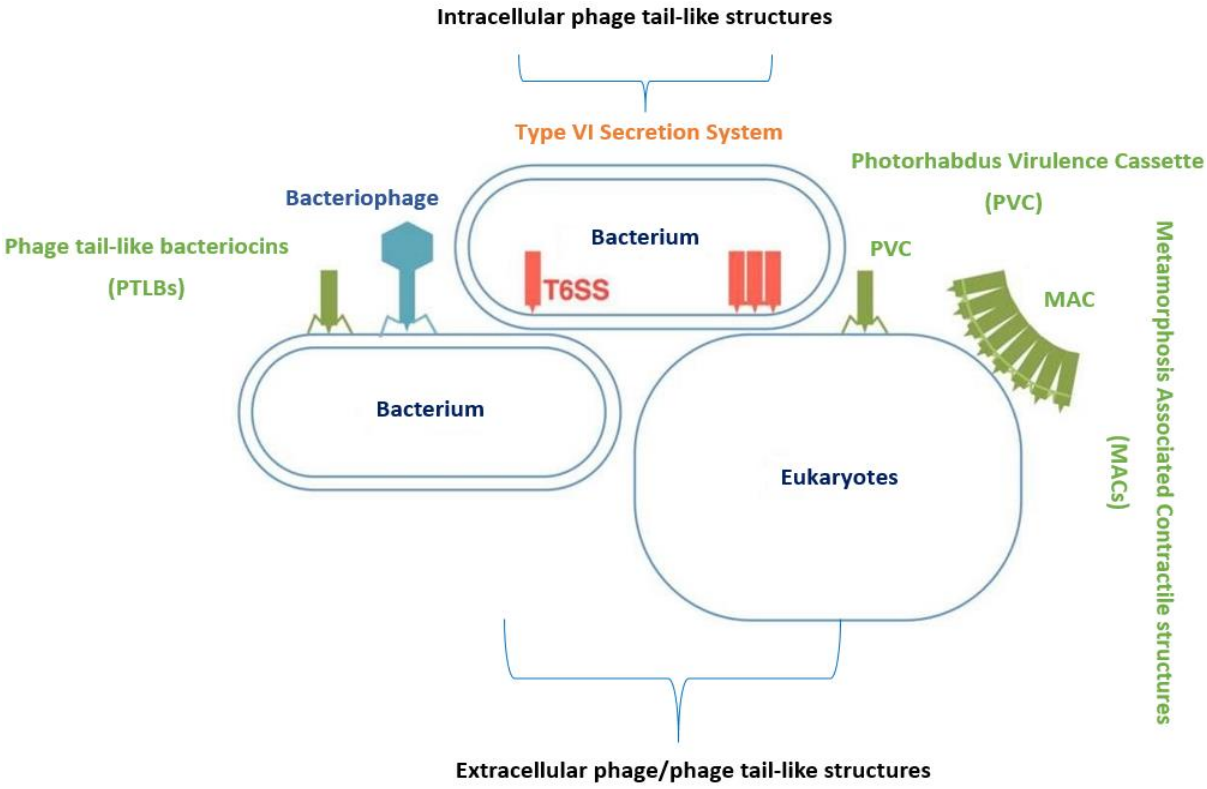

Figure 1.3 Diagrammatic presentation of phage and phage tail-like structures. Bacteriophages, phage tail-like bacteriocins (PTLBs), and phage tail-like homologous structures like PVC and MACs act extracellularly. The target of the PVC and MACs is eukaryotic cells and they are not lethal to bacterial cells. Type VI secretion system (T6SS) acts intracellularly (Sourced from: www.pilhoferlab.ethz.ch)

1.7 *Brevibacillus laterosporus*

1.7.1 *Brevibacillus laterosporus* potential as a biopesticide

Brevibacillus laterosporus (Laubach) is an often entomopathogenic, gram-positive, and spore-forming ubiquitous bacterium found in soil and water around the world (Glare et al., 2020; Hannay, 1957; Suslova et al., 2012). This broad-spectrum bacterium is classically distinguished by the production of a canoe-shaped parasporal body (CSPB) attached to one side of the spore, which defines its lateral position in the sporangium (Azizbekyan et al., 2015; Marche et al., 2017; Ruiu, 2013). The genus *Brevibacillus* was originally described as part of the *Bacillus* (Laubach et al., 1916) but was

differentiated from the genus *Bacillus* based on 16S rDNA sequencing (Shida et al., 1996). Currently, the genus *Brevibacillus* comprises 27 species (https://lpsn.dsmz.de/genus/*Brevibacillus*).

Globally, various strains of this bacterium have exhibited biocontrol potential against invertebrate pests of different insect orders including Coleoptera (Bowen et al., 2021; Salama et al., 2004; Singer, 1996), Diptera (Bedini et al., 2021; Carramaschi et al., 2015; Ruiu et al., 2006; Zubasheva et al., 2010), Lepidoptera (Ertürk & Demirbag, 2006; van Zijll de Jong et al., 2016), and also against nematodes (Zheng et al., 2016) and molluscs (De Oliveira et al., 2004; Singer et al., 1994). The insecticidal action is mostly related to the production of diverse toxins, most of which act in the insect gut after ingestion (Glare et al., 2020; Marche et al., 2018). Therefore, due to the entomocidal action of *B. laterosporus* against multifarious insect pests, there has been a surge of interest in the commercialisation of patents for future microbial pesticides development (Boets et al., 2011; Floris et al., 2011; Glare et al., 2014; Glare et al., 2018; Sampson et al., 2016).

Various strains of *B. laterosporus* can produce a wide range of enzymes and antibiotics which exhibit broad-spectrum antimicrobial activity against diversified phytopathogenic bacteria and fungi (Chandel et al., 2010). These antimicrobial peptides are resistant to heat, proteases, and pH changes, which makes them a favourable biological agent (Zhao et al., 2012b). The bacteria has long been noted for its antifungal properties when isolated from rhizosphere soil samples (Idris et al., 2008). *B. laterosporus* BPM3 isolated from mud in India inhibited the growth of the phytopathogenic fungi *Fusarium oxysporum*, *F. semitectum*, *Magnaporthe grisea,* and *Rhizoctonia oryzae* and of the gram-positive bacterium, *Staphylococcus aureus*. The broad-spectrum antimicrobial compounds responsible for the observed effects were purified and characterised (Saikia et al., 2011). *B. laterosporus* ZQ2, isolated from an apple tree rhizosphere in China, inhibited the growth of various apple tree fungal phytopathogens including *Rhizoctonia solani*, *F. oxysporum*, *F. solani*, *Aspergillus fumigatus*, *Alternaria alternata*, *Colletotrichum gloeosporioides*, *Botrytis cinerea,* and *Physalospora piricola* (Song et al., 2011). Zhao et al. (2012b) isolated and characterised a novel antimicrobial peptide BL-A60 from *B. laterosporus* strain A60. This short sequence peptide has a molecular mass of about 1.6 kD and has demonstrated activity against diverse plant pathogens including the gram-negative bacteria, *P. solanacearum* and *Xanthomonas campestris*, the gram-positive bacterium, *Bacillus subtilis*, and the fungi, *Phytophthora capsici*, *B. cinerea*, *Verticillium dahliae,* and *F. oxysporum*. This strain also enhanced the immunity of tobacco plants against infection by *B. cinerea* through secretion of the protein elicitor PeBL2 (Jatoi et al., 2019).

Some strains of *B. laterosporus* also produce chitinases that may play a major role in the degradation of the cell wall of fungi. *B. laterosporus* Lak 1210, isolated from mangrove marsh soil in India, when grown on media containing colloidal chitin, produced chitinases that were released in the culture

supernatant. The activity of these antifungal proteins was assayed against the phytopathogenic fungus *F. equiseti*. These proteins had high homology with an 89.4 kD four domain chitodextrinase and with a 69.4 kD, two domain chitinase (ChiA1) encoded by *B. laterosporus* LMG 15441 (Prasanna et al., 2013).

B. laterosporus, in addition to expressing activity against phytopathogenic bacteria and fungi, also showed activity *in vitro* against the bacterium *Paenibacillus larvae*, the causal agent of American foulbrood of honeybees (Alippi & Reynaldi, 2006). Marche et al. (2019) observed the inhibition of both *P. larvae* vegetative growth and spore germination when treated with culture supernatant of *B. laterosporus* strain F5. Mass spectrometry analyses revealed a protein complex in which the 5.7 kD bacteriocin, laterosporulin, was the major active component, followed by high-molecular weight proteins representing the different layers that make up the cell wall, and other functional (*i.e.*, enzymes) and stress-related peptides. F5-produced laterosporulin showed 100% homology with laterosporulin produced by *B. laterosporus* strains GI-9 (Singh et al., 2012) and LMG 15441 (Djukic et al., 2011), confirming that this bacteriocin is highly conserved in *B. laterosporus*. Current work highlights the potential of laterosporulin as a biological control against *P. larvae* (Marche et al., 2019). Endophytic use of this broad-spectrum bacterium can significantly reduce the intensity of various diseases like the common scab of potato caused by *Streptomyces* spp. (Chen et al., 2017), brown stripe of rice caused by *Acidovorex avenae* subsp. *avenae* (Kakar et al., 2014), and some of these strains also impart antifungal effects (Song et al., 2011; Zhou et al., 2006).

The entomocidal action and biocide effect (antibacterial & antifungal) of this useful microorganism can expand its biocontrol potential (Ghazanchyan et al., 2018). However, it is considered vital that besides determining the biocontrol potential of an entomopathogen, its effects on the agricultural ecosystem should be considered in the broadest sense. This involves the evaluation of possible effects against beneficial organisms like predators and parasites (Lacey et al., 2001). The non-lethal effects of *B. laterosporus* on natural enemies of insect pests like parasitoids (Ruiu et al., 2007) and the predator *Chrysoperla agilis* (Ruiu et al., 2020) demonstrate that it can be included in integrated pest management (IPM) programmes.

1.7.2 *Brevibacillus laterosporus* potency against *Plutella xylostella*

Diamondback moth (DBM), *Plutella xylostella* (L.) (Lepidoptera: Plutellidae) is an oligophagous pest which feeds on cruciferous crops (Furlong et al., 2013; Shelton, 2004). Globally, this obnoxious pest causes an estimated loss of US$ 4-5 billion every year (Zalucki et al., 2012) and is ranked among the world's top 10 insect pests (Avies-Riordan, 2019). The "Arthropod Pesticide Resistance" database has recently stated that the number of reported cases of insecticide resistance were greater for *P. xylostella* than any other arthropod around the world (Mota-Sanchez & Wise, 2020). Importantly, *P. xylostella* resistance involves insecticides in almost all major classes recognised by the Insecticide Resistance Action Committee (IRAC). The short life span, high reproduction rate, and the high selection pressure with insecticides are often cited for the evolving mechanism of resistance in this deadly pest (Pu et al., 2010; Zhao et al., 2002; Zhou et al., 2011). Although *B. thuringiensis* based insecticides have been used to manage its populations with considerable success (Sarfraz et al., 2005), it was the first insect to develop field resistance to the toxins produced by this biocontrol agent (Tabashnik, 1994). There are various reports of the development of resistance in the pest against *B. thuringiensis* based products (Ferré & Van Rie, 2002; Tabashnik, 1994; Wright et al., 1997).

DBM is a multivoltine pest of temperate and tropical regions with up to 20 generations per year. Females can lay over 200 eggs and 1st instar feeds primarily on spongy mesophyll tissues (Harcourt, 1957) while 2nd to 4th instars larvae are surface feeders and consume leaves, buds, flowers, siliques, the green outer layer of stems, and developing seeds within older siliques (Sarfraz et al., 2005). Populations can proliferate rapidly as moths are highly migratory and have been recorded to travel a distance of up to 1500 km at a speed of 400 to 500 km/night (Chapman et al., 2002). The pest occurs in all agricultural regions where cruciferous crops are grown, including Europe, North America, Central America, South America, Asia, Africa, Oceania, and the Caribbean (Shelton, 2004). Massive damage has been reported in different parts of the world, including Asia, Southeast Asia, and South-eastern USA (Abro et al., 1994; Ramachandran et al., 2000; Verkerk & Wright, 1996). *P. xylostella* is also a serious threat in New Zealand and growers often report that it is the most difficult pest to control (Cameron et al., 1997). Numerous factors are cited for the failure of control but generally, the inadequate application of insecticides, insecticides resistance, and favourable weather conditions are considered responsible for its intensification (Khakame et al., 2013; Sayyed & Wright, 2006). Significant efforts were made to introduce natural enemies in New Zealand such as the parasitoids *Diadegma semiclausum* and *Diadromus collaris* for its control (Sarfraz et al., 2005) but unfortunately, parasitoids could not provide effective control when the population size of the pest increases at the later stages of crop growth (Cameron et al., 1997). Fortunately, the New Zealand *B. laterosporus*

strains (1821L & 1951) demonstrated insecticidal potency against lepidopterous and dipterous insect pests (Glare et al., 2014) and especially against *P. xylostella* (Ormskirk, 2017).

1.7.3 Salient features of New Zealand *Brevibacillus laterosporus* strains (*Bl* 1821L, *Bl* 1951, *Bl* Rsp)

Insect pathogenic strains of *B. laterosporus* (1951, 1821L, Rsp) have been isolated and characterised from New Zealand. Two isolates, *Bl* 1951 and *Bl* 1821L were found in surface-sterilised brassica seeds suggesting an endophytic origin (van Zijll de Jong et al., 2016), and the third (*Bl* Rsp) was recovered from a potato plant (Bienkowski, 2012). All the isolates exhibited larvicidal activity against the diamondback moth, *P. xylostella* (Glare et al., 2014; Ormskirk, 2017; van Zijll de Jong et al., 2016). The New Zealand strains share an ability to kill some caterpillar species and mosquitoes but differ genomically in many ways from strains of other countries (Glare et al., 2020).

All three strains initially grow as vegetative cells and then form a sporangium containing a parasporal body (CSPB) and adjacent spore (Glare et al., 2014). Genome sequences of *B. laterosporus* strains are publicly available and surprisingly the high level of variation in toxin activity across the different strains provides an insight into the role of genetic regions in insect pest pathogenesis (Glare et al., 2020). Recently the genome sequences of the three New Zealand strains of *B. laterosporus* (1951, 1821L, Rsp) and two non-native strains (CCEB342 & NRS590) all with activity against *P. xylostella* and mosquito larvae were analysed and compared for the phylogenetic determinants of toxin gene distribution in their genetic makeup (Glare et al., 2020). A summary of the salient genomic features of the New Zealand strains is presented in Table 1.1.

Table 1.1 Genomic features of New Zealand *Brevibacillus laterosporus* strains (Glare et al., 2020)

Salient features	***Bl* 1951**	***Bl* 1821L**	***Bl* Rsp**
GenBank Accessions	RHPK00000000*	CP033461–4*	RHPL00000000*
Genome size (Mb)	5.48	5.56	5.39
Contigs	3	1	112
CDSs	5204	5326	5268
GC%	40.5	40.7	40.9
No. of plasmids	1	3	2
rRNAs	36	36	32
tRNAs	111	112	94

*= Bioproject PRJNA503267

The genomes of two strains (*Bl* 1821L & *Bl* 1951) harbour various crystal toxin-like (*cry*-like) genes. Ormskirk (2017) hypothesised that *cry*27-like genes identified in both *Bl* 1821L and *Bl* 1951) and the pierisin-like/*cry*35-like putative binary toxin encoding genes identified in *Bl* 1951, were responsible for the main toxicity toward diamondback moth larvae. Furthermore, it was also hypothesised that the parasporal crystals produced by *Bl* 1821L were the main agent of toxicity. However, the research findings identified a larvicidal extracellular S-layer protein, and the two putative accessory virulent genes co-located to the S-layer protein-encoding gene. S-layer protein production by a *B. laterosporus* strain has not been associated with larvicidal action against the diamondback moth before. Importantly, *Bl* 1951 S-layer protein may represent a new class of toxins active against the diamondback moth (Ormskirk, 2017).

The *B. laterosporus* strains (1821L & 1951) demonstrated significant protection against larvae of diamondback moth herbivory of cabbage plants under laboratory and field conditions when topically applied as cells or spores (Ormskirk et al., 2019; van Zijll de Jong et al., 2016). But, a loss of virulence in both the strains was noted due to the suspected infection of phages and subsequent electron microscopy of *Bl* 1821L sporulating cultures revealed the possible presence of *Tectiviridae* phages (Ormskirk, 2017). Glare et al. (2020) predicted the putative phage regions within the genomes of *B. laterosporus* strains 1821L, 1951, and Rsp using the programme PHASTER (Arndt et al., 2016). The endemic *B. laterosporus* isolates 1821L and 1951 are under development as a biopesticide however bacterial cultures during their growth cycle collapse due to the suspected activity of bacteriophages or bacteriocins. Based on the potential antagonistic effects of these bioactives and their likely

influence on the growth of the host organism, further detail on known *B. laterosporus* bioactives is outlined below.

1.8 Bacteriophages and other antimicrobials of *Brevibacillus laterosporus*

1.8.1 Bacteriophages

B. laterosporus is commonly found in beehives (Ruiu, 2013) and is regarded as one of several secondary invaders often associated with *Melissococcus plutonius* infection, the causative agent of European foulbrood in honeybees (Forsgren, 2010). The bacterial diversity within a natural beehive and their interplay with one another, as well as with their respective phages, can be a key in understanding beehive health and may intensify the efforts to prevent further collapse of bee colonies (Berg et al., 2016).

Five *B. laterosporus* phages (Jimmer1, Jimmer2, Abouo, Davies, Emery) were previously isolated and characterised, all of them belonging to the *Myoviridae* family (Merrill et al., 2014). Berg et al. (2016) isolated and characterised five novel *Brevibacillus* phages (Jenst, Osiris, Powder, SecTim467, Sundance) from honeybee debris and compared these on a genomic and cluster basis along with the identification of putative transcriptional units and proteins with the already defined phages. Powder and Osiris phages belong to the *Myoviridae* family, which is morphologically characterised by the contractile sheath and shows an analogy to the earlier reported Jimmer phage-like cluster. SecTim467, Jenst, and Sundance are the first siphoviruses to be isolated that infect *Brevibacillus* bacteria and are typically identified through the long non-contractile tail.

BLASTp analysis of both helped the authors to determine the lifestyle (temperate or lytic) of these defined phages (Berg et al., 2016). Genomic comparisons of the ten *Brevibacillus* phages revealed interesting motif features likely involved in transcriptional control, conserved and repeated proteins of interest, and a putative transposable region present in several of these phages. Furthermore, several proteins were identified that could contribute to the pathogenicity of *Brevibacillus* including a bacterial pili regulatory protein and a PAAR repeat protein, which may aid in the secretion and killing of target cells (Shneider et al., 2013), both the stage V sporulation proteins K and T, which allow for normal sporulation of the host to occur and many others.

1.8.2 Antimicrobial peptides of *Brevibacillus* species

The whole-genome sequences of *B. laterosporus* highlighted its potential to produce diverse antimicrobial peptides, polyketides, and toxins (Li et al., 2015; Ruiu et al., 2013; Zhao et al., 2012b). *Brevibacillus* species are a rich source of antimicrobial peptides (AMPs) (Yang & Yousef, 2018a) and >30 AMPs have been isolated from different species (Cochrane & Vederas, 2016). The produced bioactive peptides act as antibacterial, antifungal, and anti-invertebrate agents (Yang & Yousef, 2018a). Antibacterial action of these peptides holds significance among the insect pathogenic strains for exploration of their biocontrol potential. The AMPs of *Brevibacillus* species are either, ribosomally synthesised peptides (RSPs) or non-ribosomally synthesised peptides (NRSPs). The latter category represents the majority of known *Brevibacillus* AMPs to date (Cotter et al., 2005). However, only a limited number of RSPs produced by *B. laterosporus* have been described by various researchers (Baindara et al., 2016b; Ghadbane et al., 2013; Singh et al., 2012). An overview of the classification of antimicrobial peptides synthesised by different *Brevibacillus* spp. is presented below (Figure 1.4).

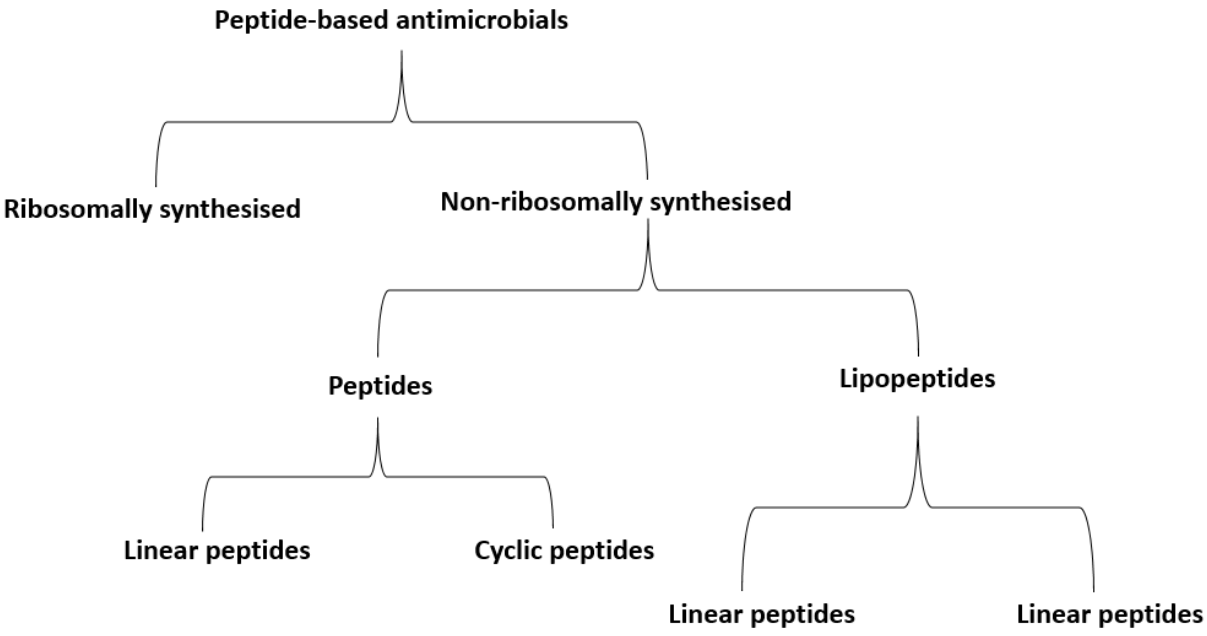

Figure 1.4 Classification of AMPs isolated from *Brevibacillus* spp. (Yang & Yousef, 2018a)

A. Ribosomally synthesised peptides produced by *Brevibacillus laterosporus*

A. Laterosporulin

B. laterosporus GI-9 is known to produce this class IId bacteriocin of 5.6 kD molecular mass (Singh et al., 2012) and its biosynthetic gene cluster and open reading frames (ORFs) analysis reveal that it consists of 49 amino acid residues (Sharma et al., 2012). Laterosporulin inactivates target cells by disrupting the function of their cytoplasmic membranes (Singh et al., 2015). The bacteriocin demonstrated broad-spectrum antimicrobial activity against a diverse range of bacteria. The cells of *E. coli* after treatment with the purified laterosporulin displayed prominent changes in shape and morphology like roughening of their surfaces with an accumulation of cell debris and lysis of bacteria (Singh et al., 2012).

B. Laterosporulin 10

Laterosporulin 10 was isolated from *B. laterosporus* SKDU by Sharma et al. (2012). The antimicrobial peptide is a class IId bacteriocin of 6 kD mass which displays 58% structural homology with laterosporulin. N-terminal sequence analysis of laterosporulin 10 illustrates that its biosynthetic cluster holds identical transcriptional regulators and dehydrogenase genes as observed in laterosporulin, but it possesses a high number of cationic amino acids.

Laterosporulin 10 was found to be active against *S. aureus* and *Mycobacterium tuberculosis* and interestingly it inactivated *M. tuberculosis* residing inside macrophages without antagonistic activity against the macrophages. Laterosporulin 10 inhibited the growth of *S. aureus* MTCC 1430 within one hour that demonstrated its bactericidal nature. The appearance of significant alteration in cell morphology and formation of clumps observed under an electron microscope also supported the hypothesis that it causes bacterial cell lysis by membrane permeabilisation (Baindara et al., 2016b).

C. Bac-GM100

Brevibacillus (=*Bacillus*) *brevis* GM100, a strain isolated from the rhizosphere of *Ononis angustissima*, an Algerian plant produces class II bacteriocin Bac-GM100 of 4.38 kD molecular weight (Ghadbane et al., 2013). N-terminal sequence analysis shows that the peptide has 65% homology with thurincin H from *B. thuringiensis*. Bac-GM100 displayed a bactericidal mode of action against gram-negative bacteria (*Salmonella enteric* ATCC 43972, *P. aeruginosa* ATCC 49189, *Agrobacterium tumefaciens* C58), gram-positive bacteria (*Enterococcus faecalis* ENSAIA 631, *S. aureus* ATCC 6538), and a fungistatic mode of action against the pathogenic fungus *Candida tropicalis* R2 (Ghadbane et al., 2013).

B. Non-ribosomally synthesised peptides produced by *Brevibacillus* species

Non-ribosomally synthesised peptides are secondary metabolites formed through peptide synthetases (Stachelhaus et al., 1999) and are categorised into peptide and lipopeptide, depending on the presence of a lipid chain acylating the N-terminal. Peptides and lipopeptides are further divided into linear and cyclic categories based on structural configuration (Cotter et al., 2005). A brief outline of *Brevibacillus* spp. synthesised peptides including the non-ribosomally synthesised class with their antimicrobial spectrum is presented in Table 1.2.

Table 1.2 Overview of AMPs isolated from *Brevibacillus* spp. (Yang & Yousef, 2018a)

Nature of peptides	Host bacterium	AMP	Antimicrobial spectrum	Reference
Ribosomally synthesised peptides	*B. laterosporus* GM-100	Bac-GM100	Broad-spectrum activity	(Ghadbane et al., 2013)
	B. laterosporus GI-9	Laterosporulin		(Singh et al., 2012)
	B. laterosporus SKDU	Laterosporulin 10		
Non-ribosomally synthesised peptides				
Non-ribosomal linear peptide	*B. brevis* XDH	Tostadin	Broad-spectrum activity	(Song et al., 2012)
	B. brevis Vm4	Edeine		(Czajgucki et al., 2006)
	B. brevis	Spergualin		(Takeuchi et al., 1981)
Non-ribosomal cyclic peptide	*B. brevis*	Gramicidin	Broad-spectrum activity	(Prenner et al., 1999)
	B. parabrevis ATCC 8185	Tyrocidines		(Munyuki et al., 2013)
	B. laterosporus VKPM B-8287	Laterocidin		(Xu et al., 2010)
	Bacillus sp. MKPNG-276A	Loloatins	Antibacterial against gram-positive	(Gerard et al., 1996)
Non-ribosomal linear lipopeptide	*Bacillus* spp.	Bogorols	Broad-spectrum activity	(Barsby et al., 2001)
	B. laterosporus OSY-I	Brevibacillin		(Yang et al., 2016)
	Brevibacillus spp.	BT peptide	Antibacterial against gram-negative	(Wu et al., 2005)
	B. laterosporus PNG276	Tauramamide	Antibacterial against gram-positive	(Desjardine et al., 2007)
	B. laterosporus A60	BL-A60	Antifungal	(Zhao et al., 2012a)
Non-ribosomal cyclic lipopeptide	*B. brevis* 342	Brevistin	Antibacterial against gram-positive	(Shoji & Kato, 1976)
Miscellaneous	*B. laterosporus* SA14	Unknown AMPs	Broad-spectrum activity	(Somsap et al., 2016)
	B. laterosporus (strains BGSP7, BGSP9, and BGSP11)			(Miljkovic et al., 2019)

1.9 Rationale for the research project

Globally, insect pest populations are witnessing a tremendous rise in resistance against pesticides including those based on gram-positive bacteria like *B. thuringiensis* and *L. sphaericus*. The insecticidal potency against pest species, non-lethal effects on natural enemies (predators and parasites), and production of antibacterial and antifungal compounds make *B. laterosporus* an excellent alternative for biopesticide synthesis. Based on the activity of New Zealand strains *Bl* 1951, *Bl* 1821L, and *Bl* Rsp towards diamondback moth caterpillars and mosquitoes the isolates are under development as a biopesticide. However, this development has been stymied by the often erratic growth behaviour of cultures. In this context, the *B. laterosporus* culture collapse during growth possibly due to the activity of bio-antagonists such as bacteriophages or bacteriocins, or other yet to be defined systems. The present study intends to define what is limiting the growth of the New Zealand strains *Bl* 1951 and *Bl* 1821L that impedes in harnessing the entomopathogenic potential of these isolates.

1.10 Main objectives of the research project

Since the discovery of the New Zealand insect pathogenic strains *Bl* 1821L, *Bl* 1951, and *Bl* Rsp their biocontrol potential has been explored. Ormskirk (2017) in her studies described the role of various virulence factors against diamondback moth and mosquitoes. Currently, the native strains are under development as a biopesticide but due to the suspected activity of *Tectiviridae* phages, there has been a loss of virulence (Ormskirk, 2017). Therefore, this research project was designed to determine the nature of bacteriophages specific to the endemic strains, what effect any phages may have on growth and virulence, and how the impacts might be overcome, to allow the harnessing of the entomopathogenic potential of this spore-forming bacterium for biopesticide synthesis.

The main objectives of the research (initially proposed) were to determine the role of putative bacteriophages in harnessing the insecticidal potential of this useful bacterium. However, the discovery of phage tail-like structures (Chapter 2) lead to the following objectives:

1. To identify the putative antibacterial structures of New Zealand *B. laterosporus* isolates *Bl* 1821L and *Bl* 1951 and define their antibacterial spectrum (Chapter 3)

2. To determine the biochemical characteristics and production kinetics of putative antibacterial proteins of New Zealand *B. laterosporus* isolates *Bl* 1821L and *Bl* 1951 (Chapter 4)

3. To purify the putative antibacterial proteins of New Zealand *B. laterosporus* isolates *Bl* 1821L and *Bl* 1951 (Chapter 5)

4. To characterise the putative antibacterial proteins of New Zealand *B. laterosporus* isolates *Bl* 1821L and *Bl* 1951 using bioinformatic analysis and express the selected genes in a gram-positive bacterium *Bacillus subtilis* WB800 (Chapter 6)

5. To determine the bactericidal activity of putative antibacterial proteins of New Zealand *B. laterosporus* isolates *Bl* 1821L and *Bl* 1951 (Chapter 7)

Chapter 2

The search for putative phages of New Zealand *Brevibacillus laterosporus* strains *Bl* 1821L and *Bl* 1951

2.1 Introduction

Bacteriophages are ubiquitous microorganisms, numerically dominating their hosts in a ratio of 10:1 (Canchaya et al., 2004; Pedulla et al., 2003), and have the faculty to regulate their numbers by inhibiting replication or inducing cell lysis (Bordenstein et al., 2006). They play a vital role in the genomic evolution of bacteria by mediating lateral gene transfer (Brüssow & Hendrix, 2002; Wommack & Colwell, 2000) and, in some cases, provide beneficial genes to their hosts (Abedon & LeJeune, 2005; Brüssow et al., 2004). Bacteriophages usually have a narrow host range (Ackermann & DuBow, 1987; Weinbauer, 2004) even though there are reports of single phages infecting different species (Tu et al., 2017). After infecting the host, bacterium phages can follow two alternative cycles of replication (Figure 1.1), lytic or lysogenic (Wang et al., 2014; Young et al., 2000). Lysogeny, a widespread phenomenon among bacterial populations (Brüssow & Hendrix, 2002), occurs when the phage genome either remains in the host as a plasmid or is integrated into the host chromosome in a form known as “prophage” and a bacterium incorporating a prophage is called “lysogen” (Young, 2014). Genome sequencing has revealed the presence of prophages in 60% to 70% of the analysed bacterial genomes, where they can constitute up to 10% to 20% of the chromosome contributing significantly to intra-species genomic differences (Casjens, 2003). However, lysogeny comes at a cost to the bacterial host due to the extra burden of replication of prophage DNA and the threat of lysogen induction, which is lethal to the host cell (Fortier & Sekulovic, 2013; Wagner & Waldor, 2002). These intact prophages are molecular time bombs that kill their hosts upon activation of the lytic cycle (Casjens, 2003; Harrison & Brockhurst, 2017a).

A prophage, under certain conditions, is induced into the lytic cycle of phage replication in response to host and/or other external danger signals (typically the host SOS response) (Grabow, 2001; Mardanov & Ravin, 2007). Numerous triggers of the SOS response include ultraviolet (UV) light, antibiotics (Mitomycin C), and physical stressors such as high pressure, which provoke activity of the restriction endonuclease to cause breakage of double-strand DNA (Aertsen & Michiels, 2005). Earlier studies have shown that various intensities of UV light induced the lysogenic phages of gram-positive and gram-negative bacteria (Marcó et al., 2010; Rodriguez et al., 2014). Mitomycin C, a radiomimetic agent is widely used to induce lysogeny among various bacterial strains harbouring

the prophages in their genomes. However, just like UV light, the sensitivity of phages to mitomycin C also varies at different concentration levels (Mobberley et al., 2010; Yuan et al., 2014). During sporulation *Bacillus thuringiensis* (*Bt*) produces crystal toxins that are highly toxic to multifarious insect pests of various orders but are harmless to vertebrates (Roh et al., 2007). *Bt* is very susceptible to phage lysis, which can present serious problems in its large-scale fermentation (Yang & Wang, 1998). Lysis can either be caused by exogenous phage infection or be due to strain lysogeny (Hyman & Abedon, 2019; Liao et al., 2008). Lysogeny is most common among *Bt* strains and about 83% of its subspecies harbour prophages (Ackermann et al., 1994). In 1960, lysogeny was reported in *Bt* subsp. *berliner* for the first time (Chapman & Norris, 1966) and Zvenigorodskii et al. (1975) identified the type phage from *Bt* subsp. *galleriae*. Since the 1960s, lysogens have been reported in various *Bt* strains (Liao et al., 2008). The molecular approaches of sequencing and gene expression became popular in the study of *Bt* phages after 2003 (Liao et al., 2008). Bam35 (Stromsten et al., 2003), GIL01 & GIL16 (Verheust et al., 2005), 0305phi8-36 (Hardies et al., 2007), MZTPO2 (Liao et al., 2008), TP21 (Klumpp et al., 2010), *Bt* CS33 (Yuan et al., 2012), BMBtp2 (Dong et al., 2013), and Smudge (Cornell et al., 2016) are the *Bt* phages that have been sequenced to date. *Tectiviridae* comprises a group of tail-less, icosahedral, membrane-containing bacteriophages that can be distinguished by their lifestyle, virulent phages infect gram-negative bacteria while the temperate phages infect gram-positive bacteria. Tectiviruses are almost 100% identical in their nucleotide composition despite having been isolated from geographically distant locations at different times (Ravantti et al., 2003; Saren et al., 2005). *Bt* specific *Tectiviridae* phages are represented by phage Bam35c, GIL01, and GIL16c (Ravantti et al., 2003; Verheust et al., 2005). *Myoviridae* family of phages is characterised by the long contractile sheath phages. The phages MZTPO2, Smudge, Hakuna, Megatron, Evoli, HoodyT, CAM003, Troll, Riley and phiCM3 belong to this family and have been isolated and characterised from different *Bt* strains (Cornell et al., 2016; Liao et al., 2008; Sauder et al., 2016; Yuan et al., 2014). *Siphoviridae* family of phages is characterised by long non-contractile tails (Yuan et al., 2014). *Bt* CS33 was the first *Siphoviridae* phage among the sequenced *Bt* phages (Yuan et al., 2012) and the other sequenced phages of this family include BMBtp2 and TP21-L (Dong et al., 2013; Klumpp et al., 2010). El-Didamony (2014) investigated the nature of five phages during a survey of insecticidal bacterium *Bt* prevalence in Yemen soils. The author isolated, purified, and morphologically characterised four phages of the *Siphoviridae* family and one phage of the *Podoviridae* family.

Five *Brevibacillus* phages (Jimmer1, Jimmer2, Abouo, Davies, Emery) belonging to the *Myoviridae* family were previously isolated and characterised (Merrill et al., 2014) and another five novel phages (Jenst, Osiris, Powder, SecTim467, Sundance) isolated from honeybee debris were

characterised (Berg et al., 2016). Structures resembling the *Tectiviridae* phages were observed under the electron microscope while looking into the structural features of the crystals and spores of the entomopathogenic strain *Bl* 1821L. The infection of *Bl* 1821L by putative phages was co-related to the collapse of cultures during the growth of host bacteria (Ormskirk, 2017), although the only evidence was the presence of virus-like particles in TEM micrographs of cells.

Viral infections can slow host cell growth (Jones et al., 2000; Wu, 1998) as viral protein expression can affect host cell resource availability and thereby host cell division (Qian et al., 2017; Shopera et al., 2017) or host cell transcription and translation (Terzi & Levinthal, 1967). Earlier research found that *Bt* phage infection during fermentation can cause a 15% to 30% reduction in yield, with instances of 50% to 80% and, to a complete loss of yield (Liao et al., 2007).

In this chapter, genome sequences of the endemic strains *Bl* 1821, *Bl* 1951, and *Bl* Rsp were analysed for the presence of putative phage regions. Subsequent research was geared towards the isolation and enumeration of the putative phages using standard protocols including plaque assays, serial dilutions test, assessment of putative phage DNA, and PCR analysis. Mitomycin C at different concentrations was evaluated to find the optimum concentration for the induction of the putative antibacterial particles. Furthermore, the induced particles were examined under the electron microscope for morphological characterisation.

2.2 Methods

2.2.1 PHASTER and Mauve analysis

PHASTER (PHAge Search Tool Enhanced Release) is a programme that locates virus-like genes and regions within bacterial genomes (Arndt et al., 2016). The putative phage regions in the *Bl* genome of native (1951, 1821L, Rsp) and non-native strains (LMG 15441, CCEB 342, B9, GI-9, NRS 590, PEG 36, UNISS 18, DSM 25) (http://ncbi.nlm.nih.gov.genome; See Table 2.4 for GenBank accessions) were analysed and compared (http://phaster.ca; accessed November 2017). Furthermore, the putative phage regions of native strains identified through the server PHASTER were aligned with Mauve (Multiple Alignment of Conserved Genomic Sequence With Rearrangements) (Darling et al., 2004).

2.2.2 Plaque assay

A plaque assay test allows visual confirmation of the presence of phage particles in a sample. In this study, the soft agar overlay method was used to propagate, isolate, and titrate phage particles (Sanders, 2012). The protocol consists of two parts, the control overlay and the phage-host bacteria overlay. For the control overlay, overnight (O/N) culture of *Bl* 1951 was prepared by inoculating a single colony of host bacteria into 5 ml of LB Broth (Luria-Bertani, Miller). The inoculated culture was placed in an orbital shaker (Conco, TU 4540, Taiwan) @ 250 rpm and 30^{o}C overnight. Soft agar (0.5%) (6.25 g LB (Miller), 1.25 g Bacteriological agar (Schau), 250 ml MQW) was prepared and 3 ml of soft agar was transferred into a 15 ml tube and placed in a heating block at 55^{o}C for 10-15 min. Then 50 µl of 1X phage buffer (10 ml 1M Tris, pH 7.5, 10 ml 1M $MgSO_4$, 4 g NaCl, 1 L ddH_2O) and 500 µl of the overnight culture were transferred into 1.7 ml microcentrifuge tube. The mixture was gently vortexed before incubation at 30^{o}C for 20 min. After incubation, the mixture (550 µl) was added into a tube containing the soft agar and the tube was rotated in between the palms to mix the contents. The soft agar mixture (control overlay) was immediately poured into LB agar plates and left it to solidify for 15-20 min. LB agar plates were placed in an incubator at 30^{o}C for 2-3 days.

The phage-host bacteria overlay was prepared by transferring 500 µl of *Bl* 1951 overnight culture and 50 µl of suspected phage lysate into a 1.7 ml microcentrifuge tube. The mixture was gently vortexed to ensure thorough mixing of the suspected phage and host bacterium. The mixture was then incubated at 30^{o}C for 20 min. After incubation, the mixture (550 µl) was added into a tube containing the soft agar and the tube was rotated in between the palms to mix the contents. The soft agar mixture was immediately poured into LB agar plates and the LB agar plates were left to solidify for 15-20 min. LB agar plates were placed in an incubator at 30^{o}C for 2-3 days enabling plaque formation by suspected phage-host bacteria overlay.

A plaque after an infection is filled with millions of identical viral particles. To retrieve the phage particles from a plaque, a plaque was picked and suspected viral particles from the plaques were re-suspended in phage buffer. The observed plaques on the lawn of *Bl* 1951 were marked by drawing a small circle around the plaque with a labelling pen. The morphology of plaques was recorded as either circular or elliptical. Aliquots of 100 µl phage buffer were prepared according to the number of plaques. The sterile tip of a 200 µl pipette was inserted into the centre of the plaque in a perpendicular position without touching the adjacent plaque. The end of the tip was placed into the phage buffer and by repeated up and down movement of the tip to dislodge the viral

particles into the corresponding tube. Soft agar overlay was performed to determine the viability of phage particles against the host bacterium.

2.2.3 Plaque assays with modified LB medium

To prepare the modified LB medium components A were autoclaved and allowed to cool to 55°C. Once the autoclaved components were cooled, components B were added after filter sterilisation (Appendix A-1) (Zeigler, 2001).

2.2.4 Plaque assay tests with mineral medium

The failure to obtain plaques in the standard plaque assay tests necessitated the use of alternative protocols to propagate and isolate the putative phages, and therefore a mineral medium was used. The soft agar overlay method of Sanders (2012) as described above (Section 2.2.2) for the enumeration of bacteriophages was pursued in the experiment, but the nature/composition of media was different from that described above. In the modified medium, 2.5-3 µg/ml of ampicillin was added in the bottom agar, which allows the formation of highly visible plaques of phages on host bacterial lawns (Loś et al., 2008). Phosphate-buffered (FB) mineral salt was used as a medium in the experiment. The bottom and top FB agars contained 1.5% and 0.7% bacteriological agar, respectively. FB plates were poured using 2X concentrated FB medium mixed with an equal volume of 3% water agar. The top agar consisted of 2X concentrated FB medium mixed with an equal volume of 1.5% water agar. FB media was supplemented with 0.4% glucose as a carbon source (Teich et al., 1998).

2.2.5 Serial dilutions assays

Serial dilution assay is a method to determine the number of phages in a sample and was employed to purify, amplify, and titre the phages. Tenfold serial dilutions are typically used to observe phage activity (Sanders, 2012). A *Bl* 1951 overnight culture was prepared by inoculating a single colony into 5 ml of LB broth and placing it in an orbital shaker (Conco, TU 4540, Taiwan) @ 250 rpm and 30°C overnight. Phage buffer (270 µl) was transferred into a 1.7 ml microcentrifuge tube and ten fold serial dilutions were prepared by adding 30 µl of undiluted phage sample to a microcentrifuge tube (270 µl) (10^{-1}) (1:10 dilution) and the sample vortexed. Ten µl of 10^{-1} solution was transferred to another microcentrifuge tube containing 90 µl of phage buffer (10^{-2}) and vortexed resulting in a

1:100 dilution of phage particles. This process was continued for successive dilutions until 10^{-8}. Three technical repeats of the sample were prepared.

The suspected phage lysate (50 µl) from each dilution (10^{-1} to 10^{-8}) was added into 500 µl of an overnight culture of host bacterium (*Bl* 1951) in each replicate and thoroughly mixed with flickering followed by 25-30 min incubation at 30°C. Three millilitres of soft agar (0.5%) was added into a 15 ml tube and was kept in a heating block at 55°C. This was transferred to a hot water bath at 46°C for 5 min of incubation. Five hundred µl of the host *Bl* 1951 and 50 µl of the suspected phage lysate sample after incubation were added into the soft agar tube, which after gentle mixing was poured into LB agar plates. LB agar plates were allowed to dry and later on left for 2-3 days at 30°C incubation to observe the number of formed plaques.

Similar to *Bl* 1951, serial dilutions assays of *Bl* 1821L were performed to examine the presence of putative phages.

2.2.6 Mitomycin C induction of putative phages

The protocol of Rybakova et al. (2014) and Hurst et al. (2018) was used to induce the putative phages in this study. *Bl* 1951 isolated single colony/colonies were used to inoculate 5 ml of LB Broth (Luria-Bertani, Miller). The inoculated culture was placed on an orbital shaker (Conco, TU 4540, Taiwan) @ 250 rpm and 30°C overnight. Aliquots (500 µl) of the overnight culture of *Bl* 1951 were made to further inoculate 25 ml of LB broth 250 ml conical flasks. This culture was allowed to grow at 30°C with shaking at 250 rpm until the culture attained turbidity (10-12 hours). Mitomycin C (Sigma) was added at different concentrations (1 µg/ml & 3 µg/ml) independently into these flasks which were then positioned on an orbital platform for incubation at ambient temperature (24°C) with rotation at 40 rpm. OD_{600nm} readings were recorded through an Ultrospec-10 spectrophotometer (Amersham Biosciences) after 2, 4, 6, and 24 hours of mitomycin C (Sigma) addition. The samples (1 ml) were drawn from each time interval flask with mitomycin C (Sigma) and control treatment to record optical density (OD_{600nm}) of cultures. The flasks were monitored to view the sign of lysis (clearing of the culture or accumulation of bacterial debris) during the mentioned time intervals and compared with the control. The flasks without the addition of mitomycin C served as control.

To extract putative phages from the induced cultures chloroform (600 µl/ml) and NaCl (1 g/ml) were added and the sample was vortexed for 20 sec. The induced culture after this vortexing was kept for 3 min and again vortexed three times but after the last vortex, the culture was let to stand for 5 min. The culture was gently decanted into a fresh centrifuge tube leaving behind the chloroform. DNase (2 µl) and RNase (1 µl) were then added and the microcentrifuge tubes inverted

and incubated at 37°C for 15 min with an occasional inversion during this process. The induced culture was centrifuged @ 16000 g for 10 min and the supernatant was decanted and kept at 4°C for overnight storage by adding two drops of chloroform. The same protocol was used to induce *Bl* 1821L and *Bl* Rsp strains.

The experiment was laid out in varied replications with randomisation form. The replications for the native strains were; *Bl* 1951 (Mitomycin C @ 1µg/ml= 6 flasks, Mitomycin C @ 3 µg/ml= 6 flasks, Control= 4 flasks), *Bl* 1821L (Mitomycin C @ 1µg/ml= 4 flasks, Mitomycin C @ 3 µg/ml= 4 flasks, Control= 3 flasks), and for *Bl* Rsp (Mitomycin C @ 1 µg/ml= 5 flasks, Mitomycin C @ 3µg/ml= 5 flasks, Control= 3 flasks) respectively. OD_{600nm} readings data at various time intervals were pooled and statistically analysed using the ANOVA (Analysis of Variance) test through Genestat-20th edition programme.

2.2.7 Extraction of putative phage DNA after mitomycin C induction

The protocol of Su et al. (1998)for the extraction of large and small scale preparation of bacteriophage λ lysate and DNA was used for the extraction of putative phage DNA of *Bl* 1951 with some modification. Mitomycin C (3 µg/ml) induced culture of *Bl* 1951 was used for DNA extraction after ultracentrifugation @ 35,000 rpm for 70 min. Nuclease mix (4 µl) was added into 1 ml of ultracentrifuged putative phage extract which was kept for incubation at 37°C for 30 min. $ZnCl_2$ (20 µl) was added into the sample at a ratio of 1:50 (1 $ZnCl_2$: 50 putative phage lysate) and incubated at 37°C for 15 min followed by centrifugation at 4,000 g for 5 min at room temperature (22°C). The supernatant was discarded and the pellet was dissolved in 700 µl of TENS buffer (50 mM Tris-HCl, pH 8.0, 100 mM EDTA, 100 mM, 100 mM NaCl, 0.3% SDS) with 4.7 µl of the proteinase-K enzyme. The mixture was mixed by pipetting up and down and incubated at 65°C for 10 min. An equal volume of phenol/chloroform/isoamyl alcohol (25:24:1) was added and the sample was centrifuged @ 4,000 g for 5 min at room temperature (22°C). The aqueous phase was collected in a new tube and phenol/chloroform/isoamyl alcohol extraction followed by centrifugation was twice repeated. After that, the aqueous phase was collected in a new tube and after the addition of an equal volume of isopropanol; the mixture was gently mixed and kept at room temperature (22°C) for 5 min. The sample was centrifuged @ 4,000 g for 10 min at room temperature (22°C) and the supernatant was gently discarded. DNA pellet was washed with 70% (700 µl) of ethanol, dried for 25-30 min under a fume hood, and then resuspended in TE buffer (10 Mm Tris-HCL, pH 8, 1 Mm EDTA).

Similar to *Bl* 1951 the putative phage DNA of *Bl* Rsp was obtained after mitomycin C (Sigma) induction (3 µg/ml). However, *Bl* 1821L culture was induced with mitomycin C (Sigma) @ 1 µg/ml to extract putative phage DNA.

2.2.8 PCR analysis of mitomycin C induced putative phage DNA

Prior to PCR, putative phage DNA concentration (ng/µl) of each sample was measured using spectrophotometry (Nanodrop 3.0.0 spectrophotometer; Nanodrop Technologies Inc., Delaware, USA). PCR master mix was prepared for each primer pair that included a negative control reaction lacking template DNA. The contents of each tube were gently pipetted up and down to ensure the thorough mixing of all the components of the reaction. Genomic DNA (1 µl) was added into 24 µl of PCR master mix (PCR buffer (Roche) 10x $MgCl_2$, dNTPs, 10 µM primer F, 10 µM primer R, Taq (Roche), PCR water). Amplification was performed in a Kyratec thermal cycler starting with an initial denaturation at 95°C for 5 min, followed by 40 cycles at 95°C for 45 sec, 60°C for 45 sec and 2 min at 72°C and a final extension of 7 min at 72°C. PCR products quality and size were assessed by agarose gel electrophoresis, using a 1% gel in 1×TAE (40 mM Tris-OH, 20 mM Acetic Acid, pH 7.8, 1 mM ethylenediaminetetraacetic acid (EDTA)). Five microliters of each PCR product along with loading dye were loaded in each lane of an agarose gel containing a DNA gel stain (0.5 x RedSafe TM). DNA ladder (Hyperladder II, Bioline, USA) of 1 kb plus was used to estimate the size of PCR products. Electrophoresis was performed at 100 V for 45 min and then visualised with exposure to UV light using a UVITEC fluorescence gel imaging system.

PCR analysis of the mitomycin C (Sigma) induced cultures of *Bl* 1821L and *Bl* Rsp was performed according to the same protocol, except for *Bl* 1821L the genomic DNA and putative phage DNA was diluted in 1: 1000 and 1: 10000 ratio for gel electrophoresis. All the primers (Tables 2.1-2.3) used in this study except 16S F (5'AGT TTG ATC CTG GCT CAG 3') and 16S R (5'GGT TAC CTT GTT ACG ACT T 3') were designed using the software Geneious basic (Kearse et al., 2012) according to the putative phage regions predicted through programme PHASTER (Arndt et al., 2016). 16S rDNA is a standard gene targeted for establishing the phylogenies of bacteria (Winand et al., 2020; Woo et al., 2008). For *B. laterosporus* there are 11-12 copies of the genes (~2500 bp) (Glare et al., 2020) and the primers targeting 1411 bp of genes in each strain were used in this study (Tables 2.1-2.3).

Table 2.1 *Bl* 1951 (RHPK01000003.1, contig 1) putative phage specific primers used in this study

Targeted gene region (bp) Annotation*	Encoded proteins of the targeted region	Primers (Genomic location**)	Sequence
495 bp	Phage protein	1951-1F (1,353,114 bp)	5' CAG GTC AAG CCA CTG GAA GT 3'
		1951-1R (1,353,609)	5' ACA TCG CGA CCC AGT TCA AT 3'
650 bp	Phage protein	1951-2F (1,559,559)	5' AGA ACA ACA GGG GCG TCA TT 3'
		1951- 2R (1,558,909)	5' TAG GAA CGA TGC TCA CGC TG 3'
548 bp	Phage tail length tape-measure protein	1951-3F (4,381,825)	5' CAG GTT TTG TGG GCG TGA AG 3'
		1951-3R (4,382,373)	5' CAA GTT CAC GCC CCA TGT TC 3'

Note: Primers were designed as specific identification tools for strains (Glare et al., 2020).
*= Based on RAST analysis (Aziz et al., 2008).
**= *Bl* 1951 (RHPK01000003.1, contig 1) GenBank accession defines the position of gene specific primers used in this study.

Table 2.2 *Bl* 1821L (NZ_CP033464.1) putative phage specific primers used in this study

Targeted gene region (bp) Annotation*	Encoded proteins of the targeted region	Primers (Genomic location)**	Sequence
621 bp	Phage related protein	1821L-1F (1,101,914)	5’ GAC CCA ACT TCC TCC TGA CG 3’
		1821L-1R (1,102,535)	5’ CCC GAT CAC ATT CAA CCC CA 3’
578 bp	Hypothetical protein	1821L-2F (2,596,129)	5’ AGG CTG GCT ACG CTT CAA AA 3’
		1821L-2R (2,596,707)	5’ CTC CTT CAC CCG TTG TGC TA 3’
624 bp	Phage-like element PBSX XkdT	1821L-3F (3,028,594)	5’ CGC GGC AAT GGA GAT TGA AG 3’
		1821L-3R (3,029,218)	5’ ATA TGT GCC GCT ACC TCT GC 3’
644 bp	Hypothetical protein	1821L-4F (5,363,003)	5’ TTC GCG CGA AAT TGA TCG TC 3’
		1821L-4R (5,363,647)	5’ GTT CAA TGC GGC TCG TGA TC 3’
625 bp	Phage protein	1821L-5F (4,523,891)	5’ GCA TCA CTG TCA CTC GTG GA 3’
		1821L-5R (4,524,516)	5’ TGC TTG ACC CTT ACC CGA AC 3’

Note: Primers were designed as specific identification tools for strains (Glare et al., 2020).

*= Based on RAST analysis (Aziz et al., 2008).

**= *Bl* 1821L (NZ_CP033464.1) GenBank accession defines the position of gene specific primers used in this study.

Table 2.3 *Bl* Rsp putative phage specific primers used in this study

Targeted gene region (bp) Annotation*	Encoded proteins of the targeted region	Primers (Genomic location)**	Sequence
647 bp	Phage terminase	Rsp-1F (contig 774)	5’ GAC CCA ACT TCC TCC TGA CG 3’
		Rsp-1R (contig 774)	5’ CCC GAT CAC ATT CAA CCC CA 3’
571 bp	Portal protein	Rsp-2F (contig 813)	5’ AGG CTG GCT ACG CTT CAA AA 3’
		Rsp-2R (contig 813)	5’ CTC CTT CAC CCG TTG TGC TA 3’
523 bp	Portal protein	Rsp-3F (contig 751)	5’ CGC GGC AAT GGA GAT TGA AG 3’
		Rsp-3R (contig 751)	5’ ATA TGT GCC GCT ACC TCT GC 3’
498 bp	Phage protein	Rsp-4F (contig 788)	5’ TTC GCG CGA AAT TGA TCG TC 3’
		Rsp-4R (contig 788)	5’ GTT CAA TGC GGC TCG TGA TC 3’
570 bp	Hypothetical protein/insecticidal toxin	Rsp-5F (contig 760)	5’ GCA TCA CTG TCA CTC GTG GA 3’
		Rsp-5R (contig 760)	5’ TGC TTG ACC CTT ACC CGA AC 3’
582 bp	Hypothetical protein	Rsp-6F (contig 763)	5’ GCA TCA CTG TCA CTC GTG GA 3’
		Rsp-6R (contig 763)	5’ GCA TCA CTG TCA CTC GTG GA 3’

Note: Primers were designed as specific identification tools for strains (Glare et al., unpublished data).

*= Based on RAST analysis (Aziz et al., 2008).

**= *Bl* Rsp strain gene specific contig

2.2.9 Transmission electron microscope (TEM) analysis of the mitomycin C induced cultures of *Brevibacillus laterosporus*

Mitomycin C induced cultures (*Bl* 1951, *Bl* 1821L, *Bl* Rsp) immediately after induction, but prior to ultracentrifugation, were analysed under an electron microscope. In addition, mitomycin C induced cultures of *Bl* 1951 and *Bl* 1821L were centrifuged @ 16,000 g for 10 min at 4^{o}C to obtain the cell free supernatants (CFS). Seven millilitres of CFS from *Bl* 1951 and *Bl* 1821L was transferred into the oak ridge centrifuge tube (PPCO; Nalgene, USA) and placed into the ultracentrifuge rotor (Beckman, J2-M1) to concentrate at 20,000 rpm for 70 min and 4^{o}C. The concentrated pellet was dissolved in 150 µl of 25 mM TBS buffer (To make 500 ml of TBS stock solution (250 mM); 40 g NaCl, 1 g KCl, 2.42 g TRIS Base, 16.5 g TRIS-HCl, dH_2o 490 ml, pH 7.4) after decanting the supernatants.

A 5 µl sample of induced culture with and without ultracentrifugation was applied to a freshly glow discharged plastic-coated hydrophilic 200 mesh EM grid (ProSciTech; Thuringowa, Australia) and kept for 2 min. The excess sample was removed using a torn filter paper (Whatman no: 1). Thereafter, the sample was stained by adding 3 µl of 0.7% uranyl acetate (UA, pH 5) to the grid and the combined solution was mixed with the micropipette tip. The mixture was left for a further 2 min and most of the solution was dried with the edge of a filter paper (Whatman no: 1). *Bl* 1951 and *Bl* 1821L samples obtained from the above two methods were subjected to analysis under an electron microscope at 18,000 to 25,000 magnification in Morgagni 268D (FEI, USA) TEM operated at 80 KeV. The images were photographed using the TENGRA camera. TEM analysis was performed at AgResearch, Lincoln, New Zealand.

2.3 Results

2.3.1 PHASTER and Mauve analysis

PHASTER analysis of the genome sequences of insect pathogenic native strains revealed the presence of several putative phage regions and some of these were reported by the programme to be “intact” (suggesting a functional virus) (Figures 2.1 & 2.2). Furthermore, the results also indicated that the New Zealand strains (*Bl* 1821L, *Bl* 1951, *Bl* Rsp) harbour more putative phage regions as compared to strains from other regions (Table 2.4). Moreover, the alignment of phage sequences of native strains through Mauve indicated that all the putative phage regions are entirely different from each other, suggesting that the phage regions among the genomes are not conserved (Figure 2.3). Therefore, in this context, it was hypothesised that these sequences can provide an insight into the lysogeny and key genes controlling random collapse during

fermentation, so isolation and identification research was undertaken to define the nature of the putative phages.

The salient genomic features of the putative phage regions of the *Bl* analysed strains identified through the programme PHASTER are diagrammatically presented in Figures 2.1 to 2.2 and Appendices A-5 to A-15.

Table 2.4 PHASTER analysis of genome sequences of *Brevibacillus laterosporus* strains

***Bl* strain**	**No. of PHASTER predicted putative phage regions**	**GenBank accession**	**Reference**
Bl 1821L	14	*NZ_CP033464.1	(Glare et al., 2020)
Bl 1951	12	*RHPK01000003.1	(Glare et al., 2020)
Bl Rsp	11	*RHPL00000000.1	(Glare et al., 2020)
Bl DSM 25	8	CP017705.1	(Lee et al., unpublished)
Bl PE 36	7	NZ_AXBT01000006.1	(Theodore et al., 2014)
Bl UNISS 18	6	MBFH00000000.1	(Camiolo et al., 2017)
Bl LMG 15441	5	CP007806.1	(Djukic et al., 2011)
Bl B9	5	JNFS01000001-3	(Li et al., 2015)
Bl GI9	4	NZ_CAGD01000001.1	(Sharma et al., 2012)
Bl NRS 590	4	*RKQC00000000.1	(Glare et al., 2020)
Bl CCEB 342	3	*RKQD00000000.1	(Glare et al., 2020)

*= Bioproject PRJNA503267 (Glare et al., 2020)

.

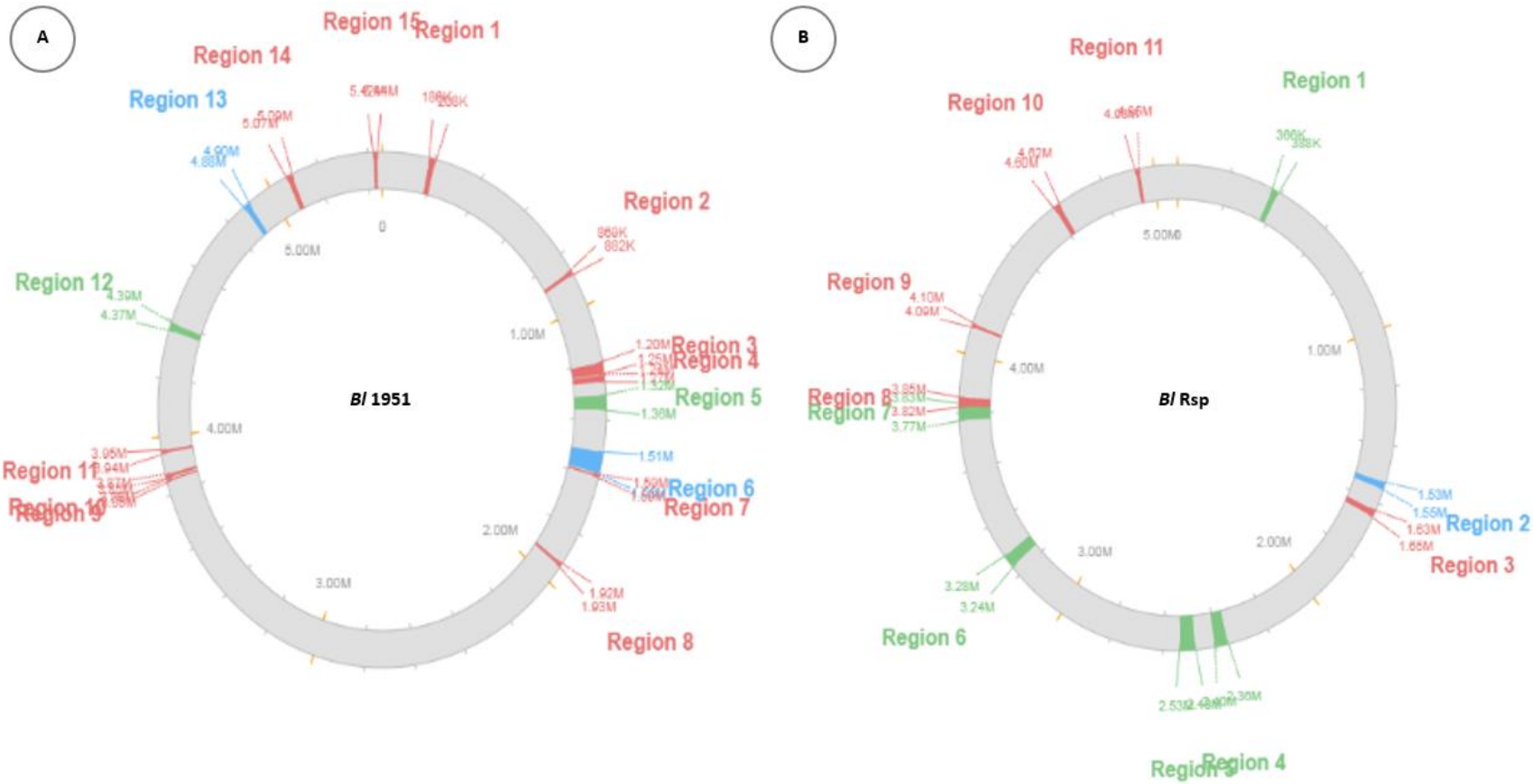
A
Region 15
Region 1
Region 14
Region 13
Region 2
Region 12
Region 3
Region 4
Region 5
Region 11
Region 6
Region 7
Region 10
Region 9
Region 8
0
1.00M
2.00M
3.00M
4.00M
5.00M
BI 1951
B
Region 11
Region 1
Region 10
Region 9
Region 8
Region 7
Region 2
Region 3
Region 6
Region 4
Region 5
1.00M
2.00M
3.00M
4.00M
5.00M
BI Rsp

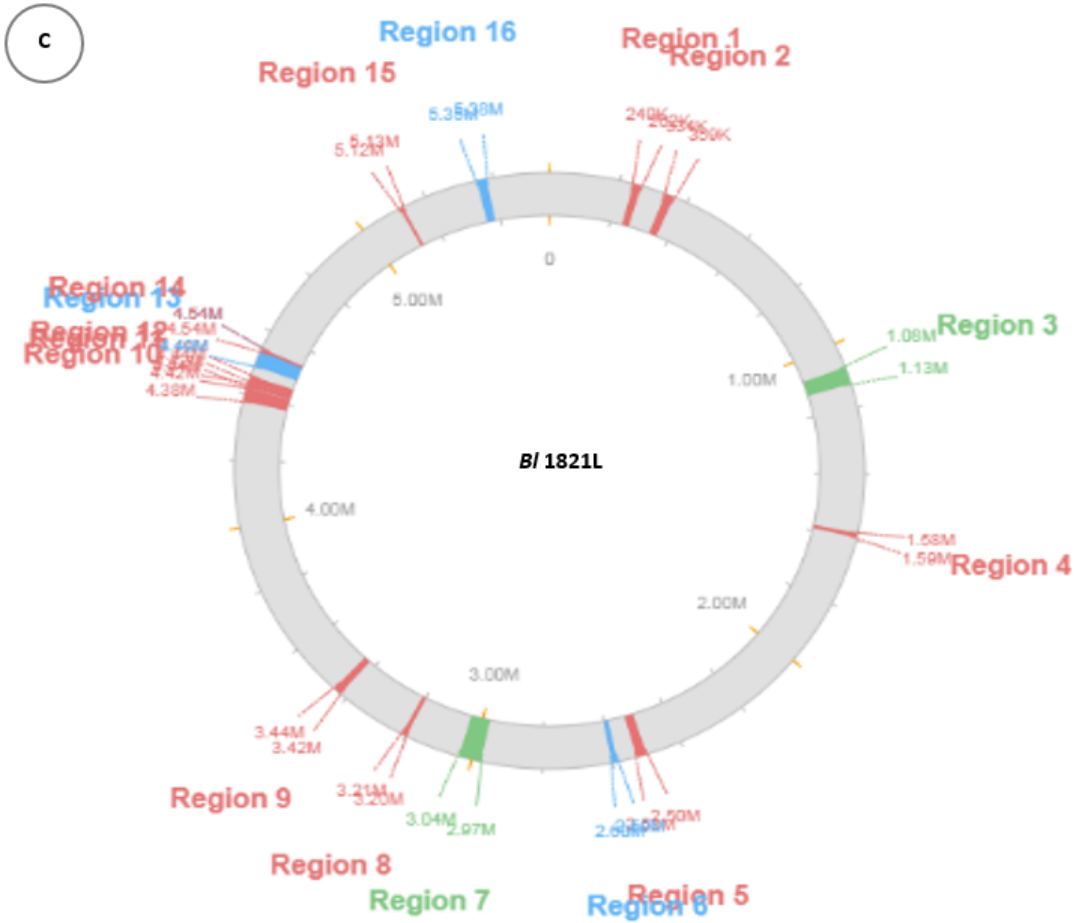

Figure 2.1 Predicted putative phage regions of the New Zealand strains of (A) *Bl* 1951 (B), *Bl* Rsp, and (C) *Bl* 1821L. Phage regions were determined using the PHASTER server, Red= Incomplete regions (score <70), Blue= Questionable regions (score 70-90), Green= Intact regions (score >90)


A
Region 1
Bl LMG15441
Region 3
Region 2
B
Region 8
Region 1
Region 2
Region 3
Bl UNISS18
Region 7
Region 6
Region 4
Region 5
C
Region 1
Region 7
Region 2
Bl PE36
Region 6
Region 3
Region 4
Region 5
D
Region 4
Region 1
Bl GI-9
Region 3
Region 2

Figure 2.2 Predicted phage regions of various *Bl* strains including (A) *Bl* LMG 15441, (B) *Bl* UNISS 18, (C) *Bl* PE 36, (D) *Bl* GI-9, (E) *Bl* CCEB 342, (F) *Bl* NRS 590, (G) *Bl* B9, and (H) *Bl* DSM 25 compared to the putative phage regions (Figure 2.1) of New Zealand strains *Bl* 1951, *Bl* 1821L, and *Bl* Rsp. Phage regions were determined using the PHASTER server, Red= incomplete (score <70), blue= questionable (score 70-90), green= intact (score >90)

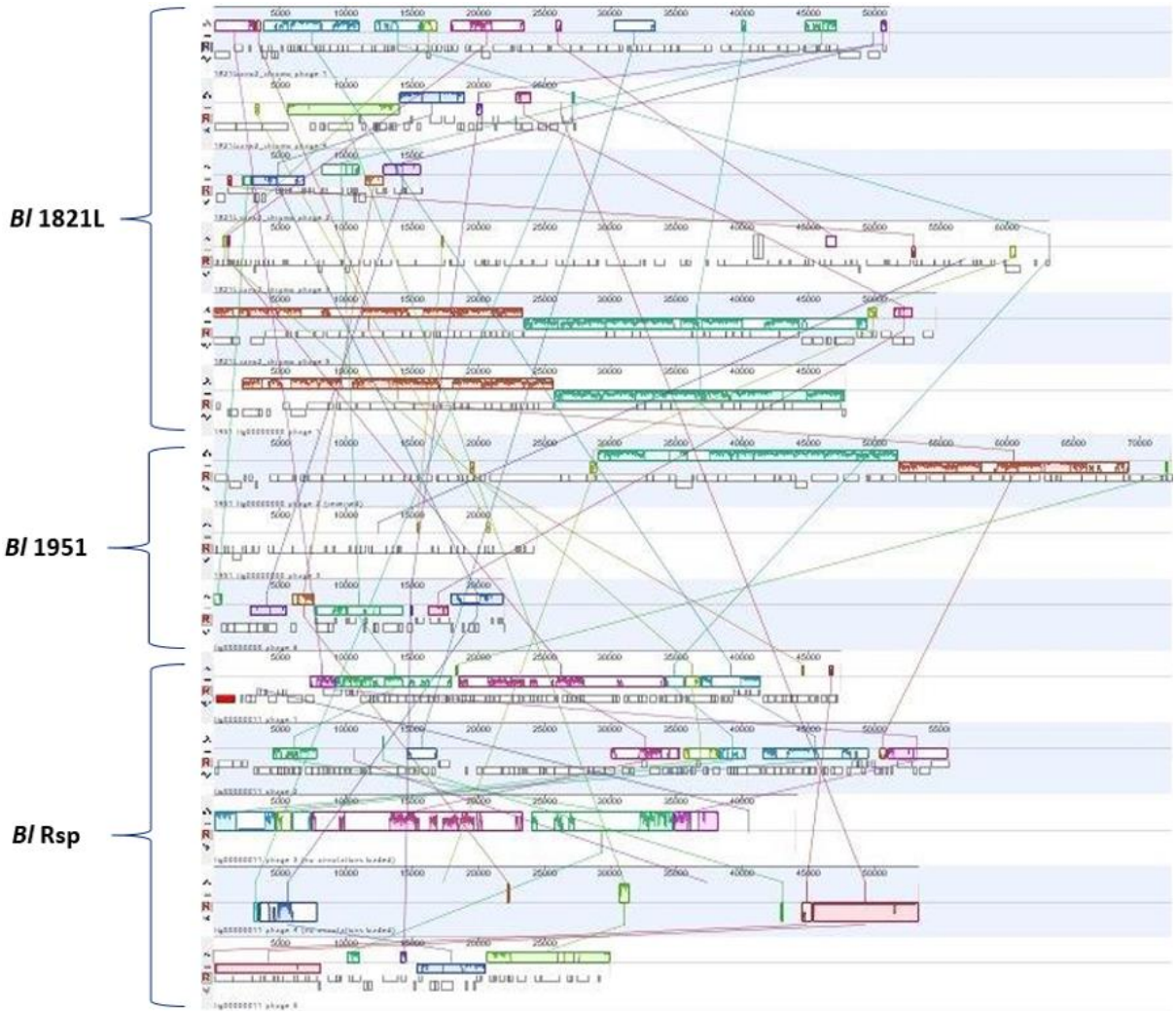

Figure 2.3 Alignment of putative "intact" phage regions of *Brevibacillus laterosporus* strains (*Bl* 821L, *Bl* 1951, *Bl* Rsp) through the programme Mauve, coloured areas denote homologous regions

2.3.2 Plaque assay tests

Plaque assay and serial dilutions are the most widely used tests to determine the existence and nature of viral particles in the host bacterium. A plaque in a sample represents a single phage particle in the original sample and therefore different phages exhibit different morphologies in plaque assays. Four *Bl* 1951 and two *Bl* 1821L isogenic culture lines (suspected collapse bacterial cultures obtained from the same source) maintained at the Bio-Protection Research Centre, New Zealand, were examined for the production of phages. *Bl* 1951 isogenic culture lines formed turbid plaques in some plates of varying dimensions. The number of plaques formed varied from 10-14 and their length fluctuated from 3 mm-18 mm and the width range was 3 mm-25 mm. The *Bl* 1951 isogenic culture line 2 formed the largest plaques that had a length of 8 mm-18 mm and width of 10 mm-25 mm (Table 2.5 & Figure

2.4). The majority of the plaques were circular while a few elliptical shapes were also noticed especially in the isogenic culture line 2. The plaques were subsequently picked and inoculated onto other LB agar plates to replicate. However, the transferred suspected phage particles did not replicate and no more plaque formation was noted. Subsequently, a serial dilution assay of the isogenic culture lines was performed to further verify the replicating capacity of the putative phages. Serial dilution assay tests of the suspected phage particles could not provide a systematic pattern of plaques at various dilutions. *Bl* 1821L did not produce any prominent plaque during the assay test but the suspected phage lysates were subjected to serial dilution tests which were negative across all the dilutions. Furthermore, the plaques formed were picked up as outlined above (Section 2.3.3) for propagation but the suspected phage particle could not exhibit any multiplication faculty. Thereafter, plaque assay tests of both the native strains (*Bl* 1951 & *Bl* 1821L) were performed after modification of media (Section 2.2.3) but no clearing zones (plaques) indicative of phage were observed.

Table 2.5 Plaque assay test of suspected phages of *Bl* 1951 isogenic culture lines

Host bacterium	Isogenic culture line no.	No. of plaques	Length of plaque (mm)	Diameter of plaque (mm)
Bl 1951	1	10	6-15	5-10
	2	11	8-18	10-25
	3	10	5-11	6-12
	4	14	3-9	2-9

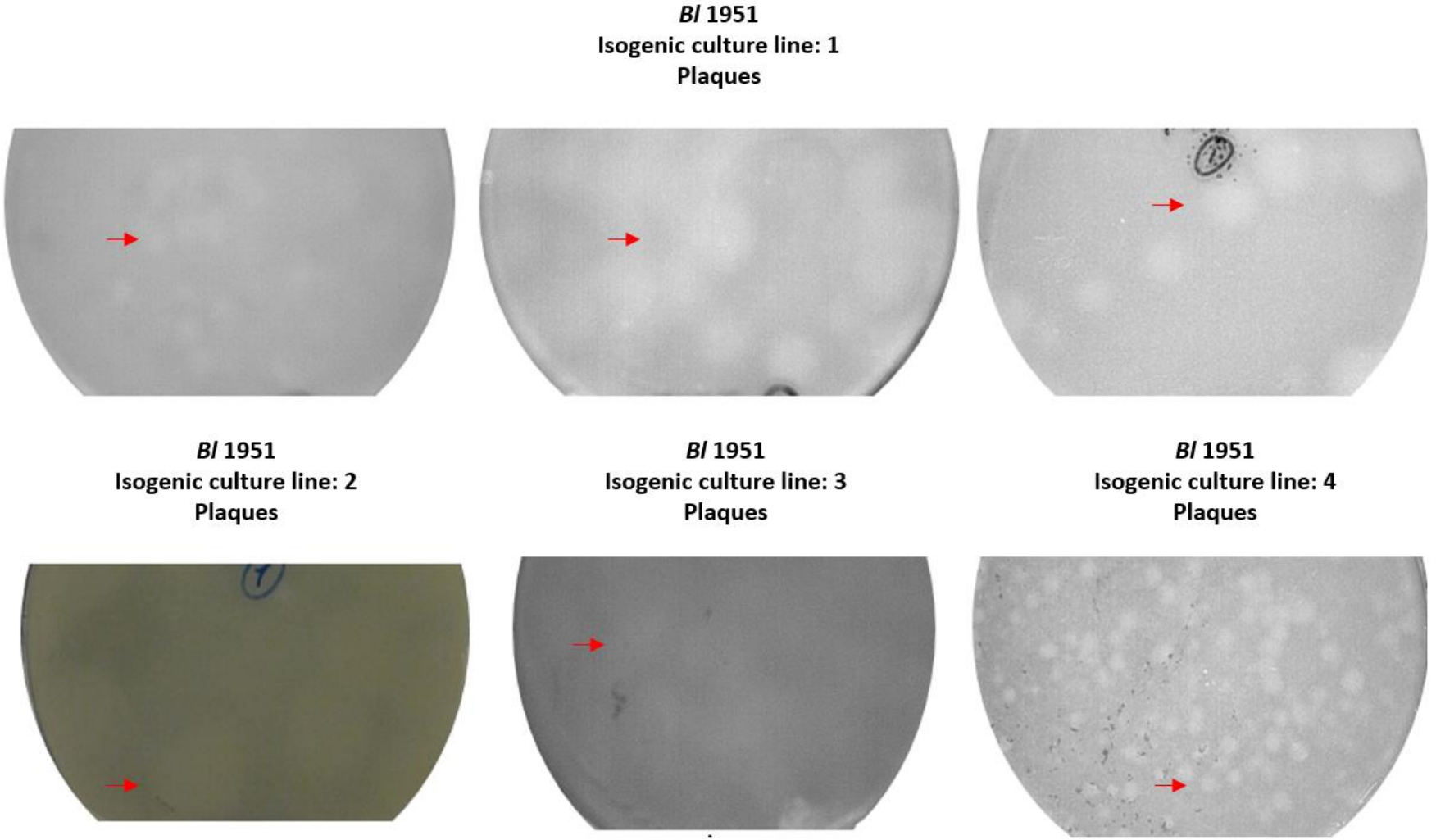

Figure 2.4 Plaque assay test of suspected phages of *Bl* 1951 isogenic lines. Arrows (red colour) denote the different types of formed plaques on the lawn of *Bl* 1951

2.3.3 Mitomycin C induction of putative phages from New Zealand *Brevibacillus laterosporus* strains

Mitomycin C at different concentrations was used to induce the putative antibacterial structures after failure to obtain the plaques. The spectrophotometer reading (OD_{600nm}) of *Bl* 1951 cultures after treatment with mitomycin C at both concentrations (1 µg/ml & 3 µg/ml) remained relatively constant up to 6 hours. However, after 24 hours it dropped to an OD_{600nm} of 0.70 and 0.20 respectively (Appendix A-2 & Figure 2.5). The mitomycin C @ 3 µg/ml treatment prominently influenced the bacterial growth and a drastic decline of 83.9% in OD_{600nm} reading was observed after 24 hours. This treatment was also significant from mitomycin C @ 1 µg/ml (Appendix A-2).

Spectrophotometer exhibited a rapid decline in OD_{600nm} reading when the mitomycin C (3 µg/ml) was added as compared to other treatments, while the control treatment (without mitomycin C) OD_{600nm} revealed an upward trend due to an increase in the turbidity *i.e.* growth of the culture. Statistically, the effect of both the concentrations of mitomycin C were significantly different from the control (Appendix A-2 & Figure 2.5).

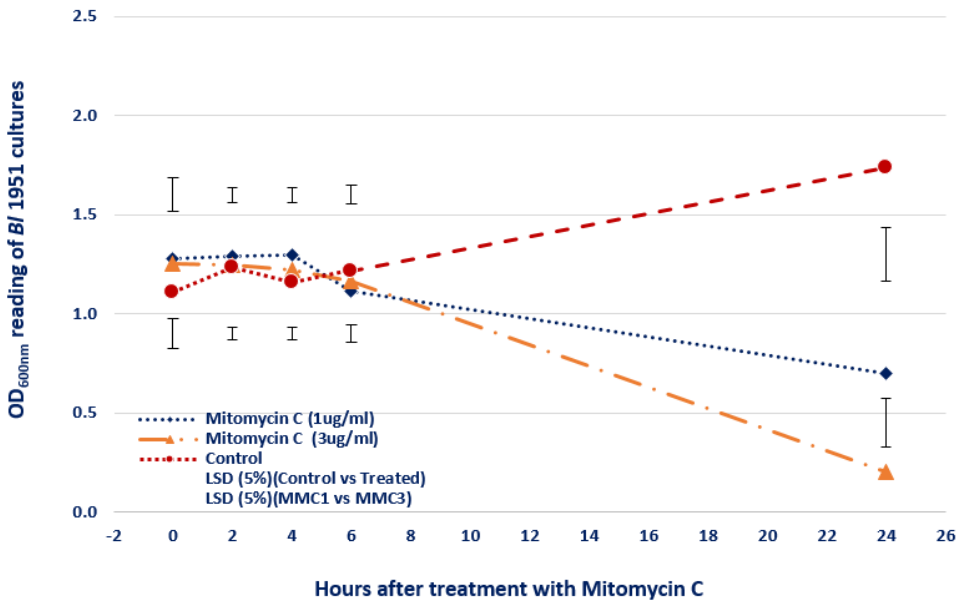

Note: LSD= Least significant difference
MMC1= Mitomycin C @ 1 µg/ml
MMC3= Mitomycin C @ 3 µg/ml

Figure 2.5 Spectrophotometric (OD_{600nm}) reading of *Bl* 1951 cultures after treatment with mitomycin C at various concentrations

After treatment with both the doses of mitomycin C (1 µg/ml & 3 µg/ml) the OD_{600nm} reading of *Bl* 1821L cultures remained almost stagnant up to 6 hours (Appendix A-3 & Figure 2.6). The spectrophotometer reading 24 hours after treatment with the mitomycin C @ 1 µg/ml indicated a fall of 49.7% due to culture lysis. Statistically, the decline in OD_{600nm} readings for the concentration of 1 µg/ml (49.7%) and 3 µg/ml (41%) did not differ significantly from each other but both were significantly different from the control. OD_{600nm} reading of the control treatment (without mitomycin C) demonstrated a slight increase of bacteria up to 6 hours from where the OD_{600nm} slowly declined through time (Appendix A-3 & Figure 2.6).

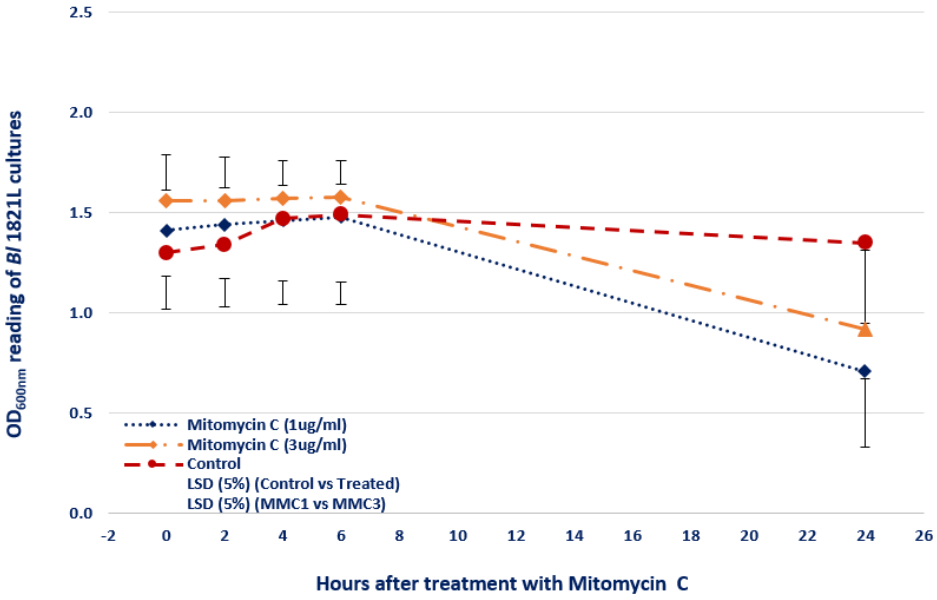

Note: LSD= Least significant difference
MMC1= Mitomycin C @ 1 µg/ml
MMC3= Mitomycin C @ 3 µg/ml

Figure 2.6 Spectrophotometric (OD_{600nm}) reading of *Bl* 1821L cultures after treatment with mitomycin C at various concentrations

OD_{600nm} reading of *Bl* Rsp cultures after treatment with mitomycin C @ 1 µg/ml started to decline (35.9%) after 6 hours, while for the other treatments the OD_{600nm} remained unchanged (Appendix A-4 & Figure 2.7). Spectrophotometer readings declined in cultures treated with the mitomycin C @ 3 µg/ml as compared to other treatments, while in the control treatment (without mitomycin C) a slight rise (14.8%) in OD_{600nm} was observed. Statistically, both the mitomycin C concentrations were significantly different from the control. However, the mitomycin C @ 3 µg/ml treatment significantly lysed the culture and a drastic decrease of 71.2% in OD_{600nm} reading was noted after 24 hours. This

treatment was also significantly different from mitomycin C @ 1 µg/ml which demonstrated a 56.9% drop in optical density (OD_{600nm}) of the *Bl* Rsp culture (Appendix A-4 & Figure 2.7).

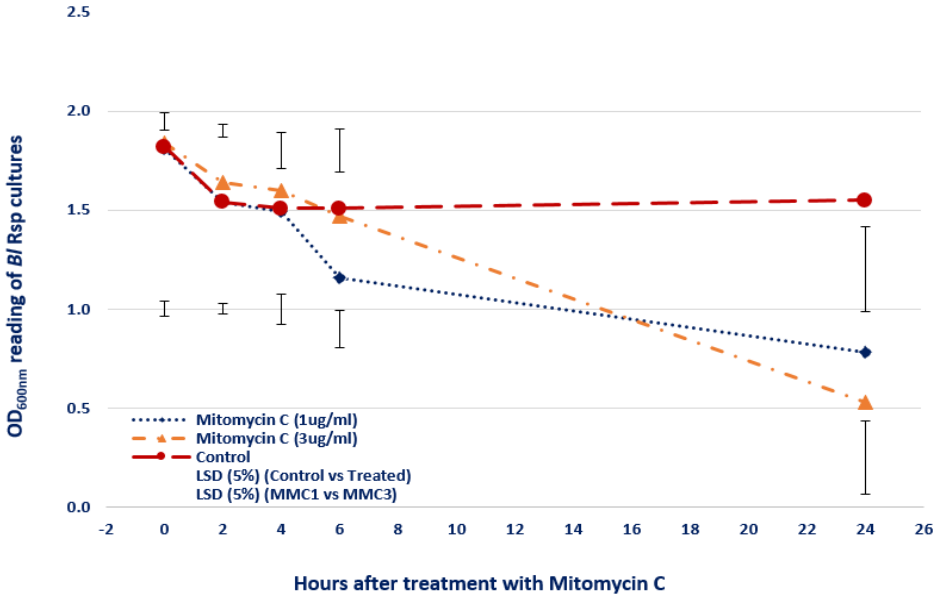

Note: LSD= Least significant difference
MMC1= Mitomycin C @ 1 µg/ml
MMC3= Mitomycin C @ 3 µg/ml

Figure 2.7 Spectrophotometric OD_{600nm} reading of *Bl* Rsp cultures after treatment with mitomycin C at various concentrations

2.3.4 Extraction of putative phage DNA and PCR analysis

Gel electrophoresis of the extracted putative phage DNA from the filtered supernatants of *Bl* 1951, *Bl* 1821L, and *Bl* Rsp displayed the bands at the same level where the chromosomal DNA was present (Figures 2.8, 2.10, 2.12). This suggested that the putative phage DNA was absent and some chromosomal carryover had occurred. However, to further affirm the results, PCR analysis was performed with the extracted DNA from the filtered supernatants.

Although standard PCR is not thought of as quantitative, stronger phage bands were expected upon amplification of suspected putative phage DNA than from standard chromosomal amplification. However, gel electrophoresis of extracted DNA of putative phage particles of *Bl* 1951, *Bl* 1821L, and *Bl* Rsp indicted that the mitomycin C treated cultures did not result in stronger amplification, suggesting no concentration of putative phage DNA (Figures 2.8, 2.10, 2.12). Putative phage specific primers of *Bl* 1951 (Table 2.1 & Figure 2.9), *Bl* 1821L (Table 2.2 & Figure 2.11), and *Bl* Rsp (Table 2.3 & Figure 2.13) could amplify the putative phage specific regions in all samples.

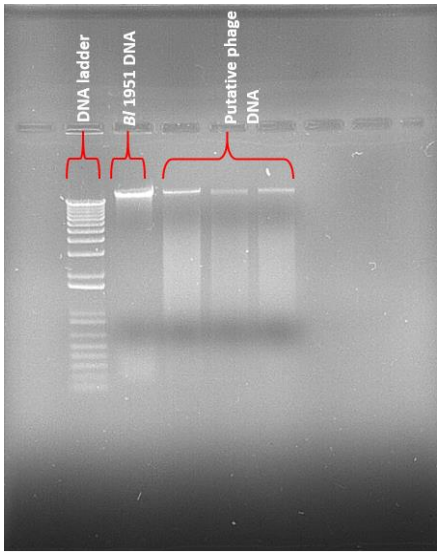

Figure 2.8 Gel electrophoresis of *Bl* 1951 genomic DNA (gDNA) and putative phage DNA showing only chromosomal DNA

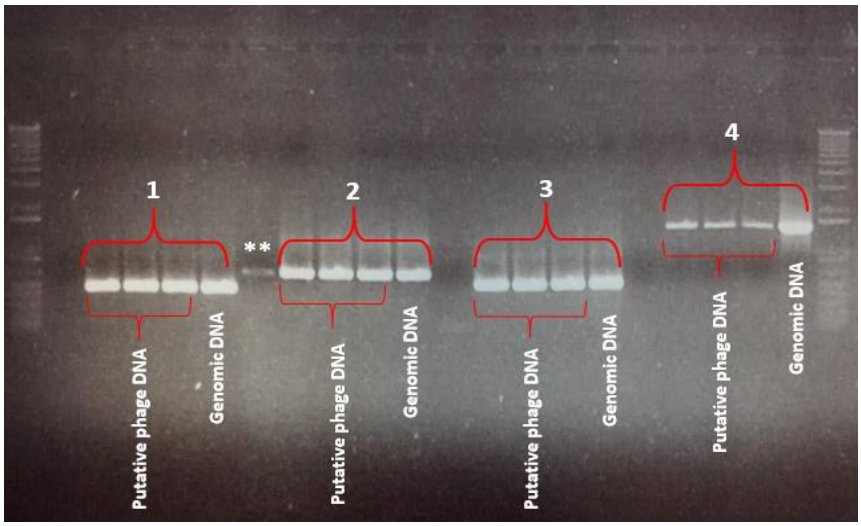

** Overflow from the adjacent well

Figure 2.9 Gel electrophoresis of *Bl* 1951 putative phage specific PCR amplicons (See Table 2.1 for numbered primers set)

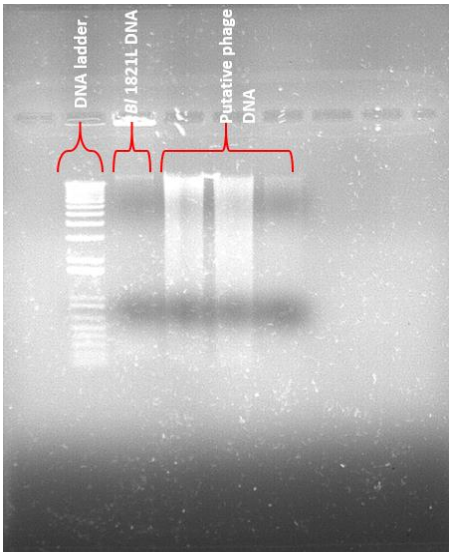

Figure 2.10 Gel electrophoresis of *Bl* 1821L genomic DNA (gDNA) and putative phage DNA showing only chromosomal DNA

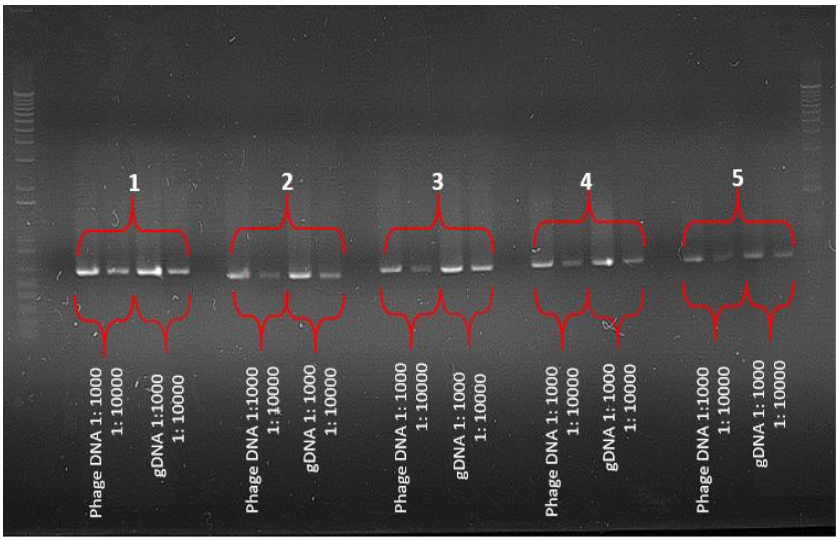

Figure 2.11 Gel electrophoresis of *Bl* 1821L putative phage specific primer amplicons (See Table 2.2 for numbered primers set)

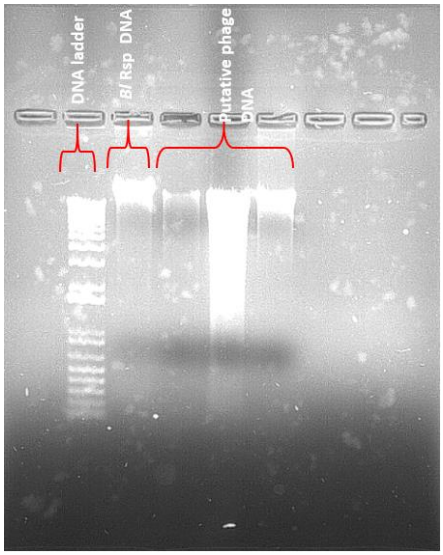

Figure 2.12 Gel electrophoresis of *Bl* Rsp genomic DNA (gDNA) and putative phage DNA showing only chromosomal DNA

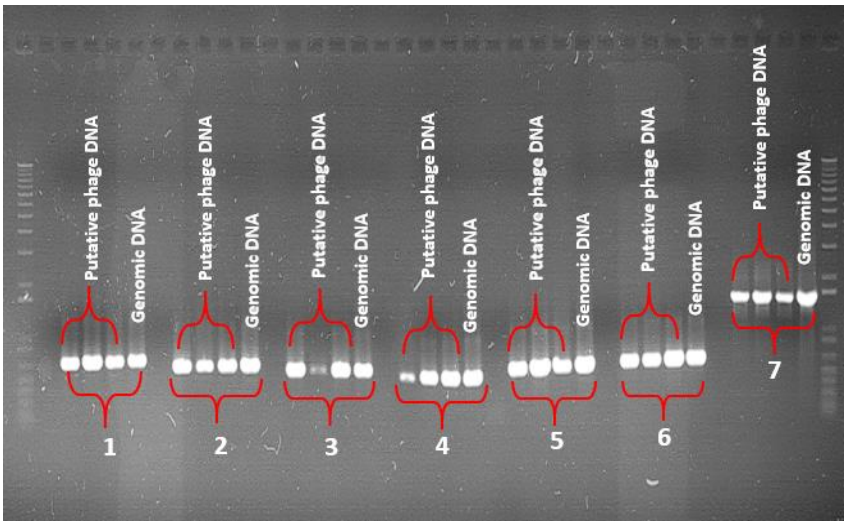

Figure 2.13 Gel electrophoresis of *Bl* Rsp putative phage specific primer amplicons (See Table 2.3 for numbered primers set)

2.3.5 TEM analysis of mitomycin C induced cultures

A. TEM analysis of *Bl* 1951 mitomycin C induced culture

TEM analysis of *Bl* 1951 cultures immediately after mitomycin C induction displayed numerous sheath structures; hollow sheaths (Figures 2.14A, 2.14C), *co*mplete contractile sheaths (Figure 2.14B), and contractile sheaths attached to their cores (Figures 2.14A, 2.14C). The concentrated lysate of *Bl* 1951 under TEM examination revealed the presence of hollow sheath structures (Figures 2.14D, 2.14F), contractile sheath structures attached with cores (Figure 2.14F), and empty hexagonal phage head-like structures (Figures 2.14D, 2.14E).

B. TEM analysis of *Bl 1*821L mitomycin C induced culture

TEM analysis of *Bl* 1821L cultures immediately after mitomycin C induction did not reveal any structures. However, electron micrographs of *Bl* 1821L taken after high-speed centrifugation revealed the predominant presence of complete contractile sheath-like structures attached to their cores, some complete contractile sheath-like structures, and hollow sheaths (Figures 2.15A-2.15D).

C. TEM analysis of *Bl* Rsp mitomycin C induced culture

TEM analysis of *Bl* Rsp cultures immediately after induction did not reveal any phage or phage tail structures, except a potential polysheath-like structure (Figure 2.16). However, due to the focus of research on *Bl* 1951 and *Bl* 1821L strain, no further work and TEM analysis of *Bl* Rsp was pursued.

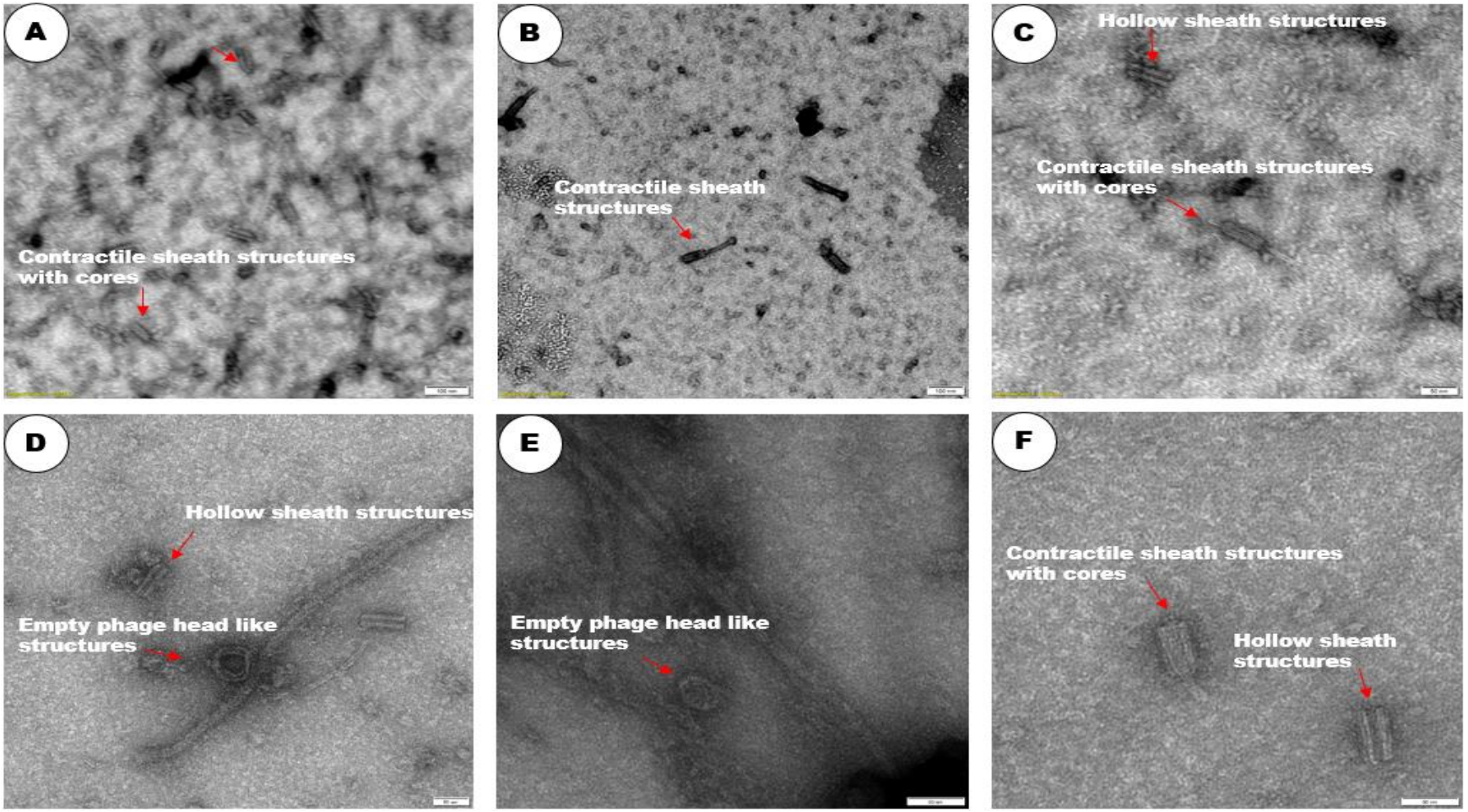

Figure 2.14 Electron micrographs of *Bl* 1951 mitomycin C induced culture. TEM images of *Bl* 1951 induced cultures without ultracentrifugation (2.14A-2.14C) and after ultracentrifugation (2.14D-2.14F). Scale bar: 100 nm (Figures 2.14A-2.14B) & 50 nm (Figures 2.14C-2.14F)

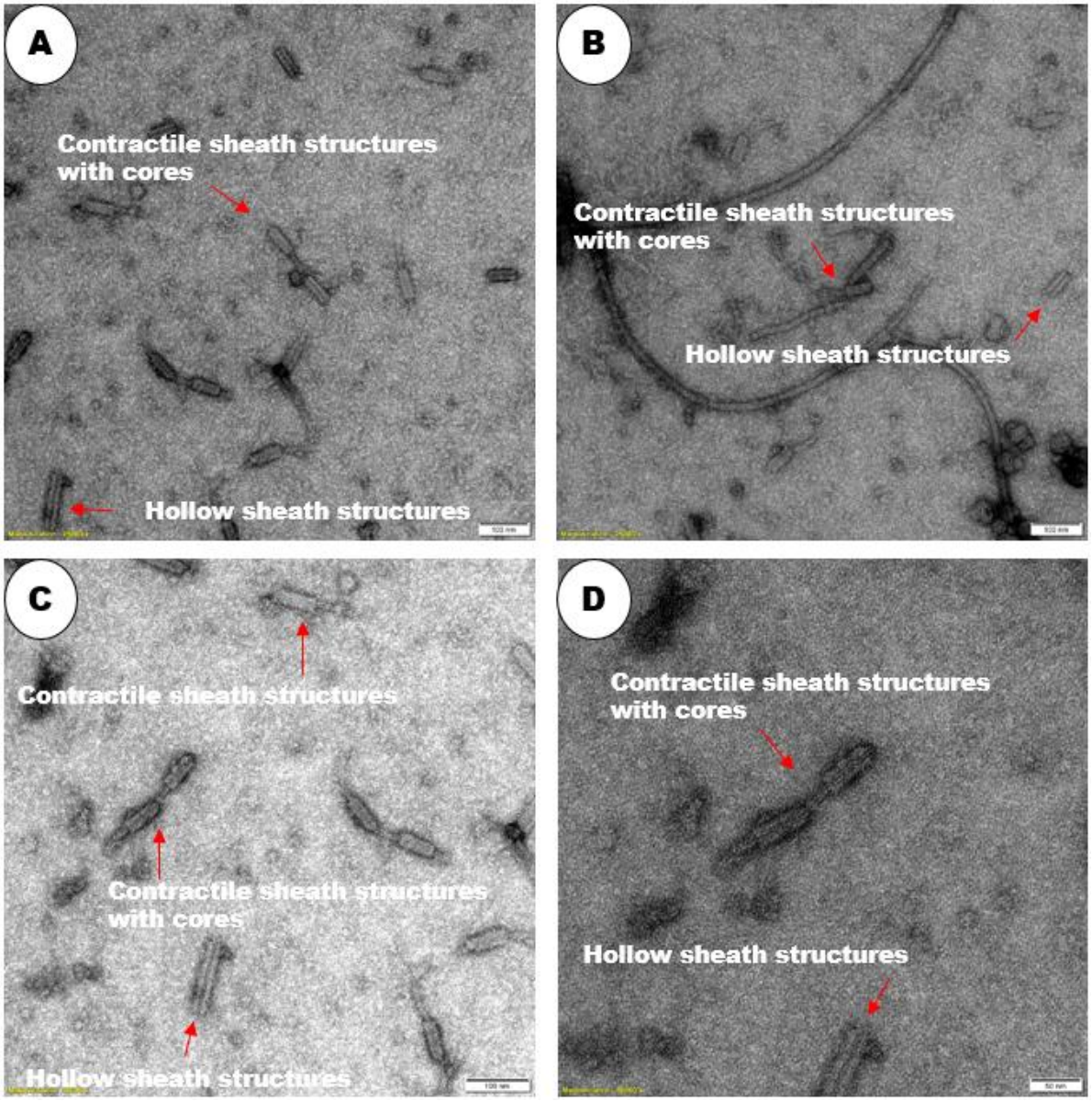

Figure 2.15 Electron micrographs of the *Bl* 1821L mitomycin C induced culture. Scale bar: 100 nm (Figures 2.15A-2.15C) & 50 nm (Figure 2.15D)

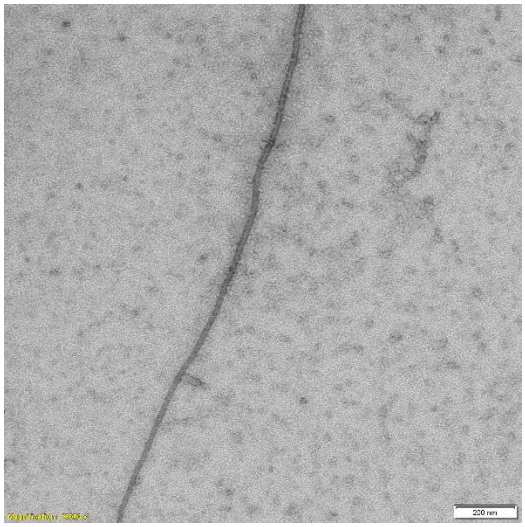

Figure 2.16 Electron micrographs of the *Bl* Rsp mitomycin C induced culture showing a putative polysheath-like structure. Scale bar: 200 nm

2.3.6 Discussion

The initial research using classical tools for the isolation and enumeration of putative phages such as plaque assays, serial dilution tests of collapsed *Bl* 1951 and *Bl* 1821L cultures, and the subsequent assessment of extracted DNA and PCR analysis of the supernatants from the mitomycin C induced cultures could not provide any substantive evidence of the presence of phage-like entities with activity towards bacteria. However, using different concentrations of mitomycin C for the induction of putative antibacterial structures from the *Bl* 1951, *Bl* 1821L, and *Bl* Rsp exhibited a negative effect on bacterial growth indicating some type of antagonism. Furthermore, TEM examination of the crude lysates of *Bl* 1951 and *Bl* 1821L after mitomycin C induction showed the presence of phage tail-like structures, which provided a base for the future research.

The term “prophage” was coined in 1952 by André Lwoff who, along with François Jacob and Jacques Monod, discovered that phages use lysogeny (Lwoff, 1953a; Ribatti, 2020) as a means to replicate, and believed that lysogeny is a window into understanding the relationship between bacteria and phages (Lwoff, 1966; Owen et al., 2020). Prophages can affect their host genome architecture by changing the genomic composition, modifying the organisation of the genome, or altering the location and the order of genes (Brüssow et al., 2004; Tan et al., 2007). Various researchers in the past have also pointed the presence of prophage regions in the bacterial genomes (Brüssow & Hendrix, 2002; Touchon et al., 2016). The alignment of putative phage regions encoded by the *Bl* 1951, *Bl* 1821L, and *Bl* Rsp genomes through the Mauve programme (Darling et al., 2004) implied that the phage specific

loci are not conserved among these strains. Yuan et al. (2014) compared the genomes of nine *Bacillus* phages and showed that different regions of the phage genome exhibited different levels of similarity. Some phage genes were highly conserved, while other genes displayed a high degree of variability. Earlier studies have also deliberated that the genetic diversity between phages and prophages in the same host bacterium can cause localised differences (Hendrix, 1999; Kwan et al., 2006).

A plaque in a bacterial lawn represents a single phage particle in the original sample and different phages exhibit different morphologies in plaque assays. Some plaques are small and clear, with a sharply defined border while others are large and can be more diffuse. The observed plaques formed due to the infection of suspected *Bl* 1951 putative phages were turbid (Figure 2.4), which is a hallmark of lysogenic phages. Generally, lysogens integrate their genome into the host bacteria and render the host immune to reinfection by a phage of the same type (Gallet et al., 2011; Goldman, 2021). Soft agar overlay is considered an integral part of bacteriophage enumeration where plaques derived from a single virus particle can be observed. Some phages form very minute or micro plaques and with a few exceptions such as the phage T7, the plaque continues to increase in size. Most phage plaques, after a period of incubation, assume a certain size and acquire a definitive boundary, either with a fuzzy or clear-cut edge (Yin, 1991, 1993), while others are almost unobservable making it challenging to quantify phage concentrations and therefore undertake phage research. Scientific literature is replete with various factors that affect the formation of plaques, like growth phase of the host bacterium (logarithmic or stationary), incubation temperature, replacing agar with agarose, media supplemented with Ca^{++} and Mg^{++}, and modifications to the double agar assay method like the use of antibiotics to trigger the SOS systems of host bacteria are the most prominent (Abedon & Yin, 2009; Kropinski et al., 2009; Lillehaug, 1997). Therefore, various modified media like Luria broth (LB) and Mineral media were attempted to obtain the plaques and isolate phages.

Modified LB media contains glucose which provides the cells with a carbon and energy source for their metabolic activities (Campbell et al., 2005), which culminate in a surge of cell growth and toxin production, thereby offsetting the inhibitory effects of phages on the host's virulence. Carbon is involved in the manufacturing of vital biological macromolecules like proteins, carbohydrates, nucleic acids (DNA & RNA), and lipids (Boundless, 2017). Therefore, it is often called the "building block of life" (Boundless, 2017). Earlier studies have demonstrated that the development of phages and cell burst sizes decrease when the cells grow more slowly (Łos et al., 2004). Furthermore, Łos et al. (2004) reported that complete inhibition of phage progeny development was achieved when the carbon source was removed from the growth medium. This phenomenon may be explained by the fact that most carbon sources used in bacterial cultures consist of glucose and, as outlined previously, glucose is an essential energy source for cellular respiration and growth. *Tectiviridae* phages were potentially

implicated in the loss of *Bl* 1821L virulence and the subsequent electron microscopy of sporulating cultures revealed the presence of similar structures. However, Ormskirk (2017) elaborated that the decrease in virulence was restored transiently when the host bacteria were cultured on NYSM (Nutrient Yeast Extract Salt Medium) or mLB (Modified Luria Bertani) medium, with a less rich carbon source. Therefore, in the present work LB media modified with the addition of glucose was used so that the nature of phages could be established after their isolation from the host. Ormskirk (2017) related susceptibility of *Bl* 1821L sporulating cultures to the presence of tailless phage, similar to CP-51 (Gillis & Mahillon, 2014). CP-51 phage can infect sporulating cells of *Bacillus cereus* in which the phage DNA stays trapped until the initiation of spore germination (Gillis & Mahillon, 2014). The sporulating cells use their DNA to produce the proteins that are necessary for spore formation and consequently the sporangium provides the invading virus with the replicative arsenal the virus needs to proliferate (McKenney et al., 2013). *E. coli* phages sometimes form either very small plaques or no plaques at all. Therefore, a modified protocol with the addition of antibiotics at the bottom agar was used to resolve the problem (Loś et al., 2008). The use of antibiotics was assessed for their ability to enhance plaque formation on the native strains (*Bl* 1951 & *Bl* 1821L) but it made no difference. There are various reports of not obtaining plaques in newly discovered bacteriophages and this issue is especially common in the case of lambdoid bacteriophages (Makino et al., 1999; Yokoyama et al., 2000).

Prophages after induction can replicate by various mechanisms. However, successful isolation of the lysogens released after induction requires a permissive host strain in which the phages can enter the lytic cycle. The lysogenic strain is then spot-tested on a lawn of the permissive strain and incubated under appropriate conditions. A lysis zone (plaques) developing around the lysogenic colonies suggests lytic propagation of induced prophages but might also be due to the release of bacteriocins (Carlson, 2004). To determine if the observed lysis zones are due to phage infection, the putative phages in the lysis zones- samples are picked using sterile pipette tips suspended in a small volume of phage diluent, and various dilutions of samples are spotted on a lawn of permissive host. The formation of plaques from the picked-up putative phage particles indicates the lytic propagation of induced phages (Carlson, 2004; Hockett & Baltrus, 2017). The lysates obtained from the collapsed cultures of *Bl* 1951 and *Bl* 1821L sometimes produced no plaques or a few plaques and even in the serial dilution assays, no systematic pattern in their activity was apparent. Based on the findings it is likely that the putative antibacterial activity of insect pathogenic strains *Bl* 1951 and *Bl* 1821L might be due to the action of bacteriocins or something else rather than bacteriophages.

Other factors that do not allow phages to show plaques include the absence of suitable phage receptors on bacterial cells (Rakhuba et al., 2010), restriction due to the restriction-modification

system of the host (Vasu & Nagaraja, 2013), superinfection immunity (McShan, 2006) or abortive infection (Chopin et al., 2005). Typically, phages use two different ways to lyse their host cells to release the progeny at the end of their lytic cycle. However, the disintegration of the bacterial cell wall is the primary target. The first mechanism is inhibition of peptidoglycan synthesis, the main constituent of the cell wall (Hatfull, 2001), and it is well illustrated in phages Qβ (Bernhardt et al., 2000) and ϕ174 (Bernhardt et al., 2001). The use of cell wall hydrolysing enzymes consisting of holin and endolysin is another common path employed by phages (Bläsi & Young, 1996). Endolysins are mureolytic enzymes designed to cleave the peptidoglycan, the main component of the bacterial cell wall, and these enzymes are instrumental for phages to achieve rapid and effective bacteriolysis (Fischetti, 2010; Loessner, 2005). Holins are hydrophobic proteins that oligomerise in the host cell cytoplasmic membrane during infection (Young & Bläsi, 1995). Importantly, these proteins are genetically programmed trigger to form holes that collapse the membrane proton motive force, leading to immediate growth cessation and cell death (Gründling et al., 2001; Wang et al., 2000). The precise regulation of host cell lysis is a key factor during phage infection. Delayed lysis can compromise the opportunity to infect new hosts whereas a premature burst results in the release of none or very few descendants (Wang et al., 2000). Kumar et al. (2012a) induced *Siphoviride* phages of *Staphyloccoccus aureus* RN4220 with mitomycin C @ 1 µg/ml and observed that >99.9% of phages adsorbed to the host cells. Since the host RN4220 is devoid of a restriction-modification system and prophages, the authors assumed that, despite successful infection and multiplication, the phage virions failed to show plaques due to its insignificant release from the cell possibly due to an insufficient level of endolysin from phage virions during phage development and assembly. Their hypothesis was substantiated by plaque formation on the lawn of host RN4220 cells when additional phage endolysin protein was supplemented via a plasmid (Kumar et al., 2012a).

Mitomycin C, an antitumor antibiotic, has been intensively used to investigate biological effects in mammalian cells, including selective inhibition of DNA synthesis, mutagenesis, stimulation of genetic recombination, chromosome breakage, sister chromatid exchange, and induction of the DNA repair (SOS) response in bacteria (López Martín, 2014; Tomasz, 1995). This antibiotic crosslinks the complementary strands of the DNA double helix and it is so lethal that a single crosslink per genome is sufficient to cause the death of the bacterial cell (Lyer & Szybalski, 1964). The effective conditions for induction depend on both the mitomycin C concentration and the cell density (Humphrey et al., 1995). Several studies have demonstrated that mitomycin C at varying concentrations ranging from 0.5 µg/ml to 3 µg/ml induced *Bt* phages (Liao et al., 2008; Yuan et al., 2014). Altenbern and Stull (1965) studying the inducible systems in the genus *Bacillus* demonstrated that the use of mitomycin C @ 1 µg/ml induced the cultures of *Bacillus* (=*Brevibacillus*) *brevis* and *Bacillus subtilis* while it prevented

lysis of *Bt*. Different concentrations (1 µg/ml & 3 µg/ml) of mitomycin C in this study were used to induce the putative antibacterial organisms (bacteriophages & bacteriocins) of *Bl* 1821L, *Bl* 1951, and *Bl* Rsp. The strain *Bl* 1821L was induced @ 1 µg/ml while *Bl* 1951 and *Bl* Rsp lysed the culture @ 3 µg/ml.

Optical density (OD_{600nm}) is often used in bacteriological research and three of the more common applications include: (a) determination and standardisation of the optimal time to induce a culture during bacterial protein expression protocols, (b) determination and standardisation of the inoculum concentration for minimum inhibitory concentration experiments, and (c) determination of the optimal time at which to harvest and prepare competent cells (Myers et al., 2013; Stevenson et al., 2016; Szermer-Olearnik et al., 2014). Rajnovic et al. (2019) determined the interaction of different concentrations of bacteria to varying concentrations of phage and their effect on optical density (OD_{600nm}) of culture. Their findings indicated that the optical density of the control increased during the first 90 min until the culture reached the stationary phase but the addition of 5 x 10^8 pfu/ml (phage forming units per millilitre) resulted in a rapid decrease of OD_{600nm} within 25-30 min due to lysis of culture. Assessments of the different concentrations of mitomycin C to induce the putative antibacterial structures from the insect pathogenic strains *Bl* 1821L, *Bl* 1951, and *Bl* Rsp exhibited no significant decline in the optical density (OD_{600nm}) in the initial 6 hours of treatment. However, after 24 hours Mitomycin C addition at a concentration of 1 µg/ml significantly decreased OD_{600nm} of *Bl* 1821L by 49.7%. For *Bl* 1951 and *Bl* Rsp, a drastic decline of 83.9% and 71.2% in OD_{600nm} was noted as compared to the control (without mitomycin C). A drastic fall in the OD_{600nm} reading and the clearing of the culture after 6 hours of treatment with the mitomycin C suggests the activation of the SOS system after this time interval. Hence, it can be assumed that the putative antibacterials (bacteriophages or bacteriocins) after their induction impeded the growth of host bacteria while the cultures without mitomycin C addition pursued their expansion. Based on a review of the literature, this is the first report defining the concentrations of mitomycin C to induce the putative antibacterial organisms (phages or bacteriocins) of the genus *Brevibacillus*

The putative antibacterial structures such like phages and phage tail-like bacteriocins are lysogenic in nature and are released upon lysis of the cells after induction (Patz et al., 2019; Scholl, 2017). While no evidence of complete bacteriophages was found, electron micrographs of the mitomycin C induced cultures of *Bl* 1951 and *Bl* 1821L showed several structural components of bacteriophages including contractile sheath-like entities with an extended core (Figures 2.14 & 2.15). The visualised morphological features of induced particles revealed the structural similarities to the previously defined phage tail-like bacteriocins (Hockett et al., 2015; Liu et al., 2013; Smarda & Benada, 2005).

2.3.7 Outcomes

The major findings of this chapter are;

1. The standard protocols including plaques assay and serial dilution tests provided no substantive evidence of the presence of the phages.
2. Mitomycin C @ 1 µg/ml induced the *Bl* 1821L culture by causing a drop of 49.7% in the optical density (OD_{600nm}). For *Bl* 1951 and *Bl* Rsp, a concentration of 3 µg/ml exhibited a fall of 83.9% and 71.2% respectively in OD_{600nm}.
3. Electron micrographs of the mitomycin C induced cultures of the *Bl* 1821L, *Bl* 1951, and *Bl* Rsp were devoid of typical intact phages. However, phage structural components including empty hexagonal phage head-like structures, hollow sheath structures, complete contractile sheath structures, and contractile sheath structures attached with the cores were seen under an electron microscope in the crude lysates of *Bl* 1821L and *Bl* 1951.

2.3.8 Conclusion

Overall, the findings indicate that the antibacterial structures similar to phage tail-like bacteriocins (PTLBs) may have a potential role in the collapse of the host bacterium and this will be further investigated in subsequent chapters.

Chapter 3

Discovery of phage tail-like bacteriocins (PTLBs) in New Zealand *Brevibacillus laterosporus* and their antibacterial spectrum

3.1 Introduction

The work reported in the previous chapter found no evidence of active phage release. However, electron micrographs of the induced cultures of *Bl* 1821L and *Bl* 1951 affirmed the presence of phage tail-like structures, which appeared to be bacteriocins. Hence, the research direction was changed from that originally proposed to pursue the presence of bacteriocins, particularly phage tail-like bacteriocins in New Zealand *Bl* 1821L and *Bl* 1951 strains.

Bacteriocins are ribosomally synthesised compounds released extracellularly by every major lineage of bacteria (Ghequire & De Mot, 2015; Riley & Wertz, 2002a). Typically, these non-replicating, proteinaceous structures are antagonistic to the closely related producer bacterial strains and species and are the immune to their own antimicrobial peptides, which is mediated by the specific immunity proteins produced by the host cells (Juturu & Wu, 2018; Kjos et al., 2011). Bacteriocins can act on related (narrow-spectrum) and non-related (broad-spectrum) species to the producing strain (Line et al., 2008; Rea et al., 2010). There are >200 bacteriocins with diverse amino acid sequences that are available in different bacteriocin databases (Baindara et al., 2016b). Different online genome databases such as BAGEL, bacterial databases such as BACTIBASE, and bioinformatic tools such as anti-SMASH and BOA (Bacteriocin operon and gene block associator) recognise bacteriocin-like operon gene arrangement and help in the identification of new bacteriocin CDS (CoDing sequence) (de Jong et al., 2006; Morton et al., 2015).

Bacteriocins are classified into two basic groups: low molecular-weight (LMW) and high molecular-weight (HMW). LMW bacteriocins are trypsin-sensitive, thermostable, and not sedimentable, whereas HMW bacteriocins are sedimentable, trypsin-resistant, thermolabile, and visible under an electron microscope as phage-like components (Bradley, 1967b; Lotz & Mayer, 1972). Literature is replete with the description of numerous low molecular-weight bacteriocins from the insect-pathogenic bacterial strains. *Bacillus thuringiensis* (*Bt*), in addition to producing the insecticidal proteins Cry, Cyt, and VIPs also synthesises bacteriocins and to date 18 bacteriocins have been defined (de la Fuente-Salcido et al., 2013). *Bt* derived bacteriocins may have either a broad or narrow killing spectrum against pathogenic bacteria. Thuricin 439 and thuricin CD have a narrow spectrum of activity (Ahern et al., 2003; Rea et al., 2010), whereas morricin 269, kurstacin 287, kenyacin 404, entomocin 420, and

tolworthcin 524 bacteriocins manifest a wide range of activity (Barboza-Corona et al., 2009; de la Fuente-Salcido et al., 2008a). *Brevibacillus* species are a rich source of antimicrobial peptides (AMPs) (Yang & Yousef, 2018b) and >30 AMPs including antibacterial, antifungal, and anti-invertebrate agents have been isolated from different species (Cochrane & Vederas, 2016; Yang & Yousef, 2018b). For *Brevibacillus laterosporus* (*Bl*) antagonistic compounds have been explicitly reviewed in recent years (Ruiu, 2013; Yang & Yousef, 2018b).

High molecular-weight or phage tail-like bacteriocins are often called "tailocins" (Ghequire & De Mot, 2014; Rybakova et al., 2013). Morphologically, tailocins resemble phage tails and a common ancestral relationship between tailocins and phages has been defined (Nakayama et al., 2000). Two morphologically distinct types of tailocins could be distinguished: the R-type tailocins are rigid and contractile particles whereas the F-type tailocins represent flexible, non-contractile structures. The common feature of the two forms is how they perpetuate in nature (Ghequire & De Mot, 2014; Ghequire & De Mot, 2015; Michel-Briand & Baysse, 2002). The best-studied examples are the colicins produced by *Escherichia coli* and the R-type pyocins of *Pseudomonas aeruginosa*. Colicin gene clusters are encoded on plasmids while pyocins are typically located on chromosomal DNA (Cascales et al., 2007; Michel-Briand & Baysse, 2002). However, similar entities have been abundantly found in other gram-negative bacteria including *Burkholderia cenocepacia* (Yao et al., 2017), *Pseudomonas syringae* (Hockett et al., 2015), *Stenotrophomonas maltophilia* (Liu et al., 2013), *Pseudomonas fluorescens* (Fischer et al., 2012), *Xenorhabdus bovienii* (Morales-Soto et al., 2012), *Budvicia aquatica* (Smarda & Benada, 2005), *Pragia fontium* (Smarda & Benada, 2005), *Serratia plymithicum* (Jabrane et al., 2002b), *Erwinia carotovora* (Nguyen et al., 2001), *Yersinia enterocolitica* (Strauch et al., 2001), *Xenorhabdus nematophilus* (Thaler et al., 1995), *Proteus mirabilis* (Senior, 1984), *Rhizobium lupine* (Lotz & Mayer, 1972), *Proteus vulgaris* (Coetzee et al., 1968), and *Vibrio cholerae* (Jayawardene & Farkas-Himsley, 1968) as well as in a limited number of gram-positive bacteria like *Listeria monocytogenes* (Lee et al., 2016), *Bacillus pumilus* (Jin et al., 2014), *Bacillus subtilis* (Nagai, 2014), *Clostridium difficile* (Gebhart et al., 2012), and *Bacillus aneurinolyticus* (Ito et al., 1986). There is no report of tailocins from the insect-pathogenic strains belonging to gram-positive bacteria so far.

Bacteriocinogenic strains spontaneously produce small amounts in culture, but the substances can also be induced by treating cells with an ultraviolet light or mitomycin C (Bradley, 1967a; Michel-Briand & Baysse, 2002). Bacteriophages and phage tail-like bacteriocins (PTLBs) rely on receptor-binding proteins (RBPs) located on tail fibres or spikes for initial and specific interaction with susceptible bacteria (Nobrega et al., 2018). Because of the host specificity of the antibacterial structures, bacterial strains can be differentiated or typed by sensitivity patterns (Holtzman et al., 2020; Ross et al., 2016). Phages kill bacteria through a lytic, replicative cycle, whereas phage-derived

bacteriocins kill the susceptible cells through membrane depolarisation in a single hit mechanism (Dams et al., 2019; Scholl, 2017).

Enzymatic or non-enzymatic methods are employed to determine the antibacterial activity of bacteriocinogenic strains (de la Fuente-Salcido et al., 2008b). Enzymatic methods rely on the immediate measurement of intracellular enzymes released after cellular lysis upon exposure to bacteriocins (Morgan et al., 1995). The non-enzymatic methods measure the inhibition of bacterial growth on solid media that may include protocols like well-diffusion or disc-diffusion assays, the soft-agar overlay method, the spot-on-lawn or the agar spot method, and deferred-antagonism plate assays (de la Fuente-Salcido et al., 2008b). The soft-agar overlay technique was originally developed over 70 years ago and has been widely used in studies of proteinaceous antibacterial structures, especially bacteriophages (as used in Chapter 2), and bacteriocins (Hockett & Baltrus, 2017).

N-terminal protein sequencing (also called Edman sequencing) information plays a vital role in modern structural and proteomics (Reim & Speicher, 2001).This is the most commonly used tool to identify unknown proteins, N-terminus, and cleavage sites of proteins (Beyer et al., 2002) and often employed to control quality control of recombinant proteins (Kaji et al., 2009).

The current chapter primarily aimed to isolate and preliminarily identify the putative antibacterial proteins (bacteriocins) of *Bl* 1821L and *Bl* 1951 strains.

3.2 Methods

3.2.1 Disc diffusion assay test of mitomycin C induced cultures

Bl 1821L and *Bl* 1951 cultures were cultivated with and without mitomycin C (Sigma) addition as described in the previous chapter (Section 2.2.6). Mitomycin C (Sigma) induced cultures of *Bl* 1821L and *Bl* 1951 were assayed through the Kirby-Bauer disc diffusion test (Bauer, 1966; Hudzicki, 2009; Kirby et al., 1956). The induced cultures were centrifuged @ 16,000 g for 10 min and the intact cells were removed from the supernatant by passing through a 0.22 µm filter. Antibacterial activity of filtered supernatants of *Bl* 1821L and *Bl* 1951 was assayed against the producer strain and vice versa. Cell free supernatants (CFS) of the treatment without mitomycin C addition were also evaluated in the assay test. For the assay, single colony/colonies of the host bacterium (*Bl* 1821L & *Bl* 1951) were inoculated into a 5 ml LB broth (Miller) and placed over an orbital shaker (Conco, TU-4540, Taiwan) @ 250 rpm and 30^{o}C for 18-20 hours to obtain overnight culture. LB agar plates were inoculated by dipping a sterile swab into the overnight culture. Excess inoculum was removed by pressing and rotating the swab against the side of a 5 ml universal vial. The swab was swabbed all over the surface

of the medium three times, rotating the plate after each application and ensuring the uniform spread of inoculum. The inoculum was left to dry for 10-15 min at room temperature (22°C). A sterile 8 mm diameter paper disc (ADVANTEC, Japan) was placed in the middle of an LB agar plate with the help of forceps and 80 µl of CFS was pipetted onto the disc. For the control treatment, sterile LB broth was pipetted onto the discs instead of CFS. LB agar plates after absorption of CFS were kept in an incubator at 30°C for 48-72 hours. Antibacterial activity of CFS of mitomycin C (Sigma) induced cultures of *Bl* 1821L and *Bl* 1951 was measured through the diameter of the zone of inhibition (including the diameter of the disc) and recorded in mm. Disc diffusion assays were performed with three technical replications.

3.2.2 Soft-agar overlay method with polyethylene glycol (PEG) precipitation

The protocol to induce *Bl* 1821L and *Bl* 1951 cultures using mitomycin C (Sigma) outlined in Chapter 2 (Section 2.2.6) was used. The induced cultures were centrifuged @ 16,000 g for 10 min and the intact cells were removed from the supernatant by passing through a 0.22 µm filter. To the filtered supernatant, 1M NaCl and 10% PEG 8000 were added and the sample was repeatedly inverted until both the NaCl and PEG 8000 were completely dissolved. The sample was incubated in an ice bath for 60 min and subsequently centrifuged @ 16,000 g for 30 min at 4°C. The supernatant was decanted and the pellet was resuspended in 1/10th volume of the original supernatant volume of buffer (10 mM Tris, 10 mM MgSO4, pH 7.0) by repeated pipetting. PEG 800 residue was removed by two sequential extractions with an equal volume of chloroform which was combined with the resuspended pellet and vortexed for 10-15 sec. The mixture was centrifuged @ 16,000 g for 10 min and the upper aqueous phase was transferred to a fresh microfuge tube. This extraction process was repeated until no white interface between the aqueous and organic phases was visible.

Overnight cultures of *Bl* 1821L and *Bl* 1951 were established by transferring a single colony/colonies of host bacterium into 5 ml LB broth (Miller) and placing the inoculated cultures on an orbital shaker (Conco, TU-4540, Taiwan) @ 250 rpm and 30°C. Soft agar (0.5%) was prepared and maintained in a water bath at 55-60°C before use. Three ml of soft agar (0.5%) was transferred into a 15 ml sterile tube and 100 µl of overnight culture was added. The tube was rotated within palms of hand for 10-15 sec and then immediately poured over an LB agar plate. LB agar plates were covered and allowed to dry for 20-30 min. Once the petri dishes were solidified, 10 µl of PEG 8000 precipitated supernatant was spotted (2 spots) on the lawn of host bacterium and the plates were kept at 30°C for 48-72 hours. Sterile LB broth was spotted on the plates in the control treatment. Antibacterial activity was evaluated by measuring the diameter of the zone of inhibition (mm) at the spotting point.

3.2.3 Antibacterial activity of cell free supernatants of mitomycin C induced cultures

Antibacterial activity of CFS of mitomycin C (Sigma) induced cultures of *Bl* 1821L and *Bl* 1951 was evaluated using the soft agar overlay protocol along with PEG 8000 precipitation (Hockett & Baltrus, 2017). Tenfold dilutions (10^{-1} to 10^{-8}) of induced cultures were prepared with LB broth (Miller) and 10 µl of each dilution was spotted separately on 1.5% LB agar plates seeded with the *Bl* 1821L and *Bl* 1951 as the host bacterium to determine susceptibility to the induced cultures. Sterile LB broth was spotted on the plates in the control treatment. Antibacterial activity of PEG 8000 precipitated CFS was evaluated by measuring the diameter (mm) of the zone of inhibition at the spotting point.

3.2.4 Antimicrobial spectrum of cell free supernatants of mitomycin C induced cultures

To study the antimicrobial spectrum of cell free supernatants of mitomycin C (Sigma) induced cultures of *Bl* 1821L and *Bl* 1951 strains against various gram-positive bacteria (*Bl* 1821L, *Bl* 1951, *Bl* Rsp, *Bl* CCEB 342, *Bl* NRS 590, *Carnobacterium maltaromaticum* 3-1, *Bacillus megaterium* 3-2, *B. megaterium* S1, *Oerskovia enterophila* 3-3, *Paenibacillus spp.* 15.12.1, *Oceanobacillus spp.* R-31213, *B. subtilis* Tp5, and *Fictibacillus rigui* FJAT 46895) (all held in the BPRC Culture Collection, Lincoln University), the soft agar overlay method with PEG 8000 precipitation was used (Hockett & Baltrus, 2017). Sterile LB broth was spotted on the plates in the control treatment. Antimicrobial activity of mitomycin C (Sigma) induced cultures of *Bl* 1821L and *Bl* 1951 after PEG 8000 precipitation was evaluated by measuring the diameter (mm) of the zone of inhibition at the spotting point.

3.2.5 Ultrafiltration of mitomycin C induced culture of *Bl* 1821L

Mitomycin C (Sigma) induced culture of *Bl* 1821L was centrifuged @ 16,000 g for 10 min to obtain the cell free supernatant (CFS). CFS was achieved by passing through a 0.22 µm filter and subsequently subjected to ultrafiltration using a 30 kD molecular weight cut off membrane (MWCO) (GE Healthcare, UK). Antibacterial activity of retentate (CFS that does not pass through the membrane) and permeate (CFS that passes through the membrane) was tested by the disc diffusion assay method (Hudzicki, 2009; Kirby et al., 1956).

3.2.6 Sodium dodecyl sulphate-polyacrylamide gel electrophoresis (SDS-PAGE) visualisation of *Bl* 1821L putative antibacterial protein

Laemmli (1970) described a method for separating proteins by electrophoresis that uses a discontinuous polyacrylamide gel as a support medium and sodium dodecyl sulphate (SDS) to denature the proteins. The method is generally known as Sodium dodecyl sulphate polyacrylamide gel electrophoresis (SDS-PAGE) (Laemmli, 1970). Ten percent resolving gel was prepared by mixing 3.96 ml MQW, 3.3 ml acrylamide (30%), 2.5 ml gel buffer (1.5 M Tris-HCl, pH 8.8), 100 µl SDS (10%), 5 µl TEMED, and 50 µl of ammonium persulphate (10% APS). Stacking gel (7.5%) was prepared by mixing 6.10 ml MQW, 1.3 ml acrylamide (30%), 2.5 ml gel buffer (0.5 M Tris-HCl, pH 6.8), 100 µl SDS (10%), 10 µl TEMED, and 50 µl of ammonium persulphate (10% APS).

The samples were prepared by adding 4 µl of 4X reducing buffer (1 ml 0.5 M Tris-HCl (pH 6.8), 0.8 ml glycerol, 1.6 ml 10% SDS, 0.4 ml 2-Mercaptoethanol, 0.4 ml 1% Bromophenol blue) and 12 µl of the ultracentrifuged sample (20,000 rpm & 70 min) which was vortexed before heating at 95^{o}C for 5 min. All the samples were kept in an icebox before gel loading. Gel plates were removed after the gel polymerised and placed inside the tank in the inward direction. The space between the plates was filled with 1X SDS buffer (To prepare 10X electrode buffer; 30.3 g Tris base, 144.0 g glycine, 10.0 g SDS dissolve all the constituents and make the volume 1000 ml with dH_2O) and the comb was removed. Ten µl of protein ladder (BIO-RAD, Precision Plus Protein^{TM} Standards) was loaded into the first well and 12.5 µl of each sample was loaded into other wells. The gel was run for 50 min at 200 volts. Glass plates were transferred into a small plastic box filled with dH_2o, left shaking for 5 min, and then washed three times in water. Gels were stained with RAMA stain (29 ml MQW, 12.5 ml CBB stock (1 gm CBB, 300 MeOH, 200 ml MQW), 3.75 ml ammonium sulphate (200 gm, 500 ml MQW), 5 ml of glacial acetic acid per gel) (Yasumitsu et al., 2010) and kept on an orbital shaker (Ratek, Australia) for 30 min at a very low speed. The gel was rinsed twice and the box was filled with dH_2o for overnight destaining.

3.2.7 N-terminal sequencing and bioinformatic analysis of *Bl* 1821L putative antibacterial protein

The following day after staining, the prominent band of an appropriate protein was excised with the help of a sterile razor and sent for N-terminal sequence analysis at AgResearch, Lincoln to identify the proteins. The short amino acid sequences obtained after N-terminal sequencing of the ~48 kD putative antibacterial protein were used to identify the encoding gene in the *Bl* 1821L genome (NZ_CP033464.1). The identified ~48 kD protein in the *Bl* 1821L genome (NZ_CP033464.1) was

searched in the Uniprot database (https://www.uniprot.org) to determine the nature of the proteins which were further subjected to BLASTp (Basic Local Alignment Search Tool) analysis to look into identical proteins (https://blast.ncbi.nlm.nih.gov). Amino acids of the ~48 kD identified putative antibacterial phage tail-sheath protein were also aligned using the programme CLUSTALO (https://www.ncbi.nlm.nih.gov).

N-terminal sequenced and identified ~48 kD putative antibacterial protein of *Bl* 1821L was bioinformatically analysed using the programme Geneious basic (Kearse et al., 2012).

3.2.8 BAGEL4 analysis of *Bl* 1821L and *Bl* 1951 genomes

BAGEL4 is a web server that that identifies and visualises gene clusters in prokaryotic DNA involved in the biosynthesis of ribosomally synthesized and post translationally modified peptides (RiPPs) and (unmodified) bacteriocins (van Heel et al., 2018). The genomes of *Bl* 1821L (NZ_CP033464.1) and *Bl* 1951(RHPK01000003.1, contig 1) were subjected to BAGEL4 analysis.

3.3 Results

3.3.1 Disc diffusion assay test of Mitomycin C induced cultures of *Bl* 1821L and *Bl* 1951

Disc assay test of cell free supernatants of mitomycin C induced culture of *Bl* 1821L produced a zone of inhibition of 11.7 mm-12.3 mm against the producer strain. A halo of 12.3 mm-13.7 mm developed when *Bl* 1951 was used as the host bacterium and no activity was seen in the control treatment (Figure 3.1). CFS of mitomycin C induced culture of *Bl* 1951 produced a zone of inhibition of 14.3 mm-15.7 mm in the assay test against *Bl 1*821L and a halo of 11.3 mm-14.7 mm against the producer strain (self) as the test bacterium (Figure 3.1). Notably, CFS of both *Bl* 1821L and *Bl* 1951 from the treatments without mitomycin C addition also demonstrated their inhibitory activities against the tested strains but at a slightly lower level than the mitomycin C induced cultures. No zone of inhibition was observed in the treatment where LB broth was used instead of CFS (Figure 3.1).

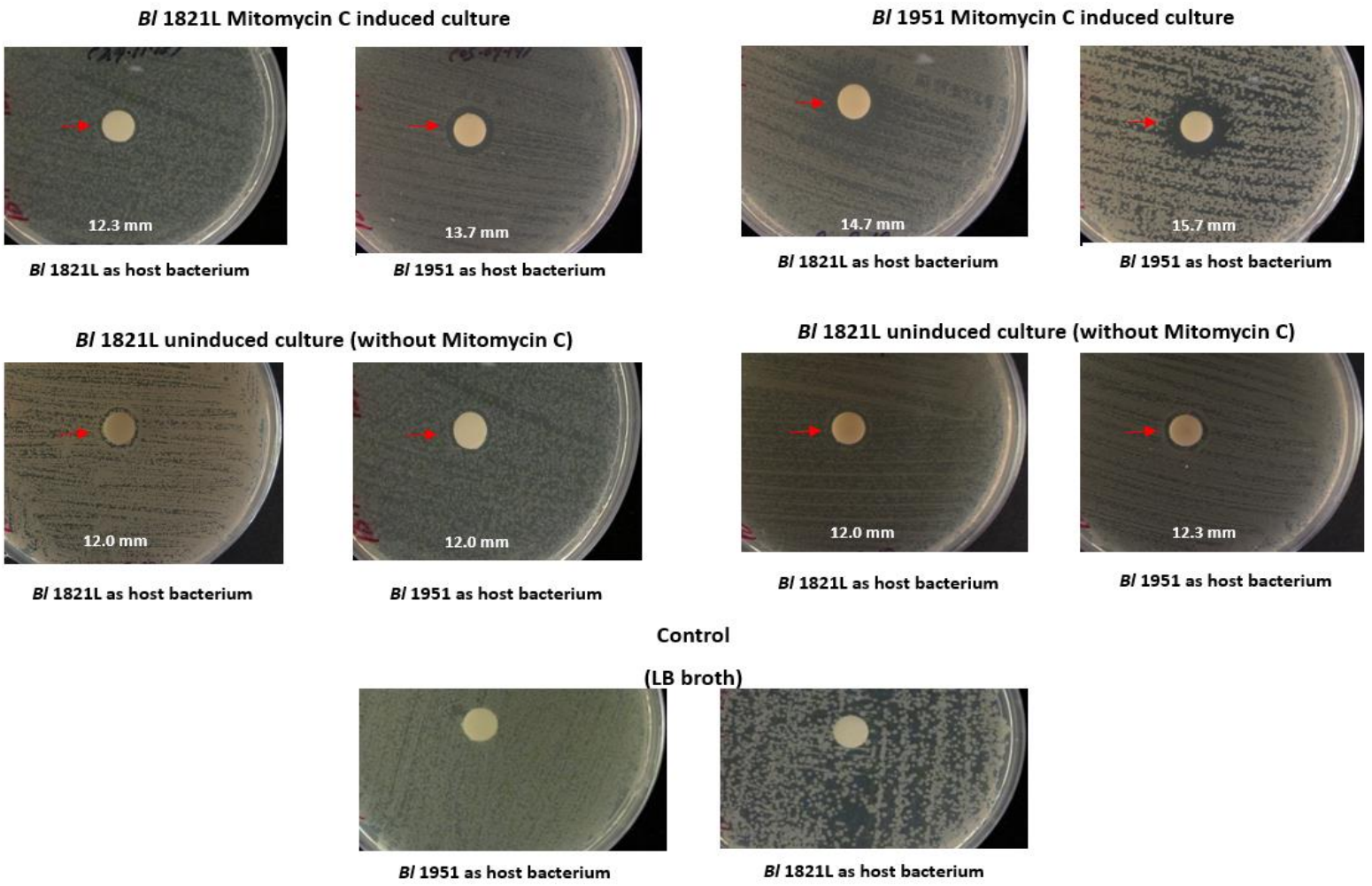

Figure 3.1 Disc diffusion assay test of *Bl* 1821L and *Bl* 1951 cultures with/without mitomycin C addition and control treatment against the producer strain and vice versa. Arrows (red colour) denote the zones of inhibition developed due to the activity of putative antibacterial proteins on the lawns of host bacteria

3.3.2 Antibacterial activity of the cell free supernatants of mitomycin C induced cultures

Antibacterial activity of bacteriophages and bacteriocins can be differentiated after PEG 8000 precipitation of mitomycin C induced bacterial cultures and the serial dilution assay testing in the soft-agar overlay. PEG 8000 precipitated cell free supernatant of *Bl* 1821L demonstrated inhibitory activity against the producer strain at the highest concentration (FS- Full strength) (Table 3.1 & Figure 3.2B) and activity of PEG 8000 precipitated *Bl* 1951 supernatant against *Bl* 1821L as the host bacterium was also observed between FS to 10^{-1} dilution (Table 3.1 & Figure 3.2C).

Table 3.1 Antibacterial activity of *Bl* 1821L and *Bl* 1951 mitomycin C induced cultures after PEG 8000 precipitation against *Bl* 1821L as the host bacterium

Antibacterial activity of *Bl* 1821L mitomycin C induced culture cell free supernatants		**Antibacterial activity of *Bl* 1951 mitomycin C induced culture cell free supernatants**	
Dilution level	**Zone of inhibition diameter (mm)**	**Dilution level**	**Zone of inhibition diameter (mm)**
*FS	12.5	FS	12.5
10^{-1}	-	10^{-1}	13.5
10^{-2}	-	10^{-2}	-**
10^{-3}	-	10^{-3}	-
10^{-4}	-	10^{-4}	-
10^{-5}	-	10^{-5}	-
10^{-6}	-	10^{-6}	-
10^{-7}	-	10^{-7}	-
10^{-8}	-	10^{-8}	-
Control	-	Control	-

* FS = Full strength
** - = No zone of inhibition

PEG 8000 precipitated cell free supernatants of *Bl* 1951 in the serial dilution assay test demonstrated no antibacterial activity against the producer strain at all the levels of dilution but a significant zone of inhibition which varied from FS to 10^{-2} or FS to 10^{-3} when *Bl* 1821L precipitated cell free supernatants (CFS) were evaluated against *Bl* 1951 as the host bacterium (Table 3.2 & Figure 3.2A).

Table 3.2 Antibacterial activity of *Bl* 1821L and *Bl* 1951 mitomycin C induced cultures after PEG 8000 precipitation against *Bl* 1951 as the host bacterium

Antibacterial activity of *Bl* 1951 mitomycin C induced culture cell free supernatants		**Antibacterial activity of *Bl* 1821L mitomycin C induced culture cell free supernatants**	
Dilution level	**Zone of inhibition diameter (mm)**	**Dilution level**	**Zone of inhibition diameter (mm)**
*FS	**-	FS	12.5
10^{-1}	-	10^{-1}	10.5
10^{-2}	-	10^{-2}	13.5
10^{-3}	-	10^{-3}	10.5
10^{-4}	-	10^{-4}	-
10^{-5}	-	10^{-5}	-
10^{-6}	-	10^{-6}	-
10^{-7}	-	10^{-7}	-
10^{-8}	-	10^{-8}	-
Control	-	Control	-

* FS = Full strength
** - = No zone of inhibition

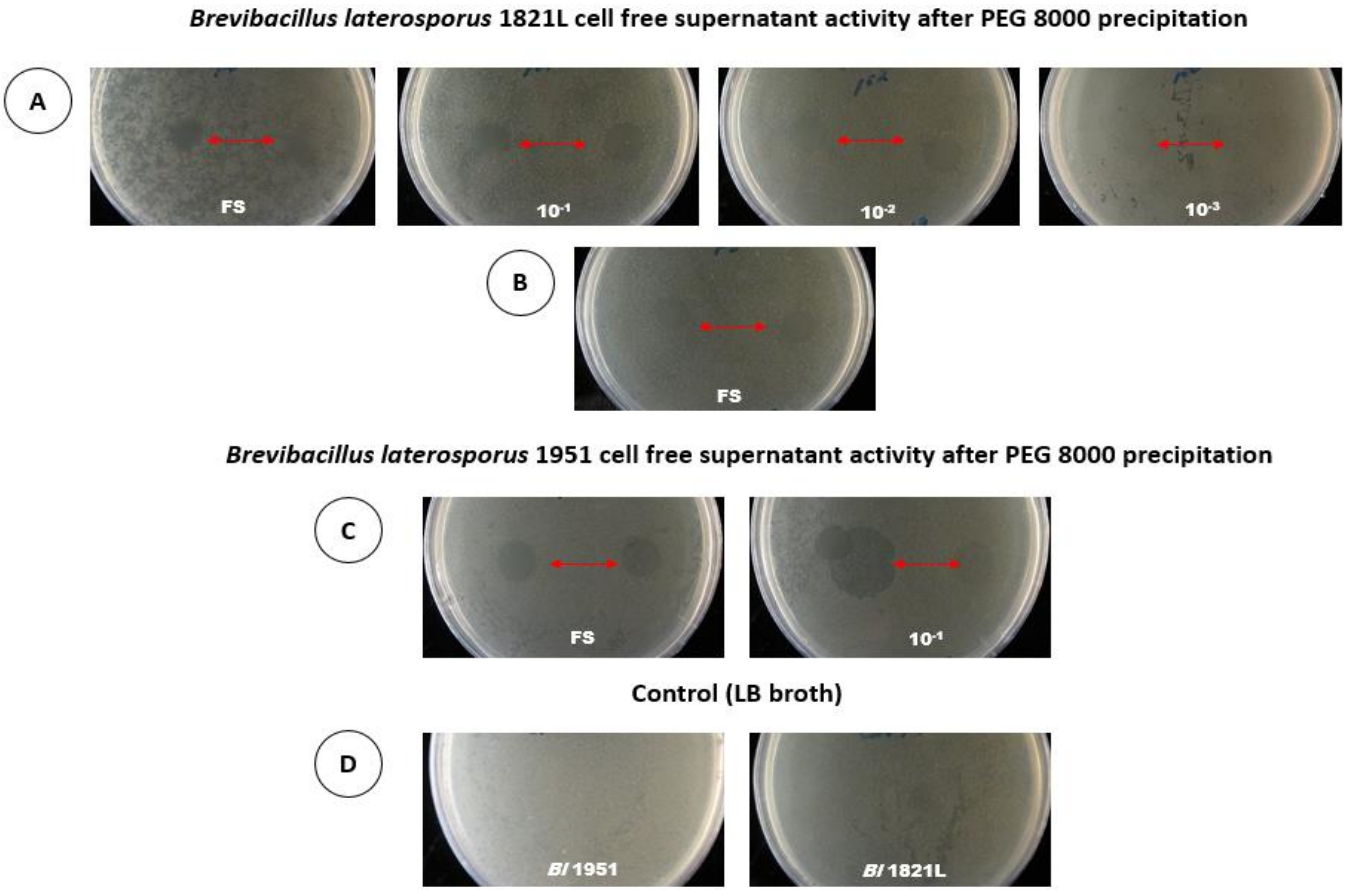

Figure 3.2 Antibacterial activity of *Bl* 1821L cell free supernatant after PEG 8000 precipitation in the serial dilutions assay test against *Bl* 1951 as the host bacterium (A) and *Bl* 1821L as the host bacterium (B). Similar to (A) and (B) antibacterial activity of *Bl* 1951 cell free supernatant after PEG 8000 precipitation in the serial dilutions assay test against *Bl* 1821L is shown in (C). Arrows (red colour) denote the zones of inhibition due to the activity of PEG 8000 precipitated putative antibacterial proteins. LB broth was used in the control treatment against *Bl* 1951 and *Bl* 1821L as the host bacterium (D).

3.3.3 Antimicrobial spectrum of cell free supernatants of mitomycin C induced cultures

Mitomycin C induced cultures of *Bl* 1821L after PEG 8000 precipitation exhibited prominent activity against all the tested strains of *Bl* except itself and *Bl* CCEB 342. All the other tested gram-positive bacterial strains showed no susceptibility to the PEG 8000 precipitated cultures of *Bl* 1821L except for the gram-positive bacterium, *C. maltaromaticum* isolate 3-1, which was slightly sensitive to their inhibitory action (Table 3.3 & Figure 3.3). PEG 8000 precipitation of *Bl* 1951 induced cultures in the soft-agar overlay showed prominent activity against all the tested *Bl* strains except the producer strain, but no effect on the other evaluated gram-positive bacterial strains. Interestingly, *Bl* CCEB 342 was not susceptible to the *Bl* 1821L crude CFS but was sensitive to *Bl* 1951 PEG 8000 precipitated CFS. Likewise, *C. maltaromaticum* 3-1, was slightly sensitive to the inhibitory action of *Bl* 1821L induced CFS but completely insensitive to *Bl* 1951 CFS (Table 3.3 & Figure 3.4).

Table 3.3 Antibacterial spectrum of *Bl* 1821L and *Bl* 1951 mitomycin C induced cultures cell free supernatants after PEG 8000 precipitation against various gram-positive bacteria

Host bacterium	Host bacterium isolate/strain	Sensitivity to induced *Bl* 1821L CFS	Sensitivity to induced *Bl* 1951 CFS
Bacillus megaterium	3-2	-	-
Bacillus megaterium	S1	-	-
Bacillus subtilis	EM-13 (Tp5)	-	-
Brevibacillus laterosporus	1951	+	-
Brevibacillus laterosporus	1821L	-	+
Brevibacillus laterosporus	Rsp	+	+
Brevibacillus laterosporus	CCEB 342	-	+
Brevibacillus laterosporus	NRS 590	+	+
Brevibacillus laterosporus	NCIMB	+	+
Carnobacterium maltaromaticum	3-1	+	-
Fictibacillus rigui	EM-14 (FJAT 46895)	-	-
Oceanobacillus spp.	EM-12 (R-31213)	-	-
Oerskovia enterophila	3-3	-	-
Paenibacillus spp.	15.12.1	-	-

* - = No zone of inhibition
** + = Zone of inhibition

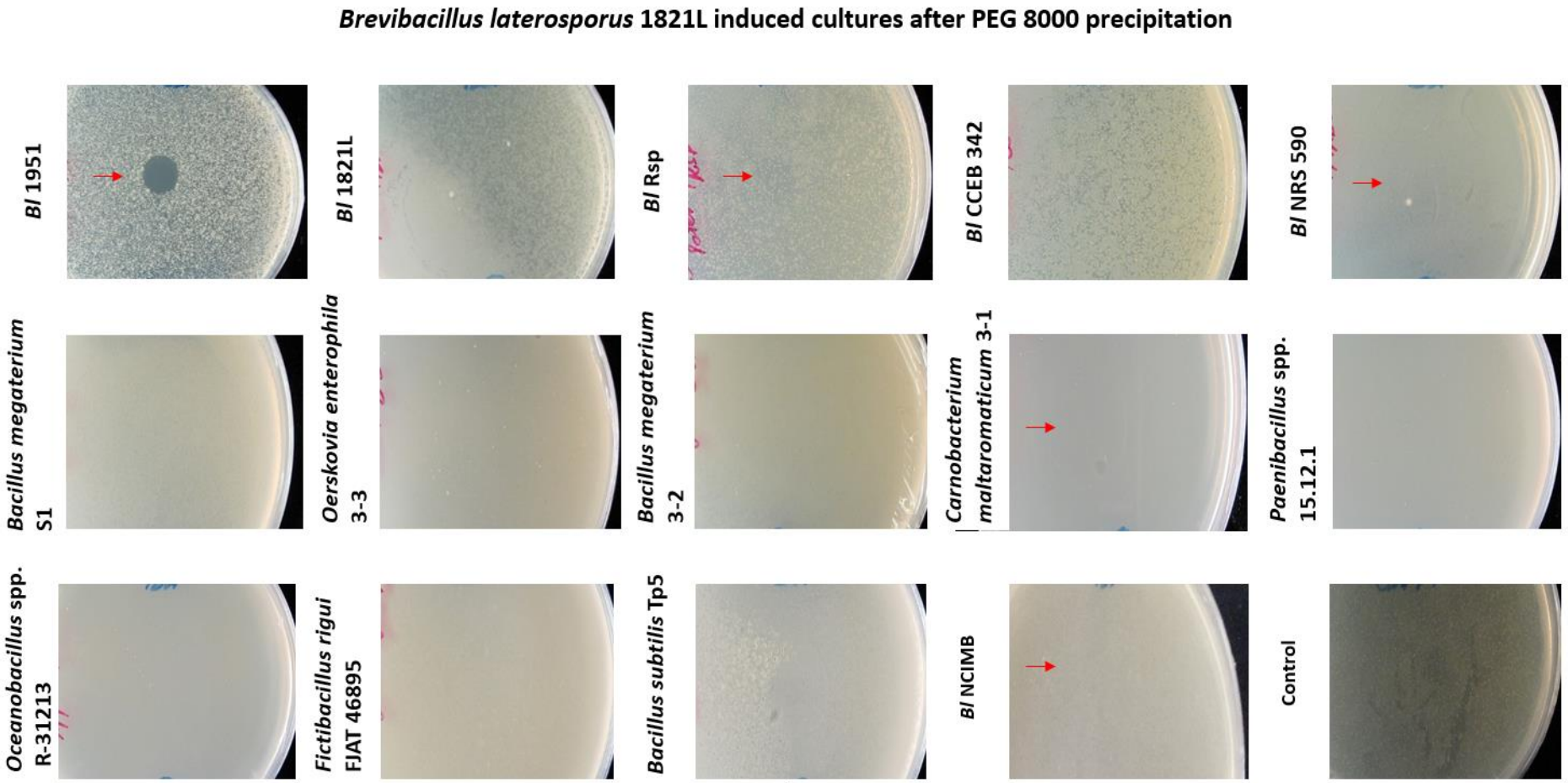

Figure 3.3 Antibacterial activity of *Bl* 1821L induced culture cell free supernatant after PEG 8000 precipitation against various gram-positive bacteria. Arrows (red colour) denote the zone of inhibition due to the activity of PEG 8000 precipitated putative antibacterial proteins

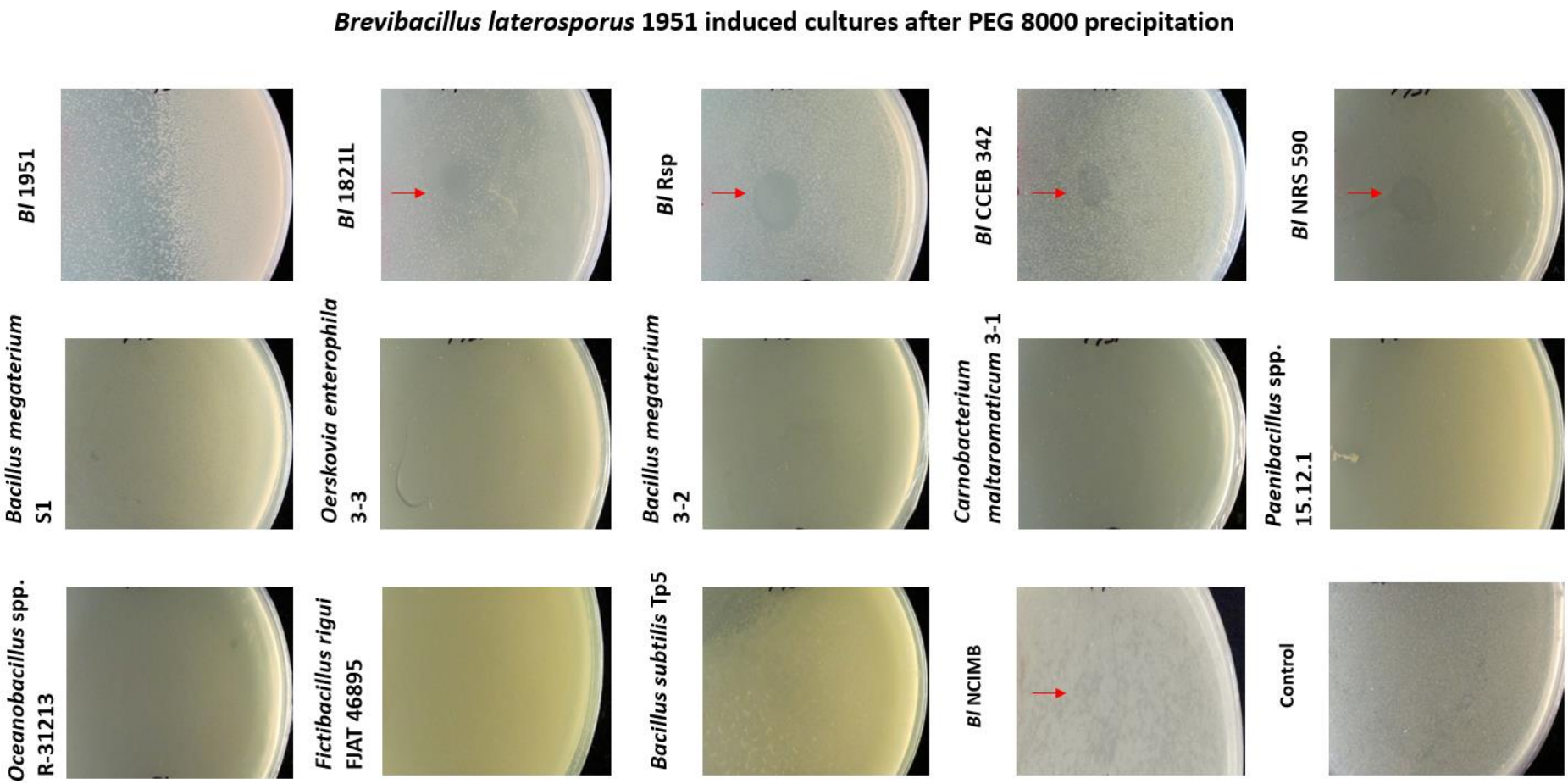

Figure 3.4 Antibacterial activity of *Bl* 1951 induced culture cell free supernatant after PEG 8000 precipitation against various gram-positive bacteria. Arrows (red colour) denote the zone of inhibition due to the activity of PEG 8000 precipitated putative antibacterial proteins

3.3.4 Ultrafiltration of mitomycin C induced culture of *Bl* 1821L

MWCO membrane (30 kD) retentate (Section 3.2.5) in the disc assay test displayed inhibitory action against the producer strain (*Bl* 1821L) and *Bl* 1951 but the tested strains were insensitive to the permeates. The expression of antibacterial activity of the retentate to the indicator strains implied that the active antimicrobial proteins are ≥30 kD in molecular mass.

3.3.5 SDS-PAGE visualisation of *Bl* 1821L putative antibacterial protein

SDS-PAGE of mitomycin C treated and untreated cultures (without mitomycin C) of *Bl* 1821L and *Bl* 1951 was performed and the *Bl* 1821L induced culture from where a prominent band of ~48 kD was observed (Figure 3.6A). Based on its dominance, it was hypothesised that this protein (~48 kD) might have a role in the antibacterial activity of *Bl* 1821L therefore the band was excised for N-terminal sequencing (Figure 3.6B).

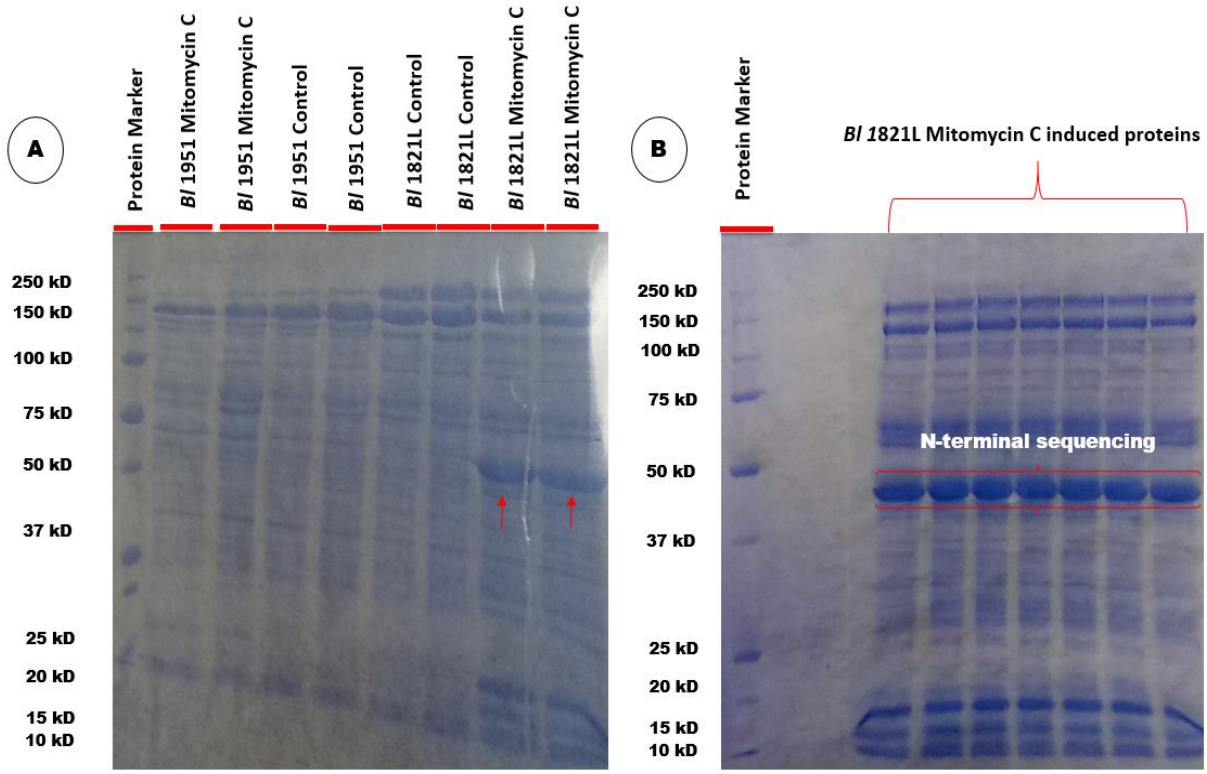

Figure 3.5 SDS-PAGE visualisation of (A) mitomycin C treated cultures of *Bl* 1951 & *Bl* 1821L along with control (without mitomycin C) treatments after ultracentrifugation (Arrows in red colour denote the prominent ~48 kD protein bands) (B). *Bl* 1821L mitomycin induced culture showing the location of prominent bands (~48 kD) which were excised for N-terminal sequencing

3.3.6 Identification of putative antibacterial protein in *Bl* 1821L genome

The resultant short sequence amino acids of N-terminal sequencing of the ~48 kD excised protein band of *Bl* 1821L exhibited several hits (covering approximately 70% of the amino acid sequence) to a predicted protein in the genome of *Bl* 1821L (NZ_CP033464.1). The predicted gene corresponding to ~48 kD putative antibacterial protein was annotated as a defective phage similar to that encoded by *Bacillus subtilis* 168 PBSX-like region gene *xkdK* (Table 3.4 & Figures 3.6 & 3.7). Defective phage gene *xkdK* occurred several times in the *Bl* 1821L genome. A second *xkdK*-like gene resided in the PBSX-like region but it displayed low homology to the identified ~48 kD protein. The amino acid region matching the phage-like element PBSX gene *xkdK* is shown in Figure 3.7 (green colour with red arrow). Notably, a gene corresponding to 41.8 kD flagellin protein (covering approximately 75% of the amino acid sequence) residing between 3,420,157 bp to 3,421,326 bp was predicted in the *Bl* 1821L genome (NZ_CP033464.1) (Table 3.4) through N-terminal sequencing of ~48 kD protein but it seems to be co-migrating on SDS-PAGE.

The identified ~48 kD phage-like element PBSX gene *xkdK* was also identified in the genome of *Bl* 1951 (RHPK01000003.1, contig 1) at the position between 1,937,150 bp to 1,935,829 bp (Figure 3.8). Furthermore, several *Bl* 1821L PBSX-like region genes such as *xkdT*, *xkdU*, and other hypothetical genes also reside in the analogous *Bl* 1951 region (Figure 3.8).

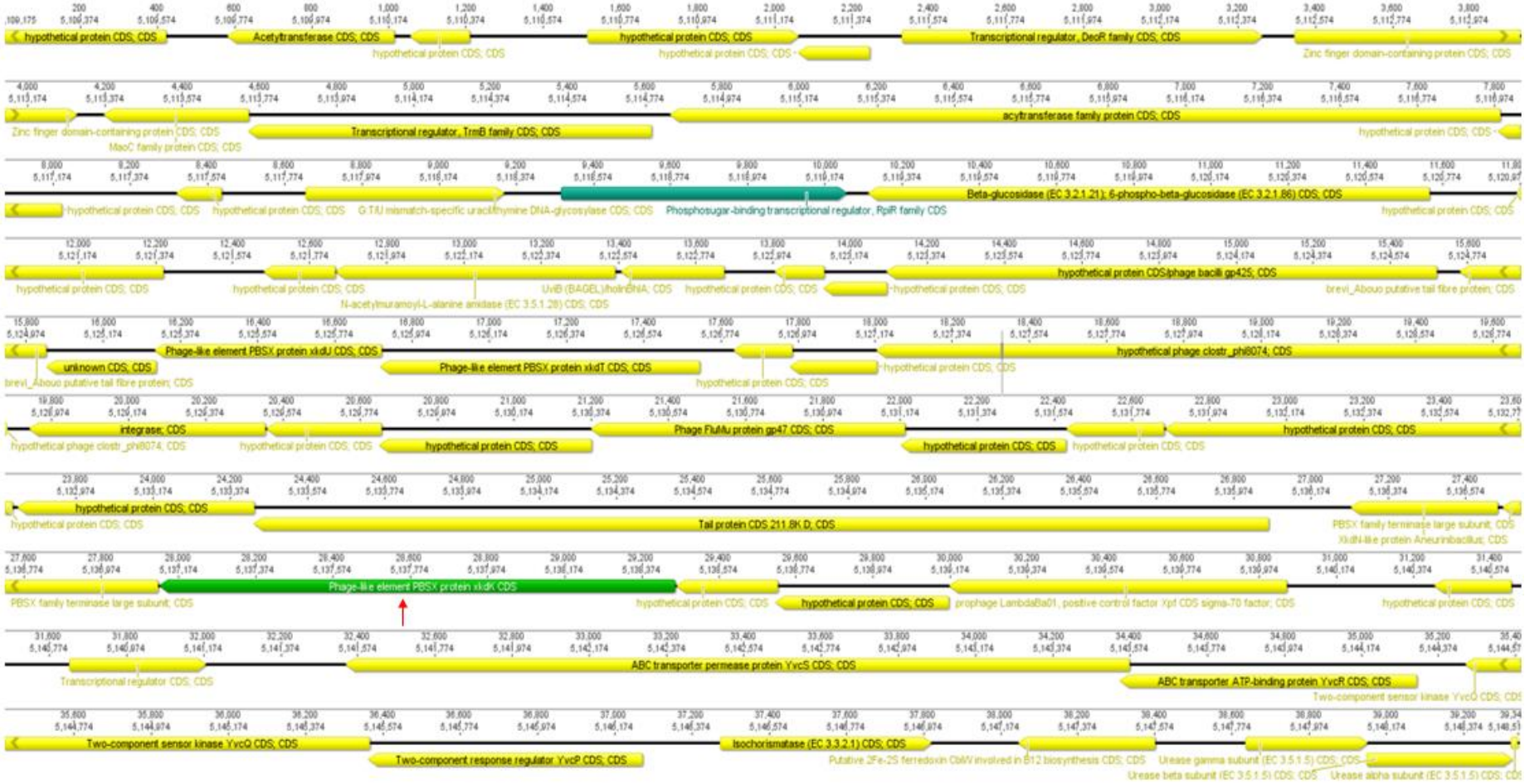

Figure 3.6 Geneious output of the phage-like element PBSX gene *xkdK* in *Bl* 1821L genome encoding a ~48 kD putative antibacterial protein similar to a *Bs* 168 defective prophage (shown in green colour with red arrow)

Figure 3.7 Geneious output of the phage-like element PBSX gene *xkdK* in *Bl* 1951 genome encoding a ~48 kD putative antibacterial protein, XkdT, and XkdU similar to a *Bs* 168 defective prophage (shown with red arrows)

3.3.7 N-terminal sequence analysis of identified 48 kD putative antibacterial protein of *Bl* 1821L

N-terminal sequencing identified ~48 kD protein through alignments with the translated 48 kD protein revealed alignment with phage tail-sheath proteins with accessions tr|A0A0F7EFA2|A0A0F7EFA2_BRELA and tr|A0A328R421|A0A328R421_BRELA in the Uniprot database (Table 3.4). BLASTp analysis of the accession tr|A0A328R421|A0A328R421_BRELA against the GenBank database shared 90% to 100% amino acid identity to the phage tail sheath subtilisin-like domain protein, phage tail protein, and phage sheath protein belonging to various *Bl* strains (Appendix B-1). Accession tr|A0A328R421|A0A328R421_BRELA is currently categorised as an obsolete entry in the Uniprot database but another equivalent accession tr|A0A518VEB0|A0A518VEB0_BRELA exists. Furthermore, accessions tr|A0A518VEB0|A0A518VEB0_BRELA and tr|A0A0F7EFA2|A0A0F7EFA2_BRELA upon BLASTp analysis against the Uniprot database also exhibited amino acid similarity to the phage tail proteins and uncharacterised proteins of the genus *Brevibacillus* (Table 3.5 & Appendix B-2). Amino acid sequence analysis of the *Bl* 1821L predicted putative phage tail-like protein through ExPasy (https://www.expasy.org) computed the molecular weight to be 48.4 kD, which was similar to the prominent band of SDS-PAGE used for N terminal sequencing (Figure 3.6B)

Table 3.4 Identification of *Bl* 1821L putative antibacterial protein (~48 kD) in the genome through the Uniprot database

Accession	Average molecular mass	Identity	Encoded proteins of identified gene	Uniprot description of identified proteins
*tr|A0A328R421|A0A328R421_BRELA tr|A0A518VEB0|A0A518VEB0_BRELA	48,361	Phage tail protein	Phage-like element PBSX XkdK protein	Phage tail protein OS= *Brevibacillus laterosporus* OX= 1465 GN= EEL30_25335 PE= 3 SV= 1
tr|A0A0F7EFA2|A0A0F7EFA2_BRELA	48,205			Phage tail protein OS= *Brevibacillus laterosporus* OX= 1465 GN= EX87_06735 PE= 3 SV= 1
tr|A0A328QKR7|A0A328QKR7_BRELA	41,717	Flagellin protein	Flagellin protein	Flagellin protein OS= *Brevibacillus laterosporus* OX=1465 GN=C2W64_03541 PE=3 SV=1

*= Currently categorised as an obsolete entry in the Uniprot database but an equivalent version tr|A0A518VEB0|A0A518VEB0_BRELA exists.

Table 3.5 Identical proteins of *Bl* 1821L N-terminal sequenced ~48 kD putative antibacterial protein in Uniprot database

Accessions	Identical proteins	Organism	Gene name	Length
tr|A0A0F7EFA2|A0A0F7EFA2_BRELA tr|A0A518VEB0|A0A518VEB0_BRELA	Phage tail sheath protein	*Brevibacillus laterosporus* LMG 15441	BRLA_c036460	462
	Uncharacterised protein	*Brevibacillus borstelensis* GI-9	BLGI_826	445
	Phage tail sheath protein	*Brevibacillus laterosporus* SKDU 10	AYJO8_14030	445
	Phage tail sheath protein	*Brevibacillus laterosporus* (*Bacillus laterosporus*)	EEL32_11960	445
	Phage tail sheath protein	*Brevibacillus laterosporus* (*Bacillus laterosporus*)	C4A76_07870, C4A77_13935, D5F52_00915	445

3.3.8 Bioinformatic analysis of 48 kD identified putative antibacterial protein of *Bl* 1821L

Assessment of ~48 kD putative antibacterial protein with the Uniprot database uncovered that the identified accessions tr|A0A518VEB0|A0A518VEB0_BRELA and tr|A0A0F7EFA2|A0A0F7EFA2_BRELA are similar proteins, and represent a similar phage tail-sheath protein (Table 3.4). The identified phage tail-sheath protein corresponded to a phage-like element PBSX gene *xkdk* mapped between 5,137,128 bp to 5,138,462 bp (Figure 3.7). In addition to a PBSX-like *xkdK* gene, several other phage-like genes are also encoded in the region. A phage FluMu Gp47 protein, a tail protein, a prophage LambdaBa01 Xpf, and two other phage-like element PBSX proteins XkdT and XkdU also reside in the PBSX-like region of *Bl* 1821L. Various hypothetical protein encoding genes are also localised in the region where the XkdK protein is encoded in the *Bl* 1821L genome (Figure 3.7). N-acetylmuramoyl-L-alanine amidase, an endolysin, hydrolytic enzyme from phages that cleaves the cell wall during the final stage of lysis, is localised along with another lysis protein holin in the region. Located at the 3' end of the phage-like element PBSX gene *xkdK* encoding region are four (ABC transporter) permease genes *yvcR*, *yvcS*, *yvcQ*, and *yvcP* (Figure 3.7). These have been implicated in the export of lipid II-binding lantibiotics, such as nisin and gallidermin (McAuliffe et al., 2001; Smits et al., 2020).

Amino acids alignment of the ~48 kD identified accessions tr|A0A518VEB0|A0A518VEB0_BRELA and tr|A0A0F7EFA2|A0A0F7EFA2_BRELA of *Bl* 1821L with the identical proteins of the genus *Brevibacillus* (Table 3.6) and phage-like element PBSX protein XkdK of the *Bs* 168 demonstrated >89.9% amino acids

similarity among the genus *Brevibacillus* proteins. However, the queried proteins of *Bl* 1821L displayed an identity of 22.7% with the similar proteins of the *Bs* 168 (Figure 3.9 & Appendix B-5). Furthermore, the distance matrices (Figure 3.10 & Appendix B-4) and the alignment of the amino acid using the programme CLUSTALO (Appendix B-3) also substantiated the findings. The genes of the defective phage *Bs* 168 presented a low level of amino acids similarity to the queried proteins of *Bl* 1821L (Appendix B-5). Bioinformatics analysis of the phage-like element PBSX protein XkdK encoding region of *Bl* 1821L revealed a similar organisational structure of the operons (Fig 3.7).

3.3.9 BAGEL4 analysis of *Bl* 1821L and *Bl* 1951genomes

Analysis of the *Bl* 1821L and *Bl* 1951 genomes predicted seven areas of interest (AOI) relevant to the putative antibacterial activity (Appendix B-6). Notably, among the seven predicted AOI, two areas matched to the core peptides (bacteriocins) (Appendix B-6) laterosporulin and UviB of *Bl* GI-9 (Singh et al., 2012) and *Bt* serovara *israelensis* ATC35646 (Anderson et al., 2005) in both the insect pathogenic strains (Appendix B-6). BAGEL4 analysis also predicted other AOI encoding sactipeptides, lanthipeptides, and latency associated peptides (LAPs) in the *Bl* 1821L and *Bl* 1951 genomes (Appendix B-6). The predicted genomic regions of the core peptides laterosporulin and UviB of *Bl* 1821L and *Bl* 1951 along with the functional motifs are presented in the Appendices B-7 and B-12.

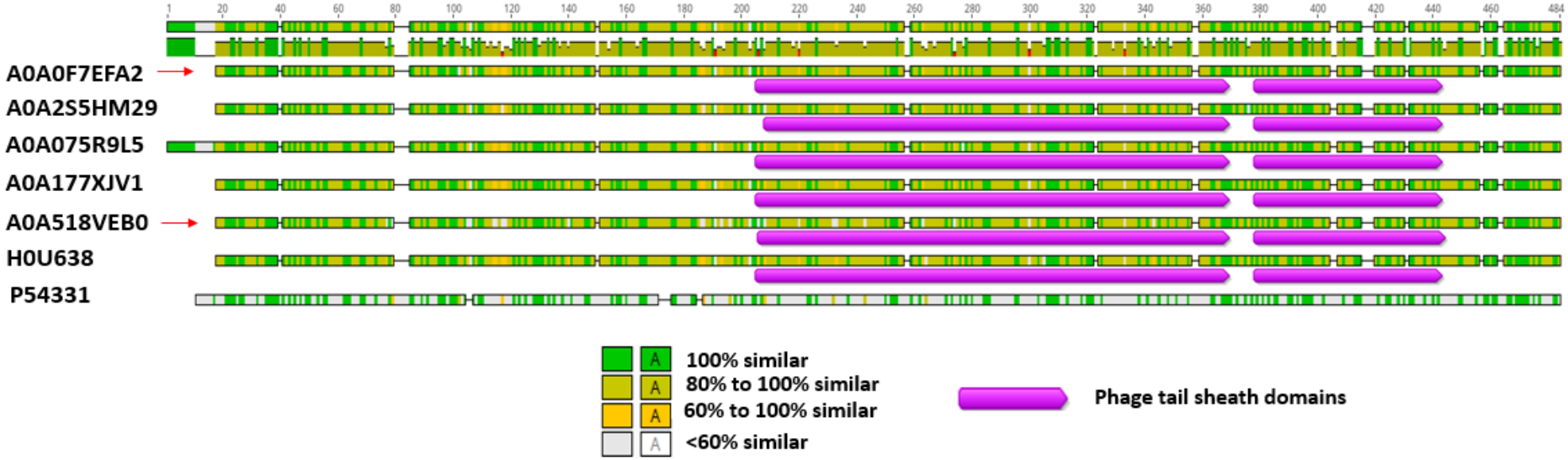

Figure 3.8 Alignment of 48 kD identified phage-like element PBSX protein XkdK accessions A0A0F7EFA2 and A0A518VEB0 (shown with red arrow) of *Bl* 1821L with the phage tail-sheath proteins of the *Bl* (A0A2S5HM29), *Brevibacillus* sp. SKDU 10 (A0A177XJV1), *Bl* LMG 15441 (A0A075R9L5), *Bl* GI-9 (H0U638), and *Bs* 168 (P54331) using the Geneious basic

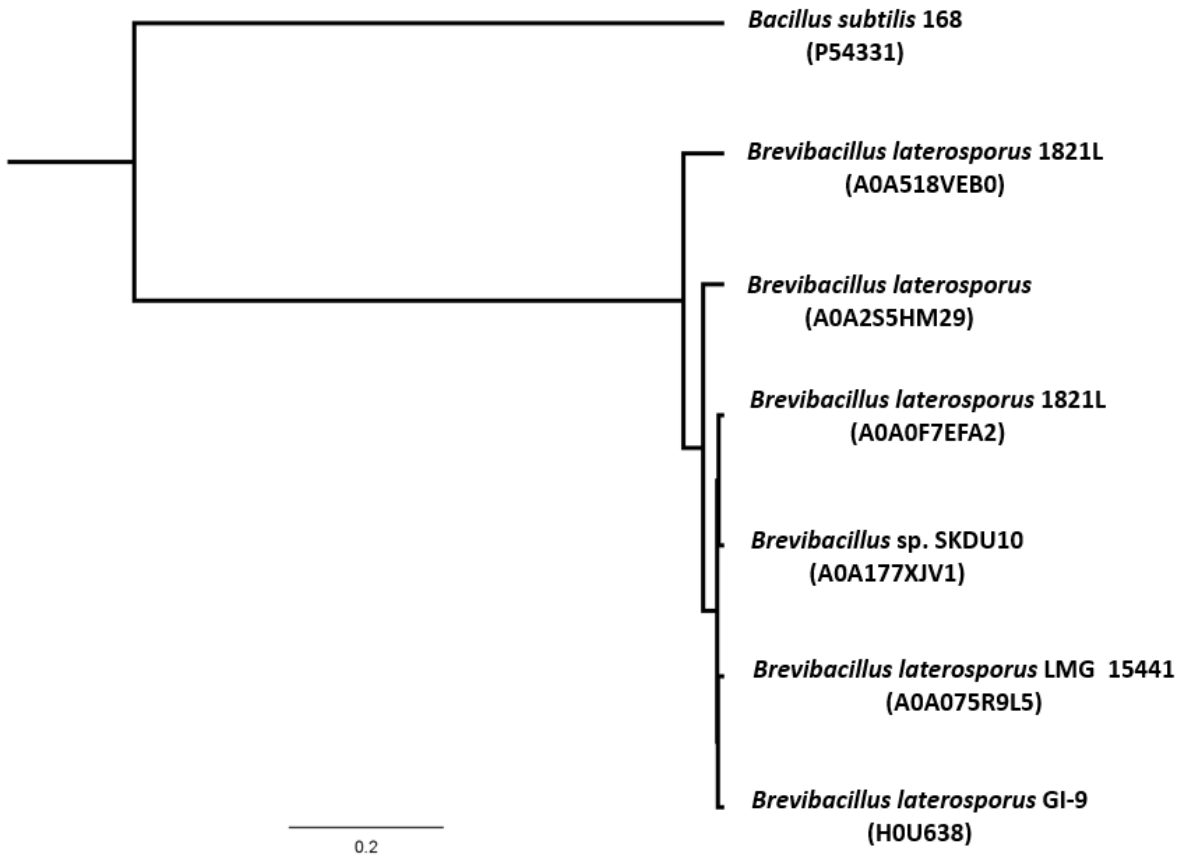

Figure 3.9 Dendrogram showing the alignment of 48 kD identified phage-like element PBSX protein XkdK of *Bl* 1821L with accessions A0A0F7EFA2 and A0A518VEB0 with the identical proteins of the genus *Brevibacillus* and the analogous protein of *Bs* 168 using Geneious basic

3.4 Discussion

Antibacterial activities of inhibitory compounds can be observed through various standard methods such as the disc diffusion assay, agar well diffusion assay, and soft agar overlay method. The disc diffusion assay and the soft agar overlay method with PEG 8000 precipitation were used to isolate and determine the antibacterial activities in the cell free supernatants of mitomycin C induced cultures of *Bl* 1951 and *Bl* 1821L. Ultrafiltration through MWCO membrane and the SDS-PAGE visualisation were employed to estimate the molecular mass (kD) of the putative antibacterial protein of *Bl* 1821L. N-terminal sequencing of ~48 kD excised band of *Bl* 1821L identified a putative antibacterial protein which was further bioinformatically analysed.

Bacteria predominantly harbour prophages in their chromosomes either in true or defective lysogenic forms (Boyd & Brüssow, 2002; Campbell, 1994; Prozorov, 1996). True lysogeny implies that the prophages of temperate phages may convert to either a lysogenic or vegetative state, while defective

lysogeny implies that the prophages cannot convert to fully functional phages because of some genetic deformation. The common products of defective phage assembly are tail parts, which attract the attention of researchers due to their killer activity against susceptible bacterial species (Boemare et al., 1992; Lee et al., 1999; Schwemmlein et al., 2018). Similar bactericidal complexes were termed "tailocin" to highlight the similarity to high molecular-weight phage tails and to avoid confusion with the low molecular-weight bacteriocins (Ghequire & De Mot, 2015). Two types of high molecular mass (>10^6 Da), phage tail-like bacteriocins, the R type and the F type, have been described from the bacterial kingdom (Michel-Briand & Baysse, 2002; Nakayama et al., 2000). Tailocins are produced intracellularly upon induction, usually of the SOS response. After intracellular assembly, the particles are released into the medium by cell lysis and can go on to kill competing target cells (Hartford & Dowds, 1992).

PBSX is a well-known induced defective phage described from *Bs* 168 (Jin et al., 2014; McDonnell & McConnell, 1994). PBSX prophage is resident in the host chromosome and is about 28 kb consisting of 38 predicted opening reading frames (ORFs) distributed between the early, middle, and late operons (Kunst et al., 1997; Moszer et al., 2002; Wood et al., 1990). The late operon encodes most of the PBSX structural and lysis genes (Wood et al., 1990). The phage particle is composed of at least 26 proteins (Mauël & Karamata, 1984b). XkdG is the main head protein, and XkdK and XkdM are the tail sheath and core proteins, respectively. XkdV is a tail fibre subunit of *Bs* 168 PBSX-like region that is involved in the killing of susceptible strains (Mauël & Karamata, 1984b; Steensma, 1981). Bioinformatic analysis of the ~48 kD identified protein of *Bl* 1821L exhibited amino acid similarities to the phage-like element PBSX protein XkdK encoded by the defective phage of *Bs* 168. Furthermore, amino acid alignment (%) and distance matrices of 48 kD putative antibacterial protein of *Bl* 1821L also showed that these proteins are distantly related but functionally alike. Numerous other genes, such as four (ABC transporter) permease genes *yvcR*, *yvcS*, *yvcQ*, and *yvcP,* also reside at the end of the phage-like bacteriocin region. These have been implicated in the export of lipid II-binding lantibiotics, such as nisin and gallidermin(McAuliffe et al., 2001; Smits et al., 2020). A search of ~48 kD phage-like element PBSX gene *xkdK* in the genome of *Bl* 1951 (RHPK01000003.1, contig 1) also indicated the presence of the *xkdK* gene along with a minority of *xkdT*, and *xkdU* like-genes of *Bs* 168. The findings manifest that the putative antibacterial phage tail-like proteins reside in the genomes of *Bl* 1821L and *Bl* 1951 (See Chapter 6; Section 6.3.7).

The disc diffusion assay was originally proposed in 1956 to test antimicrobial susceptibility (Kirby et al., 1956) but later on, it was recognised as a standardised procedure and called the "Kirby-Bauer disc diffusion test" (Bauer, 1966; Hudzicki, 2009; Kirby et al., 1956). Mitomycin C induced putative phage tail-like proteins (bacteriocins) of *Bl* 1821L (1 µg/ml) and *Bl* 1951 (3 µg/ml) and the subsequent TEM

observation in Chapter 2 (Figures 2.14 & 2.15) corroborated the release of tailocin like particles. The crude lysate harbouring phage tail-like protein (bacteriocins) from both the strains demonstrated their inhibitory activities against the producing bacteria and vice versa in the disc diffusion assay. However, the antibacterial activity was predominantly directed against the other strain with the slight difference in the diameter of zone of inhibition (mm) developed on the lawn of host bacteria (Figure 3.1). The results of the disc diffusion assay were in agreement with previous work in which the authors demonstrated the sensitivity of the producer strain, *Staphylococcus hyicus*, to its bacteriocin, hyicin 3682 (Fagundes et al., 2011).

Typically, fully functional prophages tend to undergo a round of lytic growth, resulting in plaque formation, while a substantial number of phage-like entities present in bacterial genomes only produce phage tail-like structures (Canchaya et al., 2003). Phage tail-like particles are devoid of the phage genome and can't multiply and form plaques (Hockett & Baltrus, 2017). The soft-agar overlay is the most widely utilised method to study proteinaceous antibacterial structures, especially bacteriophages and bacteriocins (Hockett & Baltrus, 2017). Gratia (1936) described this method to aid in enumerating bacteriophages but it has been used in combination with targeted genetic manipulation and PEG 8000 precipitation to distinguish among three different antimicrobial agents (a bacteriophage, a HMW bacteriocin, a LMW bacteriocin) produced by a single bacterial strain (Hockett & Baltrus, 2017; Hockett et al., 2015). Earlier work has shown that the protocol works well for *P. syringae* and would likely suffice for other gram-negative bacteria that grow vigorously under similar conditions (Hockett & Baltrus, 2017; Hockett et al., 2015; Kandel & Baltrus, 2020).

Antagonistic activities of mitomycin C induced cultures of *Bl* 1821L and *Bl* 1951 were evaluated using the soft-agar overlay after PEG 8000 precipitation. Additionally, the inhibitory activity of phages and bacteriocins was differentiated by performing a serial dilution assay test. Assay test findings were in accordance with previous work which demonstrated that performing a serial dilution on a supernatant containing bacteriophage will result in individual plaques becoming less in number with greater dilution, whereas serial dilution of a supernatant containing bacteriocin will result in a clearing zone that becomes uniformly more turbid with greater dilution (Hockett & Baltrus, 2017; Hockett et al., 2015). Furthermore, a bacteriophage will produce a clearing zone when spotted onto a fresh soft-agar overlay seeded with the same strain, whereas a bacteriocin will not produce a clearing zone when transferred to a fresh soft agar lawn, owing to the dilution of the bacteriocin (Hockett & Baltrus, 2017). Similarly, PTLBs of the gram-positive bacterium, *C. difficile*, after mitomycin C induction, were assayed for their inhibitory activities using the soft-agar overlay after PEG 8000 precipitation and the successive TEM analysis confirmed their presence (Hegarty et al., 2016).

PEG 8000 precipitated cultures of *Bl* 1821L and *Bl* 1951 did not provide any clue of the autocidal activity of the producer strains but significant activity can be seen in the disc assay tests which might be due to the use of a higher volume of cell free supernatants (Zou et al., 2018b).

Tailocins or PTLBs are bactericidal structures (Scholl & Martin, 2008). A critical feature of tailocins is their ability to recognise and bind cell receptors specific to their host. Tailocins specificity is conferred by receptors on the cell surface of the susceptible bacterium and RBPs on tailocin tail fibres (Carim et al., 2021; Scholl, 2017). Different bacterial surface components act as the receptors for phages and PTLBs, including flagella (Merino et al., 1990), pili (Waldor & Mekalanos, 1996), outer membrane proteins such as OmpA and OmpC (Morona & Henning, 1984), and lipopolysaccharides (LPS) (Köhler et al., 2010). Since the majority of R-type tailocin gene clusters contain only one tail fibre gene they have a narrow host range. However, recently up to three tail fibre genes and wide host range tailocins have been reported for plant-associated *Pseudomonas* strains (Patz et al., 2019).

Antibacterial spectrum analysis of *Bl* 1821L PEG 8000 precipitated cultures may favour a broad spectrum of action while a narrow killing activity for *Bl* 1951. *Bl* 1821L PEG 8000 precipitated cultures demonstrated their salient killing activity against all the indicator strains of the genus *Brevibacillus* except *Bl* CCEB 342, but this strain was susceptible to the PEG 8000 precipitated culture of *Bl* 1951. In addition, another gram-positive bacterium, *C. maltaromaticum* 3-1, was sensitive to *Bl* 1821L and insensitive to *Bl* 1951 precipitated cultures. No prominent activity of *Bl* 1821L and *Bl* 1951 PEG 8000 precipitated cultures was noticed against the other indicator gram-positive bacterial strains. *Brevibacillus* strains and other gram-positive bacteria sensitivity to the induced phage tail-like proteins (bacteriocins) of *Bl* 1821L and *Bl* 1951 indicate that these may share similar receptor-binding proteins. Defective phage PBP180 *o*f *Bacillus pumilus* (*Bp*) AB94180 was isolated, characterised, and compared for its antibacterial spectrum with those of PBSX, PBSZ, and PBSX4 from *Bs* 168, *Bs* W23, and *Bp* AB94044 (Jin et al., 2014). The authors showed that none of the defective phages attacked their host strains, and the killing range and degree of killing activity against the same susceptible strain of the three defective phages were different. PBSX only had killing activity against *Bs* W23. PBSZ could attack both *Bp* AB94044 and AB94180. PBP180 not only had a high level of killing activity against *Bs* W23 and *Bp* AB94044 but also displayed a medium degree of ability to attack *Bs* 168, indicating that PBP180 and PBSX possess different killing ranges. Moreover, PBSX4 possessed a low level of killing activity against *Bs* 168 and *Bs* W23 but did not attack *Bp* AB94180, suggesting that the killing spectra of PBP180 can be distinguished from that of PBSX4, even though both derived from *Bp* (Jin et al., 2014).

Previously, the antibacterial activity of R-type pyocins against other bacteria like *Campylobacter* sp. (Blackwell et al., 1982), *Haemophilus influenzae* (Phillips et al., 1990), *Haemophilus ducreyi*

(Campagnari et al., 1994; Filiatrault et al., 2001), *Neisseria gonorrhoeae* (Levin & Stein, 1996), and *Neisseria meningitidis* (Morse et al., 1976) was attributed to the common receptor sites on *P. aeruginosa* (Connelly & Allen, 1983; Filiatrault et al., 2001). The role of receptor-binding proteins in defining the inhibitory spectrum of antibacterial structures (bacteriophages, PTLBs) has been investigated by swapping their RBPs (Dams et al., 2019). R-type tailocins target recognition mechanisms have been largely analysed from *P. aeruginosa* and *B. cenocepacia*: Tailocin fibre genes encode RBPs at their C-terminus that bind to specific bacterial surface components, which are very often lipopolysaccharide residues (Buth et al., 2018; Köhler et al., 2010). Antibacterial spectra of *P. aeruginosa* have been modified by altering the RBPs of the pyocins (Williams et al., 2008). R-type tailocins were engineered (Scholl et al., 2009; Scholl et al., 2012) to extend their host range by replacing the C-terminal domain of the tailocin tail fibre (Ghequire & De Mot, 2015; Williams et al., 2008). For example, the engineering of receptor-binding proteins of F-type tailocin (Monocin) of *L. monocytogenes* altered its killing spectrum (Lee et al., 2016). R-type tailocins derived from the gram-positive bacterium, *C. difficile*, were termed "Diffocins" (Gebhart et al., 2012). The induced particles after purification from different strains indicated a different spectrum, with no single bacteriocin killing all tested *C. difficile* isolates (Gebhart et al., 2012). The authors identified the putative receptor-recognising, spectrum-determining protein for diffocins by showing that switching this one protein (200 kD) switches the bactericidal specificity of the diffocin (Gebhart et al., 2012).

Antimicrobial peptides and lipopeptides with broad-spectrum activity have been isolated and characterised from *Bl* strains (Desjardine et al., 2007; Singh et al., 2012; Zhao et al., 2012b). Laterosporulin produced by *Bl* GI-9 displayed a wide range of antibacterial activity through membrane permeabilisation (Carrillo et al., 2003; Singh et al., 2012). More recently, laterosporulin 10, produced by *Bl* SKDU 10, was characterised and considered similar to laterosporulin but it showed only 57.6% amino acids identity (Baindara et al., 2016b). Though the biosynthetic cluster of former bacteriocin contained identical transcriptional regulators, ABC transporter, and a dehydrogenase gene as observed in the latter, it contained a higher number of cationic amino acids. Laterosporulin 10 limited its inhibitory action to gram-positive bacteria due to the differences in the composition of amino acids (Baindara et al., 2016a).

3.5 Outcomes

The major findings of this chapter are;

1. N-terminal sequence analysis of a prominent band (~48 kD) of the *Bl* 1821L identified a phage tail-like protein which is typically antibacterial in nature. Bioinformatic analysis of antibacterial protein exhibited a genetic organisation similar to the PBSX-like defective prophage of *Bs* 168 (to be further explored in Chapter 6).
2. *Bl* 1821L putative antibacterial gene upon its search in the *Bl* 1951 genome showed the presence of several *xkdK*, *xkdT*, and *xkdU* genes of PBSX-like region of *Bs* 168.
3. Autocidal activity of the mitomycin C induced cultures of *Bl* 1821L and *Bl* 1951 was observed in the disc diffusion assay.
4. Antibacterial spectrum of mitomycin C induced cultures of *Bl* 1821L and *Bl* 1951 after PEG 8000 precipitation was reported. *Bl* 1821L exhibited a broad spectrum while *Bl* 1951 indicated a narrow spectrum of activity.
5. BAGEL4 analysis predicted the presence of some antibacterial motifs in the genomes of both *Bl* 1821L and *Bl* 1951.

3.6 Conclusion

Based on the present findings and the electron micrographs presented in the previous chapter, it is likely that the inherent activity of *Bl* 1821L antibacterial protein (~48 kD) is due to the phage tail-like bacteriocins which possibly have a detrimental effect on the growth of the insect pathogenic strains *Bl* 1821L and *Bl* 1951.

Chapter 4
Biochemical characterisation and production kinetics of putative antibacterial proteins of New Zealand *Brevibacillus laterosporus* strains *Bl* 1821L and *Bl* 1951

4.1 Introduction

N-terminal sequencing and the bioinformatic analysis of a putative antibacterial protein of *Bl* 1821L in the previous chapter revealed the presence of phage tail-like bacteriocins. The subsequent microbial assay tests further confirmed their nature by defining the antimicrobial spectrum and differentiating the phage tail-like bacteriocins from bacteriophages.

Ribosomally synthesised antimicrobial substances, bacteriocins, can be structurally linear or globular, and the arrangement of the amino acids sequence and formation determine their bactericidal activity, sensitivity towards enzymes, solubility, and stability at different pH and temperatures (Herzner et al., 2011; Sandiford, 2015). Therefore, bacteriocins can be subjected to a battery of biochemical characterisation assays.

Bacteriocins are proteinaceous in nature. This distinctive feature can be confirmed by testing their sensitivity to proteolytic enzymes such as chymotrypsin, pepsin, proteinase K, and trypsin and non-proteolytic enzymes such as a-amylase and catalase (Oh et al., 2000). The susceptibility of the bacteriocins to certain enzymes depends mainly on the peptide formation and amino acid sequence. Interestingly, their degree of degradation caused by different proteolytic enzymes also varies according to their amino acid composition and the bacteriocins can be partially susceptible to proteolytic enzymes (Lajis, 2020).

Prokaryotes, especially bacteria, are dependent upon the pH of their abode as very high or very low pH is not suitable for their growth and bacteriocin production may be due to the neutrophilic behaviour of the producer strain. Therefore, it is important to consider the pH of the origin of isolation (Lajis, 2020). pH directly affects the enzymatic activity of microorganisms and consequently cell growth rates and production of several metabolites, including bacteriocins (Aasen et al., 2000; Mataragas et al., 2002). Sometimes, the effect of pH on bacteriocins stability is insignificant due to their stability over a wide pH range. However, unfavourable pH conditions could reduce cell viability by disrupting the integrity of the plasma membrane. This phenomenon is attributed to the prevalence of excessive H^+ (due to pH) that weakens the membrane permeability barrier, perturbs the membrane lipid bilayers, thus causing leakage of some cellular components, and the dissipation of the electrostatic of the plasma membrane (Dominguez et al., 2007; Lee et al., 2001).

Bacteriocins are mostly heat resistant, but the optimal temperature for the highest antimicrobial activity varies depending on the species (Lajis, 2020). Typically, the optimum temperature of the bacterium allows rapid cell proliferation and enhances the synthesis of important enzymes and proteins (e.g. lanthipeptide peptidase and oxidoreductase) which catalyse the biosynthesis or modification of biologically active bacteriocins (Fickers et al., 2008).

Bacteriocinogenic strains tend to produce antimicrobial peptides during their late growth phase (Kumar et al., 2012b). Bacteriocin production, however, can be a highly regulated process, with strains requiring specific conditions and environments to induce the production of these antimicrobials (Diep et al., 2000; Maldonado-Barragán et al., 2013). These proteinaceous metabolites are synthesised by a wide variety of pathways, and both the specific genetic makeup of the producing strains and different environmental conditions can affect their activity (Ak et al., 2019; Arul Jose et al., 2013). Numerous fermentation parameters, such as incubation time, temperature, pH, aeration, and nutrient sources can influence their production in microbial systems (Turgis et al., 2016; Zhou et al., 2015).

The current study was initiated to determine biochemical features such as the proteinaceous nature and stability of crude putative antibacterial proteins (bacteriocins) of *Bl* 1821L and *Bl* 1951 at varied pH and temperatures. The production kinetics of putative antibacterial proteins (bacteriocins) of *Bl* 1821L and *Bl* 1951 at various time intervals under normal cultivating conditions was also determined.

4.2 Methods

4.2.1 Effect of enzymes on the activity of crude putative antibacterial proteins of *Bl* 1821L and *Bl* 1951

Mitomycin C (Sigma) induced culture of *Bl* 1821L was centrifuged @ 16,000 g for 10 min at 4^{o}C and the supernatant was filtered through a 0.22 µm filter. Cell free supernatant (CFS) was treated with three enzymes, viz. catalase (Sigma-Aldrich), protease (Sigma-Aldrich), and proteinase K (Sigma-Aldrich) to evaluate their effect on the activity of crude putative antibacterial proteins (bacteriocins). Enzymes, catalase (Sigma-Aldrich) and protease (Sigma-Aldrich) were prepared by dissolving in 10 mM sodium phosphate buffer and the solutions were added to the filtered supernatant of LB broth to a final concentration of 1 mg/ml. The preparations were then placed in an incubator at 30^{o}C for 6 hours followed by heating for 5 min at 85^{o}C to terminate the enzymatic activity. For the control treatment, CFS and buffer without enzymes were used.

Antibacterial activity of *Bl* 1821L crude lysate containing the phage tail-like bacteriocins was determined through the Kirby-Bauer disc diffusion assay (Bauer, 1966; Hudzicki, 2009) as outlined in

Chapter 3 (Section 3.2.1). Antibacterial activity of crude lysate of *Bl* 1821L treated with and without enzymes was examined by measuring the diameter of the zone of inhibition (including the diameter of the disc) in mm. Disc diffusion assays were performed with three technical replicates.

For determining the effect of enzymes on the activity of crude putative antibacterial proteins (bacteriocins) of *Bl* 1951 against *Bl* 1821L as the host bacterium, the same protocol as described above for crude *Bl* 1821L putative antibacterial proteins was used.

4.2.2 Effect of temperature on the activity of crude putative antibacterial proteins of *Bl* 1821L and *Bl* 1951

Mitomycin C (Sigma) induced culture of *Bl* 1821L was centrifuged @ 16,000 g for 10 min at 4°C and the supernatant was filtered through a 0.22 µm filter. Thermal stability of crude lysate of *Bl* 1821L harbouring the phage tail-like bacteriocins was evaluated by treating the filtered supernatant at 70°C, 80°C, 90°C, and 100°C for 60 min. The activity of crude putative antibacterial proteins (bacteriocins) of *Bl* 1821L was also evaluated after autoclaving at 121°C for 15 min. The samples were immediately chilled on ice after heating and assayed for activity through the Kirby-Bauer disc diffusion assay against *Bl* 1951 as the host bacterium according to the protocol described in Chapter 3 (Section 3.2.1). Aliquots (1 ml) of cell free supernatant were also exposed to 4°C and -20°C for 30 days to determine their stability in storage. Mitomycin C (Sigma) induced *Bl* 1821L filtered supernatant without heating served as a control.

Similarly to the *Bl* 1821L the effect of various temperatures on the activity of crude putative antibacterial proteins (bacteriocins) of *Bl* 1951 against *Bl* 1821L as the host bacterium was determined using the same protocol as outlined above for assessment of crude putative antibacterial proteins of *Bl* 1821L.

4.2.3 Effect of pH on the activity of crude putative antibacterial proteins of *Bl* 1821L and *Bl* 1951

To determine the effect of pH on the activity of crude lysate of *Bl* 1821L harbouring phage tail-like bacteriocins, the pH of cell free supernatant was set to 2, 4, 6, 8, 10, and 12 using either 1M HCL or 1M NaOH. The residual activity of all pH treated samples was tested through the Kirby-Bauer disc diffusion assay against *Bl* 1951 as the host bacterium according to the protocol described in Chapter 3 (Section 3.2.1). Mitomycin C (Sigma) induced *Bl* 1821L filtered supernatant without any alteration of pH served as a control.

Similarly to the *Bl* 1821L the activity of crude putative antibacterial proteins (bacteriocins) of *Bl* 1951 against *Bl* 1821L as the host bacterium was determined using the same protocol as described above for assessment of crude putative antibacterial proteins of *Bl* 1821L.

4.2.4 Production kinetics of putative antibacterial proteins of *Bl* 1821L and *Bl* 1951

Bl 1821L culture preserved (-80^{o}C) in glycerol at the Bio-Protection Research Centre (BPRC), New Zealand was streaked on an LB agar plate to cultivate a primary culture. An LB agar plate was further streaked from a colony of *Bl* 1821L primary culture to obtain a secondary culture. A single colony of the secondary culture was picked from *Bl* 1821L to inoculate 5 ml of sterile LB broth in a universal vial. *Bl* 1821L inoculated vials were placed on an orbital shaker (Conco, TU 4540, Taiwan) overnight at 30^{o}C and 250 rpm. One ml of an overnight culture of the host bacterium *Bl* 1821L was transferred into 25 ml LB broth in 250 ml flasks and placed on the shaker @ 250 rpm and 30^{o}C. Two separate flasks were used for each treatment which were taken out for assessment at the following time intervals 3, 6, 12, 18, 24, 36, 48, 60, 72, 96, 120, 144, 168, 192, 216, and 240 hours. At each time point, a sample of 1 ml was drawn from each treatment to prepare tenfold serial dilutions (10^{-1} to 10^{-6}). One hundred µl of each dilution was transferred onto an LB agar plate and spread with the help of a hockey stick, then left to dry. Two replicate LB agar plates were inoculated with the drawn sample and kept in an incubator at 30^{o}C. *Bl* 1821L colonies were counted with the help of a colony counter (Stuart, UK) after 2-3 days of spreading and converted into CFU/ml.

Bl 1821L cultures were centrifuged at 16,000 g for 10 min at 4^{o}C and the supernatants were filtered through a 0.22 µm filter. The pH of *Bl* 1821L cell free supernatants extracted at each interval was recorded with a pH meter (Orion star A211, Thermofisher).

Antibacterial activity of each time interval filtered supernatant of *Bl* 1821L was tested against *Bl* 1821L and *Bl* 1951 as the host bacterium through the Kirby-Bauer disc diffusion assay as described in Chapter 3 (Section 3.2.1). *Bl* 1821L produced bacteriocins antagonistic activity against indicator strains were examined by measuring the diameter of the zone of inhibition (including the diameter of the disc) in mm.

Three independent experiments (biological replications) were performed and data of assessed parameters, CFU/ml, pH of cell free supernatants, and diameter of lysis zones (mm) of all the experiments were pooled. CFU/ml of each experiment was converted into $\log_{10}$ CFU/ml. The cumulative data was statistically analysed using ANOVA (Analysis of Variance) through the programme Genstat (20th edition).

Likewise, the production kinetics of putative antibacterial proteins (bacteriocins) of *Bl* 1951 during the course of its host bacterium growth was determined as described for the putative antibacterial proteins of *Bl* 1821L. Various parameters, including CFU/ml, pH of cell free supernatants, and antagonistic activity of *Bl* 1951 produced bacteriocins against *Bl* 1951 and *Bl* 1821L as the host bacterium were also studied as mentioned above for *Bl* 1821L.

4.2.5 SDS-PAGE analysis of spontaneously produced putative antibacterial proteins of *Bl* 1821L and *Bl* 1951

SDS-PAGE analysis of *Bl* 1821L and *Bl* 1951 spontaneously produced putative antibacterial proteins (bacteriocins) at various time intervals was performed according to the protocol described in Chapter 3 (Section 3.2.6) (Jones & Hurst, 2016; Laemmli, 1970) after high-speed centrifugation @ 35,000 rpm (151263 x g) for 70 min at 4^{o}C. RAMA staining (Yasumitsu et al., 2010), as described in Chapter 3 (Section 3.2.6), was used to stain the gels. Mitomycin C (Sigma) induced cultures of *Bl* 1821L and *Bl* 1951 were used as a control to compare with the spontaneously induced putative antibacterial proteins (bacteriocins).

To preserve the stained gel, one piece of cellophane sheet was wetted and spread on a wet surface so that the gel could be placed on it, which was then sealed with another piece of cellophane sheet. Finally, the stained gel inside the cellophane sheet was fixed in a frame with the help of clip binders and the excess water was removed through a hole.

4.3 Results

4.3.1 Effect of enzymes on the activity of crude putative antibacterial proteins of *Bl* 1821L against *Bl* 1951 as host bacterium

Crude *Bl* 1821L filtered supernatants that contained the phage tail-like bacteriocins after treatment with the proteolytic enzymes (proteinase k & protease) lost their inhibitory activity, which proved their proteinaceous nature (Table 4.1). Catalase treatment of the mitomycin C induced culture of *Bl* 1821L did not affect the antimicrobial activity, demonstrating that the developed lysis zones on the lawns of the host bacterium were not due to the action of hydrogen peroxide (H_2O_2). The crude supernatant harbouring the putative phage tail-like bacteriocin of *Bl* 1821L in the control treatment (without enzymes) maintained the antagonistic activity (Table 4.1).

Table 4.1 Effect of enzymes on the activity of crude supernatant of *Bl* 1821L harbouring phage tail-like bacteriocins against *Bl* 1951 as the host bacterium

Enzymes	Zone of Inhibition
Proteinase-K	-
Protease	-
Catalase	+
Control (Mitomycin C)	+

4.3.2 Effect of pH on the activity of crude putative antibacterial proteins of *Bl* 1821L against *Bl* 1951 as host bacterium

Antibacterial activity of crude *Bl* 1821L supernatant harbouring phage tail-like bacteriocins against *Bl* 1951 persisted at all the evaluated pH levels except at pH 12. No zone of inhibition was observed at pH 12 (Table 4.2 & Figure 4.1).

Table 4.2 Effect of pH on the activity of crude supernatant of *Bl* 1821L harbouring phage tail-like bacteriocins against *Bl* 1951 as the host bacterium

pH	Zone of inhibition diameter (mm)
2	11.3
4	11.0
6	11.7
8	11.7
10	11.7
12	-*
Control (Mitomycin C)	15.0

*- = No zone of inhibition

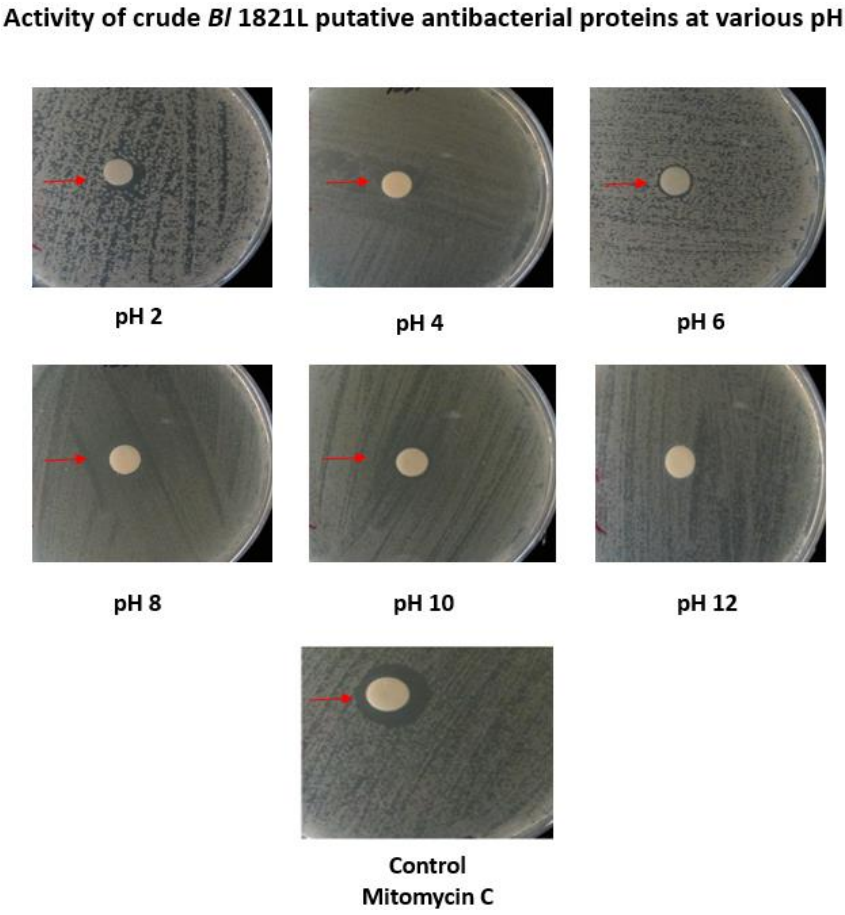

Figure 4.1 Effect of pH on the activity of crude supernatant of *Bl* 1821L harbouring phage tail-like bacteriocins against *Bl* 1951 as the host bacterium (shown with red arrow)

4.3.3 Effect of temperature on the activity of crude putative antibacterial proteins of *Bl* 1821L against *Bl* 1951 as host bacterium

The crude supernatant of *Bl* 1821L harbouring the phage tail-like bacteriocin extracted after mitomycin C induction retained thermal stability in all the treatments except at 100°C and 121°C where no zones of inhibition were observed. However, after 70°C a gradual decrease in activity was noted (Table 4.3 & Figure 4.2). The putative antibacterial proteins (bacteriocins) of *Bl* 1821L kept at 4°C and -20°C for 30 days sustained their inhibitory action against *Bl* 1951 as the host bacterium. However, the exposure to -20°C reduced the activity of crude supernatant of *Bl* 1821L.

Table 4.3 Effect of temperature on the activity of crude supernatant harbouring *Bl* 1821L phage tail-like bacteriocins against *Bl* 1951 as the host bacterium

Temperature (°C)	Zone of inhibition diameter (mm)
70	15.0
80	14.0
90	11.7
100	-*
121	-
Control (Mitomycin C)	15.7

*- = No zone of inhibition

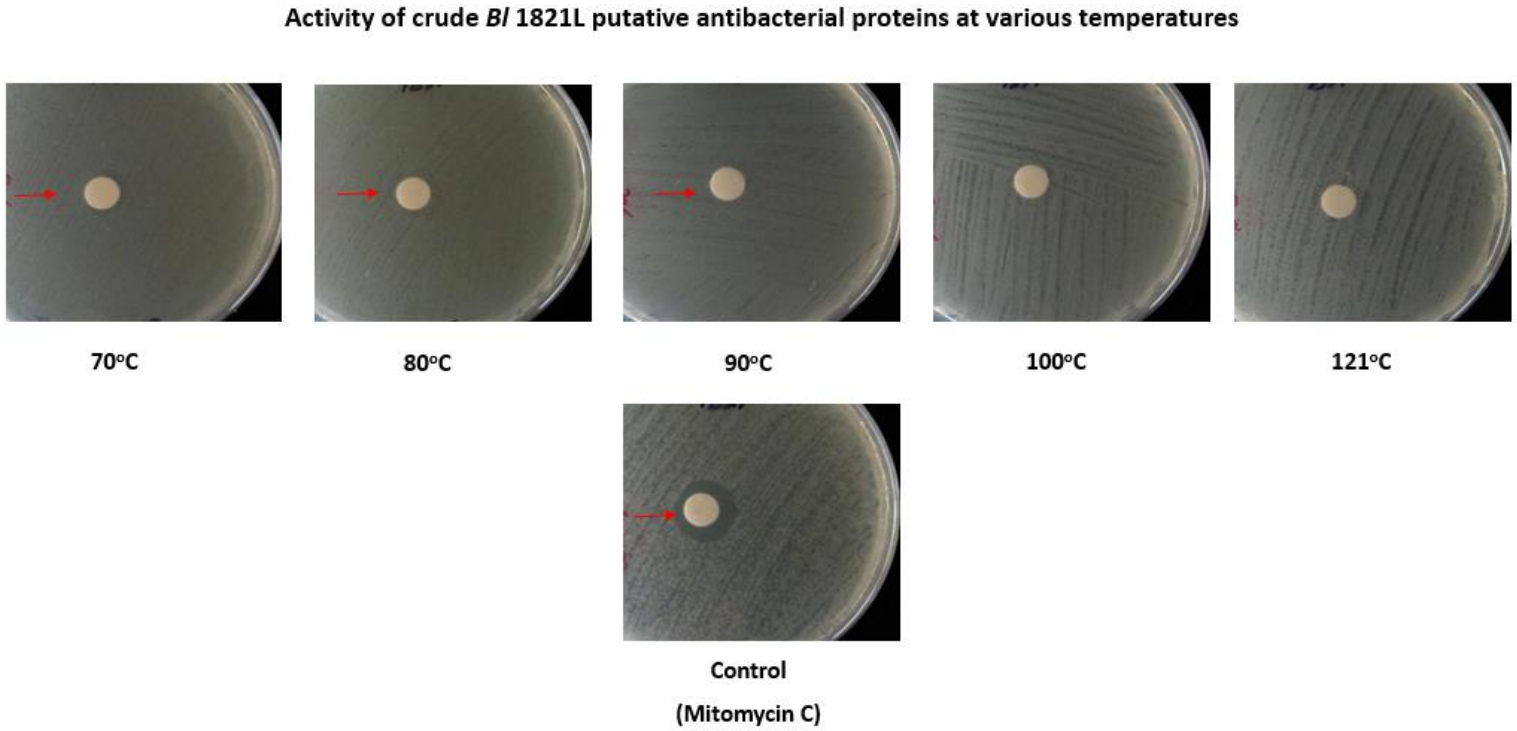

Figure 4.2 Effect of temperature on the activity of crude lysate of *Bl* 1821L harbouring the phage tail-like bacteriocins against the *Bl* 1951 as host bacterium (shown with red arrow)

4.3.4 Production kinetics of putative antibacterial proteins of *Bl* 1821L

For the production kinetics of putative antibacterial proteins (bacteriocins) of *Bl* 1821L at various time intervals during the growth, three independent replicates of experiment were performed assessing the parameters of CFU/ml, pH of filtered supernatants, and antagonistic activity of *Bl* 1821L putative antibacterial proteins (bacteriocins) against *Bl* 1821L and *Bl* 1951. To ensure a more precise representation of the number of viable cells (CFU/ml) recorded values were converted into $\log_{10}$ CFU/ml (Appendix C-1 & Figure 4.3). The results of all the experiments are included in Appendices C-2 to C-4 and the mean values of results ($\log_{10}$ CFU/ml) are presented in Figure 4.4.

Antibacterial activity of crude supernatants of *Bl* 1821L harbouring the putative phage tail-like bacteriocins against itself initiated after three hours of inoculation as indicated by a small lysis zone (11.3 mm) but CFS of 36 hours showed the highest inhibitory activity (13.7 mm) (Table 4.4). The number of viable cells started to decline gradually and after 18 hours a dip was observed. CFS extracted at this time interval (18 hours) produced a lysis zone of 13.2 mm against its own lawn (Table 4.4 & Figure 4.5). Although a dip in colony forming units ($\log_{10}$ CFU/ml) was noticed at 18 hours, it was not statistically significant when compared to 12 hours and 36 hours of growth respectively (Figure 4.4). CFS of 36 hours produced the highest halo zone of 13.7 mm on the lawns of producer strain (*Bl* 1821L) but when compared to the activity of 18 hours CFS statistically no significant difference was found in the results (Table 4.4 & Figure 4.5). pH of *Bl* 1821L filtered supernatants varied from 7.04 to 9.47 and it steadily increased up to 60 hours but the point (18 hours) where $\log_{10}$ CFU/ml demonstrated a fall indicated a significant change in pH value as compared to the pHs of 12 hours and 36 hours CFS respectively (Table 4.4).

Bl 1821L supernatants extracted after 60 hours and 72 hours exhibited the highest antagonistic activity against *Bl* 1951, producing a zone of inhibition of 15.7 mm and 15.4 mm respectively (Table 4.4 & Figure 4.6). This was the point where $\log_{10}$ CFU/ml values began to decline at an insignificant difference (statistically). Assessments of antibiotic discs with LB broth serving as a control demonstrated no antagonistic activity (Figure 4.6). However, pH of *Bl* 1821L filtered supernatants of both the time intervals statistically did not differ from each other (Table 4.4).

Table 4.4 Production kinetics of *Bl* 1821L spontaneously induced putative antibacterial proteins (bacteriocins) at various time intervals and assay test of crude cell free supernatant (CFS) harbouring *Bl* 1821L PTLBs against *Bl* 1821L and *Bl* 1951 as the host bacterium

Time interval (Hours)	log_{10} CFU/ml	pH of CFS	Zone of inhibition diameter (mm)	
			Bl 1821L as the host bacterium	*Bl* 1951 as the host bacterium
3	5.576	7.06	11.33	10.78
6	5.518	7.04	11.67	11.67
12	5.304	8.01	13.33	14.33
18	4.960	8.35	13.22	15.22
24	5.280	8.69	13.11	15.22
36	5.384	9.12	13.67	15.33
48	5.796	9.26	12.33	13.78
60	5.995	9.37	13.00	15.67
72	5.859	9.31	12.78	15.44
96	5.626	9.42	11.67	13.89
120	5.929	9.47	12.11	13.45
144	6.166	9.33	12.56	12.78
168	6.138	9.32	13.11	12.56
192	6.440	9.32	12.56	12.22
216	6.243	9.40	12.89	11.44
240	6.241	9.39	11.67	12.22
*LSD (5%)	0.636	0.317	2.221	1.922

*LSD= Least significant difference

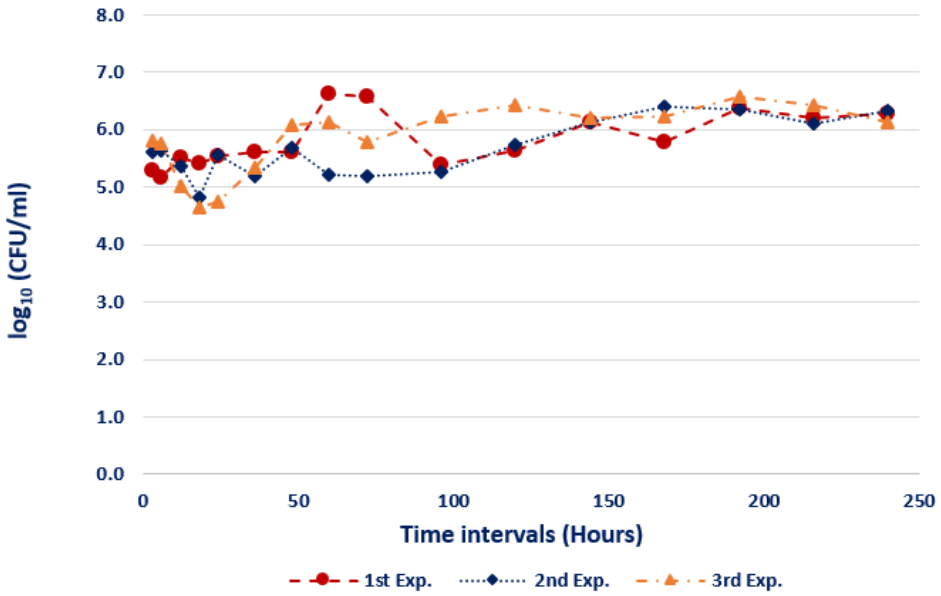

Figure 4.3 *Bl* 1821L cells growth (log_{10} CFU/ml) at various time intervals of all the experiments, grown at 30°C

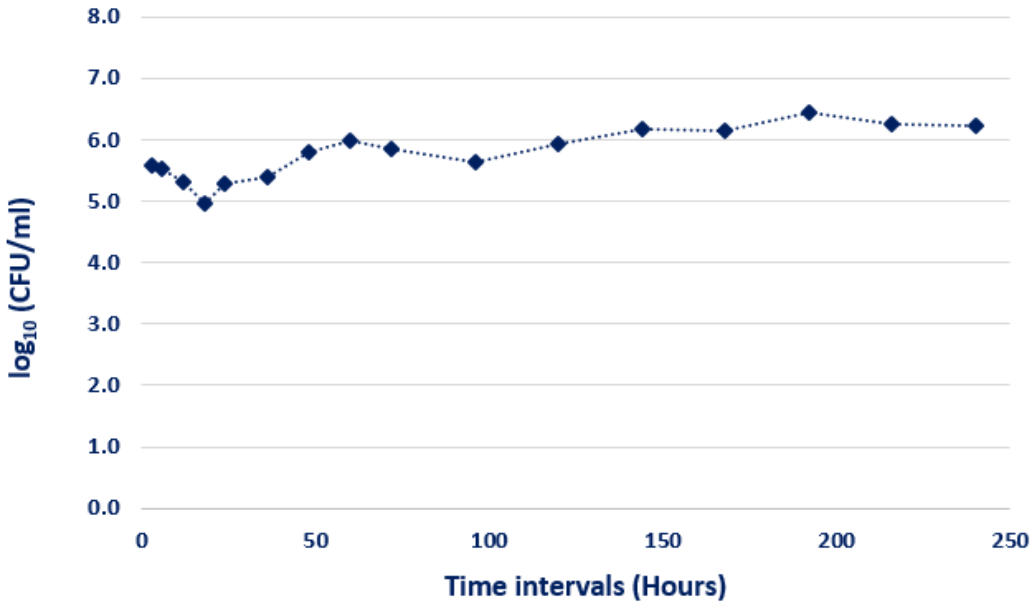

Figure 4.4 Mean values of *Bl* 1821L cells growth (log_{10} CFU/ml) at various time intervals, retrieved from the pooled data of Figure 4.3

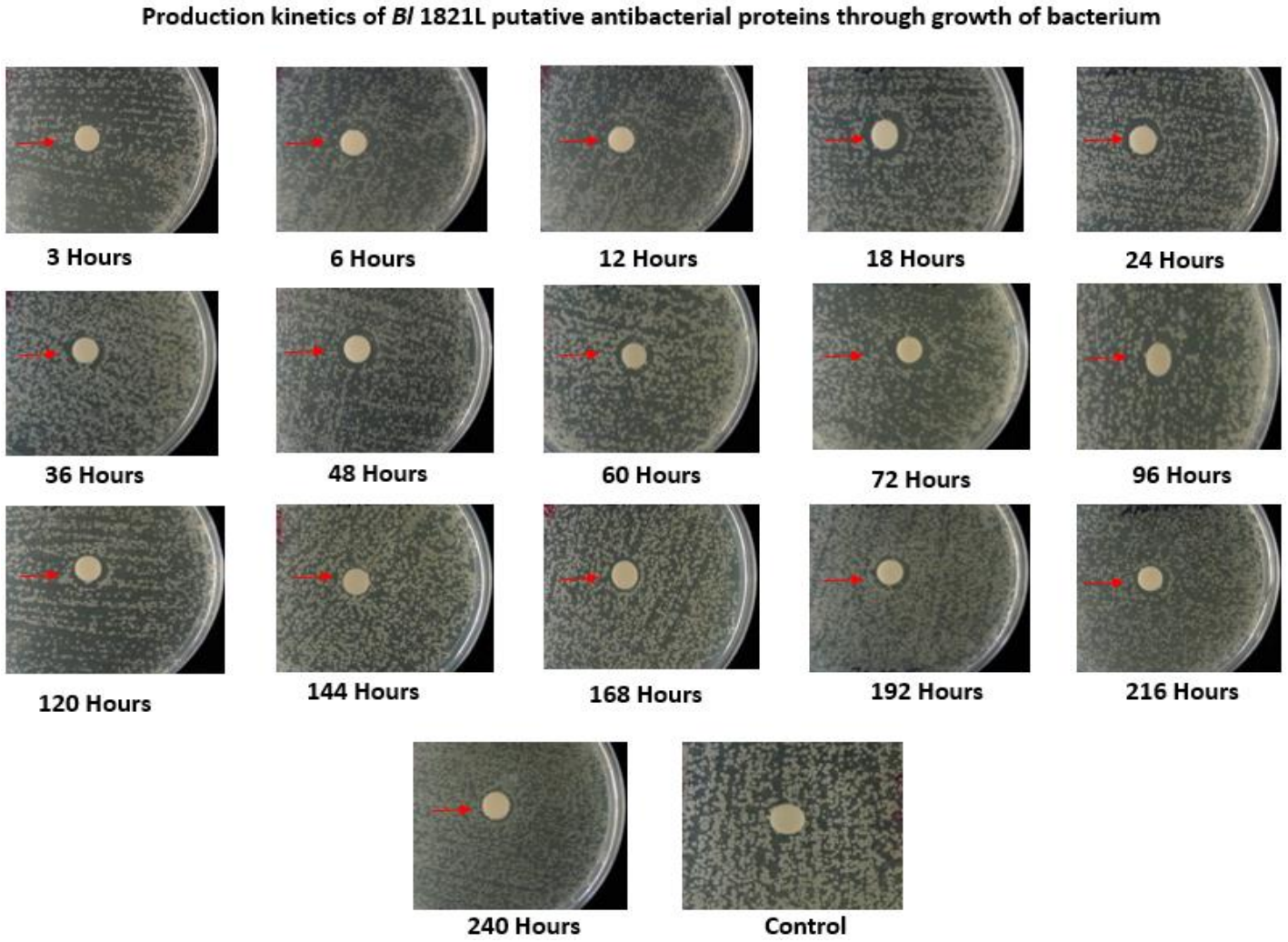

Figure 4.5 Antibacterial activity of spontaneously induced putative antibacterial proteins CFS harbouring the phage tail-like bacteriocins of *Bl* 1821L against *Bl* 1821L as the host bacterium at various time intervals during the course of its growth (shown with red arrow)

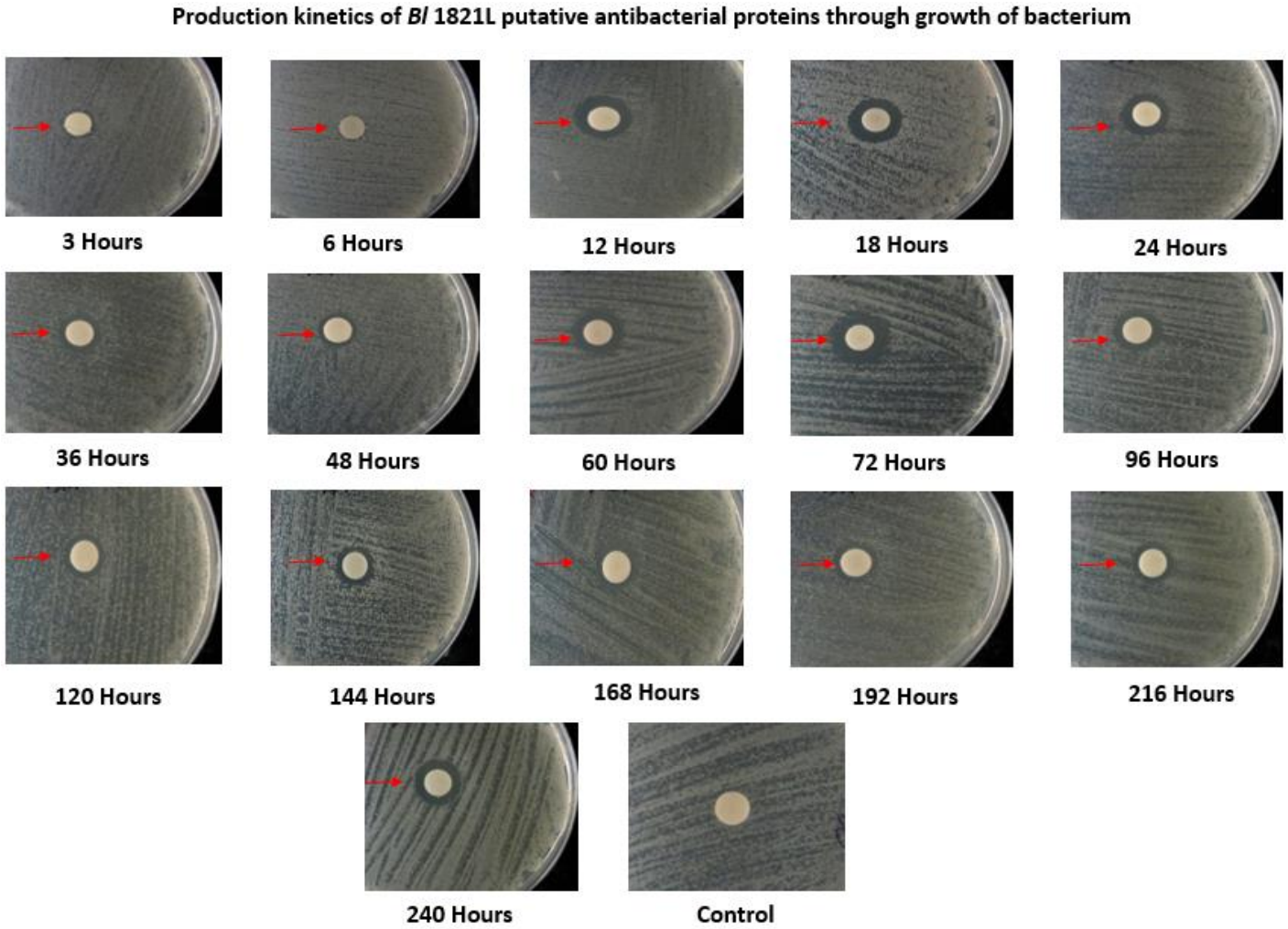

Figure 4.6 Antibacterial activity of spontaneously induced putative antibacterial proteins CFS harbouring the phage tail-like bacteriocins of *Bl* 1821L against *Bl* 1951 as the host bacterium at various time intervals during the course of its growth (shown with red arrow)

4.3.5 SDS-PAGE analysis of spontaneously induced putative antibacterial proteins of *Bl* 1821L

SDS-PAGE analysis indicated no protein bands in the initial 3-6 hours of *Bl* 1821L growth (Figure 4.7A) which is in agreement with the CFS assay test results of the same time intervals where very narrow zones of inhibition were measured (Table 4.4 & Figures 4.5-4.6). However, between 12 hours to 240 hours of growth a protein of ~48 kD, which was previously shown (Chapter 3) to represent a phage tail-like bacteriocin (Figure 3.6B), was visible on SDS-PAGE, but with a thinner band than in the mitomycin C induced cultures (Figures 4.7A-B).

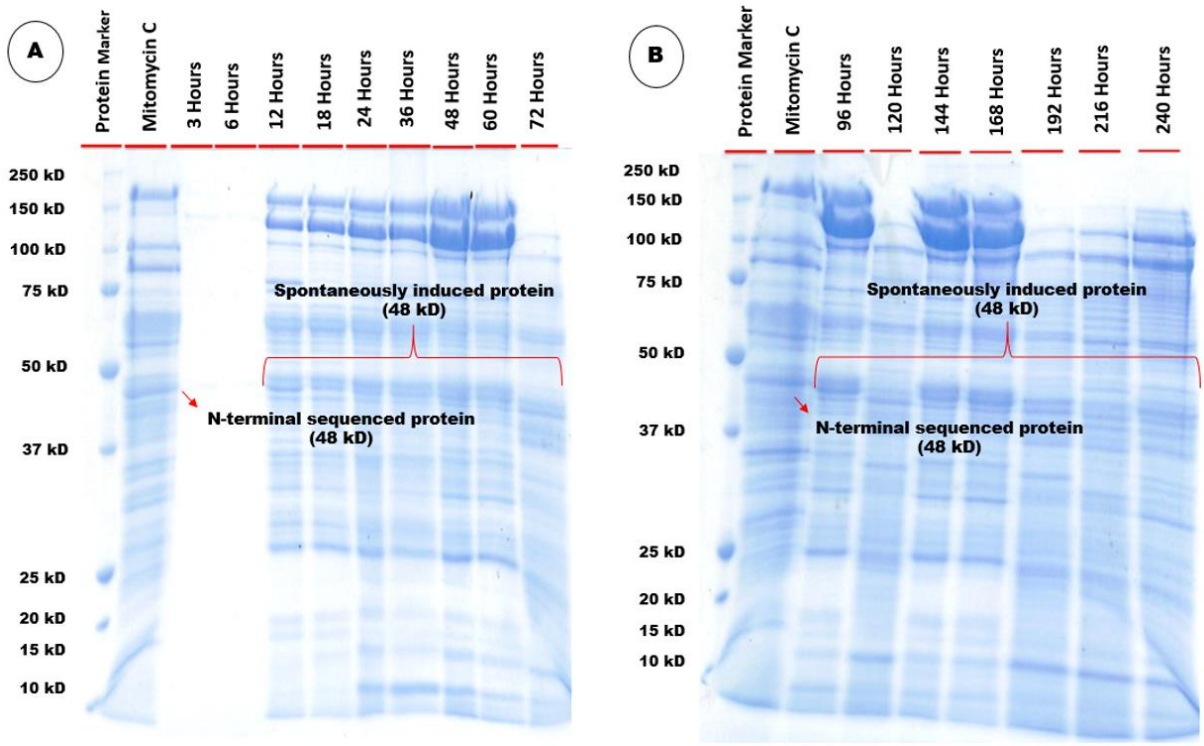

Figure 4.7 SDS-PAGE analysis of spontaneously induced putative antibacterial protein (bacteriocin) of *Bl* 1821L at various time intervals. (A) 3, 6, 12, 18, 24, 36, 48, 60, 72 hours & (B) 96, 120,144, 168, 192, 216, 240 hours

4.3.6 Effect of enzymes on the activity of crude putative antibacterial proteins of *Bl* 1951 against *Bl* 1821L as the host bacterium

The crude supernatant containing putative antibacterial proteins (bacteriocins) of *Bl* 1951 upon exposure to the proteolytic enzymes (proteinase K & protease) lost their inhibitory activity that validated their proteinaceous nature (Table 4.5). Treatment with catalase did not affect the antimicrobial activity of the mitomycin C induced filtered supernatant of *Bl* 1951 which showed that the developed lysis zones on the lawns of the host bacterium were not due to the action of hydrogen peroxide (H_2O_2). However, in the control treatment (without enzymes) the putative antibacterial proteins of *Bl* 1951 maintained their antagonistic activity (Table 4.5).

Table 4.5 Effect of enzymes on the activity of crude putative antibacterial proteins (bacteriocins) of *Bl* 1951 against *Bl* 1821L as the host bacterium

Enzymes	Zone of inhibition
Proteinase-K	-
Protease	-
Catalase	+
Control (Mitomycin C)	+

4.3.7 Effect of pH on the activity of crude putative antibacterial proteins of *Bl* 1951 against *Bl* 1821L as the host bacterium

Cell free supernatant containing the putative antibacterial proteins (bacteriocins) of *Bl* 1951 demonstrated more pronounced activity against *Bl* 1821L as the host bacterium at all the adjusted pH values except at pH 2. Antibacterial activity continued to increase from pH 4 up to pH 10, but it decreased at pH 12. A narrow zone of inhibition (10.7 mm) was measured at this value *i.e.* pH 12 (Table 4.6 & Figure 4.8).

Table 4.6 Effect of pH on the activity of crude putative antibacterial proteins (bacteriocins) of *Bl* 1951 against *Bl* 1821L as the host bacterium

pH	Zone of inhibition diameter (mm)
2	-*
4	11.67
6	20.7
8	21.0
10	21.7
12	10.7
Control (Mitomycin C)	23.0

*- = No zone of inhibition

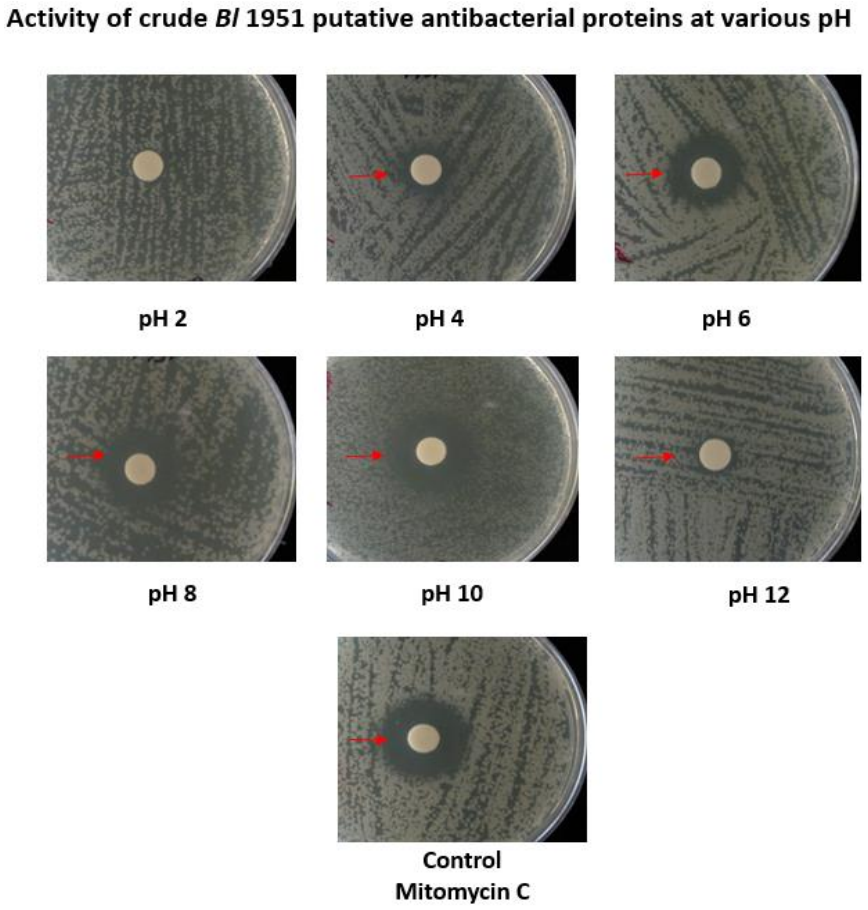

Figure 4.8 Effect of pH on the activity of crude putative antibacterial proteins (bacteriocins) of *Bl* 1951 against *Bl* 1821L as the host bacterium (shown with red arrow)

4.3.8 Effect of temperature on the activity of crude putative antibacterial proteins of *Bl* 1951 against *Bl* 1821L as the host bacterium

The crude putative antibacterial proteins (bacteriocins) of *Bl* 1951 sustained their antibacterial activity against the host bacterium *Bl* 1821L at all the evaluated temperatures except 121°C, where no zone of inhibition was observed after heating for 15 min (Table 4.7 & Figure 4.9). The crude filtered supernatant maintained at 4°C for 30 days did not lose stability when evaluated against *Bl* 1821L as the host bacterium. However, the exposure to -20°C caused a slight decrease in antagonistic activity.

Table 4.7 Effect of temperature on the activity of crude putative antibacterial proteins (bacteriocins) of *Bl* 1951 against *Bl* 1821L as the host bacterium

Temperature (°C)	Zone of inhibition diameter (mm)
70	17.0
80	18.7
90	14.3
100	14.7
121	-*
Control (Mitomycin C)	20.3

*- = No zone of inhibition

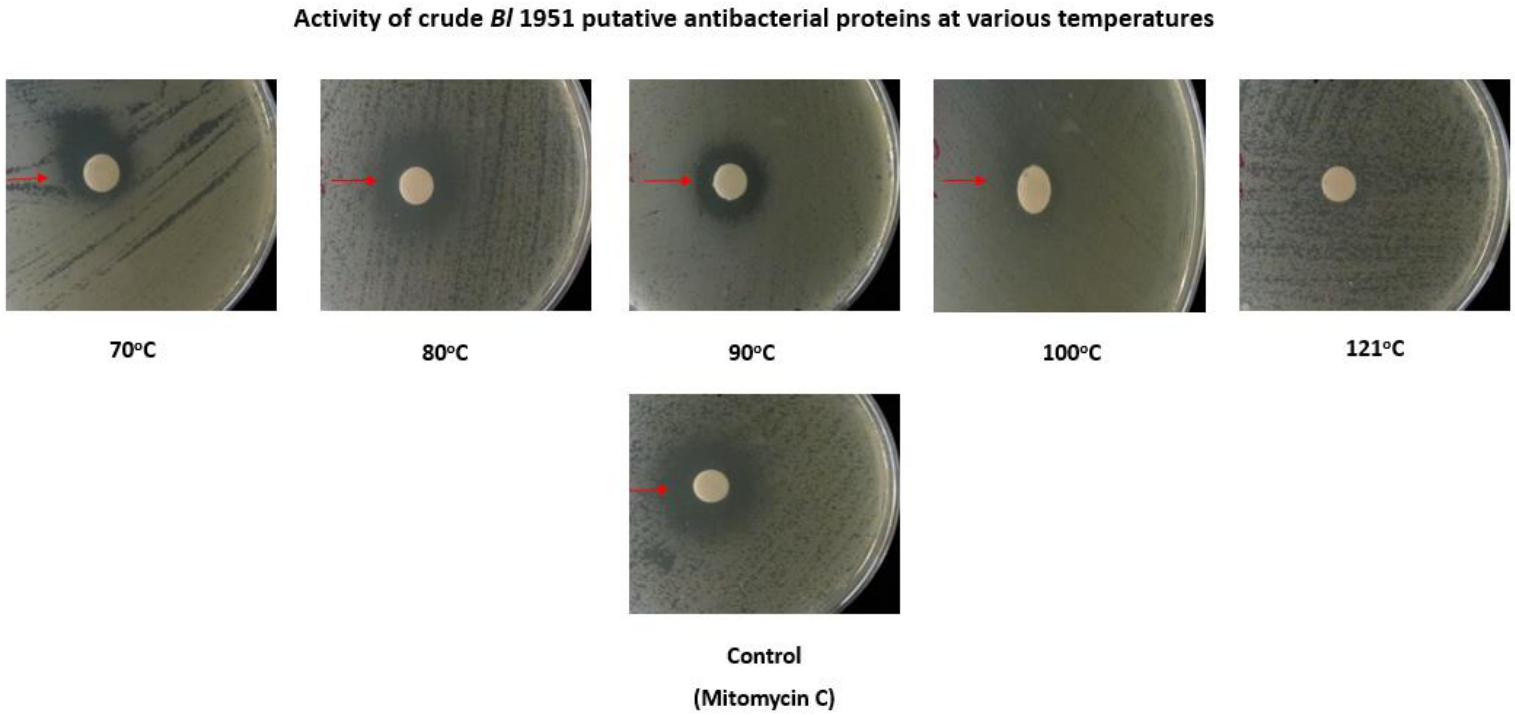

Figure 4.9 Effect of temperature on the activity of crude putative antibacterial proteins (bacteriocins) of *Bl* 1951 against *Bl* 1821L as the host bacterium (shown with red arrow)

4.3.9 Production kinetics of putative antibacterial proteins of *Bl* 1951

Similar to studies assessing crude putative antibacterial proteins (bacteriocins) of *Bl* 1821L (Section 4.2.4), three sets of independent experiments (biological replicates) were performed for determining the production kinetics of putative antibacterial proteins (bacteriocins) of *Bl* 1951 at various time intervals during the course of growth. The parameters of CFU/ml, pH of filtered supernatants, and antagonistic activity of crude proteins (bacteriocins) of *Bl* 1951 against *Bl* 1951 and *Bl* 1821L were studied. To ensure a more precise representation of the number of viable cells (CFU/ml) the recorded values were converted into $\log_{10}$ CFU/ml (Appendix C-5 & Figure 4.10). The results of all the experiments are included in Appendices C-6 to C-8 and the mean values of the results ($\log_{10}$ CFU/ml) are presented in Figure 4.11.

Antimicrobial activity of crude CFS of *Bl* 1951 harbouring the putative antibacterial proteins (bacteriocins) against *Bl* 1951 initiated after 12 hours by producing a narrow halo of 10.7 mm but against *Bl* 1821L its activity started to appear even in CFS of 3 hours (Table 4.8). The number of viable cells abruptly fell after 18-24 hours of growth (Figure 4.11). The point where the *Bl* 1951 culture experienced a dip in $\log_{10}$ CFU/ml also corresponded to the prominent antagonistic activity of CFS against *Bl* 1951 and *Bl* 1821L by developing an inhibitory zone of 13.3 mm and 15 mm respectively (Table 4.8 & Figures 4.12-4.13). No zone of inhibition was observed in the control treatment where LB broth was used (Figures 4.12-4.13). All the assessed parameters at the dipping point (18 hours) including $\log_{10}$ CFU/ml, pH of cell free supernatants, and the diameters of inhibitory zones against both the host bacteria statistically differed significantly from the initial periods (3-12 hours) of growth (Table 4.8). *Bl* 1951 cells insignificantly began to decline after 48 hours (Table 4.8 & Figure 4.11). The pH of *Bl* 1951 CFS obtained at various time intervals varied from 6.95 to 9.32 but it persistently increased slowly up to 36 hours and afterwards it almost remained static or slightly fluctuated (Table 4.8).

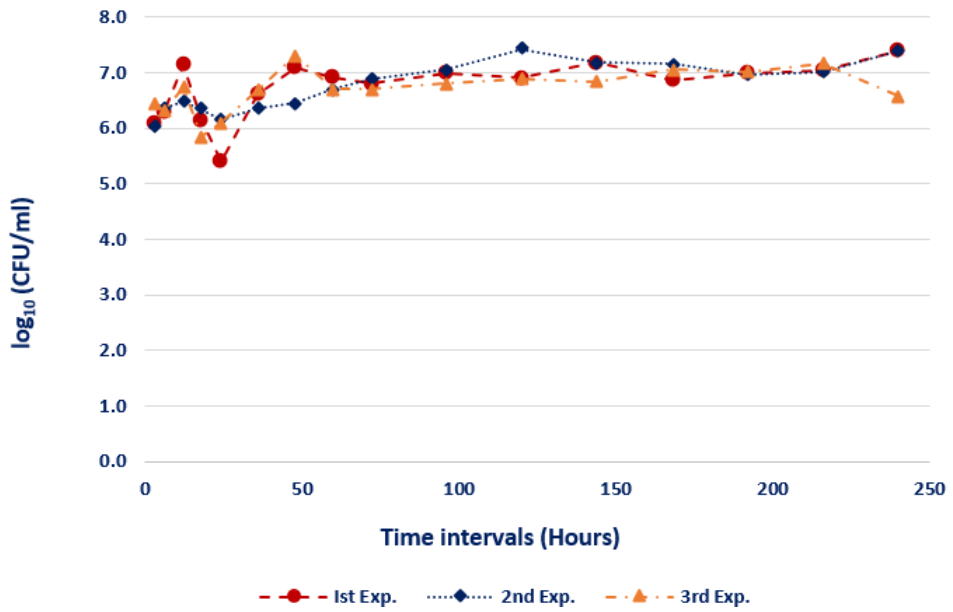

Figure 4.10 *Bl* 1951 cells growth (log_{10} CFU/ml) at various time intervals of all the experiments, grown at 30°C

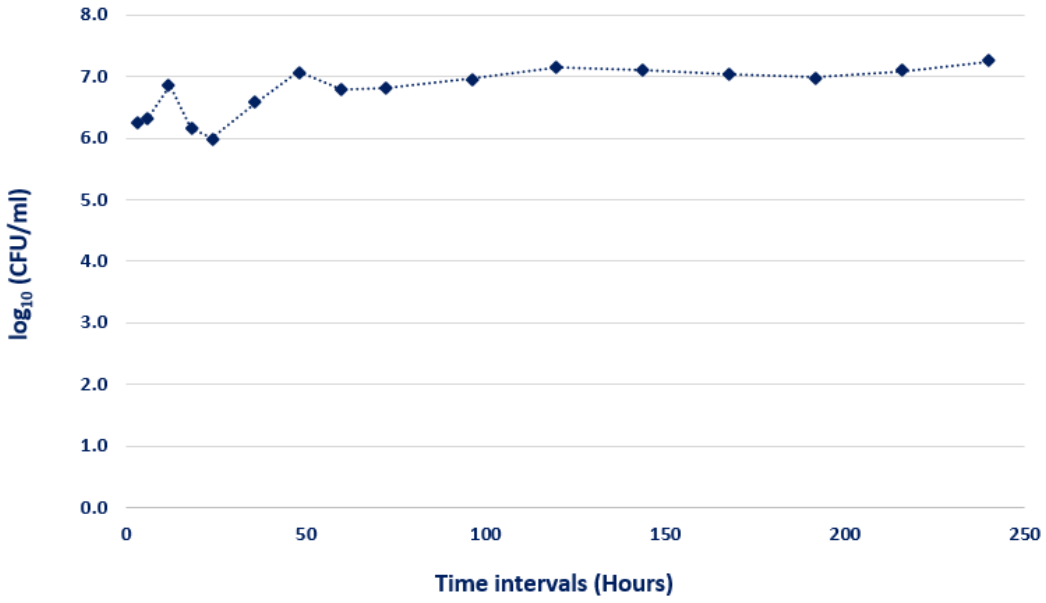

Figure 4.11 Mean values of *Bl* 1951 cell growth (log_{10} CFU/ml) at various time intervals, retrieved from the pooled data of Figure 4.10

Table 4.8 Production kinetics of *Bl* 1951 spontaneously produced putative antibacterial proteins (bacteriocins) at various time intervals and assay test of crude cell free supernatant (CFS) containing the putative antibacterial proteins of *Bl* 1951 against *Bl* 1951 and *Bl* 1821L as the host bacterium

Time interval (Hours)	log_{10} CFU/ ml	pH of CFS	Zone of inhibition diameter (mm)	
			Bl 1951 as the host bacterium	*Bl* 1821L as the host bacterium
3	6.239	6.95	0.00	12.33
6	6.315	7.08	0.00	12.22
12	6.868	7.68	10.67	13.56
18	6.156	8.18	13.33	15.00
24	6.000	8.61	11.89	13.11
36	6.574	9.05	11.67	13.11
48	7.079	9.08	12.67	12.33
60	6.795	9.12	12.22	11.56
72	6.812	9.18	12.44	12.67
96	6.968	9.24	13.78	13.11
120	7.151	9.23	12.78	12.89
144	7.103	9.24	12.22	12.78
168	7.044	9.28	12.00	14.67
192	6.988	9.29	13.11	13.67
216	7.086	9.32	11.89	13.67
240	7.253	9.20	12.78	13.56
*LSD (5%)	0.444	0.165	1.268	2.067

*LSD= Least significant difference

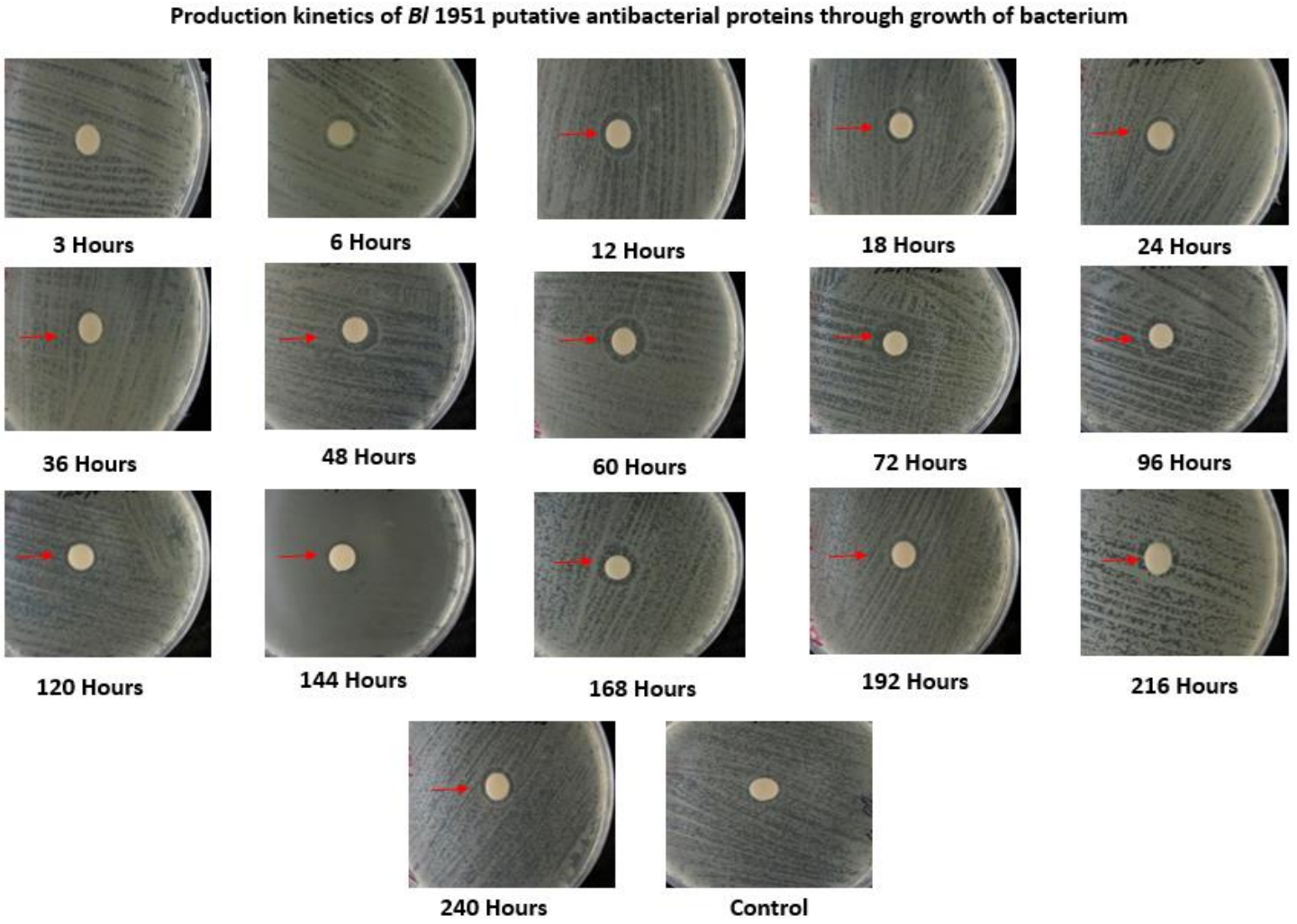

Figure 4.12 Antibacterial activity of *Bl* 1951 spontaneously produced putative antibacterial proteins (bacteriocins) CFS against *Bl* 1951 as the host bacterium at various time intervals during the course of its growth (shown with red arrow)

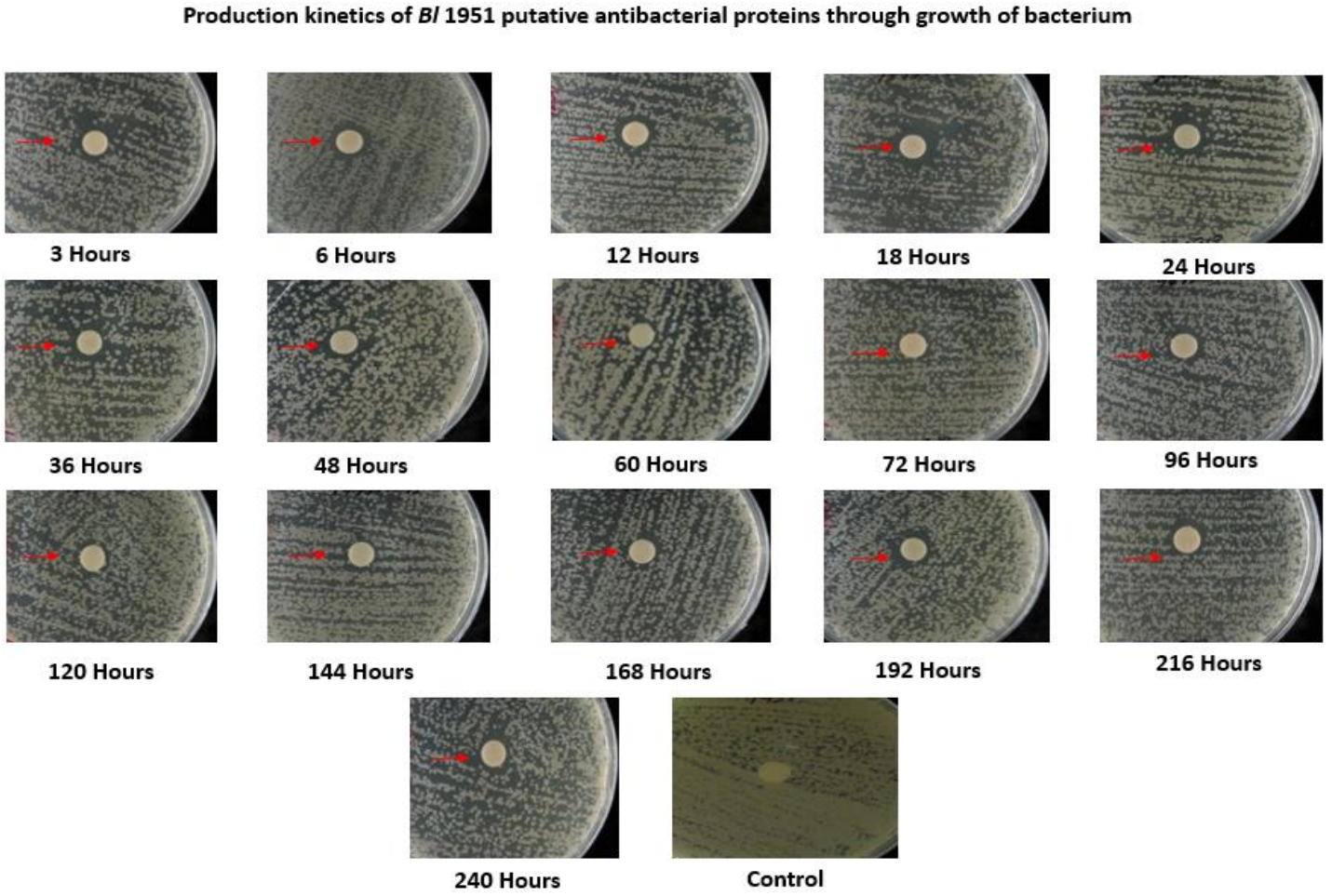

Figure 4.13 Antibacterial activity of *Bl* 1951 spontaneously produced putative antibacterial proteins (bacteriocins) CFS against *Bl* 1821L as the host bacterium at various time intervals during the course of its growth (shown with red arrow)

4.3.10 SDS-PAGE analysis of *Bl* 1951 produced putative antibacterial proteins

SDS-PAGE analysis of *Bl* 1951 spontaneously produced putative antibacterial proteins (bacteriocins) indicated minor bands during the initial times (3-6 hours) of *Bl* 1951 growth as compared to *Bl* 1821L (Figure 4.14A). As reported in the previous section, spontaneously produced putative antibacterial proteins (bacteriocins) of *Bl* 1951 started to show an inhibitory effect against *Bl* 1821L even at these early hours in the disc diffusion assay test (Table 4.8 & Figure 4.13). Mitomycin C induced culture of *Bl* 1951 indicated a prominent band of ~30 kD (which will be further purified in Chapter 5 and bioinformatically analysed in Chapter 6). Importantly, a similar protein band (~30 kD) was visualised on SDS-PAGE in the spontaneously produced putative antibacterial proteins (bacteriocins) from the early 12 hours to late 144 hours of *Bl* 1951 growth. However, afterwards this band can be observed on SDS-PAGE with a low level of protein (Figures 4.14A-B).

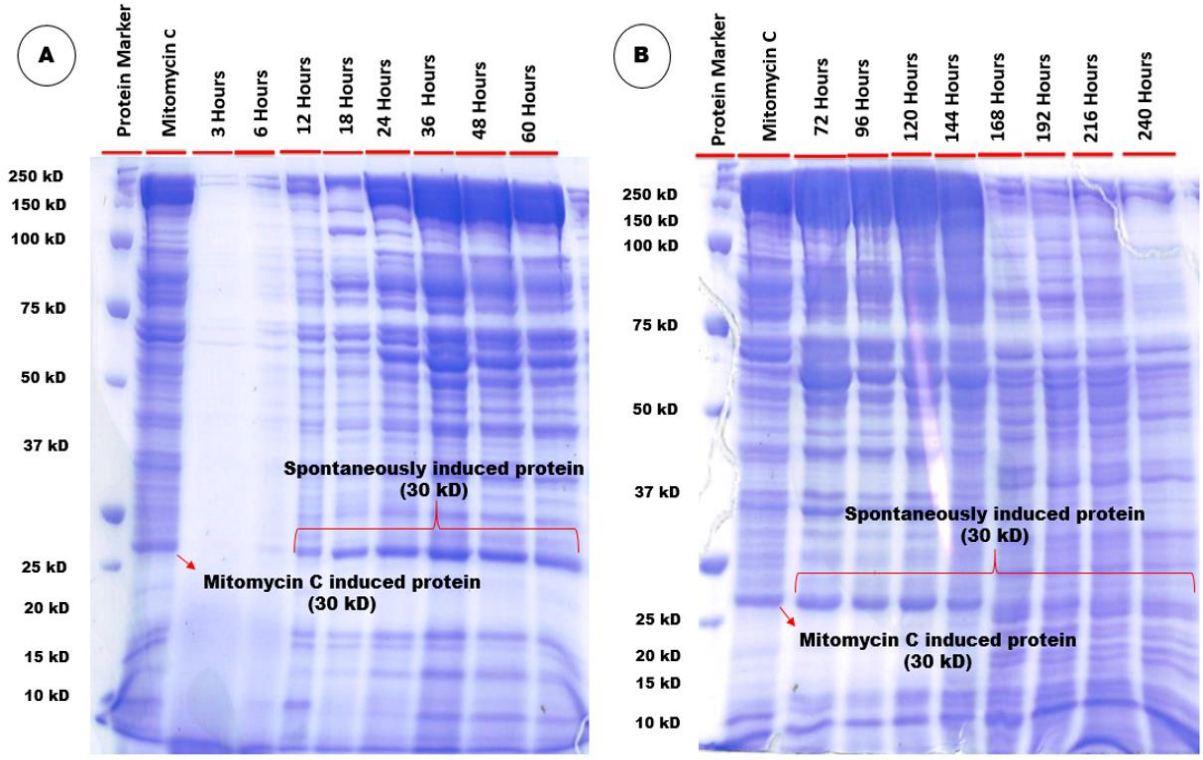

Figure 4.14 SDS-PAGE analysis of *Bl* 1951 spontaneously produced putative antibacterial proteins (bacteriocins) at various time intervals. (A) 3, 6, 12, 18, 24, 36, 48, 60, 72 hours & (B) 96, 120, 144, 68, 192, 216, 240 hours

4.4 Discussion

The current research explored biochemical features including the effect of enzymes, pH, and temperature on the activity of crude putative antibacterial proteins (bacteriocins) of *Bl* 1821L and *Bl* 1951. Furthermore, the production kinetics of *Bl* 1821L and *Bl* 1951 bacteriocins at various time intervals were investigated through disc diffusion assay tests. SDS-PAGE analysis was used to compare the spontaneously induced *Bl* 1821L and *Bl* 1951 putative antibacterial proteins at various time intervals with the mitomycin C induced cultures for the strength of the protein banding.

The production of high molecular-weight (HMW) bacteriocins (such as phage tail-like bacteriocins) is upregulated during stress. They are inducible by DNA damaging agents like UV radiation or mitomycin C and are dependent on the DNA repair and maintenance protein RecA (Sano & Kageyama, 1987; Shinomiya et al., 1983). However, under some conditions, antibacterial structures like bacteriophages and phage tail-like bacteriocins may undergo a phenomenon known as "spontaneous prophage induction" (SPI). This causes the spontaneous activation of these antibacterials in single cells of bacterial populations even in the absence of an external trigger (Nanda et al., 2015). SPI is likely due to spontaneous accumulation of DNA damage initiating the host's SOS response during cell replication (Cox et al., 2000; McCool et al., 2004; Pennington & Rosenberg, 2007). This process plays a crucial role in the population biology of temperate phages in mixtures of susceptible cells and lysogens (Nanda et al., 2015). This was first demonstrated using supernatants of *Bacillus megaterium* lysogens that spontaneously produced phages in the cultivating media under non-inducing conditions (Lwoff, 1953b). Spontaneous induction, which is often accompanied by lysis of the bacterial cell, has long been seen as a potentially detrimental process for bacterial populations, as a small percentage of cells would be lost continuously (Nanda et al., 2015). Cells of the gram-positive bacterium, *Corynebacterium glutamicum*, grown under standard conditions, spontaneously induced expression of prophage genes and this activation is caused in part by the spontaneous activity of the SOS response in single cells (Nanda et al., 2014). The simultaneous production of contractile and flexible phage tail-like bacteriocins was first reported in the bacterium *Pragia fontium* 64613 (Smarda & Benada, 2005). Maximum spontaneous production of phage tail-like particles occurred after 12 hours at 30^{o}C and heavy shaking. However, the authors demonstrated that it could be further increased by exposure to UV light at 245 nm or mitomycin C @ 1 µg/ml (Smarda & Benada, 2005). Broussard et al. (2013), while studying the non-SOS inducible mycobacteriophages, speculated that the spontaneous switching from lysogeny to the lytic state might be due to a drop in the repressor level below the threshold or to a sporadic expression of the integrase gene.

Cell free supernatants of *Bl* 1821L and *Bl* 1951 extracted at various time intervals in the assay tests demonstrated antibacterial activities. Therefore, all the filtered supernatants after high-speed

centrifugation were run on SDS-PAGE to visualise the difference between the mitomycin C induced and the spontaneously induced inhibitory compounds. A prominent band of ~48 kD from mitomycin C induced culture of *Bl* 1821L was visualised on SDS-PAGE and excised for N-terminal sequencing as reported in Chapter 3 (Figures 3.5A-B). N-terminal sequencing and further bioinformatics analysis substantiated it as a putative phage tail-like bacteriocin. SDS-PAGE analysis of spontaneously induced putative antibacterial protein of *Bl* 1821L at various time intervals also showed the presence of a ~48 kD protein band (Figures 4.7A-B). The visualisation of antibacterial protein of *Bl* 1821L across all the evaluated time intervals, except in the initial 3-6 hours, also confirmed the results of the disc assay tests against *Bl* 1821L and *Bl* 1951 as the host bacterium (Figures 4.5-4.6). Based on the availability of literature so far this is the first report of spontaneous induction of HMW bacteriocins (phage tail-like) of the insect pathogenic *Bl* 1821L strain. SDS-PAGE of *Bl* 1951 mitomycin C induced and spontaneously produced putative antibacterial proteins (bacteriocins) at various time intervals indicated a prominent ~30 kD protein. Visualisation of a spontaneously produced ~30 kD protein band on SDS-PAGE of *Bl* 1951 showed low concentrations in the initial 3-6 hours but it remained prominent up to 144 hours and at a slightly reduced level afterwards (Figures 4.14A-B). Furthermore, in this work prominent lysis zones were seen upon evaluation of *Bl* 1951 extracted CFS at all time intervals against *Bl* 1951 and *Bl* 1821L as the host bacterium. Electron micrographs of crude lysate of *Bl* 1951 presented in Chapter 2 (Figure 2.14) displayed structures similar in form to the phage tail-sheath however its involvement in the putative antibacterial activity at this stage is inconclusive due to the absence of N-terminal sequencing of ~30 kD protein of *Bl* 1951.

Microbial growth and maintenance on cultivating media in petri dishes has long been a common practice in microbiology. The preferred method for quantitative population analysis of pure and mixed cultures relies on the plating of serial dilutions and subsequent counting of CFUs (Sieuwerts et al., 2008). Numerous alternative tools like quantitative PCR (Neeley et al., 2005), fluorescent labelling (Blasco et al., 2003; Lay et al., 2005), or genome probing with microarrays (Bae et al., 2005) have gained popularity but most of these methods measure different entities*, i.e.* all cells, including non-viable cells (Liu et al., 2004). Therefore, due to the complexities involved in these protocols, colony counting is still a widely used method to enumerate microbes (Sieuwerts et al., 2008). The CFU counting method has certain distinctive features, namely the capacity for counts of any number of bacteria using dilutions, if too many, or concentrations if too few. Viable bacteria only are counted while dead bacteria and debris are excluded in this method (Hazan et al., 2012). However, the most important limitation of the CFU method is that clumps of bacteria cells can be miscounted as single colonies; the potential for counting clumps as single units is the reason the results are reported as CFU/ml rather than bacterial cells/ml. Furthermore, the results are usually obtained after 1-3 days, making the method not suitable for serial

longitudinal studies (Hazan et al., 2012). Growth curves of *Bl* 1821L and *Bl* 1951 in all the triplicate experiments did not show strong uniformity and consequently, the CFU/ml varied due to unknown factors. However, the present study revealed that the spontaneously produced putative antibacterial proteins (bacteriocins) of *Bl* 1951 caused a drastic decline in the number of viable cells (log_{10} CFU/ml) after 18 hours of growth which corresponded to the highest antagonistic activity of CFS of this particular time period against *Bl* 1821L and *Bl* 1951 as host bacterium. pH of *Bl* 1951 CFS extracted after 18 hours, like log_{10} CFU/ml and diameter of zones of inhibition (mm), were statistically significant. Although *Bl* 1821L also experienced a dip in log_{10} CFU/ml after 18 hours of growth and more pertinently this period also coincided with the highest antibacterial activity of CFS containing spontaneously induced putative antibacterial proteins (bacteriocins), but differences were not significant.

The expression of genes responsible for the production of antimicrobial peptides is largely dependent on the temperature and initial pH of the medium (Leães et al., 2013). Various metabolic mechanisms like aggregation, adsorption of bacteriocin by producing cells, and proteolytic degradation by specific or non-specific proteases, as well as post-translational modifications to produce active bacteriocins are sensitive to acidification of the cultivating media (Biswas et al., 1991; Guerra, 2014). Earlier findings mentioned that pH values decrease gradually over several hours after inoculation due to rapid bacterial growth rate (Lee et al., 2001). The gradual increase in pH of *Bl* 1951 and *Bl* 1821L up to 48 and 60 hours of growth aligns with the exponential growth and afterwards a slight fall (stationary phase) where pH values remained almost stagnant. Typically, at this stage, Bacillaceae species produce several organic acids such as malic acid, pyruvic acid, acetic acid, citric acid, succinic acid, α-ketoglutaric acid, propionic acid, and butyric acid (Lee et al., 2001). Pyruvic acid is considered as one of the key intermediates in the Tricarboxylic acid (TCA) cycle and Embden-Meyerhof-Parnas (EMP) pathways and plays a vital role in bacteriocin biosynthesis. Expression of a plasmid-encoded bacteriocin gene is attributed to the increasing level of purines and pyrimidines after the production of acetic acid (Ge et al., 2019). However, depending on the species and medium composition, the concentration of these organic acids may vary. The time when bacterial growth almost approaches the stationary phase, the concentration of organic acids decreases, as often indicated by a slight increase in fermentation pH. Therefore, optimum pH condition is important to maintain membrane potential and establish multiple ion gradients across the cytoplasmic membrane (Dominguez et al., 2007).

Proteolytic enzymes hydrolyse peptide bonds in substrate proteins, resulting in a widespread, irreversible post-translational modification of the protein's structure and biological function (Dhillon et al., 2017; Klein et al., 2018). Proteinase K is commonly used in molecular biology to digest proteins. Earlier studies have elucidated that the bacteriocins from different species can either be activated, inactivated, or do not result in any changes of antimicrobial activity (Elayaraja et al., 2014; Kang & Lee,

2005). HMW bacteriocins, BceTMilo and maltocin S16, upon exposure to the proteolytic enzymes (trypsin, α-chymotrypsin, proteinase K, protease, lipase, papain, or lysozyme) did not lose their killing activity but α-chymotrypsin caused a 75% loss in activity of maltocin S16 (Chen et al., 2019; Yao et al., 2017). Proteinase K treatment completely abrogated bactericidal activity of the phage tail-like bacteriocins, maltocin P28 and serracin P (Jabrane et al., 2002a; Liu et al., 2013). Low molecular-weight (LMW) bacteriocins of the genus *Bacillus* (Cherif et al., 2008; Flühe et al., 2013; Kaewklom et al., 2013) and *Brevibacillus* (Baindara et al., 2016b; Ghadbane et al., 2013; Singh et al., 2012) lost their antagonistic activity after treatment with proteinase K. Proteolytic enzymes (proteinase K & protease) treatment of the crude *Bl* 1821L and *Bl* 1951 bacteriocins abrogated their inhibitory activity, which proved their proteinaceous nature. Mitomycin C induced supernatants of *Bl* 1821L and *Bl* 1951 harbouring the putative antibacterial proteins (bacteriocins) retained their activity upon exposure to the catalase enzyme which confirmed that it was not caused due to hydrogen peroxide (H_2O_2).

LMW bacteriocins are mostly heat resistant, but their optimal temperature with the highest antimicrobial activity varies depending on species (Lajis, 2020; Riley & Wertz, 2002b). For example, *Bl* produced bacteriocin, laterosporulin (Singh et al., 2012), Bac-GM100 (Ghadbane et al., 2013), and laterosporulin 10 (Baindara et al., 2016b), maintain their thermal stability even after heating at 121°C for 15-20 min. The entomopathogenic bacterium, *Bt entomocidus* HD110, bacteriocins entomocin 110 and entomocin 9 retained 53% and 72% of their activity respectively even after autoclaving (Cherif et al., 2003; Cherif et al., 2008). From the available studies, the vast majority of HMW bacteriocins such as aquaticin (Smarda & Benada, 2005), fonticin (Smarda & Benada, 2005), maltocin P28 (Liu et al., 2013), maltocin S16 (Chen et al., 2019), and serracin P (Jabrane et al., 2002a) become inactive upon incubation at a temperature between 45-60°C for 10 min. The crude lysate of *Bl* 1821L harbouring phage tail-like bacteriocins retained stability between 70-90°C and the putative antibacterial proteins (bacteriocins) of *Bl* 1951 even tolerated heating up to 100°C. However, the antagonistic activities of the putative antibacterial proteins (bacteriocins) of *Bl* 1821L and *Bl* 1951 were lost after autoclaving (121°C) for 15 min. The present findings showed that the crude putative antibacterial proteins (bacteriocins) of *Bl* 1821L and *Bl* 1951 are thermally stable over a broad range as compared to the similar antibacterial agents in other bacteria.

The genus *Bacillus* bacteriocins are known to be active over a broad range of pH (Bizani & Brandelli, 2002). Laterosporulin and Bac-GM100 retained their biological activity within pH 2-10, but activity was drastically reduced at pH >10 (Ghadbane et al., 2013; Singh et al., 2012). Antimicrobial activity of laterosporulin 10 was stable over a wide range of pH (2-12) (Baindara et al., 2016b). HMW bacteriocin, BceTMilo, killing activity was stable between pH 4.8-8.8, with a 100-fold decrease in activity after 18 hours at pH 10.5 and all detectable activity was lost after 18 hours at pH 2.0 (Yao et al., 2017).

However, in the current study crude lysate harbouring the putative antibacterial proteins (bacteriocins) of *Bl* 1821L (pH 2-10) and *Bl* 1951 (pH 4-12) sustained their antibacterial activity over a wide pH range. The stability of bacteriocins over a wide pH range makes it effective but unfavourable pH conditions could reduce cell viability by disrupting the integrity of the plasma membrane. This is due to the presence of excessive H^+ (due to pH) that tend to lessen the membrane permeability barrier, perturbing the membrane lipid bilayers, thus causing leakage of some cellular components, and the dissipation of the electrostatics of the plasma membrane (Dominguez et al., 2007; Lee et al., 2001).

4.5 Outcomes

The major findings of this chapter are;

1. Biochemical characterisation of *Bl* 1821L and *Bl* 1951 putative antibacterial proteins (bacteriocins) demonstrated that they persisted in their antibacterial activity over a wide range of pHs and temperatures.
2. Proteolytic enzymes (proteinase K & protease) treatment proved the proteinaceous nature of *Bl* 1821L and *Bl* 1951 putative antibacterial proteins (bacteriocins).
3. *Bl* 1821L spontaneously induced putative antibacterial proteins harbouring a phage tail-like bacteriocin of ~48 kD molecular mass insignificantly affected the colony forming units (CFUs) of the host after 18 hours of growth.
4. *Bl* 1951 spontaneously induced a protein of ~30 kD molecular mass which is suspected (being a prominent protein band) to be involved in the antagonistic activity. A decline in the number of viable cells and significant antagonistic activity of *Bl* 1951 spontaneously induced putative antibacterial protein was found after 18 hours of growth.

4.6 Conclusion

Bl 1821L and *Bl* 1951 putative antibacterial proteins (bacteriocins) stability over a broad range of pHs and temperatures may provide an insight into their nature. Spontaneously induced putative antibacterial proteins can affect the number of viable cells of host bacteria during the course of its growth.

Chapter 5

Purification of putative antibacterial proteins of New Zealand *Brevibacillus laterosporus* isolates *Bl* 1821L and *Bl* 1951

5.1 Introduction

Biochemical characterisation and production kinetics of putative antibacterial proteins of isolates *Bl* 1821L and *Bl* 1951 in the preceding chapter demonstrated their proteinaceous nature and spontaneous production. The salient characteristics of the putative antibacterial proteins can only be ascertained if these are obtained in the purified form.

Bacteriophages are endowed with numerous structural and non-structural proteins. The former includes tail and capsid proteins represented by receptor switching in phage tail-like antibacterials (pyocins), while the latter are represented by polymerases and specialised enzymes that are well exemplified by "phage lysins" or "enzybiotics" (Kim et al., 2019). Antibacterial structures like phages and phage tail-like bacteriocins (PTLBs) are lysogenic and are released upon lysis of the cell after induction (Patz et al., 2019; Saha et al., 2021). The major components present in crude lysate apart from phage or phage tail-like bacteriocins may also include bacterial debris (mainly membranes with bacterial proteins), nucleic acids, and ribosomes (Boulanger, 2009). To identify and characterise the protein of interest it is vital to purify from this lysed homogenate (Marichal-Gallardo & Alvarez, 2012; Roy et al., 2007). Indeed, defining what a "pure protein" means is not easy. Theoretically, a protein is pure when a sample contains only a single proteins species, although in reality it is more or less impossible to achieve 100% purity (Walker, 2005). However, in practice, only four different fractionation steps are needed to purify most of the proteins and in exceptional circumstances, a single chromatographic step has been sufficient (Walker, 2005).

Various protein purification methods developed in the 1960s-1990s guided how the targeted and admixed proteins can be separated by their molecular weights, charges, hydrophobic properties, effects of salts (ammonium sulphates), and organic solvents (acetone or ethanol) (Borzenkov et al., 2014; De Vuyst & Leroy, 2007). They can also be separated by their adsorbing potentialities, resistance to pH and temperature, antibody affinity, as well as by types of substrates and inhibitors (in case of enzymes), cyanurchloride derivatives, etc. (Borzenkov et al., 2014). Size exclusion chromatography (SEC) is regarded as the standard analytical technique to separate and quantify protein oligomers. SEC separates molecules according to their hydrodynamic size, with larger-sized molecular species (which are not necessarily larger molecular mass species) eluting before smaller ones (Fekete et al., 2014; Jones &

Hurst, 2016). Ultracentrifugation is particularly useful not only in concentrating but also in purifying the phage tail-like particles in density gradients (Gebhart et al., 2012; Lawrence & Steward, 2010). PEG 8000 precipitation in combination with the salt NaCl has been employed to concentrate the antibacterial structures (such as bacteriophages and phage tail-like bacteriocins) (Hegarty et al., 2016) and to differentiate between the activity of two inhibitory compounds (Hockett & Baltrus, 2017). Ammonium sulphate precipitation has been used to purify the crude phage derived bacteriocins (Fischer et al., 2012). Purification by ammonium sulphate requires graded precipitation to obtain pure extracts. However, during ammonium sulphate precipitation, salt ions are introduced and removal of these salt ions complicates the purification process (Zou et al., 2018a).

High molecular-weight (HMW) bacteriocins (such as PTLBs) are not typically separated in a single step and therefore several steps/methods have to be employed to purify a targeted protein (Yao et al., 2017; Zou et al., 2018a). The various separation steps may exploit differences in chemical/structural/ functional properties between the target protein and other proteins in the crude mixture. Therefore, by exploiting these differences in physical and chemical properties among proteins, several different fractionation and chromatographic methods can usually be employed to design a workable purification scheme (Kallberg et al., 2012; Labrou, 2014).

The primary aim of this chapter was to purify the putative antibacterial proteins of *Bl* 1821L and *Bl* 1951 using different methods for specific identification.

5.2 Methods

5.2.1 Purification of *Bl* 1821L and *Bl* 1951 putative antibacterial proteins using size exclusion chromatography

A *Bl* 1821L culture was induced with mitomycin C (Sigma) @ 1 µg/ml as described in Chapter 2 (Section 2.2.6). The induced culture was centrifuged @ 16,000 g for 10 min and the supernatant was passed through a 0.22 µm filter. Cell free supernatant (CFS) (7.5 ml) was transferred into polypropylene centrifuge tubes (Konical, Beckman) and ultracentrifuged @ 35,000 rpm (151,263 x g) in a swing bucket rotor (41Ti, Beckman) for 70 min to concentrate the putative antibacterial proteins. The supernatant was decanted and the concentrated pellet was resuspended in 100-150 µl of TBS buffer (Tris buffer saline: 25 mM Tris-HCl, 130 mM NaCl, pH 7.5). Prior to SEC, the resuspended pellet was passed through a 0.45 µm filter. For SEC, a Bio-Rad column (1.5 x 46 cm) was used to pour the gel matrix (Sephacryl S-400) according to the manufacturer's instructions (GE Healthcare Life Sciences). An ultracentrifuged sample (800 µl) of *Bl* 1821L was injected into the column for purification. The column was connected to the BioLogic LP System. Before loading the sample into the column, it was equilibrated with TBS buffer

to a volume of approximately 150-200 ml at a flow rate of 1 ml/minute. The sample after loading into the column was run at 0.5 ml/minute and the purified/separated protein mixture was monitored by the UV slot in the BioLogic LP System measuring the absorbance at 280 nm.

For *Bl* 1951, a culture induced with mitomycin C (Sigma) @ 3 μg/ml was used in SEC purification as described for the *Bl* 1821L samples. A schematic presentation of the SEC method is illustrated in Figure 5.1.

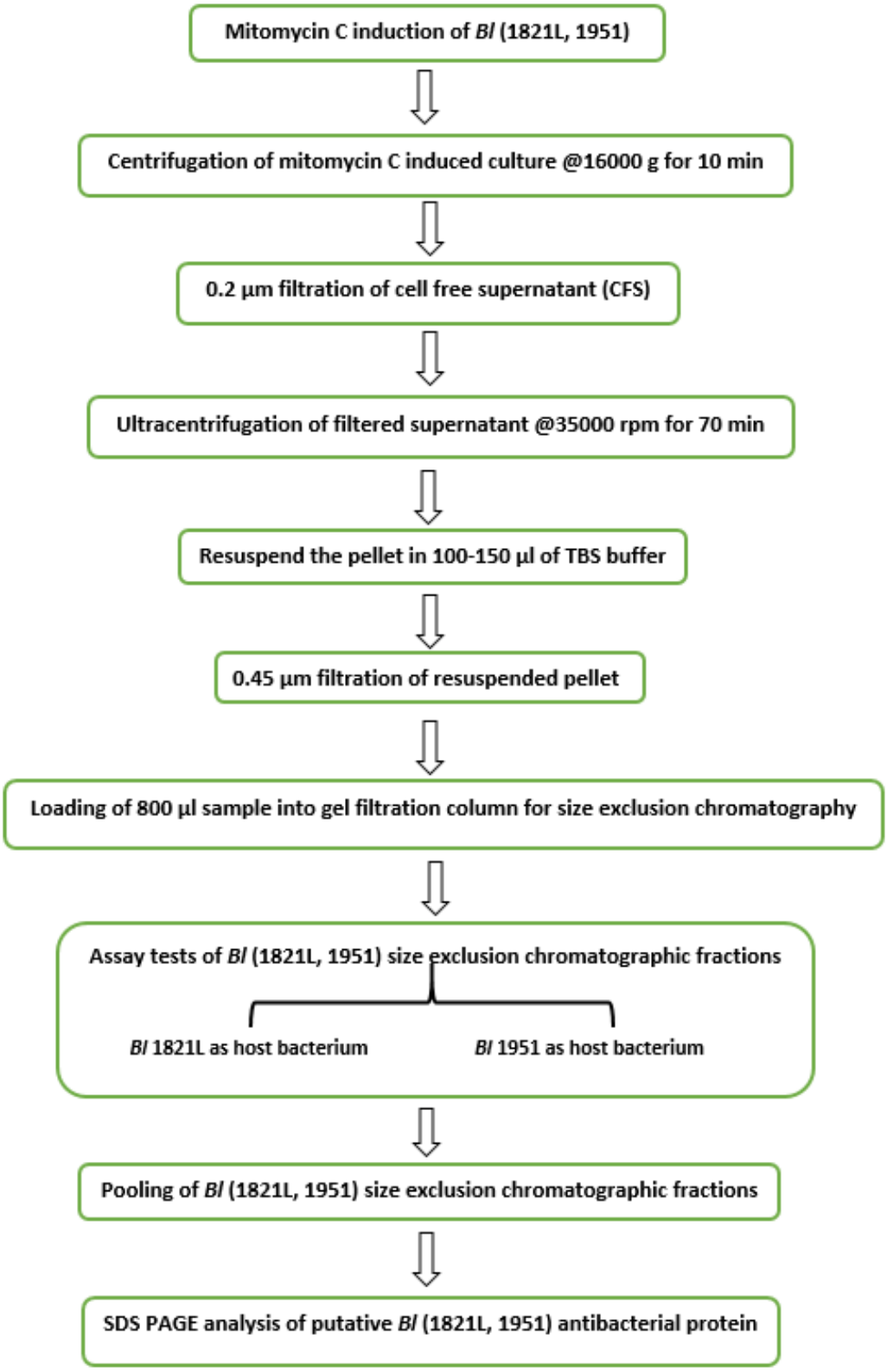

Figure 5.1 Flow chart of *Bl* (1821L, 1951) putative antibacterial proteins purification using size exclusion chromatography

A. Assay test of size exclusion chromatography fractions

Antagonistic activity of *Bl* 1821L SEC derived fractions was tested against *Bl* 1821L and *Bl* 1951 as the host bacterium through the Kirby-Bauer disc diffusion assay (Bauer, 1966; Hudzicki, 2009) as outlined in Chapter 3 (Section 3.2.1). However, in this study 80 µl of each SEC fraction was transferred to the sterile (without impregnation of antimicrobials) paper disc (ADVANTEC, Japan) of 8 mm diameter for determining its inhibitory activity against the *Bl* 1821L and *Bl* 1951 as the host bacterium. Disc diffusion assays were performed in triplicate assessing the independently undiluted *Bl* 1821L SEC fractions, from where SEC fractions exhibiting the inhibitory activities were pooled and concentrated at a high speed of 35,000 rpm (151,263 x g) in a swing bucket rotor (41Ti, Beckman) for 70 min.

Antibacterial activity of the SEC fractions of *Bl* 1951 was also evaluated through disc diffusion assay test against *Bl* 1951 and *Bl* 1821L as the host bacterium as described for *Bl* 1821L. All the SEC fractions exhibiting inhibitory activities were concentrated similar to *Bl* 1821L.

B. Protein quantification using Qubit protein assay kit

Bl 1821L and *Bl* 1951 antibacterial proteins quantification of each concentrated fraction was performed using a Qubit protein assay kit (Thermo Fisher Scientific). Qubit working solution was prepared by diluting the Qubit protein reagent 1:200 in the Qubit protein buffer. Two assay tubes were set up for the standards and each 190 µl of Qubit working solution was mixed with 10 µl of standards from the kit by vortexing for 2-3 seconds to make the final volume of 200 µl. A 20 µl putative antibacterial protein sample was added into 180 µl of Qubit working solution and vortexed for 2-3 seconds. Final volume in each *Bl* 1821L putative antibacterial protein sample was 200 µl. All the tubes were incubated at room temperature (~22^{o}C) for 15 min from where they were independently placed into the Qubit 3.0 Fluorometer (Thermo Fisher Scientific) and the protein concentration (µg/ml) readings were noted.

C. SDS-PAGE analysis of size exclusion chromatography fractions

Bl 1821L and *Bl* 1951 fractions after concentrating the putative antibacterial proteins were run on the SDS-PAGE as described in Chapter 3 (Section 3.2.6) but here the volume of loaded sample and protein ladder (BIO-RAD, Precision Plus Protein^{TM} Standards) was 20 µl and 5 µl respectively.

For staining of *Bl* 1821L and *Bl* 1951 putative antibacterial proteins, the silver straining protocol defined by Blum et al. (1987) with some modifications was used. Post SDS-PAGE the gel was washed with dH_2O and immediately transferred for fixation (Methanol 50 ml + Acetic acid 12 ml + Formalin 50 µl + dH_2O 38 ml) for 30 min on an orbital shaker (Ratek, Australia) at the lowest speed. For fixation, the gel was washed three times with 50% methanol for 5 mins. After fixation, the gel was treated with 0.1M sodium

thiosulphate (800 µl) and 100 ml dH_2O. Prior to the application of the impregnation solution (Silver nitrate 0.2 g + Formalin 75 µl + dH_2O 100 ml) to the gel for 10 min, the gel was washed three times with dH_2O for 20 sec each time. Staining was then achieved by treating the gel with the solution (Sodium carbonate 6 g + Formalin 50 µl + 0.1M Sodium thiosulphate 16 µl + dH_2O 100 ml) for 10-20 min at that time protein bands typically appear and the gel at this stage was immediately washed with dH_2O for 20 sec. To terminate the staining, the gel was treated with 10 ml 10% Acetic acid in 100 ml dH_2O for 10 min. Finally, the stained SDS-PAGE gel was washed for 20 sec in dH_2O.

D. Transmission electron microscopy of *Bl* 1821L and *Bl* 1951 putative antibacterial proteins purified using the size exclusion chromatography

TEM analysis of the *Bl* 1821L and *Bl* 1951 SEC purified and concentrated samples was performed at AgResearch, Lincoln, New Zealand according to the protocol described in Chapter 2 (Section 2.2.9).

5.2.2 Purification of *Bl* 1821L and *Bl* 1951 putative antibacterial proteins using sucrose density gradient centrifugation

Mitomycin C (Sigma) @ 1 µg/ml was used to induce *Bl* 1821L as described in Chapter 2 (Section 2.2.6). The induced culture was centrifuged @ 16,000 g for 10 min and the supernatant was passed through a 0.22 µm filter. Cell free supernatant (CFS) (7.5 ml) was transferred into polypropylene centrifuge tubes (Konical, Beckman) and ultracentrifuged @ 35,000 rpm (151,263 x g) in a swing bucket rotor (41Ti, Beckman) for 70 min to concentrate the putative antibacterial particles. The supernatant was decanted and the concentrated pellet was resuspended in 100-150 µl of TBS buffer.

Two groups of different sucrose density gradients were used in this study. Group A comprising of 10%, 20%, 30%, 40%, and 50% gradients was created by applying layers of 1.5 ml of freshly prepared sucrose solutions on top of one another. Group B comprising of 10%, 20%, 30%, 40%, 50%, and 60% gradients was created by applying layers of 1.25 ml of freshly prepared sucrose solution sequentially. The highest concentration of sucrose was applied first, followed by the lower concentrations. The *Bl* 1821L ultracentrifuged preparation (200 µl) was applied on top of each group of sucrose density gradient and centrifuged at a high speed of 35,000 rpm (151,263 x g) in a swing bucket rotor (41Ti, Beckman) for 70 min to concentrate the putative antibacterial proteins.

For loading the sucrose gradients, CFS derived from *Bl* 1821L mitomycin C (Sigma) induced culture without ultracentrifugation were independently applied (200 µl) at the top of both the groups of the sucrose density gradients. The *Bl* 1821L uninduced (without mitomycin C) culture was ultracentrifuged @ 35,000 rpm (151,263 x g) in a swing bucket rotor (41Ti, Beckman) for 70 min to concentrate the

putative antibacterial proteins. The concentrated pellet was further subjected to sucrose density gradient centrifugation for purification as performed for the mitomycin C (Sigma) induced cultures.

Like *Bl* 1821L, *Bl* 1951 cultures with/without mitomycin C (Sigma) induction were subjected to sucrose density gradient purification after ultracentrifugation. In addition, similar to *Bl* 1821L, CFS derived from mitomycin C (Sigma) induction was also purified using sucrose density gradient centrifugation. A schematic flow chart of putative antibacterial proteins purification using the sucrose density gradient centrifugation method is illustrated in Figure 5.2. The resultant protein concentration was determined through a Qubit protein assay kit (Thermo Fisher Scientific) as described above (Section 5.2.1B).

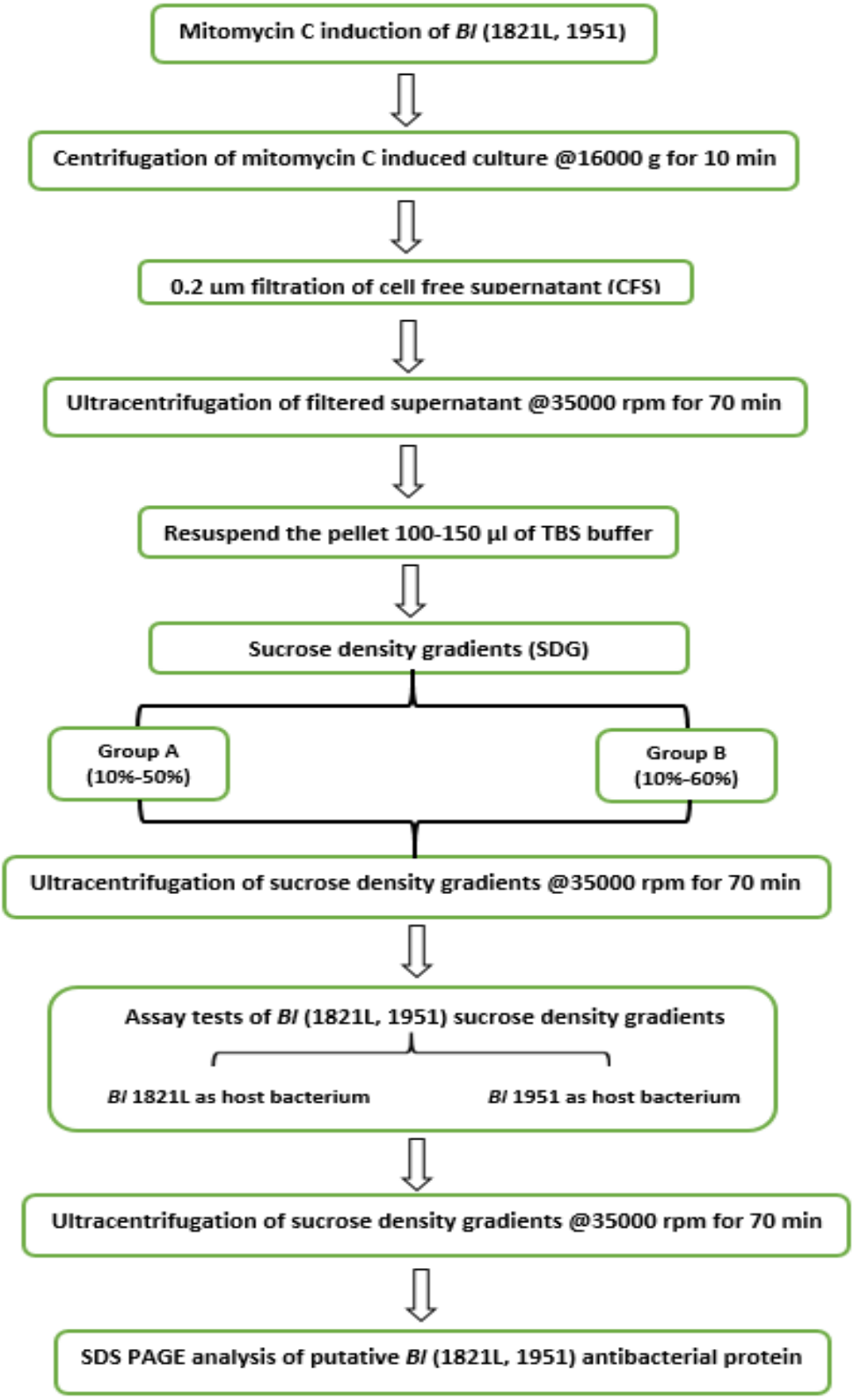

Figure 5.2 Flow chart of *BI* (1821L, 1951) putative antibacterial proteins purification using sucrose density gradient centrifugation

A. Assay test of sucrose density gradients

Sucrose density layers of *Bl* 1821L and *Bl* 1951 from each gradient were collected and evaluated for their antagonist activities. Antagonistic activity of each gradient was tested against *Bl* 1821L and *Bl* 1951 as the host bacterium through Kirby-Bauer disc diffusion assay as described above (Section 5.2.1A). All the gradients of *Bl* 1821L and *Bl* 1951 were concentrated using the same protocol as stated in Section 5.2.1A. Quantification of *Bl* 1821L and *Bl* 1951 putative antibacterial proteins of each concentrated gradient was performed using a Qubit protein assay kit (Thermo Fisher Scientific) as outlined in Section 5.2.1B.

B. SDS-PAGE analysis of sucrose density gradients

SDS-PAGE of each sucrose density gradient (*Bl* 1821L & *Bl* 1951) of both the groups (Group A 10-50% & Group B 10-60%) was run after concentrating the proteins as described in Chapter 3 (Section 3.2.6) by loading a volume of 20 µl of sample and 3 µl of protein ladder (BIO-RAD, Precision Plus Protein™ Standards) to estimate the molecular mass and purification status of putative antibacterial proteins.

Likewise, SDS-PAGE of *Bl* 1821L and *Bl* 1951 cultures after mitomycin C (Sigma) induction but without ultracentrifugation and cultures (without mitomycin C) but with ultracentrifugation were also developed. For staining, the silver stain method described above (Section 5.2.1C) was used.

C. Transmission electron microscopy of crude *Bl* 1821L and *Bl* 1951 putative antibacterial proteins

TEM analysis of the mitomycin C (Sigma) induced cultures of *Bl* 1821L and *Bl* 1951 after concentrating the putative antibacterial proteins @ 35,000 rpm (151,263 x g) in a swing bucket rotor (41Ti, Beckman) for 70 min was performed at AgResearch, Lincoln, New Zealand as described in Chapter 2 (Section 2.2.9).

D. Putative antibacterial proteins concentration

Purified *Bl* 1821L putative antibacterial proteins of ~30 kD from 20% gradient (Group A) and ~48 kD from 60% gradient (Group B) and for *Bl* 1951 purified protein of ~30 kD from 50% gradient (Group A) were further concentrated and cleaned using an Amicon Ultra-0.5 (10 kD) centrifugal filter (Millipore). Purified sucrose density gradient sample of 500 µl of each protein after ultracentrifugation was added to the Amicon ultra filter device. The capped filter device was placed into the centrifuge rotor and centrifuged @ 14,000 g for 20 min. The centricon was removed from the centrifuge and the Amicon Ultra-0.5 device filter was separated from the microcentrifuge tube. To recover the concentrated

proteins, the Amicon Ultra-0.5 device was placed upside down in a clean microcentrifuge tube and was placed in a centrifuge with an opening cap having alignment towards the centre of the rotor. It was centrifuged @ 1,000 g for 2 min to transfer the concentrated sample (putative antibacterial protein) from the device to the tube.

E. Transmission electron microscopy of *Bl* 1821L and *Bl* 1951 putative antibacterial proteins purified using sucrose density gradient centrifugation

Bl 1821L and *Bl* 1951 purified and 10 kD MWCO (Molecular weight cut off) membrane concentrated sample of 5 µl was subjected to electron microscopic analysis at AgResearch, Lincoln, New Zealand according to the protocol described in Chapter 2 (Section 2.2.9).

5.2.3 Purification of *Bl* 1821L and *Bl* 1951 putative antibacterial proteins using polyethylene glycol precipitation and sucrose density gradient centrifugation

A *Bl* 1821L culture was induced with mitomycin C (Sigma) @ 1 µg/ml to release the putative antibacterial proteins (bacteriocins) as described in Chapter 2 (Section 2.2.6). Mitomycin C (Sigma) induced culture was centrifuged @ 16,000 g for 10 min and the supernatant was passed through a 0.22 µm filter. Polyethylene glycol (PEG 8000) (10%) and 1M NaCl were added to the filtered supernatant. The mixture was incubated in an ice bath for 60 min and subsequently centrifuged @ 16,000 g for 30 min at 4^{o}C. The resultant supernatant was decanted and the pellet was resuspended in 1/10th volume of the original supernatant volume of TBS buffer (10 mM Tris, 10 mM MgSO4, pH 7.0) by repeatedly pipetting. PEG residues were removed by two sequential extractions with an equal volume of chloroform, which was combined with the resuspended pellet and vortexed for 10-15 sec. The mixture was centrifuged @ 16,000 g for 10 min and the upper aqueous phase was transferred to a fresh microcentrifuge tube. This extraction process was repeated until no white interface between the aqueous and organic phases was visible.

PEG 8000 precipitated culture of *Bl* 1821L was transferred into polypropylene centrifuge tubes (Konical, Beckman) and TBS buffer was used to make the final volume of 7.5 ml. *Bl* 1821L precipitated culture was ultracentrifuged in a swing bucket rotor (41Ti, Beckman) @ 35,000 rpm (151,263 x g) for 70 min to concentrate the putative antibacterial proteins. The supernatant was decanted and the concentrated pellet was resuspended in 100-150 µl of TBS buffer. Sucrose density gradient purification of PEG 8000 precipitated culture was performed and concentred as described above (Section 5.2.2). The same approach was used for the PEG 8000 based purification of *Bl* 1951 culture after induction with the

mitomycin C (Sigma) @ 3 µg/ml concentration. A schematic presentation of protein purification using PEG 8000 precipitation is depicted in Figure 5.3.

PEG 8000 precipitated cultures after sucrose density gradient purification with both of the groups were concentrated and the resultant samples were assessed by SDS-PAGE of each *Bl* 1821L and *Bl* 1951 gradient as outlined above (Section 5.2.1C) by loading a volume of 20 µl of sample and 3 µl of protein ladder (BIO-RAD, Precision Plus Protein^{TM} Standards) to estimate the molecular mass and purification status of putative antibacterial proteins.

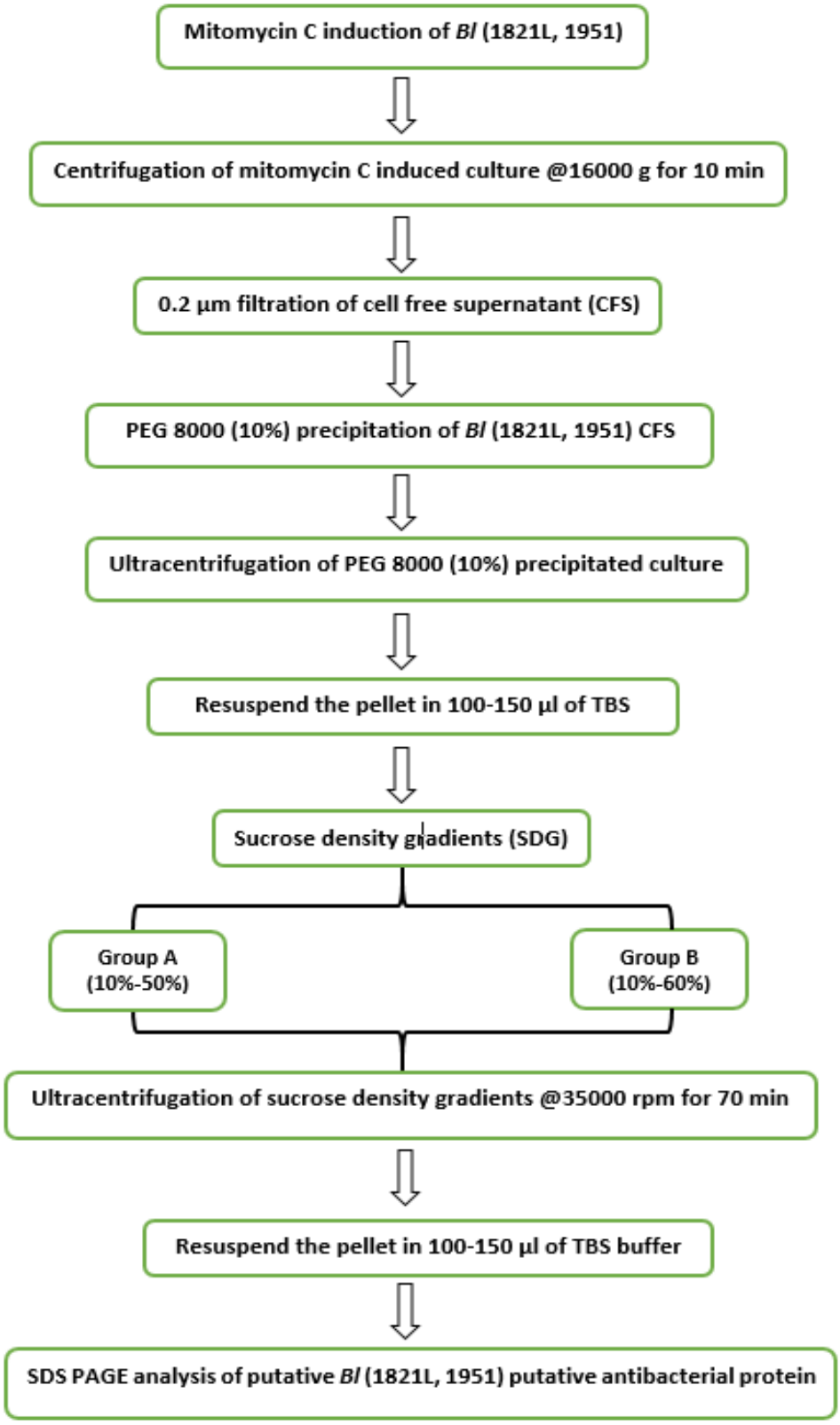

Figure 5.3 Flow chart of *Bl* (1821L, 1951) putative antibacterial proteins purification using polyethylene glycol precipitation and sucrose density gradient centrifugation

5.2.4 Purification of *Bl* 1821L and *Bl* 1951 putative antibacterial proteins using ammonium sulphate precipitation and sucrose density gradient centrifugation

A *Bl* 1821L culture was induced with the mitomycin C (Sigma) as described in Chapter 2 (Section 2.2.6). The induced culture was transferred into 50 ml tubes and centrifuged @ 10,000 g for 10 min at 4°C to spin down the cells and the supernatant was retained. The supernatant was filtered through a 0.22 µm syringe filter to remove cell debris and the volume of filtrate was measured. The supernatant was transferred into a 100 ml beaker with a magnetic stirrer and then the beaker was placed in an ice bucket ensuring that the magnetic stirrer was still stirring. The beaker containing the supernatant was kept chilled and ammonium sulphate crystals were added slowly in batches, taking into consideration that each addition was fully dissolved before adding more. Ammonium sulphate was continuously added until 85% saturation was reached (calculated 85% quantity from http://www.encorbio.com/protocols/AM-SO4.htm). The samples were left on ice for 30 min under slow stirring after the final addition. The solution after reaching saturation looked turbid and the precipitated proteins were harvested by centrifugation @ 10,000 g for 20 min. The supernatant was carefully removed and the pellet was resuspended in 5 ml of phosphate buffer + 150 mM NaCl making sure no undissolved material remained. To remove ammonium sulphate a buffer exchange was undertaken. A large size petri dish was filled with purified water (MQW) and a dialysis tube was submerged into the petri dish until both ends could be opened. One end of the dialysis tube was sealed and the sample was transferred from the other end, which was later closed. One litre of dialysis buffer (pre cooled at 4°C) was transferred into a large beaker (1 L) along with a clean magnetic stirrer. The dialysis tube with the protein precipitate was placed inside the beaker and allowed to stir slowly avoiding foaming. Phosphate buffer (pre cooled at 4°C) was replaced after every three hours. After the third buffer change, the sample within the dialysis tube was transferred into a 15 ml tube and stored at -80°C. Subsequently, precipitates were placed for 2-3 days in a freeze dryer maintained at -80°C.

Ammonium sulphate (85%) precipitated culture of *Bl* 1821L preserved at -80^{0}C was dissolved in TBS buffer and transferred into polypropylene centrifuge tubes (Konical, Beckman) to make the final volume of 7.5 ml. The tubes were placed in a swing bucket rotor (41Ti, Beckman) for high-speed centrifugation @ 35,000 rpm (151,263 x g) for 70 min to concentrate putative antibacterial proteins. The concentrated pellet was resuspended in 100-150 µl of TBS buffer. Sucrose density gradient purification of ammonium sulphate precipitated (85%) culture was performed and concentred as described in Section 5.2.2. Similarly, *Bl* 1951 culture after induction with the mitomycin C (Sigma) at a concentration of 3 µg/ml was used for ammonium sulphate precipitation (85%) and further purification with sucrose density gradient centrifugation. A schematic presentation of protein purification using ammonium sulphate precipitation (ASP 85%) is shown in Figure 5.4.

Ammonium sulphate precipitated (85%) cultures of *Bl* 1821L and *Bl* 1951 after sucrose density gradient centrifugation with both the groups were concentrated and the resultant samples were assessed by SDS-PAGE of each *Bl* 1821L and *Bl* 1951 gradient as outlined above (Sections 5.2.1C) by loading a sample of 20 µl and 3 µl of protein ladder (BIO-RAD, Precision Plus Protein™ Standards) to estimate the molecular mass and purification status of putative antibacterial proteins.

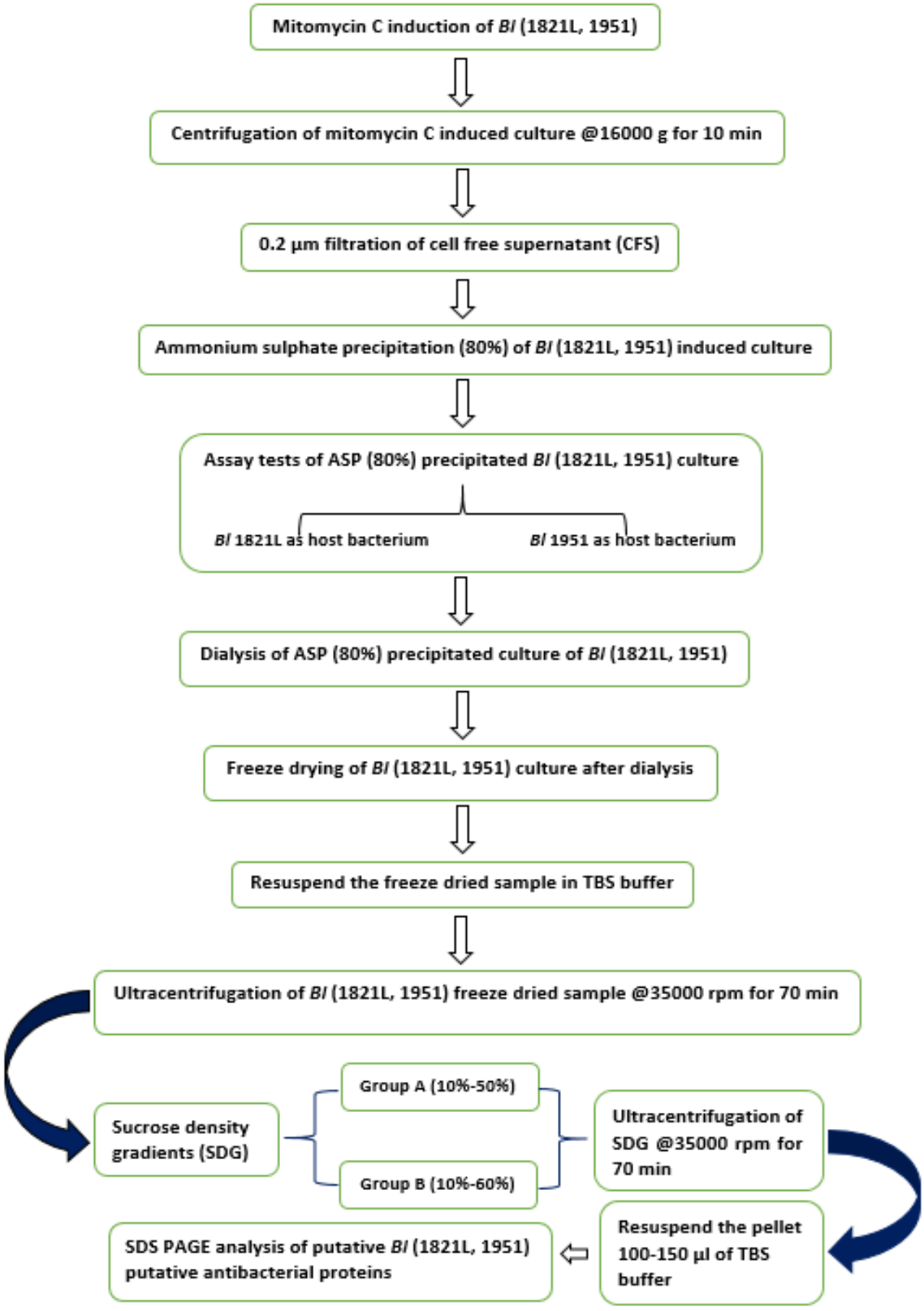

Figure 5.4 Flow chart of *Bl* (1821L, 1951) putative antibacterial proteins purification using ammonium sulphate precipitation and sucrose density gradient centrifugation

5.3 Results

5.3.1 Purification of *Bl* 1821L putative antibacterial proteins using SEC

SEC of crude *Bl* 1821L proteins at the end provided 61 fractions but the putative antibacterial activity was found in fractions 1-31 of the chromatogram as shown in Figure 5.5.

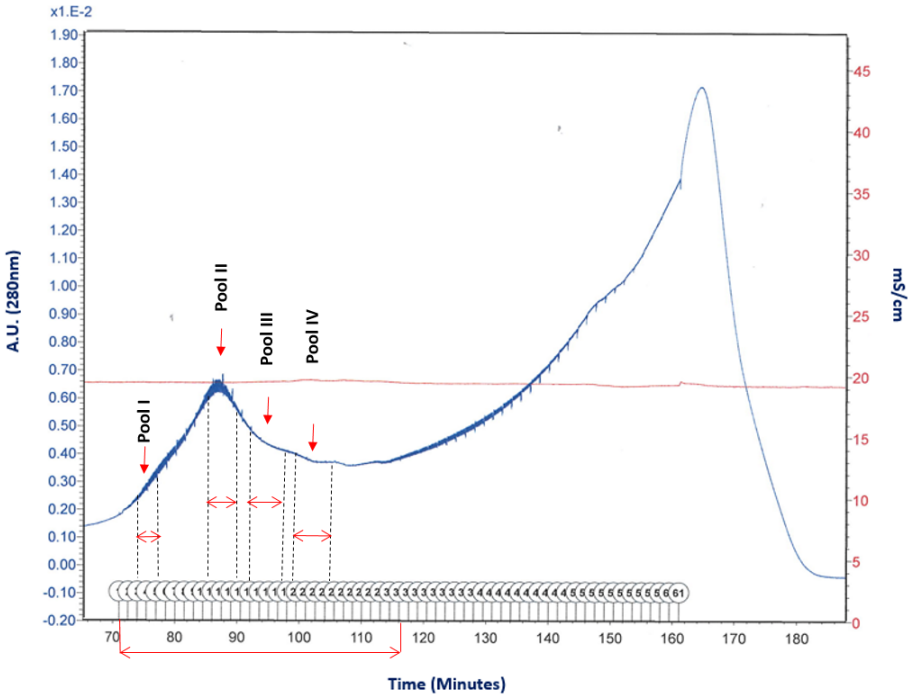

Figure 5.5 *Bl* 1821L size exclusion chromatograph of the ultracentrifuged supernatant of mitomycin C induced culture. SEC fractions (pooled) showing putative antibacterial activity upon assessment in the disc diffusion assay are indicated

5.3.2 Assay test of *Bl* 1821L SEC fractions

All 61 fractions were tested through the Kirby-Bauer disc diffusion test for their antagonistic activity against *Bl* 1821L and *Bl* 1951 as the host bacteria. A prominent zone of inhibition was observed when using 32 of the SEC fraction against *Bl* 1821L while 27 fractions inhibited the growth of *Bl* 1951 (Table 5.1). Fractions exhibiting prominent activities were pooled (Table 5.2 & Figure 5.5). Assay test results exhibited pronounced activity differences among the pooled groups as shown in Table 5.2. Pooled I fractions (3, 4, 5) demonstrated antibacterial activity against both *Bl* 1821L and *Bl* 1951, but the pooled fractions II (11, 12, 13, 14, 15) and III (16, 17, 18, 19) had antagonistic activities only against the *Bl* 1821L. Pooled IV fractions (20, 21, 22, 23, 24) displayed antibacterial activity only against *Bl* 1951, except fraction no. 21 which was active against both the hosts (*Bl* 1821L & *Bl* 1951) (Table 5.2 & Figure 5.5).

Protein contents of all the active fractions (pooled) were measured (Table 5.2) using a Qubit protein assay kit (Thermo Fisher Scientific). Quantification of *Bl* 1821L putative antibacterial proteins illustrated that the pool IV fractions contained the highest protein contents (Table 5.3).

Table 5.1 *Bl* 1821L size exclusion chromatography active fractions of the assay test

Host bacterium	Size exclusion chromatographic fractions	Total fractions
Bl 1821L as the host bacterium	2, 3, 4, 5, 6, 7, 8, 9, 10, 11, 12, 13, 14, 15, 16, 17, 18, 19, 21, 26, 27, 34, 37 , 39, 40, 41, 42, 45, 49, 52, 53, 55, 58	32
Bl 1951 as the host bacterium	2, 3, 4, 5, 7, 8, 10, 20, 21, 22, 23, 24, 25, 26, 27, 28, 29, 30, 31, 32, 41, 42, 47, 49, 52, 59, 61	27

Table 5.2 *Bl* 1821L putative antibacterial proteins assay test and quantification of SEC fractions

Pooled fractions group	SEC fractions no.	Protein concentration (µg/ml)	Zone of inhibition diameter (mm)	
			***Bl* 1821L as host bacterium**	***Bl* 1951 as host bacterium**
Pooled I	3	16.2	16.0	15.0
	4	13.3	14.0	14.0
	5	16.4	14.0	16.0
Pooled II	11	13.1	12.0	-
	12	14.9	13.0	-
	13	13.5	13.0	-
	14	15.9	15.0	-
	15	17.9	13.0	-
Pooled III	16	17.7	14.0	-
	17	19.0	15.0	-
	18	54.1	15.0	-
	19	20.4	14.0	-
Pooled IV	20	19.2	-	13.0
	21	20.4	12.0	14.0
	22	19.2	-	12.0
	23	26.8	-	12.0
	24	19.7	-	12.0

Table 5.3 *Bl* 1821L size exclusion chromatography fractions pooling for SDS-PAGE analysis

Pooled	Size exclusion chromatography pooled fractions	Protein content (µg/ml)
Pooled I	3-5	152
Pooled II	11-14	163
Pooled III	15-19	159
Pooled IV	20-24	167

5.3.3 SDS-PAGE analysis of *Bl* 1821L putative antibacterial proteins purified using size exclusion chromatography

SDS-PAGE analysis of *Bl* 1821L putative antibacterial proteins purified using SEC showed two prominent bands of ~30 kD and ~48 kD molecular mass. Pooled fractions II and III indicated both the protein bands while pooled fraction IV displayed a prominent protein of ~30 kD (Figure 5.6). No protein was observed on the SDS-PAGE of pooled fraction I (Figure 5.6), although the protein was present (Table 5.3).

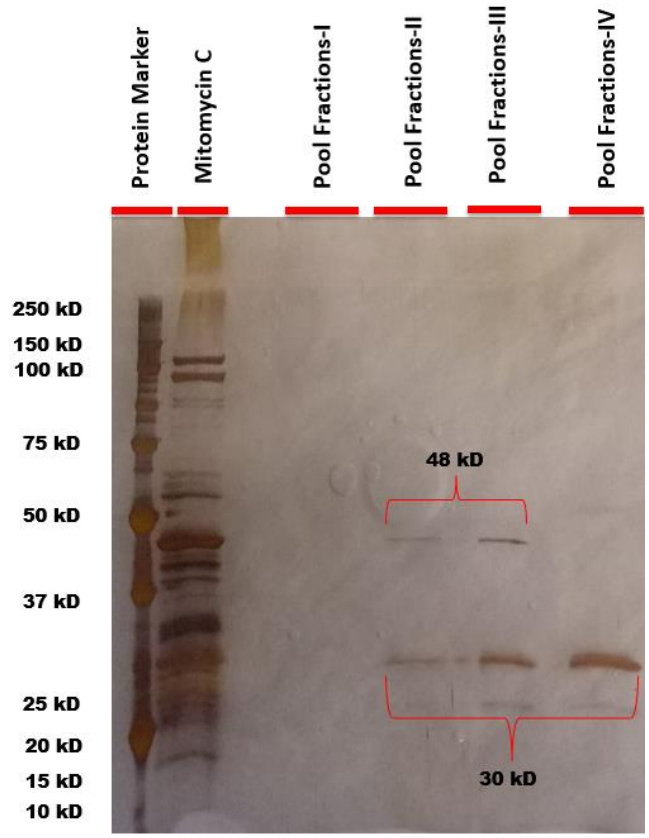

Figure 5.6 SDS-PAGE analysis of *Bl* 1821L putative antibacterial proteins purified using size exclusion chromatography (See Table 5.2 for fraction numbers of pooled samples & TEM images of purified putative antibacterial proteins in Figs. 5.7A-B)

5.3.4 Transmission electron microscopy of *Bl* 1821L putative antibacterial proteins purified using size exclusion chromatography

Purification of putative antibacterial proteins of *Bl* 1821L using SEC yielded two prominent bands of ~30 kD and ~48 kD (Figure 5.6). SEC pooled III and pooled IV fractions were used for TEM analysis. Electron micrograph of negatively stained pooled III fraction showed a hollow tube-like structure (Figure 5.7A) and in the pooled IV fraction (~30 kD) hexagonal phage capsid-like structures of uniform sizes were seen (Figure 5.7B).

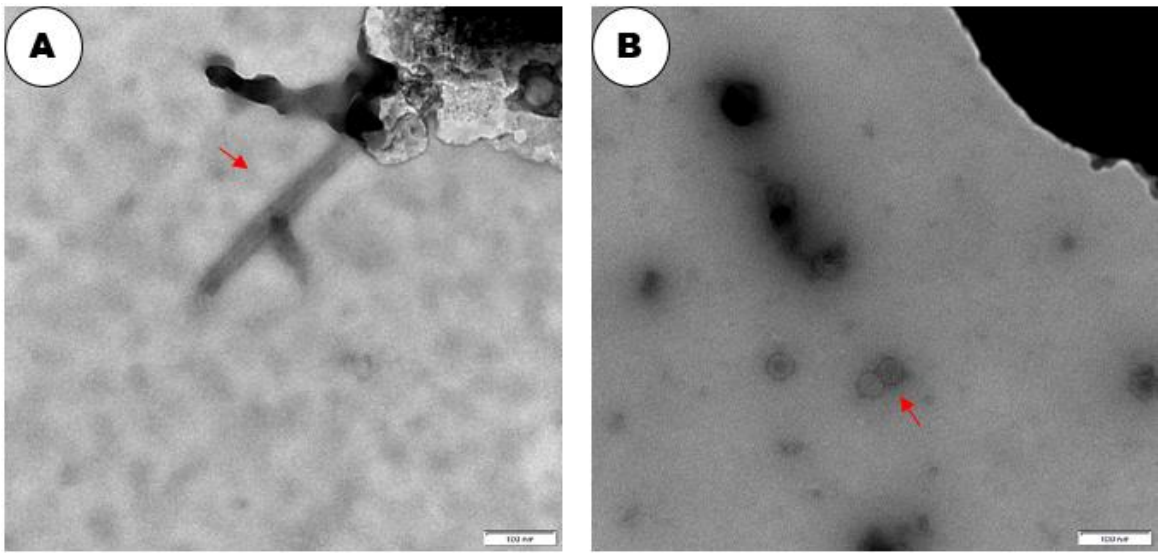

Figure 5.7 Electron micrographs of *Bl* 1821L putative antibacterial proteins purified using size exclusion chromatography. (A) Pooled-III and (B) Pooled-IV of SEC fractions. The red arrows denote a hollow tube-like structure (Fig. 5.7A) and a hexagonal phage capsid-like structure of uniform size (Fig. 5.7B). Scale bar = 100 nm

5.3.5 Purification of *Bl* 1951 putative antibacterial protein using SEC

Of the 61 fractions of *Bl* 1951 collected, SEC fractions indicated that the initial 6-22 fractions (Figure 5.8) displayed prominent antagonistic activity. Protein contents of SEC purified and concentrated fractions (Table 5.5) were determined as outlined in Section 5.2.1B.

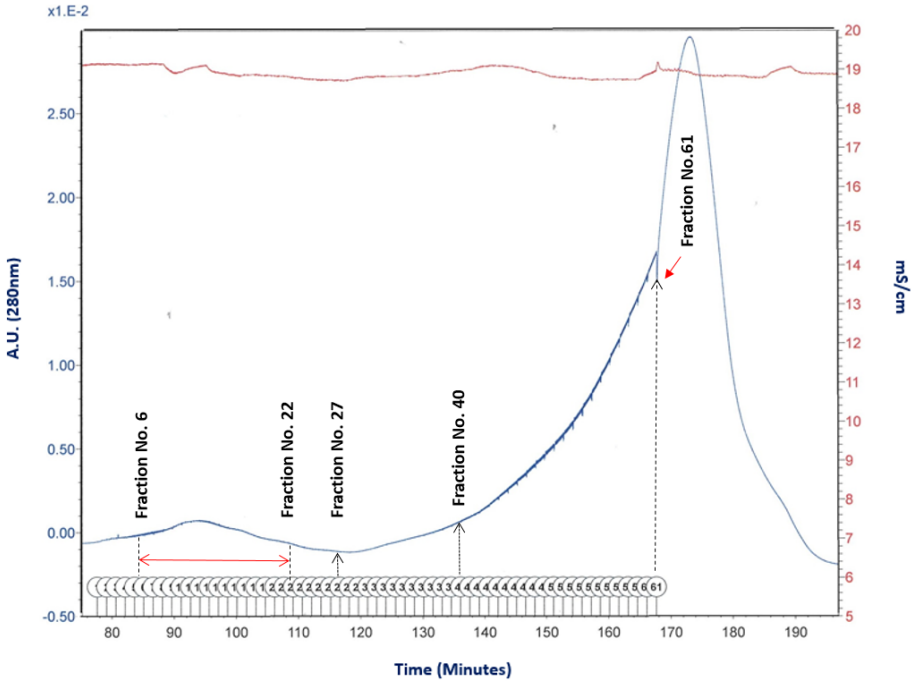

Figure 5.8 *Bl* 1951 size exclusion chromatograph of the ultracentrifuged supernatant of mitomycin C induced culture. SEC fractions showing putative antibacterial activity upon assessment in the disc diffusion assay are indicated

5.3.6 Assay test of *Bl* 1951 SEC fractions

Bl 1951 SEC also comprised 61 fractions, which similar to the *Bl* 1821L SEC derived fractions, were evaluated for activity against *Bl* 1951 and *Bl* 1821L as the host bacterium. Antagonistic activity was observed in 16 fractions against *Bl* 1951 and 11 fractions against *Bl* 1821L as the host bacterium (Table 5.4). Unexpectedly, while assessing the inhibitory activity of *Bl* 1951 SEC fractions (11, 12, 13, 14, 15, 21, 40) against *Bl* 1821L, instead of producing a prominent zone of inhibition, growth of the host bacterium around the antibiotic discs was observed (Figure 5.9). These growing cells might be resistance cells, technically termed "persister cells". These resistant cells were retrieved and cultivated as an overnight culture. Subsequent assessment of *Bl* 1951 mitomycin C induced filtered supernatant against the cultivated lawn of *Bl* 1821L persister cells produced a prominent zone of inhibition which suggests their transient nature *i.e.* as shown by the loss of resistance (Figure 5.10).

Table 5.4 *Bl* 1951 size exclusion chromatography active fractions using disc assay test

Host bacterium	Size exclusion chromatographic fractions	Total fractions
Bl 1951 as the host bacterium	6, 9, 16, 21, 22, 27, 28, 31, 34, 40, 47, 50, 52, 55, 58, 61	16
Bl 1821L as the host bacterium	8, 10, 11, 12, 13, 14, 15, 16, 18, 19, 40	11

Table 5.5 *Bl* 1951 putative antibacterial proteins assay test and quantification of SEC fractions

SEC fractions no.	Protein concentration (µg/ml)	Zone of inhibition diameter (mm)	
		***Bl* 1951 as host bacterium**	***Bl* 1821L as host bacterium**
12	300	-	12.5
13	308	-	13.0
14	280	-	12.0
15	292	-	14.0
18	310	-	13.0
21	276	13.5	-
22	318	12.5	-
27	262	14.0	-
28	308	12.0	-
40	324	-	11.0
61	368	13.0	-

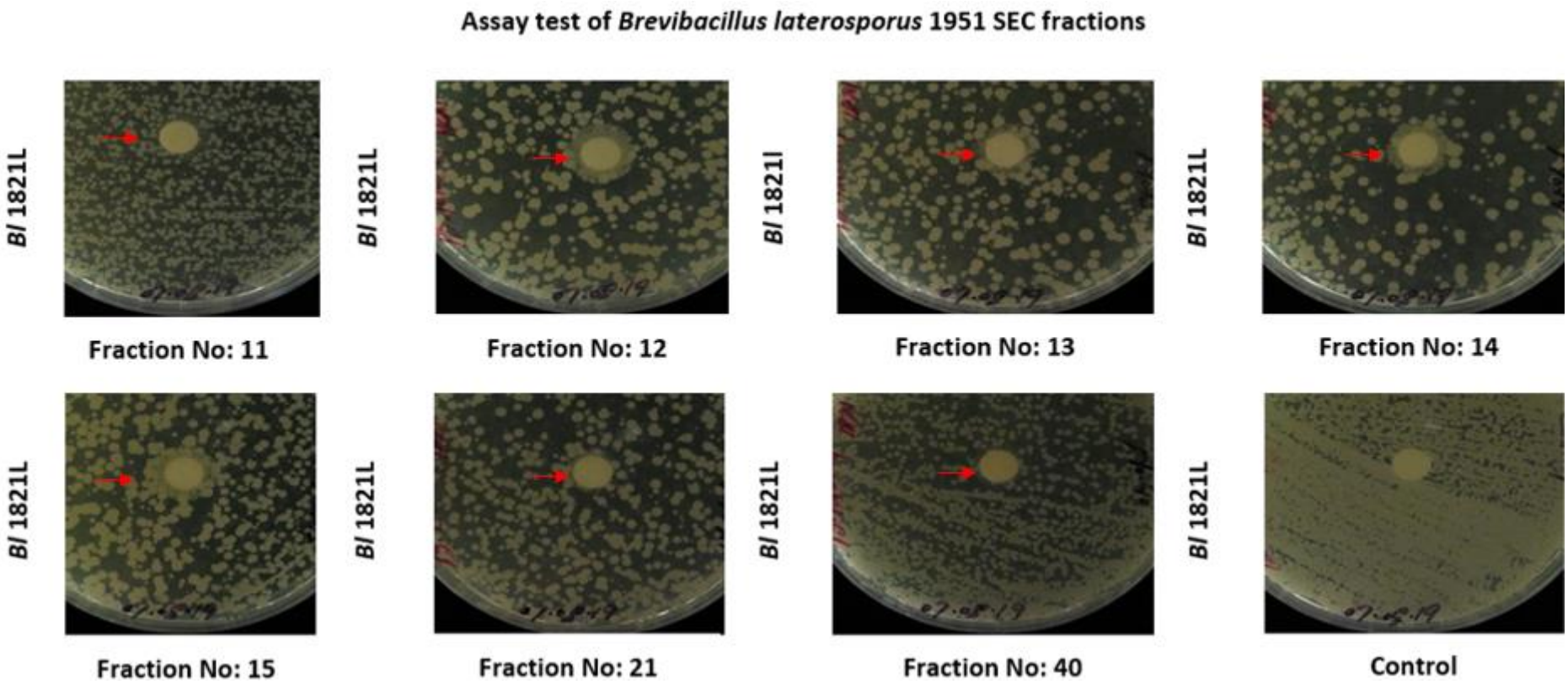

Figure 5.9 Assay test of *Bl* 1951 size exclusion chromatographic fractions against *Bl* 1821L as the host bacterium. The red arrow denotes the formed persister cells

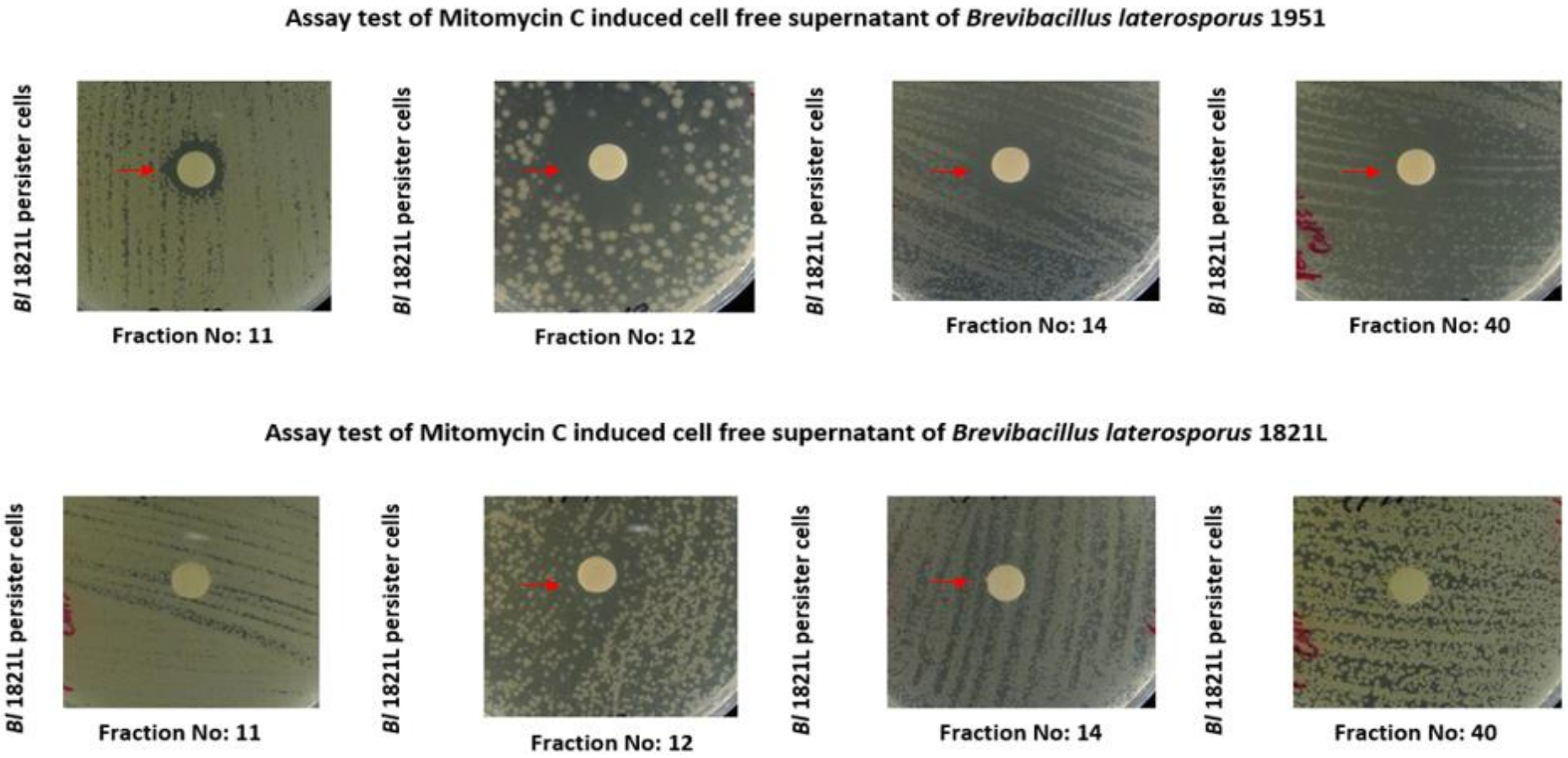

Figure 5.10 Assay test of *Bl* 1821L and *Bl* 1951 mitomycin C induced cell free supernatants against *Bl* 1821L persister cells. The red arrow denotes the zone of inhibition due to the activity of mitomycin C induced cell free supernatants against the *Bl* 1821L persister cells

5.3.7 SDS-PAGE analysis of *Bl* 1951 putative antibacterial protein purified using size exclusion chromatography

Similar to *Bl* 1821L, some of the *Bl* 1951 SEC fractions (12, 13, 14, 15, 40) were active against *Bl* 1821L and some (18, 21, 22, 27, 28, 61) active against *Bl* 1951 (Table 5.5 & Figure 5.8). Assessment of these fractions by SDS-PAGE revealed the presence of a shared ~30 kD protein (Figures 5.11A-B).

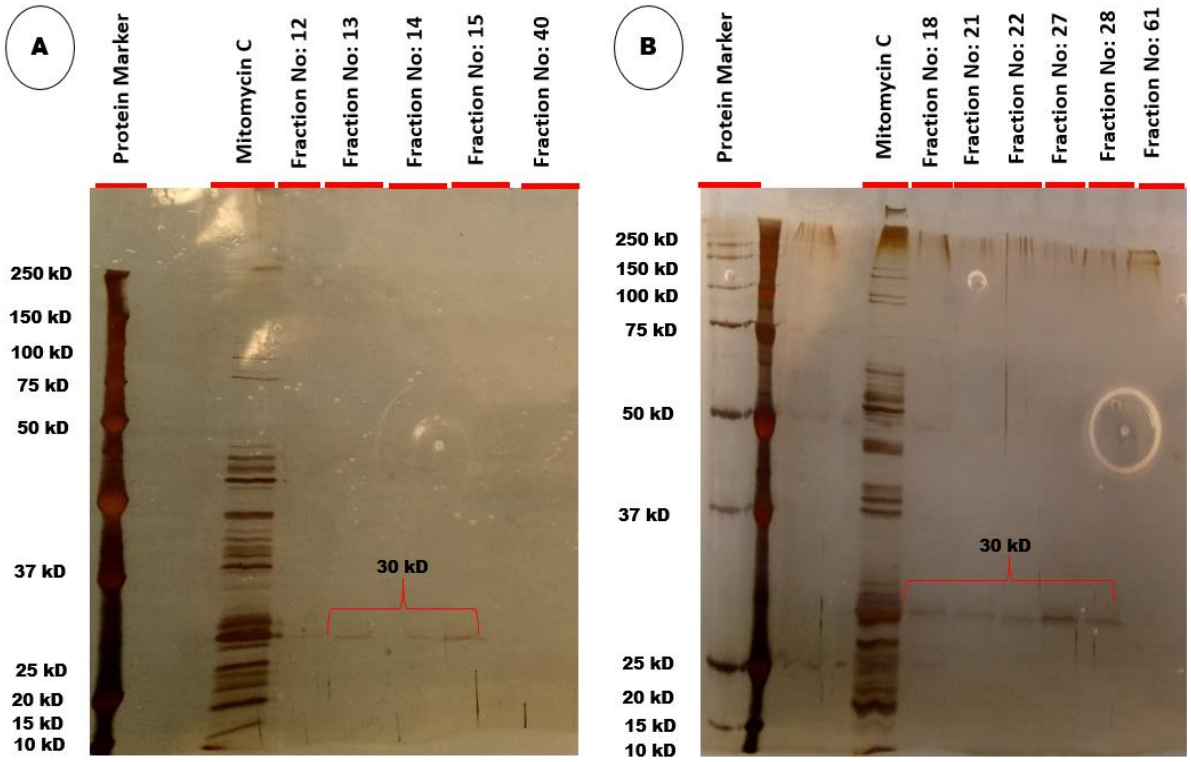

Figure 5.11 SDS-PAGE analysis of *Bl* 1951 putative antibacterial protein purified using size exclusion chromatography. (A) SEC fractions 12, 13, 14, 15, 40 and (B) SEC fractions 18, 21, 22, 27, 28, 61 (See SEC chromatogram Fig. 5.8 & TEM images of purified fractions no. 15 and no. 27 in Figs. 5.12A-B)

5.3.8 Transmission electron microscopy of *Bl* 1951 putative antibacterial protein purified using size exclusion chromatography

SDS-PAGE of purified *Bl* 1951 putative antibacterial protein indicated a band of ~30 kD molecular mass among the active fractions. Purified fractions no. 15 and no. 27 were subjected to electron microscopic examination from where hexagonal phage capsid-like structures of a consistent size were observed in both fractions (Figures 5.12A-B).

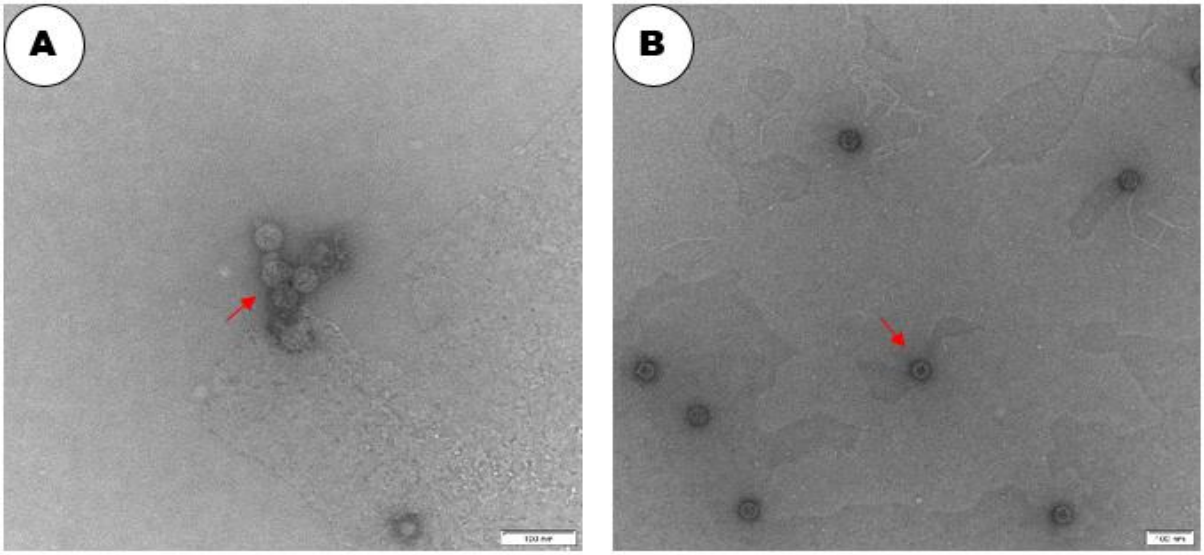

Figure 5.12 Electron micrographs of *Bl* 1951 putative antibacterial protein purified using size exclusion chromatography. (A) SEC fraction no. 15 and (B) SEC fraction no. 27. The red arrows denote uniform sized phage capsid-like structures (Figs. 5.12A-B). Scale bar = 100 nm

5.3.9 Assay test of *Bl* 1821L sucrose density gradients

Antibacterial activity of *Bl* 1821L group A gradients (10-50%) showed narrow zones of inhibition (9-10.5 mm) against *Bl* 1821L as the host bacterium (Table 5.6). While parallel assessments of the group B gradients (10-60%) showed zones of inhibition that varied from 9-14 mm (Table 5.7). However, for *Bl* 1951 as the host bacterium treatment with the purified sucrose A and B gradients of both the groups resulted in similar halo sizes (Tables 5.6 & 5.7).

5.3.10 Protein quantification using Qubit protein assay kit

Protein contents of group A (10-50%) gradients varied from 74.9-116 µg/ml. The concentrations of proteins in this group showed a steady increase from the top to bottom gradients (Table 5.6). Group B gradients (10-60%) protein contents varied from 84.1-117 µg/ml, but the lowest concentration of protein was recorded at the bottom gradient *i.e.* 60% (Table 5.7).

Table 5.6 *Bl* 1821L putative antibacterial proteins assay test and quantification of group A (10-50%) sucrose density gradients

Sucrose density gradients (%)	Protein concentration (µg/ml)	Zone of inhibition diameter (mm)	
		***Bl* 1821L as host bacterium**	***Bl* 1951 as host bacterium**
10	75.5	9.0	12.5
20	74.9	9.5	12.0
30	89.3	10.5	12.0
40	87.2	9.0	11.5
50	116.0	10.0	10.5

Table 5.7 *Bl* 1821L putative antibacterial proteins assay test and quantification of group B (10-60%) sucrose density gradients

Sucrose density gradients (%)	Protein concentration (µg/ml)	Zone of inhibition diameter (mm)	
		***Bl* 1821L as host bacterium**	***Bl* 1951 as host bacterium**
10	101.0	12.0	9.5
20	117.0	14.0	10.5
30	101.0	12.5	11.0
40	100.0	12.0	11.0
50	90.1	11.0	9.5
60	84.1	9.00	9.0

5.3.11 SDS-PAGE analysis of *Bl* 1821L putative antibacterial proteins purified using sucrose density gradient centrifugation

SDS-PAGE analysis of *Bl* 1821L sucrose density gradients revealed the presence of two protein bands of ~30 kD and ~48 kD. A purified putative antibacterial protein of ~30 kD molecular mass in gradients 20% and 30% of group A (Figure 5.13A) and ~48 kD band can be prominently visualised in 20%, 40%, and 50% gradients (Figure 5.13A). However, purified protein of ~48 kD was also prominently observed in group B gradients (40% to 60%) (Figure 5.13B).

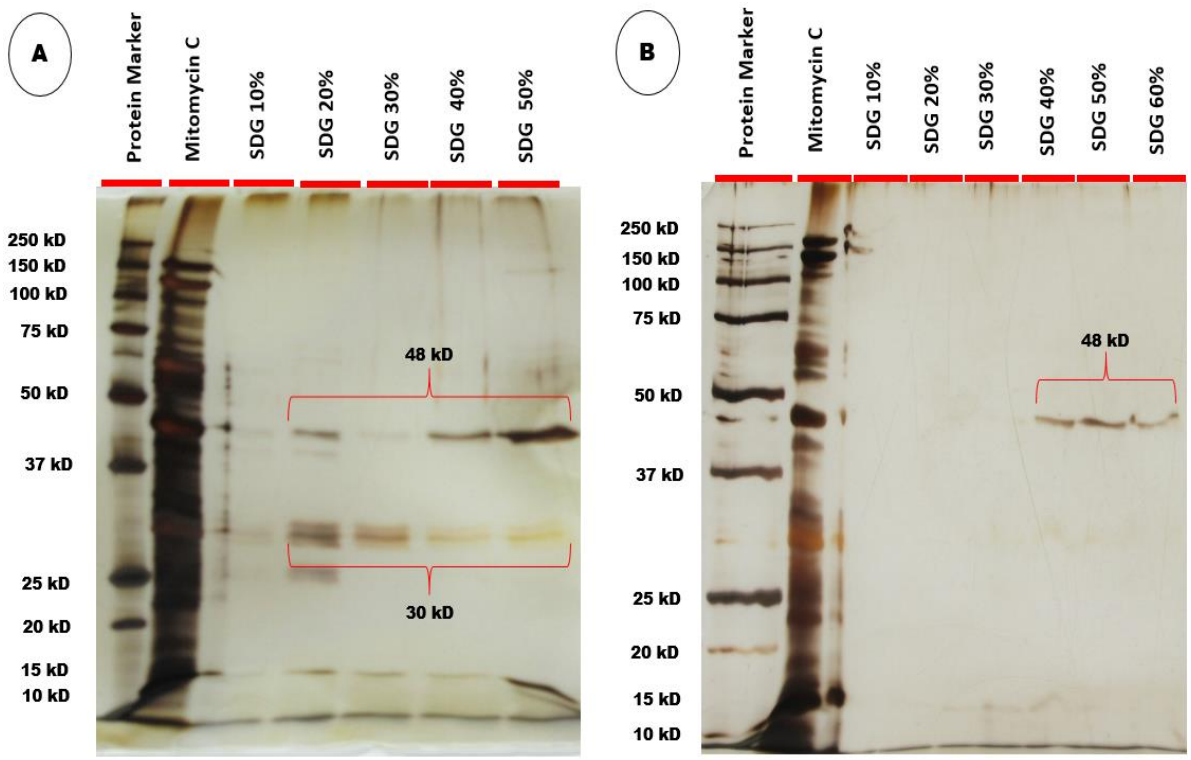

Figure 5.13 SDS-PAGE analysis of *Bl* 1821L putative antibacterial proteins purified using sucrose density gradient (SDG) centrifugation. (A) Group A (10-50%) and (B) group B (10-60%) gradients

5.3.12 SDS-PAGE analysis of *Bl* 1821L putative antibacterial proteins (without mitomycin C) purified using sucrose density gradient centrifugation

SDS-PAGE analysis of uninduced *Bl* 1821L ultracentrifuged supernatant was assessed to define differences between the mitomycin C treated and untreated cultures. A purified protein of ~30 kD was observed on the gel from 20% to 50% gradients of group A (Figure 5.14A). Both the proteins (30 kD & 48 kD) were purified and visible in group B gradients (10-60%) but ~48 kD protein was observed in the gradients 40% to 60% (Figure 5.14B).

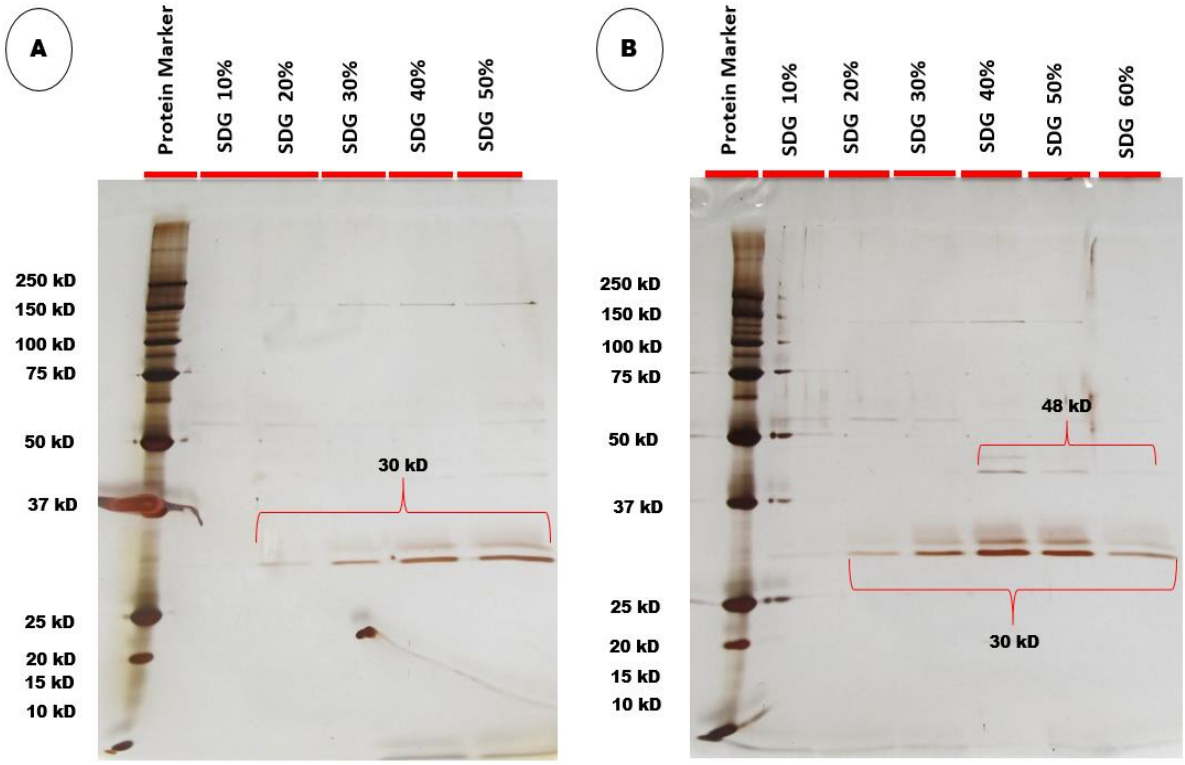

Figure 5.14 SDS-PAGE analysis of *Bl* 1821L putative antibacterial proteins from the culture without mitomycin C treatment purified using sucrose density gradient (SDG) centrifugation. (A) Group A (10-50%) and (B) Group (B) (10-60%) gradients

5.3.13 SDS-PAGE analysis of *Bl* 1821L putative antibacterial proteins from cell free supernatants purified using sucrose density gradient centrifugation

Mitomycin C induced CFS of *Bl* 1821L without high-speed centrifugation was also run on SDS-PAGE with both the groups of gradients and only the ~30 kD protein was visualised in the group A gradients of 30% and 40% (Figure 5.15).

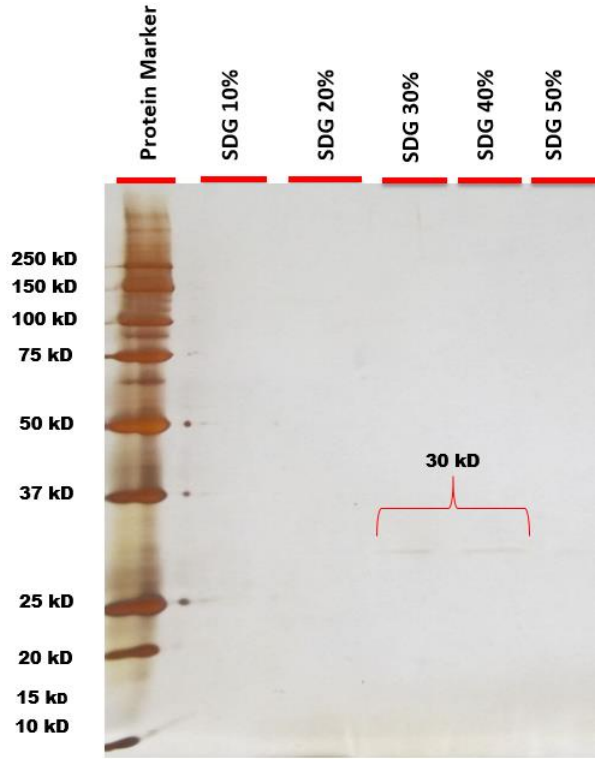

Figure 5.15 SDS-PAGE analysis of *Bl* 1821L (CFS) putative antibacterial protein purified using sucrose density gradients (SDG) centrifugation

5.3.14 Transmission electron microscopy of crude *Bl* 1821L putative antibacterial proteins

Ultracentrifuged *Bl* 1821L filtered supernatant after mitomycin C induction was used as a crude lysate for TEM analysis. Assessment of the electron micrographs revealed that the *Bl* 1821L crude lysate yielded numerous phage structural components. The most numerous particles were contractile sheath-like structures (Figure 5.16E), hollow tubes with one end opening (Figure 5.16C) or two ends opening like a sieve (Figure 5.16B), and hollow tubes at some points were connected through a knot-like structure or without it to form a polysheath (Figures 5.16B-D). In addition to these, cog wheel-like structures (Figure 5.16A) and empty phage head-like hexagonal structures (Figure 5.16E) were often observed.

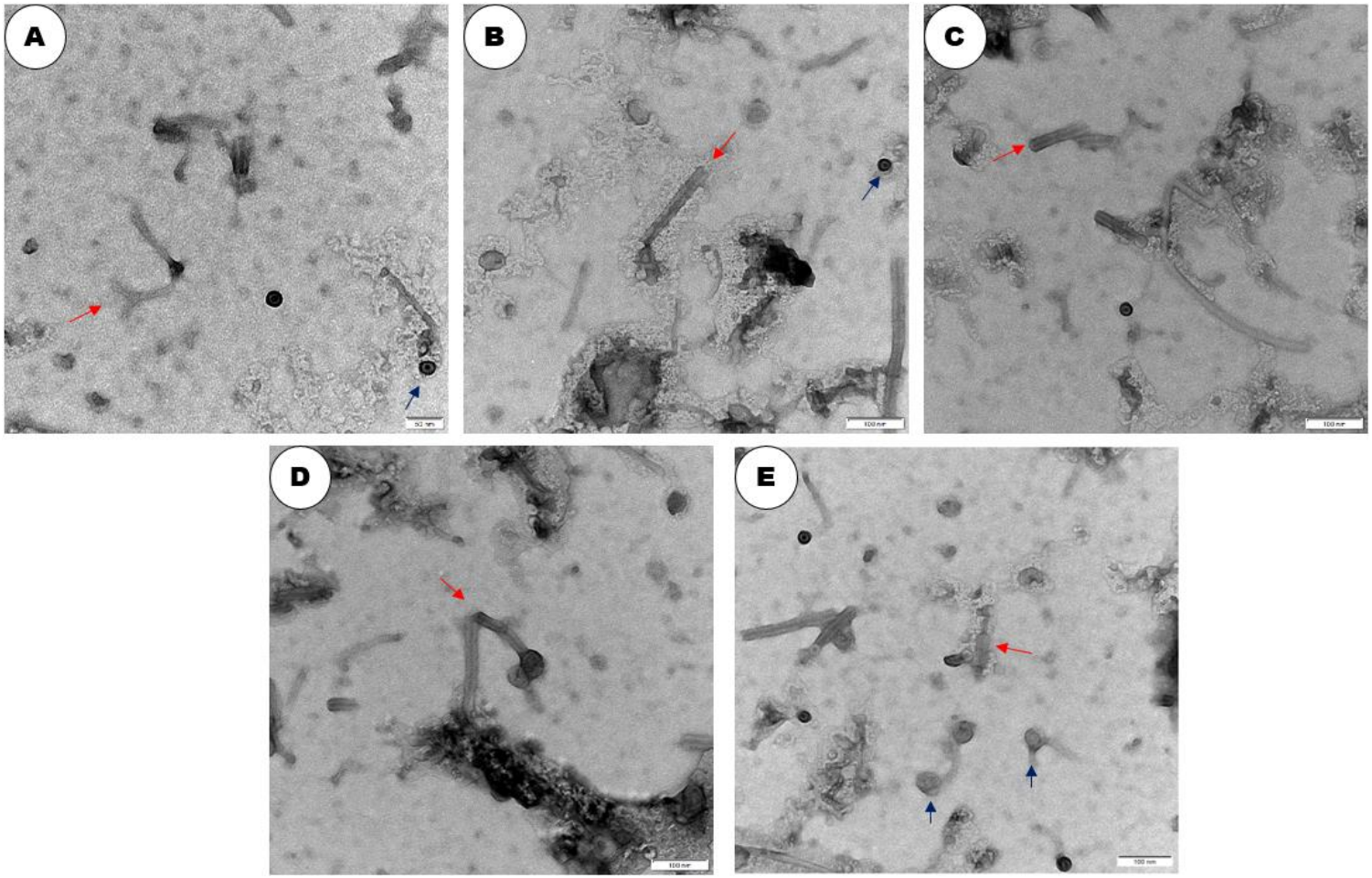

Figure 5.16 Electron micrographs of crude *Bl* 1821L putative antibacterial proteins. The dark blue arrows denote cog wheel-like (Figs. 5.16A-B) and empty phage head-like hexagonal structures (Fig. 5.16E) while the red arrows point the fork-shaped hollow tube (Fig. 5.16A), hollow tube with two end openings (Fig. 5.16B), hollow tube with one end opening (Fig. 5.16C), polysheath-like (Fig. 5.16D), and contractile sheath-like structures (Fig.5.16E). Scale bar A= 50 nm & B, C, D, E= 100 nm

5.3.15 Transmission electron microscopy of sucrose density gradient centrifugation purified and 10 kD MWCO membrane concentrated putative antibacterial proteins of *Bl* 1821L

Sucrose density gradient centrifugation purified the two putative antibacterial proteins of ~30 kD and ~48 kD molecular mass. Electron micrographs of the ~30 kD protein predominantly showed the presence of empty round or hexagonal structures that resembled phage capsids (Figures 5.17A-B). Assessments of the TEM images of the purified ~48 kD putative antibacterial protein revealed the presence of long and ordered nanotubular structures similar in form to a "polysheath". Furthermore, analysis uncovered that the hollow tube structures joined each other at various points through knot-like structures (Figure 5.18B) or without these to form the polysheaths (Figures 5.18A, 5.18C-F).

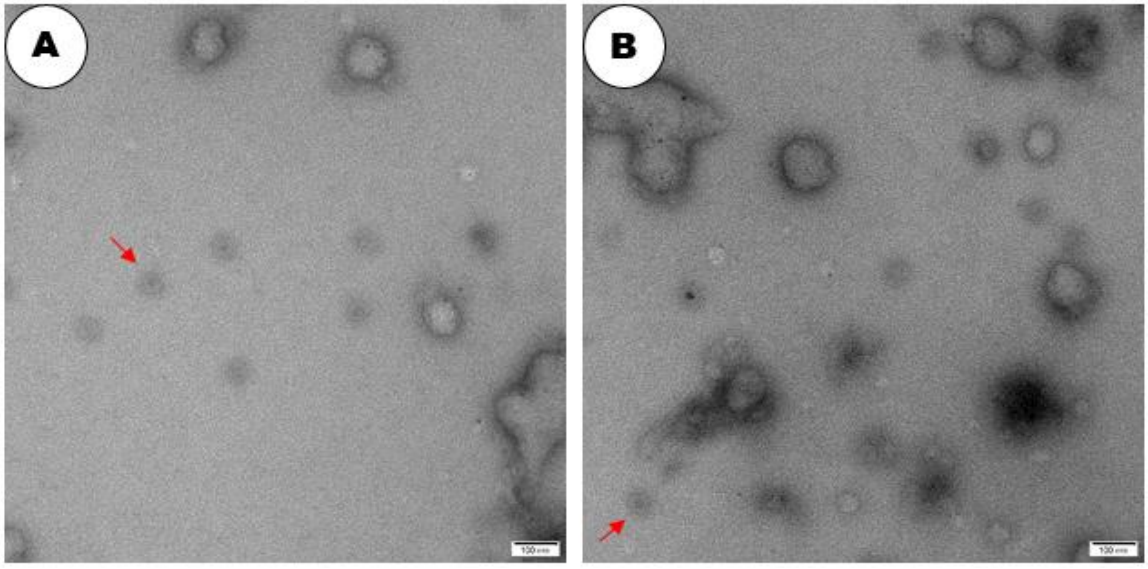

Figure 5.17 Electron micrographs of *Bl* 1821L (30 kD) putative antibacterial protein purified using sucrose density gradient centrifugation. The red arrows denote empty round (Fig. 5.17A) and phage capsid-like structures (Fig. 5.17B). Scale bar= 100 nm

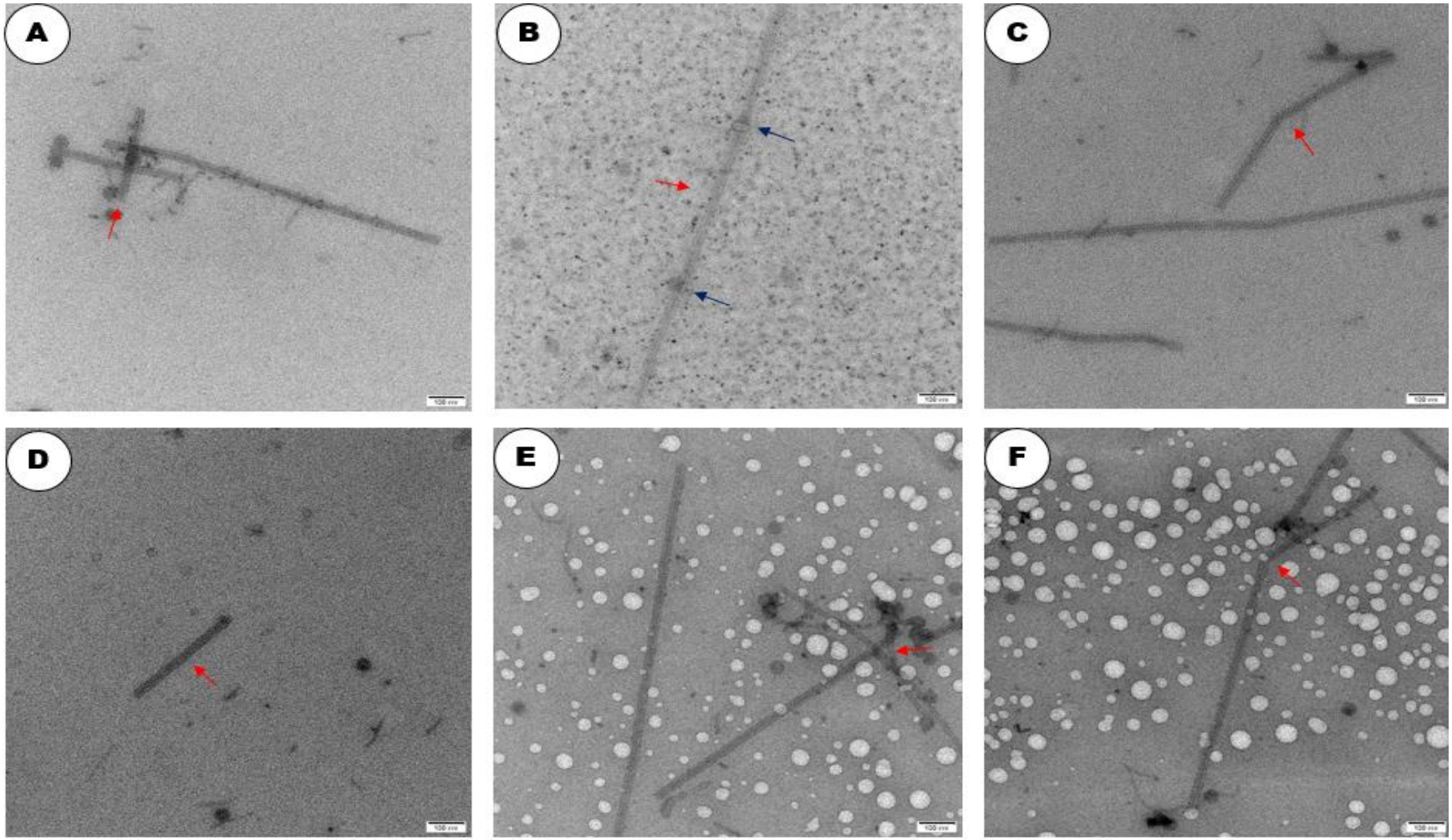

Figure 5.18 Electron micrographs of *Bl* 1821L (48 kD) putative antibacterial protein purified using sucrose density gradient centrifugation. The red arrows denote a long rigid polysheath structure (Figure 5.18A-F), a hollow tube intermittently joined through knot-like structures (Fig. 5.18B shown with dark blue arrow), and without knot-like structures (Fig. 5.18C-D) to form a polysheath. Scale bar= 100 nm

5.3.16 Assay test of *Bl* 1951 sucrose density gradients

Bl 1951 group A sucrose density gradients (10-50%) exhibited similar antagonistic activity against both the hosts (*Bl* 1951 & *Bl* 1821L) causing narrow zones of inhibition (9-11.5 mm) (Table 5.8). Likewise, the activity of the *Bl* 1951 derived group B gradients was similar across all the gradients but slightly differed in activity from each other against the tested bacterium (Table 5.9).

5.3.17 Protein quantification using Qubit protein assay kit

Protein contents of group A gradients (10-50%) varied from 75.2-92.6 µg/ml (Table 5.8) and for group B (10-60%) it ranged from 97.5-119 µg/ml (Table 5.9).

Table 5.8 *Bl* 1951 putative antibacterial protein assay test and quantification of group A (10-50%) sucrose density gradients

Sucrose density gradients (%)	Protein concentration (µg/ml)	Zone of inhibition diameter (mm)	
		***Bl* 1951 as host bacterium**	***Bl* 1821L as host bacterium**
10	88.9	9.5	9.0
20	84.9	9.5	9.5
30	77.7	9.0	9.0
40	75.2	9.5	10.0
50	92.6	9.5	11.0

Table 5.9 *Bl* 1951 putative antibacterial protein assay test and quantification of group B (10-60%) sucrose density gradients

Sucrose density gradients (%)	Protein concentration (µg/ml)	Zone of inhibition diameter (mm)	
		***Bl* 1951 as host bacterium**	***Bl* 1821L as host bacterium**
10	115.0	11.5	10.0
20	97.5	11.5	9.0
30	119.0	11.0	9.0
40	118.0	11.0	10.0
50	111.0	10.5	10.5
60	109.0	10.5	9.0

5.3.18 SDS-PAGE analysis of *Bl* 1951 putative antibacterial protein purified using sucrose density gradient centrifugation

Sucrose density gradient centrifugation purified a putative antibacterial protein of ~30 kD molecular mass from the crude lysate of *Bl* 1951. Excluding the 10% sucrose density gradient of both the groups (A & B) all the gradients purified the active putative antibacterial protein (Figures 5.19A-B), though in Figure 5.19A some other co-purified proteins were also visualised.

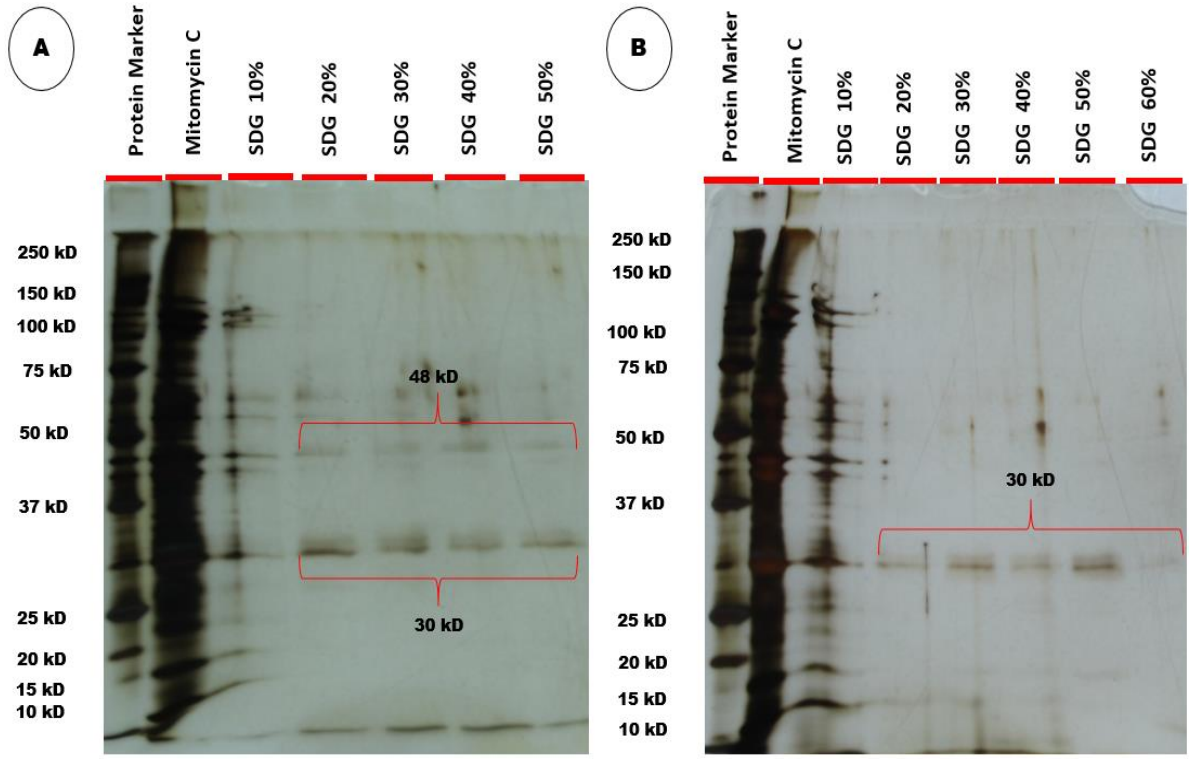

Figure 5.19 SDS-PAGE analysis of *Bl* 1951 putative antibacterial proteins purified using sucrose density gradient (SDG) centrifugation. (A) Group A (10-50%) and (B) Group B (10-60%) gradients

5.3.19 SDS-PAGE analysis of *Bl* 1951 putative antibacterial protein (without mitomycin C) purified using sucrose density gradient centrifugation

Gel electrophoresis of *Bl* 1951 culture without mitomycin C treatment after ultracentrifugation was performed with sucrose density gradients of both the groups (A & B) for purification. Purified protein of ~30 kD molecular mass can be visualised on SDS-PAGE across all the gradients of group A and group B except for the 10% gradient (Figures 5.20A-B). Furthermore, all the sucrose density gradients of group A excluding the uppermost (10%) and group B gradients (40% to 60%) also showed a purified protein of ~48 kD (Figures 5.20A-B).

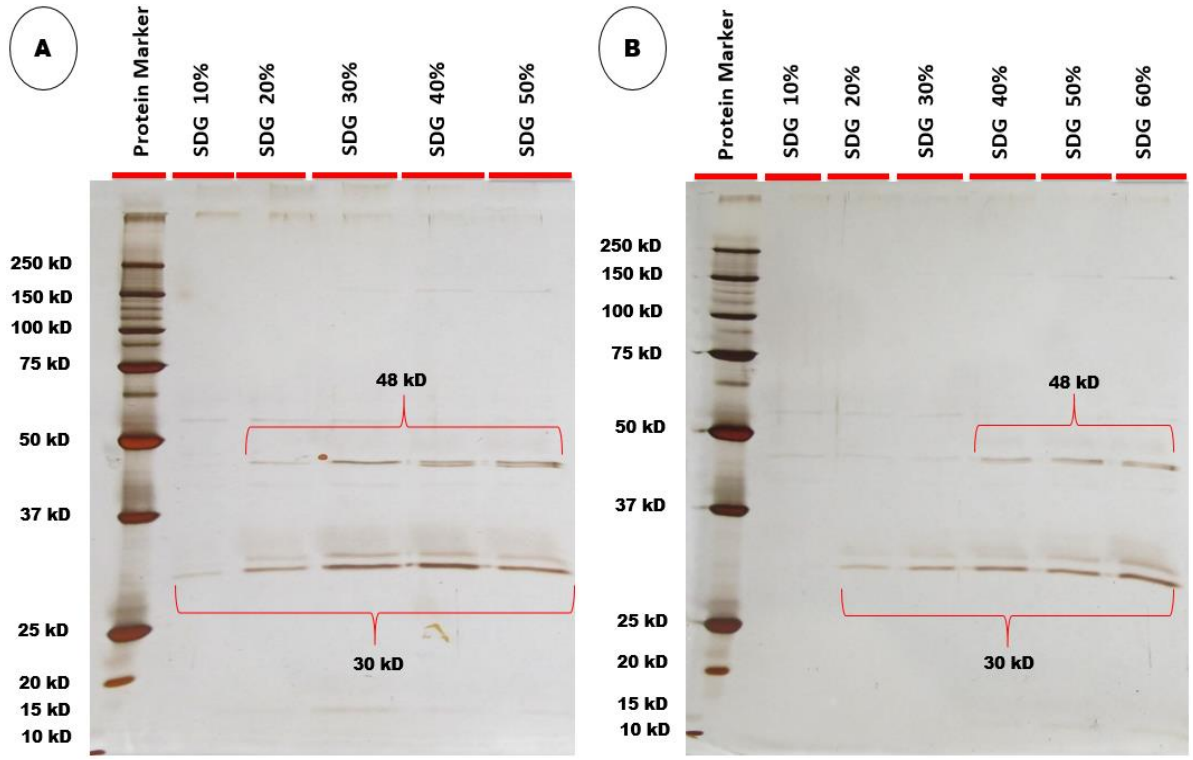

Figure 5.20 SDS-PAGE analysis of *Bl* 1951 putative antibacterial proteins from the culture without mitomycin C treatment purified using sucrose density gradient (SDG) centrifugation. (A) Group A (10-50%) and (B) Group B (10-60%) gradients

5.3.20 SDS-PAGE analysis *Bl* 1951 putative antibacterial protein from cell free supernatant purified using sucrose density gradient centrifugation

The cell free supernatant of *Bl* 1951 mitomycin C induced culture without ultracentrifugation was also run on SDS-PAGE with the gradients of both the groups (A & B) and the two protein bands of ~30 kD and ~48 kD were visualised in the top gradients (10% & 20%) of group B (Figure 5.21). Furthermore, a faint band of ~30 kD protein was also visualised in 40 % gradient of group B (Figure 5.21).

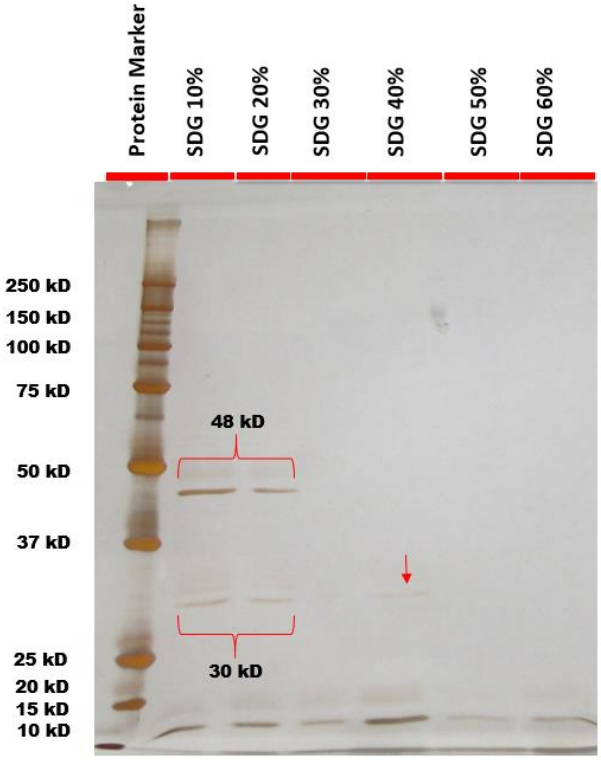

Figure 5.21 SDS-PAGE analysis of *Bl* 1951 (CFS) putative antibacterial protein purified using sucrose density gradient (SDG) centrifugation. The red arrow denotes a faint band of ~30 kD in SDG 40%

5.3.21 Transmission electron microscopy of crude *Bl* 1951 putative antibacterial protein

TEM analysis of crude lysate of *Bl* 1951 showed numerous hollow tube-like structures with both ends opening and polysheaths (Figures 5.22A-B). In addition to, a few empty hexagonal or phage head-like structures were also observed (Figure 5.22A).

5.3.22 Transmission electron microscopy of sucrose density gradient centrifugation purified and 10 kD MWCO membrane concentrated putative antibacterial protein of *Bl* 1951

Purification of putative antibacterial protein of *Bl* 1951 using sucrose density gradient centrifugation revealed a prominent protein of ~30 kD molecular mass. Electron micrographs of purified and 10 kD MWCO membrane concentrated protein of *Bl* 1951 displayed hexagonal phage capsid-like structures and long nanotubes like polysheaths (Figure 5.23A). Polysheaths with intermittent joints through knot-like structures were also observed (Figure 5.23B).

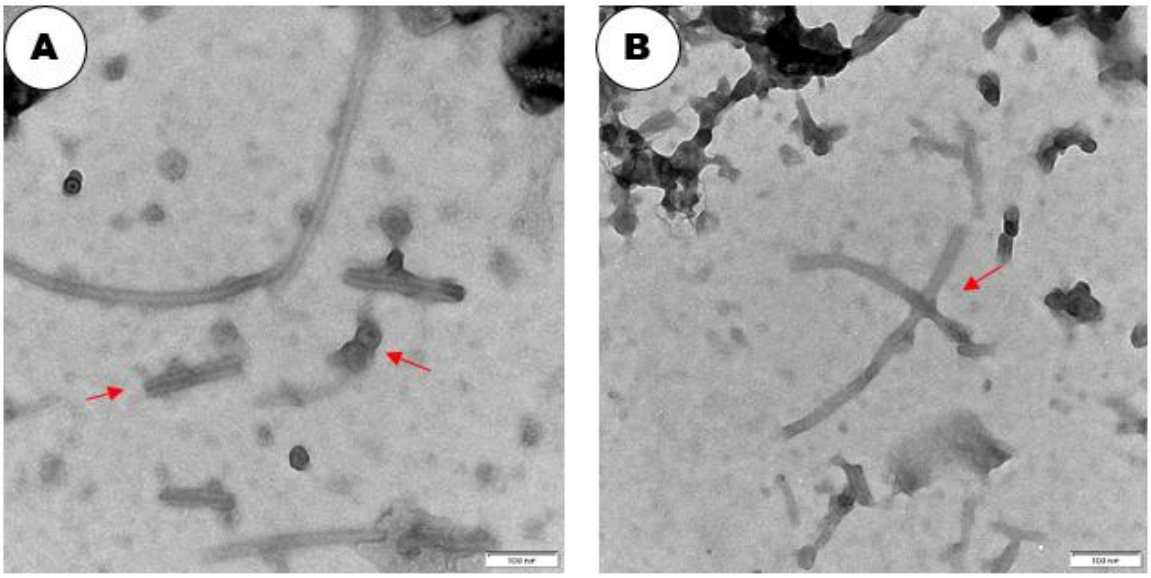

Figure 5.22 Electron micrographs of crude *Bl* 1951 putative antibacterial proteins. The red arrows denote an empty phage head-like structure, a hollow tube-like structure with both ends opening, (Fig. 5.22A), and a polysheath-like structure (Fig. 5.22B). Scale bar = 100 nm

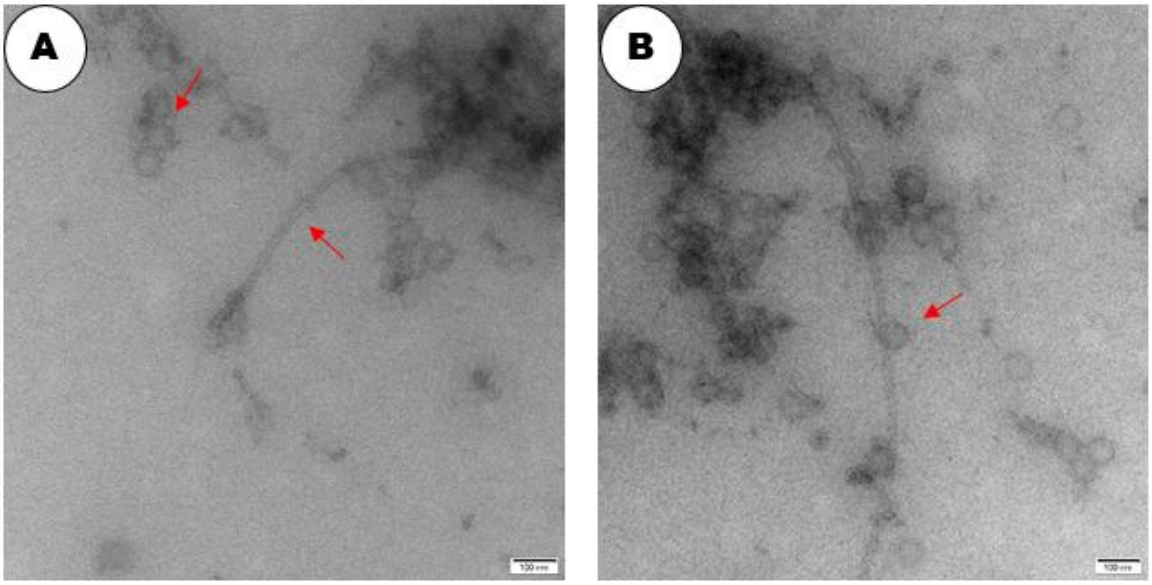

Figure 5.23 Electron micrographs of *Bl* 1951 (~30 kD) putative antibacterial protein purified using sucrose density gradient centrifugation. The red arrows denote phage capsid-like and polysheath-like structures (Fig. 5.23A), and a polysheath-like structure joined at various points through knot-like structures (Fig. 5.23B). Scale bar= 100 nm

5.3.23 SDS-PAGE analysis of sucrose density gradient centrifugation purified and 10 kD MWCO membrane concentrated putative antibacterial proteins of *Bl* 1821L and *Bl* 1951

Sucrose density gradient centrifugation purified and 10 kD MWCO membrane concentrated putative antibacterial proteins of *Bl* 1821L and *Bl* 1951 after TEM analysis were run on the SDS-PAGE to affirm the molecular masses. SDS-PAGE analysis revealed that the purified *Bl* 1821L sample (Group A 20% gradient) observed under TEM (Figures 5.17A-B) was of ~30 kD (Figure 5.24) molecular mass while electron micrographs (Figures 5.18A-F) of group B (60% gradient) exhibited a prominent band of ~48 kD (Figure 5.24). The *Bl* 1951 purified sample analysed under TEM (Figures 5.23A-B) was of ~30 kD molecular mass (Figure 5.25).

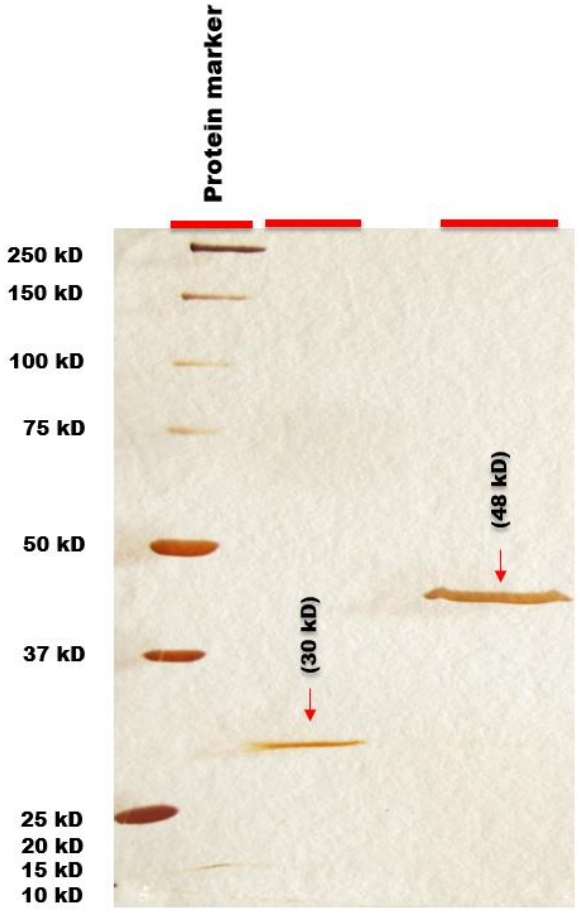

Figure 5.24 SDS-PAGE analysis of *Bl* 1821L sucrose density gradient purified, 10 kD MWCO membrane concentrated, and TEM analysed putative antibacterial proteins (See TEM images of purified ~30 kD (Figs. 5.17A-B) and ~48 kD (Figs. 5.18A-F) putative antibacterial proteins)

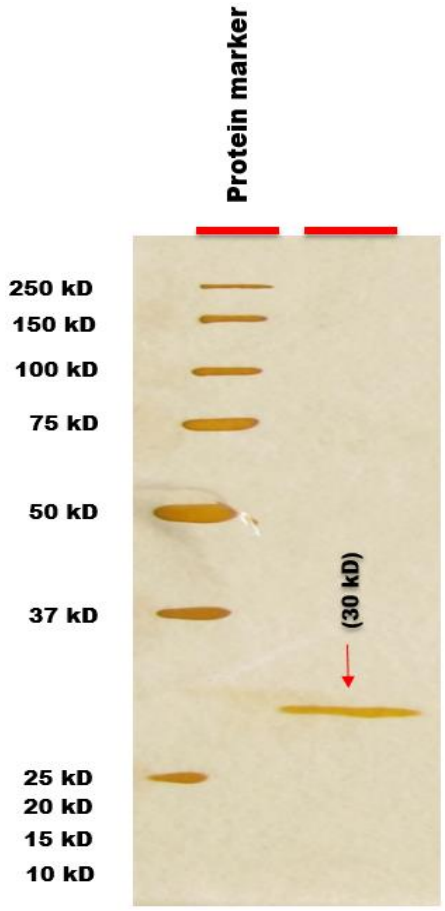

Figure 5.25 SDS-PAGE analysis of *Bl* 1951 sucrose density gradient purified, 10 kD MWCO membrane concentrated, and TEM analysed putative antibacterial protein (See TEM images of purified ~30 kD (Figs. 5.23A-B) putative antibacterial protein)

5.3.24 SDS-PAGE analysis of *Bl* 1821L putative antibacterial proteins purified using polyethylene glycol precipitation and sucrose density gradient centrifugation

Bl 1821L antibacterial proteins were precipitated with PEG 8000 (10%) and further purified using sucrose density gradient centrifugation. Antibacterial proteins of ~30 kD and ~48 kD were purified with group B (10-60%) gradients. The purified band of ~48 kD protein was very minor when compared to ~30 kD and the former was observed only in sucrose density gradients of 40% and 60% (Figure 5.26). Attempts to purify *Bl* 1951 putative antibacterial protein after PEG 8000 (10%) precipitation and further purification using sucrose density gradient centrifugation were not successful.

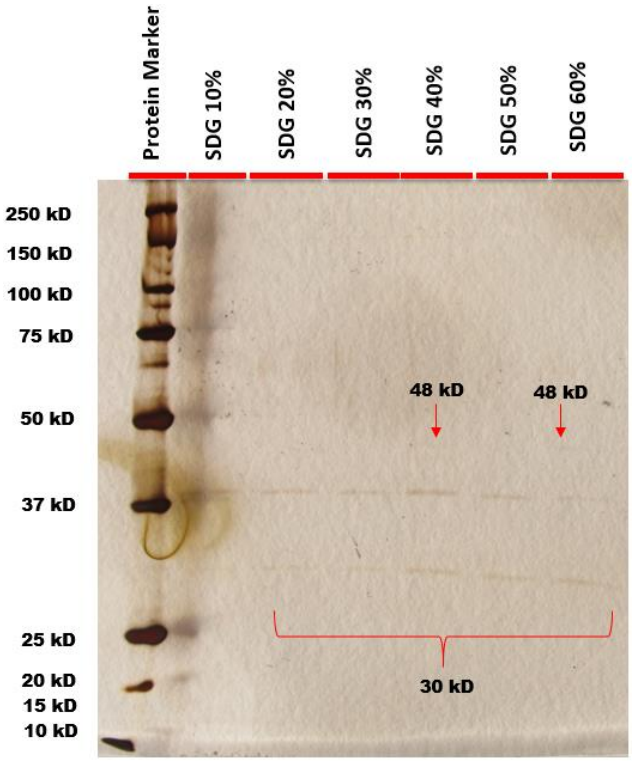

Figure 5.26 SDS-PAGE analysis of *Bl* 1821L putative antibacterial proteins purified using PEG 8000 (10%) precipitation and sucrose density gradient (SDG) centrifugation

5.3.25 SDS-PAGE analysis of *Bl* 1821L putative antibacterial proteins purified using ammonium sulphate precipitation and sucrose density gradient centrifugation

The putative antibacterial proteins of *Bl* 1821L were precipitated with ammonium sulphate (85%) and further purified using sucrose density gradient centrifugation. Group B (10-60%) gradients purified an antibacterial protein of ~50 kD and this protein band was observed on SDS-PAGE in the bottom 50% and 60% gradients (Figure 5.27).

Attempts to purify the ammonium sulphate (85%) precipitated culture of *Bl* 1951 similar to *Bl* 1821L could not be successful.

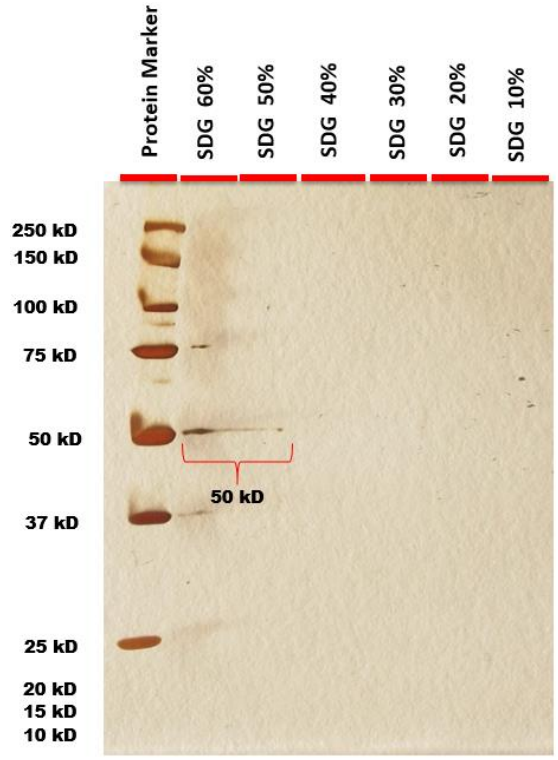

Figure 5.27 SDS-PAGE analysis of *Bl* 1821L putative antibacterial proteins purified using ammonium sulphate (85%) precipitation and sucrose density gradient (SDG) centrifugation

5.4 Discussion

Protein purification is an intrinsic step to understand the nature of a targeted protein (Roy et al., 2007). Therefore, various methods such as size exclusion chromatography, sucrose density gradient centrifugation, polyethylene glycol precipitation, and ammonium sulphate precipitation were undertaken to purify the putative antibacterial proteins of *Bl* 1821L and *Bl* 1951 isolates. Two putative antibacterial proteins (~30 kD & ~48 kD) of *Bl* 1821L and one ~30 kD of *Bl* 1951 was purified. Electron micrographs of purified proteins showed different phage structural components similar to the defective phages. Furthermore, the purification of uninduced cultures (without mitomycin C) showed the same protein bands. A population of resistant cells (persisters) in the *Bl* 1821L strain was noted.

Since the early 1960s, the concentration of virus particles with ultracentrifugation has been preferred due to its rapidity and cost, but there are also reports that the structural components of viruses may be damaged due to the high speed (Børsheim et al., 1990). Despite its limitations, density gradient ultracentrifugation is a common technique used to isolate and purify biomolecules and cell structures (Lawrence & Steward, 2010). Purification of *Bl* 1821L putative antibacterial proteins using sucrose density gradient centrifugation showed two prominent bands of ~30 kD and ~48 kD molecular mass.

Bl 1821L purified antagonistic proteins were concentrated through 10 kD MWCO membrane to remove sucrose residues for TEM analysis. Electron micrographs of *Bl* 1821L purified putative antibacterial proteins displayed remarkable structural differences. Phage encapsulating (capsid-like) structures were observed in ~30 kD containing gradient (Figure 5.17) and polysheath-like structures were seen in ~48 kD containing purified gradient (Figure 5.18). Polysheaths are aberrant assemblies of tail material in a structure identical with a contracted sheath and may be found in a "smooth" or "helical" form (Kellenberger & Boy de la Tour, 1964). Polysheaths were classified as phage tail-like defective bacteriophages together with rhapidosomes and particularly bacteriocins such as R-pyocins (Lotz, 1976). Previously, bacteria producing the long and ordered nanotube-like structures (polysheaths) were believed to harbour a true prophage, but over time, the genetic information for the phage has decreased to such an extent that the information for the sheaths is the only structural information left (Gumpert & Taubeneck, 1968; Kellenberger & Boy de la Tour, 1964). Polysheaths structures are very stable and can withstand treatments with various chemical and physical factors (Arisaka et al., 1981; Kurochkina et al., 2018; Šimoliūnas et al., 2019). The findings herein were in agreement with the Chapter 2 TEM examination (Figure 2.15) and the Chapter 3 N-terminal sequencing and bioinformatic analysis, which identified ~48 kD protein as "phage tail-like bacteriocin" or "phage-like element PBSX protein XkdK".

In addition, sucrose density gradient centrifugation of *Bl* 1951 putative antibacterial protein indicated a protein band of ~30 kD molecular mass. TEM analysis of ~30 kD purified and concentrated protein showed the hexagonal capsids-like structures and polysheaths (Figure 5.23) which corresponded to the preceding electron microscopic examination of Chapter 2 (Figure 2.14). SDS-PAGE analysis of *Bl* 1951 production kinetics experiment in Chapter 4 also showed a prominent band of ~30 kD protein (Figure 4.14) but its function was unknown. However, in the current chapter, the role of ~30 kD purified protein in antibacterial activity was demonstrated in the assay tests, and substantiated by following TEM analysis (Figure 5.23). Electron micrographs of the polysheaths in the current study were in agreement with previous work in various bacteria (Baechler & Berk, 1974; Bradley & Dewar, 1966; Kurochkina et al., 2018; Šimoliūnas et al., 2019).

Non-induced crude lysate of *Bl* 1821L and *Bl* 1951 upon purification with the sucrose density gradient centrifugation showed two protein bands of ~30 kD and ~48 kD molecular masses (Figures 5.14 & 5.20). Purification of *Bl* 1821L and *Bl* 1951 putative antibacterial proteins from the crude lysate of non-induced cultures (without mitomycin C) may be related to the phenomenon of spontaneous prophage induction (SPI). Spontaneous prophage induction is the activation of bacteriophages and prophage elements, pathogenicity islands, and phage morons (an extra gene in a prophage genome without a function) from the bacterial cells in the absence of an external trigger (Nanda et al., 2015; Taylor et

al., 2019). This phenomenon is potentially considered a detrimental process for bacterial populations as a small percentage of cells would be lost continuously due to the lysis of the bacterial cells (Nanda et al., 2015). Earlier studies have reported the spontaneous release of free bacteriophage and phage tail-like particles in the supernatant of non-induced cultures of various lysogenic bacteria (Lwoff, 1953b; Smarda & Benada, 2005). The findings were in agreement with the Chapter 4 production kinetics experiments where spontaneously produced putative antibacterial proteins of *Bl* 1951 (~30 kD) and *Bl* 1821L (~48 kD) were proposed to be involved in the putative antibacterial activity (Figures 4.7 & 4.14).

Size exclusion chromatography or gel filtration is a technique that is widely used to separate macromolecules based on their relative size (Hong et al., 2012a; Jones & Hurst, 2016). This method purified one putative antibacterial protein of ~30 kD from *Bl* 1951 crude lysate and two putative antibacterial proteins of ~30 kD and ~48 kD from *Bl* 1821L. Electron micrographs of ~30 kD purified putative antibacterial protein exhibited hexagonal capsid-like structures (Figure 5.7B) and hollow sheath-like structures (Figure 5.7A) were seen with ~48 kD protein which through purity is also likely composed of ~30 kD subunits (Figure 5.6). In addition to the structural differences between the two putative antibacterial proteins, the current study found that the ~30 kD putative antibacterial protein harbouring fractions demonstrated antagonistic activity against *Bl* 1951 while the pooled fractions that exhibited ~30 kD and ~48 kD bands exhibited the activity against the host bacterium *Bl* 1821L. Typically, the putative antibacterial proteins (bacteriocins) are antagonistic to the kin population of bacteria and the producer strains are immune to their toxic effects (Michel-Briand & Baysse, 2002; Scholl, 2017). However, some members of a genetically identical population can kill (autocidal) their siblings (González-Pastor et al., 2003; Popp & Mascher, 2019). An example is a bacteriocin, hyicin 3682, which exhibited its antagonistic activity against the producer strain, *Staphylococcus hyicus* (Fagundes et al., 2011). The antagonistic activity of ~30 kD encapsulating protein of *Bl* 1821L against *Bl* 1951 was in line with the work of various studies (Eppert et al., 1997; Valdés-Stauber & Scherer, 1994). Notably, some of the *Bl* 1951 SEC fractions in the assay, instead of producing a prominent zone of inhibition on the lawns of *Bl* 1821L, caused the growth of cells around the antimicrobial discs which, based on the literature, are proposed to be persister cells (Figure 5.9). All the known lineages of bacterial populations are known to harbour a small fraction of transiently antibiotic-tolerant cells known as “persisters” (Wilmaerts et al., 2019). These cells are characterised by their dormant nature and reduced metabolic activity (Lewis, 2010; Shah et al., 2006). The genetic basis of persister cells formation is attributed to the role of toxin-antitoxin (TA) systems in dormancy induction (Jayaraman, 2008). Several TA systems have been suggested as the basis of persister cell formation (Hong et al., 2012b; Kim & Wood, 2010; Lewis, 2010). TA systems typically consist of a stable toxin (always a

protein) that disrupts an essential cellular process (e.g., translation via mRNA degradation) and a labile antitoxin (either RNA or a protein) that prevents toxicity (Schuster & Bertram, 2013; Van Melderen & Saavedra De Bast, 2009). Numerous environmental stimuli are also involved in the persister cells formation (Michiels et al., 2016). Dörr et al. (2010) demonstrated that DNA damage in *Escherichia coli* inducing the SOS response led to the formation of persisters by stimulating the expression of TisB toxin. Growth phase of the bacterium plays a crucial role in determining the number of persisters, with the highest percentage of persisters found at the stationary phase (Keren et al., 2004). Persisters are typically absent in the early exponential phase of growth, but by the mid-exponential phase, persisters begin to appear in the population, and a maximum of approximately 1% is reached during the stationary phase (Keren et al., 2004; Lewis, 2008; Spoering & Lewis, 2001). Therefore, it might be possible that in the current study, *Bl* 1821L persister cells were produced in the mid/late exponential phase and a small percentage of these cells exhibited resistance against some of the *Bl* 1951 SEC fractions. However, *Bl* 1821L persister cells lost their resistance upon treatment with the mitomycin C induced supernatant of *Bl* 1951, confirming their transient nature.

Protein purification through precipitation by using various salts like ammonium sulphate (AS) and polyethylene glycol (PEG) is also in use as a method to purify viral proteins (phages). PEG precipitation is considered the best method to concentrate virus particles (proteins) due to its ability to maintain the intactness of structural components (Colombet et al., 2007; Tardieu et al., 2002) but often fails to obtain sufficient volume of pure phage preparations (Boulanger, 2009). PEG precipitation in combination with salts such as NaCl has also been employed to recover various viruses from different growing media (Lewis & Metcalf, 1988). PEG and monovalent salts are good inductors of interactions that preferentially crystallise biological macromolecules, such as DNA and viruses, in the inter-polymer spaces between PEG molecules (Tardieu et al., 2002). Effective pegylation occurs when the concentration of DNA and viruses exceeds their solubility (Polson, 1993). Mitomycin C induced cultures of various bacteria have been subjected to concentrate and purify phage tail-like particles by using PEG 8000 in conjunction with the NaCl (Gnezda-Meijer et al., 2006; Hegarty et al., 2016; Kandel & Baltrus, 2020). PEG 8000 (10%) precipitated *Bl* 1821L culture was further subjected to the purification of putative antibacterial proteins using sucrose density centrifugation in this study. SDS-PAGE showed a low abundance of the ~48 kD band in group B sucrose density gradients 40% and 60% however, comparatively, the ~30 kD purified protein band was readily visualised (Figure 5.26).

Ammonium sulphate precipitation method is often used to purify bacteriocins, commonly immediately after elimination of cell debris. Bacteriocins after removal of cell debris and following dialysis, either maintain their full activity at 50-60% saturation or lose it up to 40% even at saturation of 75-80% (dialysis sacs to purify proteins are used) (Parente & Ricciardi, 1999; Stern et al., 2006). The

concentration of ammonium sulphate required is dependent on the type of bacteriocin (Pingitore et al., 2007). However, it is not the preferred method for purifying low molecular-weight bacteriocins (proteins) as the proteins precipitate poorly even at 75-80% saturation, and when passing through dialysis tubing they can be eliminated fully or in part (Borzenkov et al., 2014). A putative antibacterial protein of ~50 kD was purified from *Bl* 1821L strain after ammonium sulphate precipitation (85%) and subsequent sucrose density gradient centrifugation in the bottom gradients *i.e*. 50% and 60% respectively. Since each purification step necessarily involves loss of some of the targeted proteins (Walker, 2005) it is possible that both the precipitation methods could not purify *Bl* 1951 putative antibacterial protein due to the involvement of several purification steps *i.e.* it was lost through successive purification steps.

5.5 Outcomes

The major findings of this chapter are;

1. Using various methods one putative antibacterial protein (~30 kD) of *Bl* 1951 and two putative antibacterial proteins (~30 kD & ~48 kD) of *Bl* 1821L were purified.

2. Antagonistic potency of *Bl* 1821L proteins differed from each other as the pooled fractions (II & III) showing both ~30 kD & ~48 kD protein bands exhibited inhibitory activity against *Bl* 1821L only while pooled fractions (IV) displaying a protein band of ~30 kD was found active against *Bl* 1951 as the host bacterium.

3. TEM analysis of purified ~30 kD and ~48 kD putative antibacterial proteins of *Bl* 1821L showed the structural differences.

4. Purification of non-induced (without mitomycin C) cultures of *Bl* 1821L and *Bl* 1951 crude lysate using sucrose density gradient centrifugation displayed two prominent bands of ~30 kD and ~48 kD which suggested their spontaneous induction.

5. Persister cells formation in the population of *Bl* 1821L was noted due to the effect of some of the SEC purified *Bl* 1951 fractions which might be due to the presence of a toxin-antitoxin system.

5.6 Conclusion

The putative antibacterial proteins of *Bl* 1821L and *Bl* 1951 were purified using different purification methods and subsequently identified under an electron microscope comprising of phage capsids-like and polysheath-like structures.

Chapter 6

N-terminal sequencing, bioinformatic analyses, and expression of putative antibacterial proteins in a gram-positive bacterium *Bacillus subtilis* WB800

6.1 Introduction

Various purification methods employed in the preceding chapter enabled the isolation of two putative antibacterial proteins (~30 kD & ~48 kD) of *Bl* 1821L but only one putative antibacterial protein (~30 kD) of *Bl* 1951. Subsequent TEM examination of purified putative antibacterial proteins of *Bl* 1821L affirmed the presence of encapsulin (~30 kD) and polysheath (~48 kD) like structures. Although only the ~30 kD protein was purified from *Bl* 1951, both structures were seen in this strain under TEM.

Biological macromolecules such as proteins play a vital role in the metabolic functioning of living organisms (Cristea et al., 2004). To demonstrate the importance of these molecules, scientists coined the term "proteomics" which can be defined as the overall protein content of a cell that is characterised with regard to its localisation, interactions, post-translational modifications, and turnover at a particular time (Domon & Aebersold, 2006; Wilkins et al., 1996). Proteomics is one of the most significant tools for understanding the functioning of a gene (Aslam et al., 2017; Lander et al., 2001). Genome sequencing provides information of the identified genes (Blackstock & Weir, 1999) including biochemical features that can suggest the role and biological functions of the gene products (mostly proteins) (Cox & Mann, 2007; Shendure & Aiden, 2012).

Bacteriophages encapsulate their genome in a proteinaceous structure called "capsid" (Burns et al., 1990; Stockley et al., 2016) and many phages have a tail connected to the capsid (Nobrega et al., 2018). Phage tails are molecular machines that specifically recognise bacterial host cells, penetrate the cell envelope, and deliver the phage genome into the cytoplasm. Phages may have a long, contractile tail (*Myoviridae*) or long, non-contractile tail (*Siphoviridae*) (Ackermann & Prangishvili, 2012). Contractile phage tail-like structures that are homologous to phage components but performing other biological functions have been identified in a wide range of bacteria (Scholl, 2017). Phage tail-like particles are commonly known as defective bacteriophages or cryptic phages (Bobay et al., 2014; Sarris et al., 2014) due to their distinctive feature to accommodate bacterial chromosomal DNA and killing potency against sensitive bacteria without injecting DNA (Bradley, 1967b; Jin et al., 2014). In evolutionary terms, these structures are related to *Myoviridae* phages and share a conserved protein core (tail

tube, tail spike, baseplate, and often receptor-binding proteins) (Nobrega et al., 2018). Defective phages are widely found in members of the genus *Bacillus* (Krogh et al., 1996). PBSH, PBSX, PBSV, PBSW, PBSY, PBSZ, and PBP180 are some of the identified defective phages of *Bacillus subtilis* 168, *Bacillus licheniformis*, *B. subtilis* var. *vulgatus*, *B. subtilis* S31, *B. subtilis* W23, and *Bacillus pumilus* AB94180 respectively (Haas & Yoshikawa, 1969; Jin et al., 2014; Wood et al., 1990). Importantly, all of these are bactericidal in nature, and PBSX, being the most widely studied phage-like element, is considered a model organism (Jin et al., 2014; Seaman et al., 1964).

Encapsulating proteins (capsids) derived from viral capsids often display antibacterial properties against gram-positive and gram-negative bacteria (Dias et al., 2017). The bactericidal action of encapsulating proteins is related to the presence of cell penetrating motifs (Freire et al., 2015b; Madani et al., 2011). Viral capsid protein derived from human hepatitis B virus, HBc ARD (Chen et al., 2013), and PepR from dengue virus (Alves et al., 2010) are the most prominent examples.

Heterologous expression of proteins is the expression of recombinant proteins in cells where they do not naturally occur (Fakruddin et al., 2013). The gram-positive bacterium, *Bacillus subtilis* (*Bs*), is extensively used for the expression of foreign genes (Su et al., 2020). Numerous transformation methods including the competent transformation method (Spizizen, 1958), protoplast transformation method (Chang & Cohen, 1979), alkali metal ions method (Ano et al., 1990), and protoplast electroporation method (Kusaoke et al., 1989) have been used to insert foreign genes in *Bs* (Lu et al., 2012). Since the first application of an electroporation method on *Bs* 168 (McDonald et al., 1995) it has become the commonly used method to move plasmids expressing foreign proteins into *Bs* (Jeong et al., 2018*)*. Different operating parameters like field strength, the composition of cultivating and electroporation media, competent cells concentration, and plasmid type influence the transformation efficiency of the electroporation method (Jeong et al., 2018).

This chapter describes analyses of N-terminal sequencing of purified putative antibacterial proteins of *Bl* 1821L and *Bl* 1951 and subsequent bioinformatic analyses. Furthermore, the identified putative encapsulating protein (~30kD) of *Bl* 1821L was transformed into a gram-positive bacterium, *Bs* WB800, to affirm the bactericidal activity of the corresponding protein.

6.2 Methods

6.2.1 N-terminal sequencing of *Bl* 1821L and *Bl* 1951 putative antibacterial proteins and bioinformatic analyses

Mitomycin C (Sigma) was used to induce *Bl* 1821L and *Bl* 1951 putative antibacterial proteins as described in Chapter 2 (Section 2.2.6). Induced *Bl* 1821L putative antibacterial proteins (30 kD & 48 kD) were purified from group A (20%) and group B (60%) sucrose density gradients and, for *Bl* 1951, group A gradient (50%) was used according to the protocol outlined in Chapter 5 (Section 5.2.2). N-terminal sequencing of the sucrose density gradient purified *Bl* 1821L and *Bl* 1951 protein bands was performed at AgResearch, Lincoln, New Zealand, as outlined in Chapter 3 (Section 3.2.7). Bioinformatic analyses of N-terminal sequenced proteins of *Bl* 1821L and *Bl* 1951 putative antibacterial proteins were performed using the programme Geneious basic (Kearse et al., 2012).

6.2.2 Identification of *Bl* 1821L and *Bl* 1951 putative antibacterial proteins

Identified proteins of *Bl* 1821L and *Bl* 1951 were explored in the Uniprot database (https://www.uniprot.org) to determine the nature of putative antibacterial proteins and were further subjected to BLASTp (Basic Local Alignment Search Tool) to look for similar proteins (https://blast.ncbi.nlm.nih.gov; https://www.uniprot.org). Identified proteins molecular weights were calculated through ExPasy (https://www.expasy.org).

6.2.3 Bactericidal determinants of *Bl* 1821L and *Bl* 1951 putative antibacterial proteins

Bioinformatic tools AMPA (Torrent et al., 2012) and CellPPD (Gautam et al., 2013) were used to search for motifs related to the bactericidal activity and cell penetrating peptides (CPPs) potency of 30 kD putative encapsulating protein of *Bl* 1821L and *Bl* 1951. Likewise, the putative phage tail-like protein (48 kD) sequence of *Bl* 1821L was subjected to AMPA analysis to search for motifs related to known bactericidal activity (Gautam et al., 2013).

6.2.4 Comparison of identified *Bl* 1821L phage-like element PBSX protein XkdK with the similar proteins of other gram-positive bacteria

Identified (48 kD) phage like-element PBSX protein (XkdK) of *Bl* 1821L (NZ_CP033464.1) was aligned with XkdK proteins of other gram-positive bacteria using the programme Geneious basic (Kearse et

al., 2012) and a dendrogram was produced using the same programme. Amino acid sequence of *Bl* 1821L was also aligned using the programme CLUSTALO to determine differences among the aligned XkdK proteins (https://www.uniprot.org).

6.2.5 Expression of a hypothetical protein (25 kD), putative encapsulating protein (30 kD), and both (25 kD & 30 kD) in a gram-positive bacterium *Bacillus subtilis* WB800N

A collaborative research project was initiated with Dr. Campbell Sheen and Dr. Barbara Koch of Callaghan Innovation's Protein Science & Engineering team based at the University of Canterbury, New Zealand, for the transformation of putative antibacterial proteins in a gram-positive bacterium *Bs* WB800N. All the expression work was performed by the collaborators at the University of Canterbury, New Zealand. The assay tests, purification process, and SDS-PAGE analysis of transformed *Bl* 1821L pHT01-*hypo* (25 kD), pHT01-*encap* (30 kD), and pHT01- *hypo*.*encap* genes encoding both the 25 kD and 30 kD proteins were performed by me at the Bio-Protection Research Centre and Replacement for Hilgendorf (RFH) building laboratories of Lincoln University, New Zealand.

6.2.6 *Bl* 1821L genomic DNA extraction and amplification

Genomic DNA of *Bl* 1821L (NZ_CP033464.1) was extracted using the DNeasy Blood & Tissue Kit (250) (QIAGEN, Germany) according to the manufacturer's instructions. In this study, identified *Bl* 18 21L genes corresponding to a hypothetical protein (25 kD) residing at 18,917 bp to 19,564 bp (648 bp), a putative encapsulating protein (30 kD) encoded at 19,592 bp to 20,434 bp (843 bp), and both the genes encoding 25 kD and 30 kD proteins (Figure 6.1) were used for transformation in a gram-positive bacterium *Bs* WB800N. The three constructs developed were named accordingly *i.e.* pHT01-*hypo* (25 kD), pHT01-*encap* (30 kD), and pHT01-*hypo*.*encap* containing both the genes (25 kD & 30 kD). Primers were designed to amplify these regions. Primer combinations were used (Table 6.1) to amplify coding regions using CloneAmp (TakaRa Bio, USA) master mix according to the manufacturer's instructions with a 1/500 dilution of genomic DNA diluted in water as a template. A 10 µl aliquot of the PCR reaction was electrophoresed on a 1% (w/v) agarose gel (1× TAE buffer) until separated. The bands of appropriate size were visualised and excised on a DarkReader blue light table (Clare Chemical Research, USA) before purification using a NucleoSpin gel and PCR purification kit (Macherey-Nagel, USA) according to the manufacturer's instructions.

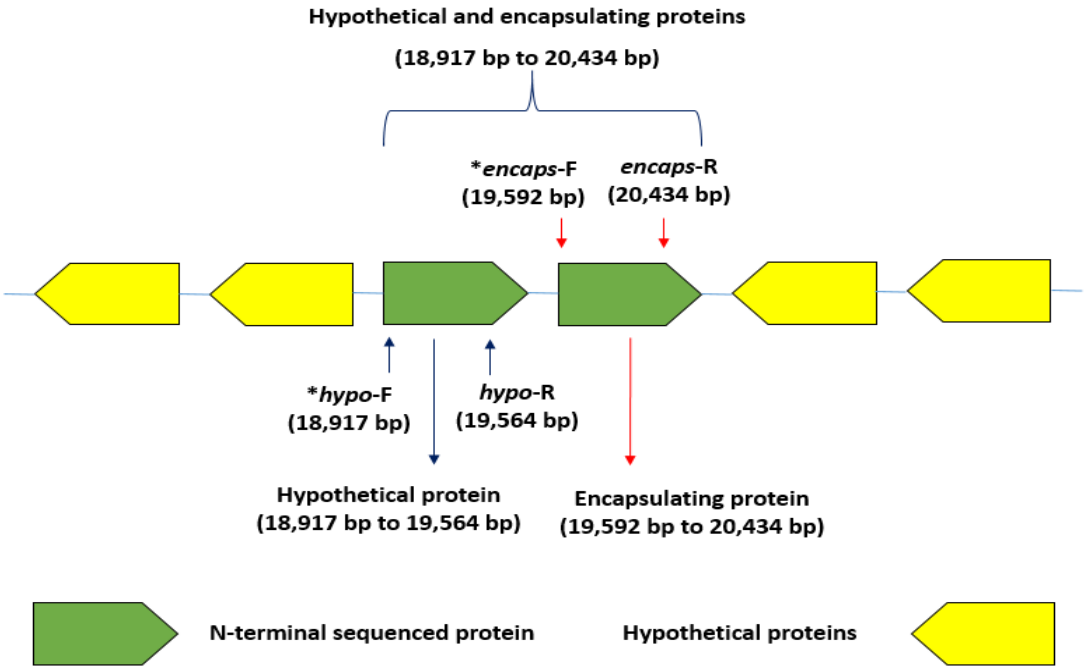

Note: The short amino acid sequences of ~30 kD N-terminal sequenced protein of *Bl* 1821L identified a hypothetical and an encapsulating gene in *Bl* 1821L genome.

Figure 6.1 Schematic presentation of genes encoding proteins in *Bl* 1821L genome corresponding to the constructs used in this study for expression in *Bs* WB800N. Identified genes of the 25 kD hypothetical protein (dark blue arrows) and 30 kD putative encapsulating protein (red arrows) are shown in green colours

Table 6.1 Primers used for amplification of a hypothetical- *hypo* (25 kD), putative encapsulating gene- *encaps* (30 kD), and both the genes- *hypo.encap* (25 kD & 30 kD)

**hypo*-F	5′-CAATTAAAGGAGGAAGGATCCATGATGCAAGAAATCAAGCAGCTCC
hypo-R	5′-CATTAGGCGGGCTGCCCCGGGTTATACGTGACGATTGAGATGACGCAG
**encaps*-F	5′-CAATTAAAGGAGGAAGGATCCATGGATAAAGCACAGAAATTCCCAGAC
encaps-R	5′-CATTAGGCGGGCTGCCCGGGCTATTCTTCTGTCATTTCCAATGTGCAA

Note: Red colour indicates pHT01 (plasmid) homology region, underline indicates BamHI (GGATCC) or XmaI (CCCGGG) restriction sites and blue indicates *Bl* 1821L genome specific primer sequence (NZ_CP033464.1)

**hypo* was amplified using *hypo*-F/R
**encaps* was amplified using *encaps*-F/R
**operon* was amplified using *hypo*-F/*encaps*-R

6.2.7 Cloning of the genes of putative hypothetical (25 kD) and encapsulating (30 kD) proteins into pHT01

PCR amplified sequences were cloned into plasmid pHT01 (MoBiTec, Germany) (Figure 6.2) using an Infusion HD cloning kit (TakaRa Bio, USA). Briefly, plasmid pHT01 was digested with BamHI and XmaI (The New England BioLabs, NEB) then gel purified as above. Purified linear plasmid and respective PCR products were used in the infusion cloning reaction according to the manufacturer's instructions. Cloning reactions were then used to transform *Escherichia coli* stellar cells (Clonetech Laboratories, TakaRa Bio, USA), according to manufacturer's instructions, with selection on LB agar containing 100 µg/ml carbenicillin. Plasmid DNA was extracted using a NucleoSpin Plasmid Mini kit (Macherey-Nagel, USA). Plasmids were sequenced by Macrogen (Korea) and sequencing data were aligned to those of the respective constructs using Geneious Prime-2020 (Biomatters, New Zealand) and then manually curated. Plasmid DNA from one correct construct was used to transform *Bs* WB800N.

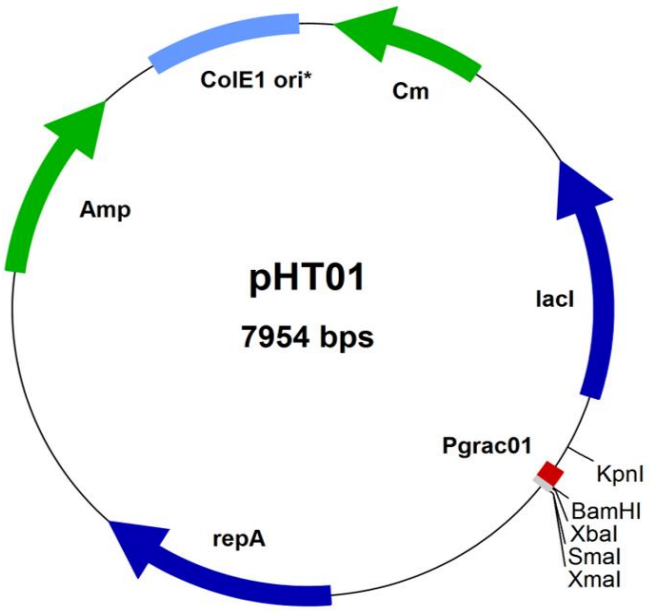

Figure 6.2 Schematic presentation of plasmid pHT01 used in this study with promoter P*grac*01 (BamHI (GGATCC) or XmaI (CCCGGG))

Gram-positive bacterium, *Bs* WB800N (*nprE aprE epr bpr mpr::ble nprB::bsr Δvpr wprA::hyg cm::neo;* NeoR) was used for transformation (Jeong et al., 2018; Wu et al., 2002). A fresh colony of *Bs* WB800N was inoculated into 5 ml of LB (Miller) and placed in an orbital shaking incubator (Conco, TU-4540, Taiwan) @ 250 rpm at 37^0C for 12 hours. After 12 hours, 1 ml of the culture was transferred into 40 ml of LB broth (Miller) containing 0.5 M/L sorbitol and incubated at 37°C to a logarithmic phase.

Subsequently, the culture was cooled on ice for 5 min and centrifuged @ 5,000 g for 10 min and 4°C to pellet the cells, followed by washing four times with the electroporation buffer (0.5 M/L sorbitol, 0.5 M/L mannitol, 0.5 M/L trehalose, 10% glycerol). The cells were ultimately suspended with an appropriate volume of electroporation buffer and stored at -70°C. For electroporation, 60 µl of the competent cells were mixed with 1 µl (50 ng/µl) plasmid and then put into an ice-cold electroporation cuvette (1 mm gap). The cells after 5-10 min of incubation were shocked using a pulser (Micro Pulser; Bio-Rad, Hercules, CA) resulting in time constants of 5-5.8 ms. Immediately, 1 ml of recovery medium (LB containing 0.5 M/L sorbitol & 0.5 M/L mannitol) was added to the cells. After incubation at 37°C for 3 hours, the bacteria were plated onto the LB plate with the antibiotic chloramphenicol @ 5 µg/ml and incubated at 37°C overnight.

Genes corresponding to the 25 kD hypothetical (pHT01-*hypo*), 30 kD putative encapsulating protein (pHT01-*encap*), and pHT01-*hypo*.*encap* with both the proteins (25 kD & 30 kD) were transformed separately into *Bs* WB800N enabling their expression and the determination of the putative antibacterial activity of each protein. After transformation two single colonies of pHT01-*hypo* (A1 & A2) and pHT01-*encap* (B1 & B2) containing *Bs* WB800N colonies and one colony from pHT01-*hypo*.*encap* was streaked onto an LB agar plate. The streaked colonies were cultivated overnight until the culture attained OD_{600nm} 0.7-0.8 and aliquoted into two parts. An aliquot (7.5 ml) was induced with 1 mM IPTG and the other was uninduced. Both induced and uninduced samples were drawn after 3.5 and 24 hours of treatment. The resultant cultures were centrifuged @ 6,000 g for 10 min at 4°C to spin down the cells. Cell pellets were stored at -20°C and the supernatant was sterilised by passing twice through a 0.22 µm filter.

6.2.8 Assay test of transformed hypothetical (25 kD) and putative encapsulating (30 kD) proteins activity

Cell free supernatants (CFS) of *Bs* WB800N containing the induced proteins corresponding to the pHT01-*hypo* (25 kD), pHT01-*encap* (30 kD), and pHT01-*hypo*.*encap* containing both the genes (25 kD & 30 kD) were evaluated using the Kirby-Bauer disc diffusion test (Bauer, 1966; Hudzicki, 2009) as described in Chapter 3 (Section 3.2.1) against *Bl* 1821L and *Bl* 1951 as the host bacteria. For the control treatment, CFS of *Bs* WB800N without transformation of plasmids was used.

6.2.9 Purification and SDS-PAGE analysis of transformed hypothetical (25 kD) and putative encapsulating (30 kD) proteins

Transformed *Bs* WB800N (pHT01-*hypo*, pHT01-*encap*, pHT01-*hypo*.*encap*) CFS demonstrating antagonistic activities were concentrated and purified using the group B (10-60%) sucrose density gradients centrifugation method as outlined in Chapter 5 (Section 5.2.2). Purified and expressed proteins (pHT01-*hypo*, pHT01-*encap*, pHT01-*hypo*.*encap*) CFS were again concentrated before running on gel electrophoresis and SDS-PAGE was stained with silver as described in Chapter 5 (Section 5.2.2D). For the control SDS-PAGE of sucrose density, gradient purified *Bs* WB800N CFS without transformation of plasmids was used.

Overall, in this Chapter bioinformatic analyses of putative antibacterial proteins of insect pathogenic strains *Bl* 1821L and *Bl* 1951 were performed (Table 6.2).

Table 6.2 Overview of *in silico* analysis of putative antibacterial proteins of *Bl* 1821L and *Bl* 1951

Bacterium strain	Accession #	Estimated molecular weight of purified putative antibacterial proteins	Identification of purified putative antibacterial proteins	Analysis performed	
Bl 1821L	tr|A0A502IA18|A0A502IA18_BRELA tr|A0A2S5H3X5|A0A2S5H3X5_BRELA	*30 kD	Putative encapsulating protein	N-terminal sequencing	Bioinformatic analysis
	tr|A0A518VEB0|A0A518VEB0_BRELA tr|A0A0F7EER1|A0A0F7EER1_BRELA	48 kD	Phage-like element PBSX protein XkdK		
Bl 1951	tr|A0A502IA18|A0A502IA18_BRELA tr|A0A2S5H3X5|A0A2S5H3X5_BRELA	*30 kD	Putative encapsulating protein		

*=N-terminal sequencing of 30 kD purified protein also identified a 25 kD hypothetical protein with accession tr|A0A502I846|A0A502I846_BRELA in both the strains (*Bl* 1821L & *Bl* 1951) which appears to be a co-located protein.

6.3 Results

6.3.1 Identification of putative antibacterial protein (30 kD) in *Bl* 1821L and *Bl* 1951 genomes

The short amino acids sequences obtained after N-terminal sequencing of the purified ~30 kD protein band were used to predict the corresponding gene in the *Bl* 1821L (NZ_CP033464.1) genome. Analysis identified several match hits to a hypothetical protein (covering 57% of the amino acid sequence) and an adjacent bacteriocin family protein (covering 78% of the amino acid sequence) residing in the *Bl* 1821L genome (Appendix D-1 & D-2). The gene regulating the putative bacteriocin family protein (30 kD) was identified between 19,592 bp to 20,431 bp and at 3' end, the hypothetical protein (25 kD) regulating gene was encoded between 18,917 bp to 19,561 bp (Table 6.3 & Figure 6.3). Importantly, it was also shown through N-terminal sequencing of the 30 kD protein to be another potentially co-migrating protein. Identified (30 kD) *Bl* 1821L bacteriocin family protein (tr|A0A502IA18|A0A502IA18 _BRELA & tr|A0A2S5H3X5|A0A2S5H3X5_BRELA) and 25 kD hypothetical protein (tr|A0A502I846| A0A502I846_BRELA) regulating genes were also searched in the *Bl* 1951 genome (RHPK01000003.1, contig 1). The gene corresponding to the 30 kD bacteriocin family protein was mapped between 2,359,628 bp to 2,360,467 bp and immediately downstream, a gene encoding the predicted 25 kD hypothetical protein resided between 2,358,953 bp to 2,359,597 bp (Figures 6.1 & 6.5).

Through N-terminal sequencing of the purified *Bl* 1951 protein band (~30 kD), several short amino acid sequences were used to define the corresponding gene in the *Bl* 1951 genome (RHPK01000003.1, contig 1). Alignment of the N-terminal short amino acid sequences revealed amino acid identity to a hypothetical protein (tr|A0A502I846|A0A502I846_BRELA) and a putative bacteriocin family protein (tr|A0A502IA18|A0A502IA18_BRELA & tr|A0A2S5H3X5|A0A2S5H3X5_BRELA) (Figure 6.5 & Appendix D-1 to D-2). For *Bl* 1951, the genes encoding the proteins are labelled as putative encapsulating protein for a DyP-type peroxidase or ferritin-like protein (30 kD) and hypothetical protein (25 kD) (Figure 6.5). Based on BLASTp analysis both the amino acid sequences of the *Bl* 1951 and *Bl* 1821L 25 kD and 30 kD proteins shared 100% amino acid identity (Appendix D-3 & D-4).

6.3.2 N-terminal sequence analysis of *Bl* 1821L and *Bl* 1951 identified 30 kD putative antibacterial protein

The identified putative antibacterial protein (30 kD) of *Bl* 1821L was further assessed using the Uniprot database. Assessment of the *Bl* 1821L purified ~30 kD N-terminal sequenced band through alignment with the 30 kD genome revealed putative bacteriocin and uncharacterised protein with accessions tr|A0A502IA18|A0A502IA18_BRELA, tr|A0A2S5H3X5|A0A2S5H3X5_BRELA, and tr|A0A502I846|A0A502I846_BRELA in the Uniprot database (Table 6.3). Identified accessions tr|A0A502IA18|A0A502IA18_BRELA and tr|A0A2S5H3X5|A0A2S5H3X5_BRELA expressed >97% amino acids similarity to the Linocin M18 bacteriocin family protein of *Bl* LMG 15441 and *Bl* GI-9. The rest of the predicted identical proteins corresponded to the putative bacteriocins of other *Bl* strains (Table 6.4). Accession tr|A0A502I846|A0A502I846_BRELA exhibited similar identity to the uncharacterised proteins from several *Bl* stains (Table 6.5). Amino acid sequence analysis through ExPasy computed the molecular weight of purified *Bl* 1821L putative bacteriocin family protein of 31.4 kD, which was within the expected range estimated by SDS-PAGE analysis *i.e*. ~30 kD (Figure 5.24). BLASTp analysis of the accessions tr|A0A502IA18|A0A502IA18_BRELA and tr|A0A2S5H3X5|A0A2S5H3X5_BRELA against Uniprot database identified 97.1% and 99.3% amino acid similarity to the Linocin M18 bacteriocin family protein of *Bl* LMG 15441 and several other proteins exhibiting ≥70% amino acid similarity were identified (Table 6.4 & Appendix D-5). Accession tr|A0A502I846|A0A502I846_BRELA displayed 90.7% amino acids similarity to an uncharacterised protein of *Bl* LMG 15441. Furthermore, a *Brevibacillus centrosporus* encapsulating protein with 57.8% amino acid similarity and other uncharacterised proteins belonging to several *Bl* strains showing 54.8% to 57.6% amino acid identity to the Uniprot identified proteins were found (Table 6.5 & Appendix D-6).

In the preceding section, it was shown that the genes corresponding to the hypothetical protein (25 kD) and putative bacteriocin family protein (30 kD) in both the strains (*Bl* 1821L & *Bl* 1951) were 100% identical (Appendix D-3 & D-4).

Table 6.3 Identification of *Bl* 1821L and *Bl* 1951 putative antibacterial gene and protein (30 kD) in the genome and Uniprot database

Accession	Average molecular mass	Identity	Identified genes	Uniprot description of identified proteins
tr|A0A502IA18|A0A502IA18_BRELA	31404	Putative bacteriocin	Currently gene is labelled as a putative bacteriocin family protein in *Bl* 1821L genome.	Uncharacterised protein OS= *Brevibacillus laterosporus* OX= 1465 GN= C2W64_00537 PE= 4 SV= 1
tr|A0A2S5H3X5|A0A2S5H3X5_BRELA	31409		Currently gene is labelled as a putative encapsulating protein for a DyP-type peroxidase or ferritin-like protein family protein in *Bl* 1951 genome.	Bacteriocin OS= *Brevibacillus laterosporus* OX= 1465 GN= C4A76_22885 PE= 4 SV= 1
tr|A0A502I846|A0A502I846_BRELA	25006	Hypothetical protein	Currently gene is labelled as hypothetical protein downstream to the gene corresponding to the putative bacteriocin family protein/encapsulating protein for a DyP-type peroxidase or ferritin-like in *Bl* 1821L and *Bl* 1951 genomes.	Uncharacterised protein OS= *Brevibacillus laterosporus* OX= 1465 GN= C2W64_00536 PE= 4 SV= 1

Table 6.4 Identical proteins of *Bl* 1821L and *Bl* 1951 N-terminal sequenced putative encapsulating protein of 30 kD with accessions tr|A0A502IA18|A0A502IA18_RELA and tr|A0A2S5H3X5|A0A2S5H3X5_BRELA in the Uniprot database

Accession	Identical proteins	Organism	Gene name	Length
tr|A0A502IA18|A0A502IA18_BRELA tr|A0A2S5H3X5|A0A2S5H3X5_BRELA	Bacteriocin	*Brevibacillus laterosporus* (*Bacillus laterosporus*)	C4A76_22885, D5F52_25150	280
	Linocin M18 bacteriocin family protein	*Brevibacillus laterosporus* LMG 15441	BRLA_c039240	280
	Bacteriocin	*Brevibacillus laterosporus* (*Bacillus laterosporus*)	EX87_10870	280
	Linocin M18 bacteriocin family protein	*Brevibacillus laterosporus* GI-9	BLGI_2572	280
	Bacteriocin	*Brevibacillus laterosporus* (*Bacillus laterosporus*)	C4A77_24310	280
	Bacteriocin	*Brevibacillus* sp. SKDU 10	AYJ08_06900	280
	Bacteriocin	*Brevibacillus laterosporus* (*Bacillus laterosporus*)	EEL30_01270, EEL32_19195	280

Table 6.5 Identical proteins of *Bl* 1821L and *Bl* 1951 identified hypothetical protein of 25 kD with accession tr|A0A502I846|A0A502I846_BRELA in the Uniprot database

Accession	Identical proteins	Organism	Gene name	Length
tr|A0A502I846|A0A502I846_BRELA	Uncharacterised protein	*Brevibacillus laterosporus* (*Bacillus laterosporus*)	EX87_10875	215
	Uncharacterised protein	*Brevibacillus laterosporus* LMG 15441	BRLA_c039230	215
	Uncharacterised protein	*Brevibacillus laterosporus* GI-9	BLGI_2573	215
	Uncharacterised protein	*Brevibacillus laterosporus* (*Bacillus laterosporus*)	C4A77_24315	215
	Uncharacterised protein	*Brevibacillus laterosporus* (*Bacillus laterosporus*)	C4A76_22880	215
	Uncharacterised protein	*Brevibacillus laterosporus* (*Bacillus laterosporus*)	D5F52_25155	215
	Uncharacterised protein	*Brevibacillus* sp. SKDU 10	AYJ08_06905	215

6.3.3 Bioinformatic analysis of identified *Bl* 1821L and *Bl* 1951 putative antibacterial protein (30 kD) genomic region

Identified putative bacteriocin family protein in the *Bl* 1821L genome at the 5' end is flanked by two hypothetical proteins (Table 6.3 & Figures 6.1 & 6.4). Another hypothetical protein (25 kD) encoding gene at the 3' end of the gene encoding the putative 30 kD bacteriocin family protein residing between 18,917 bp to 19,561 bp was identified (Table 6.3 & Figures 6.3-6.4). The proteins appear to be co-migrating on SDS-PAGE (Table 6.3). Different families of transcriptional regulator proteins including PadR, MarR, Helix-turn-Helix (HEH), and other domain containing proteins such as the trypsin-like peptidase, and bacillithiol system redox-active protein (YtxJ) are located in this genomic region (Figure 6.4). As outlined earlier, the *Bl* 1951 genes corresponding to the putative encapsulating protein for a DyP-type peroxidase or ferritin-like oligomers and hypothetical proteins are 100% identical to the bacteriocin family protein and hypothetical protein of *Bl* 1821L (Appendix D-3 & D-4) and are also flanked with uncharacterised genes (Table 6.3 & Figures 6.5 & 6.6). The gene localised at the immediate position (21,077 bp to 20,604 bp) corresponding to a hypothetical protein expressed 100% amino acid similarity to a corresponding *Bl* 1951 gene (RHPK01000003.1, contig 1) encoded between 2,361,116 bp to 2,360,643 bp (Figures 6.3 & 6.5 & Appendix D-7A). In the upstream position of this gene another gene encoded a hypothetical protein (21,684 bp to 21,391 bp) with 99% similarity to a gene residing between 2,361,723 bp to 2,361,430 bp in the *Bl* 1951 genome (RHPK01000003.1, contig 1) (Figures 6.3 & 6.5 & Appendix D-7B). The *Bl* 1821L gene encoding the stress protein (YtxJ) in *Bl* 1821L is localised between 2,353,005 bp to 2,353,331 bp (Figure 6.3), and in the *Bl* 1951 strain it is labelled as Pyridoxamine 5'-phosphate oxidase (EC 1.4.3.5) CDS (Figure 6.5). Furthermore, the genomic organisation of the putative encapsulating region is similar between strains (Figures 6.4 & 6.6).

A schematic presentation of the predicted 3D structures of identified 25 kD hypothetical and 30 kD putative encapsulating protein for a DyP-type peroxidase or ferritin-like protein oligomers is shown in Figures 6.7A and 6.7C. Electron micrograph of putative encapsulating 30 kD protein (Figure 6.7B), and genomic organisation of *Bl* 1821L and *Bl* 1951 is presented (Figure 6.7D).

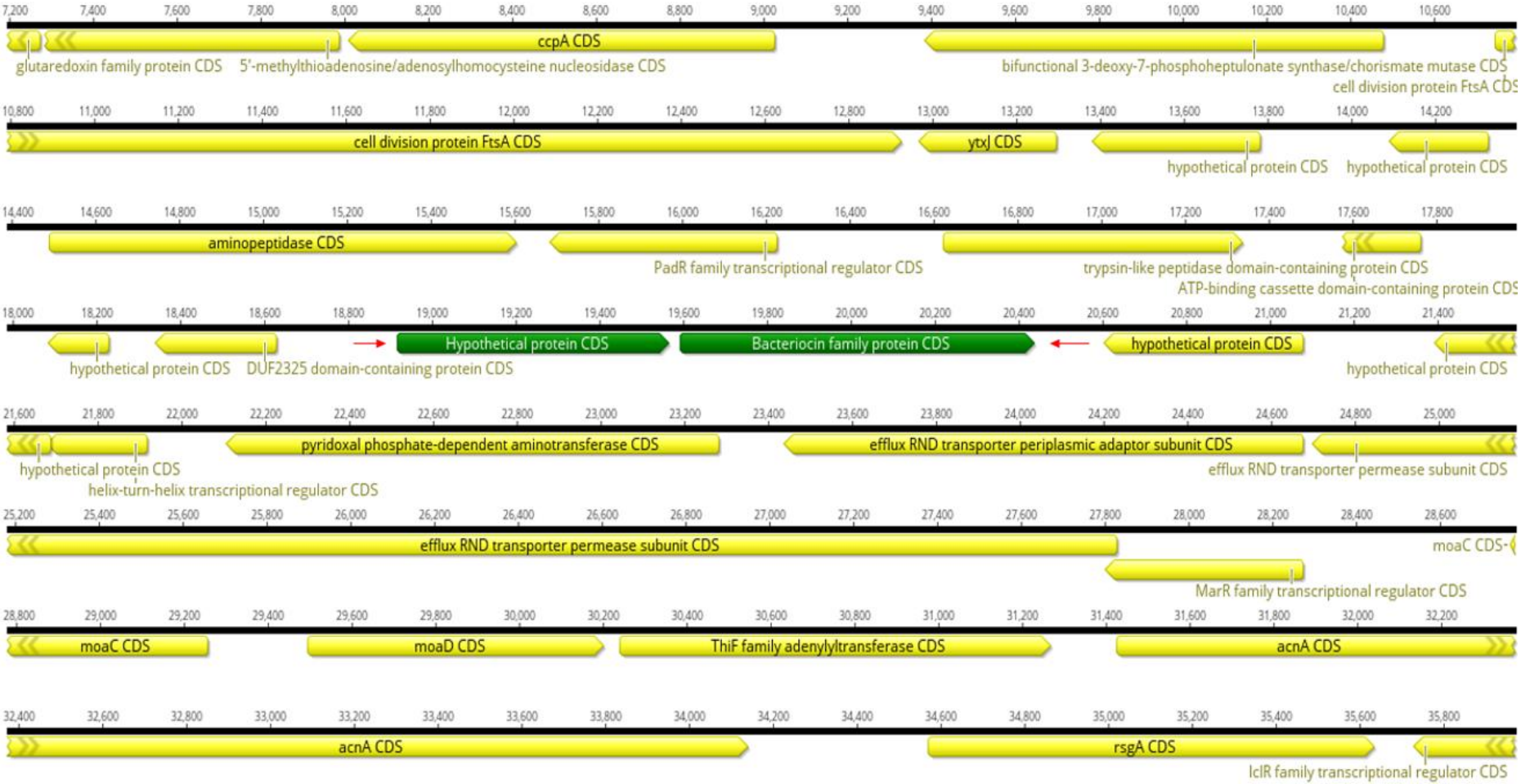

Figure 6.3 Geneious output of the 30 kD N-terminal sequence of *Bl* 1821L identifying genes corresponding to a hypothetical protein (25 kD) and a bacteriocin family protein (30 kD) in *Bl* 1821L genome (shown in green colour with red arrow)

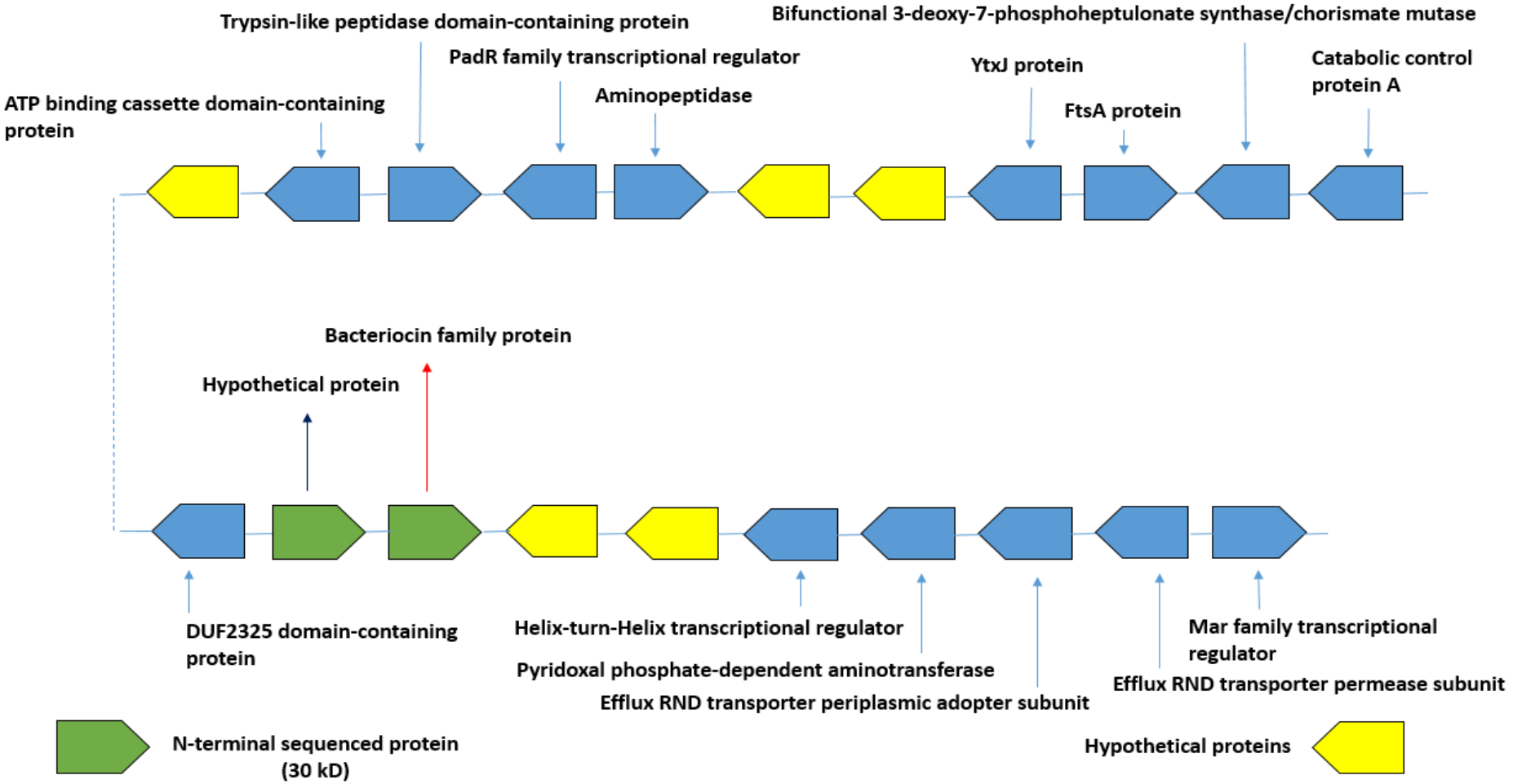

Figure 6.4 Genomic architecture of the 30 kD N-terminal sequence of *Bl* 1821L showing identified genes of a 25 kD hypothetical protein (dark blue arrow) and a 30 kD bacteriocin family protein (red arrow) residing in *Bl* 1821L genome along with other genes of the region. Vertical dash denotes the flow of genes in the genome

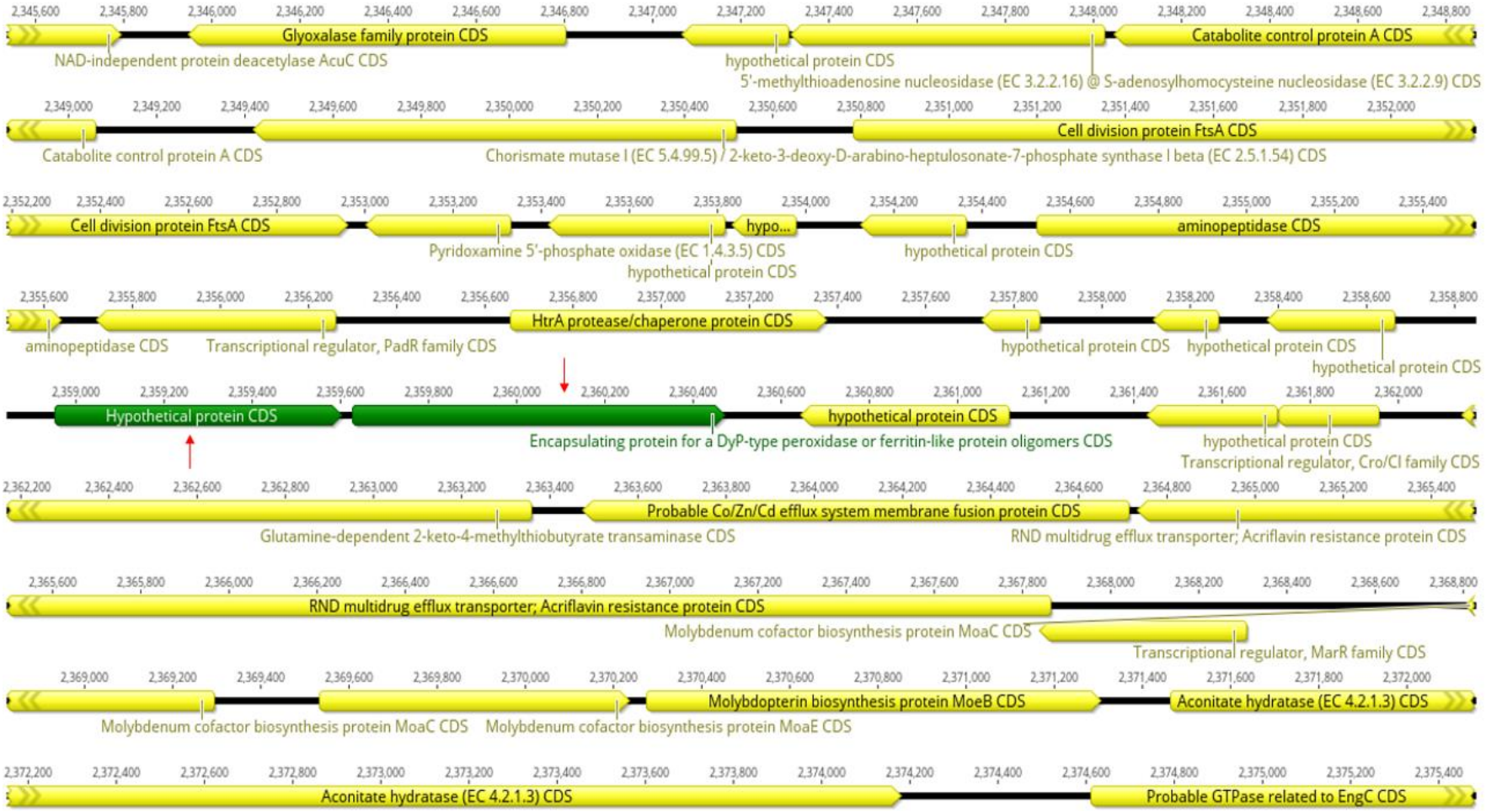

Figure 6.5 Geneious output of the 30 kD N-terminal sequence of *Bl* 1951 identifying genes corresponding to a hypothetical protein (25 kD) and a putative encapsulating protein (30 kD) in *Bl* 1951 genome (shown in green colour with red arrow)

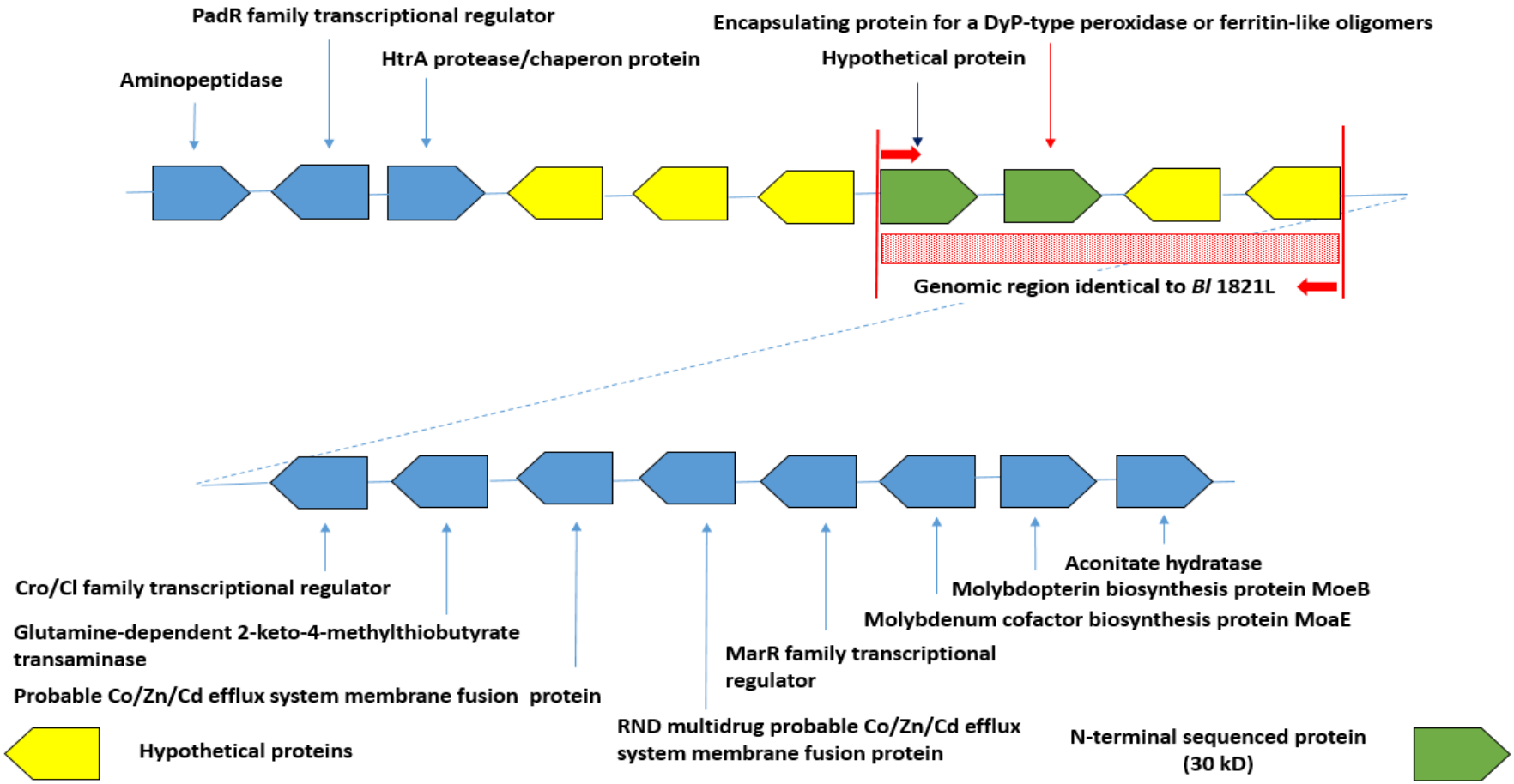

Figure 6.6 Genomic architecture of the 30 kD N-terminal sequence of *Bl* 1951 showing identified genes of a 25 kD hypothetical protein (dark blue arrow) and a 30 kD putative encapsulating protein (red arrow) residing in *Bl* 1951 genome along with other genes of the region. *Bl* 1951 genomic region identical to *Bl* 1821L genome is highlighted with red shaded box region. Diagonal dash denotes the flow of genes in the genome

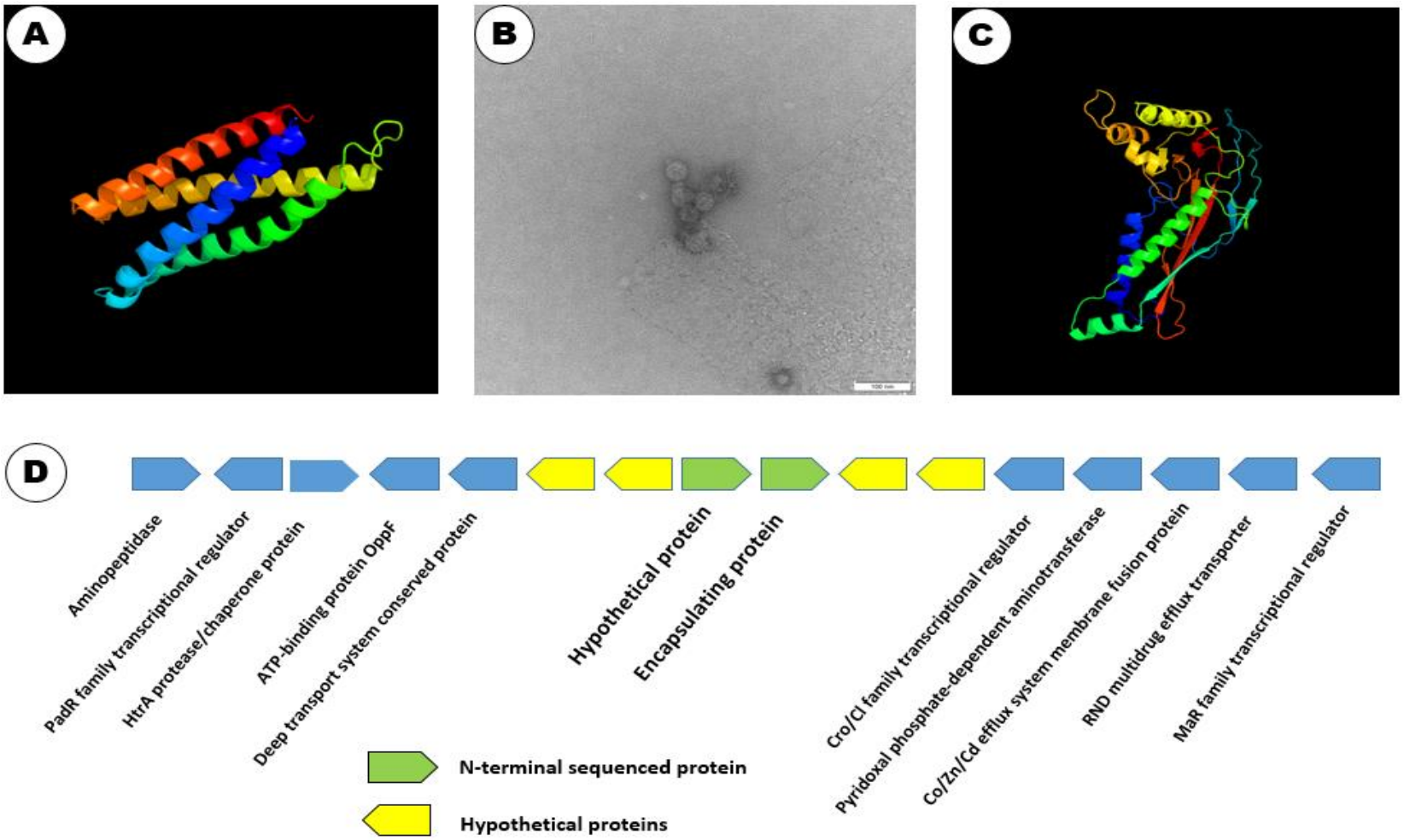

Figure 6.7 Predicted 3D structures of identified 25 kD hypothetical (A) and 30 kD putative encapsulating (C) proteins of *Bl* 1821L and *Bl* 1951 generated using Phyre[2] (Kelley et al., 2015). (B). Morphological presentation of putative encapsulating protein (30 kD) under TEM (Scale bar= 100 nm). (D). Identical genomic region of *Bl* 1821L and *Bl* 1951 encoding putative hypothetical and encapsulating genes (filled green arrows)

6.3.4 Bactericidal determinant of *Bl* 1821L and *Bl* 1951 putative encapsulating protein (30 kD)

AMPA is an automated web server used to predict the antimicrobial regions in a protein. It is based on an antimicrobial propensity scale that takes into account the physical and chemical properties of each amino acid, like hydrophobicity and amphipathicity, and the relevance of amino acid position for antimicrobial activity (Torrent et al., 2012). An antimicrobial index (AI) < 0.225 was considered a positive hit for an AMP in this study. AMPA analysis of the ~30 kD putative encapsulating protein sequence of *Bl* 1821L revealed an index value (AI) below the threshold level, which illustrated its bactericidal potency (Figure 6.8). The region of amino acid similarity covered amino acids, -2 to 279 as shown in Figure 6.9 in the red area with a propensity value of 0.001 (0%) and a mean value of 0.001. CellPPD is a support vector machine (SVM) that scores each amino acid residue with an SVM score and an SVM > 0 is considered a positive CPP hit (Gautam et al., 2013). Cell penetrating peptides (CPPs) specific amino acids and motifs identified in the *Bl* 1821L (identical to the *Bl* 1951) encapsulating protein (30 kD) sequence are presented below (Table 6.6 & Figure 6.9).

Identified genes and the amino acid content of N-terminal sequenced and bioinformatically analysed *Bl* 1951 (~30 kD) protein band were identical to the identified *Bl* 1821L putative encapsulating protein (~30 kD) (Appendix D-3 & D-4). Therefore, the resultant bactericidal activity predicted through bioinformatic tools AMPA and CellPPD is likely to be similar.

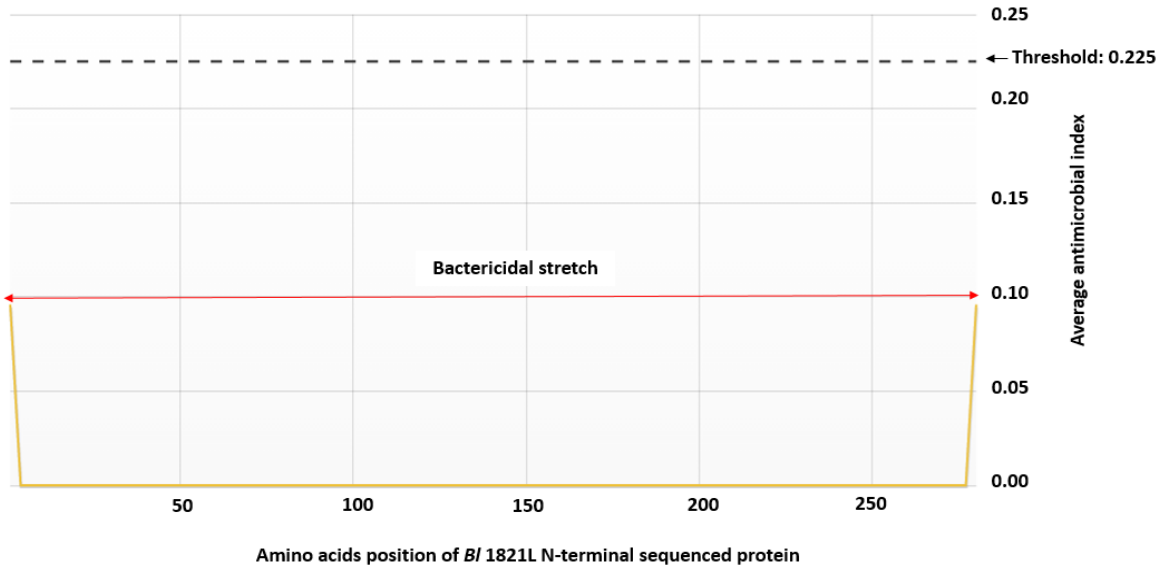

Figure 6.8 AMPA analysis of 30 kD putative encapsulating protein of *Bl* 1821L spanning -2 to 279 amino acid residues of the protein

Figure 6.9 CPPs motifs identified (shown in red) in putative encapsulating protein (30 kD) of *Bl* 1821L

Table 6.6 CPPs identified in *Bl* 1821L putative encapsulating protein (30 kD) using CellPPD

Peptide sequence	Mutation position	SVM score	Hydrophobicity	Hydropathicity	Hydrophilicity	Charge	Molecular wt.
MARRQLVGRR	No mutation	0.36	-0.60	-1.02	0.71	4.00	1242.65
ARRQLVGRRF	No mutation	0.22	-0.56	-0.93	0.59	4.00	1258.63
RRQLVGRRFI	No mutation	0.10	-0.52	-0.66	0.46	4.00	1300.72
KGRLTHIKSD	No mutation	0.01	-0.41	-1.26	0.78	2.50	1154.48
ARNKLLKMGH	No mutation	0.14	-0.33	-0.81	0.33	3.50	1167.59
ECAVLRIKRP	No mutation	0.06	-0.32	-0.12	0.54	2.00	1184.60
CAVLRIKRPS	No mutation	0.11	-0.29	0.15	0.27	3.00	1142.56
AVLRIKRPSA	No mutation	0.05	-0.27	0.08	0.32	3.00	1110.50

6.3.5 Identification of putative antibacterial protein (48 kD) in *Bl* 1821L genome

N-terminal sequencing of purified (~48 kD) putative antibacterial protein provided several short sequence amino acids which were used to identify the regulating gene in the *Bl* 1821L genome (NZ_CP033464.1). Genome analysis uncovered that the predicted sequenced protein (~48 kD) reads had several hits (covering approximately 34% of the amino acid sequence) to an identified defective prophage protein, similar to that encoded by the *Bs* 168 phage-like element PBSX gene *xkdK* (Table 6.7 & Appendix D-8). This is also a confirmation of the results of *Bl* 1821L in Chapter 3.

6.3.6 N-terminal sequence analysis of *Bl* 1821L identified 48 kD putative antibacterial protein

Identified *Bl* 1821L putative phage-like element PBSX XkdK protein (48 kD) residing in the *Bl* 1821L genome was used to search in the Uniprot database to determine the nature of proteins. The region of *Bl* 1821L genome encoding the predicted XkdK protein (48 kD) shared amino acid identity with a phage tail protein accession tr|A0A0F7EER1|A0A0F7EER1_BRELA and an uncharacterised protein with accession tr|A0A328R421|A0A328R421_BRELA. An equivalent accession tr|A0A518VEB0|A0A518VEB0_BRELA to tr|A0A328R421|A0A328R421_BRELA exists in the Uniprot database (Table 6.7). Amino acid sequence analysis through ExPasy computed the molecular weight of purified *Bl* 1821L putative phage tail protein of 48.5 kD, which was similar to the location of the band on SDS-PAGE (Table 6.7 & Figure 5.24).

BLASTp analysis of the accessions tr|A0A518VEB0|A0A518VEB0_BRELA and tr|A0A0F7EER1|A0A0F7EER1_BRELA against Uniprot database identified 90.3% and 73.5% amino acid similarity to the phage tail-sheath protein of *Bl* LMG 15441 (Appendix D-9). Furthermore, BLASTp analysis revealed similar identity to a phage tail protein, phage sheath protein, and uncharacterised proteins belonging to various *Bl* strains (Table 6.8 & Appendix D-9).

Table 6.7 Identification of *Bl* 1821L putative antibacterial gene and protein (48 kD) in the genome and Uniprot database

Accession	Average molecular mass	Identity	Identified gene	Uniprot description of identified proteins
tr|A0A518VEB0|A0A518VEB0_BRELA	48361.09	Phage tail protein	Phage-like element PBSX *xkdK* gene	Phage tail protein OS= *Brevibacillus laterosporus* OX= 1465 GN= EEL30_25335 PE= 3 SV= 1
tr|A0A0F7EER1|A0A0F7EER1_BRELA	48490.93			Phage tail protein OS= *Brevibacillus laterosporus* OX= 1465 GN= EX87_02320 PE= 4 SV= 1

Table 6.8 Identical proteins of *Bl* 1821L N-terminal sequenced putative phage tail protein of 48 kD with accessions tr|A0A518VEB0|A0A518VEB0_BRELA and tr|A0A0F7EER1|A0A0F7EER1_ BRELA) in the Uniprot database

Accessions	Identical proteins	Organism	Gene name	Length
tr|A0A518VEB0|A0A518VEB0_BRELA tr|A0A0F7EER1|A0A0F7EER1_BRELA	Phage tail protein	*Brevibacillus laterosporus* (*Bacillus laterosporus*)	C4A76_07870, C4A77_13935, D5F52_00915	445
	Phage tail protein	*Brevibacillus laterosporus* (*Bacillus laterosporus*)	EX87_06735	445
	Phage tail-sheath protein	*Brevibacillus laterosporus* LMG 15441	BRLA_c036460	462
	Uncharacterised protein	*Brevibacillus borstelensis* GI-9	BLGI_826	445
	Phage tail protein	*Brevibacillus laterosporus* (*Bacillus laterosporus*)	EEL32_11960	445
	Phage tail protein	*Brevibacillus laterosporus* SKDU 10	AYJO8_14030	445
	Phage tail protein	*Brevibacillus laterosporus* (*Bacillus laterosporus*)	EX87_02320	445
	Phage tail protein	*Brevibacillus laterosporus* (*Bacillus laterosporus*)	D5F52_16160	445
	Phage tail protein	*Brevibacillus laterosporus* (*Bacillus laterosporus*)	C4A76_21720	445

6.3.7 Bioinformatic analysis of identified *Bl* 1821L putative antibacterial protein (48 kD) genomic region

Identified phage-like element PBSX gene *xkdK* of *Bl* 1821L is encoded between 5,137,125 bp to 5,138,462 bp (Figure 6.10). An uncharacterised protein tr|A0A518VE83|A0A518VE83_BRELA residing in *Bl* 1821L genome (NZ_CP033464.1) between 15,854 bp to 15,582 bp shared low amino acid identity with the putative *Brevibacillus* phage Abouo tail fibre protein (Kearse et al., 2012). The genome of *Brevibacillus* phage Abouo (KC595517) encodes two tail fibre proteins; the first is putative tail fibre protein (tr|S5MNY5|S5MNY5_9CAUD) and the second is tail fibre protein (tr|S5M627|S5M627_ 9CAUD). The tail fibre protein of *Bl* 1821L was aligned with both of these proteins. Alignment of *Bl* 1821L tail fibre protein tr|A0A518VE83|A0A518VE83_BRELA with the tail fibre protein tr|S5M627| S5M627_9CAUD and putative tail fibre protein tr|S5MNY5|S5MNY5_9CAUD of *Brevibacillus* phage Abouo using the programme Geneious basic (Kearse et al., 2012) illustrated a low amino acids similarity of 3.5% and 30% with the queried proteins (Appendix D-10 & D-11).

An upstream gene resembling the putative bacteriocin UviB of *Bs* 168 having a precursor of holin BhlA along with other phage-like element PBSX genes *xkdT* and *xkdU* (Figure 6.10) is localised in the genomic region. The gene regulating the holin protein (BhlA) was bioinformatically extracted and subjected to BLASTp analysis and exhibited 100% amino acid identity to an uncharacterised protein of *Bl* LMG 15441, in addition to similar uncharacterised proteins from different *Bl* phages (Table 6.9). A hydrolytic enzyme, N-acetylmuramoyl-L-alanine amidase, a regulating gene, is next to the UviB/holin BhlA in the genomic region (Figure 6.10). Furthermore, several other phage-like proteins including a tail protein, phage FluMu protein Gp47, and a prophage LambdaBa01 Xpf encoded in the PBSX-like region of *Bl* 1821L are also annotated. Various hypothetical protein encoding genes are also localised in the region where the XkdK protein resides in the *Bl* 1821L genome. Located at the 3' end of the phage-like element PBSX x*kdK* gene encoding region are four (ABC transporter) permease genes *yvcR*, *yvcS*, *yvcQ*, and *yvcP* (Figure 6.10). The translated products of these genes have been implicated in the export of lipid II-binding lantibiotics, such as nisin and gallidermin (McAuliffe et al., 2001; Smits et al., 2020).

Bl 1821L phage tail-sheath like encoding region exhibiting homology to the PBSX-like region of *Bs* 168 was also identified in the genome of *Bl* 1951 (RHPK01000003.1, contig 1) at the position between 1,937,150 bp to 1,935,813 bp (Figure 6.12). At the 5' end of XkdK protein encoding gene two hypothetical proteins reside. Therefore, BLASTp analysis of hypothetical proteins was performed to affirm the nature of proteins. An uncharacterised protein with accession tr|A0A502IL32|A0A502IL32_BRELA identical to the predicted protein immediate upstream of XkdK protein is localised. However, the adjacent upstream hypothetical protein tr|A0A502IL09|A0A502IL09_BRELA showed 96% amino acids similarity with the XkdN protein of *Bl* LMG 15441 having accession tr|A0A075R977|A0A075R977_BRELA (Figures 6.12 & 6.13). Analysis of the genomic region revealed the presence of genes involved in phage lysis activities including N-acetylmuramoyl-L-alanine amidase and holins. Furthermore, in the *Bl* 1951 genome sequence several other PBSX-like region genes such as *xkdT* and *xkdU* as well as other phage-relevant and hypothetical genes are encoded (Figure 6.12).

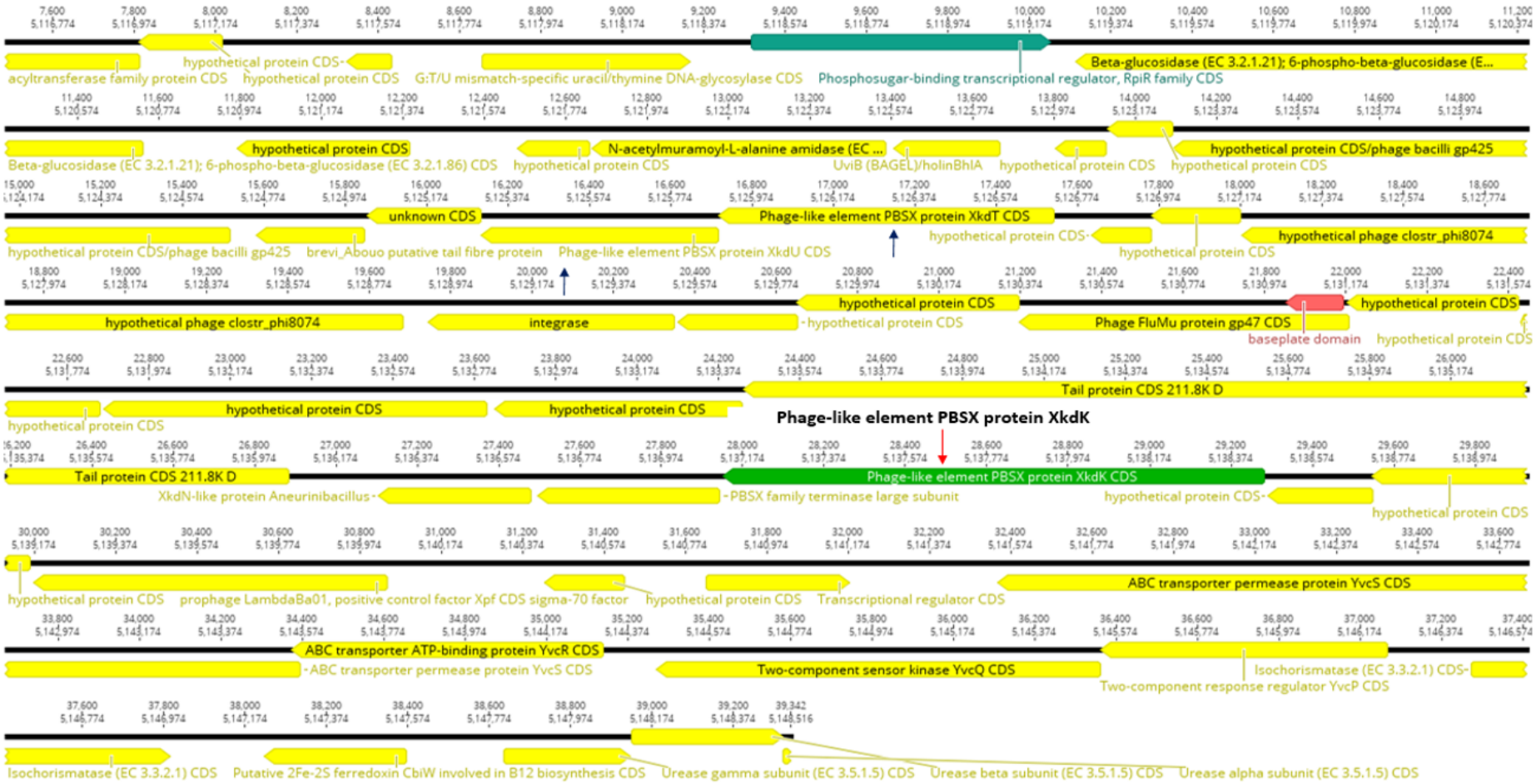

Figure 6.10 Geneious output of the 48 kD N-terminal sequence of *Bl* 1821L identifying a putative phage-like element PBSX gene *xkdK* (shown in green with red arrow) and dark blue arrows point to other phage-like element PBSX genes (*xkdT* & *xkdU*) residing in *Bl* 1821L genome

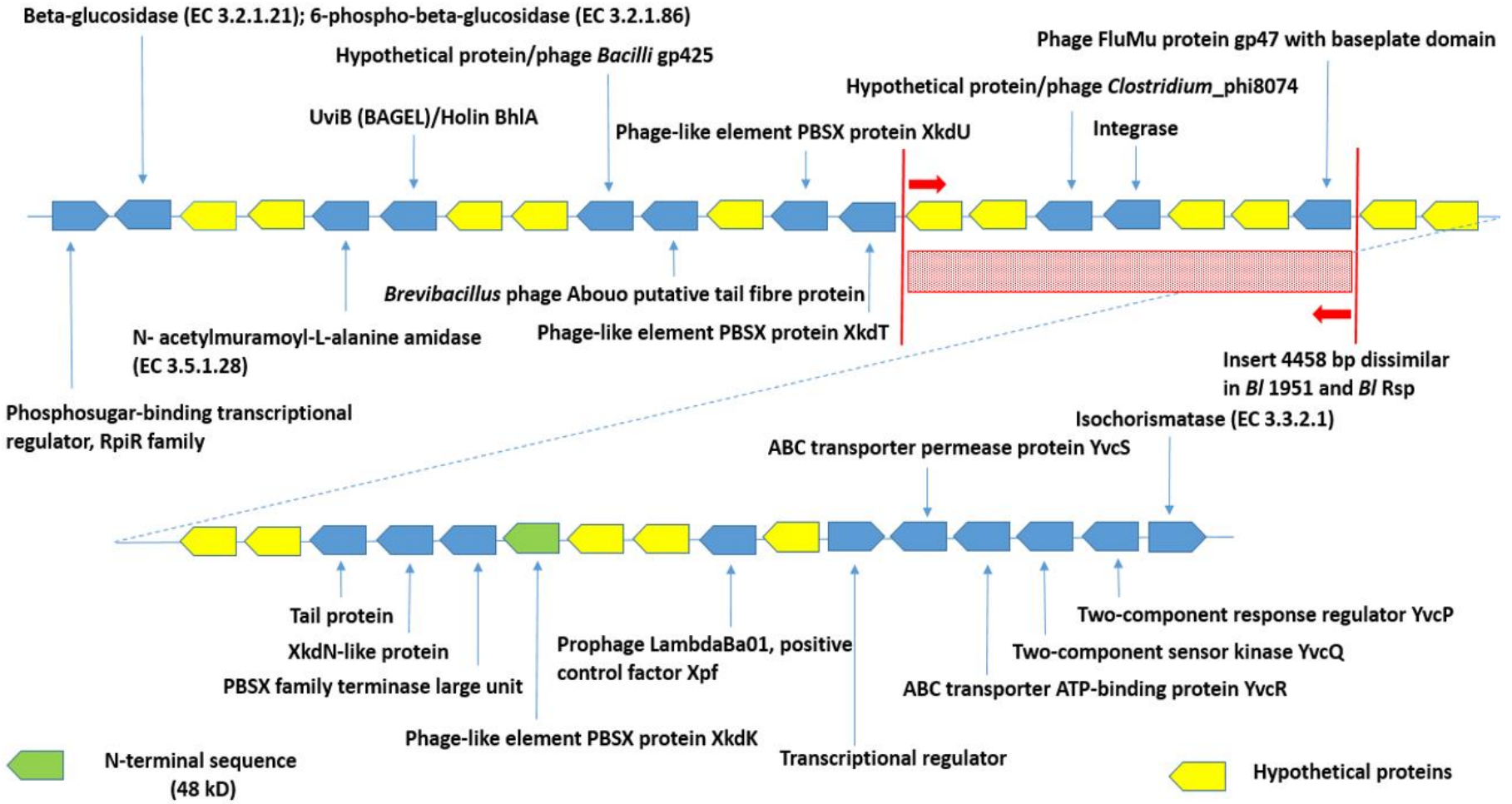

Figure 6.11 Genomic architecture of the 48 kD N-terminal sequence of *Bl* 1821L showing identified phage-like element PBSX gene *xkdK* along with other genes of the region. The red shaded box denotes the region of difference between *Bl* 1821L and *Bl* 1951

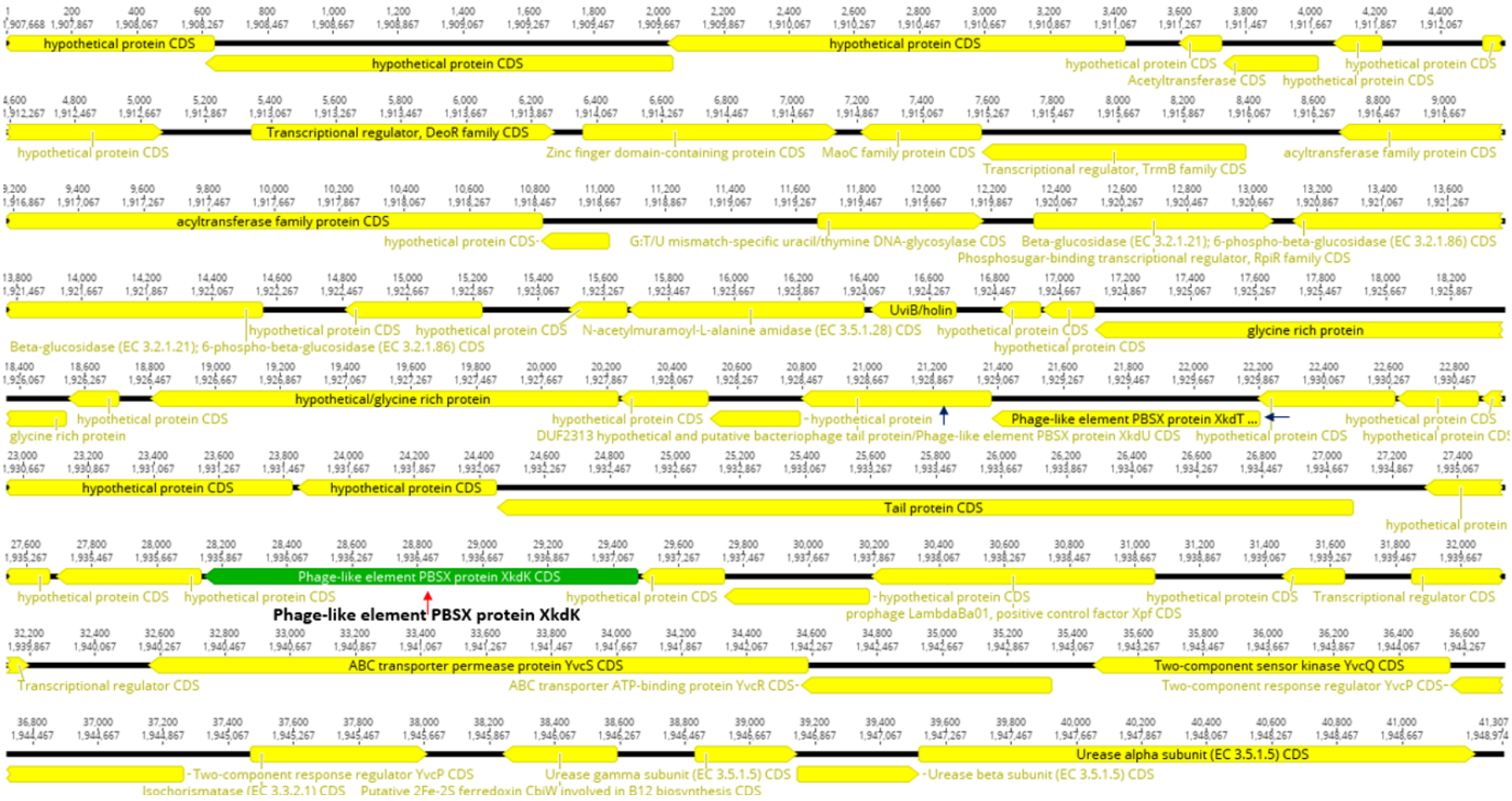

Figure 6.12 Geneious output of the 48 kD N-terminal sequence of *Bl* 1821L identifying a putative phage-like element PBSX gene *xkdK* (shown in green with red arrow) and dark blue arrows point to other phage-like element PBSX genes (*xkdT* & *xkdU*) residing in *Bl* 1951 genome

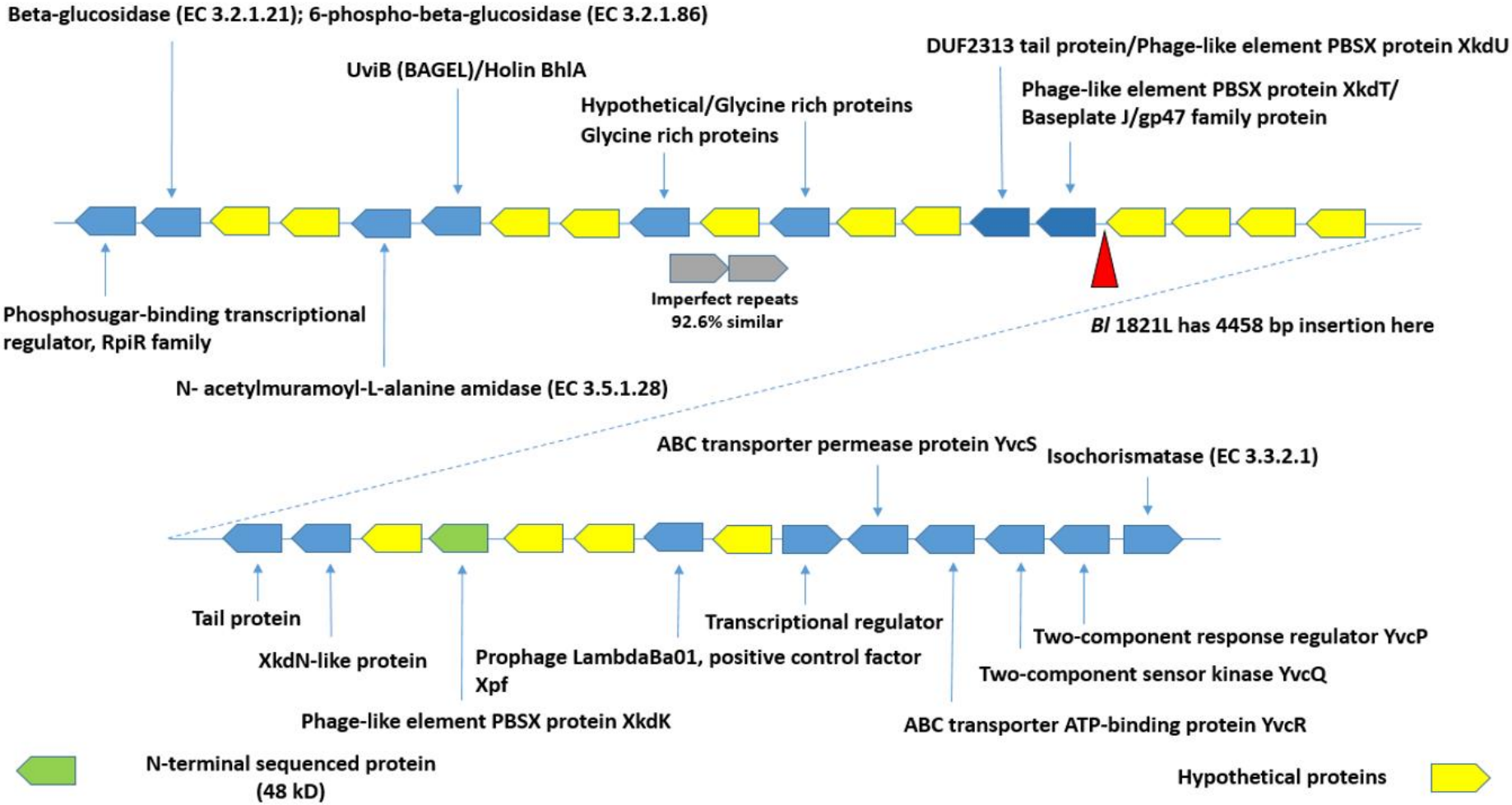

Figure 6.13 Genomic architecture of the 48 kD N-terminal sequence of *Bl* 1821L showing identified phage-like element PBSX gene *xkdK* encoding region in *Bl* 1951 along with other genes of the region. The filled red wedge points to the integration of the red shaded region of *Bl* 1821L (Fig. 6.11) in the *Bl* 1951 genome

Table 6.9 Protein orthologues of *Bl* 1821L UviB (BAGEL)/Holin BhlA protein in the Uniprot database

Accession	Homologous protein	Organism	% identity
tr|A0A075R9K7|A0A075R9K7_BRELA	Uncharacterised protein	*Brevibacillus laterosporus* LMG 15441	100
tr|S5M5U3|S5M5U3_9CAUD	Bacteriocin UviB	*Brevibacillus* phage Emery	92.0
tr |S5M6A1|S5M6A1_9CAUD	Uncharacterised protein	*Brevibacillus* phage Davies	90.8
tr|S5MNE1|S5MNE1_9CAUD	Uncharacterised protein	*Brevibacillus* phage Jimmer 1	90.8
tr|A0A0K2CND1|A0A0K2CND1_9CAUD	Uncharacterised protein	*Brevibacillus* phage Osiris 1	90.8

Bioinformatic analysis of the PBSX-like region in both the strains (*Bl* 1821L & *Bl* 1951) displayed a similar organisational structure of the operons (Figure 6.14B). However, the alignment of the two regions indicate that for *Bl* 1951 in the upstream region of XkdK there are genes encoding glycine rich proteins and the phage-like element similar to PBSX gene *xkdU*. Interestingly, two imperfect repeats of glycine rich proteins (1700 bp long) residing in the *Bl* 1951 genome (Figure 6.12) exhibited 92.6% similarity to each other (Figure 6.14B). For *Bl* 1821L, this part of the genome differed from *Bl* 1951 as the PHASTER programme identified a putative phage region (Figure 6.14B). In the upstream region of the *Bl* 1821L putative phage region and the imperfect repetitive region of *Bl* 1951 the encoding genes have only minor differences between the two strains (Figure 6.14B). Likewise, analysis of the genomic region of both *Bl* 1821L and *Bl* 1951 using the programme Mauve (Darling et al., 2004) substantiated the findings by indicating the region of differences as shown in Figure 6.14A (blank areas).

Furthermore, in the upstream region of *Bl* 1821L where putative phage-like element PBSX gene *xkdK* was found and hypothetical phage *Clostridium*_phi8074, integrase, phage Flu protein Gp47 with baseplate domain, and other hypothetical proteins relevant genes are encoded, differ by 4458 bp from *Bl* 951 and *Bl* Rsp strains (Figure 6.11). Like the *Bl* 1821L genomic region, both holin and N-acetylmuramoyl-L-alanine amidase encoding genes, which are an integral part of bacterial lysis systems, are also localised (Figure 6.12).

A schematic of the PBSX-like region of *Bl* 1821L with identified 48 kD XkdK protein is presented in Figure 6.15D along with the 3D structure (Figure 6.15A) and morphological features of XkdK protein (Figure 6.15C) corresponding to a typical tailed phage (*Myoviridae*) structural proteins (Figure 6.15B) is shown.

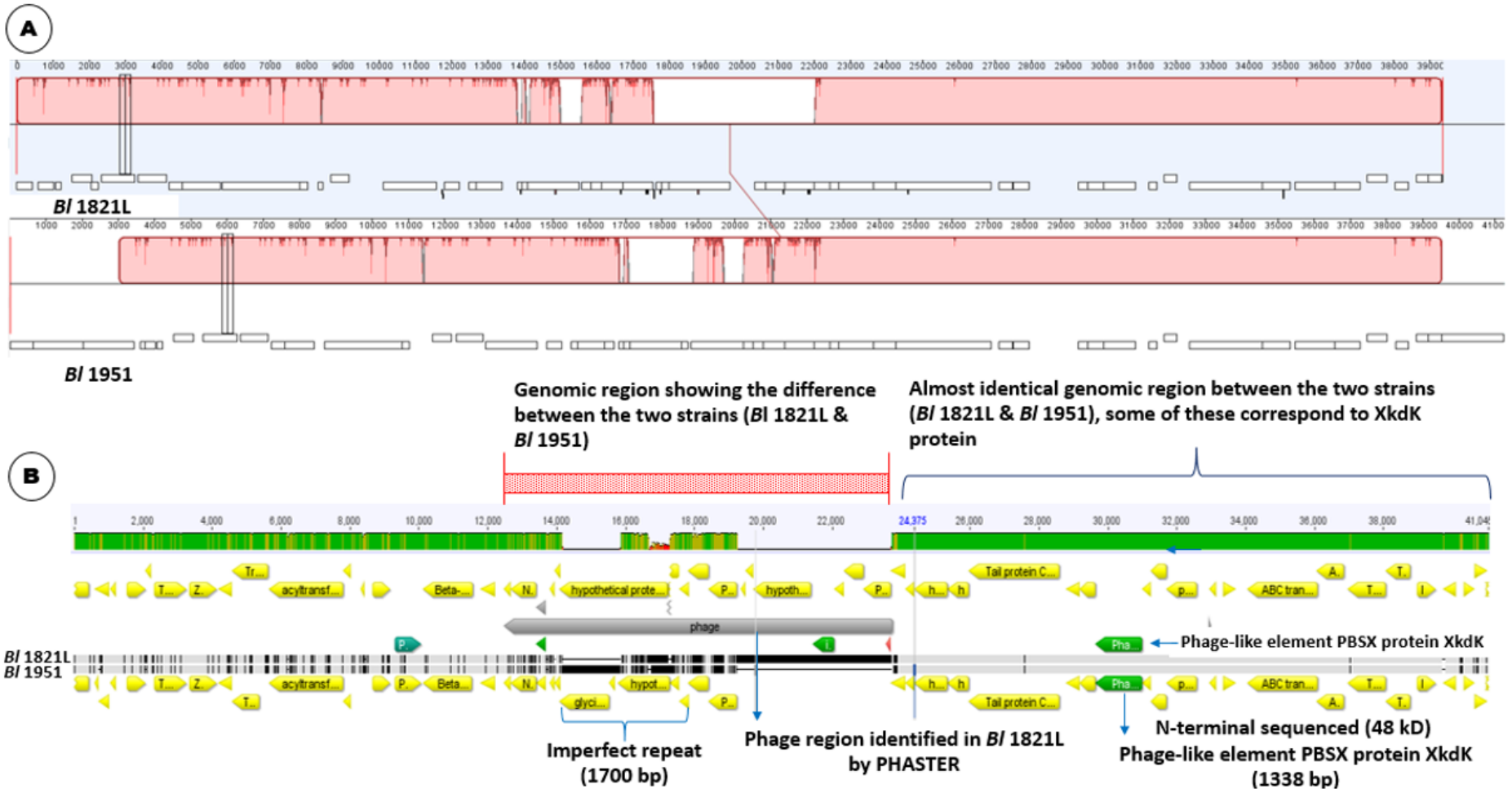

Figure 6.14 (A) Mauve analysis of the *Bl* 1821L and *Bl* 1951 genomic regions. (B) Annotation of the *Bl* 1821L and *Bl* 1951 genomic regions including 48 kD encoded phage-like element PBSX gene *xkdK* (1338 bp long) showing the region of differences between the two strains (shown in red shaded box). PBSX like region in *Bl* 1951 encodes genes of 1700 bp long imperfect repeats of glycine rich proteins and in an analogous *Bl* 1821L genomic region a putative phage region is predicted

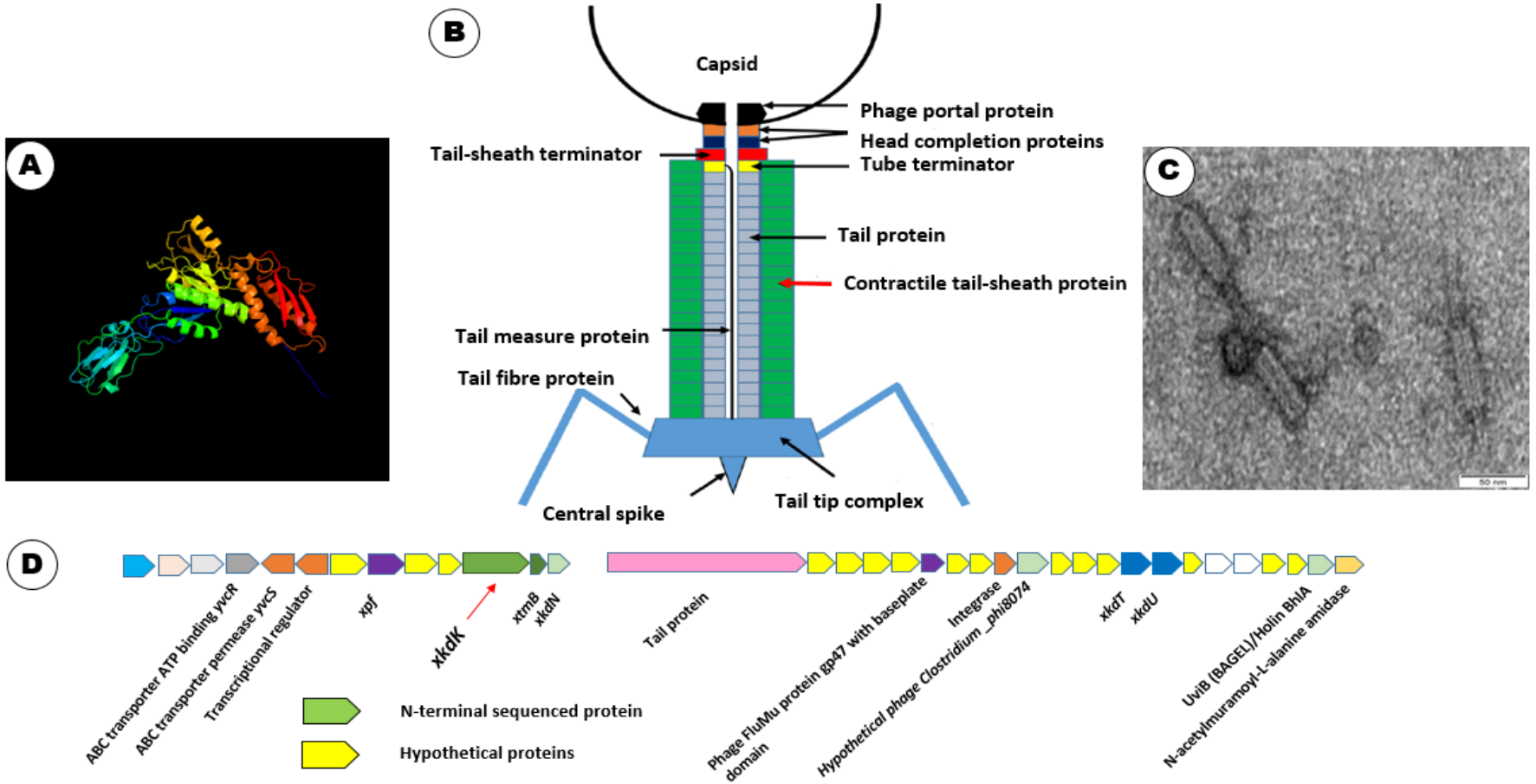

Figure 6.15 (A). Predicted 3D structure of 48 kD identified phage-like element PBSX protein XkdK of *Bl* 1821L generated using Phyre[2] (Kelley et al., 2015). (B). Schematic presentation of structural proteins of a contractile-tailed bacteriophage (*Myoviridae*) (Fokine & Rossmann, 2014). (C). Electron micrograph showing the contractile sheath-like structure (Scale bar= 50 nm) similar to a typical *Myoviridae* phage (shown with red arrow in Fig. 6.15B). (D). Genomic organisation of *Bl* 1821L PBSX-like region with identified *xkdK* gene (shown in green with red arrow)

6.3.8 Comparison of 48 kD identified *Bl* 1821L and *Bl* 1951 phage-like element PBSX protein XkdK with the similar proteins of other gram-positive bacteria

Phage like-element PBSX protein (XkdK) of *Bl* 1821L (NZ_CP033464.1) and *Bl* 1951 (RHPK01000003.1, contig 1) identified with accession tr|A0A518VEB0|A0A518VEB0_BRELA was aligned with BLASTp analysed and identical XkdK proteins/phage tail-sheath proteins of other gram-positive bacteria (Table 6.10) using Geneious basic (Kearse et al., 2012), and a dendrogram was also drawn using the same programme.

Table 6.10 Encoded phage-like element PBSX protein XkdK and phage tail-sheath proteins in different gram-positive bacteria

Accession	Protein name	Organism
tr|A0A0D1WNL8|A0A0D1WNL8_ANEMI	Phage tail sheath	*Aneurinibacillus migulanus*
tr|A0A410KN98|A0A410KN98_9BACI	Phage tail sheath	*Bacillus aerophilus*
tr|R4JQA6|R4JQA6_9CAUD	Structural protein	*Bacillus* phage PBP180
tr|A0A5B0B6Z4|A0A5B0B6Z4_9BACI	Phage-like element PBSX XkdK	*Bacillus* sp. ANT_WA51
tr|A0A410QZ71|A0A410QZ71_9BACI	Phage-like element PBSX XkdK	*Bacillus* sp. WR11
tr|A0A6H0H1P2|A0A6H0H1P2_BACIU	Phage-like element PBSX XkdK	*Bacillus subtilis* subsp. s*ubtilis* str. SMY
tr|P54331|XKDK_BACSU	Phage-like element PBSX XkdK	*Bacillus subtilis168*
tr|C0Z5G9|C0Z5G9_BREBN	Uncharacterised protein	*Brevibacillus brevis* (strain 47/JCM 6285/NBRC 100599)
tr|A0A3M8B733|A0A3M8B733_9BACL	Phage tail	*Brevibacillus gelatini*
tr|A0A075R9L5|A0A075R9L5_BRELA	Phage tail sheath	*Brevibacillus laterosporus* LMG 15441
tr|Q18BN0|Q18BN0_CLOD6	Phage-like element PBSX XkdK	*Clostridioides difficile* 630
tr|A0A061P351|A0A061P351_9BACL	Phage-like element PBSX XkdK	*Geomicrobium* sp. JCM 19039

Alignment of the *Bl* 1821L and *Bl* 1951 XkdK amino acid sequence (48 kD) with orthologous proteins of the genus *Aneurinibacillus*, *Bacillus*, *Brevibacillus*, *Clostridoides*, and *Geomicrobium* provided an

insight into their phylogenic relationships. The alignment of XkdK proteins encoded in the PBSX region revealed that all of these were distantly related to each other (Figure 6.17). PBSX is considered a model phage tail sheath-like protein (XkdK) representative of *Bs* 168 but had only 21.2% amino acid similarity with the queried XkdK protein (tr|A0A518VEB0|A0A518VEB0_BRELA) of *Bl* 1821L and *Bl* 1951 (Appendix D-14). While this is low for the specific gene, the similarity of the whole operon is of interest and suggests shared origins. Comparatively, *Bl* 1821L and *Bl* 1951 predicted XkdK protein (48 kD) exhibited 89.1%, 69%, and 68% homology to the phage tail-sheath, phage tail, and an uncharacterised protein of *Bl* LMG 15441, *B. gelatini*, and *B. brevis* 47/JCM 6285/NBRC 100599 respectively (Appendix D-14). Likewise, the XkdK protein of *Bs* 168 shared 100% amino acid similarity with the *Bacillus* sp. WR11, *Bacillus* sp. ANT_WA51, *Bs* subsp. *subtilis* SMY, 64.8% with *B. aerophilus* and *B. pumilus* AB94180, 51.7% with *Geomicrobium* sp. JCM 19039, and 41.5% with *Aneurinibacillus migulanus* (Appendix D-14). XkdK protein of *C. difficile* 630 displayed a low homology (19.9%) with the 48 kD protein and the same trend was followed for other aligned proteins (Appendix D-14). Furthermore, distance matrices of aligned XkdK proteins (Figure 6.17 & Appendix D-13) and amino acids alignment using Geneious basic (Kearse et al., 2012) (Figure 6.16 & Appendix D-14) and CLUSTALO (Appendix D-12) substantiated the findings.

6.3.9 Comparison of identified putative phage tail-sheath protein (48 kD) of *Bl* 1821L and *Bl* 1951 with the phage tail-sheath protein of different *Bl* phages

The identified 48 kD putative phage tail-sheath protein (XkdK) of *Bl* 1821L and *Bl* 1951 with accession tr|A0A518VEB0|A0A518VEB0_BRELA was aligned with the phage tail-sheath protein of different *Bl* phages including Abouo (tr|S5MUG6|S5MUG6_9CAUD), Jimmer1 (tr|S5MNC1|S5MNC1_9CAUD), Davies (tr|S5MCF5|S5MCF5_9CAUD), Jimmer2, (tr|S5MBG7|S5MBG7_9CAUD), Powder (tr|A0A0K2FLW7|A0A0K2FLW7_9CAUD), and Osiris (tr|A0A0K2CNL4|A0A0K2CNL4_9CAUD) (Berg et al., 2016). Alignment of *Bl* 1821L and *Bl* 1951 identified phage tail-sheath protein with the similar protein of different *Bl* phages suggests its nature. *Bl* specific phages Abouo, Jimmer1, Davies, Jimmer2, Powder, and Osiris phage tail-sheath proteins were prominently (>97%) similar to each other, but exhibited low amino acids similarity (21.9%) to the putative phage tail-sheath protein of *Bl* 1821L and *Bl* 1951 (Figure 6.18 & Appendix D-17). Furthermore, distance matrices of aligned phage tail-sheath proteins (Figure 6.19 & Appendix D-16) and amino acids alignment using CLUSTALO (Appendix D-15) also substantiated the findings.

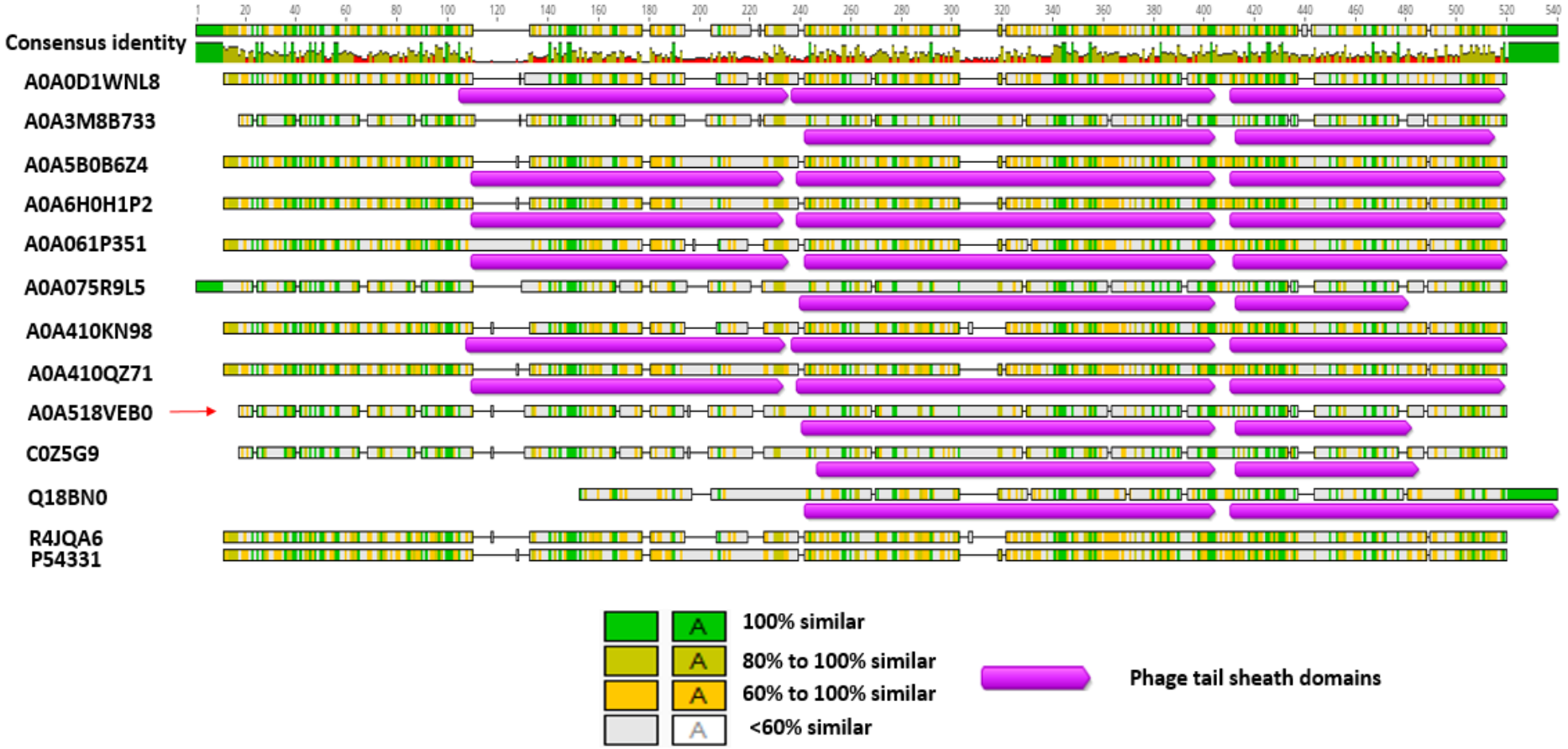

Figure 6.16 Alignment of 48 kD identified phage-like element PBSX protein XkdK accession A0A518VEB0 (shown with red arrow) of *Bl* 1821L and *Bl* 1951 with the phage tail-sheath proteins of *Aneurinibacillus migulanus* (A0A0D1WNL8), *Bacillus aerophilus* (A0A410KN98), *Brevibacillus gelatini* (A0A3M8B733), *Brevibacillus laterosporus* LMG 15441 (A0A075R9L5); uncharacterised protein of *Brevibacillus brevis* (strain 47/JCM 6285/NBRC 100599), and similar proteins of other gram-positive bacteria including *Bacillus* phage PBP180 (R4JQA6), *Bacillus* sp. ANT_WA51 (A0A5B0B6Z4), *Bacillus* sp.WR11 (A0A410QZ71), *Bacillus subtilis* subsp. *subtilis* str. SMY (A0A6H0H1P2), *Bacillus subtilis* 168 (P54331), *Clostridioides difficile* 630 (Q18BN0), and *Geomicrobium* sp. JCM 19039 (A0A061P351) using the Geneious basic

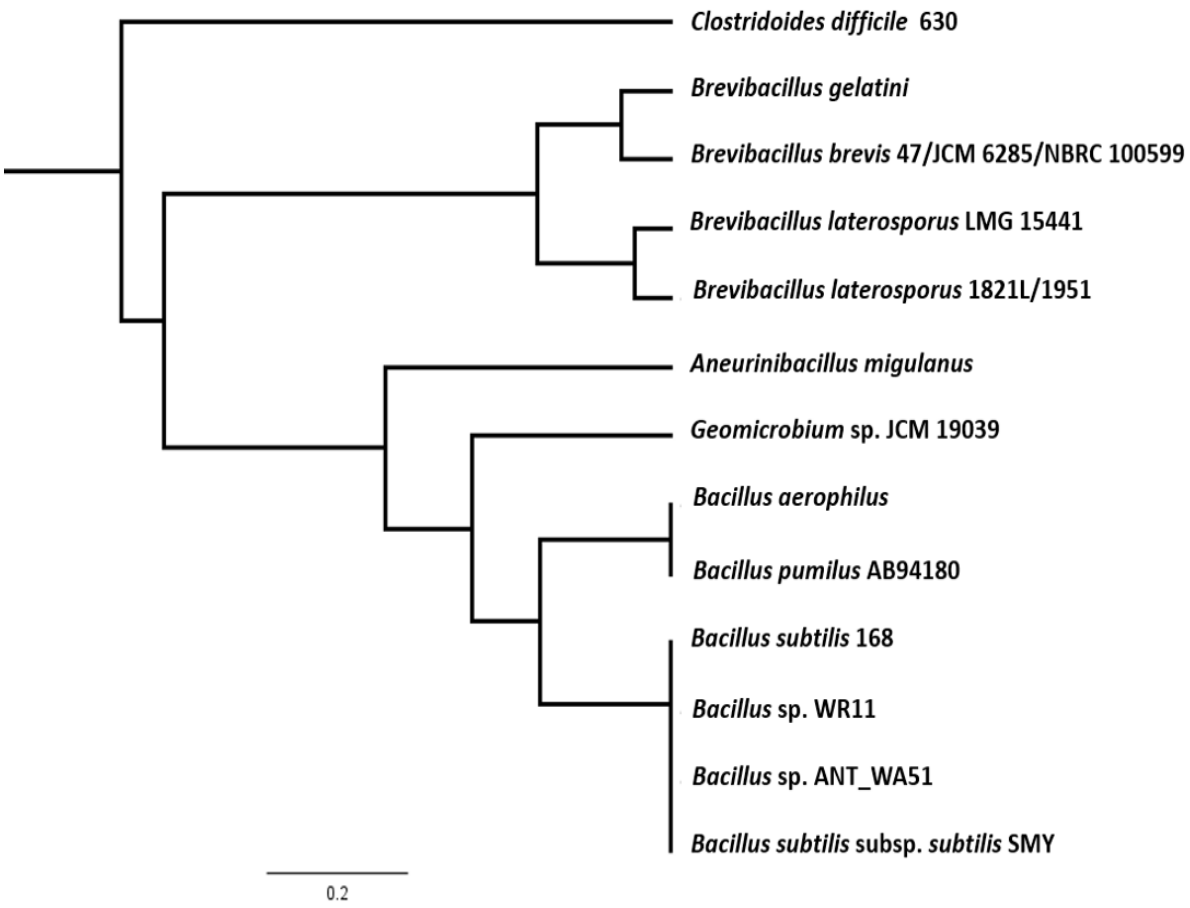

Figure 6.17 Dendrogram showing alignment *Bl* 1821L and *Bl* 1951 identified (A0A518VEB0) phage-like element PBSX protein XkdK (48 kD) with similar proteins of other gram-positive bacteria

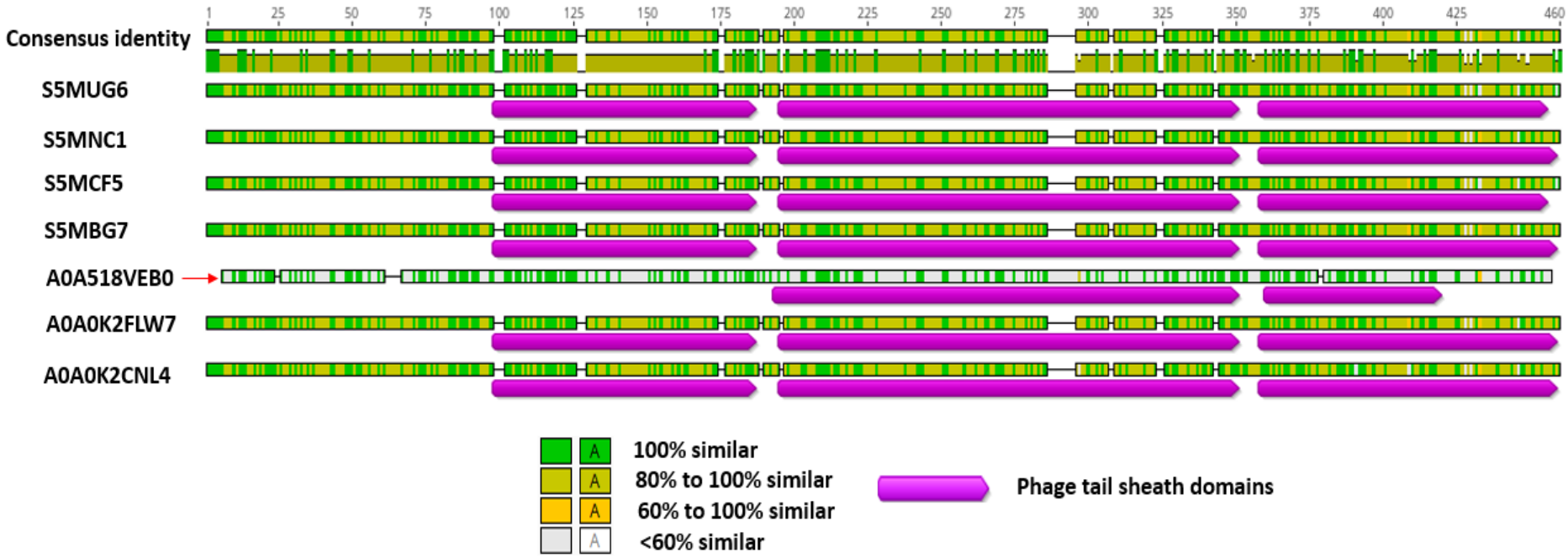

Figure 6.18 Amino acids alignment of 48 kD identified putative phage tail-sheath protein accession A0A518VEB0 (shown with red arrow) of *Bl* 1821L and *Bl* 1951 with similar proteins of different *Bl* phages including Abouo (S5MUG6), Jimmer1 (S5MNC1), Davies (S5MCF5), Jimmer2, (S5MBG7), Powder (A0A0K2FLW7), and Osiris (A0A0K2CNL4) using Geneious basic

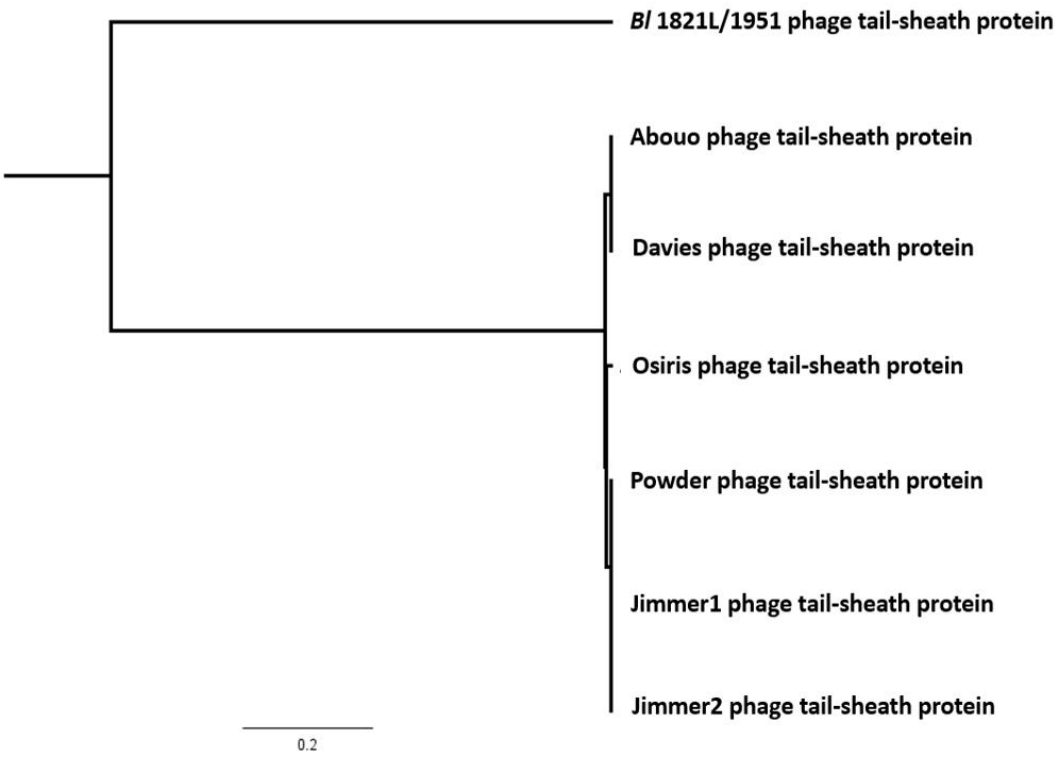

Figure 6.19 Dendrogram showing the alignment of identified (48 kD) putative phage tail-sheath protein (A0A518VEB0) of *Bl* 1821L and *Bl* 1951 with similar protein of different *Bl* phages

6.3.10 Genomic comparison of the *Bl* 1821L and *Bl* 1951 PBSX-like region with the similar region of defective prophages PBSZ, PBSX, and PBP180

The genomic organisation of the identified *Bl* 1821L (NZ_CP033464.1) and *Bl* 1951 (RHPK01000003.1, contig 1) PBSX-like region displayed similarities as shown in Figures 6.20 and 6.21. However, some variations were also found in the PBSX-like regions of both strains (Figure 6.14). Therefore, the PBSX-like regions of *Bl* 1821L and *Bl* 1951 were compared with the defective prophages PBSZ, PBSX, and PBPB180 of *B. subtilis* W23, *B. subtilis* 168, and *Bacillus* phage PBP180 (Jin et al., 2014). Amino acids content of *Bl* 1821L and *Bl* 1951 XkdK protein (48 kD) tr|A0A518VEB0|A0A518VEB0_BRELA was compared with the similar proteins of PBSZ (tr|E0U1S9|E0U1S9_BACPZ), PBSX (sp|P54331|XKDK_ BACSU), and PBP180 (tr|R4JQA6|R4JQA6_9CAUD). Likewise, amino acid residues of the tail protein (tr|A0A518VEA0|A0A518VEA0_BRELA) residing in *Bl* 1821L and *Bl* 1951 PBSX-like region was Compared with the similar proteins of defective prophages PBSZ (tr|E0U1T3|E0U1T3_BACPZ), PBSX (sp|P54334|XKDO_BACSU), and PBP180 (tr|R4JJ03|R4JJ03_9CAUD) (Jin et al., 2014).

N-acetylmuramoyl-L-alanine amidase (XlyA) is one of the lysis proteins of the phage lysis system so a corresponding protein (tr|A0A518VEA4|A0A518VEA4_BRELA) encoded in the *Bl* 1821L and *Bl* 1951 PBSX-like region was compared with the similar proteins of PBSZ (tr|E0U1U7|E0U1U7_BACPZ), PBSX

(sp|P39800|XLYA_BACSU), and PBP180 (tr|R4JMV0|R4JMV0_9CAUD). Holin (XhlB), another lysis protein (tr|A0A075R9K7|A0A075R9K7_BRELA) residing in the PBSX-like region of *Bl* 1821L and *Bl* 1951 was also compared with the similar proteins of defective prophages PBSZ (tr|E0U1U5|E0U1U5_ BACPZ), PBSX (sp|Q99163|XHLB_BACSU), and PBP180 (tr|R4JHG4|R4JHG4_9CAUD) (Jin et al., 2014). Genomic organisation of the *Bl* 1821L PBSX-like region with that of the PBSZ, PBSX, and PBP180 indicated significant differences. Phage-like element PBSX protein XkdK (48 kD) encoding gene of *Bl* 1821L at the 5' end is flanked by a large terminase unit (*xtmB*) gene and *xkdN* while uncharacterised proteins and a prophage LambdaBa01, positive control factor *xpf* reside at the 3'end (Figure 6.20). The gene *xkdM* residing immediately upstream in the other *Bacillus* strains was absent in the *Bl* 1821L. Immediately upstream of *xkdN* gene encoding the tail protein corresponding to *xkdO* gene of PBSX, PBSZ and PBP180 is encoded in the *Bl* 1821L genome but in other *Bacillus* strains, gene *xkzB* is located before the tail protein. XkdP, a murein binding protein resides immediately upstream of the tail protein of the *Bacillus* strains and afterwards several hypothetical proteins (XkdQ, XkdR, XkdS) are present (Figure 6.20). Similarly, for *Bl* 1821L four hypothetical proteins adjacent to the tail protein (XkdO) are localised. The genomic region where *xkdT* and *xkdU* genes reside, is almost the same in its organisation but in *Bl* 1821L uncharacterised proteins reside both upstream and downstream of these genes. However, other proteins, including phage FluMu protein with baseplate domain, hypothetical proteins, integrase protein, and a hypothetical phage *Clostridium*_ phi8074, are also found in this area (Figure 6.20). In the PBP180 phage XkdK protein encoding region operons ORF30, 33, and 35 demonstrated some similarity to XkdV proteins of PBSX but differences were reported (Jin et al., 2014). A low homology tail fibre protein to that of *Brevibacillus* phage Abouo and phage *Bacilli* Gp425 is present in this region of *Bl* 1821L. Lysis genes (*xepA*, *xhlA, xhlB*, *xlyA*) reside in PBSZ, PBSX, and PBP180 defective prophages. Although in *Bl* 1821L PBSX-like region genes corresponding to phage lysis *xhlB* (holin) and endolysin (*xlyA*) are encoded but at the 3' end of holins two hypothetical proteins are localised (Figure 6.20).

Similar to *Bl* 1821L, the encoded PBSX-like region in the *Bl* 1951 genome was analysed to compare the genomic organisation with that of PBSZ, PBSX, and PBP180 (Figure 6.21). A gene corresponding to a hypothetical protein is encoded at the 5' end of *xkdK*. Despite similarities in the genomic architecture in the upstream and downstream of *xkdK* gene some prominent differences exist. *Bl* 1951 genomic region where the genes encoding XkdT and XkdU proteins reside includes some hypothetical and glycine rich proteins. For *Bl* 1951 in this region, imperfect repeats of glycine rich proteins (1700 bp long) are encoded where a putative phage region is located in *Bl* 1821L (Figure 6.14). This is the region where the genes encoding XkdV and hypothetical proteins reside in *Bacillus* strains (Figure 6.20).

Amino acid alignment of XkdK protein (48 kD) of *Bl* 1821L and *Bl* 1951 expressed a low amino acid identity of 22.9%, 22.9%, and 21.6% with the respective protein orthologues PBSZ, PBSX and PBP180 (Figure 6.22 & Appendix D-20). However, XkdK proteins of *Bacillus* strains had a high level of amino acid similarity to each other as compared to those in *Bl* 1821L and *Bl* 1951 (Appendix D-20). Furthermore, distance matrices of the aligned XkdK proteins using Geneious basic (Kearse et al., 2012) (Figure 6.23 & Appendix D-19) and amino acids alignment using CLUSTALO (Appendix D-18) substantiated the findings.

Tail protein residing in the PBSX-like region of *Bl* 1821L and *Bl* 1951 demonstrated 50% similarity with the corresponding protein of PBSZ prophage but had no alignment with the PBSX and PBP180 defective prophage tail proteins. However, PBSX protein showed 51.1% and 37% amino acids similarity with the PBSZ and PBP180 tail proteins (Appendix D-23). Furthermore, distance matrices of aligned tail proteins calculated using Geneious basic (Kearse et al., 2012) (Appendix D-22) and amino acids alignment using CLUSTALO (Appendix D-21) substantiated the findings.

The holin protein (XhlB) of PBSX expressed high amino acid similarity with PBSZ (89.8%) and PBP180 (61.4%) but comparatively, the *Bl* 1821L and *Bl* 1951 holin protein (BhlA) exhibited a low level of 11.4% to 13.6% analogy with PBP180, PBSZ, and PBSX (Appendix D-26 & D-27B). Furthermore, the distance matrices using Geneious basic (Kearse et al., 2012) (Appendix D-25 & D-27A) and amino acids alignment using CLUSTALO (Appendix D-24) substantiated the findings. N-acetylmuramoyl-L-alanine is an endolysin related protein (XlyA) localised in the *Bl* 1821L and *Bl* 1951 genomes, which had a low sequence similarity of 15.4%, 15.4%, and 7.7% to PBSZ, PBSX, and PBP180 respectively (Appendix D-30 & D-31A). These proteins were quite similar to each other; PBSX having amino acids similarity of 95.3% with PBSZ and 53.9% with PBP180 (Appendix D-30 & D-31A). Furthermore, the distance matrices (Appendix D-29 & D-31B) and amino acids alignment using CLUSTALO (Appendix D-28) substantiated the findings.

A summary of amino acids (%) alignment of tail-sheath protein (XkdK), tail protein (XkdO), N-acetylmuramoyl-L-alanine (XlyA), and holin (XhlB) residing in the PBSX-like region of *Bl* 1821L and *Bl* 1951 with similar proteins of defective prophages PBSZ, PBSX, and PBP180 is presented below (Table 6.11). Likewise, a comparative summary of amino acids (%) alignment of PBSX with the PBSZ, PBP180, and PBSX-like region of *Bl* 1821L and *Bl* 1951 is also presented in Table 6.12.

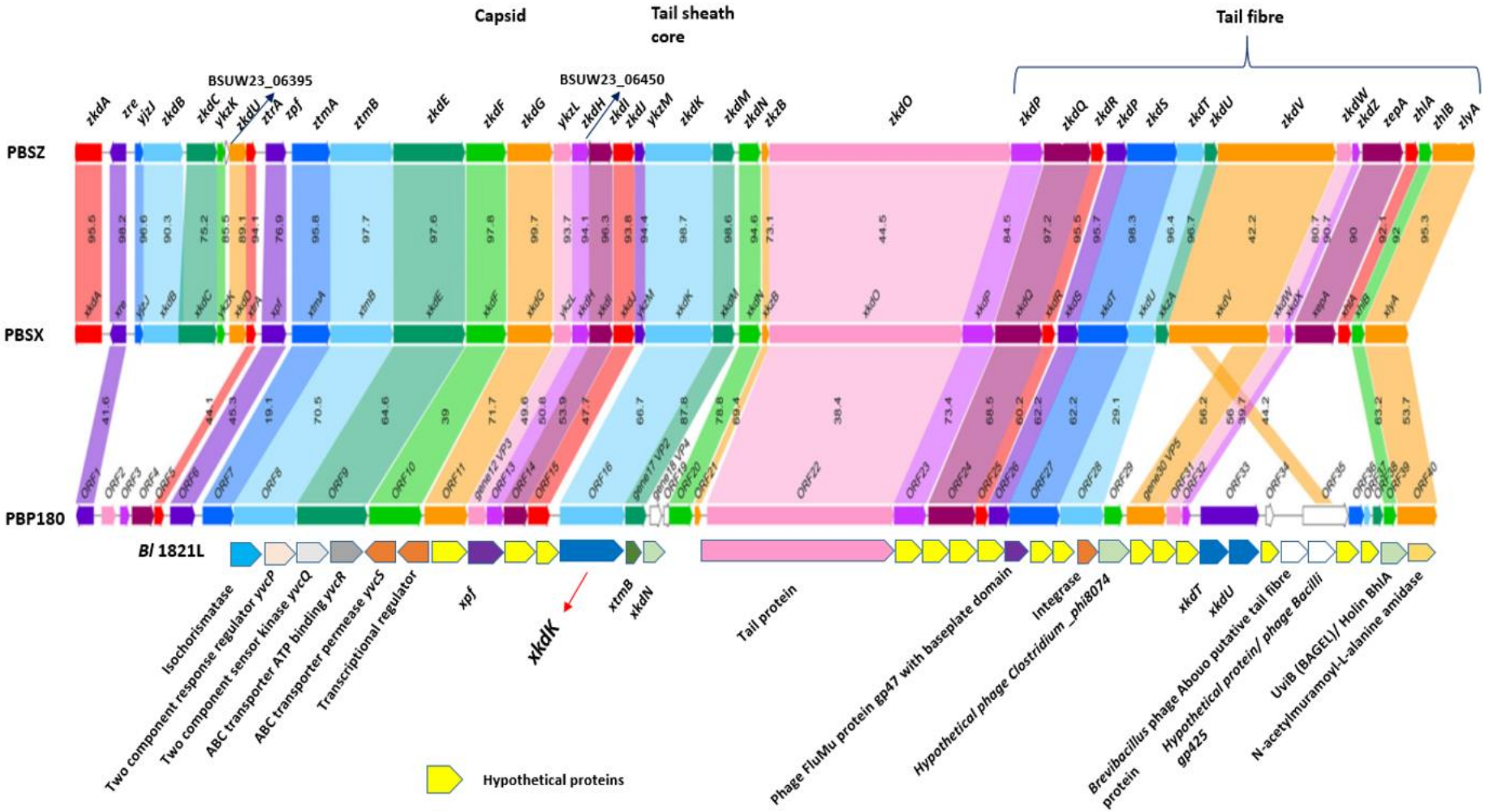

Figure 6.20 Schematic genomic alignment of identified phage-like element PBSX gene *xkdK* (shown with red arrow) encoding region in the *Bl* 1821L genome with defective prophages PBSZ, PBSX, and PBP180 of *B. subtilis* subsp. *spizzenii* W23, *B. subtilis* 168, and *Bacillus* phage PBP180 (Jin et al., 2014)

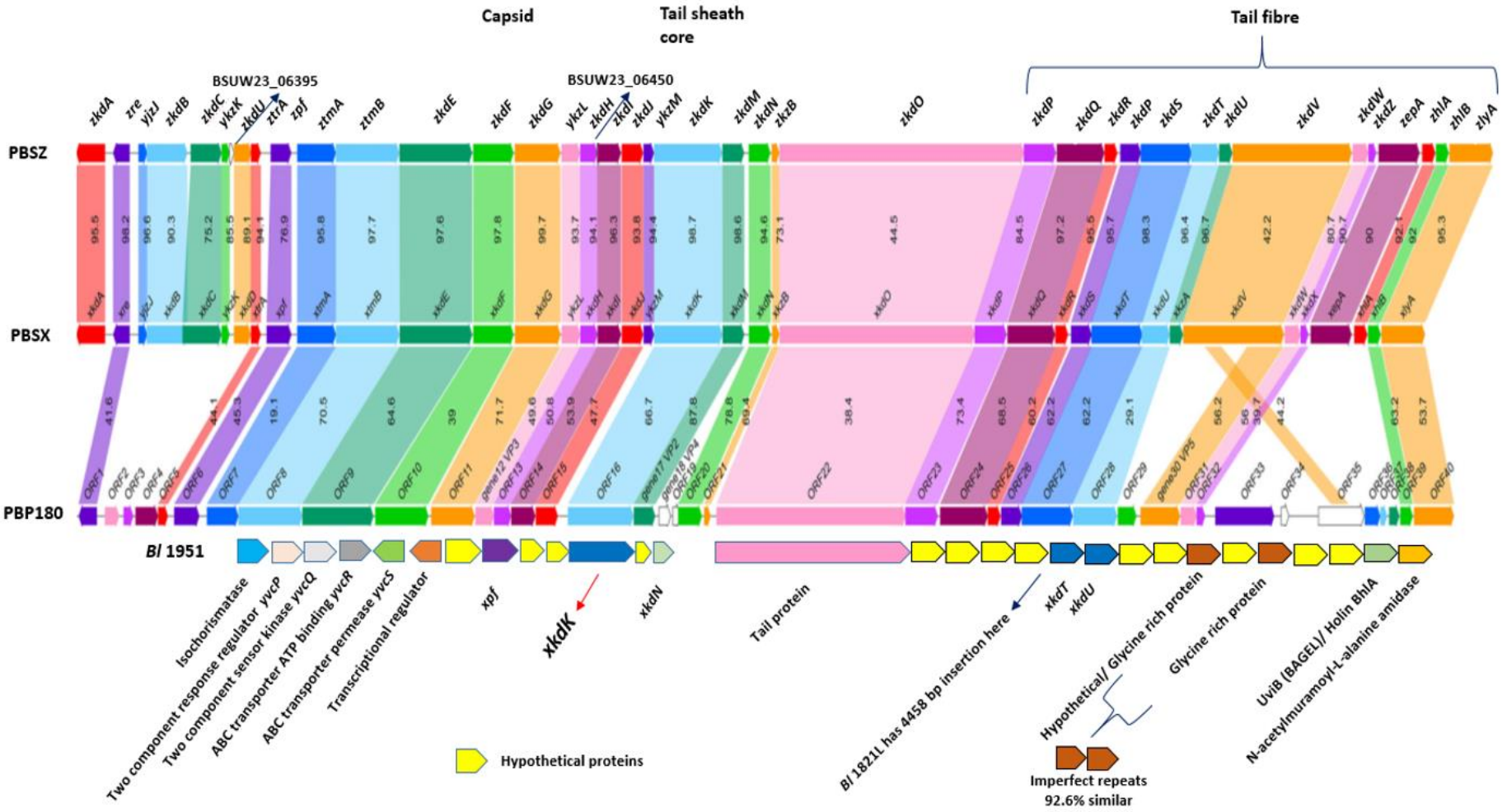

Figure 6.21 Schematic genomic alignment of identified phage-like element PBSX gene *xkdK* (shown with red arrow) encoding region in the *Bl* 1951 genome with defective prophages PBSZ, PBSX, and PBP180 of *B. subtilis* subsp. *spizzenii* W23, *B. subtilis* 168, and *Bacillus* phage PBP180 (Jin et al., 2014)

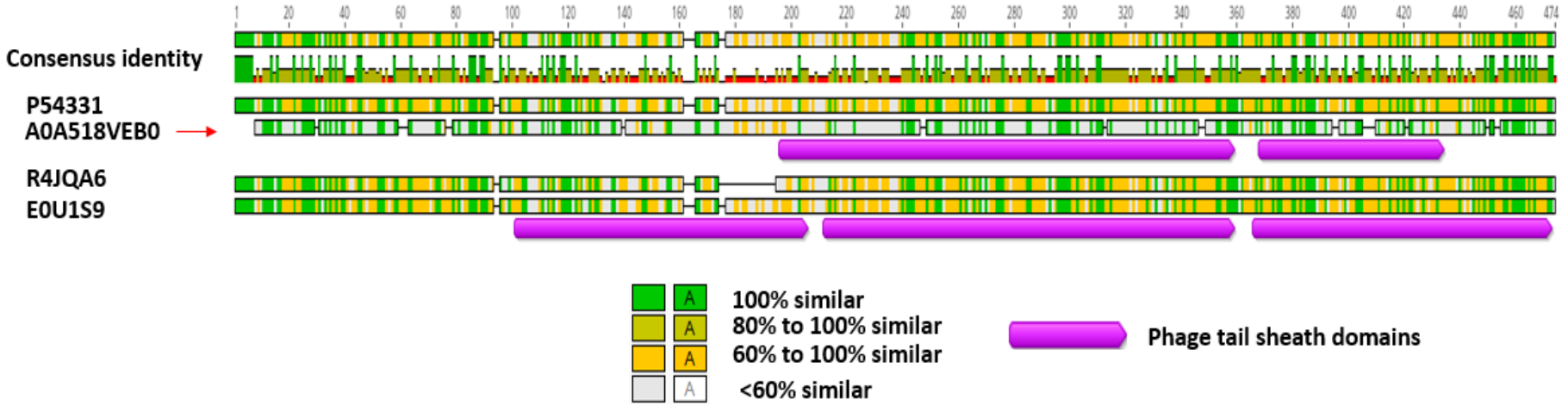

Figure 6.22 Amino acids alignment of 48 kD identified phage-like element PBSX protein XkdK accession A0A518VEB0 (shown with red arrow) of *Bl* 1821L and *Bl* 1951 with similar proteins of defective prophages of *B. subtilis* subsp. *spizzenii* W23 (E0U1S9), *B. subtilis* 168 (P54331), and *Bacillus* phage PBP180 (R4JQA6) using the Geneious basic

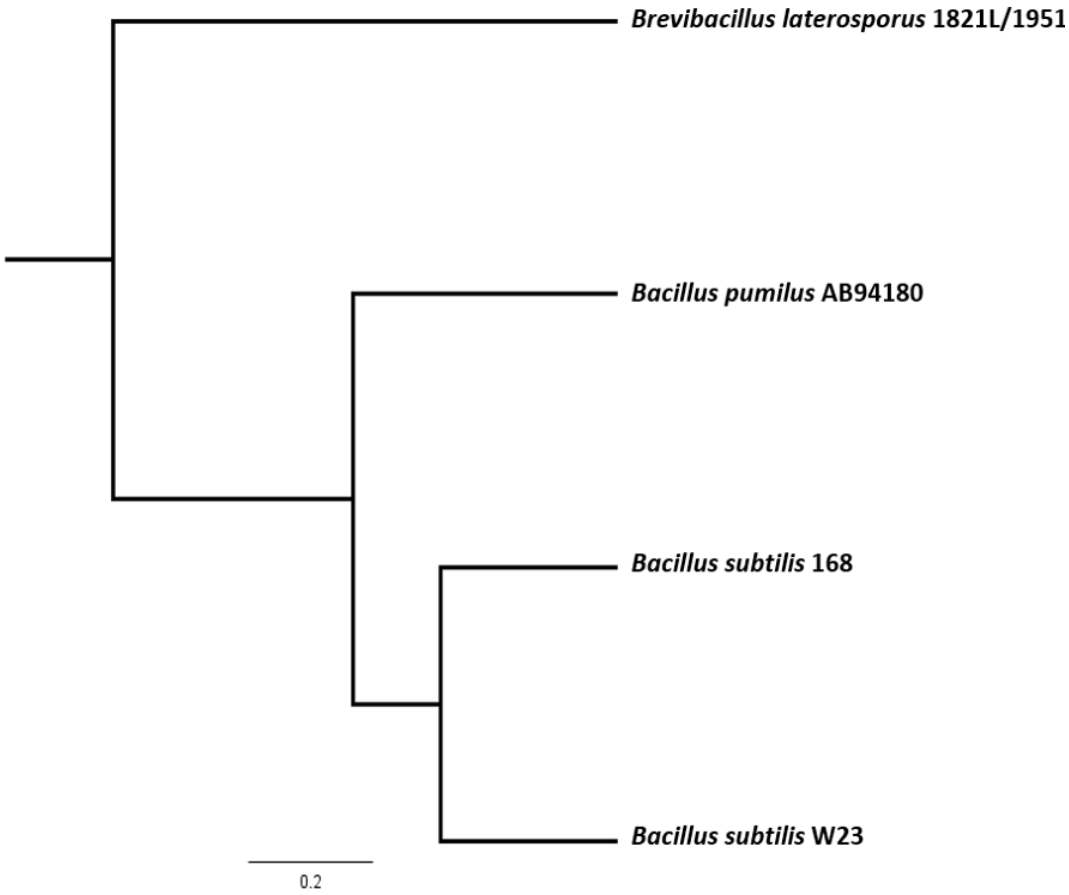

Figure 6.23 Dendrogram showing alignment of the identified (48 kD) phage-like element PBSX protein XkdK (A0A518VEB0) of *Bl* 1821L and *Bl* 1951 with similar proteins of defective prophages of *B. subtilis* subsp. *spizzenii* W23 (E0U1S9), *B. subtilis* 168 (P54331), and *Bacillus* phage PBP180 (R4JQA6)

Table 6.11 Summary of comparison of amino acid similarity (%) of different proteins encoded in the PBSX-like region of *Bl* 1821L and *Bl* 1951 with the analogous proteins of defective prophages PBSZ, PBSX, and PBP180

Defective phages	Encoded proteins in PBSX-like region			
	Tail-sheath protein (XkdK)	Tail protein (XkdO)	Holin protein (XhlB)	N-acetylmuramoyl-L-alanine protein (XlyA)
PBSZ	22.9	50.0	13.6	15.4
PBSX	22.9	0.0	13.6	15.4
PBP180	21.6	0.0	11.4	7.7

Table 6.12 Summary of comparison of amino acids similarity (%) of different proteins encoded in the PBSX-like region of *Bs* 168 with the analogous proteins of defective prophages PBSX-like *Bl* 1821L, *Bl* 1951, PBSZ, and PBP180

Defective phages	Encoded proteins in PBSX-like region			
	Tail-sheath protein (XkdK)	Tail protein (XkdO)	Holin protein (XhlB)	N-acetylmuramoyl-L-alanine protein (XlyA)
PBSX-like *Bl* 1821L & *Bl* 1951 defective prophage	22.9	0.0	13.6	15.4
PBSZ	66.5	51.1	89.8	95.3
PBP180	98.7	37.5	61.4	53.9

6.3.11 Bactericidal determinant of *Bl* 1821L putative phage tail-like protein (48 kD)

Antimicrobial index (AI) of N-terminal sequence-identified *Bl* 1821L phage tail-sheath protein (48.5 kD) was below the threshold level (< 0.225) indicating a bactericidal potency (Figure 6.24, shown with red arrow). AMPA result showed that bactericidal stretch was found from 360 to 373 amino acids (NKKFAKNIVRVLD) having a propensity value of 0.223 for the sequenced phage tail-like protein of *Bl* 1821L (Figure 6.25, shown in red).

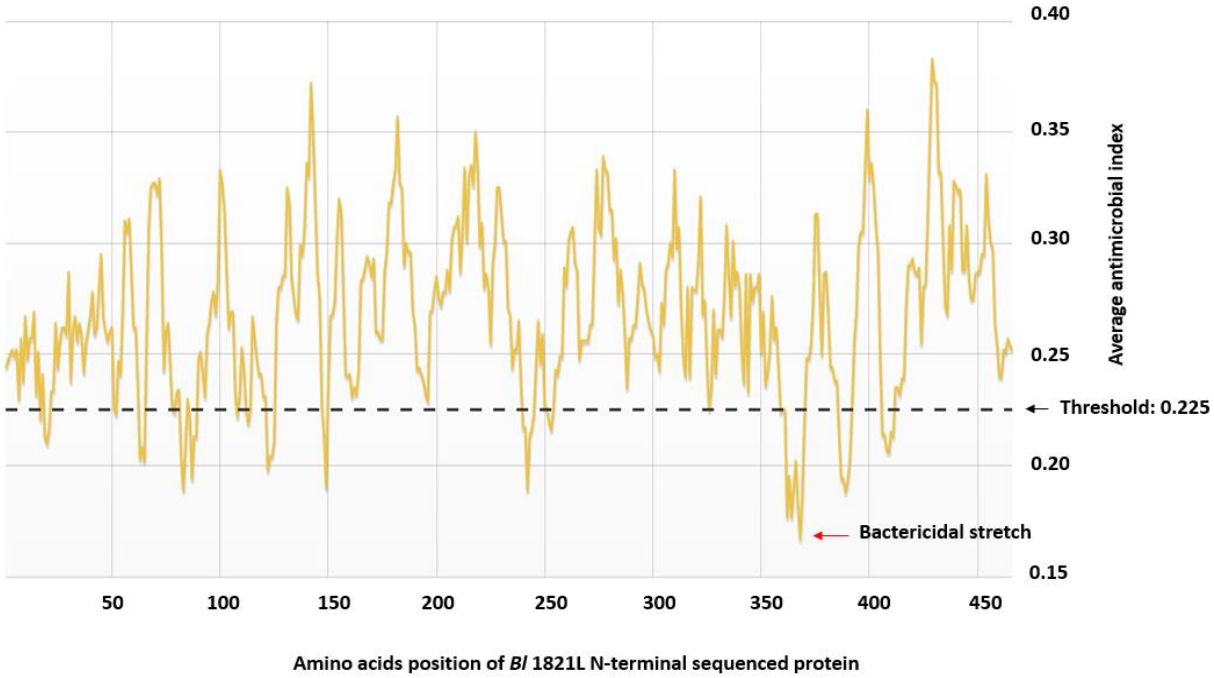

Figure 6.24 AMPA analysis of 48 kD identified phage tail-sheath protein of *Bl* 1821L

1 MNGGTFTTGKEKERAGIYFNFKTTAQERVSLSERGTVALPVASSWGEAKTFVSISSVEDL

61 NKKVGLSIDDPSLLLLREAKKNAKTVLMYRLTEGVRASADIAEGVKATAVYGGTKGNDII

121 IRINQNVLDANSFDVTTYMDESEVDKQTVKKAEELTANGYVTFTGTGDLSSTIPLTGSEG

181 DTAAETLNASAGIRLSGGTDKAPVNSDYTDFLAAAETESFDVIALPVAEGDQLKATFAAF

241 IKRLRDGQGQKVQGVTANYAGDYEGIINVTEGVLLEDGTEVTPDKATAWVAGASAGATN

301 QSLTFVEYEGAVDVLHRLDHDTIVERLGKGEFLFTFDARDKSVSVEKDINSLVTFTAEKN

361 KKFAKNKIVRVLDAVNNDLTRELKALIKSRKGSGSDIPASEDGLQYVKTMITQYMTTLQD

421 AGGITGFDSDEDITISMNEDRDGFLIDLAVQPVDAAEKFYFNVEVN

Figure 6.25 AMPA analysis of 48 kD identified phage tail-sheath protein of *Bl* 1821L. Amino acids (360-373) corresponding to the bactericidal stretch are highlighted in red colour

6.3.12 Expression of the 25 kD hypothetical protein, 30 kD putative encapsulating protein, and both the 25 kD and 30 kD proteins in the gram-positive bacterium *Bacillus subtilis* WB800N

The collaborating researchers based at the University of Canterbury, New Zealand, provided the cell free supernatants of the expressed 25 kD hypothetical protein (pHT01-*hypo*), 30 kD putative encapsulating protein (pHT01-*encap*), and the both 25 kD and 30 kD (pHT01-*hypo*.*encap*) proteins after twice passing through a 0.22 µm filter for further analysis.

Bs WB800N (pHT01-*hypo*, A1) supernatant expressing the 25 kD hypothetical protein demonstrated antagonistic activity against *Bl* 1951 by developing a zone of inhibition of 11.7 mm and 12 mm with induced and uninduced cultures respectively after 3.5 hours of induction. For *Bl* 1821L, the same supernatant demonstrated no significant activity (Tables 6.13-6.14 & Figure 6.26). Similarly, 25 kD hypothetical protein (pHT01-*hypo*, A2) after 3.5 hours of induction exhibited similar activity against both the strains (*Bl* 1821L & *Bl* 1951) by developing a zone of inhibition of 11.7 mm and 11 mm respectively. However, after 24 hours of induction antagonistic activity was almost absent (Tables 6.13-6.14 & Figure 6.27). Purification of the corresponding protein was only visualised on SDS-PAGE with the 25 kD hypothetical protein sample (pHT01-*hypo*, A1) (Figure 6.31) and no protein bands were seen with the other concentrated protein (pHT01-*hypo*, A2). Unexpectedly, a defined band of ~48 kD in 40% gradient, faint bands of the same level in other gradients, and prominent protein bands of

>50 kD in the 20% gradient were visualised on SDS-PAGE with the purified and concentrated 25 kD hypothetical protein (pHT01-*hypo*, A1) (Figure 6.31).

For the control treatment, CFS of *Bs* WB800N without any transformation of plasmid (pHT01-*hypo*, pHT01-*encap*, pHT01-*hypo*.*encap*) was evaluated against *Bl* 1821L and *Bl* 1951 but no zones of inhibition were produced (Tables 6.13-6.14 & Figure 6.36). No bands were observed on silver stained SDS-PAGE analysis of concentrated supernatant from the *Bs* WB800N control (Figure 6.36).

Table 6.13 Assay of *Bs* WB800N supernatant containing 25 kD hypothetical protein (pHT01-*hypo*), 30 kD putative encapsulating protein (pHT01-*encap*), and both 25 kD and 30 kD proteins (pHT01-*hypo*.*encap*) against *Bl* 1821L as the host bacterium

Cell free supernatants (CFS)	Zone of inhibition diameter (mm)			
	Time after induction (3.5 Hours)		Time after induction (24 Hours)	
	Induced	Uninduced	Induced	Uninduced
Hypothetical protein (pHT01-*hypo*, A1)	-*	-	-	9.0
Hypothetical protein (pHT01-*hypo*, A2)	11.7	-	9.7	-
Encapsulating protein (pHT01-*encap*, B1)	-	10.3	12.3	11.7
Encapsulating protein (pHT01-*encap*, B2)	-	-	11.0	-
Hypothetical and encapsulating proteins (pHT01-*hypo*.*encap*)	9.3	-	11.0	-
**Control	-	-	-	-

*= No zone of inhibition

**= For control cell free supernatant of *Bs* WB800N without (pHT01-*hypo*, pHT01-*encap*, pHT01 *hypo*.*encap*) expression was used against both the strains *Bl* 1821L & *Bl* 1951

Table 6.14 Assay of *Bs* WB800N supernatant containing 25 kD hypothetical protein (pHT01-*hypo*), 30 kD putative encapsulating protein (pHT01-*encap*), and both 25 kD and 30 kD proteins (pHT01-*hypo*.*encap*) against *Bl* 1951 as the host bacterium

Cell free supernatants (CFS)	Zone of inhibition diameter (mm)			
	Time after induction (3.5 Hours)		Time after induction (24 Hours)	
	Induced	Uninduced	Induced	Uninduced
Hypothetical protein (pHT01-*hypo*, A1)	11.7	12.0	-*	-
Hypothetical protein (pHT01-*hypo*, A2)	11.0	-	-	-
Encapsulating protein (pHT01-*encap*, B1)	10.3	10.0	11.0	-
Encapsulating protein (pHT01-*encap*, B2)	-	-	-	-
Hypothetical and encapsulating proteins (pHT01-*hypo*.*encap*)	10.0	-	12.3	-
**Control	-	-	-	-

*= No zone of inhibition

**= For control cell free supernatant of *Bs* WB800N without (pHT01-*hypo*, pHT01-*encap*, pHT01-*hypo*.*encap*) expression was used against both the strains *Bl* 1821L & *Bl* 1951

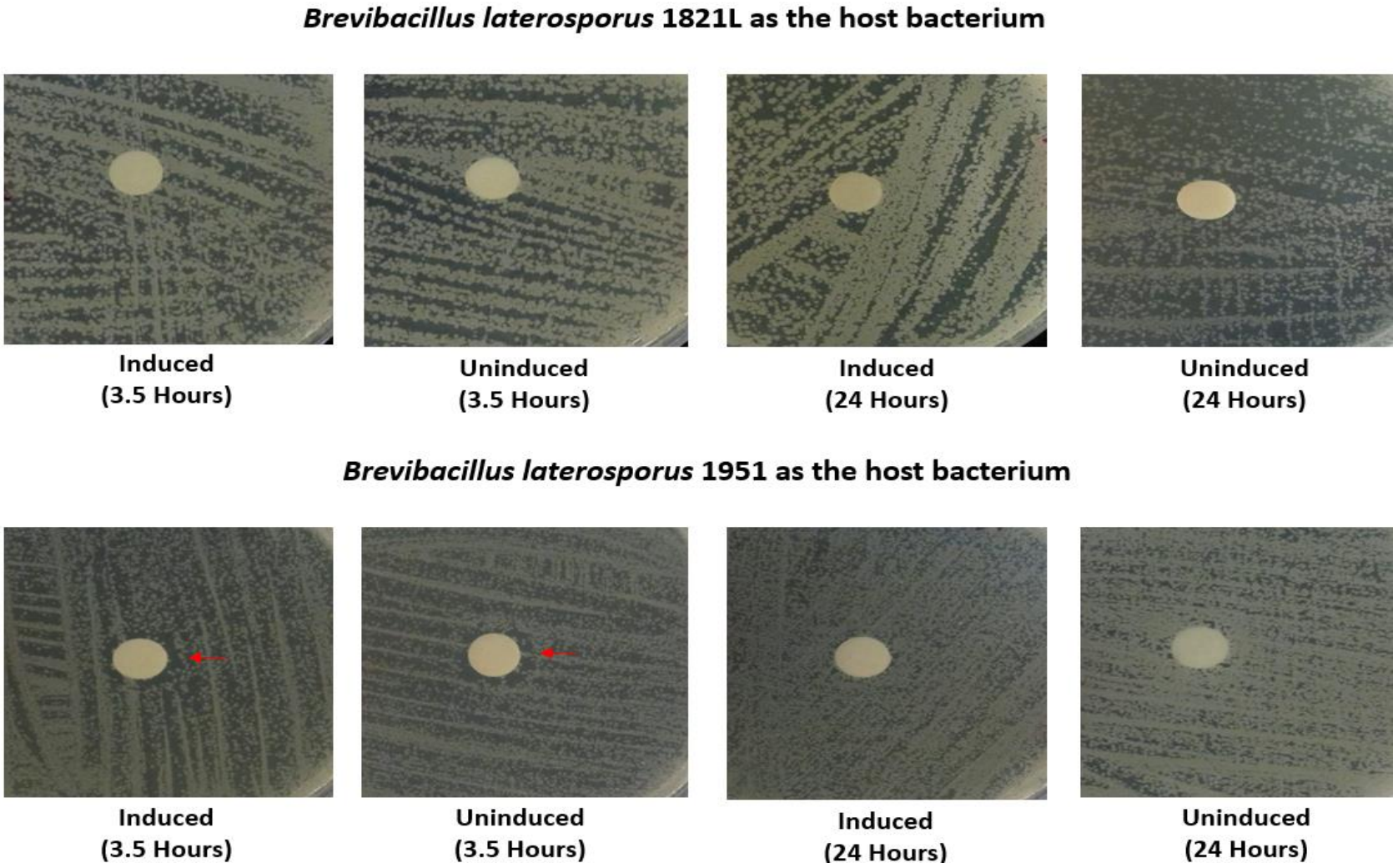

Figure 6.26 Assay test of CFS from *Bs* WB800N (pHT01-*hypo*, A1) expressing 25 kD hypothetical protein against *Bl* 1821L and *Bl* 1951 as the host bacterium. Arrows (red) denote the zones of inhibition showing a diameter of ≥ 11 mm

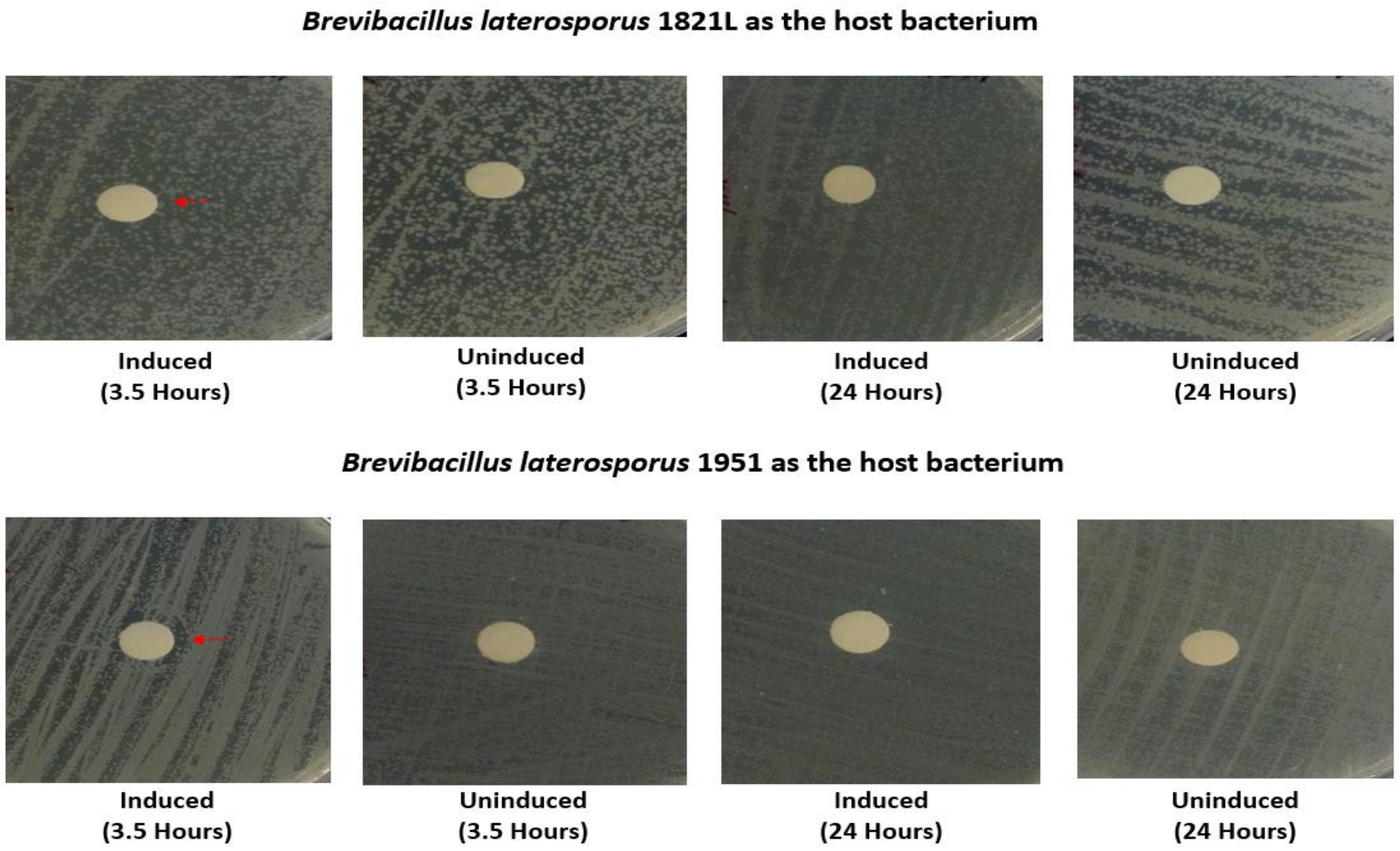

Figure 6.27 Assay test of CFS from *Bs* WB800N (pHT01-*hypo*, A2) expressing 25 kD hypothetical protein against *Bl* 1821L and *Bl* 1951 as the host bacterium. Arrows (red) denote the zones of inhibition showing a diameter of ≥ 11 mm

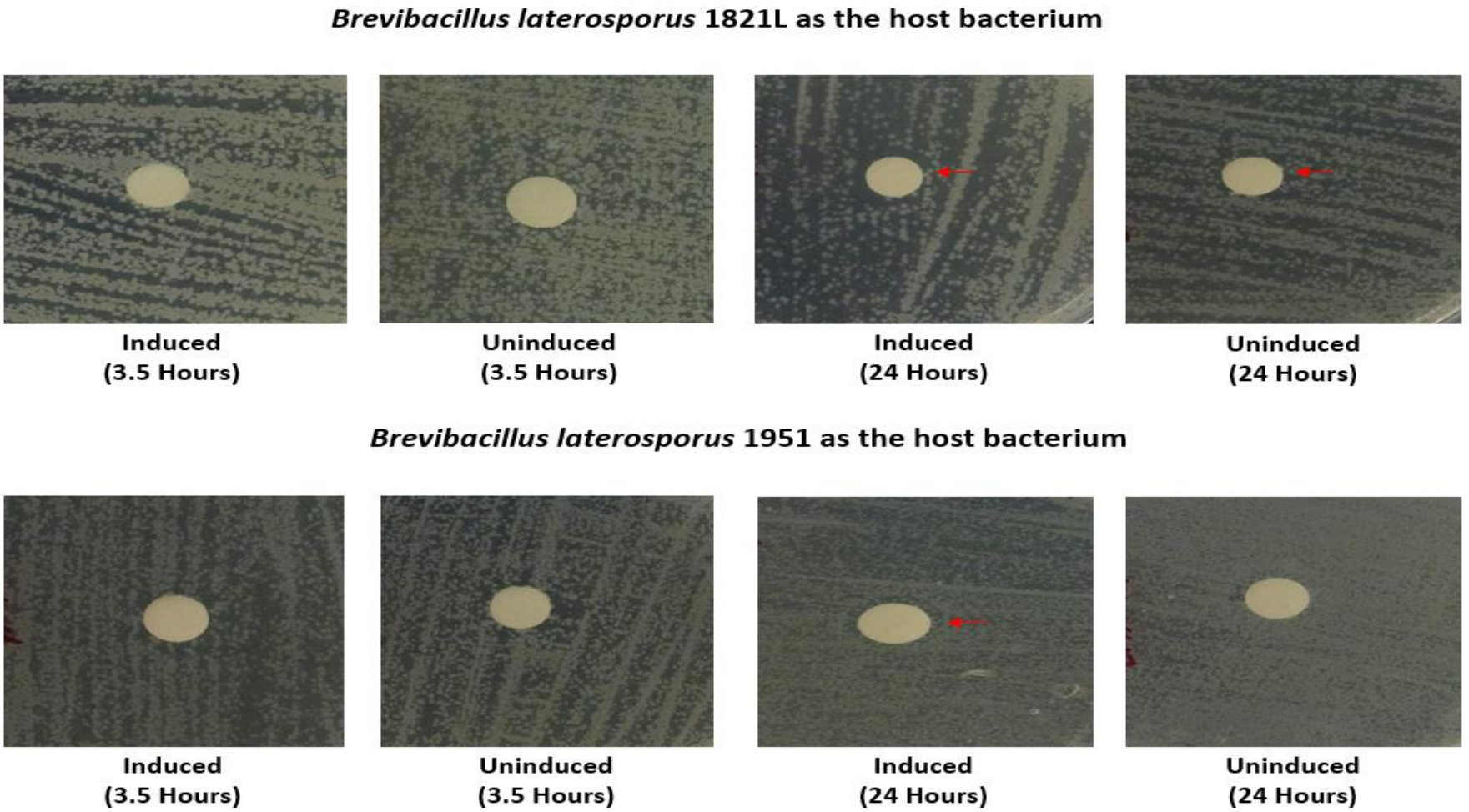

Figure 6.28 Assay test of CFS from *Bs* WB800N (pHT01-*encap*, B1) expressing 30 kD putative encapsulating protein against *Bl* 1821L and *Bl* 1951 as the host bacterium. Arrows (red) denote the zones of inhibition showing a diameter of ≥ 11 mm

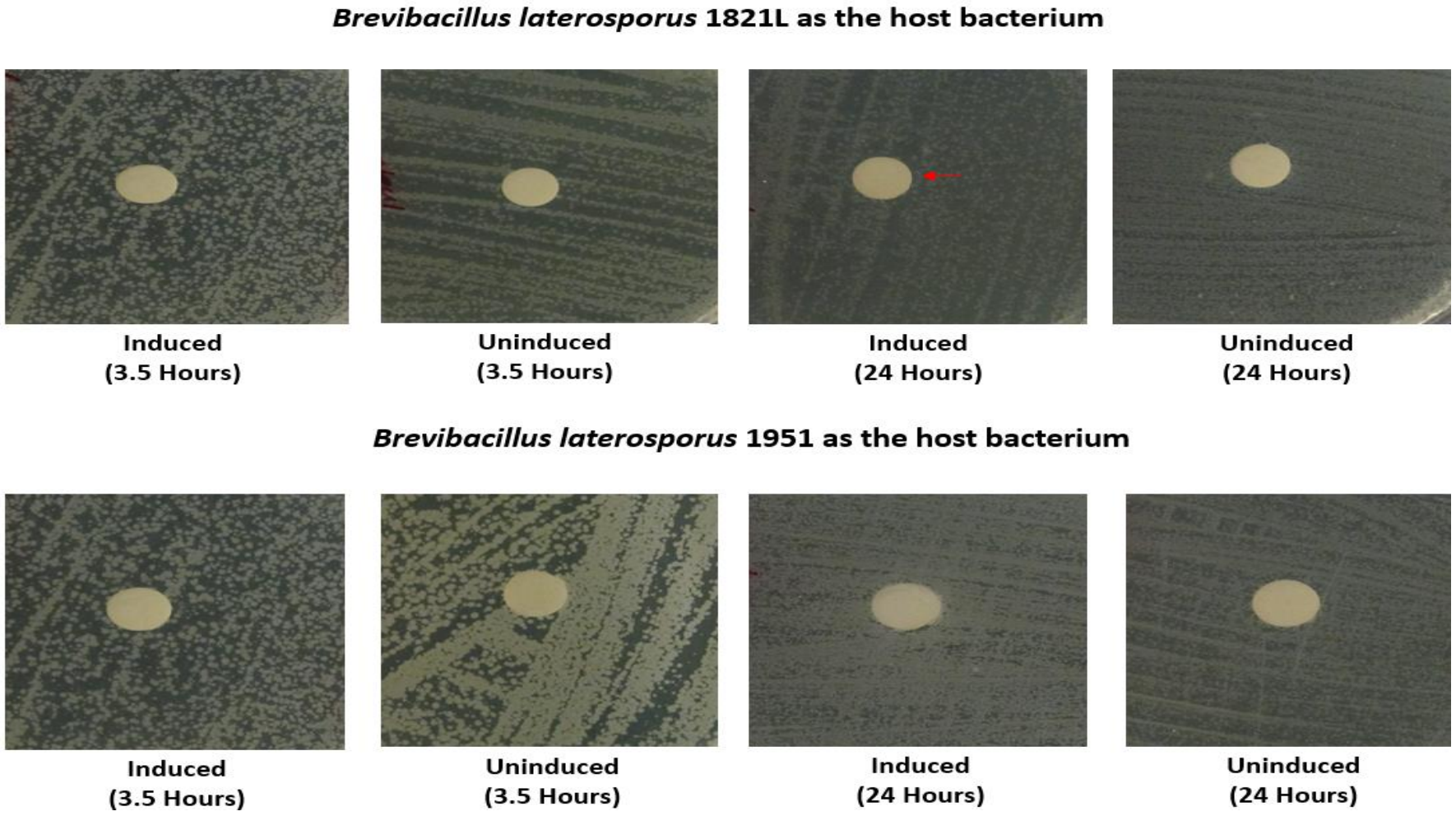

Figure 6.29 Assay test of CFS from *Bs* WB800N (pHT01-*encap*, B2) expressing 30 kD putative encapsulating protein against *Bl* 1821L and *Bl* 1951 as the host bacterium. Arrows (red) denote the zones of inhibition showing a diameter of ≥ 11 mm

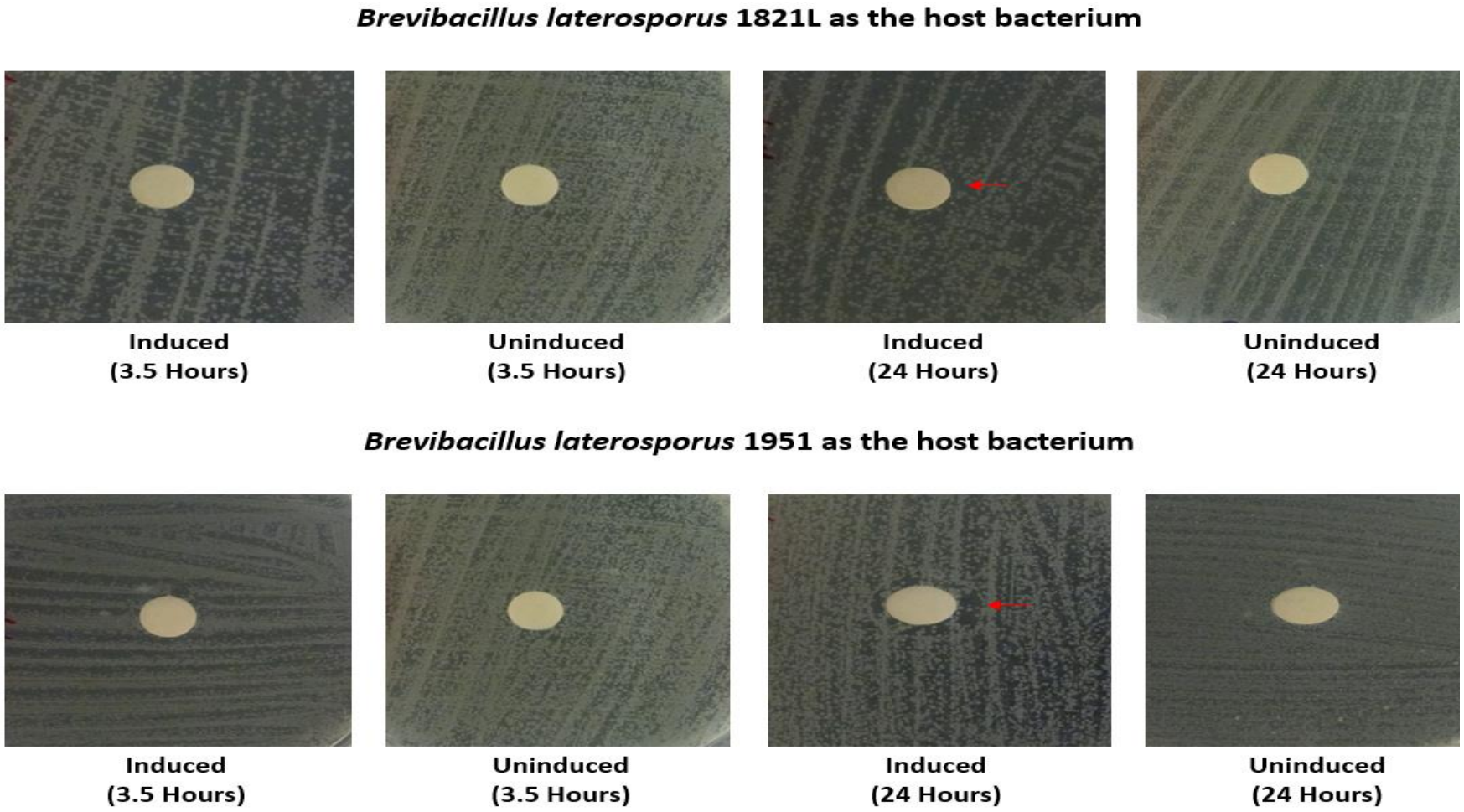

Figure 6.30 Assay test of CFS from *Bs* WB800N (pHT01-*hypo.encap*) expressing both 25 kD hypothetical and 30 kD putative encapsulating proteins against *Bl* 1821L and *Bl* 1951 as the host bacterium. Arrows (red) denote the zones of inhibition showing a diameter of ≥ 11 mm

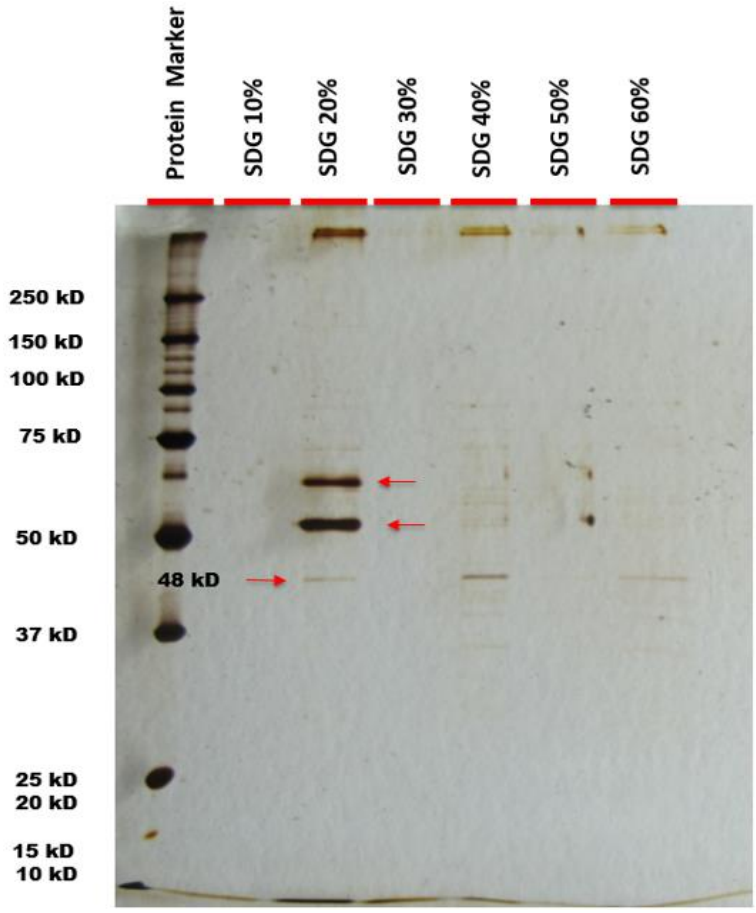

Figure 6.31 SDS-PAGE analysis of supernatant from *Bs* WB800N (pHT01-*hypo*, A1) expressing 25 kD hypothetical protein after 3.5 hours of induction. The red arrows denote sucrose density gradient purified proteins

Antibacterial activity was found in CFS (pHT01-*encap*, B1) containing 30 kD putative encapsulating protein against *Bl* 1821L as the host bacterium, developing a lysis zone of 12.3 mm after 24 hours of induction and 11.7 mm without induction (Table 6.13 & Figure 6.28). For *Bl* 1951, a halo zone of 11 mm was noted 24 hours after induction (Table 6.13 & Figure 6.28). SDS-PAGE analysis of the 30 kD concentrated putative encapsulating protein (pHT01-*encap*, B1) after 3.5 hours of induction displayed a very faint band of ~30 kD (Figure 6.33A) but after 24 hours of induction, in addition to the ~30 kD band, other proteins were also present (Figure 6.33B). Putative 30 kD encapsulating protein (pHT01-*encap*, B2) solely exhibited inhibitory activity against *Bl* 1821L as the host bacterium by producing a zone of inhibition of 11 mm after 24 hours of incubation (Tables 6.13-6.14 & Figure 6.29) and a purified band of ~30 kD in 40% gradient was visualised on SDS-PAGE (Figure 6.34).

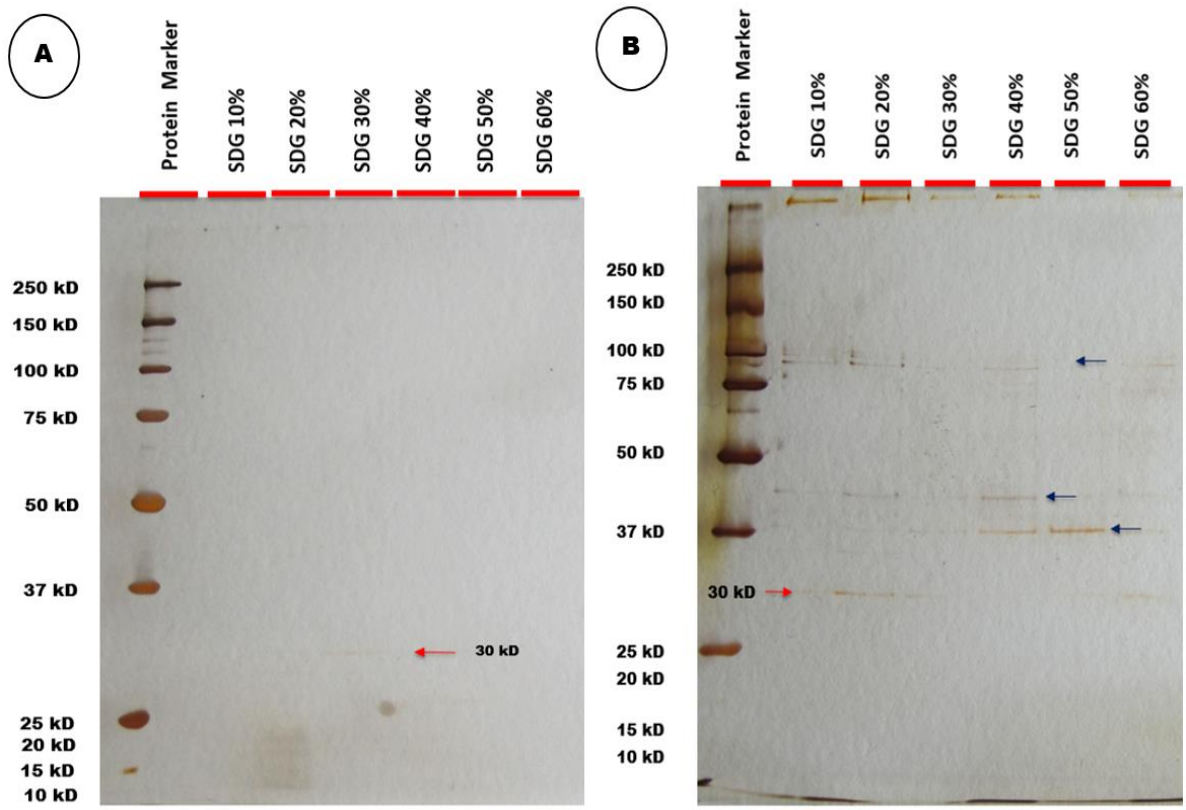

Figure 6.32 SDS-PAGE analysis of 30 kD putative encapsulating protein expressed after 3.5 hours (A) and 24 hours (B) of induction from *Bs* WB800N (pHT01-*encap*, B1). Arrows denote sucrose density gradient purified ~30 kD encapsulating protein (red colour) and other proteins (dark blue colour)

Bs WB800N supernatant expressing (pHT01-*hypo*.*encap*) both the hypothetical (25 kD) and putative encapsulating (30 kD) proteins displayed prominent antibacterial activity against *Bl* 1821L and *Bl* 1951 after 24 hours of induction by causing inhibition zones of 11 mm and 12 mm respectively (Tables 6.13-6.14 & Figure 6.30). SDS-PAGE analysis of purified and concentrated culture (pHT01-*hypo*.*encap*) displayed numerous bands with a good intensity including a ~30 kD protein in the 60% gradient (Figure 6.35).

Post purification the expressed proteins were visualised on SDS-PAGE at a low intensity. Therefore, it was hypothesised that the hypothetical (25 kD) and putative encapsulin (30 kD) proteins might be trapped in the cell pellets, so the pellets were further treated with lysis buffer (0.4 ml 2N NaOH, 0.4 ml 10% SDS, 3.2 ml dH_2O= 4 ml). Disc diffusion assay of lysed pellets showed some activity but no prominent bands were observed on SDS-PAGE.

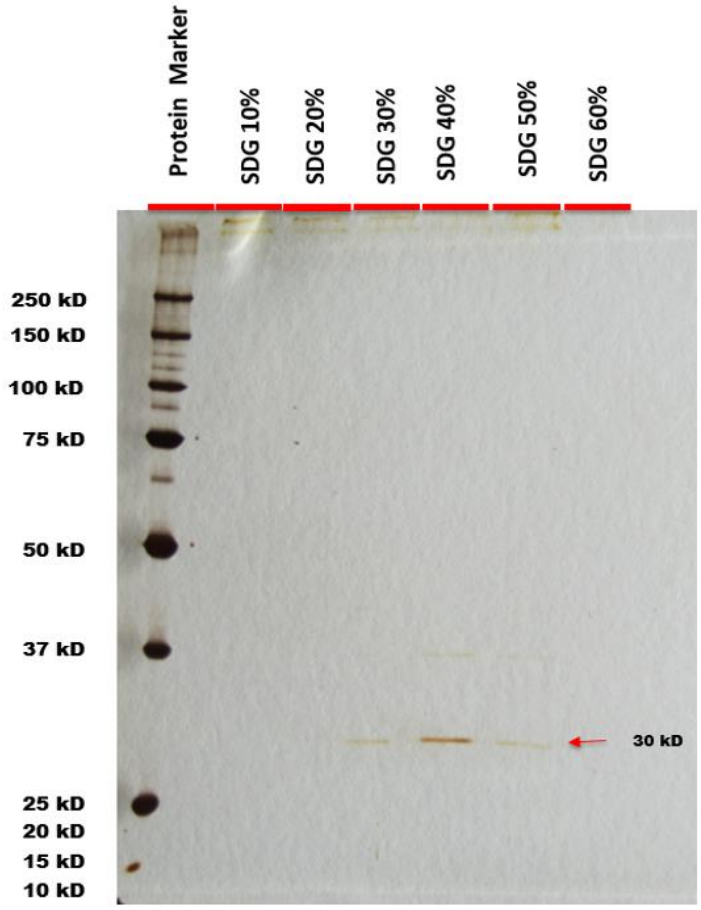

Figure 6.33 SDS-PAGE analysis of 30 kD putative encapsulating protein expressed after 24 hours of induction from *Bs* WB800N (pHT01-*encap*, B2). The red arrow denote sucrose density gradient purified putative encapsulating protein (~30 kD)

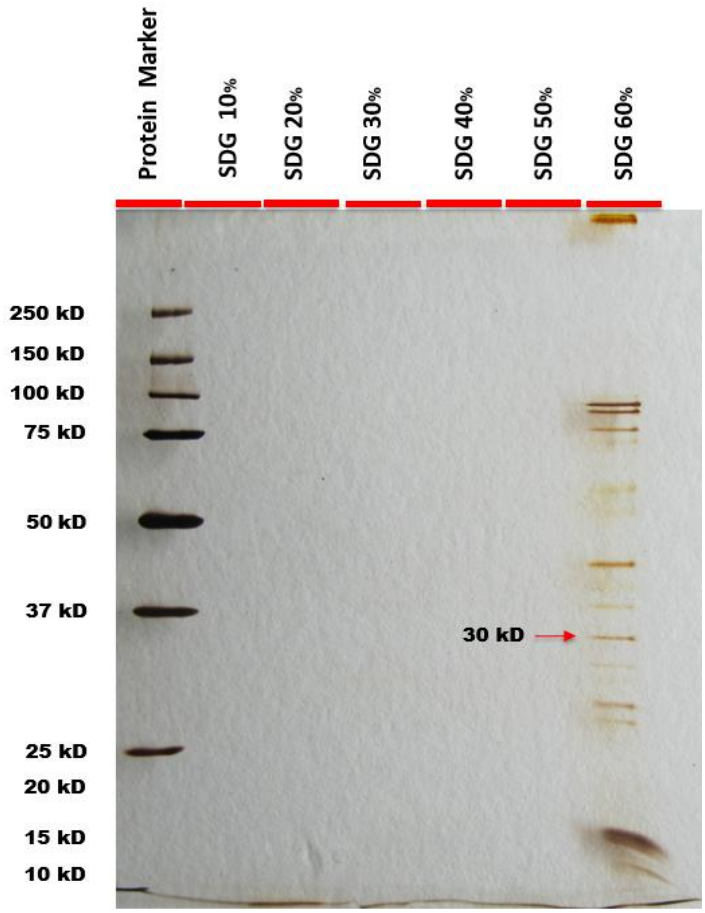

Figure 6.34 SDS-PAGE analysis of the expression of both the 25 kD hypothetical and 30 kD putative encapsulating proteins after 24 hours of induction from *Bs* WB800N (pHT01-*hypo.encap*). The red arrow denote sucrose density gradient purified encapsulating protein (~30 kD)

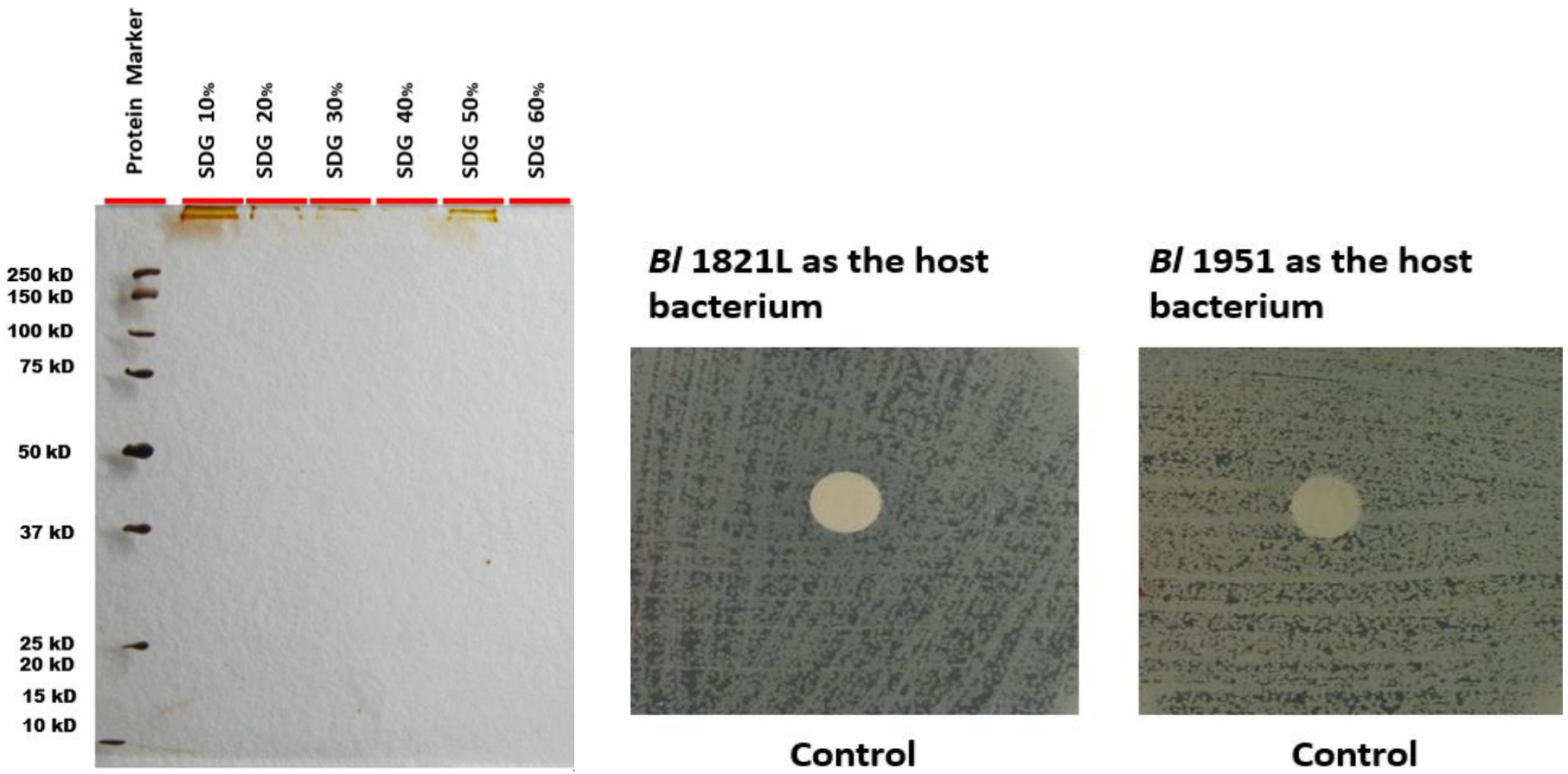

Figure 6.35 SDS-PAGE analysis of *Bs* WB800N concentrated CFS protein without any hypothetical (25 kD) and putative encapsulating (30 kD) protein expression (left side image). Assay tests of CFS of *Bs* WB800N without transformation (pHT01-*hypo*, pHT01-*encap*, pHT01-*hypo*.*encap*) against *Bl* 1821L and *Bl* 1951 as the host bacterium (right side image)

6.4 Discussion

Through N-terminal sequencing of the purified *Bl* 1821L (~30 kD & ~48 kD) and *Bl* 1951 (~30 kD) bactericidal protein bands, the putative encoding genes were located in the genomes of both strains. A 25 kD hypothetical protein at the 3' end of the putative encapsulating protein (30 kD) was also identified in *Bl* 1821L and *B*l 1951. Bioinformatic analysis of the ~30 kD putative encapsulating protein sequence using the tools AMPA and CellPPD identified the potential bactericidal motifs. Furthermore, the genes encoding the 25 kD hypothetical protein, putative encapsulating protein (30 kD), and the operon containing both 25 kD and 30 kD proteins of *Bl* 1821L were transformed in a gram-positive bacterium *Bs* WB800N for heterologous expression (Jeong et al., 2018).

Bioinformatic analysis of *Bl* 1821L putative phage tail-sheath protein in the *Bl* 1821L genome identified a phage-like element with low homology (34%) to the PBSX protein XkdK. Genes corresponding to the PBSX family terminase large unit (*xtmB*) and phage tail assembly chaperon (*xkdN*) upstream and hypothetical proteins downstream of *xkdK* gene are encoded (Figure 6.20). Genomes of numerous bacteria harbour defective prophages where they fail to complete a viral replication cycle and multiply in their hosts as healthy prophages (Bobay et al., 2014; Ramisetty & Sudhakari, 2019). Defective prophages often package random DNA fragments derived from various sites of the host chromosome instead of their own genomes (Jin et al., 2014). The gram-positive bacterium, *Bs,* is known to produce defective phage-like particles (Garro & Marmur, 1970; Hemphill & Whiteley, 1975). PBSX, the best-studied resident defective prophage (Lang et al., 2012; McDonnell et al., 1994), is described from *Bs* 168 and comprised of 38 predicted opening reading frames (ORFs) distributed between the early, middle, and late operons (Moszer et al., 2002; Westers et al., 2003). The early operon encodes an essential regulatory gene, *xre*, whose product maintains the PBSX DNA in a repressed state in the host chromosome (McDonnell & McConnell, 1994; Wood et al., 1990). The gene *xre* controls the induction of PBSX by binding to multiple promoters within the *Bacillus* genome (McDonnell et al., 1994) and controlling the expression of positive control factor (*xpf*), whose product resembles a sigma factor for the transcription of late genes (Krogh et al., 1998). Seven ORFs belonging to a single transcriptional unit reside in the middle operon and the functions of most ORFs within this region are unknown. Most of the structural and lysis genes are located in the late operon (Longchamp et al., 1994; Wood et al., 1990). PBSX phage particle is composed of at least 26 polypeptides. XkdG is the main capsid protein, and XkdK and XkdM are the tail sheath and core proteins, respectively. XkdV is presumably a fibre subunit that is involved in the killing of susceptible strains (Mauël & Karamata, 1984a; Steensma, 1981).

The predominant population of tailed DNA phages and some eukaryotic viruses utilise a molecular machine to package their genomic DNA into a preformed empty capsid (procapsid or proheads) (Rao & Feiss, 2008; Sun et al., 2010). The DNA packaging machine includes a small terminase and a large terminase component. The former plays a role in initiating the packaging of the viral genome, whereas the latter is responsible for the ATP-powered translocation of DNA from the capsid (Sun et al., 2012). Long tails of the phages may be in a contractile (*Myoviridae)* or non-contractile (*Siphoviridae*) form and the morphogenesis of the tail is largely dependent on the production of the XkdN protein (Pell et al., 2013). XtmB proteins (phage terminase large subunit) in other PBSX-like structures reside in the capsid region and often accompany the small terminase subunit protein XtmA. However, in the *Bl* 1821L putative PBSX-like region, their location in the upstream region suggests a possible role in the adhesion of tail protein with the putative phage tail-sheath protein (Figure 6.20). Temperate phages integrating into the genome of the susceptible host attach themselves with an enzyme known as integrase (Groth & Calos, 2004). An integrase encoding gene was found between 5,129,530 bp to 5,128,919 bp and is presumed to be a site of attachment of XkdK-like protein in the *Bl* 1821L genome. Other phage-like element PBSX proteins XkdT and XkdU are also seen at the 5' end of integrase.

A putative tail fibre protein encoded upstream of XkdU protein shared low amino acid homology to the *Brevibacillus* phage Abouo. Amino acid alignment *Bl* 1821L putative tail fibre protein with *Brevibacillus* phage Abouo tail fibre protein (S5M627) and putative tail fibre protein (S5MNY5) showed only 3.51% and 30% amino acids similarity. Phage tails are the molecular machines that play a decisive role in determining the host specificity and infection process of respective phages (Holtzman et al., 2020; Islam et al., 2019). Tail fibres, tail spikes, and tail tips located at the distal end of tailed phages act as RBPs to interact with the bacterial cell surface receptors (Nobrega et al., 2018). Variations in tail fibre proteins caused differences in the killing spectrum of defective phages PBP180, PBSX, and the PBSX-like phages of *Bacillus pumilus* AB94044 (Jin et al., 2014). Phage-induced bacterial lysis relies on the concerted action of two proteins (lytic enzymes), holin and endolysin (Hyman & Abedon, 2019; Young, 2014). Holins are small hydrophobic proteins that are thought to form stable and non-specific lesions in the cell membrane and thereby admit the endolysins to pass the membrane and access the cell wall target (Young, 2013). The timing of lysis, which is critical for viral reproduction, is somehow "programmed" into the structure of the holin (Young et al., 2000). Bioinformatic analysis identified a holin protein (BhlA) in PBSX-like region of *Bl* 1821L similar to that found in *Bs* prophage SPBeta than the PBSX holin XhlA, a sign of genomic plasticity that phages and phage-related particles have (Fernández-Fernández et al., 2021)**.** However, the localisation of lysis genes holin BhlA (*xhlB*) and endolysin enzyme N-acetylmuramoyl-L-alanine amidase (*xlyA*) suggests that the identified lysis genes

of the *Bl* 1821L PBSX-like region may follow a pathway similar to the phages in host cell lysis. However, earlier studies demonstrated that four genes *(xepA*, *xhlA*, *xhlB*, *xlyA*) displaying expected characteristics of a host cell lysis system reside within the late operon of PBSX (Krogh et al., 1998). Genes *xhlA* (encoding a putative membrane associated protein), *xlyA* (encoding a putative endolysin), and *xhlB* (encoding a putative holin) are vital for cell lysis, whereas *xepA* (encoding an export protein) has no known role in lysis (Krogh et al., 1998). Furthermore, the work illustrated that the expression of both *xhlA* and *xhlB* is necessary to effect *Bs* cell lysis. However, expression of *xhlB* together with *xlyA* has no effect on cell lysis, indicating that the PBSX lysis system differs from the ones identified in phages of gram-negative bacteria (Krogh et al., 1998). With the exception of *Clostridium difficile* 630 (Gebhart et al., 2012), *Bacillus* is the only example where PBSX phage-like elements are described in the literature. However, the *C. difficile* 630 is devoid of functioning lysis genes (Gebhart et al., 2012). Based on the current literature, the identified *Bl* 1821L PBSX phage-like element is a new addition from a gram-positive bacterium and the first report of the genus *Brevibacillus*.

Interestingly, identified *Bl* 1821L phage-like element PBSX protein XkdK residing between 1,937,150 bp to 1.935,813 bp in the genome of *Bl* 1951 (RHPK01000003.1, contig 1) exhibited similar genomic organisation (Figures 6.11 & 6.13). However, the further analysis uncovered some differences (Figure 6.14). An insertion region (4458 bp) was found at the 3' end of XkdT protein in *Bl* 1821L compared to *Bl* 1951. Localised XkdK protein in the upstream position is flanked by a hypothetical protein and XkdN protein. In the upstream region of XkdT and XkdU proteins, imperfect repeats of glycine rich proteins are found in *Bl* 1951 (Figures 6.13 & 6.14). The tips of phage tail fibres are reported to be rich in glycines (Dunne et al., 2018; Trojet et al., 2011). Glycine-rich proteins are considered vital in sustaining the unusual conformations found in the tail fibre structures (Islam et al., 2019). Therefore, it is likely that the glycine-rich proteins of *Bl* 1951 might be involved in conformations of tail fibres for adhesion to its host. Furthermore, it also suggests that the encoding of glycine rich proteins with imperfect repeats might have a role in causing the differences in antimicrobial activity of *Bl* 1821L and *Bl* 1951 against various gram-positive bacteria (Chapter 3). Mean pairwise consensus identity analysis of imperfect repeats (1700 bp long) using Geneious basic exhibited 92.6% similarity but for *Bl* 1821L the PHASTER programme identified it as a putative phage region. Furthermore, in the upstream of this genomic region, several minor differences are seen compared to *Bl* 1821L.

Comparative analysis of the genomic architecture of the *Bl* 1821L PBSX-like region with the defective prophages PBSZ, PBSX, and PBP180 demonstrated similarities and differences. Genomic organisation of the *Bl* 1821L PBSX-like region displayed localisation of a large terminal subunit protein (XtmB) upstream of the XkdK encoding region, but in the defective *Bacillus* phages, it resides in the capsid region. Conserved hypothetical proteins in the adjacent upstream position of a tail protein (XkdO)

reside in the *Bl* 1821L PBSX-like region and for defective *Bacillus* phages PBSZ, PBSX, and PBP180, the corresponding region encodes hypothetical proteins XkdQ, XkdR, and XkdS. Although the *Bl* 1821L PBSX-like region resembles the defective phages PBSZ, PBSX, and PBP180 in the genomic organisation, there was only a low level of amino acid similarity to XkdK, XkdO, XhlB, and XlyA proteins of *Bl* 1821L with the similar proteins of defective phages PBSZ, PBSX, and PBP180. *Bl* 1821L XkdK protein showed 22.9%, 22.9%, and 21.9% amino acids similarity to the XkdK proteins of PBSZ, PBSX, and PBP180. PBSX presented a high level of amino acids alignment of 98.7% and 66.5% with PBSZ and PBP180. These findings are in agreement with the work of Jin et al. (2014) who deliberated that in spite of similar genomic organisation, XkdV, a putative tail fibre region of PBSX, differed from the defective prophage PBP180 corresponding operons ORF30, ORF33, and ORF35. Based on the similarities in operon architecture and differences of *Bl* 1821L with the identical regions it is likely that all evolved from a common distant ancestor.

N-terminal sequencing analysis of ~30 kD purified putative antibacterial protein of *Bl* 1821L and *Bl* 1951 affirmed that both the homologous proteins originate from the same gene and share >97% amino acids similarity to the Linocin M18 bacteriocin family of protein. Linocin M18 family proteins are found in eubacteria and archaea (McHugh et al., 2014; Valdes-Stauber & Scherer, 1996) often referred to as "encapsulins" due to the formation of nanocompartments within the bacterium that contains ferritin-like compounds or peroxidase enzymes (Kerfeld et al., 2010; Yeates et al., 2011). The distinctive nanocompartments allow cells to compartmentalise materials and enzymatic reactions to increase the metabolic activity, protect them from proteolysis or other challenges, and sequester toxic products (Diekmann & Pereira-Leal, 2013). Ferritin family proteins include three sub-families; classical ferritin (Ftn), bacterioferritin (Bfr), and the DNA-binding protein from starved cells (Dps) (Andrews, 2010; Theil et al., 2013). The first two categories (Ftn & Bfr) perform diverse functions including ribonucleotide reductase (Åberg et al., 1993), protecting DNA from oxidative damage (Grant et al., 1998), and iron storage (Bradley et al., 2014a). However, Dps proteins are unique and are involved in iron detoxification as opposed to storage (McHugh et al., 2014). Importantly, a failure to detoxify iron may prove fatal to the cells (Giessen & Silver, 2017; He et al., 2016a). Furthermore, a search of identified Linocin M18 family protein in the Pfam database revealed its association with the clan (CL0373) of phage coat superfamily proteins (Mistry et al., 2021). The clan CL0373 contains nine families including DUF1884, DUF2184, Gp23 (PF07068), *Lactococcus lactis* bacteriophage major capsid protein (PF06673), Linocin M18 (PF04454), P22 coat protein (PF11651), phage major capsid protein E (PF03864), phage major capsid protein P2 (PF05125), and phage capsid (PF05065) (Mistry et al., 2021). Encapsulin proteins seize a fold of a capsid protein of lambdoid bacteriophage HK97 in their shell protein (formerly referred to as Linocin-like protein) (Sutter et al., 2008; Wikoff et al., 2000). Since

then, the HK97 fold has been observed in the capsid proteins of several other tailed bacteriophages (Gabashvili et al., 2020; Orlova et al., 2012). Therefore, it is likely that encapsulins and the capsid proteins of tailed phages have evolved from a common ancestor (Abrescia et al., 2012; Heinemann et al., 2011). However, viral capsids and encapsulin nanocompartments functionally differ: the former transport viral genomes from one cell to another and the latter are involved in metabolic activities (McHugh et al., 2014). Bioinformatic analysis of ~30 kD purified putative encapsulating protein in this study and TEM examination in Chapter 5 also substantiate the findings.

The adjacent identified hypothetical (25 kD) and putative encapsulating (30 kD) proteins in *Bl* 1821L and *Bl* 1951, both upstream and downstream, are flanked by hypothetical proteins. Significant transcriptional regulators family proteins (PadR & MarR) also reside in the region. The PadR family is a large group of transcriptional regulators that function as environmental sensors (Park et al., 2017) and are involved in various cellular survival processes, such as toxin production, detoxification, multidrug resistance (Lubelski et al., 2006; Nguyen et al., 2011), antibiotic biosynthesis (Florez et al., 2015), and carbon catabolism (Park et al., 2017). This family interacts with the operator DNA using a winged helix-turn-helix (wHTH) motif and exhibits a high structural similarity to the multiple antibiotic resistance regulator (MarR) family in the wHTH superfamily (Alekshun et al., 2001; De Silva et al., 2005). Microorganisms, including bacteria, sense and respond dynamically to both beneficial and harmful environmental changes and stresses (Imlay, 2015; Lee et al., 2017). For instance, to avoid the toxicity of phenolic acids some bacterial species, such as *Bs* (Tran et al., 2008), *Bacillus pumilus* (Degrassi et al., 1995), *C. difficile* (Gury et al., 2004), *Lactobacillus plantarum* (Silva et al., 2011), and *Pediococcus pentosaceus* (Barthelmebs et al., 2000) express phenolic acid decarboxylase (*padC* gene product in *Bs*), which converts antimicrobial phenolic acids into less toxic vinyl derivatives, as a defence mechanism known as the phenolic acid stress response (Lee et al., 2017; Park et al., 2017). The regulation of transcriptional gene *padC* is governed by a negative transcription factor, phenolic acid decarboxylase regulator (*padR*), in a substrate-inducible manner (Gury et al., 2004; Nguyen et al., 2011). Localisation of another stress protein YtxJ in the genome of *Bl* 1821L and *Bl* 1951 in proximity to PadR may provide a plausible explanation for the identified putative encapsulating proteins to likely act as an antimicrobial peptide for its defence against some unknown stresses.

Bioinformatic tools including AMPA and CellPPD were used to substantiate the bactericidal role of 30 kD putative encapsulating protein of *Bl* 1821L and *Bl* 1951. AMPA analysis revealed the bactericidal potential of the putative encapsulating protein (Figure 6.8) and CellPPD identified the motifs in the bactericidal stretch (Figure 6.9) that have the faculty to penetrate the cells. The findings of the current study suggest that the putative encapsulating proteins of *Bl* 1821L and *Bl* 1951 are likely to act as cell penetrating peptides to lyse the cells. Typically, cell penetrating peptides (CPPs) are short cationic

peptides, usually 5-30 amino acid residues, which can be found in a wide range of natural sources from microbes to plants and animals (Milletti, 2012). Furthermore, the results align with the work of researchers who identified the potential of encapsulating proteins to act as antimicrobial peptides (Dias et al., 2017; Pinto et al., 2019). Based on the literature, this is the first report of the involvement of putative encapsulating protein of the genus *Brevibacillus* in antibacterial activity.

The gram-positive bacterium, *Bs*, is a more effective expression system for foreign proteins due to the structural differences in the outer cell membrane compared to the gram-negative bacterium, *E. coli* (Su et al., 2020; Zweers et al., 2008). However, the expression of recombinant secretory proteins in *Bs* has often been hampered due to the degradation of secreted proteins by extracellular proteases (Westers et al., 2004). *Bs* has eight extracellular proteases, known as NprE, AprE, Epr, Bpr, Mpr, NprB, Vpr, and WprA (Jeong et al., 2018). Therefore, to enhance the stability of secreted proteins, an extracellular-protease-deficient mutant *Bs* WB800N was used in this study (Jeong et al., 2018; Nguyen et al., 2011). The putative encapsulating protein (30 kD) of *Bl* 1821L was successfully expressed in *Bs* WB800N at low levels. N-terminal sequencing of the excised ~30 kD putative antibacterial protein band identified genes that corresponded to a 25 kD hypothetical protein and a 30 kD putative encapsulating protein. Identified 25 kD hypothetical protein appears to be a co-migrating protein. Furthermore, amino acid analysis of identified *Bl* 1821L putative encapsulating proteins calculated the molecular mass of ~31 kD through ExPasy. Heterologously expressed 25 kD hypothetical protein (pHT01-*hypo*) localised between 18,917 bp to 19,564 bp CFS demonstrated activity but SDS-PAGE analysis showed only purified bands of ≥48 kD. The absence of expected protein band might be due to the loss of transformed protein in the multiple purification steps (Walker, 2005) or low expression of proteins of interest (Lu et al., 2012). Assay of *Bs* WB800N (pHT01-*encap*) supernatant containing 30 kD putative encapsulating protein encoded between 19,592 bp to 20,434 bp exhibited antibacterial activity against *Bl* 1821L and a prominent purified band of ~30 kD was visualised on SDS-PAGE. However, activity of the 30 kD putative encapsulating protein (pHT01-*encap*, B1) was found against *Bl* 1821L and *Bl* 1951, which might be due to the variation in the expression of pHT01-*encap*, B1 and pHT01-*encap*, B2. Expression of both hypothetical (25 kD) and putative encapsulating proteins (30 kD) in *Bs* WB800N (pHT01-*hypo*.*encap*) displayed an inhibitory action against both the strains (*Bl* 1821L & *Bl* 1951) and purification of the corresponding supernatant yielded a protein band of ~30 kD along with other proteins. All the constructs used in this study expressed the antibacterial activity in *Bs* WB800N, which is otherwise absent in this strain.

6.5 Outcomes

The major findings of this chapter are;

1. N-terminal sequencing of ~48 kD excised protein band identified a phage-like element PBSX protein XkdK corresponding to a phage tail-sheath protein of *Bl* 1821L which was also an authentication of the Chapter 3 findings. For the *Bl* 1951 genome, a similar analogous gene was present. Although PBSX-like genes were found in both strains and exhibited high similarity to each other, analysis revealed some differences between the regions around the genes.
2. BLASTp analysis of *Bl* 1821L ~48 kD identified protein accessions with >90% amino acid similarity to the phage tail-sheath protein of *Bl* LMG 15441.
3. Comparative genomic analysis of the genomic organisation of the *Bl* 1821L PBSX-like region with the defective prophages PBSZ, PBSX, and PBP180 revealed notable differences and similarities. XkdK, XkdO, XlyA, XhlB proteins of the *Bl* 1821L PBSX-like region displayed a low level of amino acids sequence identity with the similar proteins of PBSZ, PBSX, and PBP180. Based on the similarities in genetic architecture and gene content differences it is suggested that they evolved from a common ancestor.
4. AMPA analysis determined the bactericidal stretch of the ~48 kD putative phage tail-sheath protein of *Bl* 1821L. Furthermore, phage lysis genes including N-acetylmuramoyl-L-alanine amidase (*xlyA*) and holins (*xhlB*) encoding in the XkdK-like region of *Bl* 1821L and *Bl* 1951 suggests that a phage-like lysis system may be involved in cell lysis.
5. N-terminal sequencing of purified ~30 kD protein band from *Bl* 1821L and *Bl* 1951 identified genes corresponding to a 25 kD hypothetical and a 30 kD putative encapsulating protein. Furthermore, localisation of transcriptional regulator family proteins (PadR & MarR) and YtxJ protein in the genomic region suggests that the 30 kD putative encapsulating protein is likely to be produced under some unknown stresses.
6. BLASTp analysis of *Bl* 1821L and *Bl* 1951 purified protein (~30 kD) identified >97% amino acid identity to the Linocin M18 bacteriocin family protein of *Bl* LMG 15441 and *Bl* GI-9 which are encapsulating in nature. Ferritin family proteins constituting encapsulins often prove fatal to the cells due to the failure to detoxify iron. Hence, this phenomenon may be one of the possible causes of the collapse of endemic bacterial cultures.
7. AMPA analysis determined the bactericidal stretch of the putative encapsulating protein of *Bl* 1821L and *Bl* 1951 and CellPPD identified the cell penetrating peptides motif in the encapsulating protein sequence. Based on the findings it is likely that the putative encapsulating proteins can lyse the cells using cell penetrating peptides pathway.

8. Expression of bactericidal activity of putative encapsulation protein (~30 kD) in a gram-positive bacterium *Bs* WB800N affirmed the antibacterial role.

6.6 Conclusion

Bioinformatics analyses substantiated the bactericidal features of putative encapsulating protein (~30 kD) and phage-like element PBSX protein XkdK (~48 kD) of endemic strains *Bl* 1821L and *Bl* 1951. An insight into the genomic analysis revealed the ~30 kD putative encapsulating protein might act as antibacterial through the cell penetrating peptides, the activation of the stress proteins, or failure of ferritin protein to detoxify the excessive iron. Bactericidal activity of ~48 kD phage-like element PBSX protein XkdK is likely due to the contractile injection system of phages by the formation of pores in the sensitive cells.

Chapter 7

Bactericidal activity of putative antibacterial proteins of New Zealand *Brevibacillus laterosporus* isolates of *Bl* 1821L and *Bl* 1951

7.1 Introduction

N-terminal sequencing of two purified *Bl* 1821L protein bands (~30 kD & ~48 kD) and one protein of *Bl* 1951 (~30 kD) identified the proteins in the preceding chapter. Bioinformatics analysis of the amino acid sequence to which the purified *Bl* 1821L proteins N- terminal shared amino acid identity, affirmed a putative encapsulating protein of 30 kD and phage tail-sheath protein of 48 kD. A 25 kD hypothetical protein, which corresponded to the gene adjacent to the 30 kD encoding gene was also identified. The ~30 kD purified *Bl* 1951 protein was found to be identical to the putative encapsulating protein of *Bl* 1821L. Furthermore, the bactericidal regions and motifs of the sequenced proteins were also identified.

Tailocins or phage tail-like bacteriocins (PTLBs) are bactericidal structures (Ge et al., 2020; Saha et al., 2021) first identified as R-type and F-type pyocins produced by *Pseudomonas aeruginosa* (Ge et al., 2015; Scholl, 2017). They resemble phage tails, with the R-type pyocins corresponding to the contractile tails of myophages such as T4 and the F-type pyocins corresponding to the flexible, non-contractile tails of siphophages such as T1 (Schwemmlein et al., 2018; Taylor et al., 2016). Both the nanotube like antibacterials rely on receptor-binding proteins (RBPs) located on tail fibres or spikes for initial and specific interaction with susceptible bacteria (Böck et al., 2017; Scholl, 2017). Phages kill bacteria through a lytic, replicative cycle, whereas PTLBs kill the target cell through membrane depolarisation in a single hit mechanism (Figure 7.1A-B) (Dams et al., 2019; Ge et al., 2020). Homologous bactericidal phage-like element PBSX protein defined within the gram-positive bacteria of the genus *Bacillus* (Jin et al., 2014; Wood et al., 1990) are known to employ a similar killing mechanism as perpetrated by the tailocins (Ghequire & De Mot, 2015; Yao et al., 2017).

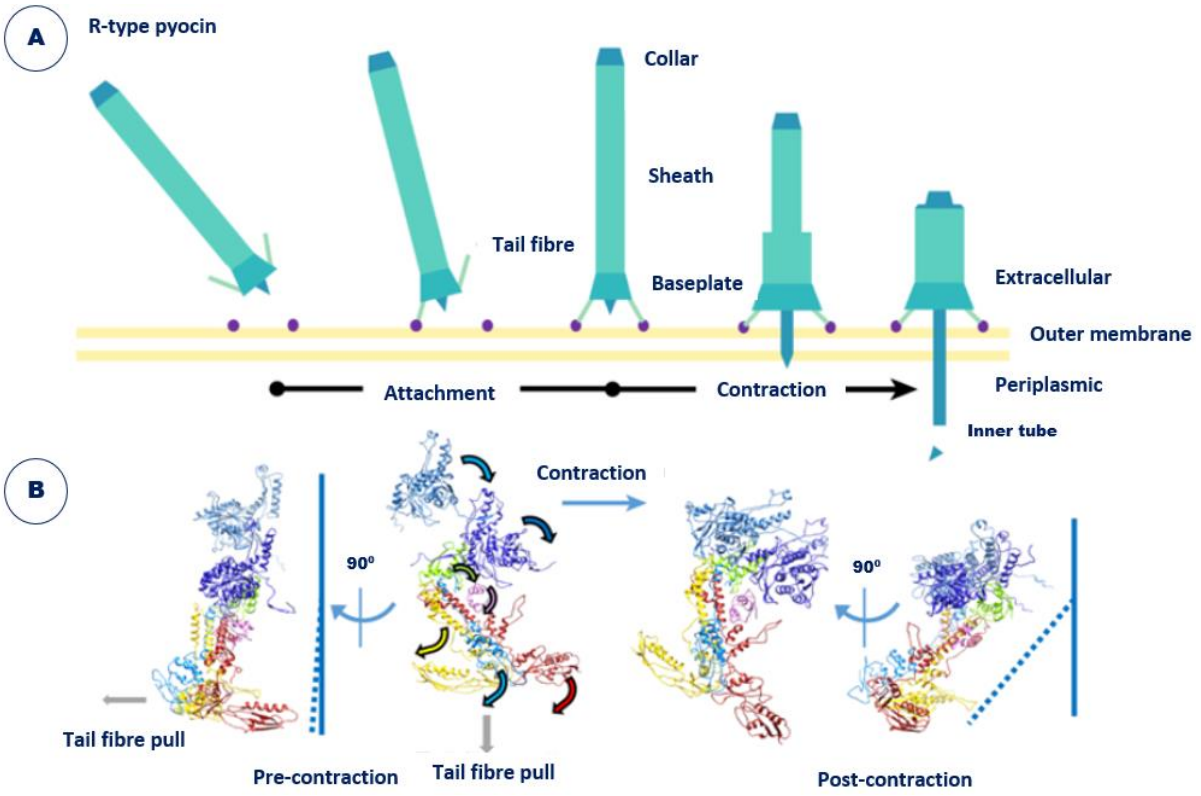

Figure 7.1 Bactericidal activity of R-type pyocins. (A). Bactericidal activity of R-type pyocin initiates after attachment to the sensitive cells and the contractile sheath upon contraction injects the effectors (toxins) into the susceptible cells. (B). Bactericidal activity of R-type pyocin illustrated in 3D crystal form (Ge et al., 2020)

Virus structural proteins (capsid) often encode various bioactive peptides such as antimicrobial peptides (AMPs) and cell-penetrating peptides (CPPs) (Freire et al., 2015a; Järver & Langel, 2006). CPPs are short, water-soluble, partly hydrophobic, and/or polybasic peptides (at most 30-35 amino acid residues) with a net positive charge at physiological pH (Järver & Langel, 2006). Based on the structural similarities and activity between these two groups of peptides, it has been proposed that CPPs are not distinct from AMPs (Henriques et al., 2006; Splith & Neundorf, 2011). Different models including carpet-like, toroid-pore, and barrel stave have been used to describe the killing mechanism of both the AMPs and CPPs (Figure 7.2) (Sanderson, 2005; Yeaman & Yount, 2003).

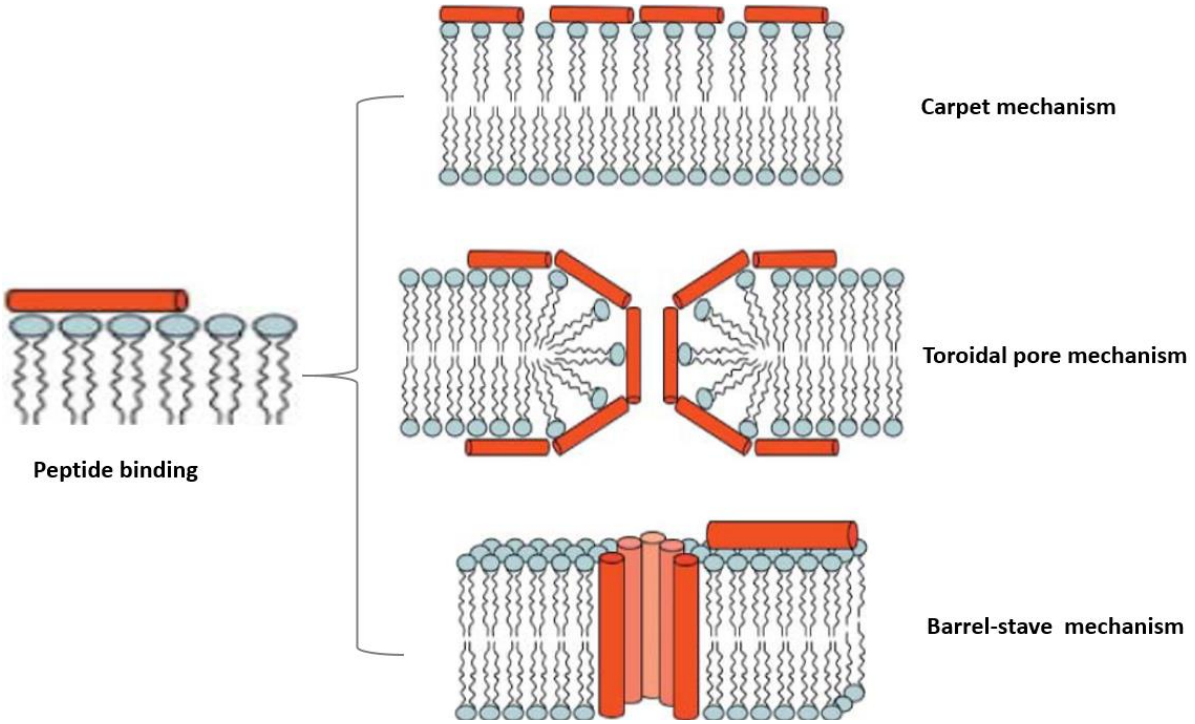

Figure 7.2 Pore-forming mechanism of antimicrobial peptides (Sanderson, 2005)

Intact cell membrane, metabolic activity, and reproducibility are the three accepted general parameters for the viability assessment of microorganisms (Oliver, 2005). The conventional colony-forming unit (CFU) counting method takes into account only one of these parameters, reproducibility, and provides only information about viable and culturable cells. The method is prone to errors due to the factors involved in bacterial growth on agar plates (Davis, 2014). However, an alternative to culture-based detection is the assessment of cell viability using fluorescent dyes, including membrane potential and membrane integrity (Berney et al., 2007; Stiefel et al., 2015) while various commercially available kits based on fluorescent dyes are being employed to determine bacterial viability (Asadishad et al., 2011; Joux & Lebaron, 2000). LIVE/DEAD® BacLight™ bacterial viability assay kit (LIVE/DEAD staining) is the most widely used in microbiological studies (Berney et al., 2007). LIVE/DEAD staining differentiates live and dead cells using membrane integrity as a proxy for cell viability and is based on a dual staining procedure using SYTO 9 and propidium iodide (PI) (Berney et al., 2007; Stiefel et al., 2015). Viable cells are characterised by intact and tight cell membranes while dead cells are considered to have disrupted and/or broken membranes (Oliver, 2010; Robertson et al., 2019). SYTO 9, which has a green fluorescence emission, stains both live and dead bacterial DNA, while propidium iodide (PI), which has a red fluorescence emission, penetrates only damaged cell membranes (Freire et al., 2015b; Stiefel et al., 2015).

Turbidimetry is one of the established methods to monitor bacterial growth since optical density (OD) measurements at 600_{nm} make it possible to follow bacterial population growth in real-time. Some authors have attempted to derive growth parameters from optical density measurements (Begot et al., 1996; Hudson & Mott, 1994).

Therefore, in the present work several methods including CFUs (growth) assay, turbidimetric assay, and LIVE/DEAD staining were employed to determine the bactericidal activity of crude and purified ~30 kD and ~48 kD putative antibacterial proteins of *Bl* 1821L and *Bl* 1951.

7.2 Methods

7.2.1 Bactericidal activity of crude *Bl* 1821L and *Bl* 1951 putative antibacterial proteins

Bl 1821L and *Bl* 1951 cultures were independently maintained on LB agar plates, a single colony was picked to inoculate 5 ml sterile LB broth (Miller) into universal vials as described in Chapter 4 (Section 4.2.4). Inoculated vials were placed on a shaking incubator (Conco, TU 4540, Taiwan) overnight at 30^{o}C and 250 rpm. One ml of an overnight culture of the host bacterium (*Bl* 1821L & *Bl* 1951) was transferred into 25 ml LB broth in 250 ml flasks and was placed on the shaking incubator with a speed of 250 rpm at 30^{o}C for 10-12 hours until the cultures attained sufficient turbidity. Mitomycin C (Sigma) @ concentration of 1 µg/ml was used to induce *Bl* 1821L culture as described in Chapter 2 (Section 2.2.6). *Bl* 1821L induced cultures were centrifuged at 16,000 g for 10 min to remove the intact cells and cell free supernatant (CFS) was passed through a 0.22 µm filter. Filtered supernatant containing a mixture of putative antibacterial proteins (encapsulating & phage tail-like proteins) in the crude state was added (500 µl) into a 250 ml flask containing the turbid cultures of the host bacterium. The turbidity of the culture was achieved by transferring 1 ml of an overnight culture of the host bacterium (*Bl* 1821L & *Bl* 1951) into 25 ml LB broth in 250 ml flasks and placing on the shaking incubator (Conco, TU 4540, Taiwan) with a speed of 250 rpm at 30^{o}C for 10-12 hours. Host bacterium (*Bl* 1821L & *Bl* 1951) cultures with the addition of LB broth (500 µl) served as a control for the corresponding strains. All the flasks with/without cell free supernatant containing *Bl* 1821L putative antibacterial proteins (crude) were kept at 30^{o}C in a standing incubator.

A sample (3 ml) was drawn from each treatment after 1, 3, 6, 12, 18, and 24 hours of incubation to determine the number of viable cells (CFU/ml) and OD_{600nm}. Cell biomass (OD_{600nm}) was measured through the Ultrospec-10 spectrophotometer (Amersham Biosciences) by transferring 1 ml of host bacterium with/without crude *Bl* 1821L putative antibacterial proteins into a cuvette and three

readings were taken for each sample, which were pooled to obtain a mean value for statistical analysis (Genstat 20th Edition).

A sample of 1 ml from each treatment after 1, 3, 6, 12, 18, and 24 hours of incubation was used to make tenfold serial dilutions for determining the number of viable cells (CFU/ml). After preparations of tenfold serial dilutions (10^{-1} to 10^{-6}) 100 µl of each dilution was spread in duplicate on two independent LB agar plates and the plates were incubated at 30°C. *Bl* 1821L and *Bl* 1951 colonies were counted using a colony counter (Stuart, UK) 2-3 days after spreading and converted into CFU/ml. Four sets of independent experiments (biological replicates) were performed and data for OD_{600nm} readings and CFU/ml of all the experiments were pooled to obtain a mean value for statistical analysis. Number of viable cell count (CFU/ml) was converted into $\log_{10}$ CFU/ml to have a precise presentation of data. To determine the effect of crude solution (lysate) containing putative antibacterial proteins, percentage (%) decrease/ increase in the number of viable cells from the control treatment (without putative antibacterial proteins) was calculated. All the data were statistically analysed using ANOVA (Analysis of Variance) through Genstat (20th Edition).

7.2.2 Bactericidal activity of purified putative antibacterial proteins of *Bl* 1821L and *Bl* 1951

Bactericidal activity of purified *Bl* 1821L and *Bl* 1951 putative antibacterial proteins was determined using the same protocol as described above (Section 7.2.1) for cell free supernatant (crude). For this study, group A (sucrose density gradient 20%) and group B (sucrose density gradient 60%) as described in Chapter 5 (Section 5.2.2) were used to purify *Bl* 1821L putative encapsulating protein (~30 kD) and phage tail-like protein (~48 kD). Likewise, group A (sucrose density gradient 50%) as outlined in Chapter 5 (Section 5.2.2) was used to purify ~30 kD putative encapsulating protein of *Bl* 1951. For determining the killing activity of purified putative antibacterial proteins, one experiment was performed with three LB agar plates used for each treatment to determine the number of viable cells (CFU/ml) as described above (Section 7.2.1). Similar to the crude lysate, the CFUs/ml were converted to $\log_{10}$ CFU/ml. The effect of percentage change in viable cells compared to the control treatment (without putative antibacterial proteins) after treatment with purified putative antibacterial proteins was calculated.

For spectrophotometer readings (OD_{600nm}) at various time intervals, the same method as described above (Section 7.2.1) was used on the data of three pooled values, to determine the percentage increase/decrease in OD_{600nm}.

7.2.3 LIVE/DEAD staining of bacterial cells after treatment with purified putative antibacterial proteins of *Bl* 1821L and *Bl* 1951

Overnight cultures of *Bl* 1821L and *Bl* 1951 were produced as described above. Ten millilitres of each host bacterium were aliquoted into two parts. One part was treated with the purified putative antibacterial protein and the other part, serving as the control, was treated with the TBS buffer. Two concentrations (100 µl & 200 µl) of purified putative antibacterial proteins were used. Solutions containing the purified putative antibacterial proteins (100 µl & 200 µl) were added into a 5 ml culture of the host bacterium (*Bl* 1821L & *Bl* 1951); a similar volume of TBS was used for the control treatment. All the treatments with/without TBS or putative antibacterial proteins were incubated at 30^{o}C and the samples were drawn from each treatment (1, 3, 6, 12, 18, 24 hours) for LIVE/DEAD staining.

For fluorescent microscopy, 5 µl of SYTO 9/PI stain (LIVE/DEAD® BacLight^{TM} bacterial viability assay kit ; Invitrogen, Carlsbad, CA, USA) was mixed with an equal volume of host bacteria with/without putative antibacterial protein for 5 mins in a UV-safe tube. Five µl of this mixture was pipetted onto a slide and a small volume (3 µl) of molten agarose (0.1%) was added to reduce cell movement. Cells were examined under a BX51 light microscope (Olympus) at x 100 magnification for fluorescent microscopy. Olympus DP74 camera (Japan) attached to the microscope was used to take the images with the help of CellSens 2.1 software. SYTO 9 (green) stain was visualised using a FITC filter with excision of 550 nm wavelength and for PI stain (red) a 650 nm wavelength was used. Immediately, both the images were overlapped using the CellSens 2.1 software to visualise the status of cells (alive or dead).

7.3 Results

7.3.1 Bactericidal activity of crude *Bl* 1821L putative antibacterial proteins (ABPs)

All the experimental data regarding the effect of putative antibacterial proteins of *Bl* 1821L in the crude form on the number of viable cells and optical density (OD_{600nm}) of the host bacterium (*Bl* 1821L & *Bl* 1951) are presented in Appendices E-2 to E-9. The mean values of the pooled data after statistical analysis are presented below and in Appendix E-1.

Bl 1821L culture after 6 hours of incubation at 30^{o}C with the crude *Bl* 1821L CFS containing putative antibacterial proteins of 30 kD (encapsulating protein) and 48 kD (phage tail-like protein) had a decrease of 30.1% in the number of viable cells (Table 7.1 & Figure 7.3) as compared to the control (without ABPs) and preceding time intervals (1 & 3 hours). Statistical analysis (ANOVA) found this decrease to be non-significant (Table 7.1). However, the number of viable cells in both the treatments exhibited a similar trend afterwards, with increasing cell counts, but post 18 hours of incubation the

number of colony forming unit in the control treatment indicated a decline of 23.6% as compared to the treated cultures (Table 7.1 & Figure 7.3).

Treatment of *Bl* 1951 culture with the crude *Bl* 1821L containing putative antibacterial proteins (encapsulating & phage tail-like proteins) in the filtered supernatant caused no alterations in the number of viable cells across all the time intervals. Even the number of CFUs of *Bl* 1951 treated culture demonstrated an upward trend as compared to the control (without ABPs). The number of viable cells increased from 31.9% to 55.2% up to 6 hours, but after this started to decrease when treated with the putative antibacterial proteins in the crude state (Table 7.1 & Figure 7.3).

The spectrophotometer reading (OD_{600nm}) decreased from the beginning (1 hour) to the end (24 hours) of the incubation (Table 7.2). For *Bl* 1821L, OD_{600nm} reading dropped by 40.7% in 24 hours after treatment with the crude ABPs which was slightly higher for the control (without ABPs) having a decrease of 37.2%. Likewise, for *Bl* 1951, a similar trend was noted as the ABPs treated culture had a decrease of 37.9% as compared to the control (without ABPs) where a decline of 32.8% was recorded (Table 7.2). However, OD_{600nm} reading of the treatments of *Bl* 1821L and *Bl* 1951 with/without crude ABPs addition to the turbid cultures did not display any prominent changes across all the time intervals. Variations in OD_{600nm} across all the time intervals of the treatments fluctuated from 0.0% to 8.4% (Table 7.2 & Figure 7.4).

Table 7.1 Effect of crude *Bl* 1821L putative antibacterial proteins (ABPs) on the number of viable cells of *Bl* 1821L and *Bl* 1951 after incubation at 30°C for various time intervals. Data presents the mean values of four experiments. Values of % decrease/increase in the number of viable cells are calculated from CFUs values of corresponding time intervals

Time intervals (Hours)	*Bl* 1821L	*Bl* 1821L + *Bl* 1821L crude ABPs	% Decrease/increase in no. of viable cells	*Bl* 1951	*Bl* 1951 + *Bl* 1821L crude ABPs	% Decrease/increase in no. of viable cells	*LSD (5%)
1	4.46E+06 (6.650)**	5.56E+06 (6.745)	-24.65	3.18E+06 (6.502)	4.19E+06 (6.622)	-31.89	0.350
3	3.70E+06 (6.568)	3.85E+06 (6.585)	-4.05	3.64E+06 (6.561)	4.93E+06 (6.692)	-35.40	0.281
6	3.58E+06 (6.553)	2.50E+06 (6.398)	30.07	3.74E+06 (6.573)	5.80E+06 (6.763)	-55.18	0.377
12	1.18E+07 (7.071)	1.10E+07 (7.043)	6.36	9.15E+06 (6.961)	1.33E+07 (7.123)	-45.22	0.312
18	1.35E+07 (7.131	1.67E+07 (7.223)	-23.57	1.05E+07 (7.023)	1.17E+07 (7.068)	-11.03	0.228
24	1.72E+07 (7.236)	1.50E+07 (7.177)	12.71	5.58E+06 (6.746)	7.89E+06 (6.897)	-41.48	0.317

*=Least significant difference

**=The values in parenthesis indicate the converted value of number of viable cells (CFU/ml) into $\log_{10}$ CFU/ml.

Table 7.2 Effect of crude *Bl* 1821 putative antibacterial proteins (ABPs) on the OD_{600nm} reading of *Bl* 1821L and *Bl* 1951 after incubation at 30°C for various time intervals. Data presents the mean values of four experiments

Time intervals (Hours)	*Bl* 1821L	*Bl* 1821L + *Bl* 1821L crude ABPs	% Decrease/increase in OD_{600nm} reading	*Bl* 1951	*Bl* 1951 + *Bl* 1821L crude ABPs	% Decrease/increase in OD_{600nm} reading	*LSD (5%)
1	1.99	1.99	0.00	1.92	1.90	1.14	0.061
3	1.87	1.85	0.67	1.74	1.73	0.43	0.121
6	1.65	1.63	1.21	1.58	1.55	1.51	0.148
12	1.29	1.26	2.32	1.45	1.39	4.57	0.135
18	1.23	1.21	1.63	1.24	1.25	-0.10	0.227
24	1.25	1.18	5.51	1.29	1.18	8.36	0.237
% Decrease from the start (1 hour) to the end (24 hours) of incubation	37.2%	40.7%		32.8%	37.9%		

*=Least significant difference

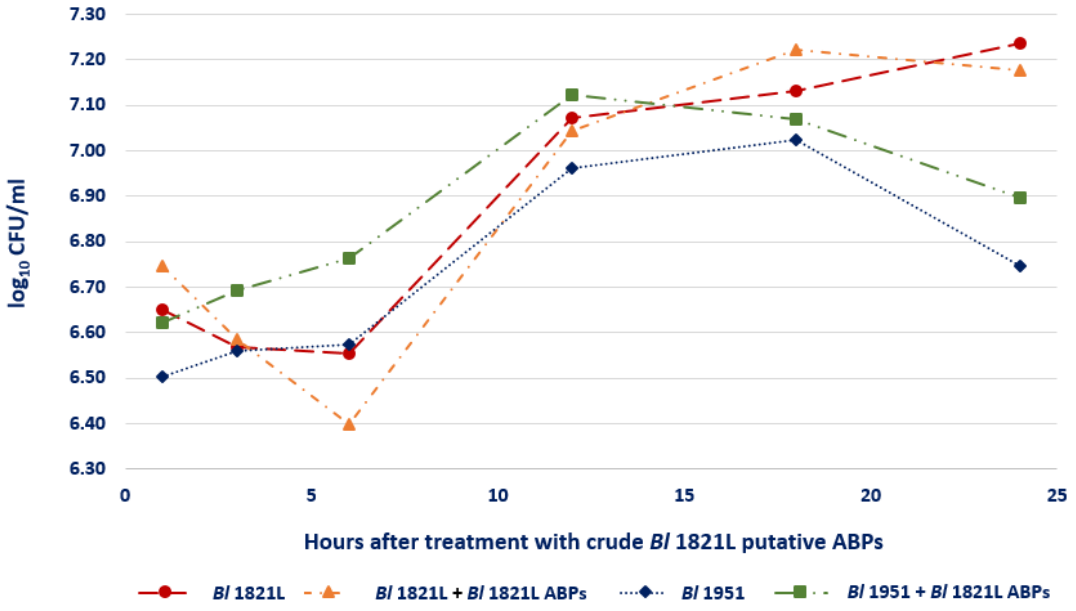

Figure 7.3 Number of viable cells (log_{10} CFU/ml) of *Bl* 1821L and *Bl* 1951 with/without treatment of crude *Bl* 1821L putative antibacterial proteins (ABPs) after incubation at 30°C for various time intervals

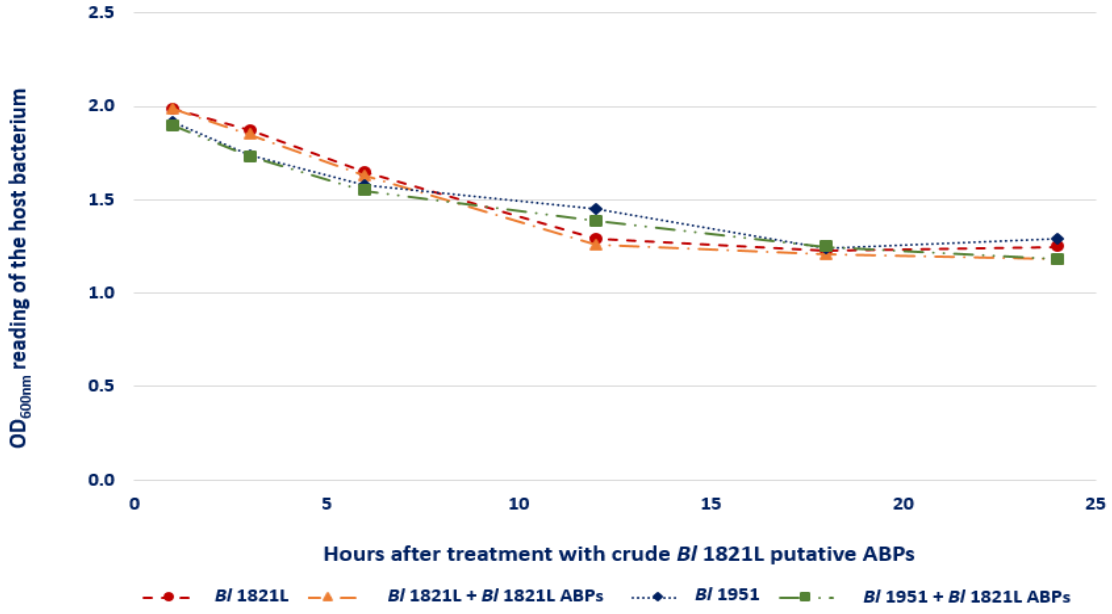

Figure 7.4 Effect of crude *Bl* 1821 putative antibacterial proteins (ABPs) on the OD_{600nm} reading of *Bl* 1821L and *Bl* 1951 after incubation at 30°C for various time intervals

7.3.2 Bactericidal activity of purified *Bl* 1821L putative encapsulating protein (30 kD)

The *Bl* 1821L culture after treatment with the purified putative encapsulating protein (EP) of ~30 kD (Figures 5.17A-B & 5.24) exhibited a steady increase in the number of cells at the start (1-3 hours) of incubation. But, the number of viable cells underwent a decline of 48.9% after 6 hours of incubation at 30^{o}C and subsequently *Bl* 1821L treated culture exhibited an exponential increase relative to the control treatment (without EP) (Table 7.3 & Figure 7.5).

A similar trend in the antibacterial activity against *Bl* 1951 cells was observed. Encapsulating protein treated *Bl* 1951 culture displayed a similar growth trend to the control treatment (without EP) at the beginning (1-3 hours). However, after 6 hours post incubation (HPI), there was a decline of 43.8% in the number of viable cells which then increased from 12 to 24 hours (Table 7.3 & Figure 7.5).

Spectrophotometric reading (OD_{600nm}) of *Bl* 1821L treated culture exhibited a change from 1 to 24 HPI. A decrease in OD_{600nm} reading of control treatment (without EP) of 49.7% was recorded, slightly higher than for the treated culture (46.9%). For *Bl* 1951, the difference between the OD_{600nm} readings between the treated and control treatment was not as prominent as the former with a decline of 53.9% and the latter 52.4% (Table 7.4). However, OD_{600nm} readings of all the treatments with/without EP across various time intervals revealed very small changes (0% to 12%) (Table 7.4 & Figure 7.6).

Table 7.3 Effect of purified *Bl* 1821L 30 kD putative encapsulating protein (EP) on the number of viable cells of *Bl* 1821L and *Bl* 1951 after incubation at 30°C for various time intervals. Data presents the mean values of one experiment. Values of % decrease/increase in the number of viable cells are calculated from CFUs values of corresponding time intervals

Time intervals (Hours)	*Bl* 1821L	*Bl* 1821L + *Bl* 1821L EP	% Decrease/increase in no. of viable cells	*Bl* 1951	*Bl* 1951 + *Bl* 1821L EP	% Decrease/increase in no. of viable cells
1	5.30E+06 (6.724)*	5.65E+06 (6.752)	-6.60	6.65E+06 (6.823)	8.40E+06 (6.924)	-26.32
3	2.35E+06 (6.371)	2.85E+06 (6.455)	-21.28	6.35E+06 (6.803)	6.75E+06 (6.829)	-6.30
6	7.05E+06 (6.848)	3.60E+06 (6.556)	48.94	8.00E+06 (6.903)	4.50E+06 (6.653)	43.75
12	2.14E+07 (7.330)	2.79E+07 (7.445)	-30.14	2.08E+07 (7.318)	2.14E+07 (7.330)	-2.88
18	1.12E+07 (7.049)	1.67E+07 (7.221)	-48.66	1.21E+07 (7.081)	1.67E+07 (7.221)	-38.17
24	1.28E+07 (7.109)	1.82E+07 (7.259)	-42.35	1.24E+07 (7.093)	1.51E+07 (7.179)	-21.77

*=The values in parenthesis indicate the converted value of number of viable cells (CFU/ml) into $\log_{10}$ CFU/ml.

Table 7.4 Effect of purified *Bl* 1821L 30 kD putative encapsulating protein (EP) on the OD_{600nm} reading of *Bl* 1821L and *Bl* 1951 after incubation at 30°C for various time intervals. Data presents the mean values of one experiment

Time intervals (Hours)	*Bl* 1821L	*Bl* 1821L + *Bl* 1821L EP	% Decrease/increase in OD_{600nm} reading	*Bl* 1951	*Bl* 1951 + *Bl* 1821L EP	% Decrease/increase in OD_{600nm} reading
1	3.02	2.90	3.97	2.90	2.93	-1.03
3	2.76	2.43	11.96	1.91	1.95	-1.83
6	1.93	1.93	0.00	1.93	1.92	0.52
12	1.69	1.73	-2.07	1.88	1.93	-2.39
18	1.53	1.58	-3.27	1.41	1.33	5.67
24	1.41	1.33	5.67	1.38	1.35	2.17
% Decrease from the start (1 hour) to the end (24 hours) of incubation	49.7%	46.9%		52.4%	53.9%	

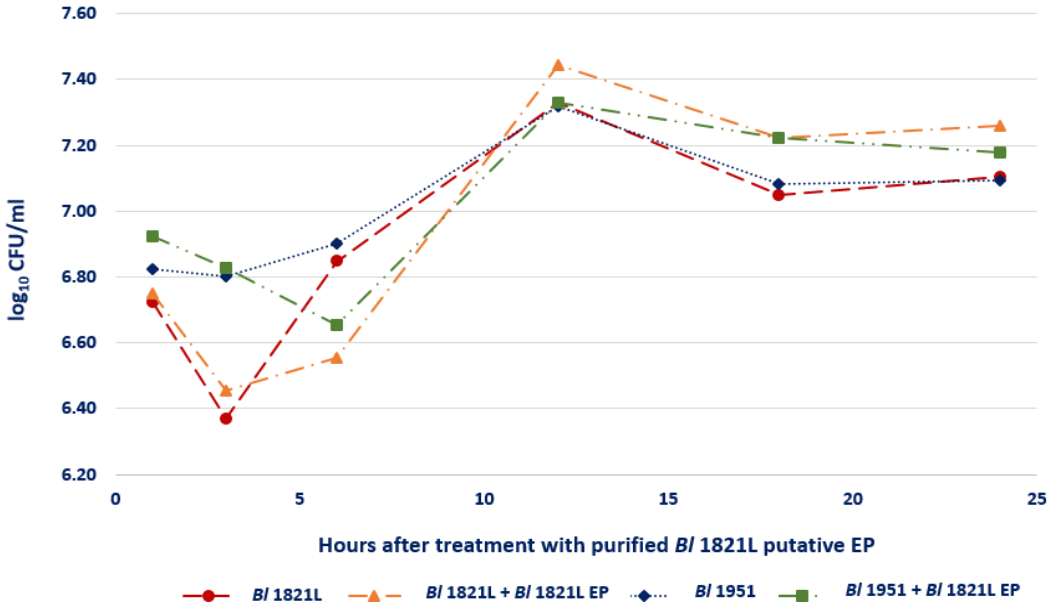

Figure 7.5 Number of viable cells (log_{10} CFU/ml) of *Bl* 1821L and *Bl* 1951 with/without treatment of purified *Bl* 1821L putative encapsulating protein (30 kD) after incubation at 30°C for various time intervals

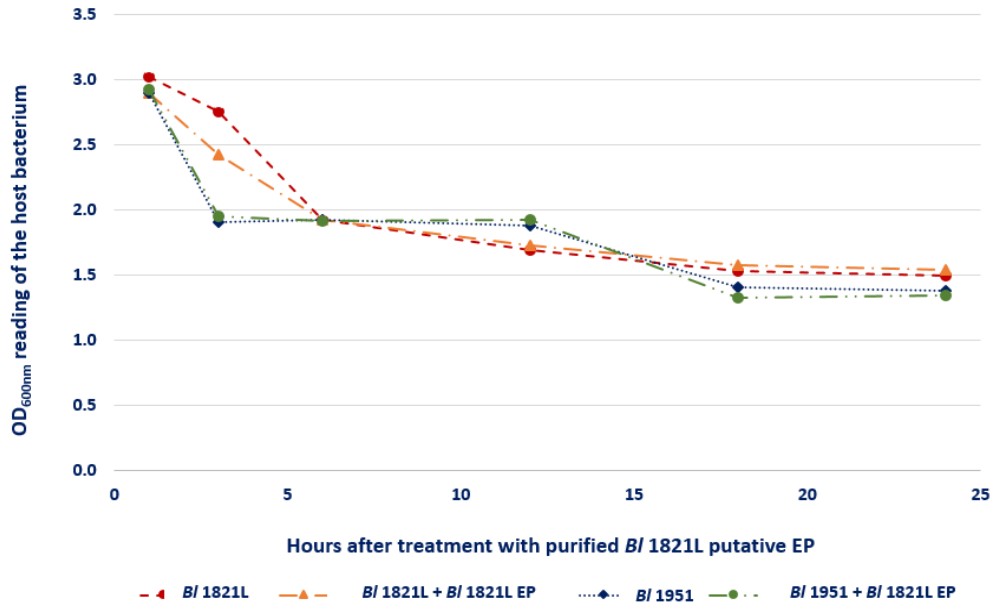

Figure 7.6 Effect of purified *Bl* 1821L putative encapsulating protein (30 kD) on the OD_{600nm} reading of *Bl* 1821L and *Bl* 1951 after incubation at 30°C for various time intervals

7.3.3 LIVE/DEAD staining of *Bl* 1821L cells after treatment with the purified *Bl* 1821L putative encapsulating protein (30 kD)

Live/Dead staining of *Bl* 1821L treated culture with the purified *Bl* 1821L putative ~30 kD encapsulating protein (EP) did not show a higher population of red cells (cells with compromised membranes) after 1 hour of incubation. However, in the control treatment (without EP) more red cells were present (Figure 7.7). *Bl* 1821L cells with compromised cell membranes (red) were prominent after 6 and 12 hours of incubation with the purified EP, which was similar to the control. Notably, the appearance of red cells coincided with the decrease in the number of viable cells (48.9%) 6 hours after treatment with the purified EP but in contrast to the 12 hours treatment (Table 7.3 & Figures 7.5, 7.7). On a percentage basis, 6 hours after treatment 58.8% of the EP treated and 37.5% of the untreated cells were red (Figures 7.7 & 7.8). However, 3 hours after treatment with the purified EP, more red cells were seen compared to the control where yellow/orange colour cells were predominant (Figure 7.7). Live/Dead staining of *Bl* 1821L treated culture with the purified *Bl* 1821L putative ~30 kD EP at a higher concentration resulted in more cells with compromised membranes (red) from the initial 1 hour of incubation up to 6 hours when compared to the control (without EP). However, yellow/orange cells in the *Bl* 1821L culture with the purified ~30 kD EP were dominant from 12 to 24 hours of incubation at 30^{o}C (Figure 7.9).

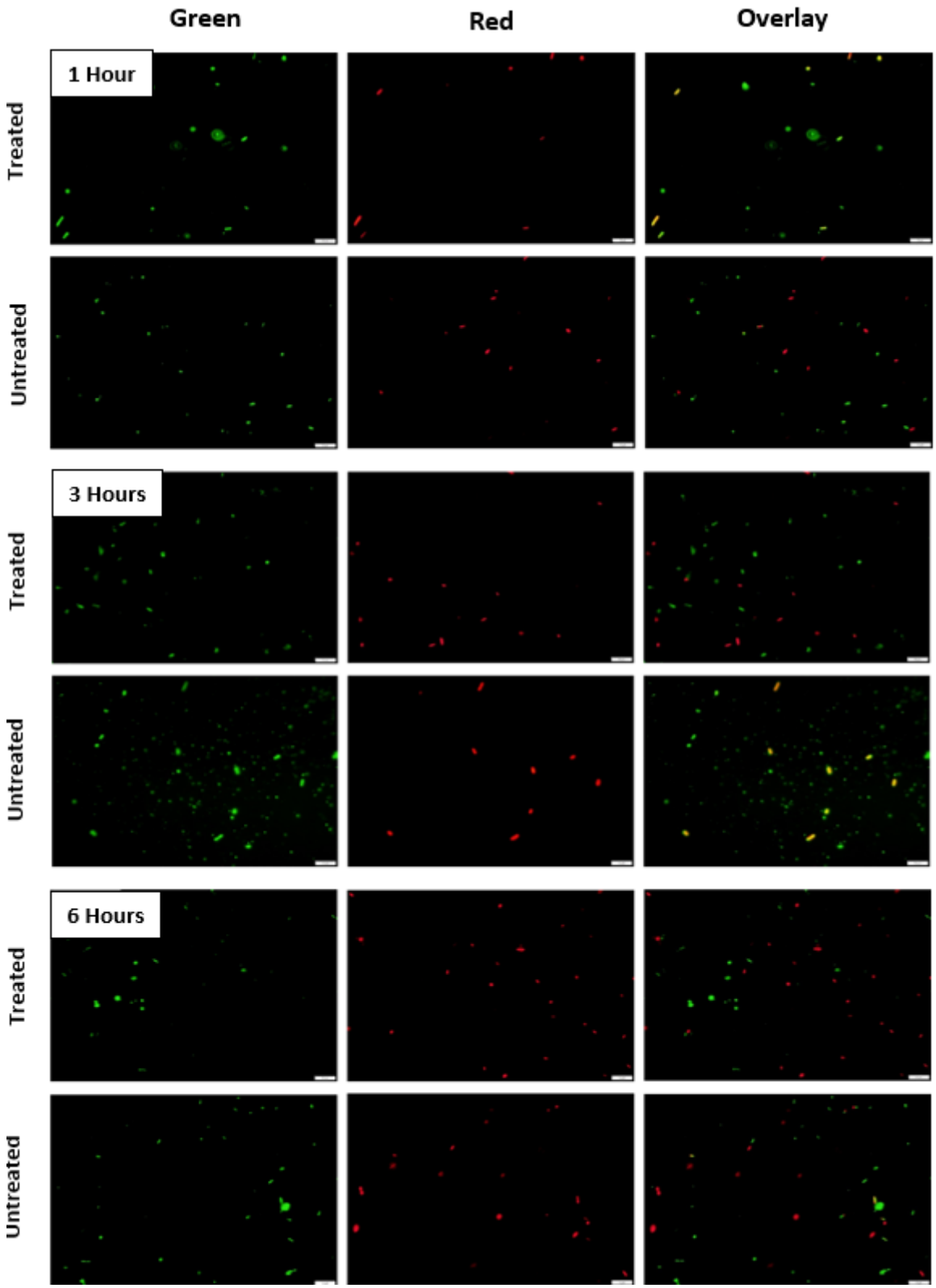
Green
Red
Overlay
1 Hour
Treated
Untreated
3 Hours
Treated
Untreated
6 Hours
Treated
Untreated

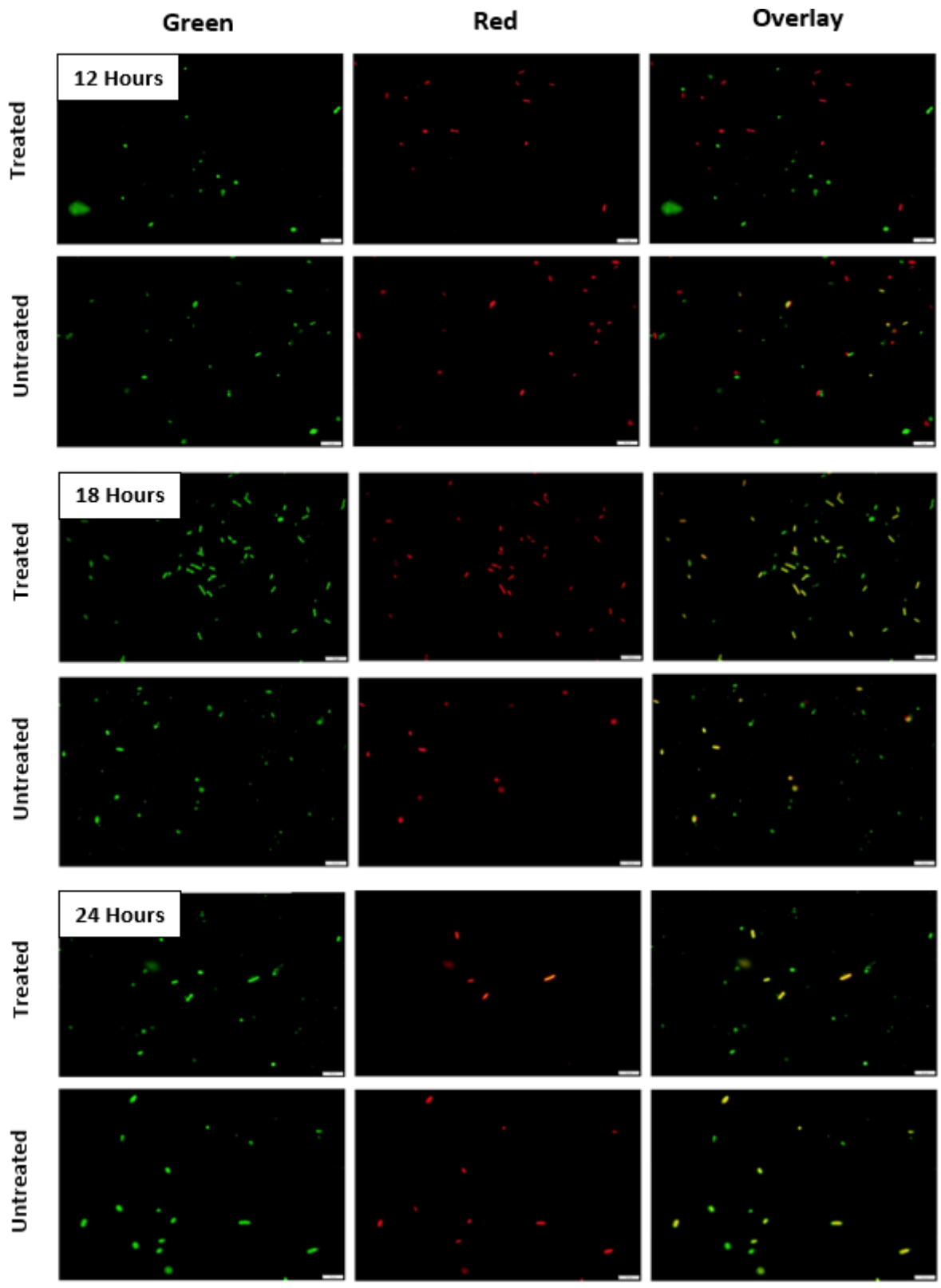

Figure 7.7 LIVE/DEAD staining of *Bl* 1821L cells after treatment with the purified *Bl* 1821L putative encapsulating protein (30 kD). Scale bar = 10 µm

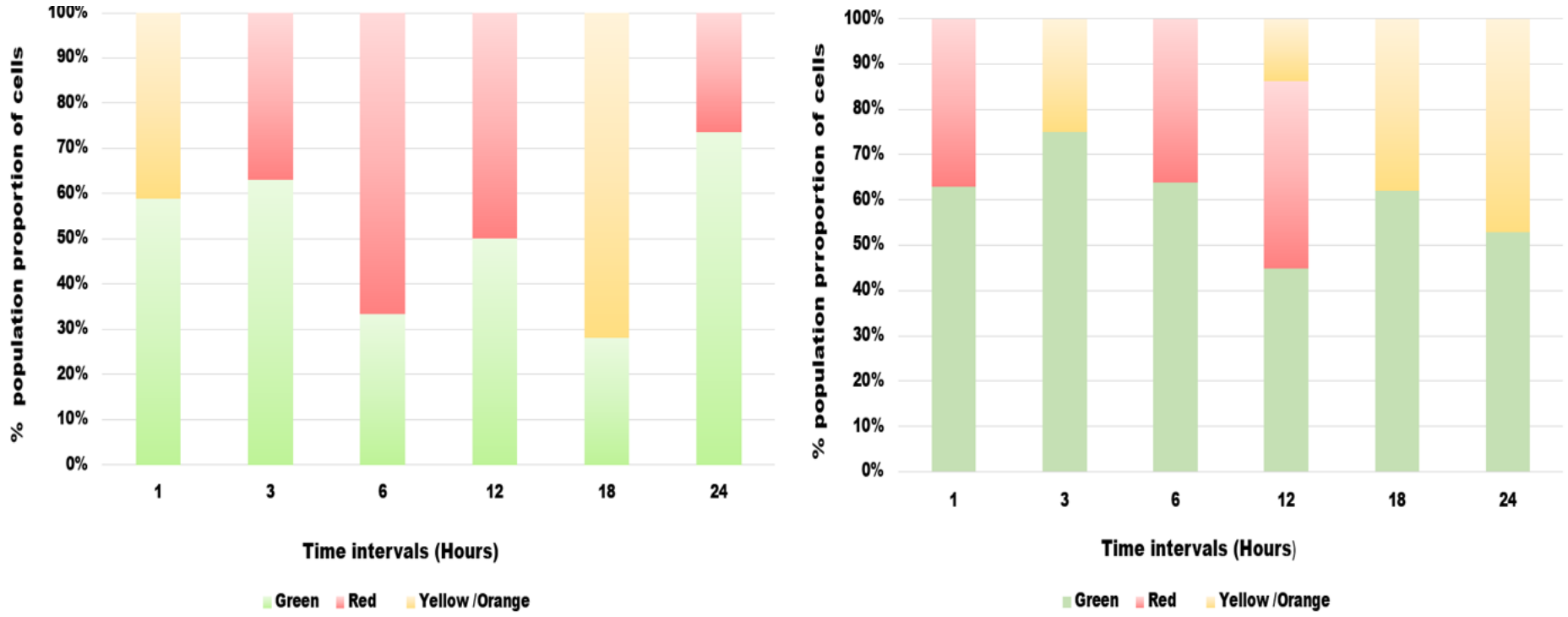

Figure 7.8 LIVE/DEAD stained percentage population proportion of *Bl* 1821L cells after treatment (left side graph) with the 30 kD purified putative encapsulating protein of *Bl* 1821L and without treatment (right side graph)

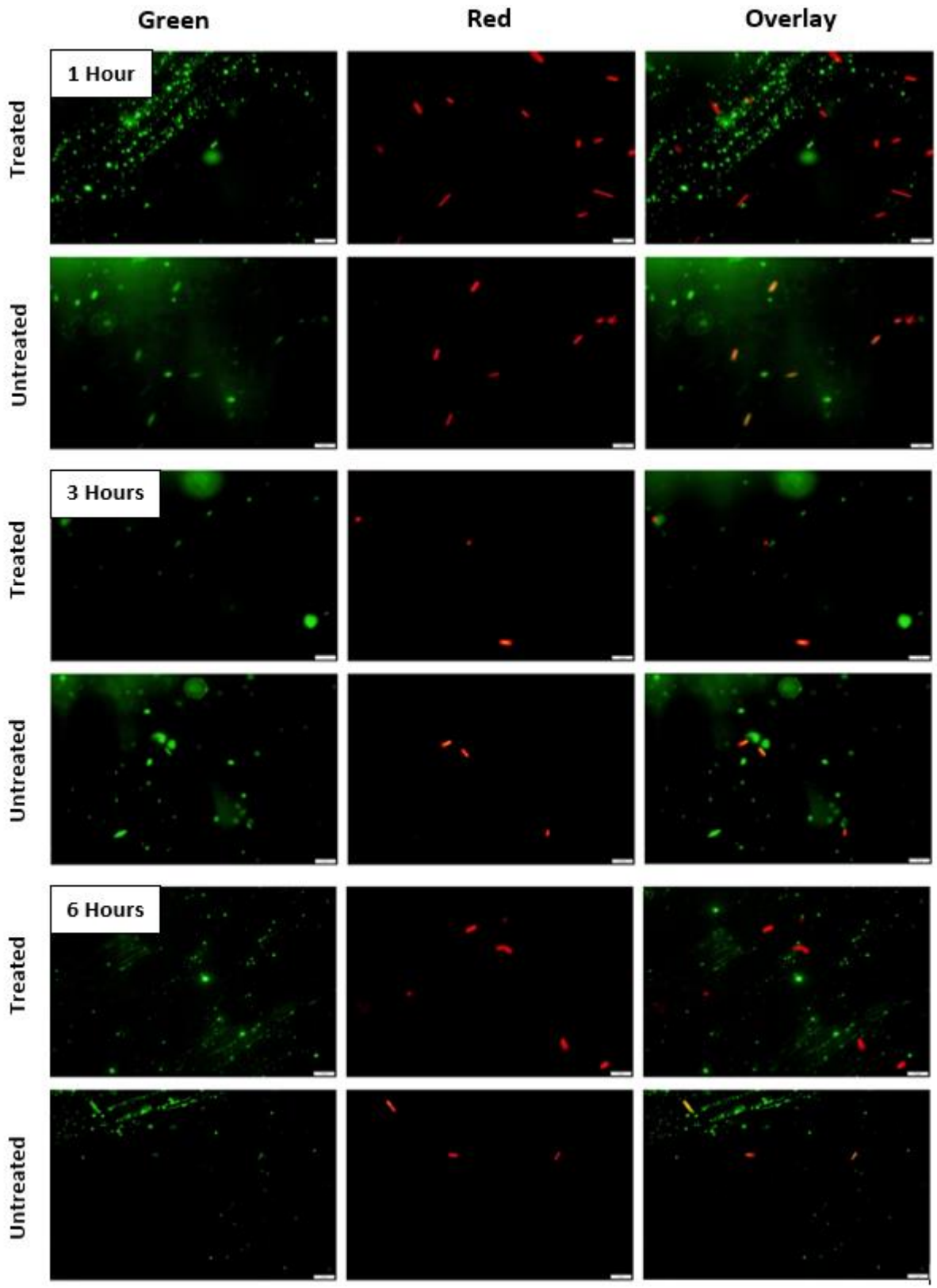
Green
Red
Overlay
1 Hour
Treated
Untreated
3 Hours
Treated
Untreated
6 Hours
Treated
Untreated

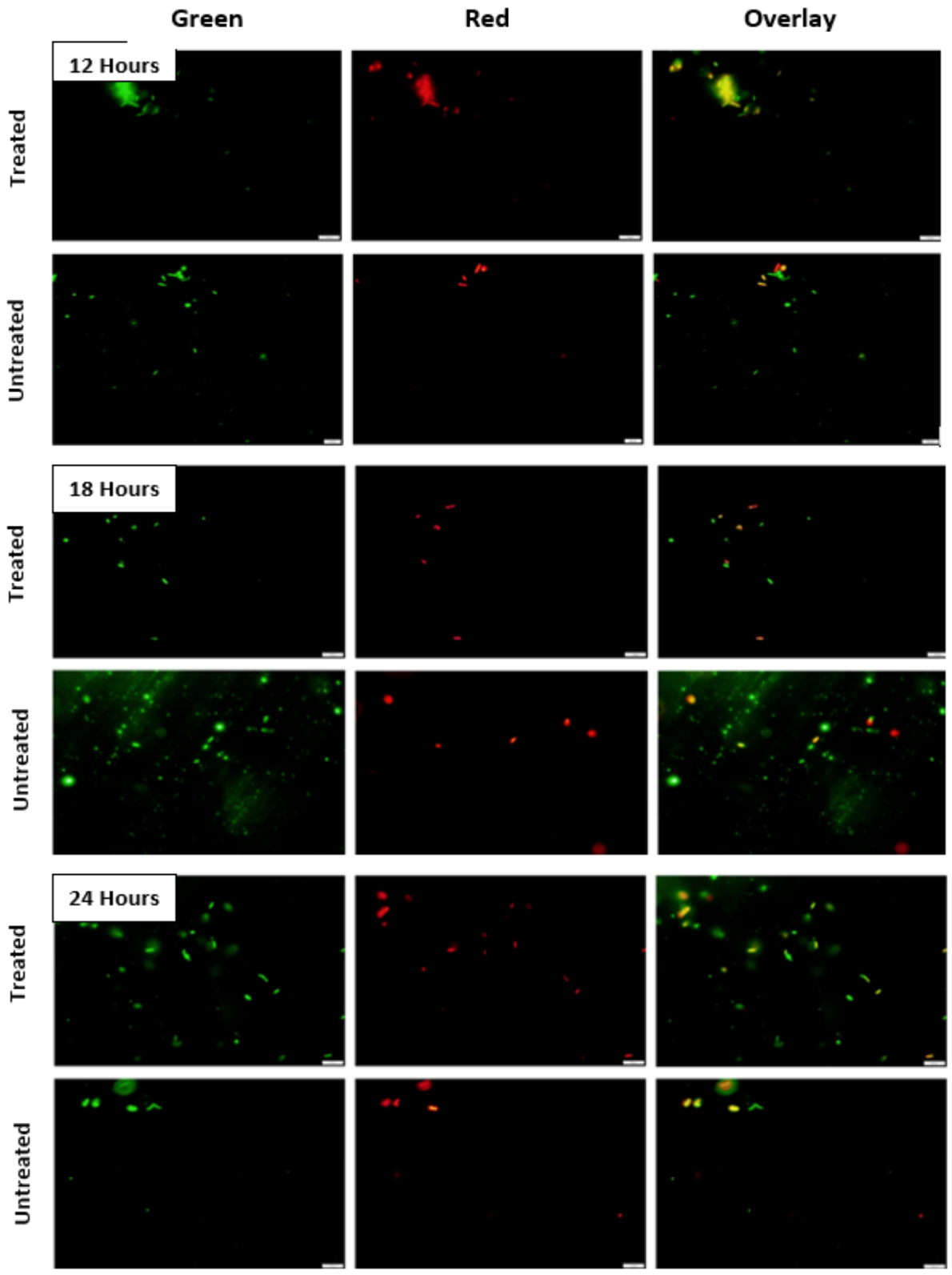

Figure 7.9 LIVE/DEAD staining of *Bl* 1821L cells after treatment with the purified *Bl* 1821L putative encapsulating protein (30 kD) at a higher concentration. Scale bar = 10 µm

7.3.4 LIVE/DEAD staining of *Bl* 1951 cells after treatment with the purified *Bl* 1821L putative encapsulating protein (30 kD)

Fluorescent microscopy of the *Bl* 1951 culture after addition of the purified *Bl* 1821L putative encapsulating protein (~30 kD) revealed a mixed population of a few green and the majority of red and yellow/orange cells, whereas the TBS treated (control) had a higher population of green and yellow/ orange cells (Figure 7.10). Cells with compromised cell membranes (red) were more often seen after 3 and 24 HPI when EP was added and yellow/orange cells were noticed after 6, 12, and 18 hours of treatment (Figure 7.10).

Treatment of *Bl* 1951 cells with the purified *Bl* 1821L EP at a higher concentration showed a dominating population of red cells after 1 and 6 hours of incubation at 30^{o}C but at later time intervals (12, 18, 24 hours) yellow/orange cells were seen (Figure 7.11).

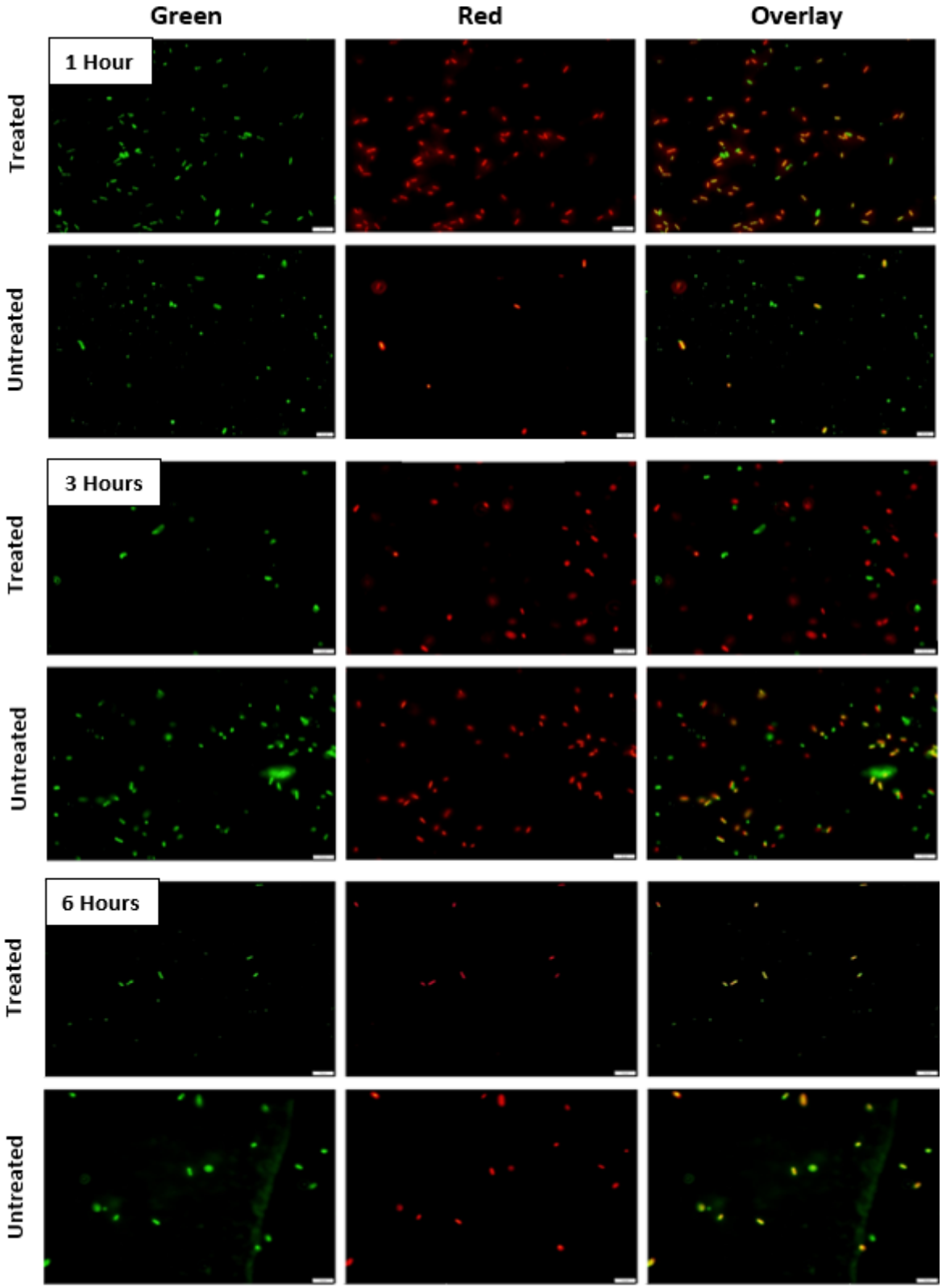
Green
Red
Overlay
1 Hour
Treated
Untreated
3 Hours
Treated
Untreated
6 Hours
Treated
Untreated

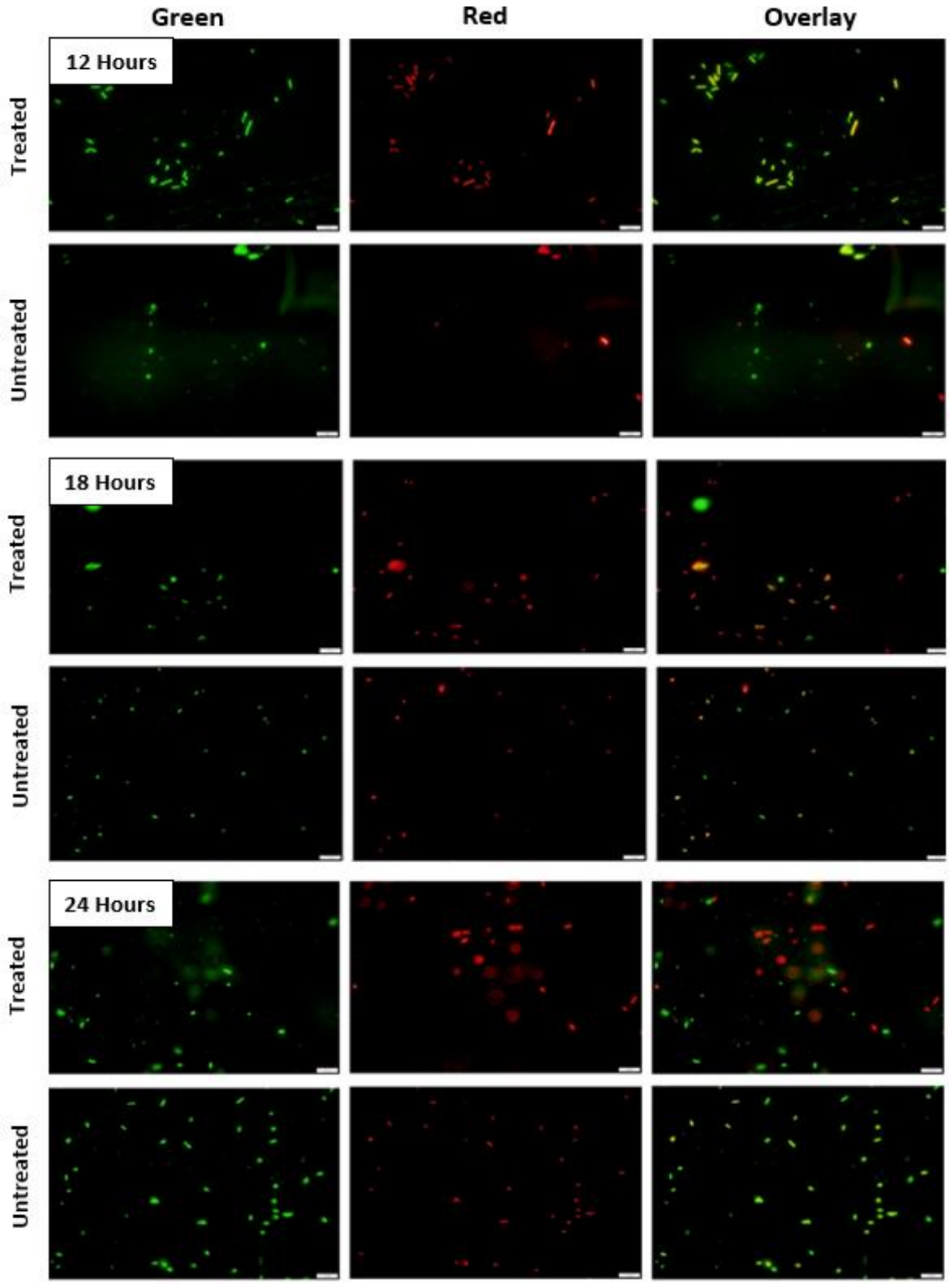

Figure 7.10 LIVE/DEAD staining of *Bl* 1951 cells after treatment with the purified *Bl* 1821L putative encapsulating protein (30 kD). Scale bar = 10 µm

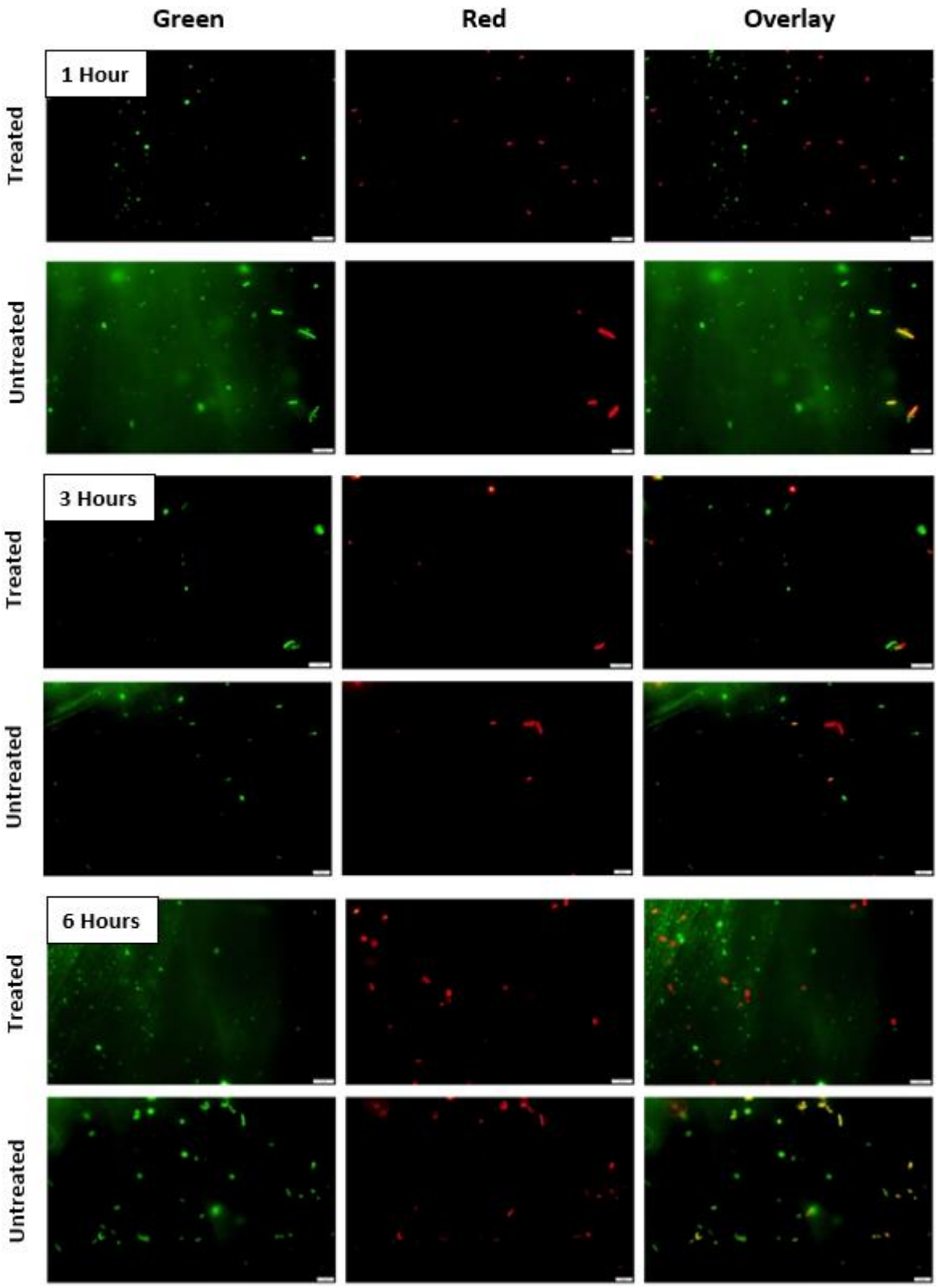
Green
Red
Overlay
1 Hour
Treated
Untreated
3 Hours
Treated
Untreated
6 Hours
Treated
Untreated

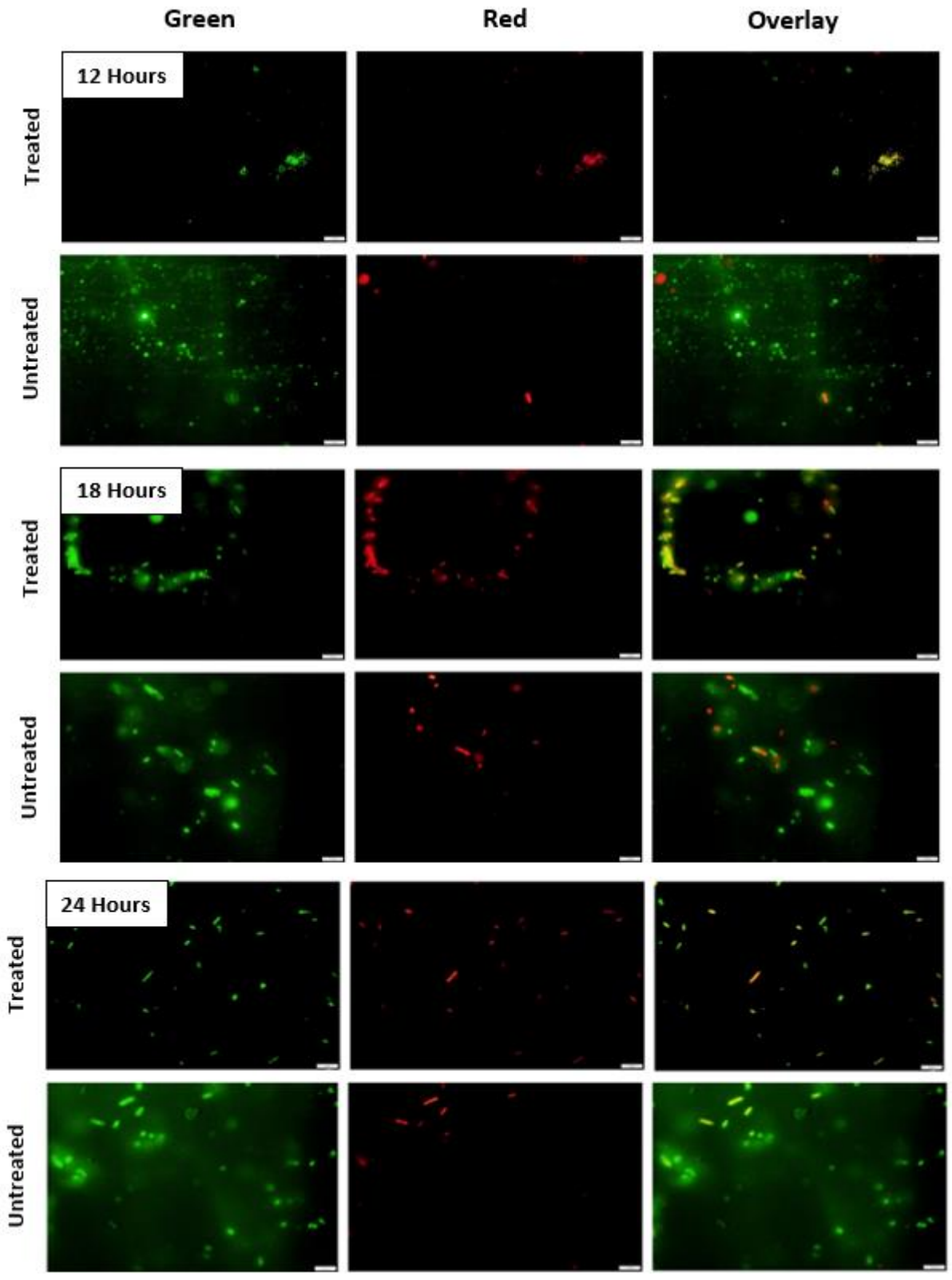

Figure 7.11 LIVE/DEAD staining of *Bl* 1951 cells after treatment with the purified *Bl* 1821L putative encapsulating protein (30 kD) at a higher concentration. Scale bar = 10 µm

7.3.5 Bactericidal activity of purified *Bl* 1821L putative phage tail-like protein (48 kD)

Upon addition of *Bl* 1821L purified ~48 kD phage tail-like protein (PTLP) (Figures 5.18A-F & 5.24) into *Bl* 1821L culture, there was no pronounced change in the number of viable cells. However, relative to the control treatment (without PTLP) there was an increase in the number of viable cells across the time intervals, except at 3 and 12 HPI (Table 7.5 & Figure 7.12).

The number of viable cells showed a consistent increase for an hour post incubation of *Bl* 1951 with the purified PTLP, after which cell numbers steadily declined. Twelve and 18 hours after treatment of *Bl* 1951 cells with the purified PTLP, there was a decline of 22.1% and 34.2% in the number of viable cells as compared to the control (without PTLP) (Table 7.5 & Figure 7.12).

OD_{600nm} reading of *Bl* 1821L treated cultures exhibited a change from the beginning (1 hour) to the end (24 hours) of incubation. OD_{600nm} reading of *Bl* 1821L culture without PTLP (control) decreased 66.5%, which was slightly higher than that of the treated ones (62.2%). For *Bl* 1951, the difference in the OD_{600nm} readings between the treated and control treatment was not prominent as the former showed a decline of 50.5% and the latter 48.3% (Table 7.6). OD_{600nm} reading of all the treatments of *Bl* 1821L and *Bl* 1951 with/without purified PTLP added to the cultures did not exhibit any prominent changes across different time intervals. Variations in OD_{600nm} across various time intervals of all the treatments fluctuated from 0% to 6% (Table 7.6 & Figure 7.13).

Table 7.5 Effect of purified *Bl* 1821L putative 48 kD phage tail-like protein (PTLP) on the number of viable cells of *Bl* 1821L and *Bl* 1951 after incubation at 30°C for various time intervals. Data presents the mean values of one experiment. Values of % decrease/increase in the number of viable cells are calculated from CFUs values of corresponding time intervals

Time intervals (Hours)	*Bl* 1821L	*Bl* 1821L + *Bl* 1821L PTLP	% Decrease/increase in no. of viable cells	*Bl* 1951	*Bl* 1951 + *Bl* 1821L PTLP	% Decrease/increase in no. of viable cells
1	1.74E+07 (7.241)*	2.81E+07 (7.448)	-61.21	9.05E+06 (6.957)	1.66E+07 (7.220)	-83.43
3	2.41E+07 (7.381)	2.16E+07 (7.334)	10.19	6.20E+06 (6.792)	8.80E+06 (6.944)	-41.94
6	1.13E+07 (7.051)	1.64E+07 (7.215)	-45.78	1.17E+07 (7.066)	1.08E+07 (7.031)	7.73
12	2.34E+07 (7.369)	2.14E+07 (7.330)	8.55	2.58E+07 (7.411)	2.01E+07 (7.302)	22.14
18	1.68E+07 (7.224)	2.78E+07 (7.443)	-65.67	2.37E+07 (7.375)	1.56E+07 (7.193)	34.18
24	2.33E+07 (7.366)	2.87E+07 (7.457)	-23.23	1.87E+07 (7.271)	2.03E+07 (7.307)	-8.85

*=The values in parenthesis indicate the converted value of number of viable cells (CFU/ml) into $\log_{10}$ CFU/ml.

Table 7.6 Effect of purified *Bl* 1821L 48 kD putative phage tail-like protein (PTLP) on the OD_{600nm} reading of *Bl* 1821L and *Bl* 1951 after incubation at 30°C for various time intervals. Data presents the mean values of one experiment

Time intervals (Hours)	*Bl* 1821L	*Bl* 1821L + *Bl* 1821L PTLP	% Decrease/increase in OD_{600nm} reading	*Bl* 1951	*Bl* 1951 + *Bl* 1821L PTLP	% Decrease/increase in OD_{600nm} reading
1	3.40	3.20	5.88	2.89	2.90	-0.35
3	1.99	1.98	0.50	1.93	1.91	1.04
6	1.70	1.61	5.01	1.76	1.79	-1.70
12	1.26	1.30	-3.59	1.65	1.68	-1.82
18	1.19	1.27	-6.30	1.58	1.59	-0.63
24	1.14	1.21	-6.14	1.43	1.50	-4.90
% Decrease from the start (1 hour) to the end (24 hours) of incubation	66.5%	62.2%			50.5%	48.3%

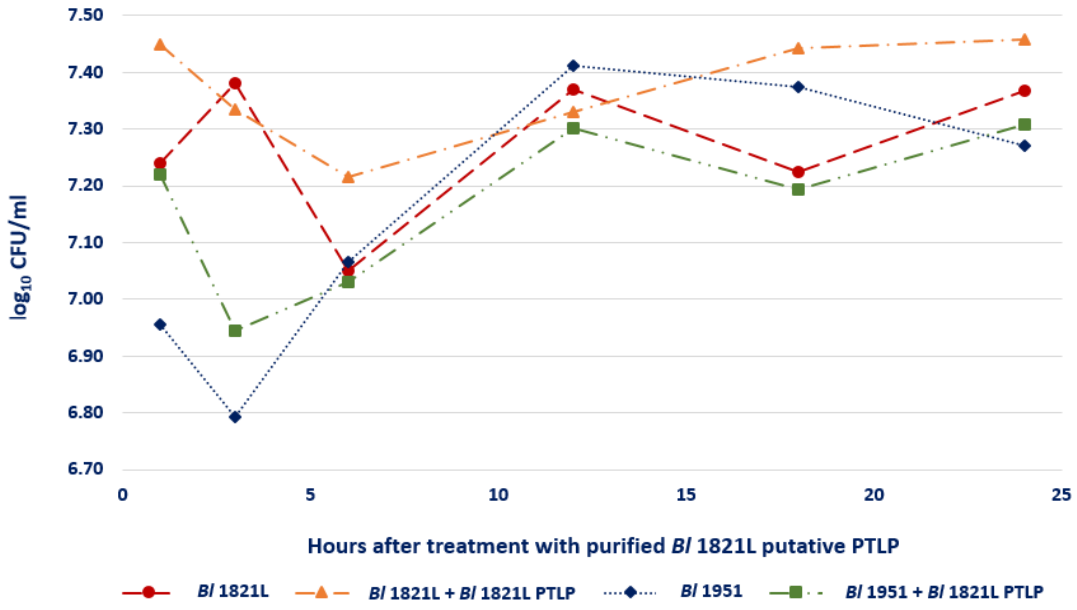

Figure 7.12 Number of viable cells (log_{10} CFU/ml) of *Bl* 1821L and *Bl* 1951 with/without treatment of purified *Bl* 1821L putative phage tail-like protein (48 kD) after incubation at 30^{o}C for various time intervals

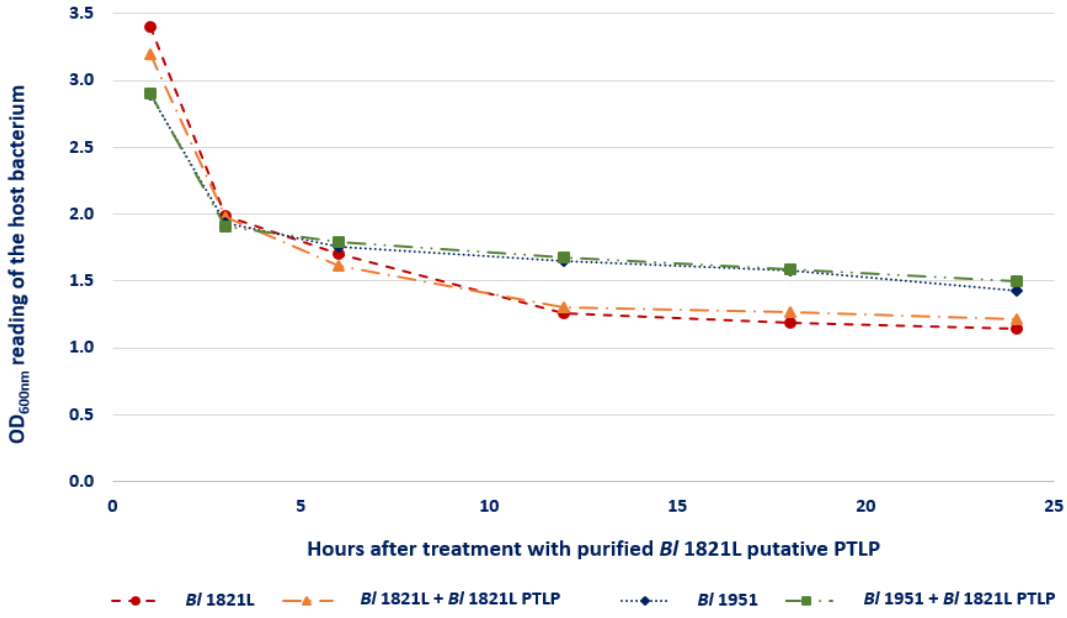

Figure 7.13 Effect of purified *Bl* 1821 putative phage tail-like protein (48 kD) on the OD_{600nm} reading of *Bl* 1821L and *Bl* 1951 after incubation at 30°C for various time intervals

7.3.6 LIVE/DEAD staining of *Bl* 1951 cells after treatment with the purified *Bl* 1821L putative phage tail-like protein (48 kD)

LIVE/DEAD staining of *Bl* 1951 cells after treatment with the purified ~48 kD putative phage tail-like protein (PTLP) indicated a minor population of red cells at 3 hours but cells with compromised membranes (red) were seen after 18 hours of incubation with the PTLP at 30^{o}C, although less in number than green cells (cells with intact membranes). Post treatment of *Bl* 1951 cells with the purified ~48 kD PTLP after 6, 12, and 24 hours showed the prevalence of yellow/orange cells in the population (Figure 7.14).

Purified *Bl* 1821L PTLP addition to the *Bl* 1951 culture at a higher concentration exhibited more *Bl* 1951 cells with compromised membranes (red) from 1 hour to 6 hours however, a similar percentage of red cells were also seen in the control treatment (without PTLP) (Figure 7.15). Cells with intact membranes (green) were more frequent after 18 and 24 hours of incubation at 30^{o}C as compared to the cells with compromised membranes (red). However, yellow/orange colour cells were obvious 12 hours after treatment with the purified *Bl* 1821L PTLP (Figure 7.15).

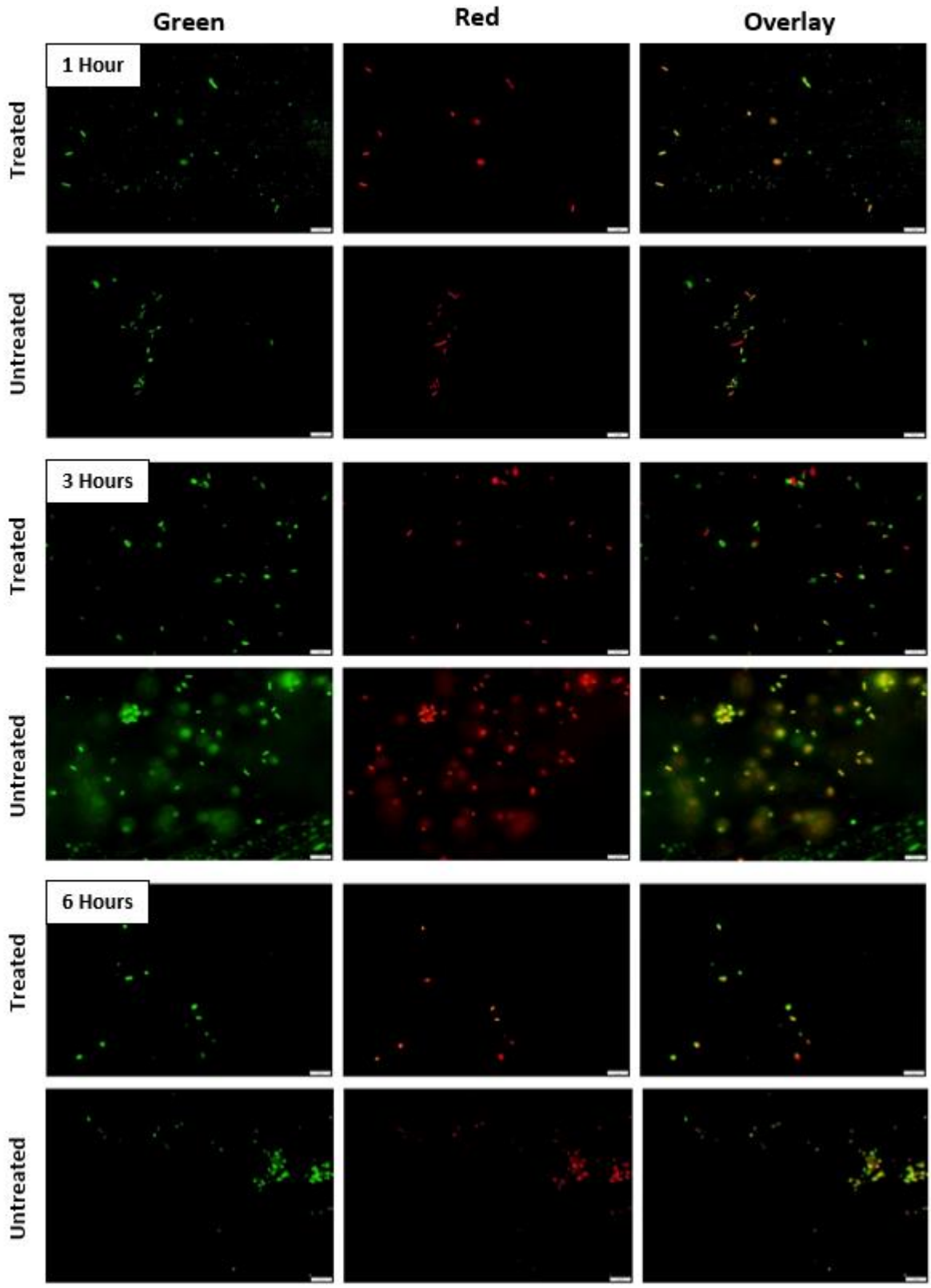
Green
Red
Overlay
1 Hour
Treated
Untreated
3 Hours
Treated
Untreated
6 Hours
Treated
Untreated

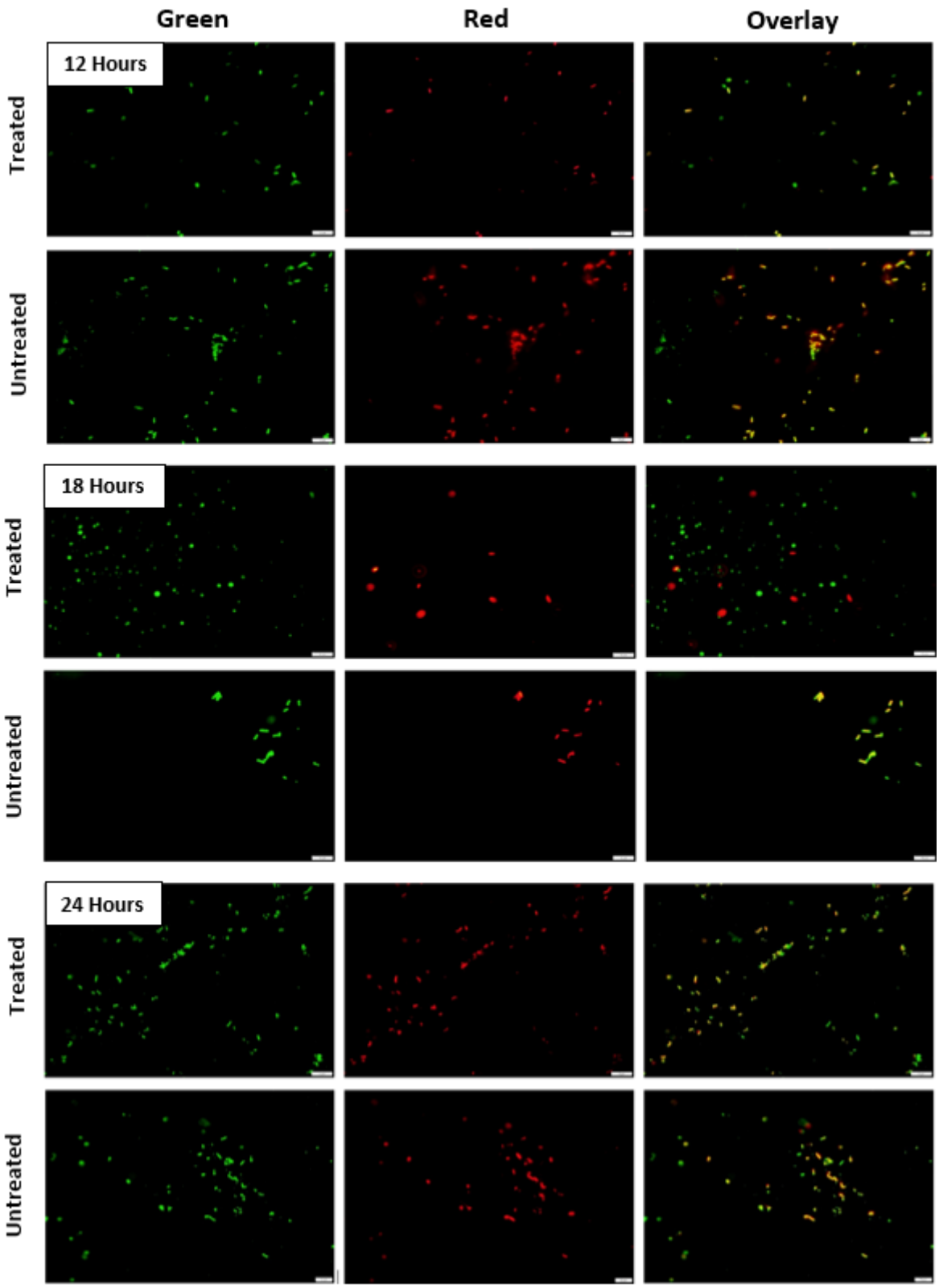

Figure 7.14 LIVE/DEAD staining of *Bl* 1951 cells after treatment with the purified *Bl* 1821L putative phage tail-like protein (48 kD). Scale bar = 10 µm

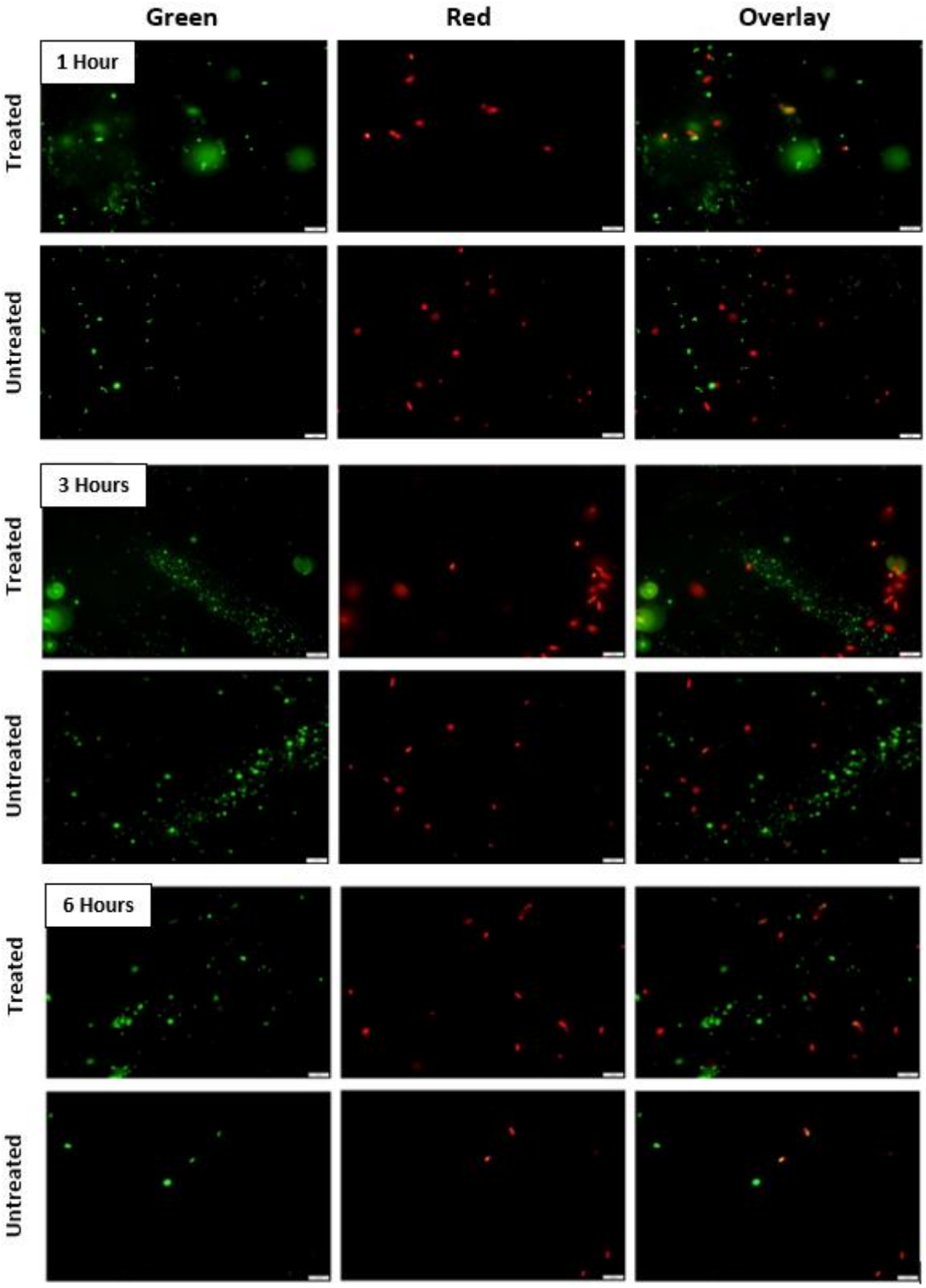
Green
Red
Overlay
1 Hour
Treated
Untreated
3 Hours
Treated
Untreated
6 Hours
Treated
Untreated

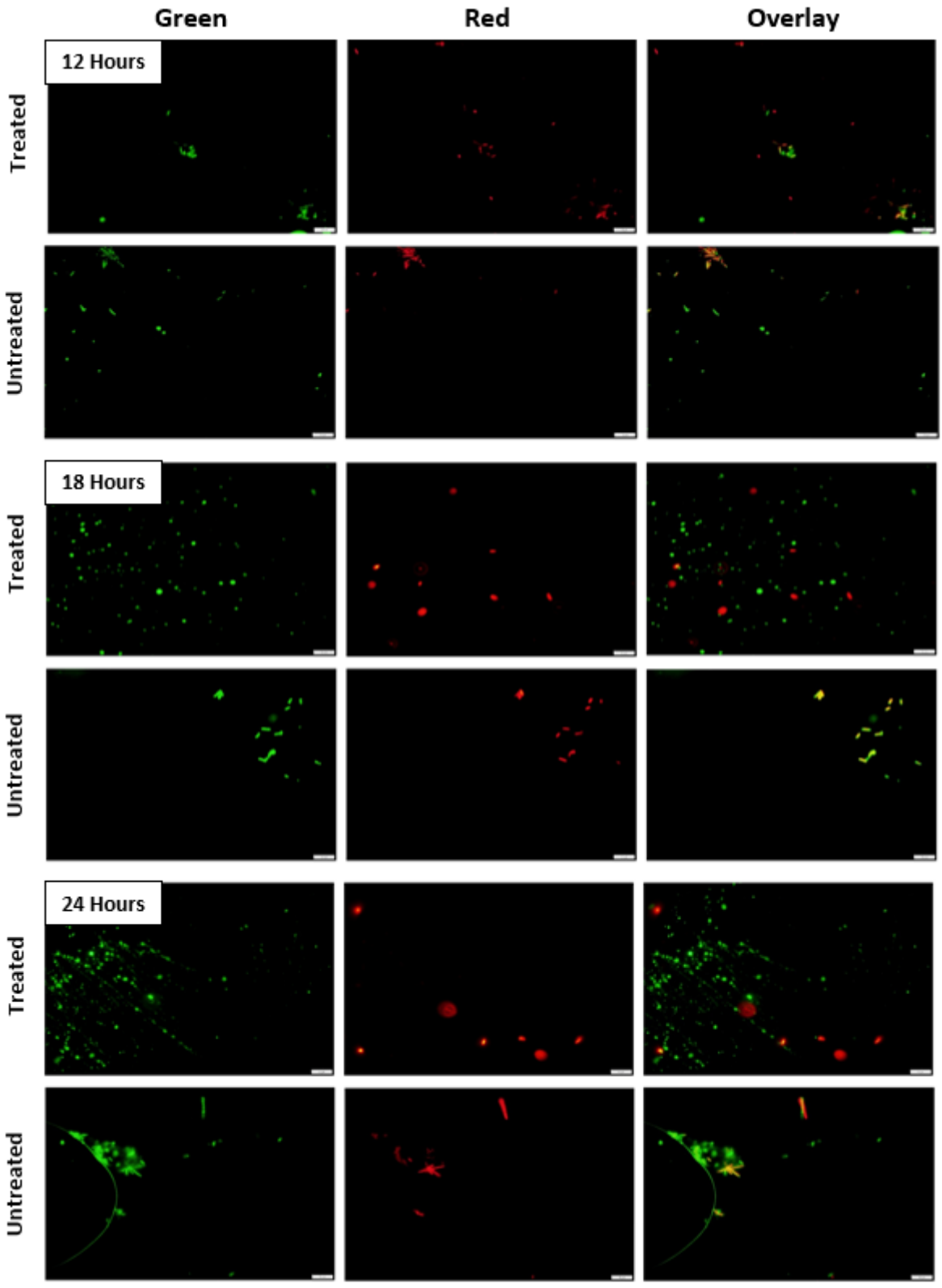

Figure 7.15 LIVE/DEAD staining of *Bl* 1951 cells after treatment with the purified *Bl* 1821L putative phage tail-like protein (48 kD) at a higher concentration. Scale bar = 10 µm

7.3.7 Bactericidal activity of crude *Bl* 1951 putative antibacterial proteins (ABPs)

Crude lysate of *Bl* 1951 harbours both encapsulating and contractile tail-sheath like structures as evidenced by TEM analysis in Chapter 2 (Figure 2.14). N-terminal sequencing and bioinformatic analysis of a purified ~30 kD band in Chapter 6 identified it as an "encapsulating protein". The molecular mass of phage tail-sheath protein in this study is unconfirmed due to the absence of N-terminal sequencing of the band from *Bl* 1951. However, in the purification of crude lysate in Chapter 5, proteins of ~48 kD and ~30 kD were visualised on SDS-PAGE (Figures 5.19A, 5.20A-B, 5.21). Furthermore, bioinformatic analysis (Chapter 6) revealed the encoding of a 48 kD phage-like element similar to PBSX protein XkdK in the *Bl* 1951 genome, identical to that in *Bl* 1821L (Figure 6.9). Based on these findings, it is likely that the 48 kD protein in *Bl* 1951 corresponds to a putative PTLP (Table 7.11).

The experimental data relating to the effect of putative antibacterial proteins of *Bl* 1951 in the crude form on cell viability and optical density (OD_{600nm}) of *Bl* 1951 and *Bl* 1821L are presented in Appendices E-11 to E-18. The mean values of the pooled data table after statistical analysis are explained below and in Appendix E-10.

Bl 1951 culture treated with crude supernatant (lysate) containing putative antibacterial proteins (encapsulating & phage tail-like proteins) of *Bl* 1951 caused an increase in the number of viable cells (17.4%) relative to the TBS control (without ABPs) after an hour of incubation from where it slowly decreased (Table 7.7 & Figure 7.15). Decrease in the number of viable cells the *Bl* 1951 treated cultures after 3, 6, and 12 hours relative to the control (without ABPs) was 16.4%, 25.5%, and 48.4% respectively. The highest decrease (48.4%) in the number of viable cells was found after 12 hours and then declined afterwards as compared to the control (without ABPs) (Table 7.7 & Figure 7.15). However, statistically the decrease (48.4%) in the number of viable cells was insignificant (Table 7.7). Treatment of crude *Bl* 1951 ABPs to the *Bl* 1821L turbid culture did not show any prominent decrease in the number of viable cells. Control treatments (without ABPs) even exhibited a decrease in the number of cells after 3, 18, and 24 hours of incubation (Table 7.7 & Figure 7.16).

The spectrophotometer reading (OD_{600nm}) decreased from the beginning (1 hour) to the end (24 hours) of incubation (Table 7.8). For *Bl* 1951, the OD_{600nm} reading after treatment with the crude ABPs decreased by 37.4% in 24 hours which was slightly lower than the control (without ABPs) having a value of 45.9% (Table 7.8). But, for *Bl* 1821L, ABPs treated cultures indicated a slightly higher value of 41.4% as compared to 39.9% for the control (without ABPs) (Table 7.8). However, OD_{600nm} reading of *Bl* 1821L and *Bl* 1951 treatments with/without crude ABPs to the turbid cultures did not display any prominent changes across the various time intervals. Variations in OD_{600nm} reading of different time intervals of the treatments fluctuated from 0.0% to 5.7% (Table 7.8 & Figure 7.17).

Table 7.7 Effect of crude *Bl* 1951 putative antibacterial proteins (ABPs) on the number of viable cells of *Bl* 1951 and *Bl* 1821L after incubation at 30°C for various time intervals. Data presents the mean values of four experiments. Values of % decrease/increase in the number of viable cells are calculated from CFUs values of corresponding time intervals

Time intervals (Hours)	*Bl* 1951	*Bl* 1951 + *Bl* 1951 crude ABPs	% Decrease/increase in no. of viable cells	*Bl* 1821l	*Bl* 1821L + *Bl* 1951 crude ABPs	% Decrease/increase in no. of viable cells	*LSD (5%)
1	8.54E+06 (6.931)**	1.00E+07 (7.001)	-17.28	2.08E+07 (7.318)	1.92E+07 (7.284)	7.51	0.853
3	4.81E+06 (6.682)	4.03E+06 (6.605)	16.36	6.58E+06 (6.818)	9.89E+06 (6.995)	-50.38	0.339
6	3.29E+06 (6.517)	2.45E+06 (6.389)	25.48	1.15E+07 (7.062)	1.03E+07 (7.013)	10.63	0.606
12	9.33E+06 (6.970)	4.81E+06 (6.682)	48.39	1.08E+07 (7.033)	9.23E+06 (6.965)	14.48	0.550
18	8.01E+06 (6.904)	9.60E+06 (6.982)	-19.81	7.03E+06 (6.847)	8.68E+06 (6.938)	-23.49	0.359
24	7.56E+06 (6.879)	5.99E+06 (6.777)	20.83	1.08E+07 (7.033)	1.27E+07 (7.1032)	-17.27	0.311

*=Least significant difference

**=The values in parenthesis indicate the converted value of number of viable cells (CFU/ml) into $\log_{10}$ CFU/ml.

Table 7.8 Effect of crude *Bl* 1951 putative antibacterial proteins (ABPs) on the OD_{600nm} reading of *Bl* 1951 and *Bl* 1821L after incubation at 30°C for various time intervals. Data presents the mean values of four experiments.

Time intervals (Hours)	*Bl* 1951	*Bl* 1951 + *Bl* 1951 crude ABPs	% Decrease/increase in OD_{600nm} reading	*Bl* 1821l	*Bl* 1821L + *Bl* 1951 crude ABPs	% Decrease/increase in OD_{600nm} reading	*LSD (5%)
1	1.81	1.79	0.90	2.83	2.68	5.35	0.817
3	1.59	1.66	-4.31	1.82	1.76	3.16	0.286
6	1.44	1.54	-7.03	1.69	1.59	5.70	0.225
12	1.46	1.38	5.31	1.40	1.36	2.78	0.380
18	1.07	1.19	-11.74	1.28	1.23	3.81	0.296
24	0.98	1.12	-14.47	1.12	1.11	1.01	0.141
% Decrease from the start (1 hour) to the end (24 hours) of incubation	45.86%	37.43%		39.58%	41.42%		

*=Least significant difference

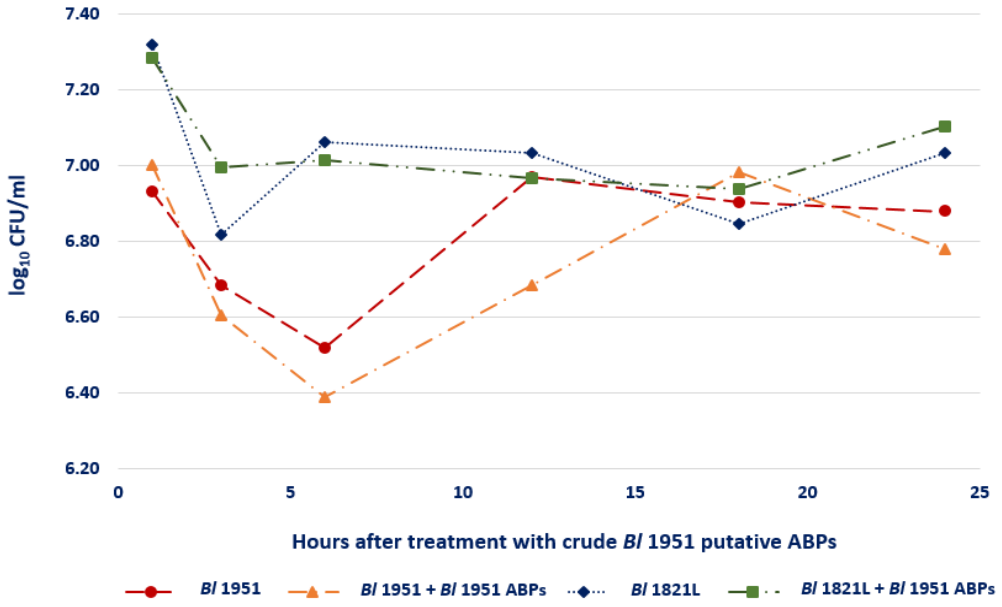

Figure 7.16 Number of viable cells (log_{10} CFU/ml) of *Bl* 1951 and *Bl* 1821L with/without treatment of crude *Bl* 1951 putative antibacterial proteins (ABPs) after incubation at 30°C for various time intervals

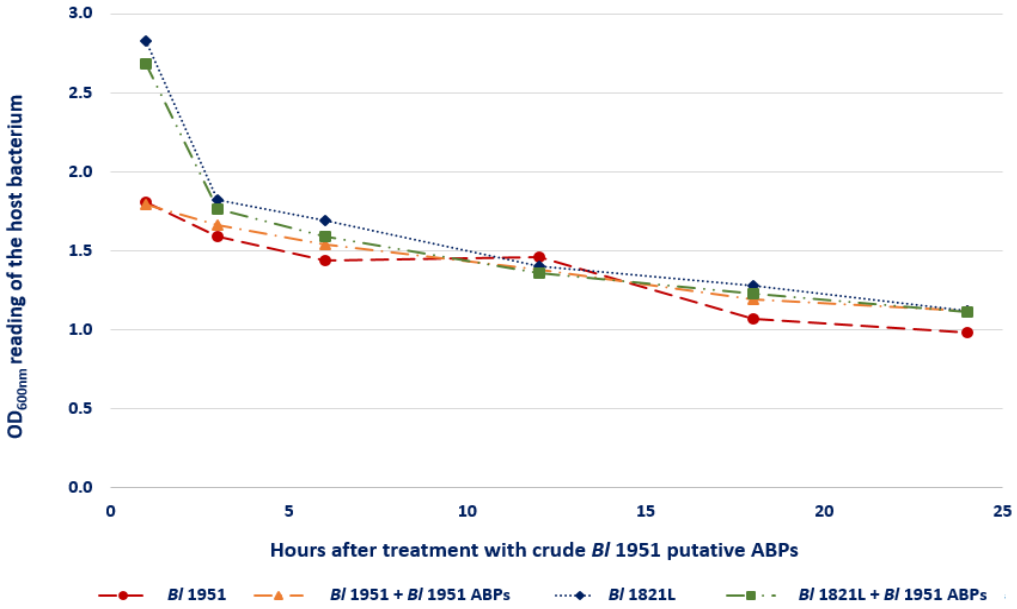

Figure 7.17 Effect of crude *Bl* 1951 putative antibacterial proteins (ABPs) on the OD_{600nm} reading of *Bl* 1951 and *Bl* 1821L after incubation at 30°C for various time intervals

7.3.8 Bactericidal activity of purified *Bl* 1951 putative encapsulating protein (30 kD)

Purified *Bl* 1951 ~30 kD EP (Figures 5.23A-B & 5.25) caused a 27.1% decrease in the number of viable cells after 3 hours of incubation with *Bl* 1951 as the host bacterium compared to the control treatment (without EP). The number of cells of *Bl* 1951 treated culture after a slight increase steadily declined to 15.3%, 20.3% and 21.6% 12, 18, and 24 HPI respectively (Table 7.9 & Figure 7.18).

For *Bl* 1821L, as shown in Figure 7.18 at the beginning (1 hour) of incubation, the difference in the number of viable cells of both the *Bl* 1951 EP treated and control cultures was not very prominent. However, after 3 hours of incubation, treated *Bl* 1821L culture showed a decline of 30.2% in the number of viable cells. Following that the number of viable cells of treated culture started to increase as compared to the control (without EP) (Table 7.9 & Figure 7.18).

All the treatments exhibited a decline in spectrophotometer reading (OD_{600nm}) from the beginning (1 hour) to the end (24 hours) of incubation. Decrease in OD_{600nm} reading of the *Bl* 1951 turbid culture after treatment with the purified *Bl* 1951 EP was 29.8%, slightly higher as compared to the TBS control (without EP) (26.1%) (Table 7.10). Likewise, for *Bl* 1821L, EP treated cultures showed a slightly higher value of 20.9% as compared to 16.2% for the control (without EP) (Table 7.10). However, the OD_{600nm} readings of *Bl* 1821L and *Bl* 1951 treatments with/without purified EP addition to the turbid cultures did not change across the various time intervals. Variations in OD_{600nm} of the treatments fluctuated from 0.0% to 7.7% across all the time intervals (Table 7.10 & Figure 7.19).

Table 7.9 Effect of purified *Bl* 1951 30 kD putative encapsulating protein (EP) on the number of viable cells of *Bl* 1951 and *Bl* 1821L after incubation at 30°C for various time intervals. Data presents the mean values of four experiments. Values of % decrease/increase in the number of viable cells are calculated from CFUs values of corresponding time intervals

Time intervals (Hours)	*Bl* 1951	*Bl* 1951 + *Bl* 1951 EP	% Decrease/increase in no. of viable cells	*Bl* 1821l	*Bl* 1821L + *Bl* 1951 EP	% Decrease/increase in no. of viable cells
1	3.05E+06 (6.484)*	4.10E+06 (6.613)	-34.43	5.30E+06 (6.724)	5.65E+06 (6.752)	-6.60
3	3.50E+06 (6.544)	2.55E+06 (6.407)	27.14	4.80E+06 (6.681)	3.35E+06 (6.525)	30.21
6	5.40E+06 (6.732)	5.50E+06 (6.740)	-1.85	4.40E+06 6.643	4.80E+06 6.681	-9.09
12	9.45E+06 (6.975)	8.00E+06 (6.903)	15.34	1.02E+07 (7.009)	1.14E+07 (7.055)	-11.27
18	1.04E+07 (7.015)	8.25E+06 (6.916)	20.29	9.80E+06 (6.991)	1.46E+07 (7.164)	-48.98
24	1.67E+07 (7.221)	1.31E+07 (7.116)	21.62	2.50E+07 (7.397)	2.57E+07 (7.409)	-2.81

*=The values in parenthesis indicate the converted value of number of viable cells (CFU/ml) into $\log_{10}$ CFU/ml.

Table 7.10 Effect of purified *Bl* 1951 30 kD putative encapsulating protein (EP) on the OD_{600nm} reading of *Bl* 1951 and *Bl* 1821L after incubation at 30°C for various time intervals. Data presents the mean value of one experiment

Time intervals (Hours)	*Bl* 1951	*Bl* 1951 + *Bl* 1951 EP	% Decrease/increase in OD_{600nm} reading	*Bl* 1821l	*Bl* 1821L + *Bl* 1951 EP	% Decrease/increase in OD_{600nm} reading
1	1.76	1.78	-1.42	1.98	1.96	0.76
3	1.68	1.68	0.00	1.92	1.95	-1.30
6	1.58	1.555	1.27	1.91	1.87	1.84
12	1.03	1.01	1.94	1.41	1.33	6.03
18	1.04	0.96	7.69	1.37	1.32	3.30
24	1.30	1.25	3.85	1.66	1.55	6.63
% Decrease from the start (1 hour) to the end (24 hours) of incubation	26.2%	29.8%		16.2%	20.9%	

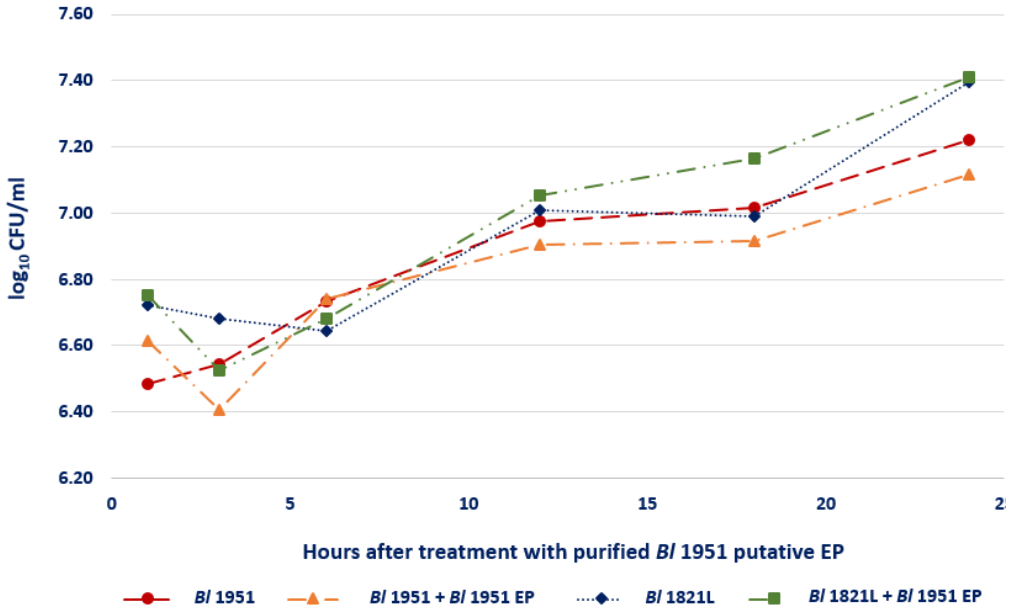

Figure 7.18 Number of viable cells (log_{10} CFU/ml) *Bl* 1951 and *Bl* 1821L with/without treatment of purified *Bl* 1951 putative encapsulating protein (30 kD) after incubation at 30°C for various time intervals

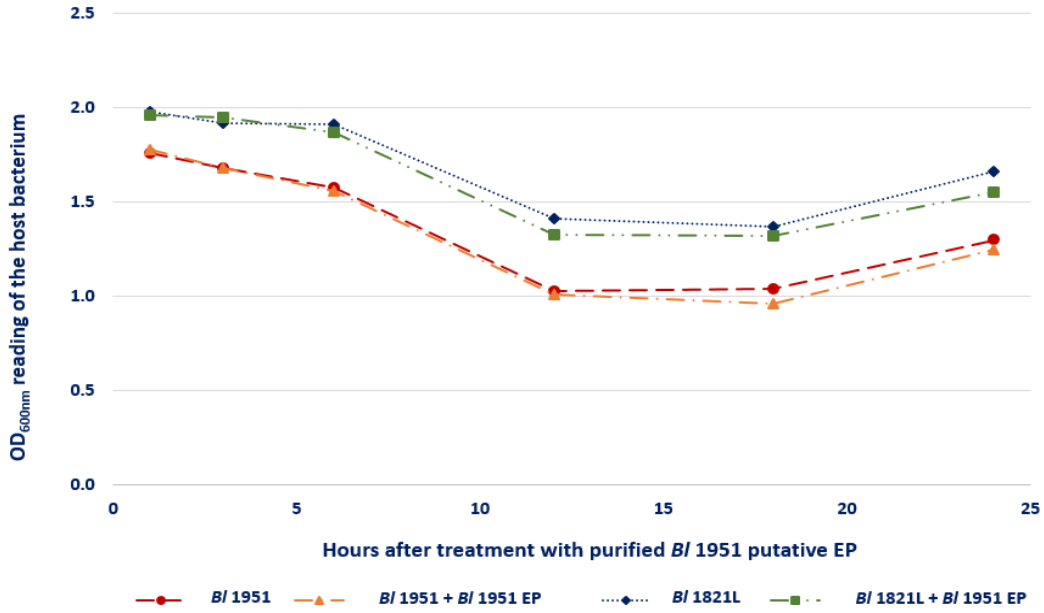

Figure 7.19 Effect of purified *Bl* 1951 putative encapsulating protein (30 kD) on the OD_{600nm} reading of *Bl* 1951 and *Bl* 1821L after incubation at 30°C for various time intervals

7.3.9 LIVE/DEAD staining of *Bl* 1951 cells after treatment with the purified *Bl* 1951 putative encapsulating protein (30 kD)

LIVE/DEAD staining of *Bl* 1951 cells after treatment with the purified ~30 kD putative encapsulating protein of *Bl* 1951 across all the time intervals showed the presence of more yellow/orange cells than red or green, except after 6 hours where a few cells with the compromised cell membranes (red) were noticed (Figure 7.20). Treatment of *Bl* 1951 cells with the purified *Bl* 1951 EP at a higher concentration showed the prevalence of more yellow/orange cells as compared to the control (without EP) across all the time intervals except after 18 hours (Figure 7.21).

7.3.10 LIVE/DEAD staining of *Bl* 1821L cells after treatment with the purified *Bl* 1951 putative encapsulating protein (30 kD)

Treatment of *Bl* 1821L cells with the purified *Bl* 1951 EP displayed yellow/orange colour cells across all the time intervals (Figure 7.22). However, the addition of ~30 kD purified *Bl* 1951 EP into the *Bl* 1821L culture at a higher concentration resulted in a few cells with the deformed membranes (red) at 1 and 12 HPI, and more yellow/orange cells were seen after 3, 6, 18, and 24 hours of treatments than in the controls (without EP) (Figure 7.23).

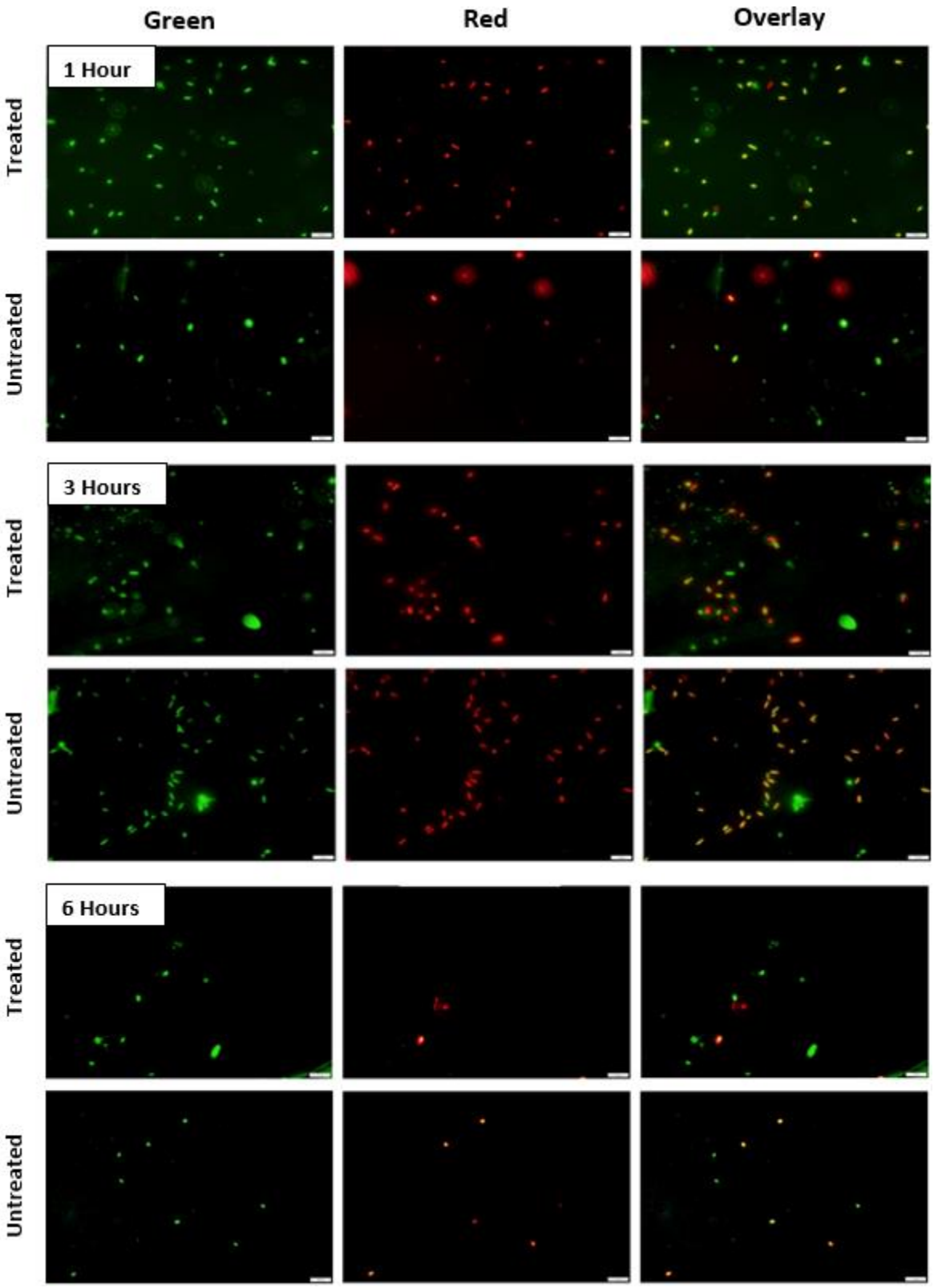
Green
Red
Overlay
1 Hour
Treated
Untreated
3 Hours
Treated
Untreated
6 Hours
Treated
Untreated

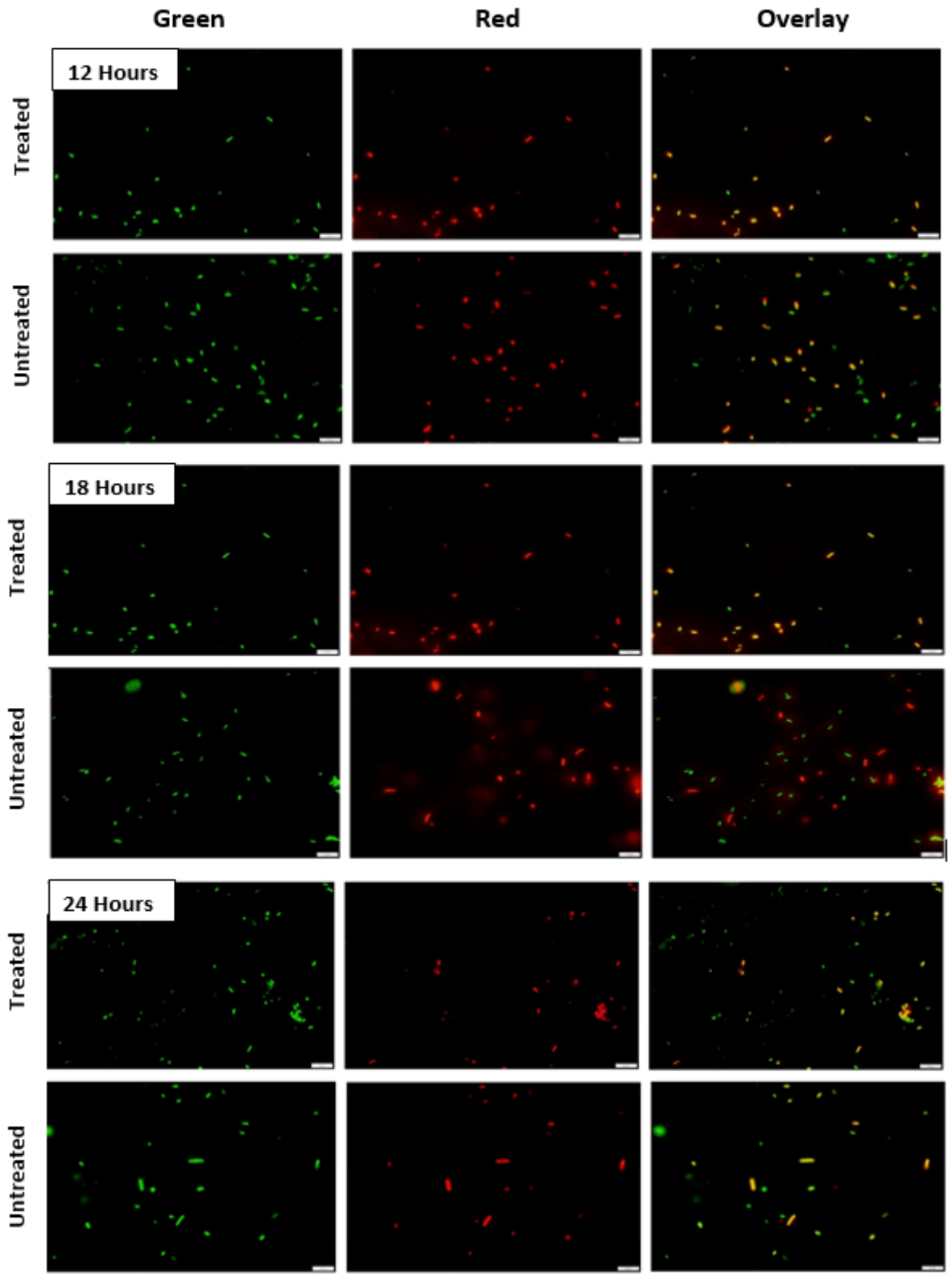

Figure 7.20 LIVE/DEAD staining of *Bl* 1951 cells after treatment with the purified *Bl* 1951 putative encapsulating protein (30 kD). Scale bar = 10 µm

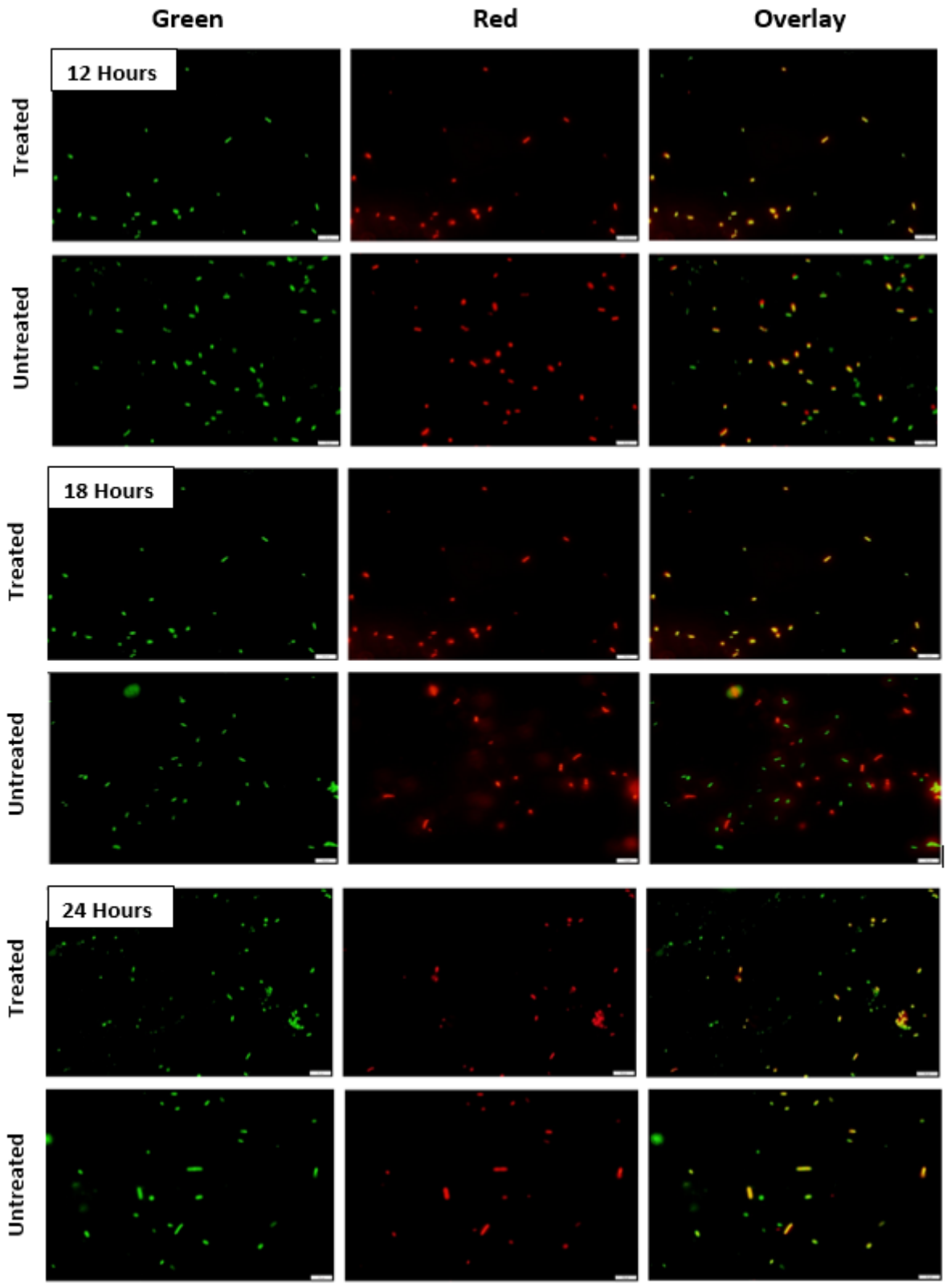

Figure 7.21 LIVE/DEAD staining of *Bl* 1951 cells after treatment with the purified *Bl* 1951 putative encapsulating protein (30 kD) at a higher concentration. Scale bar = 10 µm

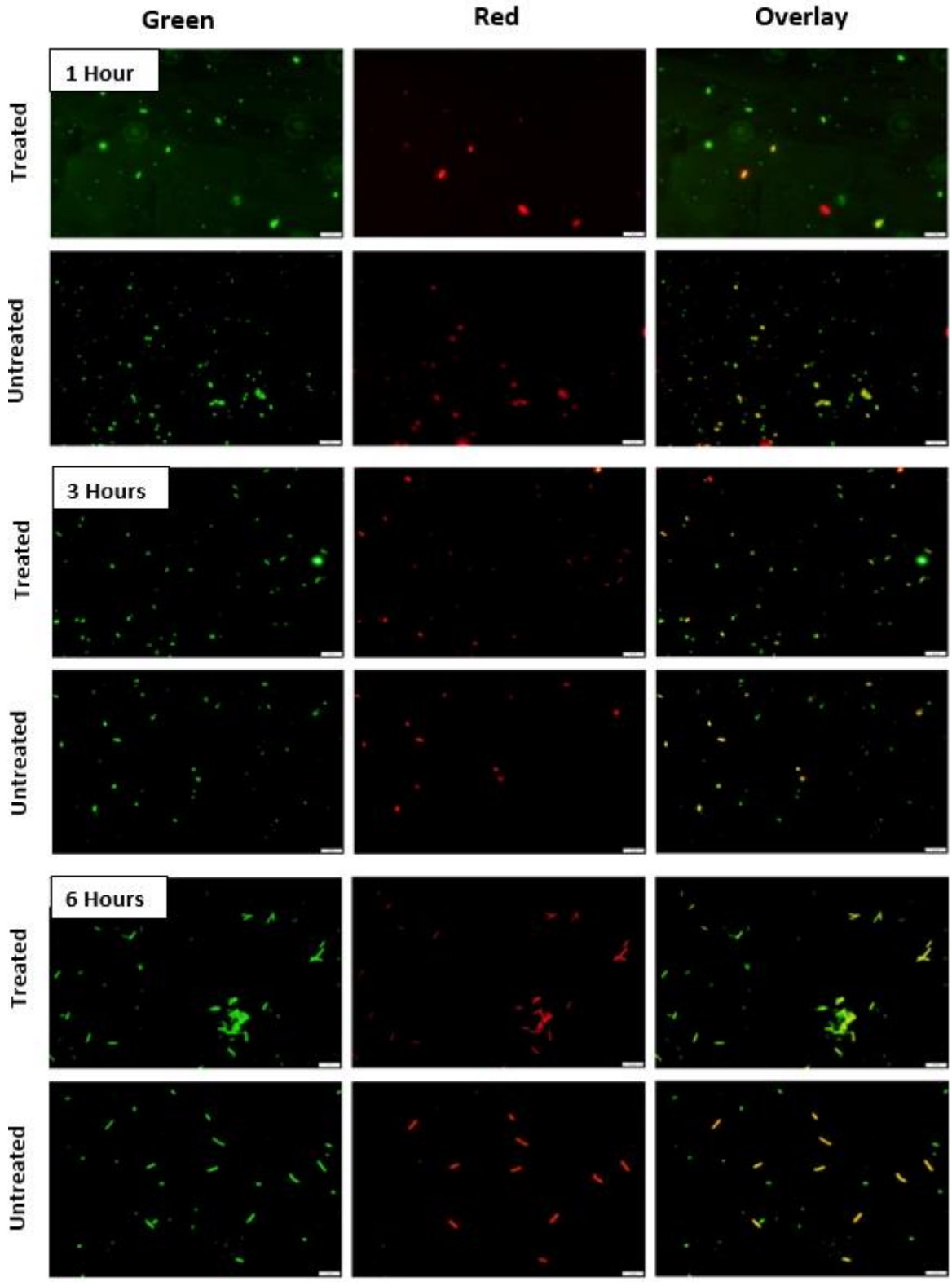
Green
Red
Overlay
1 Hour
Treated
Untreated
3 Hours
Treated
Untreated
6 Hours
Treated
Untreated

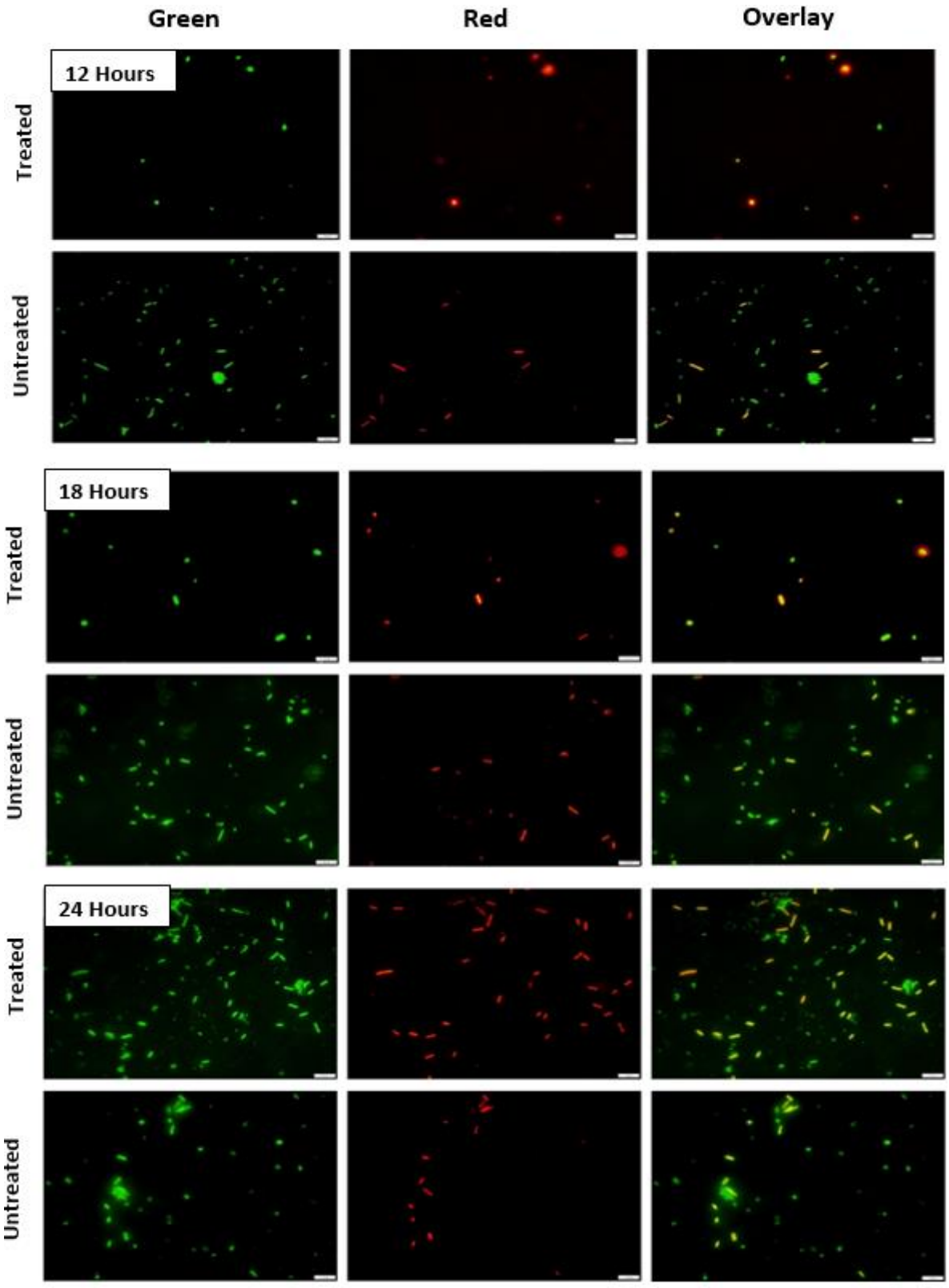

Figure 7.22 LIVE/DEAD staining of *Bl* 1821L cells after treatment with the purified *Bl* 1951 putative encapsulating protein (30 kD). Scale bar = 10 µm

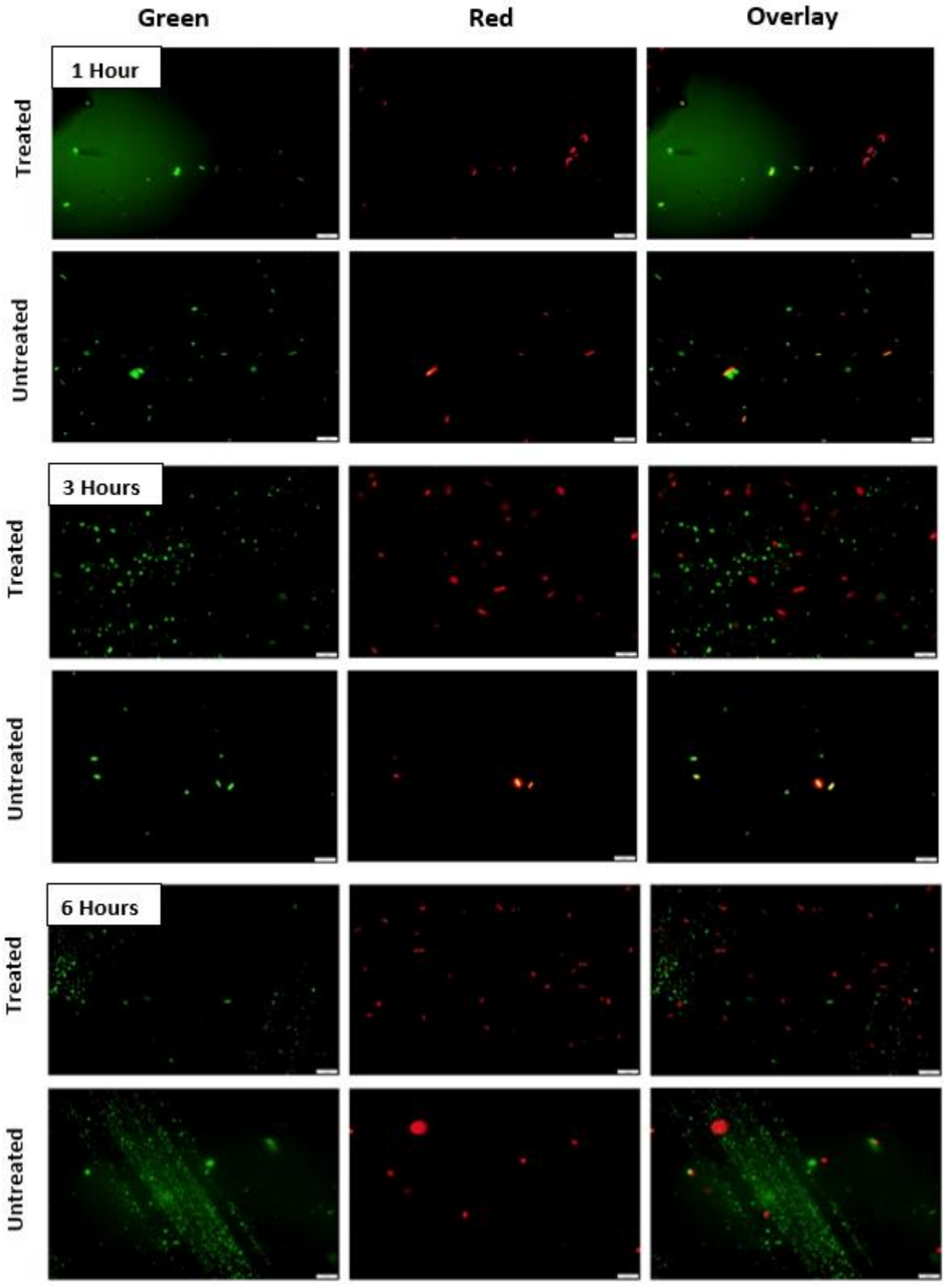
Green
Red
Overlay
1 Hour
Treated
Untreated
3 Hours
Treated
Untreated
6 Hours
Treated
Untreated

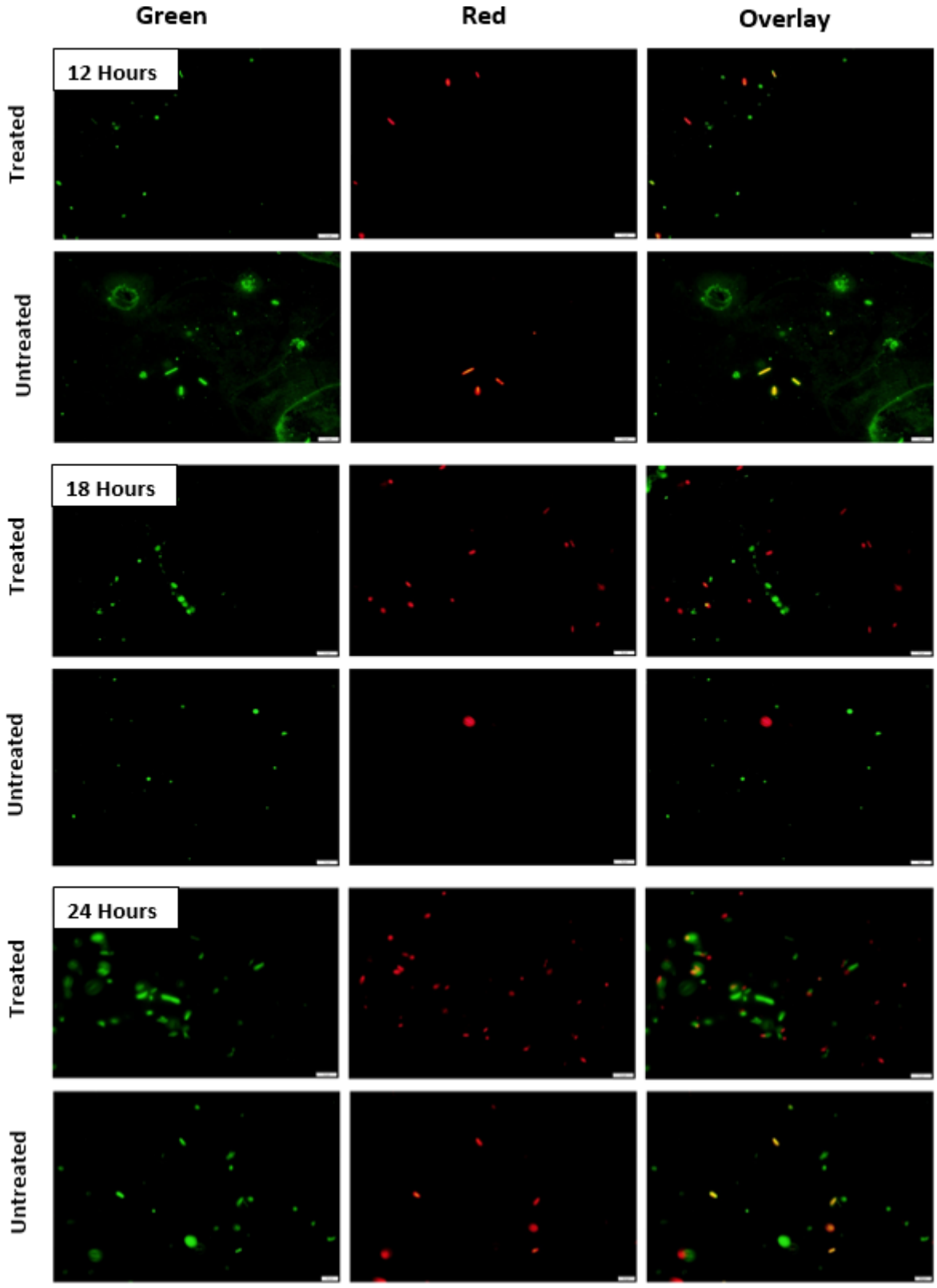

Figure 7.23 LIVE/DEAD staining of *Bl* 1821L cells after treatment with the purified *Bl* 1951 putative encapsulating protein (30 kD) at a higher concentration. Scale bar = 10 µm

In consistent antibacterial activity of the crude lysate of *Bl* 1821L and *Bl* 1951 containing putative encapsulating protein (30 kD) and phage tail-sheath protein (48 kD) was found against the producer strains only. However, purified putative encapsulating protein (~30 kD) of *Bl* 1821L and *Bl* 1951 demonstrated antagonistic action against both the strains as the host bacterium. Bactericidal activity of purified putative phage tail-sheath protein (~48 kD) of *Bl* 1821L in this study was active solely against *Bl* 1951 (Table 7.11). Overall, a summary of the activity of putative antibacterial proteins of *Bl* 1821L and *Bl* 1951 in crude and purified forms is presented in Table 7.11.

Table 7.11 Summary of bactericidal activity of putative antibacterial proteins of *Bl* 1821L and *Bl* 1951

Putative antibacterial proteins (ABPs)			**Time interval (Hours)**	**% Decrease in number of viable cells**	
Host bacterium	**Status**	**Estimated molecular wt.**		***Bl* 1821L**	***Bl* 1951**
Bl 1821L	*Crude	30 kD + 48 kD	6	30.1	-55.2
	Purified	30 kD	6	48.9	43.7
	Purified	48 kD	18	-65.7	34.2
Bl 1951	*Crude	30 kD + 48 kD**	12	14.5	48.4
	Purified	30 kD	3	30.2	27.1

*= Figures relative to the bactericidal activity of putative antibacterial proteins in crude form represent the mean values of four experiments whereas, for purified putative antibacterial (~30 kD or ~48 kD) mean values of one experiment is presented

**= Based on findings of the earlier chapters of this study as explained above

7.4 Discussion

The present study examined the killing activity of putative antibacterial proteins from *Bl* 1821L and *Bl* 1951 in both crude and purified forms. Furthermore, the results of purified proteins in the growth assay (CFUs count) were corroborated with the LIVE/DEAD staining using a BacLight^{TM} bacterial viability assay kit.

Virus structural proteins, particularly capsid and tail-sheath proteins, often demonstrate antibacterial activity against both gram-negative and gram-positive bacteria (Dias et al., 2017; Ge et al., 2020; Jin et al., 2014). In this study, the antagonistic activity of putative antibacterial proteins of *Bl* 1821L and *Bl* 1951 in both crude and purified forms was determined. Crude lysate of *Bl* 1951 and *Bl* 1821L harbours putative encapsulating (30 kD) and phage tail-sheath (48 kD) proteins (Figures 2.14 & 2.15). Antagonistic activity of *Bl* 1821L putative antibacterial proteins not only varied between the different proteins but also with the state of the proteins (crude or purified). *Bl* 1821L crude lysate caused a decrease of 30.1% in the number of viable cells of *Bl* 1821L as compared to the control (without ABPs) 6 hours after treatment, but no effect of the same lysate was noticed against *Bl* 1951. Interestingly, the bactericidal activity of purified ~30 kD and ~48 kD putative antibacterial proteins *Bl* 1821L differed markedly (Table 7.11).

Purified *Bl* 1821L putative encapsulating protein (~30 kD) displayed antibacterial activity against *Bl* 1821L and *Bl* 1951 by causing a decrease of 48.9% and 43.5% in the number of viable cells as compared to the TBS control (without EP) 6 hours after treatment. The decrease in the number of viable cells of *Bl* 1951 due to the ~30 kD putative encapsulating protein was in line with the findings of Chapter 5 where *Bl* 1821L size exclusion chromatographic (SEC) fractions demonstrated antibacterial activity against *Bl* 1951 in the disc diffusion assay test (Table 5.2). Bioinformatic analysis of the purified ~30 kD protein of *Bl* 1821L and *Bl* 1951 in Chapter 6 identified a similar gene corresponding to the putative encapsulation protein for a DyP-type peroxidase or ferritin-like protein oligomers (Figures 6.3 & 6.5). Furthermore, amino acids of identified 30 kD protein shared >97% identity to the Linocin M18 bacteriocin family of protein. Encapsulating proteins were first identified in 1994 as a high molecular-weight complex in the cell free supernatant of the bacterium *Brevibacterium linens*, displaying a bacteriostatic action against various strains of *Arthrobacter*, *Bacillus, Brevibacterium*, *Corynebacterium*, and *Listeria* (Valdés-Stauber & Scherer, 1994; Winter et al., 1995). The encapsulins were initially characterised as bacteriocins and possibly protease, but the bactericidal activity could not be established upon purification (Hicks et al., 1998; Sutter et al., 2008; Valdés-Stauber & Scherer, 1994). Since then, encapsulins have been identified in various bacteria including *Mycobacterium leprae* (Winter et al., 1995), *M. tuberculosis* (Rosenkrands et al., 1998), *Thermotoga maritima* (Hicks et al., 1998), *Streptomyces coilicolor* (Kawamoto et al., 2001), and

Quasibacillus thermotolerans (Giessen et al., 2019). Genes encoding encapsulin proteins are typically located downstream of genes for dye-dependent per-oxidase (DyP) family enzymes (Roberts et al., 2011), or encapsulin-associated ferritins (EncFtn) (He & Marles-Wright, 2015). DyP family enzymes usually demonstrate activity against polyphenolic compounds such as azo dyes and lignin breakdown products (Ahmad et al., 2010) although their physiological function and natural substrates are not known (Roberts et al., 2011). Ferritin family proteins play a decisive role in sustaining various physiological processes (Giessen & Silver, 2017) including storage of iron in a bioavailable form (Giessen et al., 2019). Iron is an integral component of various enzymes that participate in different life processes such as energy production and metabolism (Andrews et al., 2003). Iron is indispensable for metabolic functioning of the bacteria however there are exceptions including lactic acid bacteria which uses manganese and cobalt instead of iron (Bruyneel et al., 1989; Weinberg, 1997) and *Borrelia burgdoferi* which utilises manganese in place of iron (Posey & Gherardini, 2000). Importantly, iron can also present a hazard to organisms because of the Fe^{2+} triggered Fenton/Haber-Weiss reaction which produces harmful reactive oxygen species (ROS) such as superoxide (O^{2-}), hydrogen peroxide (H_2O_2), and the highly destructive hydroxyl radical (OH) (Cornelis et al., 2011). The aerobic microorganisms 'accidentally' generate ROS during respiration via incomplete reduction of O_2 and through Flavin-mediated reductive processes (Imlay, 2002). ROS are also produced deliberately during competition between organisms as a result of redox-cycling antibiotics, as generated by plants and microbes (Cornelis et al., 2011). By reacting with the oxygen these ROS may prove lethal to the cells inflicting damage to the DNA, proteins, and the membranes that surround cells (He et al., 2016b). Hence, to balance the cell's need for iron against its potential detrimental effects, organisms have evolved iron storage proteins termed "ferritins". These proteins residing in bacterial genomes are known to participate in the conversion of iron into a less reactive form that is mineralised and safely stored in the central cavity of the ferritin cage and is available for cells when they need it (Bradley et al., 2014b). Often the genomes of some bacteria like *Quasibacillus thermotolerans* encode no ferritin protein but can deposit the iron in these specialised nanocompartments to mitigate oxidative stress (Gabashvili et al., 2020; Giessen et al., 2019). McHugh et al. (2014) demonstrated that under stress conditions like amino acids starvation, encapsulins of the bacterium *Myxococcus Xanthus* releases the stored iron with the cargo proteins to lessen the oxidative stress. Based on the results of this study it might be possible that a deprivation of iron in the host cells might have weakened the defence system or the failure to detoxify iron into a less harmful form proved fatal to *Bl* 1821L and *Bl* 1951 cells. In addition, the encapsulating proteins often harbour cell penetrating peptides, which exhibit antibacterial activities (Pinto et al., 2019). Interestingly, bioinformatic analysis including AMPA and CellPPD in Chapter 6 identified the bactericidal and cell penetrating peptide motifs of putative encapsulating

protein (30 kD) of *Bl* 1821L (Figures 6.8 & 6.9) which suggested their likely involvement in the antibacterial activity. In this instance, the findings corroborate with a recent study of a peptide derived from the dengue virus capsid protein, PepR, which demonstrated rapid bactericidal activity against *Staphylococcus aureus* (Pinto et al., 2019). Other authors also deliberated that the viral protein-derived peptide (vAMP 059) and viral protein-derived cell penetrating peptides (vCPP 0769 & vCPP 2319) are all bactericidal in nature and derived from viral capsids (Dias et al., 2017; Freire et al., 2015a). Bacterial genomes often harbour genes encoding a small toxin protein of approximately 100 amino acid residues in length. This toxin may inhibit cell growth by halting essential cellular processes, including DNA replication, mRNA stability, protein synthesis, cell-wall biosynthesis, and ATP synthesis (Pandey & Gerdes, 2005; Yarmolinsky, 1995). These toxins are co-transcribed and co-translated with their cognate antitoxins from an operon called a toxin-antitoxin (TA) operon (Yamaguchi et al., 2011). Typically, the antitoxin consists of two distinct domains: a DNA-binding domain and a toxin-binding domain. The fundamental role of the antitoxin is to neutralise the lethal effect of its cognate toxin mediated by the toxin-binding domain. The toxin-binding domain of antitoxins is distinctively structured for neutralisation of the toxicity of their cognate toxins (Van Melderen & Saavedra De Bast, 2009). The structural models of several of the TA complexes reveal that the interaction between toxin and its cognate antitoxin is mediated through a combination of hydrophobic and electrostatic interactions however, the electrostatic interaction primarily defines the specificity of the antitoxin binding to the cognate toxin (Dalton & Crosson, 2010; Kamada et al., 2003). Variation in the bactericidal activity of crude lysate containing both the 30 kD putative encapsulating and 48 kD phage tail-like protein and the purified ones alone suggests that a toxin-antitoxin (TA) system is operating in the endemic strains that nullifies the effect of either 30 kD or 48 kD. Furthermore, the findings also align with the formation of persister cells on the *Bl* 1821L lawn against the activity of some of the *Bl* 1951 SEC purified fractions of this study (Chapter 5). The formation of persister cells is also attributed due to the prevalence of TA systems in bacteria (Paul et al., 2019; Ronneau & Helaine, 2019).

LIVE/DEAD staining method permits detection of cell states other than live and dead, as those unable to grow, including live injured (where membrane integrity is compromised) cells that are unable to grow on agar plates (Davis, 2014; Léonard et al., 2016; Stiefel et al., 2015). Furthermore, it allows the loss of membrane integrity to be visualised over time (Nocker et al., 2017). Detection of cell viability using the LIVE/DEAD staining (BacLight^{TM}) offers numerous advantages as compared to colony counting on agar plates. Therefore, LIVE/DEAD staining was performed in this study to look into the status of host cells after treatment with the purified putative antibacterial proteins of *Bl* 1821L (~30 kD & ~48 kD) and *Bl* 1951 (~30 kD) and to corroborate with the results of the growth assay

(CFUs count). Subsequent LIVE/DEAD staining of *Bl* 1821L cells after treatment with the purified encapsulating protein (~30 kD) displayed more *Bl* 1821L cells with compromised membranes (red) 6 to 12 hours after treatment and a more pronounced effect was noted with an increasing concentration of purified putative antibacterial protein. Interestingly, the appearance of red cells occurred at the same time as a decrease in the number of viable cells at 6 hours after treatment with the purified putative EP as compared to the control (Figure 7.7). The cells with compromised cell membranes (red) comprised a population of 58.8% as compared to 37.5% of control (without EP) (Figure 7.8). However, a decrease in the number of viable cells 12 hours after treatment contrasted with the LIVE/DEAD staining. Likewise, LIVE/DEAD staining of *Bl* 1951 cells with the purified encapsulating protein (~30 kD) showed the prevalence of red cells 3 hours after treatment and, at a higher concentration, cells with deformed membranes (red) were noted even after 1 hour of incubation. A decrease in the colony count and a concurrent increase in the number of cells with compromised cell membranes (red) in LIVE/DEAD staining assay suggests that the cell penetrating peptides residing in the putative encapsulating protein (30 kD) may be involved in the formation of pores to lyse the susceptible cells (Sanderson, 2005). Bioinformatic analysis of 30 kD putative encapsulating protein also suggested other potential killing mechanisms like the failure of encoded ferritin protein to detoxify the harmful compounds or the iron malnutrition (Chapter 6).

On the other hand, purified *Bl* 1821L putative phage tail-like protein (~48 kD) treatment decreased the number of viable cells of *Bl* 1951 by 34.2% 18 hours after treatment as compared to the control (without PTLP), but no antagonistic activity against *Bl* 1821L. This decrease in the number of viable cells of *Bl* 1951 due to bactericidal activity of purified *Bl* 1821L putative phage tail-like protein (~48 kD) aligns with previous work which showed that virus structural proteins, particularly R-type tailocins, act as specialised weapons against kin bacteria (Yao et al., 2017). Furthermore, LIVE/DEAD staining of *Bl* 1951 cells substantiated the results by showing a minor population of cells with compromised membranes (red). However, the use of a higher concentration of purified putative *Bl* 1821L PTLP resulted in more red cells even 3 to 6 hours after treatment compared to the control (without PTLP). Contractile phage tail-sheath structures reproduce the initial steps of a phage infection cycle and after specific adsorption to a phage receptor, there is a conformational change in the tail structure that punctures the cytoplasmic membrane of the host bacterium (Ge et al., 2020; Scholl, 2017). The resultant pores depolarise the membrane (Strauch et al., 2001; Uratani & Hoshino, 1984) by affecting the protein and nucleic acid synthesis in sensitive cells, which is followed by cell death (Scholl et al., 2009; Williams et al., 2008). This killing is very efficient as the attachment of only a single particle may result in cell death (Hegarty et al., 2016; Leiman & Shneider, 2012). Earlier studies reported bactericidal activity of various phage tail-like structures against susceptible strains at varying

concentrations by causing a decrease in the number of viable cells (CFU/ml) include maltocin P28 (Liu et al., 2013), enterocoliticin (Strauch et al., 2001), and xenorhabdicin (Thaler et al., 1995). A decrease in the number of viable cells and the appearance of red cells in the LIVE/DEAD staining suggests that the putative purified *Bl* 1821L PTLP of ~48 kD lysed the cell through pore formation using contractile injection system mechanism of phages (Scholl, 2017; Yao et al., 2017). A genomic, morphological, and 3D structural presentation of 48 kD putative phage tail-sheath protein is shown in Figure 6.15.

Electron micrographs of crude lysate of *Bl* 1951 in Chapter 2 (Figure 2.14) displayed both the encapsulating and contractile tail-sheath structures (proteins). Similar to *Bl* 1821L, the antibacterial activity of *Bl* 1951 in crude and purified forms differed. Crude lysate of *Bl* 1951 demonstrated a prominent activity against its host bacterium *i.e. Bl* 1951 by causing a decrease of 48.4% in the number of viable cells as compared to the control (without ABPs). However, this decrease in the number of viable cells was statistically insignificant due to the heterogeneity in the data of all four experiments. Interestingly, an analysis of the data of all the four experiments uncovered a decrease in the number of viable cells 12 hours after treatment by 23.1%, 64.7%, 44.1%, and 29.1% respectively (Appendices E-11 to E-14). Furthermore, the analysis also showed the decline in the number of viable cells 3 hours after treatment for the 3rd and 4th replicated experiment (Appendix E-13 & E-14) and for 6 hours after treatment in the 2nd and 4th replicated experiment of the study (Appendix E-12 & E-14). These findings are in agreement with previous work where researchers encountered variations and inconsistencies in plate counts within and between different experiments while using the spread-plating technique (Thomas et al., 2012) despite taking into consideration the likely causes of inequality in CFUs such as the presence of clumps (Bettencourt et al., 2010), errors while preparing and dispensing dilutions, or the improper drying of plates (Corry et al., 2007; Hedges, 2002).

Purified putative encapsulating protein (~30 kD) of *Bl* 1951 caused a reduction of 30.2% and 27.1% in the number of viable cells of *Bl* 1821L and *Bl* 1951 as compared to the control (without EP). LIVE/DEAD staining of *Bl* 1821L and *Bl* 1951 cells after 3 hours of incubation with the ~30 kD purified putative encapsulating protein indicated the population of yellow/orange cells, while with an increasing concentration of putative encapsulating protein, more cells with compromised membranes (red) were seen. The yellow/orange cells cropped up after LIVE/DEAD staining of host cells with/without the purified putative encapsulating protein of *Bl* 1821L and *Bl* 1951 in the overlay images. The cause might be insufficient replacement of SYTO 9 with PI and the retention of both the dyes within the cells at the same time (Kirchhoff & Cypionka, 2017; Lu et al., 2014). Typically, cells with compromised membranes (red) are considered to be dead or approaching death (Oliver, 2010; Robertson et al., 2019). However, some authors also include yellow/orange coloured cells in the category of dead (Leuko et al., 2004; Lu et al., 2014; Stiefel et al., 2015). Hu et al. (2017) also observed yellow cells while using LIVE/DEAD stain

(BacLight™) with glutaraldehyde fixation for the measurement of bacterial abundance and viability in rainwater. Bioinformatic analysis of the 30 kD purified putative encapsulating protein of *Bl* 1951 in Chapter 6 substantiated that the corresponding gene is the same as identified for *Bl* 1821L. Furthermore, the turbidimetric assay and LIVE/DEAD staining results also suggest that the 30 kD protein of *Bl* 1951 is likely to act similarly to the 30 kD putative encapsulating protein of *Bl* 1821L.

7.5 Outcomes

The major findings of this chapter include:

1. Crude putative antibacterial proteins of *Bl* 1821L and *Bl* 1951 displayed prominent activity against the producer strains by causing a decrease of 30.1% and 48.4% in the number of viable cells without any prominent alteration in the optical density (OD_{600nm}) after 6 and 12 hours.
2. Bactericidal activity of purified ~30 kD and ~48 kD putative antibacterial proteins of *Bl* 1821L differed from each other.

   I). *Bl* 1821L encapsulating protein (~30 kD) exhibited antibacterial activity by causing a decrease of *Bl* 1821L (48.9%) and *Bl* 1951 (43.5%) in the number of viable cells after 6 hours without any prominent alteration in the optical density (OD_{600nm}). In this instance, the cell penetrating peptides (CPPs) of encapsulating protein (~30 kD) are likely to be involved in the pore formation and consequently killing mechanism. Furthermore, the role of iron malnutrition or failure to detoxify iron by Ferritin protein can't be ruled out.

   II). Purified *Bl* 1821L putative phage tail-like protein (~48 kD) demonstrated its bactericidal activity by causing a decline of 34.2% in the number of viable cells without any prominent alteration in the optical density (OD_{600nm}) of *Bl* 1951 after 18 hours. Pore formation of *Bl* 1951 cells is likely due to the activity of the contractile injection system of putative phage tail-like protein and consequently killing mechanism.
3. Variation in the bactericidal activity of crude lysate and purified putative antibacterial proteins suggest that a toxin-antitoxin system is operating to neutralise the effect of either 30 kD putative encapsulating or 48 kD phage tail-like protein in the crude form.
4. Purified *Bl* 1951 putative encapsulating protein (~30 kD) displayed bactericidal activity through the cell penetrating peptides like *Bl* 1821L by causing a reduction of 27.1% and 30.2% in the number of viable cells of *Bl* 1951 and *Bl* 1821L respectively without any prominent alteration in the optical density (OD_{600nm}) after 3 hours.

7.6 Conclusion

The results shed light on the bactericidal activity and mode of action of the ~30 kD putative encapsulating protein of *Bl* 1821L and *Bl* 1951 and ~48 kD phage tail-like protein of *Bl* 1821L. A decrease in the number of viable cells can affect the insecticidal potential of this useful entomopathogenic bacterium.

Chapter 8

General Discussion

Discovery of phage tail-like structures (bacteriocins) in New Zealand *Brevibacillus laterosporus* isolates *Bl* 1821L and *Bl* 1951

A decade ago, an entomopathogenic, gram-positive, spore-forming bacterium, *Brevibacillus laterosporus* (Laubach) was discovered in New Zealand. Two isolates *Bl* 1951 and *Bl* 1821L were found in surface-sterilised brassica seeds (van Zijll de Jong et al., 2016) and the third one (*Bl* Rsp) was recovered from a potato plant (Bienkowski, 2012). While commonly found around the world, this was the first New Zealand description of this useful bacterium. Based on genome comparisons of different strains New Zealand *B. laterosporus* strains were found to be genetically distinct compared to the rest of the world (Glare et al., 2020) and were highly pathogenic to diamondback moth larvae (Ormskirk, 2017; van Zijll de Jong et al., 2016). Therefore, efforts were geared to harness the biocontrol potential of the endemic strains *Bl* 1821L, *Bl* 1951, and *Bl* Rsp. Unfortunately, a loss of virulence against the diamondback moth was observed during the research and TEM analysis of sporulating cultures of *Bl* 1821L revealed the presence of tailless virus-like structures (Tectivirus) (Ormskirk, 2017). The scholar hypothesised the involvement of *Tectiviridae* phages in the stymied growth and loss of virulence of *Bl* 1821L (Ormskirk, 2017). Based on these observations the current research project aimed to isolate and characterise the suspected bacteriophage (Tectivirus-like structures), cure the bacteria of the invading phage particles, compare the virulence of phage cured and uncured strains against the diamondback moth, and enable the stable repeatable culture of *Bl.*

Initial work involving classical phage isolation and enumeration assays (plaque and serial dilutions) and electron microscopic examination could not substantiate the presence of putative phage particles, despite bioinformatic prediction indicating the presence of intact phages in *Bl* 1821L, *Bl* 1951, and *Bl* Rsp genomes (Chapter 2). However, the following efforts enabled the isolation, and preliminary identification of putative phage tail-like structures (bacteriocins) not only under an electron microscope but also through partial purification, subsequent SDS-PAGE analysis, and through N-terminal sequencing (Chapter 3). The findings raised several questions, such as how these phage tail-like structures are produced; whether they are involved in the disruption of growth, and most importantly how do they interfere with the insecticidal potential of this useful bacterium? Once the high molecular-weight (HMW) bacteriocins (antibacterial agents) were analysed, further questions emerged, such as is there any evolutionary relationship of these phage tail-like structures with the bacteriophages?

Bacteriophages (or phages for short), due to their ubiquity and numerical abundance, play a vital role in bacterial population dynamics (Bordenstein et al., 2006; Dion et al., 2020). Although all phages can propagate horizontally between cells, temperate phages also propagate vertically in bacterial (lysogenic) lineages, typically by integrating into the bacterial chromosome as prophages (Casjens, 2003; Howard-Varona et al., 2017). Interestingly, the vast majority of the prophages residing in the bacterial genomes are cryptic (defective) and in a state of mutational decay (Casjens, 2003; Srividhya et al., 2007). Sequence analysis defined numerous ways in which prophages shape the genome of their host bacteria (Brüssow & Hendrix, 2002; Owen et al., 2020). The mutation rate of viruses is much higher than that of cellular organisms (Duffy et al., 2008; Sanjuán et al., 2010). Growing evidence suggests most of the resident defective prophages have mutated and are unable to excise from the host chromosome, cannot lyse host cells, or produce infectious phage particles (Bobay et al., 2014; Ramisetty & Sudhakari, 2019). Defective prophages do not confer immunity to superinfection, meaning they are incapable of preventing lytic attack by related viruses (Campbell, 1996). They may offer integration sites for incoming phages and other genetic elements (Lawrence, 2004; Lichens-Park et al., 1990). Numerous molecular systems presumably derived from defective prophages including gene transfer agents (GTAs) that transfer random pieces of chromosomal DNA to other cells (Lang et al., 2012), phage-derived bacteriocins (Patz et al., 2019; Scholl, 2017), and Type 6 secretion systems (T6SSs) (Howard & Filloux, 2019; Leiman et al., 2009) that are involved in bacterial antagonistic associations often reside in the bacterial genomes (Figure 8.1). Phage-derived elements, like GTAs or T6SSs, are streamlined and genetically very stable (Bobay et al., 2014). However, genomes contain some phage-derived elements that are less able to be assigned to the aforementioned categories and likely perform other functions with varying degrees of efficiency (Nobrega et al., 2018): they parasite other phages, kill other bacteria, or transfer host DNA (Campbell, 1977).

The failure to isolate and identify the putative phage particles (Chapter 2) led to the assessment of Mitomycin C induced cultures, assay tests of PEG 8000 precipitated cultures, TEM examination, N-terminal sequencing of a prominent protein (~48 kD) on SDS-PAGE of *Bl* 1821L, and the discovery of phage tail-like structures (bacteriocins). Based on this finding, an alteration in the originally proposed research project was required. Hence, the subsequent research efforts were directed to find out whether the newly discovered putative phage tail-like particles (bacteriocins) have any role in the stymied growth of endemic strains that thwarts the exploitation of the insecticidal potential of this beneficial bacterium.

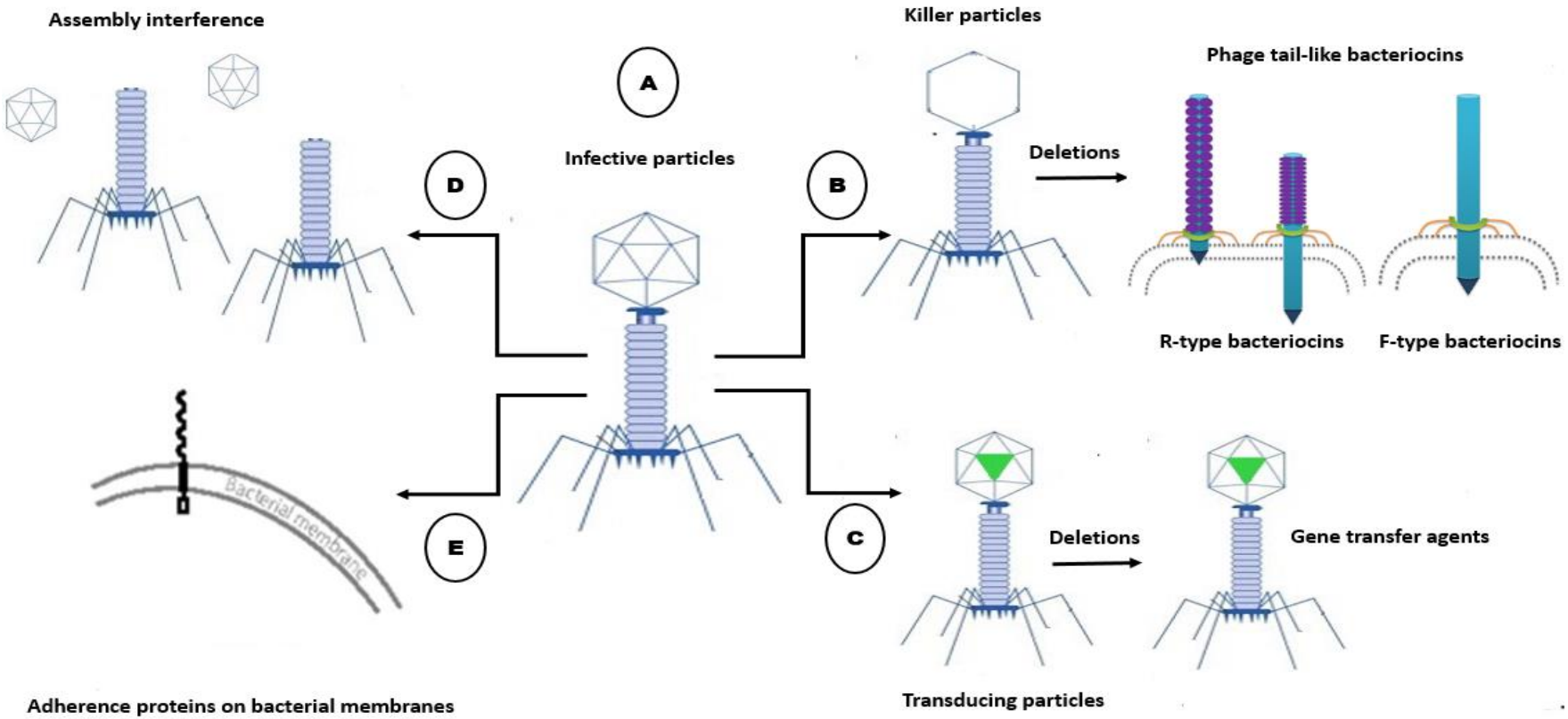

Figure 8.1 Putative functions of orthologous prophages conserved in their hosts (Bobay et al., 2014). (A). Functional prophages can be used as molecular weapons to kill non-lysogens through the production of infective particles. (B) Defective prophages can produce non-infective particles (Phage killer particles & R/F-type bacteriocins) that kill sensitive cells. (C) Prophages can form transducing particles and gene transfer agents (GTAs) that promote host DNA exchange (shown in green colour). (D) Degraded prophages might interfere with the assembly of other phages leading to the formation of defective particles. (E) Prophage structural proteins often display Immunoglobulin (Ig)-like domains that might be used by their hosts for adherence in niche colonisation

Is there any detrimental effect of putative antibacterial proteins (bacteriocins) on the growth of host bacterium?

Often the antibacterial structures (phages and PTLBs) are induced under some conditions without the aid of an external trigger. This phenomenon is termed "spontaneous prophage induction" (SPI) (Nanda et al., 2015) and occurs due to spontaneous accumulation of DNA damage initiating the host's SOS response during cell replication (Cox et al., 2000; McCool et al., 2004; Pennington & Rosenberg, 2007). SPI, plays a critical role in the population biology of temperate phages in mixtures of susceptible cells and lysogens (Nanda et al., 2015). While studying the production kinetics of putative antibacterial structures of *Bl* 1821L under natural growth conditions it was found that the identified ~48 kD phage tail-like protein (bacteriocin) (Chapter 3) was also spontaneously induced as shown in assay tests and SDS-PAGE analysis (Chapter 4). SPI of putative phage tail-like protein (bacteriocin) of *Bl* 1821L insignificantly affected the number of viable cells after 18 hours of growth (Chapter 4). Although putative phage tail-like structures were examined under TEM of Mitomycin C induced lysate of *Bl* 1951 (Chapter 2), due to absence of N-terminal sequencing at that time its nature was not defined. Based on the electron micrographs (Chapter 2) where hexagonal or phage head-like and phage contractile-sheath like structures were observed and the assays of PEG 8000 precipitated culture (Chapter 3), putative antibacterial activity was perceived to be due to the phage tail-like proteins (bacteriocins). Through SDS-PAGE analysis of *Bl* 1951 during the growth phases a prominent ~30 kD band was observed from the early 12 hours to the late 144 hours of post inoculation, and even persisted afterwards, but at a low intensity (Chapter 4). This corresponded to the spontaneous production of putative antibacterial proteins (bacteriocins) of *Bl* 1951 and significantly affected the number of viable cells after 18 hours of growth and this decrease in viable cells corresponded to the highest antagonistic activity of supernatants against *Bl* 1821L and *Bl* 1951 as determined through the disc assay tests (Chapter 4). Assessments of pH of *Bl* 1951 CFS extracted after 18 hours, in terms of the number of viable cells and the diameter of zones of inhibition (mm), were statistically significant. Typically, pH values of the bacterial cultures after inoculation gradually decrease within several hours likely due to the rapid growth rate of the bacteria (Lee et al., 2001). The gradual increase in pH of *Bl* 1951 and *Bl* 1821L up to 60 hours of growth aligned with the exponential growth and afterwards was followed by a slight fall (stationary phase) where pH values remained almost static (Chapter 4). Based on the literature, this is the first report of the spontaneous induction of putative antibacterial structures having detrimental effects on the growth of the insect pathogenic strains *Bl* 1821L and *Bl* 1951.

Antibacterial spectrum of putative phage tail-like proteins (bacteriocins): broad or narrow?

While assessing the host range of PEG 8000 precipitated cultures of *Bl* 1821L and *Bl* 1951 against different gram-positive bacteria, it was found that all the *Bl* strains were susceptible to their toxic effects, except *Bl* CCEB 342. The strain *Bl* CCEB 342 was susceptible to the putative antibacterial proteins (bacteriocins) of *Bl* 1951 but insensitive to those of *Bl* 1821L. Of the other assessed gram-positive bacteria, the strain *Carnobacterium maltaromaticum* 3-1 was slightly sensitive to the PEG 8000 precipitated culture of *Bl* 1821L harbouring the putative phage tail-like bacteriocins and insensitive to that of *Bl* 1951 (Chapter 3). Hence, in this context the putative antibacterial protein (PTLB) of *Bl* 1821L is considered to be broad-spectrum.

The host range (antibacterial spectrum) is the breadth of bacteria (species or strains) that a bacteriophage or phage tail-like bacteriocin can kill (Hyman & Abedon, 2010). Therefore, the interaction between phages or phage tail-like particles and their bacterial hosts is crucial to understand how they influence their biology (Dowah & Clokie, 2018). Antibacterial structures (phages and PTLBs) typically exhibit a narrow host range (Boeckaerts et al., 2021). Numerous host-specific factors including defence mechanisms such as CRISPR-Cas (Barrangou et al., 2007) and restriction-modification systems (Gormley et al., 2001), presence of phage receptors (Smith et al., 2007), abiotic factors (Fister et al., 2016), and features encoded by the phage receptor-binding proteins (RBPs) (Yosef et al., 2017) influence the host range. Both the antibacterial structures (phages and PTLBs) employ the same primary determinant of specificity, *i.e*., one and more RBPs for binding to the cell surface of the sensitive host bacterium (Holtzman et al., 2020). This initial recognition subsequently leads to infection of the bacterium by phages or the depolarisation of its membrane by PTLBs (Ge et al., 2020; Simpson et al., 2016). There are several examples in the past where the host range of antibacterial structures (phages and PTLBs) has been expanded due to modifications in the tail fibre proteins (Dams et al., 2019; Williams et al., 2008). Holtzman et al. (2020) recently deliberated how a continuous evolutionary mechanism causes contraction in the host range of bacteriophage T7. The authors showed that T7 phage grown in the presence of five restrictive strains and one permissive host, each with a different lipopolysaccharides (LPS) form, gradually avoided recognition of the restrictive strains. Interestingly, avoidance of the restrictive strains was repeated in different experiments using six different permissive hosts. The evolved phages carried mutations that changed their specificity as determined by RBPs genome sequences. This system demonstrated a major role of RBPs in contracting the range of futile infections (Holtzman et al., 2020).

An exceptional example of the role of the receptor-binding proteins of phage-derived bacteriocins in determining the antimicrobial spectrum is found in the gram-negative bacterium *Pseudomonas chlororaphis* 30-84 (Dorosky et al., 2017). Contractile phage tail-like structures (R-type pyocins)

typically encode one tail fibre protein. However, genomic analysis of *P. chlororaphis* 30-84 found the presence of three tail fibre-resembling genes in the tailocin 2 genetic modules that caused a differential antimicrobial spectrum (Dorosky et al., 2018).

Electron micrographs of the crude lysate of *Bl* 1821L and *Bl* 1951 in this study displayed numerous hexagonal or phage head-like (encapsulating) and phage tail-sheath like structures (Chapter 2). Furthermore, the soft agar overlay assay involving PEG 8000 precipitation of the Mitomycin C induced cultures of *Bl* 1821L and *Bl* 1951 affirmed the activity of putative antibacterial proteins (bacteriocins) instead of intact phages (Chapter 3). N-terminal sequencing of prominent protein (~48 kD) on SDS-PAGE revealed the presence of putative phage tail-sheath protein (Chapter 3). However, due to the absence of N-terminal sequencing of putative antibacterial proteins for *Bl* 1951 at that stage their nature was not defined (Chapter 3). Based on TEM analysis (Chapter 2) and the following assay tests (Chapter 3), it is likely that the susceptibility of strain *Bl* CCEB 342 to *Bl* 1951 and insensitivity to *Bl* 1821L precipitated lysates suggested a form of host specificity which might be due to the differential RBPs of harboured PTLBs in each of the strains. The specificity of putative antibacterial structures (phages and PTLBs) against different bacteria suggested that similar RBPs are likely involved. For instance, the marine bacterium *Prochlorococcus*, accounting for half of the photosynthetic biomass harbours cyanophages that infect *Prochlorococcus* (Lindell et al., 2004). Most of these phages are host-strain-specific while others cross-infect with the closely related marine bacterium, *Synechococcus*, suggesting a mechanism for horizontal gene transfer (Figure 8.2) (Zeidner et al., 2005). Interestingly, high-light adapted *Prochlorococcus* hosts yielded *Podoviridae* phages exclusively, which were extremely host-specific, whereas low-light adapted *Prochlorococcus* and all strains of *Synechococcus* yielded primarily *Myoviridae* phages, which have a broad host range (Sullivan et al., 2003). As explained above there is a possibility that the identified bactericidal contractile sheath PBSX-like structures of *Bl* 1821L might have evolved after losing some of the structural components like carotovoricins due to mutations (Nguyen et al., 1999). Likewise, bacteriophages are always undergoing the process of evolution due to the exchange of genetic material among the microbial community in natural environments. In a recent article, Moura de Sousa et al. (2021) elaborated on the occurrence of genetic transfer between distantly related phages. An interesting example of gene flux between distantly related phages is the homologous recombination between virulent phages (935 & c2) and prophage (P335) in *Lactococcus lactis* (Figure 8.2) (Bouchard & Moineau, 2000; Labrie & Moineau, 2007). Moura de Sousa et al. (2021) suggested genetic transfer between temperate phages with different host genera through virulent phages along with the above cited examples (Figure 8.2).

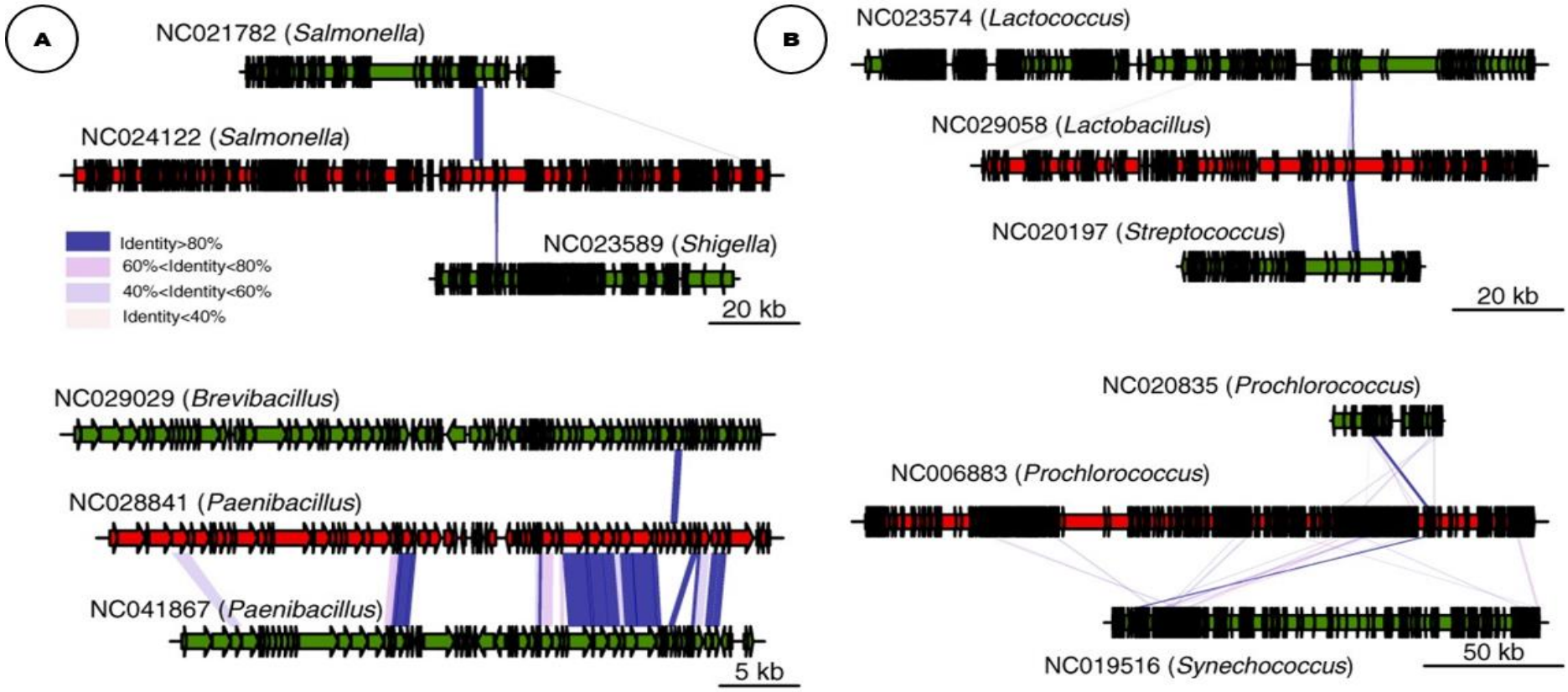

Figure 8.2 Genetic transfers between temperate phages with different host genera through virulent phages (Moura de Sousa et al., 2021). (A) Examples of virulent phages (red) with genes transferred from/to two temperate phages (green) infecting distinct bacterial genera. (B) Analogous to (A) but representing transfers with the virulent phage that involve the exact same protein in both temperate phages. Colours in the blocks linking the phages indicate the level of sequence similarity between homologs

Do the putative phage tail-like structures have any role in the interbacterial competition?

The antibacterial spectrum of putative phage-tail like structures (bacteriocins) of *Bl* 1821L and *Bl* 1951 against the kin *Bl s*trains (1821L, 1951, Rsp, CCEB 342, NRS 590, NCIMB) (Chapter 3) is striking from the interbacterial point of view. As explained earlier, putative antibacterial proteins (PTLBs) of *Bl* 1821L exhibited broad-spectrum activity as compared to those of *Bl* 1951. In the context of interbacterial competition, it is interesting that the putative antibacterial proteins (bacteriocins) from both strains (*Bl* 1821L & *Bl* 1951) exhibited prominent antagonistic activity against the kin strains except for *Bl* CCEB 342 which showed some form of host specificity. Importantly, all the other evaluated gram-positive bacteria were insensitive to their toxic effects, except for *C. maltaromaticum* 3-1. The strain *Bl* CCEB 342 was not susceptible to the putative bacteriocins of *Bl* 1821L but was sensitive to the *Bl* 1951 bacteriocins. Similarly, the strain *C. maltaromaticum* 3-1 was slightly sensitive to the putative bacteriocins of *Bl* 1821L and insensitive to those from *Bl* 1951. These findings may define the role of putative antibacterial proteins such as phage tail-like bacteriocins in the interbacterial competition of the endemic strains (*Bl* 1821L & *Bl* 1951) and provide an insight into complex relationships within bacterial communities.

Bacteria seldom exist in isolation and generally reside within diverse microbial communities (Klein et al., 2020). A fundamental requirement for survival in these complex environments is to gain access to scarce resources *i.e.* nutrients and space, by competing with the other inhabitants. The bacteria are not only in competition with distantly related microorganisms but also with the phylogenetically related kin bacteria who are likely the contenders for the same ecological niche (Hibbing et al., 2010; Klein et al., 2020). Therefore, competition with the kin bacteria requires highly specific mechanisms to outcompete them but not to kill individuals from the same clonal population (strains having identical genomes). Hence, the arsenal employed against kin needs to be highly specialised with a narrow spectrum of activity (Brown et al., 2009; Foster & Bell, 2012). To combat the competitors, bacteria have evolved a diverse array of weapons (Granato et al., 2019) including mechanisms for chemical warfare via toxins (e.g. T6SSs), complex mechanical weapons that punch holes (e.g. tailocins), and the use of viruses (phages) in biological warfare (Brown et al., 2009). However, deployment of these weapons is considered costly as a cell has to sacrifice for the survival of others (Catalão et al., 2013). Numerous species employ multiple types of weapons and occasionally multiple variants of each type (Granato et al., 2019). An example is a gram-negative bacterium, *Pseudomonas aeruginosa*, where a single cell has the option to produce a vast arsenal including many different types of diffusing protein toxins (including S-type pyocins) (Michel-Briand & Baysse, 2002), multiple types of poisoned molecular speargun (T6SSs) (Russell et al., 2014), poisonous proteinaceous sticks (contact-dependent growth inhibition system) (Mercy et al., 2016), two different mechanical weapons that punch holes in

other cells (R-type & F-type pyocins) (Ghequire & De Mot, 2014), and viruses (phages) that kill non-clone mates (Davies et al., 2016).

Vacheron et al. (2021) proposed a model where certain R-tailocins are targeted and efficient weapons in microscale interbacterial competitions between kin bacteria (Figure 8.3). The authors suggested that R-tailocins may be induced either, spontaneously or by external stressors (such as Mitomycin C), including interference competition signals (Ghoul & Mitri, 2016; Gonzalez & Mavridou, 2019) or competitor toxins (Granato & Foster, 2020). After induction, R-tailocins are synthesised at the center of the cell and migrate to the cell poles. Once R-tailocins have migrated, produced cells undergo lysis in a two-step process, firstly by forming spheroblasts and secondly through complete lysis of the cells. Following explosive cell lysis, the contractile phage tail-like particles are released into the extracellular environment where they have to face the competing bacteria. Generally, R-tailocins specifically bind and kill kin bacteria that are ecological niche competitors while more distantly related strains are exempted. This kin-exclusion strategy allows the reduction of kin bacteria and may favour the flux of new genes from the phylogenetically more distant bacteria within the community. However, clonal cells are not disturbed by the R-tailocins in the environment as bacteria seem to be immune to their own R-tailocins. A similar mechanism is likely to be involved for *Bl* 1821L and *Bl* 1951 phage tail-like structures (bacteriocins) as both demonstrated antagonistic activities against the evaluated kin strains except that *Bl* 1821L could not inhibit the *Bl* CCEB 342 strain (Chapter 3). Furthermore, BAGEL4 analysis of *Bl* 1821L and *Bl* 1951 predicted other antimicrobial peptides including the two core peptides laterosporulin (Singh et al., 2012) and UviB (Anderson et al., 2005) (Chapter 3). Although functional analysis of the predicted core peptides of *Bl* 1821L and *Bl* 1951 was beyond the scope of this research project. However, it is likely that the simultaneous existence of phage tail-like bacteriocins and the core peptides (laterosporulin and UviB) in the natural environment might have implications for the survival of the bacterium due to the aforementioned kin exclusion strategy.

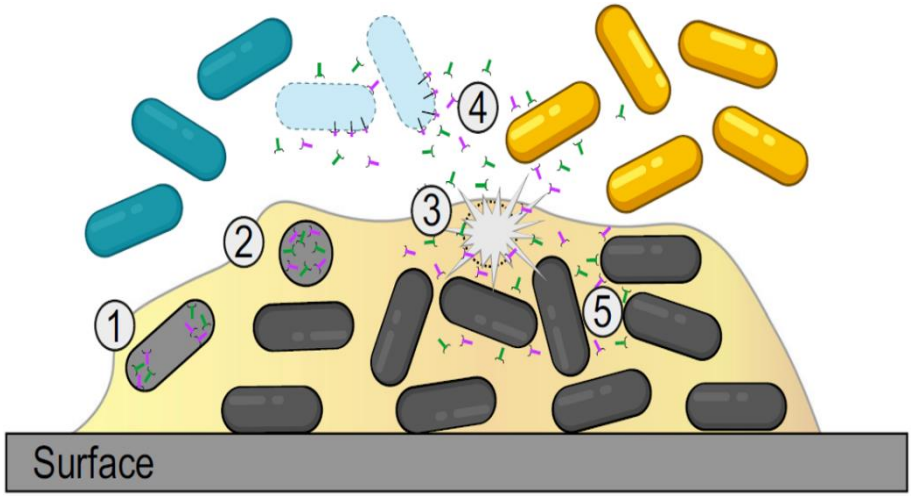

Figure 8.3 Model of the ecological role of R-tailocins in interbacterial competitiveness (Vacheron et al., 2021). (1) Some cells are induced upon environmental stress and synthesise R-tailocins that are produced at the center of the cell and migrate to the cell poles. (2) Subsequently to the migration of the R-tailocins, the cell lyses, firstly by forming a spheroblast. (3) Secondly, the cell lyses completely and explosively, thereby thrusting its R-tailocins into the environment. (4) Once in the medium, R-tailocins specifically bind to kin bacteria and kill them whereas more distantly related bacteria are spared. (5) Clonal cells are immune and are therefore protected from the R-tailocins released in the environment

Is the autocidal activity of the endemic strains *Bl* 1821L and *Bl* 1951 an altruistic suicide or social killing?

Bacteria produce "chemical weapons" (bacteriocins) to protect themselves from competitors in the ecological niche (Ghequire & De Mot, 2015; Riley & Wertz, 2002b). These proteinaceous weapons are inherently designed to inhibit growth, to kill a broad array of microbial species, or just closely related strains of the same species, and the producer strains are immune to their toxic effects (Heng et al., 2007; Kjos et al., 2011). However, some members of a genetically identical population can kill (autocidal) their siblings (González-Pastor et al., 2003; Popp & Mascher, 2019). An example is a bacteriocin, hyicin 3682, which exhibited its antagonistic activity against the producer strain, *Staphylococcus hyicus* (Fagundes et al., 2011).

A test for assessing and differentiating the inhibitory activities of putative antibacterials (phages and bacteriocins) is PEG 8000 precipitation followed by soft agar overlay (Hockett & Baltrus, 2017). In the current study, the role of phage tail-like bacteriocins in the putative antibacterial activity was affirmed (Chapter 3) but any autocidal activity was not substantiated, possibly due to the usage of lower volumes of the supernatants (Zou et al., 2018b). However, the disc diffusion assay tests (Bauer, 1966; Hudzicki, 2009) of Mitomycin C induced supernatants of *Bl* 1821L and *Bl* 1951 prominently showed

autocidal activity (Chapter 4). While purifying the putative antibacterial proteins using various methods, different size exclusion chromatographic fractions and sucrose density gradients in the assay tests also demonstrated the autocidal activity (Chapter 5). Importantly in this study, purified putative encapsulating protein (30 kD) of *Bl* 1951 and *Bl* 1821L exhibited an autocidal activity in the liquid assays by causing a decrease of 27.1% and 48.9% in the number of viable cells after 3 and 6 hours of growth respectively (Chapter 7). Through recombinant expression, this activity was extenuated by the co-expression of the 25 kD hypothetical protein. Late in the project, adjacent genes encoding both the 30 kD putative encapsulating and the 25 kD hypothetical proteins were shown to have activity through recombinant expression. The fact that the 25 kD hypothetical protein was involved in the antagonistic activity was not known for the majority of the study, but given the co-migration on the proteins (due to size similarity) and the use of semi-pure supernatant in most assays, this protein was likely contributing to the activity attributed to the 30 kD protein.

Is there any biological significance of autocidal activity?

What could be the biological relevance of producing such autocidal toxins and how do bacteria control their toxic activity to avoid eradicating themselves? The best-understood examples of antimicrobial compounds that act against the producing organism itself are so-called toxin-antitoxin (TA) systems. Initially, TA systems were identified on plasmids (Engelberg-Kulka & Glaser, 1999) but subsequently were also found on bacterial chromosomes and were regarded as responsible for bacterial programmed cell death (PCD) in the context of population traits (Popp & Mascher, 2019). The genes encoding the toxin and the antitoxin are normally encoded in an operon and constantly expressed under normal growth conditions. While the toxin is a stable gene product, the antitoxin is not. There is no harm to the cell as long as a constant expression of the operon ensures resupply of the antitoxin, the cells survive. However, as soon as the expression of the operon or translation of its mRNA terminates, for example, in response to stress conditions, the difference in protein stability causes an increasing imbalance between the stable toxin and the fading antitoxin, ultimately unleashing the lethal activity of the toxin, resulting in PCD (Popp & Mascher, 2019).

The crude lysate of *Bl* 1821L and *Bl* 1951 harbouring the putative antibacterial proteins of 30 kD (encapsulating) and 48 kD (phage contractile-sheath) in the growth assays (CFUs) prominently exhibited the autocidal activity by causing a decrease of 30.1% and 48.4% respectively in the number of viable cells and a minor effect on vice versa analysis (Chapter 7). As explained above the putative antibacterial proteins (bacteriocins) are active against the competitors or the kin strains but the producer strains are immune to their lethal effects (Riley & Wertz, 2002b). In the light of these findings

(Chapter 7), a toxin-antitoxin (TA) system is likely functioning to mask the effect of either 30 kD or 48 kD putative antibacterial protein in *Bl* 1821L and *Bl* 1951.

Based on the bioinformatic analysis (Chapter 6) and the findings of the liquid assay (Chapter 7), the autocidal activity of 30 kD putative encapsulating protein of *Bl* 1821L and *Bl* 1951 might be due to the activation of stress triggered transcriptional regulator family proteins (PadR & MarR) and YtxJ protein under some stresses such as iron malnutrition. The gram-positive bacterium *Bacillus subtilis* (*Bs*) is an example which demonstrates the self-killing tendency under nutritional stress (Höfler et al., 2016). Importantly, *Bs* cells at the onset of sporulation secrete extracellular killing factors and lyse the sibling non-sporulating cells that have not developed immunity to these toxins. Furthermore, the resultant lysis also releases nutrients from the dead cells into the starved medium that the surviving sporulating cells can feed on therefore this behaviour was called “cannibalism” (González-Pastor et al., 2003). The cannibalistic phenomenon has some biological significance for the bacterial populations as the *Bs* population could be at risk if most of the members engage in sporulation at once (González-Pastor, 2011; Höfler et al., 2016). Spore formation consumes plenty of energy and time to be completed, and it is reversible only up to a certain point (Parker et al., 1996). For instance, sporulating cells and spores could not resume growth as efficiently as vegetative cells or even resting cells if nutrients were available again in the medium. In natural environments, other microorganisms, many of them non-sporulating, surround *Bs* communities and *Bs* cells committed to sporulate or spores could be at disadvantage relative to them. Here, cannibalism helps to sustain a mixed population during the stationary phase with a small percentage of spores and a high percentage of growing cells for a longer period of time, which might be beneficial to the community (González-Pastor, 2011).

Is 25 kD hypothetical or 30 kD putative encapsulating protein involved in the antibacterial activity?

N-terminal sequence of purified ~30 kD putative antibacterial protein of *Bl* 1821L and *Bl* 1951 identified several matches to the homologous 25 kD hypothetical and 30 kD putative encapsulating protein in each strain, a likely result of their potential co migration on SDS-PAGE (Chapter 6). Identified 30 kD putative encapsulating protein of *Bl* 1821L and *Bl* 1951 shared >97% amino acid similarity to the Linocin M18 bacteriocin family of protein (Chapter 6) (McHugh et al., 2014; Valdes-Stauber & Scherer, 1996) which are termed “encapsulins” due to the formation of nanocompartments within the bacterium that contains ferritin-like compounds or peroxidase enzymes (Kerfeld et al., 2010; Yeates et al., 2011). Furthermore, electron micrograph of the 30 kD purified protein displayed hexagonal or phage capsids-like structures (encapsulating) alluding that the 30 kD assembles as a hexagonal composite (Chapter 5). The gene encoding the second identified 25 kD hypothetical protein of

unknown function was located at the 3' end of the gene encoding the 30 kD putative encapsulating protein (Chapter 6). BLASTp analysis of 25 kD hypothetical protein showed 90.7% amino acid similarity to an uncharacterised protein of *Bl* LMG 15441, 57.8% to the putative encapsulating protein of *Brevibacillus centrosporus*, and uncharacterised proteins of different *Bl* strains (Chapter 6, Appendix D-6).

The role of genes encoding the 25 kD hypothetical and 30 kD putative encapsulating proteins in the antagonistic activity was affirmed by expressing the corresponding genes individually (pHT01-*hypo*, 25 kD), (pHT01-*encap*, 30 kD), and the both pHT01-*hypo*.*encap* (25 kD & 30 kD) in a gram-positive positive bacterium *Bs* WB800N (Chapter 6). Notably, in the disc assay tests each expressed hypothetical (pHT01-*hypo*, 25 kD), encapsulating (pHT01-*encap*, 30 kD), and the pHT01-*hypo*.*encap* encoding both the proteins (25 kD & 30 kD) expressed their antagonistic activity (Chapter 6). Interestingly, 25 kD expressed hypothetical protein (pHT01-*hypo*) was more potent in activity as compared to 30 kD putative encapsulating protein (pHT01-*encap*). Encapsulin, a novel class of prokaryotic nanocompartments resembling viral capsid-like structures has been implicated in the antibacterial activities (McHugh et al., 2014; Valdes-Stauber & Scherer, 1996). Linocin M18, an encapsulating protein of 31 kD molecular mass, derived from the cell free supernatant of *Brevibacterium linens* M18 inhibited the growth of *Listeria* spp., several coryneform, and other gram-positive bacteria but no activity against gram-negative bacteria was reported (Valdés-Stauber & Scherer, 1994).

The purified putative encapsulating protein (30 kD) of *Bl* 1821L in this study caused a decline of 48.9% and 43.5% in the number of viable cells of *Bl* 1821L and *Bl* 1951 after 6 hours of treatment in the liquid assay. Furthermore, LIVE/DEAD staining of *Bl* 1821L cells treated with the 30 kD purified putative encapsulating protein also substantiated the findings by showing 58.8% red cells (dead) as compared to the untreated (37.5%) ones (Chapter 7). Likewise, the purified 30 kD purified encapsulating protein of *Bl* 1951 reduced the number of viable cells of *Bl* 1821L (27.1%) and *Bl* 1951 (30.2%) after 3 hours of treatment (Chapter 7). Ferritin-like or peroxidase enzymes of the encapsulating proteins are involved in performing multifarious cellular functions including the storage of iron (Kerfeld et al., 2010; Yeates et al., 2011). Iron is an essential nutrient for almost all microbes for sustaining their metabolic activities (Moreira et al., 2020). Although iron is essential, excess free iron is potentially toxic for the cells because it catalyses the production of reactive oxygen radicals by a Fenton reaction, leading to oxidative damage. Thus, a balanced quantity is needed for their survival (Harrison & Arosio, 1996). However, to store the excessive iron, microorganisms have evolved two types of proteins, ferritins (Ftn) and bacterioferritins (Bfr) which are distinguishable by the presence of heme in the latter (Cornelis et al., 2011). The primary function of Ftn and Bfr is to store iron during iron adequacy and

supply it to the cell for various functions (Cornelis et al., 2011; Smith, 2004). *Mycobacterium tuberculosis*, a pathogenic bacterium harbours two putative iron storage proteins namely, BfrA (Rv1876) a bacterioferritin, and BfrB (Rv3841) a ferritin-like protein. The expression of both *bfrA* and *bfrB* is regulated by the binding of iron-activated *ideR* (iron-dependent regulator) to the tandem operator sites present at the 5' end of the iron storage gene (Cole et al., 1998). Reddy et al. (2012) generated mutants *bfrA* (Rv1876) and *bfrB* (Rv3841) lacking the functional genes. Interestingly, the authors found that the mutant bacterium under iron-deficient conditions not only showed a significant decrease in growth but was vulnerable to oxidative stress (Reddy et al., 2012). In this context, it is possible that the identified 30 kD putative encapsulating proteins of *Bl* 1821L and *Bl* 1951 might be undergoing an iron deficiency, or the ferritin proteins failed to detoxify the excessive iron which contributed towards the stymied growth of both the strains. Furthermore, the bioinformatic analysis of 30 kD putative encapsulating protein of *Bl* 1821L also identified the motifs relevant to the bactericidal activity and the potency of the amino acids to penetrate the cells (Chapter 6).

Based on this, different killing mechanisms of putative 30 kD encapsulating proteins of *Bl* 1821L and *Bl* 1951 are proposed. These include the activation of stress relevant transcriptional regulator family proteins (PadR & MarR) or YtxJ protein under some stresses (such as malnutrition of iron), failure of ferritin protein to detoxify iron, and cell penetrating peptides activity.

Is there any evolutionary mechanism responsible for multiple functioning of the putative phage tail-like structures?

Bioinformatic analysis of the ~48 kD putative phage tail-sheath protein identified a similarity to the PBSX protein XkdK (Chapter 6) and further, the region around the encoding gene for the ~48 kD protein was similar to the genomic architecture of the defective prophage PBSX in *Bs* 168 (Bradley, 1967b; Wood et al., 1990). Despite sharing a low protein similarity with the different *Bacillus* defective prophages, the regions perform a similar function (bactericidal). The bactericidal role of contractile-sheath tail-like structures (R-type pyocins) has been demonstrated in gram-negative bacteria (Michel-Briand & Baysse, 2002) and the diffocins from a gram-positive bacterium (*Clostrioides difficile* 630) is the only exception so far (Gebhart et al., 2012; Schwemmlein et al., 2018).

The genes of tailed phages from the gram-negative bacteria underwent an evolutionary shift to become fundamental components of bacterial nanomachines such as secretion systems or pyocins (Veesler & Cambillau, 2011). Based on these bacterial systems, phage contractile-sheath tails in terms of morphology, size, and even function are the Type 6 secretion systems (T6SSs) (Bönemann et al., 2010), the R-type and F-type pyocins (Michel-Briand & Baysse, 2002), antifeeding prophage (Afp) particles from *Serratia entomophila* (Hurst et al., 2004), and the virulence cluster from *Photorhabdus*

luminescens (PVC) (Yang et al., 2006). Interestingly, all these elements, despite architectural (genome) similarities, perform varied functions: R-type and F-type pyocins are involved in antibacterial activity against closely related bacteria through pore formation (Scholl, 2017), whereas T6SS has a dual role: it attacks not only bacterial cells (Hood et al., 2010)but can also induce morphological changes in the cytoskeleton of eukaryotic cells (Ma & Mekalanos, 2010). Afp/PVC were initially grouped with R-type pyocins due to their genetic homology however, functional studies disclosed their toxicity against insects (Yang et al., 2016). The bacterium harbouring these phage tail-like structures maintains the basic organisation of the corresponding contractile tail consisting of the main tube, the outer sheath, and the baseplate all of which are plasmid encoded (Heymann et al., 2013). Furthermore, the T6SSs, R-type, and F-type pyocins share an ancestral origin with T4, P2, and λ phages respectively (Sarris et al., 2014; Scholl, 2017). Carotovoricins, phage tail-like high molecular-weight bacteriocins resembling the *Myoviridae* phages, are produced by the gram-negative bacterium, *Erwinia carotovora* (Nguyen et al., 1999). Subsequent nucleotide sequence analysis and genomic organisation revealed that it was likely that the carotovoricins evolved from the same ancestor as *Salmonella typhi* prophage by losing head, lysogeny, and DNA replication genes (Yamada et al., 2006).

Antibacterial structures resembling contractile-tailed phages of the *Myoviridae* family (R-type pyocins) (Gebhart et al., 2012) and non-contractile tailed phages of the *Siphoviridae* family (F-type pyocins) (Saha et al., 2021) are found in gram-positive bacteria. However, most of the prophage families may not fit well with the description of R-type or F-type bacteriocins but could correspond to phage killer particles. Interestingly, these elements behave like bacteriocins but are very diverse genetically, displaying features ranging from streamlined phage tail-like bacteriocins (PTLBs) to nearly complete phages (Campbell, 1977; Michel-Briand & Baysse, 2002). Defective phages can easily give rise to phage killer particles (Bobay et al., 2014). Therefore, for the defective prophages the term “phage killer particles or protophages” was coined to include PBSX and other non-infectious defective phage particles acting as de facto bacteriocins (Bradley, 1967b; Wood et al., 1990). PBSX of *Bs* 168, one of the most widely studied defective phage is considered a model organism (Jin et al., 2014). This phage is induced by the SOS response and results in cell lysis (Brito et al., 2018). Induction is suicidal for both the phage and bacterial cell (Krogh et al., 1996). In this stance, Mitomycin C at a concentration of 1 µg/ml (*Bl* 1821L) and 3 µg/ml (*Bl* 1951) induced the putative antibacterial structures by causing a decrease of 49.7% and 83.9% in the optical density (OD_{600nm}) of cultures and the following TEM analysis showed the empty hexagonal or phage head like (encapsulating) and contractile phage tail-sheath like structures (Chapter 2). Disc assay tests of the Mitomycin C induced cultures of *Bl* 1821L and *Bl* 1951 showed prominent autocidal activity besides the vice versa (Chapter 3). Importantly, the non-induced (without Mitomycin C) cultures of *Bl* 1821L and *Bl* 1951 also displayed a similar pattern (Chapter 3)

but at a lower rate (Chapter 4) which is an indication of spontaneous induction of putative antibacterial structures (Nanda et al., 2015) (Chapter 4).

The identification of the *Bl* 1821L bactericidal phage-like element PBSX protein XkdK (contractile tail-sheath) is the first report of this type of protein in the genus *Brevibacillus* and an addition among the gram-positive bacteria as these structures have been defined before only in the genus *Bacillus* and in *Clostrioides difficile* 630 (R-type pyocins) (Gebhart et al., 2012; Schwemmlein et al., 2018). Nevertheless, there is a paucity of knowledge regarding the evolution of these bactericidal structures in gram-positive bacteria. However, the evolutionary mechanism might have caused the switching of the bactericidal structures from the gram-negative to the gram-positive bacteria to perform a similar role.

Future outlook

1. N-terminal sequencing of ~30 kD purified putative antibacterial protein of *Bl* 1821L and *Bl* 1951 identified homologous 25 kD hypothetical and 30 kD putative encapsulating proteins. Antibacterial activity of 25 kD expressed hypothetical protein (pHT01-*hypo*) was more pronounced as compared to the 30 kD putative encapsulating protein (pHT01-*encap*). Therefore, an extensive study involving the 25 kD hypothetical protein of *Bl* 1821L and *Bl* 1951 in the future will be needed.
2. Bactericidal activity of ~30 kD putative encapsulating protein is proposed to be due to the activation of transcriptional regulator family proteins (PadR & MarR) and YtxJ protein under some unknown stresses like iron deficiency or failure of the ferritin protein to detoxify the excessive iron or antibacterial activity of the cell penetrating peptides. Extensive research to decipher the plausible role of each factor may provide an insight into the killing mechanism of the 30 kD putative encapsulating protein of *Bl* 1821L and *Bl* 1951.
3. The identified ~48 kD phage-like element PBSX protein XkdK of *Bl* 1821L could not be successfully expressed in the gram-positive bacterium *Bs* WB800N. Therefore, to affirm the role of 48 kD putative phage tail-sheath protein in bacterial lysis optimisation of the expression system needs to be undertaken. The lysis system of phages and the orthologous structures is mostly dependent upon the activity of two important proteins *i.e.* endolysin and holin. It will be useful to determine the role of lysis relevant proteins in the activity of the *Bl* 1821L PBSX-like region for future studies.
4. Variation in the antibacterial spectrum of crude lysates of *Bl* 1821L and *Bl* 1951 suggests the need for a thorough investigation into the tail fibre proteins of both the strains. Furthermore, the differences in the bactericidal activity of crude lysate (containing the 30 kD putative encapsulating protein and 48 kD phage tail-liker protein) and the purified ones suggests a toxin-antitoxin system may be involved in neutralising the effect of either 30 kD or 48 kD putative antibacterial protein which needs to be further studied. Future research will help to define the basis of the persister cell formation in the population of the *Bl* 1821L strain.
5. Assessing the expression of the 25 kD hypothetical, ~30 kD putative encapsulating, and ~48 kD phage tail-sheath proteins through culture growth by qPCR analysis to further augment the role of relevant genes in the bactericidal activity will be required in the future.

Conclusion

The present study isolated, purified, and characterised the putative antibacterial proteins of the insect pathogenic strains *Bl* 1821 and *Bl* 1951. Different plausible mechanism of bactericidal action of two putative antibacterial proteins of ~30 kD (encapsulating) and ~48 kD (phage contractile-tail sheath) in *Bl* 1821L and one putative encapsulating protein (~30 kD) of *Bl* 1951 were defined. The identified ~30 kD and ~48 kD putative antibacterial proteins are proposed to be involved in cell lysis by depolarisation of the bacterial cell membranes which results in the stymied growth of endemic strains. A 25 kD hypothetical protein with more potent bactericidal activity was also identified in *Bl* 1821L and *Bl* 1951 but it needs further investigation. To counter the detrimental effects of these bactericidal proteins it is proposed to utilise fresh bacterial cultures as the old cultures are more vulnerable to autocidal activity. The supplementation of iron in the cultivating media may lessen the cell lysis due to malnutrition of iron. The population of *Bl* 1821L cells (persister) which tolerated the lethal effects of some of the size exclusion chromatographic fractions of *Bl* 1951 can be exploited for future use. The host range of phage tail-like antibacterial structures such as diffocins, monocins, and syringacins, has been altered in the previous studies using modern molecular tools so it is possible to use these technologies to protect the insect pathogenic bacterium from their deleterious effects. Overall, this research project provided a wealth of knowledge that will be useful in synthesising a biopesticide from this bacterium.

References

Aasen, I. M., Møretrø, T., Katla, T., Axelsson, L., & Storrø, I. (2000). Influence of complex nutrients, temperature and pH on bacteriocin production by *Lactobacillus sakei* CCUG 42687. *Applied Microbiology and Biotechnology, 53*(2), 159-166. doi:https://doi.org/10.1007/s002530050003

Abedon, S. T. (2012). Bacterial 'immunity' against bacteriophages. *Bacteriophage, 2*(1), 50-54. doi:https://doi.org/10.4161/bact.18609

Abedon, S. T., & LeJeune, J. T. (2005). Why bacteriophage encode exotoxins and other virulence factors. *Evolutionary Bioinformatics, 1*, 117693430500100001.

Abedon, S. T., & Yin, J. (2009). Bacteriophage plaques: Theory and analysis. In M. R. J. Clockie & A. M. Kropinski (Eds.), *Bacteriophages* (Vol. 1, pp. 161-174): Springer.

Åberg, A., Nordlund, P., & Eklund, H. (1993). Unusual clustering of carboxyl side chains in the core of iron-free ribonucleotide reductase. *Nature, 361*(6409), 276-278.

Abrescia, N. G., Bamford, D. H., Grimes, J. M., & Stuart, D. I. (2012). Structure unifies the viral universe. *Annual Review of Biochemistry, 81*, 795-822.

Abro, G., Jayo, A., & Syed, T. (1994). Ecology of diamondback moth, *Plutella xylostella* (L.) in Pakistan. Host plant preference. *Pakistan Journal of Zoology, 26*(1), 35-38.

Ackermann, H., & DuBow, M. (1987). Phage multiplication. *Viruses of Prokaryotes, 1*, 49-85.

Ackermann, H. W. (2001). Frequency of morphological phage descriptions in the year 2000. *Archives of Virology, 146*(5), 843-857. doi:https://doi.org/10.1007/s007050170120

Ackermann, H. W. (2007). 5500 Phages examined in the electron microscope. *Archives of Virology, 152*(2), 227-243.

Ackermann, H. W., Azizbekyan, R., Konjin, H. E., Lecadet, M.-M., Seldin, L., & Yu, M. (1994). New *Bacillus* bacteriophage species. *Archives of Virology, 135*(3-4), 333-344.

Ackermann, H. W., & Prangishvili, D. (2012). Prokaryote viruses studied by electron microscopy. *Archives of Virology, 157*(10), 1843-1849.

Aertsen, A., & Michiels, C. W. (2005). Diversify or die: generation of diversity in response to stress. *Critical Reviews in Microbiology, 31*(2), 69-78.

Ahern, M., Verschueren, S., & van Sinderen, D. (2003). Isolation and characterisation of a novel bacteriocin produced by *Bacillus thuringiensis* strain B439. *FEMS Microbiology Letters, 220*(1), 127-131. doi:https://doi.org/10.1016/s0378-1097(03)00086-7

Ahmad, M., Taylor, C. R., Pink, D., Burton, K., Eastwood, D., Bending, G. D., & Bugg, T. D. (2010). Development of novel assays for lignin degradation: comparative analysis of bacterial and fungal lignin degraders. *Molecular Biosystems, 6*(5), 815-821.

Ahmed, I., Yokota, A., Yamazoe, A., & Fujiwara, T. (2007). Proposal of *Lysinibacillus boronitolerans* gen. nov. sp. nov., and transfer of *Bacillus fusiformis* to *Lysinibacillus fusiformis* comb. nov. and *Bacillus sphaericus* to *Lysinibacillus sphaericus* comb. nov. *International Journal of Systematic and Evolutionary Microbiology, 57*(5), 1117-1125. doi:https://doi.org/10.1099/ijs.0.63867-0

Ak, A. U., Demirkan, E., Cengiz, M., Sevgi, T., Zeren, B., & Abdou, M. (2019). Optimisation of culture medium for the production and partial purification and characterisation of an antibacterial activity from *Brevibacillus laterosporus* strain EA62. *Romania Biotechnology Letter, 4*(24), 705-713.

Alekshun, M. N., Levy, S. B., Mealy, T. R., Seaton, B. A., & Head, J. F. (2001). The crystal structure of MarR, a regulator of multiple antibiotic resistance, at 2.3 A resolution. *Nature Structure Biology, 8*(8), 710-714. doi:https://doi.org/10.1038/90429

Alippi, A. M., & Reynaldi, F. J. (2006). Inhibition of the growth of *Paenibacillus* larvae, the causal agent of American foulbrood of honeybees, by selected strains of aerobic spore-forming bacteria isolated from apiarian sources. *Journal of Invertebrate Pathology, 91*(3), 141-146.

Altenbern, R. A., & Stull, H. B. (1965). Inducible lytic systems in the genus *Bacillus*. *Microbiology, 39*(1), 53-62.

Alvarez-Sieiro, P., Montalbán-López, M., Mu, D., & Kuipers, O. P. (2016). Bacteriocins of lactic acid bacteria: extending the family. *Applied Microbiology and Biotechnology, 100*(7), 2939-2951. doi:https://doi.org/10.1007/s00253-016-7343-9

Alves, C. S., Melo, M. N., Franquelim, H. G., Ferre, R., Planas, M., Feliu, L., . . . Santos, N. C. (2010). *Escherichia coli* cell surface perturbation and disruption induced by antimicrobial peptides BP100 and pepR. *Journal of Biological Chemistry, 285*(36), 27536-27544.

Anderson, I., Sorokin, A., Kapatral, V., Reznik, G., Bhattacharya, A., Mikhailova, N., . . . Walunas, T. (2005). Comparative genome analysis of *Bacillus cereus* group genomes with *Bacillus subtilis*. *FEMS Microbiology Letters, 250*(2), 175-184. doi: https:// doi.org/ 10.1016/ j.femsle. 2005. 07. 008

Andrews, N. C. (2010). Ferrit (in) ing out new mechanisms in iron homeostasis. *Cell Metabolism, 12*(3), 203-204.

Andrews, S. C., Robinson, A. K., & Rodríguez-Quiñones, F. (2003). Bacterial iron homeostasis. *FEMS Microbiology Review, 27*(2-3), 215-237. doi:https://doi.org/10.1016/s0168-6445(03)00055

Ano, T., Kobayashi, A., & Shoda, M. (1990). Transformation of *Bacillus subtilis* with the treatment by alkali cations. *Biotechnology Letters, 12*(2), 99-104.

Arisaka, F., Engel, J., & Klump, H. (1981). Contraction and dissociation of the bacteriophage T4 tail sheath induced by heat and urea. *Progress in Clinical and Biological Research, 64*, 365-379.

Arndt, D., Grant, J. R., Marcu, A., Sajed, T., Pon, A., Liang, Y., & Wishart, D. S. (2016). PHASTER: a better, faster version of the PHAST phage search tool. *Nucleic Acids Research, 44*(W1), W16-21. doi:https://doi.org/10.1093/nar/gkw387

Arnison, P. G., Bibb, M. J., Bierbaum, G., Bowers, A. A., Bugni, T. S., Bulaj, G., . . . Clardy, J. (2013). Ribosomally synthesised and post-translationally modified peptide natural products: Overview and recommendations for a universal nomenclature. *Natural Product Reports, 30*(1), 108-160.

Aronson, A. I., Beckman, W., & Dunn, P. (1986). *Bacillus thuringiensis* and related insect pathogens. *Microbiological Reviews, 50*(1), 1-24.

Arul Jose, P., Sivakala, K. K., & Jebakumar, S. R. D. (2013). Formulation and statistical optimisation of culture medium for improved production of antimicrobial compound by *Streptomyces* sp. JAJ06. *International Journal of Microbiology, 2013*.

Asadishad, B., Ghoshal, S., & Tufenkji, N. (2011). Method for the direct observation and quantification of survival of bacteria attached to negatively or positively charged surfaces in an aqueous medium. *Environmental Science and Technology, 45*(19), 8345-8351.

Aslam, B., Basit, M., Nisar, M. A., Khurshid, M., & Rasool, M. H. (2017). Proteomics: technologies and their applications. *Journal of Chromatographic Science, 55*(2), 182-196.

Avies-Riordan, K. (2019). *10 insect pests that that threaten the world's plants*. Retrieved 01st June, 2021,from https://www.kew.org/read-and-watch/insect-pests-biggest-threat-plants

Aziz, R. K., Bartels, D., Best, A. A., DeJongh, M., Disz, T., Edwards, R. A., . . . Zagnitko, O. (2008). The RAST server: rapid annotations using subsystems technology. *BMC Genomics, 9*, 75. doi:https://doi.org/10.1186/1471-2164-9-75

Azizbekyan, R., Didenko, L., Smirnova, T., Kuzin, A., Shevlyagina, N., Zubasheva, M., & Nikolaenko, M. (2015). Biofilm formation and sporulation in *Brevibacillus laterosporus*. *Applied Biochemistry and Microbiology, 51*(9), 866-872.

Bae, J. W., Rhee, S. K., Park, J. R., Chung, W. H., Nam, Y. D., Lee, I., . . . Park, Y. H. (2005). Development and evaluation of genome-probing microarrays for monitoring lactic acid bacteria. *Applied and Environmental Microbiology, 71*(12), 8825-8835. doi:https://doi.org /10.1128/ AEM. 71.12. 8825-8835.2005

Baechler, C. A., & Berk, R. S. (1974). Electron microscopic observations of *Pseudomonas aeruginosa*. *Zeitschrift Für Allgemeine Mikrobiologie, 14*(4), 267-281. doi:https://doi.org/10.1002/jobm. 19740140402

Baindara, P., Singh, N., Ranjan, M., Nallabelli, N., Chaudhry, V., Pathania, G. L., . . . Korpole, S. (2016a). Laterosporulin10: a novel defensin like class IId bacteriocin from *Brevibacillus* sp. strain SKDU10 with inhibitory activity against microbial pathogens. *Microbiology, 162*(8),1286-1299 https://.doi: 10. 1099/mic.0.000316

Baindara, P., Singh, N., Ranjan, M., Nallabelli, N., Chaudhry, V., Pathania, G. L., . . . Korpole, S. (2016b). Laterosporulin10: a novel defensin like Class IId bacteriocin from *Brevibacillus* sp. strain SKDU 10 with inhibitory activity against microbial pathogens. *Microbiology 162*(8), 1286-1299. doi:https://doi.org/10.1099/mic.0.000316

Baquero, F., & Moreno, F. (1984). The microcins. *FEMS Microbiology Letters, 23*(2-3), 117-124.

Barboza-Corona, J. E., de la Fuente-Salcido, N., Alva-Murillo, N., Ochoa-Zarzosa, A., & López-Meza, J. E. (2009). Activity of bacteriocins synthesised by *Bacillus thuringiensis* against *Staphylococcus aureus* isolates associated to bovine mastitis. *Veterniary Microbiology, 138*(1-2), 179-183. doi:https://doi.org/10.1016/j.vetmic.2009.03.018

Barrangou, R., Fremaux, C., Deveau, H., Richards, M., Boyaval, P., Moineau, S., . . . Horvath, P. (2007). CRISPR provides acquired resistance against viruses in prokaryotes. *Science, 315*(5819), 1709-1712.

Barsby, T., Kelly, M. T., Gagné, S. M., & Andersen, R. J. (2001). Bogorol A produced in culture by a marine *Bacillus* sp. reveals a novel template for cationic peptide antibiotics. *Organic Letters, 3*. doi:https://doi.org/10.1021/ol006942q

Barthelmebs, L., Lecomte, B., Divies, C., & Cavin, J. F. (2000). Inducible metabolism of phenolic acids in *Pediococcus pentosaceus* is encoded by an autoregulated operon which involves a new class of negative transcriptional regulator. *Journal of Bacteriology, 182*(23), 6724-6731. doi:https://doi.org/10.1128/JB.182.23.6724-6731.2000

Basler, M. (2015). Type VI secretion system: secretion by a contractile nanomachine. *Philosophical Transactions of the Royal Society B: Biological Sciences, 370*(1679), 20150021.

Basler, M., Ho, B., & Mekalanos, J. (2013). Tit-for-tat: type VI secretion system counterattack during bacterial cell-cell interactions. *Cell, 152*(4), 884-894.

Bastos, M., Ceotto, H., Coelho, M., & Nascimento, J. (2009). *Staphylococcal* antimicrobial peptides: relevant properties and potential biotechnological applications. *Current Pharmaceutical Biotechnology, 10*(1), 38-61.

Bauer, A. (1966). Antibiotic susceptibility testing by a standardised single disc method. *American Journal of Clinical Pathology, 45*, 149-158.

Baur, M., & Fuxa, J., & L. S. U. A. Center. (2007). *Factors affecting the survival of entomopathogens* [Bulletin]. Louisiana State University Agricultural Center USA: Southern Cooperative Series Bulletin 400.

Bedini, S., Conti, B., Hamze, R., Muniz, E. R., Fernandes, É. K., & Ruiu, L. (2021). Lethal and sub-lethal activity of *Brevibacillus laterosporus* on the mosquito *Aedes albopictus* and side effects on non-target water-dwelling invertebrates. *Journal of Invertebrate Pathology*, 107645.

Beegle, C. C., Rose,RI, Ziniu,Y. (1991). Mass production of *Bacillus thuringiensis* and *Bacillus sphaericus* for microbial control of insect pests. *In: Maramorosch, K. (Ed.), Biotechnology for Biological Control of Pests and Vectors. CRC Press, Boca Raton*, 195-216.

Begot, C., Desnier, I., Daudin, J. D., Labadie, J. C., & Lebert, A. (1996). Recommendations for calculating growth parameters by optical density measurements. *Journal of Microbiological Methods, 25*(3), 225-232. doi:https://doi.org/10.1016/0167-7012(95)00090-9

Berg, J. A., Merrill, B. D., Crockett, J. T., Esplin, K. P., Evans, M. R., Heaton, K. E., . . . Grose, J. H. (2016). Characterisation of five novel *Brevibacillus* bacteriophages and genomic comparison of *Brevibacillus* phages. *Plos One, 11*(6), e0156838-e0156838. doi:https://doi.org/10.1371/journal.pone.0156838

Berling, M., Blachere-Lopez, C., Soubabere, O., Lery, X., Bonhomme, A., Sauphanor, B., & Lopez-Ferber, M. (2009). *Cydia pomonella* granulovirus genotypes overcome virus resistance in the codling moth and improve virus efficiency by selection against resistant hosts. *Applied and Environmental Microbiology, 75*(4), 925-930.

Bernardi, D., Salmeron, E., Horikoshi, R. J., Bernardi, O., Dourado, P. M., Carvalho, R. A., . . . Omoto, C. (2015). Cross-resistance between Cry1 proteins in fall armyworm (*Spodoptera frugiperda*) may affect the durability of current pyramided *Bt* maize hybrids in Brazil. *Plos One, 10*(10), e0140130.

Berney, M., Hammes, F., Bosshard, F., Weilenmann, H.-U., & Egli, T. (2007). Assessment and interpretation of bacterial viability by using the LIVE/DEAD BacLight Kit in combination with flow cytometry. *Applied and Environmental Microbiology, 73*(10), 3283-3290.

Bernhardt, T. G., Roof, W. D., & Young, R. (2000). Genetic evidence that the bacteriophage ϕX174 lysis protein inhibits cell wall synthesis. *Proceedings of the National Academy of Sciences, 97*(8), 4297-4302.

Bernhardt, T. G., Wang, N., Struck, D. K., & Young, R. (2001). A protein antibiotic in the phage Qβ virion: diversity in lysis targets. *Science, 292*(5525), 2326-2329.

Berry, C. (2012). The bacterium, *Lysinibacillus sphaericus*, as an insect pathogen. *Journal of Inverteberate Pathology, 109*(1), 1-10.

Bettencourt, P., Pires, D., Carmo, N., & Anes, E. (2010). Application of confocal microscopy for quantification of intracellular mycobacteria in macrophages. *Microscopy: Science, Technology, Applications and Education, 614*.

Beveridge, T. J. (2001). Use of the gram stain in microbiology. *Biotechnic and Histochemistry, 76*(3), 111-118. doi:https://doi.org/10.1080/bih.76.3.111.118

Beyer, K., Bardina, L., Grishina, G., & Sampson, H. A. (2002). Identification of sesame seed allergens by 2-dimensional proteomics and Edman sequencing: seed storage proteins as common food allergens. *Journal of Allergy and Clinical Immunology, 110*(1), 154-159. doi:https://doi.org/10.1067/mai.2002.125487

Bienkowski, D. (2012). *Biological control of Rhizoctonia diseases of potato* (Doctoral Thesis). Lincoln University. Retrieved from https://researcharchive.lincoln.ac.nz

Bierbaum, G., & Sahl, H. G. (2009). Lantibiotics: mode of action, biosynthesis and bioengineering. *Current Pharmaceutical Biotechnology, 10*(1), 2-18. doi:https://doi.org/10.2174/138920109787048616

Bingle, L. E., Bailey, C. M., & Pallen, M. J. (2008). Type VI secretion: a beginner's guide. *Current Opinion in Microbiology, 11*(1), 3-8.

Biswas, S. R., Ray, P., Johnson, M. C., & Ray, B. (1991). Influence of growth conditions on the production of a bacteriocin, Pediocin AcH, by *Pediococcus acidilactici* H. *Applied and Environmental Microbiology, 57*(4), 1265-1267. doi:https://doi.org/10.1128/aem.57.4.1265-1267.1991

Bizani, D., & Brandelli, A. (2002). Characterisation of a bacteriocin produced by a newly isolated *Bacillus* sp. strain 8 A. *Journal of Applied Microbiology, 93*(3), 512-519. doi:https://doi.org/ 10.1046/j.1365-2672.2002.01720.x

Blackstock, W. P., & Weir, M. P. (1999). Proteomics: quantitative and physical mapping of cellular proteins. *Trends in Biotechnology, 17*(3), 121-127. doi:https://doi.org/10.1016/S0167-799(98)01245-1

Blackwell, C. C., Winstanley, F., & Brunton, W. T. (1982). Sensitivity of thermophilic campylobacters to R-type pyocines of *Pseudomonas aeruginosa*. *Journal of Medical Microbiology, 15*(2), 247-251.

Blasco, L., Ferrer, S., & Pardo, I. (2003). Development of specific fluorescent oligonucleotide probes for in situ identification of wine lactic acid bacteria. *FEMS Microbiology Letters, 225*(1), 115-123.

Bläsi, U., & Young, R. (1996). Two beginnings for a single purpose: the dual-start holins in the regulation of phage lysis. *Molecular Microbiology, 21*(4), 675-682.

Blow, F., Ankrah, N. Y. D., Clark, N., Koo, I., Allman, E. L., Liu, Q., . . . Ruby, E. G. (2020). Impact of facultative bacteria on the metabolic function of an obligate insect-bacterial symbiosis. *mBio, 11*(4), e00402-00420. doi:https://doi.org/10.1128/mBio.00402-20

Blum, H., Beier, H., & Gross, H. J. (1987). Improved silver staining of plant proteins, RNA and DNA in polyacrylamide gels. *Electrophoresis, 8*(2), 93-99.

Bobay, L.-M., Touchon, M., & Rocha, E. P. (2014). Pervasive domestication of defective prophages by bacteria. *Proceedings of the National Academy of Sciences, 111*(33), 12127-12132.

Böck, D., Medeiros, J. M., Tsao, H.-F., Penz, T., Weiss, G. L., Aistleitner, K., . . . Pilhofer, M. (2017). In situ architecture, function, and evolution of a contractile injection system. *Science, 357*(6352), 713. doi:https://doi.org/10.1126/science.aan7904

Boeckaerts, D., Stock, M., Criel, B., Gerstmans, H., De Baets, B., & Briers, Y. (2021). Predicting bacteriophage hosts based on sequences of annotated receptor-binding proteins. *Scientific Reports, 11*(1), 1467. doi:https://doi.org/10.1038/s41598-021-81063-4

Boemare, N. E., Boyer-Giglio, M. H., Thaler, J. O., Akhurst, R. J., & Brehelin, M. (1992). Lysogeny and bacteriocinogeny in *Xenorhabdus nematophilus* and other *Xenorhabdus* spp. *Applied and Environmental Microbiology, 58*(9), 3032-3037. doi:https://doi.org/10.1128/AEM.58.9.3032-3037.1992

Boets, A., Arnaut, G., Van Rie, J., & Damme, N., &. (2011). *Toxins*: US Patent No. 7,919,609 B2. Washington, DC: U.S. Patent and Trademark Office.

Bönemann, G., Pietrosiuk, A., & Mogk, A. (2010). Tubules and donuts: a type VI secretion story. *Molecular Microbiology, 76*(4), 815-821.

Bordenstein, S. R., Marshall, M. L., Fry, A. J., Kim, U., & Wernegreen, J. J. (2006). The tripartite associations between bacteriophage, *Wolbachia*, and arthropods. *Plos Pathogens, 2*(5), e43.

Borges, H. D., & Hussey, N. W. (1971). *Microbial control of insects and mites*: New York, London: Academic Press. Retrieved from https://www.cabdirect.org/cabdirect/abstract/19722900132. Retrieved from CABDirect database.

Børsheim, K. Y., Bratbak, G., & Heldal, M. (1990). Enumeration and biomass estimation of planktonic bacteria and viruses by transmission electron microscopy. *Applied and Environmental Microbiology, 56*(2), 352-356. doi:10.1128/AEM.56.2.352-356.1990

Borzenkov, V., Surovtsev, V., & Dyatlov, I. (2014). Obtaining bacteriocins by chromatographic methods. *Advances in Bioscience and Biotechnology, Vol.05* (05), 6. doi:https://doi.org/10.4236/abb.2014.55054

Botstein, D. (1980). A theory of modular evolution for bacteriophages. *Annals of the New York Academy of Sciences, 354*(1), 484-491.

Botstein, D., & Herskowitz, I. (1974). Properties of hybrids between *Salmonella* phage P22 and coliphage λ. *Nature, 251*(5476), 584-589.

Bouchard, J. D., & Moineau, S. (2000). Homologous recombination between a lactococcal bacteriophage and the chromosome of its host strain. *Virology, 270*(1), 65-75.

Boulanger, P. (2009). Purification of bacteriophages and SDS-PAGE analysis of phage structural proteins from ghost particles. In M. R. J. Clockie & A. M.Kropinski (Eds.), *Methods in Molecular Biology* (Vol. 2, pp. 227-238). doi:https://doi.org/10.1007/978-1-60327-565-1

Boundless. (2017). *The chemical basis of life*. Retrieved 20 th November 2017,from https://www.boundless.com

Bowen, D., Yin, Y., Flasinski, S., Chay, C., Bean, G., Milligan, J., . . . Buckman, K. (2021). Cry75Aa (Mpp75Aa) insecticidal proteins for controlling the Western corn rootworm, *Diabrotica virgifera virgifera* LeConte (Coleoptera: Chrysomelidae), isolated from the insect-pathogenic bacterium *Brevibacillus laterosporus*. *Applied and Environmental Microbiology, 87*(5), e02507-02520.

Boyd, E. F., & Brüssow, H. (2002). Common themes among bacteriophage-encoded virulence factors and diversity among the bacteriophages involved. *Trends in Microbiology, 10*(11), 521-529. doi:https://doi.org/10.1016/s0966-842x(02)02459-9

Brackmann, M., Nazarov, S., Wang, J., & Basler, M. (2017). Using force to punch holes: mechanics of contractile nanomachines. *Trends in Cell Biology, 27*(9), 623-632.

Bradley, D., & Dewar, C. A. (1966). The structure of phage-like objects associated with non-induced bacteriocinogenic bacteria. *Microbiology, 45*(3), 399-408.

Bradley, D. E. (1967a). Ultrastructure of bacteriophage and bacteriocins. *Bacteriological Reviews, 31*(4), 230-314.

Bradley, D. E. (1967b). Ultrastructure of bacteriophage and bacteriocins. *Bacteriological Reviews, 31*(4), 230-314.

Bradley, J. M., Moore, G. R., & Le Brun, N. E. (2014a). Mechanisms of iron mineralization in ferritins: one size does not fit all. *Journal of Biological Inorganic Chemistry, 19*(6), 775-785.

Bradley, J. M., Moore, G. R., & Le Brun, N. E. (2014b). Mechanisms of iron mineralization in ferritins: one size does not fit all. *Journal of Biological Inorganic Chemistry, 19*(6), 775-785.

Braun, V., Pilsl, H., & Groß, P. (1994). Colicins: structures, modes of action, transfer through membranes, and evolution. *Archives of Microbiology, 161*(3), 199-206. doi:https://doi.org/10.1007/BF00248693

Bravo, A., Likitvivatanavong, S., Gill, S. S., & Soberón, M. (2011a). *Bacillus thuringiensis*: a story of a successful bioinsecticide. *Insect Biochemistry & Molecular Biology, 41*(7), 423-431.

Bravo, A., Likitvivatanavong, S., Gill, S. S., & Soberón, M. (2011b). *Bacillus thuringiensis*: a story of a successful bioinsecticide. *Insect Biochemistry and Molecular biology, 41*(7), 423-431.

Brito, P. H., Chevreux, B., Serra, C. R., Schyns, G., Henriques, A. O., & Pereira-Leal, J. B. (2018). Genetic competence drives genome diversity in *Bacillus subtilis*. *Genome Biology and Evolution, 10*(1), 108-124.

Broussard, G. W., Oldfield, L. M., Villanueva, V. M., Lunt, B. L., Shine, E. E., & Hatfull, G. F. (2013). Integration-dependent bacteriophage immunity provides insights into the evolution of genetic switches. *Molecular Cell, 49*(2), 237-248. doi:https://doi.org/10.1016/j.molcel.2012.11.012

Brown, S. E., Cao, A. T., Hines, E. R., Akhurst, R. J., & East, P. D. (2004). A novel secreted protein toxin from the insect pathogenic bacterium *Xenorhabdus nematophila*. *Journal of Biological Chemistry, 279*(15), 14595-14601.

Brown, S. P., Fredrik Inglis, R., & Taddei, F. (2009). SYNTHESIS: Evolutionary ecology of microbial wars: within-host competition and (incidental) virulence. *Evolutionary Applications, 2*(1), 32-39.

Brüssow, H., Canchaya, C., & Hardt, W. D. (2004). Phages and the evolution of bacterial pathogens: from genomic rearrangements to lysogenic conversion. *Microbiology and Molecular Biology Reviews, 68*(3), 560-602. doi:https://doi.org/10.1128/mmbr.68.3.560-602.2004

Brüssow, H., & Hendrix, R. W. (2002). Phage Genomics: Small Is Beautiful. *Cell, 108*(1), 13-16. doi:https://doi.org/10.1016/S0092-8674(01)00637-7

Bruyneel, B., Vande Woestyne, M., & Verstraete, W. (1989). Lactic acid bacteria: microorganisms able to grow in the absence of available iron and copper. *Biotechnology Letters, 11*(6), 401-406.

Bubici, G. (2018). *Streptomyces* spp. as biocontrol agents against *Fusarium* species. *CAB Review, 13*, 050.

Burns, C. M., Chan, H. L., & DuBow, M. S. (1990). In vitro maturation and encapsidation of the DNA of transposable Mu-like phage D108. *Proceedings of Natlonal Academy of Sciences U S A, 87*(16), 6092-6096. doi:https://doi.org/10.1073/pnas.87.16.6092

Buth, S. A., Shneider, M. M., Scholl, D., & Leiman, P. G. (2018). Structure and analysis of R1 and R2 pyocin receptor-binding fibres. *Viruses, 10*(8), 427. doi:https://doi.org/10.3390/v10080427

Cai, H., Wang, Y., WAN, H.-g., JIANG, D.-h., WANG, H.-l., & ZHAO, Z.-s. (2011). Research progress of spinosad produced by *Saccharopolyspora spinosa*. *China Biotechnology, 31*(02), 124-129.

Cameron, P., Shelton, A., Walker, G., & Tang, J. (1997). Comparative insecticide resistance of New Zealand and North American populations of diamondback moth, *Plutella xylostella* (Lepidoptera: Plutellidae). *New Zealand Journal of Crop and Horticultural Science, 25*(2), 117-122.

Camiolo, S., Porceddu, A., & Ruiu, L. (2017). Genome sequence of *Brevibacillus laterosporus* UNISS 18, a pathogen of mosquitoes and flies. *Genome Announcements, 5*(21), e00419-00417.

Campagnari, A. A., Karalus, R., Apicella, M., Melaugh, W., Lesse, A. J., & Gibson, B. W. (1994). Use of pyocin to select a *Haemophilus ducreyi* variant defective in lipooligosaccharide biosynthesis. *Infection and Immunity, 62*(6), 2379-2386. doi:https://doi.org/10.1128/iai.62.6.2379-2386.1994

Campbell, A. (1977). Defective Bacteriophages and Incomplete Prophages. In H. Fraenkel-Conrat & R. R. Wagner (Eds.), *Regulation and Genetics: Bacterial DNA Viruses* (1st ed., pp. 259-328). Boston, MA: Springer US. doi:https://doi.org/10.1007/978-1-4684-2715-8_3

Campbell, A. (1994). Comparative molecular biology of lambdoid phages. *Annual Review of Microbiology, 48*, 193-222. doi:https://doi.org/10.1146/annurev.mi.48.100194.001205

Campbell, A. (1996). Cryptic prophages. *Escherichia coli and Salmonella: Cellular and Molecular Biology, 2*, 2041-2046.

Campbell, N., Reece, J., & Mitchell, L. (2005). A tour of the cell. *Biology*, 1-1390.

Canchaya, C., Desiere, F., McShan, W. M., Ferretti, J. J., Parkhill, J., & Brüssow, H. (2002). Genome analysis of an inducible prophage and prophage remnants integrated in the *Streptococcus pyogenes* strain SF370. *Virology, 302*(2), 245-258.

Canchaya, C., Fournous, G., & Brüssow, H. (2004). The impact of prophages on bacterial chromosomes. *Molecular Microbiology, 53*(1), 9-18.

Canchaya, C., Fournous, G., Chibani-Chennoufi, S., Dillmann, M.-L., & Brüssow, H. (2003). Phage as agents of lateral gene transfer. *Current Opinion in Microbiology, 6*(4), 417-424. doi:https://doi.org/10.1016/S1369-5274(03)00086-9

Carim, S., Azadeh, A. L., Kazakov, A. E., Price, M. N., Walian, P. J., Lui, L. M., . . . Arkin, A. P. (2021). Systematic discovery of pseudomonad genetic factors involved in sensitivity to tailocins. *The ISME Journal*. doi:https://doi.org/10.1038/s41396-021-00921-1

Carlson, K. (2004). Working with bacteriophages: Common techniques and methodological approaches. In E. Kutter & A. Sulakvelidze (Eds.), *Bacteriophages: Biology and applications* (pp. 437- 494): CRC Press.

Carramaschi, I. N., Pereira, L. d. A., Queiroz, M. M. d. C., & Zahner, V. (2015). Preliminary screening of the larvicidal effect of *Brevibacillus laterosporus* strains against the blowfly *Chrysomya megacephala* (Fabricius, 1794)(Diptera: Calliphoridae). *Revista da Sociedade Brasileira de Medicina Tropical, 48*, 427-431.

Carrillo, C., Teruel, J. A., Aranda, F. J., & Ortiz, A. (2003). Molecular mechanism of membrane permeabilisation by the peptide antibiotic surfactin. *Biochimica et Biophysica Acta-Biomembranes, 1611*(1), 91-97. doi:https://doi.org/10.1016/S0005-2736(03)00029-4

Cascales, E., Buchanan, S. K., Duché, D., Kleanthous, C., Lloubes, R., Postle, K., . . . Cavard, D. (2007). Colicin biology. *Microbiology and Molecular Biology Reviews, 71*(1), 158-229.

Casjens, S. (2003). Prophages and bacterial genomics: what have we learned so far? *Molecular Microbiology, 49*(2), 277-300.

Catalão, M. J., Gil, F., Moniz-Pereira, J., São-José, C., & Pimentel, M. (2013). Diversity in bacterial lysis systems: bacteriophages show the way. *FEMS Microbiology Reviews, 37*(4), 554-571. doi:https://doi.org/10.1111/1574-6976.12006

Chandel, S., Allan, E. J., & Woodward, S. (2010). Biological control of *Fusarium oxysporum* f.sp. *lycopersic*i on tomato by *Brevibacillus brevis*. *Journal of Phytopathology, 158*. doi:https://doi.org/10.1111/j.1439-0434.2009.01635,x

Chang, S., & Cohen, S. N. (1979). High frequency transformation of *Bacillus subtilis* protoplasts by plasmid DNA. *Molecular and General Genetics, 168*(1), 111-115.

Chapman, H. M., & Norris, J. (1966). Four new bacteriophages of *Bacillus thuringiensis*. *Journal of Applied Bacteriology, 29*(3), 529-535.

Chapman, J. W., Reynolds, D. R., Smith, A. D., Riley, J. R., Pedgley, D. E., & Woiwod, I. P. (2002). High-altitude migration of the diamondback moth *Plutella xylostella* to the UK: a study using radar, aerial netting, and ground trapping. *Ecological Entomology, 27*(6), 641-650.

Chavan, M. A., & Riley, M. A. (2007). Molecular evolution of bacteriocins in gram-negative bacteria. In M. A. Riley & M. A. Chavan (Eds.), *Bacteriocins: Ecology and evolution* (1 ed., pp. 19-43). Berlin, Heidelberg: Springer Berlin Heidelberg. doi:https://doi.org/10.1007/978-3-540-36604-1_3

Chawla, S. (2015). *Genome sequence and the iIdentification of mosquitocidal toxin operons in Clostridium bifermentans subsp. Malaysia* (Doctoral Thesis). University of California, Riverside. Retrieved from https://www.proquest.com/openview

Chen, H. L., Su, P. Y., Chang, Y. S., Wu, S. Y., Liao, Y. D., Yu, H. M., . . . Shih, C. (2013). Identification of a novel antimicrobial peptide from human hepatitis B virus core protein arginine-rich domain (ARD). *Plos Pathogens, 9*(6), e1003425.

Chen, J., Zhu, Y., Yin, M., Xu, Y., Liang, X., & Huang, Y. P. (2019). Characterisation of maltocin S16, a phage tail-like bacteriocin with antibacterial activity against *Stenotrophomonas maltophilia* and *Escherichia coli*. *127*(1), 78-87. doi:https://doi.org/10.1111/jam.14294

Chen, S., Zhang, M., Wang, J., Lv, D., Ma, Y., Zhou, B., & Wang, B. (2017). Biocontrol effects of *Brevibacillus laterosporus* AMCC100017 on potato common scab and its impact on rhizosphere bacterial communities. *Biological Control, 106*, 89-98.

Cherif, A., Chehimi, S., Limem, F., Hansen, B. M., Hendriksen, N. B., Daffonchio, D., & Boudabous, A. (2003). Detection and characterisation of the novel bacteriocin entomocin 9, and safety evaluation of its producer, *Bacillus thuringiensis* ssp. *entomocidus* HD9. *Journal of Applied Microbiology, 95*(5), 990-1000. doi:https://doi.org/10.1046/j.1365-2672.2003.02089.x

Cherif, A., Rezgui, W., Raddadi, N., Daffonchio, D., & Boudabous, A. (2008). Characterisation and partial purification of entomocin 110, a newly identified bacteriocin from *Bacillus thuringiensis* subsp. *entomocidus* HD110. *Microbiological Research, 163*(6), 684-692.

Chibani-Chennoufi, S., Dillmann, M.-L., Marvin-Guy, L., Rami-Shojaei, S., & Brüssow, H. (2004). *Lactobacillus plantarum* bacteriophage LP65: a new member of the SPO1-like genus of the family *Myoviridae*. *Journal of Bacteriology, 186*(21), 7069-7083.

Chopin, M.-C., Chopin, A., & Bidnenko, E. (2005). Phage abortive infection in *lactococci*: variations on a theme. *Current Opinion in Microbiology, 8*(4), 473-479.

Cianfanelli, F. R., Monlezun, L., & Coulthurst, S. J. (2016). Aim, load, fire: the type VI secretion system, a bacterial nanoweapon. *Trends in Microbiology, 24*(1), 51-62.

Clarke, D. J. (2020). *Photorhabdus*: a tale of contrasting interactions. *Microbiology, 166*(4), 335-348.

Cleveland, J., Montville, T. J., Nes, I. F., & Chikindas, M. L. (2001). Bacteriocins: safe, natural antimicrobials for food preservation. *International Journal of Food Microbiology, 71*(1), 1-20.

Cochrane, S. A., & Vederas, J. C. (2016). Lipopeptides from *Bacillus* and *Paenibacillus* spp.: a gold mine of antibiotic candidates. *Medical Research Review, 36*(1), 4-31. doi:https://doi.org/10.1002/med.21321

Coetzee, H. L., De Klerk, H. C., Coetzee, J. N., & Smit, J. A. (1968). Bacteriophage-tail-like particles associated with intra-species killing of *Proteus vulgaris*. *The Journal of General Virology, 2*(1), 29-36. doi:https://doi.org/10.1099/0022-1317-2-1-29

Cohen, E., Rozen, H., Joseph, T., Braun, S., & Margulies, L. (1991). Photoprotection of *Bacillus thuringiensis kurstaki* from ultraviolet irradiation. *Journal of Invertebrate Pathology, 57*(3), 343-351. doi:https://doi.org/10.1016/0022-2011(91)90138-G

Cole, S., Brosch, R., Parkhill, J., Garnier, T., Churcher, C., Harris, D., . . . Barry, C. r. (1998). Deciphering the biology of *Mycobacterium tuberculosis* from the complete genome sequence. *Nature, 396*(6707), 190-190.

Colombet, J., Robin, A., Lavie, L., Bettarel, Y., Cauchie, H. M., & Sime-Ngando, T. (2007). Virioplankton 'pegylation': Use of PEG (polyethylene glycol) to concentrate and purify viruses in pelagic ecosystems. *Journal of Microbiological Methods, 71*(3), 212-219. doi:https://doi.org/10.1016/j.mimet.2007.08.012

Connelly, M. C., & Allen, P. Z. (1983). Chemical and immunochemical studies on lipopolysaccharides from pyocin 103-sensitive and -resistant *Neisseria gonorrhoeae*. *Carbohydrate Research, 120*, 171-186. doi:https://doi.org/10.1016/0008-6215(83)88015.x

Cordova-Kreylos, A. L., Fernandez, L. E., Koivunen, M., Yang, A., Flor-Weiler, L., & Marrone, P. G. (2013). Isolation and characterisation of *Burkholderia rinojensis* sp. nov., a non-*Burkholderia cepacia* complex soil bacterium with insecticidal and miticidal activities. *Applied and Environmental Microbiology, 79*(24), 7669-7678.

Cornelis, P., Wei, Q., Andrews, S. C., & Vinckx, T. (2011). Iron homeostasis and management of oxidative stress response in bacteria. *Metallomics, 3*(6), 540-549. doi:https://doi.org/10.1039/c1mt00022e

Cornell, J. L., Breslin, E., Schuhmacher, Z., Himelright, M., Berluti, C., Boyd, C., . . . Gilliam, B. (2016). Complete genome sequence of *Bacillus thuringiensis* bacteriophage Smudge. *Genome Announcements, 4*(4), e00572-00516.

Corry, J. E., Jarvis, B., Passmore, S., & Hedges, A. (2007). A critical review of measurement uncertainty in the enumeration of food micro-organisms. *Food Microbiology, 24*(3), 230-253.

Cotter, P. D., Hill, C., & Ross, R. P. (2005). Bacteriocins: developing innate immunity for food. *Nature Reviews Microbiology, 3*. doi:https://doi.org/10.1038/nrmicro1273

Couch, T. L., & Jurat-Fuentes, J. L. (2014). Commercial production of entomopathogenic bacteria. In J. A.Morales-Ramos, M. G. Rojas & D. I. S. Ilan (Eds.), *Mass Production of Beneficial Organisms* (pp. 415-435): Elsevier.

Cox, J., & Mann, M. (2007). Is proteomics the new genomics? *Cell, 130*(3), 395-398.

Cox, M. M., Goodman, M. F., Kreuzer, K. N., Sherratt, D. J., Sandler, S. J., & Marians, K. J. (2000). The importance of repairing stalled replication forks. *Nature, 404*(6773), 37-41. doi:https://doi.org/10.1038/35003501

Crickmore, N. (2006). Beyond the spore-past and future developments of *Bacillus thuringiensis* as a biopesticide. *Journal of Applied Microbiology, 101*(3), 616-619.

Crickmore, N., Zeigler, D., Feitelson, J., Schnepf, E., Van Rie, J., Lereclus, D., . . . Dean, D. (1998). Revision of the nomenclature for the *Bacillus thuringiensis* pesticidal crystal proteins. *Microbiology and Molecular Biology Reviews, 62*(3), 807-813.

Crickmore, N., Zeigler, D., Schnepf, E., Van Rie, J., Lereclus, D., Baum, J., . . . Dean, D. (2016). *Bacillus thuringiensis toxin nomenclature*. Retrieved 20th March, 2020,from http://www.btnomenclature.info

Cristea, I. M., Gaskell, S. J., & Whetton, A. D. (2004). Proteomics techniques and their application to hematology. *Blood, 103*(10), 3624-3634.

Czajgucki, Z., Andruszkiewicz, R., & Kamysz, W. (2006). Structure activity relationship studies on the antimicrobial activity of novel edeine A and D analogues. *Journal of Peptide Science, 12*. doi:https://doi.org/10.1002/psc.775

Dalton, K. M., & Crosson, S. (2010). A conserved mode of protein recognition and binding in a ParD-ParE toxin- antitoxin complex. *Biochemistry, 49*(10), 2205-2215.

Dams, D., Brøndsted, L., Drulis-Kawa, Z., & Briers, Y. (2019). Engineering of receptor-binding proteins in bacteriophages and phage tail-like bacteriocins. *47*(1), 449-460. doi:https://doi.org/10.1042/bst20180172

Dara, S. K. (2017). Insect resistance to biopesticides. *UCANR E-Journal of Entomology and Biologicals*.

Darling, A. C., Mau, B., Blattner, F. R., & Perna, N. T. (2004). Mauve: multiple alignment of conserved genomic sequence with rearrangements. *Genome Research, 14*(7), 1394-1403.

Davies, E. V., Winstanley, C., Fothergill, J. L., & James, C. E. (2016). The role of temperate bacteriophages in bacterial infection. *FEMS Microbiology Letters, 363*(5). doi:https://doi.org/10.1093/femsle/fnw015

Davis, C. (2014). Enumeration of probiotic strains: review of culture-dependent and alternative techniques to quantify viable bacteria. *Journal of Microbiological Methods, 103*, 9-17.

de Jong, A., van Hijum, S. A., Bijlsma, J. J., Kok, J., & Kuipers, O. P. (2006). BAGEL: a web-based bacteriocin genome mining tool. *Nucleic Acids Res, 34*(Web Server issue), W273-279. doi:https://doi.org/10.1093/nar/gkl237

de la Fuente-Salcido, N., Alanís-Guzmán, M. G., Bideshi, D., Salcedo-Hernández, R., Bautista-Justo, M., & Barboza-Corona, J. (2008a). Enhanced synthesis and antimicrobial activities of bacteriocins produced by Mexican strains of *Bacillus thuringiensis*. *Archives of MIicrobiology, 190*(6), 633-640. doi:https;//doi.org/10.1007/s00203-008-0414-2

de la Fuente-Salcido, N., Guadalupe Alanís-Guzmán, M., Bideshi, D. K., Salcedo-Hernández, R., Bautista-Justo, M., & Barboza-Corona, J. E. (2008b). Enhanced synthesis and antimicrobial activities of bacteriocins produced by Mexican strains of *Bacillus thuringiensis*. *Archives of Microbiology, 190*(6), 633-640. doi:https;//doi.org/10.1007/s00203-008-0414-2

de la Fuente-Salcido, N. M., Barboza-Corona, J. E., Espino Monzón, A., Pacheco Cano, R., Balagurusamy, N., Bideshi, D. K., & Salcedo-Hernández, R. (2012). Expanding the use of a fluorogenic method to determine activity and mode of action of *Bacillus thuringiensis* bacteriocins against gram-positive and gram-negative bacteria. *The Scientific World Journal, 2012*.

de la Fuente-Salcido, N. M., Casados-Vázquez, L. E., & Barboza-Corona, J. E. (2013). Bacteriocins of *Bacillus thuringiensis* can expand the potential of this bacterium to other areas rather than limit its use only as microbial insecticide. *Canadian Journal of Microbiology, 59*(8), 515-522. doi:https://doi.org/10.1139/cjm-2013-0284

De Oliveira, E. J., Rabinovitch, L., Monnerat, R. G., Passos, L. K. J., & Zahner, V. (2004). Molecular characterisation of *Brevibacillus laterosporus* and its potential use in biological control. *Applied and Environmental Microbiology, 70*(11), 6657-6664.

De Silva, R. S., Kovacikova, G., Lin, W., Taylor, R. K., Skorupski, K., & Kull, F. J. (2005). Crystal structure of the virulence gene activator AphA from *Vibrio cholerae* reveals it is a novel member of the winged helix transcription factor superfamily. *Journal of Biological Chemistry, 280*(14), 13779-13783.

De Vuyst, L., & Leroy, F. (2007). Bacteriocins from lactic acid bacteria: production, purification, and food applications. *Journal of Molecular Microbiology and Biotechnology, 13*(4), 194-199. doi:https://doi.org/10.1159/000104752

Deegan, L. H., Cotter, P. D., Hill, C., & Ross, P. (2006). Bacteriocins: biological tools for bio-preservation and shelf-life extension. *International Dairy Journal, 16*(9), 1058-1071.

Degrassi, G., Polverino De Laureto, P., & Bruschi, C. V. (1995). Purification and characterisation of ferulate and p-coumarate decarboxylase from *Bacillus pumilus*. *Applied and Environmental Microbiology, 61*(1), 326-332.

Desfosses, A., Venugopal, H., Joshi, T., Felix, J., Jessop, M., Jeong, H., . . . Gutsche, I. (2019). Atomic structures of an entire contractile injection system in both the extended and contracted states. *Nature Microbiology, 4*(11), 1885-1894.

Desjardine, K., Pereira, A., Wright, H., Matainaho, T., Kelly, M., & Andersen, R. J. (2007). Tauramamide, a lipopeptide antibiotic produced in culture by *Brevibacillus laterosporus* isolated from a marine habitat: structure elucidation and synthesis. *Journal of Natural Products, 70*(12), 1850-1853. doi:https://doi.org/10.1021/np070209r

Destoumieux-Garzón, D., Thomas, X., Santamaria, M., Goulard, C., Barthélémy, M., Boscher, B., . . . Rebuffat, S. (2003). Microcin E492 antibacterial activity: evidence for a TonB-dependent inner membrane permeabilisation on *Escherichia coli*. *Molecular Microbiology, 49*(4), 1031-1041. doi:https://doi.org/10.1046/j.1365-2958.2003.03610.x

Dhillon, A., sharma K, Rajulapati V, & A., G. (2017). Proteolytic enzymes In *Current Developments in Biotechnology and Bioengineering* (pp. 149-173): Elesvier, Radarweg 29, PO Box 211, 1000 AE Amsterdam, Netherlands. The Boulevard, Langford Lane, Kidlington, Oxford OX5 1GB, United Kingdom. 50 Hampshire Street, 5th Floor, Cambridge, MA 02139, United States. doi:https://doi.org/10.1016/B978-0-444-63662-1.00007-5

Dias, S. A., Freire, J. M., Pérez-Peinado, C., Domingues, M. M., Gaspar, D., Vale, N., . . . Castanho, M. A. (2017). New potent membrane-targeting antibacterial peptides from viral capsid proteins. *Frontiers in Microbiology, 8*, 775.

Diekmann, Y., & Pereira-Leal, J. B. (2013). Evolution of intracellular compartmentalisation. *Biochemical Journal, 449*(2), 319-331.

Diep, D. B., Axelsson, L., Grefsli, C., & Nes, I. F. (2000). The synthesis of the bacteriocin sakacin A is a temperature-sensitive process regulated by a pheromone peptide through a three-component regulatory system. *Microbiology 146 (Pt 9)*, 2155-2160. doi:https://doi.org/10.1099/00221287-146-9-2155

Dieppois, G., Opota, O., Lalucat, J., & Lemaitre, B. (2015). *Pseudomonas entomophila*: a versatile bacterium with entomopathogenic properties. In *Pseudomonas* (pp. 25-49): Springer.

Dimopoulos, G. (2003). Insect immunity and its implication in mosquito–malaria interactions. *Cellular Microbiology, 5*(1), 3-14. doi:https://doi.org/10.1046/j.1462-5822.2003.00252.x

Dion, M. B., Oechslin, F., & Moineau, S. (2020). Phage diversity, genomics and phylogeny. *18*(3), 125-138. doi:https://doi.org/10.1038/s41579-019-0311-5

Djukic, M., Poehlein, A., Thürmer, A., & Daniel, R. (2011). Genome sequence of *Brevibacillus laterosporus* LMG 15441, a pathogen of invertebrates. *Journal of Bacteriology, 193*(19), 5535-5536. doi:https://doi.org/10.1128/jb.05696-11

Dominguez, A. P. M., Bizani, D., Cladera-Olivera, F., & Brandelli, A. (2007). Cerein 8A production in soybean protein using response surface methodology. *Biochemical Engineering Journal, 35*(2), 238-243. doi:https://doi.org/10.1016/j.bej.2007.01.019

Domon, B., & Aebersold, R. (2006). Challenges and opportunities in proteomics data analysis. *Molecular and Cellular Proteomics, 5*(10), 1921-1926.

Dong, Z., Peng, D., Wang, Y., Zhu, L., Ruan, L., & Sun, M. (2013). Complete genome sequence of *Bacillus thuringiensis* bacteriophage BMBtp2. *Genome Announcements, 1*(1), e00011-00012.

Dorosky, R. J., Pierson III, L. S., & Pierson, E. A. (2018). *Pseudomonas chlororaphis* produces multiple R-tailocin particles that broaden the killing spectrum and contribute to persistence in rhizosphere communities. *Applied and Environmental Microbiology, 84*(18), e01230-01218.

Dorosky, R. J., Yu, J. M., Pierson III, L. S., & Pierson, E. A. (2017). *Pseudomonas chlororaphis* produces two distinct R-tailocins that contribute to bacterial competition in biofilms and on roots. *Applied and Environmental Microbiology, 83*(15), e00706-00717.

Dörr, T., Vulić, M., & Lewis, K. (2010). Ciprofloxacin causes persister formation by inducing the TisB toxin in *Escherichia coli*. *Plos Biology, 8*(2), e1000317.

Dowah, A. S. A., & Clokie, M. R. J. (2018). Review of the nature, diversity and structure of bacteriophage receptor binding proteins that target gram-positive bacteria. *Biophysics Review, 10*(2), 535-542. doi:https://doi.org/10.1007/s12551-017-0382-3

Duckworth, D. H. (1970). The metabolism of T4 phage ghost-infected cells: I. Macromolecular synthesis and transport of nucleic acid and protein precursors. *Virology, 40*(3), 673-684.

Duffy, S., Shackelton, L. A., & Holmes, E. C. (2008). Rates of evolutionary change in viruses: patterns and determinants. *Nature Reviews Genetics, 9*(4), 267-276.

Dunne, M., Hupfeld, M., Klumpp, J., & Loessner, M. J. (2018). Molecular basis of bacterial host interactions by gram-positive targeting bacteriophages. *Viruses, 10*(8), 397.

Durand, E., Zoued, A., Logger, L., Pehau-Arnaudet, G., Aschtgen, M.-S., Spinelli, S., . . . Roussel, A. (2015). Biogenesis and structure of a type VI secretion membrane core complex. *Nature, 523*(7562), 555-560.

Dykhuizen, D. (2005). Species numbers in bacteria. *Proceedings of California Academy of Sciences, 56*(6 Suppl 1), 62-71.

Dykhuizen, D. E. (1998). Santa Rosalia revisited: why are there so many species of bacteria? *Antonie van Leeuwenhoek, 73*(1), 25-33.

Ehlers, R. U. (2001). Mass production of entomopathogenic nematodes for plant protection. *Applied Microbiology and Biotechnology, 56*(5), 623-633.

El-Didamony, G. (2014). Occurrence of *Bacillus thuringiensis* and their phages in Yemen soil. *Virus Disease, 25*(1), 107-113.

Elayaraja, S., Annamalai, N., Mayavu, P., & Balasubramanian, T. (2014). Production, purification and characterisation of bacteriocin from *Lactobacillus murinus* AU06 and its broad antibacterial spectrum. *Asian Pacific Journal of Tropical Biomedicine, 4*(Suppl 1), S305-311. doi:https://doi.org/10.12980/apjtb.4.2014c537

Engelberg-Kulka, H., & Glaser, G. (1999). Addiction modules and programmed cell death and antideath in bacterial cultures. *Annual Review of Microbiology, 53*(1), 43-70. doi:https://doi.org/10.1146/annurev.micro.53.1.43

Ennahar, S., Sashihara, T., Sonomoto, K., & Ishizaki, A. (2000). Class IIa bacteriocins: biosynthesis, structure and activity. *FEMS Microbiology Reviews, 24*(1), 85-106.

Eppert, I., Valdés-Stauber, N., Götz, H., Busse, M., & Scherer, S. (1997). Growth reduction of *Listeria* spp. caused by undefined industrial red smear cheese cultures and bacteriocin-producing *Brevibacterium lines* as evaluated in situ on soft cheese. *Applied and Environmental Microbiology, 63*(12), 4812-4817.

Ericson, C. F., Eisenstein, F., Medeiros, J. M., Malter, K. E., Cavalcanti, G. S., Zeller, R. W., . . . Shikuma, N. J. (2019). A contractile injection system stimulates tubeworm metamorphosis by translocating a proteinaceous effector. *E-Life, 8*, e46845.

Ertürk, Ö., & Demirbag, Z. (2006). Studies on bacterial flora and biological control agent of *Cydia pomonella* L. (Lepidoptera: Tortricidae). *African Journal of Biotechnology, 5*(22).

Fagundes, P. C., Ceotto, H., Potter, A., de Paiva Brito, M. A. V., Brede, D., Nes, I. F., & de Freire Bastos, M. d. C. (2011). Hyicin 3682, a bioactive peptide produced by *Staphylococcus hyicus* 3682 with potential applications for food preservation. *Research in Microbiology, 162*(10), 1052-1059.

Fakruddin, M., Mohammad Mazumdar, R., Bin Mannan, K. S., Chowdhury, A., & Hossain, M. (2013). Critical factors affecting the success of cloning, expression, and mass production of enzymes by recombinant *Escherichia coli*. *International Scholarly Research Notices, 2013*.

Fekete, S., Beck, A., Veuthey, J. L., & Guillarme, D. (2014). Theory and practice of size exclusion chromatography for the analysis of protein aggregates. *Journal of Pharmaceutical and Biomedical Analysis, 101*, 161-173. doi:https://doi.org/10.1016/j.jpba.2014.04.011

Fernández-Fernández, A., Osuna, A., & Vilchez, S. (2021). *Bacillus pumilus* 15.1, a strain active against *Ceratitis capitata*, contains a novel phage and a phage-related particle with bacteriocin activity. *International Journal of Molecular Sciences, 22*(15), 8164.

Ferrari, J., & Vavre, F. (2011). Bacterial symbionts in insects or the story of communities affecting communities. *Philosophical Transactions of the Royal Society of London. Series B, Biological Sciences, 366*(1569), 1389-1400. doi:https://doi.org/10.1098/rstb.2010.0226

Ferré, J., & Van Rie, J. (2002). Biochemistry and genetics of insect resistance to *Bacillus thuringiensis*. *Annual Review of Entomology, 47*(1), 501-533.

Fickers, P., Leclère, V., Guez, J.-S., Béchet, M., Coucheney, F., Joris, B., & Jacques, P. (2008). Temperature dependence of mycosubtilin homologue production in *Bacillus subtilis* ATCC6633. *Research in Microbiology, 159*(6), 449-457.

Filiatrault, M. J., Munson Jr, R. S., & Campagnari, A. A. (2001). Genetic analysis of a pyocin-resistant lipooligosaccharide (LOS) mutant of *Haemophilus ducreyi*: restoration of full-length LOS restores pyocin sensitivity. *Journal of Bacteriology, 183*(19), 5756-5761.

Filloux, A. (2011). Protein secretion systems in *Pseudomonas aeruginosa*: an essay on diversity, evolution, and function. *Frontiers in Microbiology, 2*, 155.

Fischer, S., Godino, A., Quesada, J. M., Cordero, P., Jofré, E., Mori, G., & Espinosa-Urgel, M. (2012). Characterisation of a phage-like pyocin from the plant growth-promoting rhizobacterium *Pseudomonas fluorescens* SF4c. *Microbiology 158*(Pt 6), 1493-1503. doi:https://doi.org/10.1099/mic.0.056002-0

Fischetti, V. A. (2010). Bacteriophage endolysins: a novel anti-infective to control gram-positive pathogens. *International Journal of Medical Microbiology, 300*(6), 357-362.

Fisher, T., & Garczynski, S. (2012). Isolation, culture, preservation, and identification of entomopathogenic bacteria of the *Bacilli*. In L. A. Lacey (Ed.), *Manual of Techniques in Invertebrate Pathology. Academic Press, London* (2 ed., pp. 75-98): Elsevier.

Fister, S., Robben, C., Witte, A. K., Schoder, D., Wagner, M., & Rossmanith, P. (2016). Influence of environmental factors on phage-bacteria interaction and on the efficacy and infectivity of phage P100. *Frontiers in Microbiology, 7*, 1152.

Florez, A. B., Alvarez, S., Zabala, D., Brana, A. F., Salas, J. A., & Mendez, C. (2015). Transcriptional regulation of mithramycin biosynthesis in *Streptomyces argillaceus*: dual role as activator and repressor of the PadR-like regulator MtrY. *Microbiology, 161*(2), 272-284.

Floris, I., Ruiu, L., Satta, A., Delrio, G., Rubino, S., Paglietti, B., . . . Pantaleoni, R. A., &. (2011). *Brevibacillus laterosporus strain compositions containing the same and method for the biological control of dipters*. US Patent No. 8,076,119 B2 Washington, DC: U.S. Patent and Trademark Office..

Flühe, L., Burghaus, O., Wieckowski, B. M., Giessen, T. W., Linne, U., & Marahiel, M. A. (2013). Two [4Fe-4S] clusters containing radical SAM enzyme SkfB catalyze thioether bond formation during the maturation of the sporulation killing factor. *Journal of American Chemical Society, 135*(3), 959-962. doi:https://doi.org/10.1021/ja310542g

Fokine, A., & Rossmann, M. G. (2014). Molecular architecture of tailed double-stranded DNA phages. *Bacteriophage, 4*(1), e28281-e28281. doi:https://doi.org/10.4161/bact.28281

Forsgren, E. (2010). European foulbrood in honey bees. *Journal of Invertebrate Pathology, 103*, S5-S9. doi:https://doi.org/10.1016/j.jip.2009.06.016

Fortier, L.-C. (2017). The contribution of bacteriophages to the biology and virulence of pathogenic *Clostridia*. *Advances in Applied Microbiology, 101*, 169-200.

Fortier, L.-C., & Sekulovic, O. (2013). Importance of prophages to evolution and virulence of bacterial pathogens. *Virulence, 4*(5), 354-365.

Foster, K. R., & Bell, T. (2012). Competition, not cooperation, dominates interactions among culturable microbial species. *Current Biology, 22*(19), 1845-1850. doi:https://doi.org/10.1016/j.cub.2012.08.005

Frankenhuyzen, K. v. (2009). Insecticidal activity of *Bacillus thuringiensis* crystal proteins. *Journal of Invertebrate Pathology, 101*(1), 1-16. doi:https://doi.org/10.1016/j.jip.2009.02.009

Freire, J. M., Almeida Dias, S., Flores, L., Veiga, A. S., & Castanho, M. A. (2015a). Mining viral proteins for antimicrobial and cell-penetrating drug delivery peptides. *Bioinformatics, 31*(14), 2252-2256.

Freire, J. M., Santos, N. C., Veiga, A. S., Da Poian, A. T., & Castanho, M. A. (2015b). Rethinking the capsid proteins of enveloped viruses: multifunctionality from genome packaging to genome transfection. *The FEBS Journal, 282*(12), 2267-2278.

Furlong, M. J., Wright, D. J., & Dosdall, L. M. (2013). Diamondback moth ecology and management: problems, progress, and prospects. *Annual Review of Entomology, 58*, 517-541.

Gabashvili, A. N., Chmelyuk, N. S., Efremova, M. V., Malinovskaya, J. A., Semkina, A. S., & Abakumov, M. A. (2020). Encapsulins-bacterial protein nanocompartments: Structure, properties, and application. *Biomolecules, 10*(6), 966. doi:https://doi.org/10.3390/biom10060966

Galán, J. E., & Waksman, G. (2018). Protein-injection machines in bacteria. *Cell, 172*(6), 1306-1318. doi:https://doi.org/10.1016/j.cell.2018.01.034

Gallet, R., Kannoly, S., & Wang, I.-N. (2011). Effects of bacteriophage traits on plaque formation. *BMC Microbiology, 11*(1), 181. doi:https://doi.org/10.1186/1471-2180-11-181

Garnier, M., Foissac, X., Gaurivaud, P., Laigret, F., Renaudin, J., Saillard, C., & Bové, J. (2001). Mycoplasmas, plants, insect vectors: a matrimonial triangle. *Comptes Rendus de l'Académie des Sciences-Series III-Sciences de la Vie, 324*(10), 923-928.

Garro, A. J., & Marmur, J. (1970). Defective bacteriophages. *Journal of Cellular Physiology, 76*(3), 253-263.

Gautam, A., Chaudhary, K., Kumar, R., Sharma, A., Kapoor, P., Tyagi, A., & Raghava, G. P. (2013). In silico approaches for designing highly effective cell penetrating peptides. *Journal of Translational Medicine, 11*(1), 1-12.

Ge, J., Kang, J., & Ping, W. (2019). Effect of acetic acid on bacteriocin production by gram-positive bacteria. *Journal of Microbiology and Biotechnology, 29*(9), 1341-1348. doi:https://doi.org/10.4014/jmb.1905.05060

Ge, P., Scholl, D., Leiman, P. G., Yu, X., Miller, J. F., & Zhou, Z. H. (2015). Atomic structures of a bactericidal contractile nanotube in its pre-and postcontraction states. *Nature Structural and Molecular Biology, 22*(5), 377-382.

Ge, P., Scholl, D., Prokhorov, N. S., Avaylon, J., Shneider, M. M., Browning, C., . . . Ding, K. (2020). Action of a minimal contractile bactericidal nanomachine. *Nature, 580*(7805), 658-662.

Gebhart, D., Williams, S. R., Bishop-Lilly, K. A., Govoni, G. R., Willner, K. M., Butani, A., . . . Scholl, D. (2012). Novel high-molecular-weight, R-type bacteriocins of *Clostridium difficile*. *Journal of Bacteriology, 194*(22), 6240-6247.

Gerard, J., Haden, P., Kelly, M. T., & Andersen, R. J. (1996). Loloatin B, a cyclic decapeptide antibiotic produced in culture by a tropical marine bacterium. *Tetrahedron Letters, 37*. doi:https://doi.org/10.1016/0040-4039(96)01624-3

Ghadbane, M., Harzallah, D., Laribi, A. I., Jaouadi, B., & Belhadj, H. (2013). Purification and biochemical characterisation of a highly thermostable bacteriocin isolated from *Brevibacillus brevis* strain GM100. *Bioscience, Biotechnology, and Biochemistry*, 120681.

Ghazanchyan, N., Kinosyan, M., Tadevosyan, P., Khachaturyan, N., & Afrikian, E. (2018). *Brevibacillus laterosporus* as perspective source of new bioinsecticides. *Annals of Agrarian Science, 16*(4), 413-415.

Ghequire, M. G., & De Mot, R. (2014). Ribosomally encoded antibacterial proteins and peptides from *Pseudomonas*. *FEMS Microbiology Review, 38*(4), 523-568. doi:https://doi.org/10.1111/1574-6976.12079

Ghequire, M. G., & De Mot, R. (2015). The tailocin tale: peeling off phage tails. *Trends in Microbiology, 23*(10), 587-590.

Ghoul, M., & Mitri, S. (2016). The ecology and evolution of microbial competition. *Trends in Microbiology, 24*(10), 833-845.

Giessen, T. W., Orlando, B. J., Verdegaal, A. A., Chambers, M. G., Gardener, J., Bell, D. C., . . . Silver, P. A. (2019). Large protein organelles form a new iron sequestration system with high storage capacity. *E-Life, 8*, e46070. doi:https://doi.org/10.7554/eLife.46070

Giessen, T. W., & Silver, P. A. (2017). Widespread distribution of encapsulin nanocompartments reveals functional diversity. *Nature Microbiology, 2*, 17029. doi:https://doi.org/10.1038/nmicrobiol.2017.29

Gillis, A., & Mahillon, J. (2014). Phages preying on *Bacillus anthracis*, *Bacillus cereus*, and *Bacillus thuringiensis*: past, present and future. *Viruses, 6*(7), 2623-2672.

Gillor, O., Kirkup, B. C., & Riley, M. A. (2004). Colicins and microcins: the next generation antimicrobials. *Advances in Applied Microbiology, 54*(18), 129-146.

Glare, T., Caradus, J., Gelernter, W., Jackson, T., Keyhani, N., Köhl, J., . . . Stewart, A. (2012). Have biopesticides come of age? *Trends in Biotechnology, 30*(5), 250-258.

Glare, T. R., Durrant, A., Berry, C., Palma, L., Ormskirk, M. M., & Cox, M. P. (2020). Phylogenetic determinants of toxin gene distribution in genomes of *Brevibacillus laterosporus*. *Genomics, 112*(1), 1042-1053.

Glare, T. R., Hampton, J. G., Cox, M. P., & Bienkowski, D. A., &. (2014). *Novel strains of Brevibacillus laterosporus as biocontrol agents against plant pests, particularly lepidoptera and diptera*.

International Publication No. WO 2014/045131 A9. World Intellectual Property Organisation International Bureau. Google Patent

Glare, T. R., Hampton, J. G., Cox, M. P., & Bienkowski, D. A., &. (2018). *Biocontrol compositions*. USA Patent No. 10,004,236 B2. Washington, DC: U.S. Patent and Trademark Office.

Glare, T. R., Jurat-Fuentes, J. L., & O'Callaghan, M. (2017). Basic and applied research: Entomopathogenic bacteria. In L. A. Lacey (Ed.), *Microbial control of insect and mite pests from theory to practice* (pp. 47-67): Elsevier. Retrieved from https://www.sciencedirect.com/science/article/pii/B9780128035276000044. doi:https://doi.org/10.1016/B978-0-12-803527-6.00004-4

Glare, T. R., & O'Callaghan, M. (2000). *Bacillus thuringiensis: Biology, ecology and safety.* : John Wiley & Sons.

Gnezda-Meijer, K., Mahne, I., Poljsak-Prijatelj, M., & Stopar, D. (2006). Host physiological status determines phage-like particle distribution in the lysate. *FEMS Microbiology Ecology, 55*(1), 136-145. doi:https://doi.org/10.1111/j.1574-6941.2005.00008.x

Goldman, E. (2021). Plaque assay for bacteriophage. In L. H. Green & E. Goldman (Eds.), *Practical Handbook of Microbiology* (4th ed., pp. 71-74): CRC Press.

Gong, H., Meng, X., & Wang, H. (2010). Plantaricin MG active against gram-negative bacteria produced by *Lactobacillus plantarum* KLDS1. 0391 isolated from "Jiaoke", a traditional fermented cream from China. *Food Control, 21*(1), 89-96.

González-Pastor, J. E. (2011). Cannibalism: a social behavior in sporulating *Bacillus subtilis*. *FEMS Microbiology Reviews, 35*(3), 415-424. doi:https://doi.org/10.1111/j.1574-6976.2010.00253.x

González-Pastor, J. E., Hobbs, E. C., & Losick, R. (2003). Cannibalism by sporulating bacteria. *Science, 301*(5632), 510-513. doi:https://doi.org/10.1126/science.1086462

Gonzalez, D., & Mavridou, D. A. (2019). Making the best of aggression: the many dimensions of bacterial toxin regulation. *Trends in Microbiology, 27*(11), 897-905.

Gordon, D. M., Oliver, E., & Littlefield-Wyer, J. (2007). The diversity of bacteriocins in gram-negative bacteria. In M. A. Riley & M. A. Chavan (Eds.), *Bacteriocins: Ecology and evolution* (1st ed., pp. 5-18). Berlin, Heidelberg: Springer Berlin Heidelberg. doi:https://doi.org/10.1007/978-3-540-36604-12

Gormley, N. A., Watson, M. A., & Halford, S. E. (2001). Bacterial restriction-modification systems. *E-Life Science*.

Govan, J. (1974). Studies on the pyocins of *Pseudomonas aeruginosa*: production of contractile and flexuous pyocins in *Pseudomonas aeruginosa*. *Microbiology, 80*(1), 17-30.

Grabow, W. O. K. (2001). Bacteriophages : update on application as models for viruses in water. *Water SA, 27*(2), 251-268. doi:https://doi.org/10.4314/wsa.v27i2.4999

Gram, C. (1884). Ueber die isolirte Farbung der Schizomyceten in Schnitt-und Trockenpraparaten. *Fortschritte der Medicin, 2*, 185-189.

Granato, E. T., & Foster, K. R. (2020). The evolution of mass cell suicide in bacterial warfare. *Current Biology, 30*(14), 2836-2843. e2833.

Granato, E. T., Meiller-Legrand, T. A., & Foster, K. R. (2019). The evolution and ecology of bacterial warfare. *Current Biology, 29*(11), R521-R537.

Grant, R., Filman, D., Finkel, S., Kolter, R., & Hogle, J. (1998). The crystal structure of Dps, a ferritin homolog that binds and protects DNA. *Nature Structural Biology, 5*(4), 294-303.

Gratia, A. (1925). Sur un remarquable exemple d'antagonisme entre deux souches de coilbacille. *CR Seances Soc. Biol. Fil., 93*, 1040-1041.

Gratia, A. (1936). The numerical relation between lysogenic bacteria and the phage particles which they carry. *Annual Institute of Pasteur, 57*, 652-676.

Grimont, P. A., Grimont, F., & Lysenko, O. (1979). Species and biotype identification of *Serratia* strains associated with insects. *Current Microbiology, 2*(3), 139-142.

Groth, A. C., & Calos, M. P. (2004). Phage integrases: Biology and applications. *Journal of Molecular Biology, 335*(3), 667-678. doi:https://doi.org/10.1016/j.jmb.2003.09.082

Gründling, A., Manson, M. D., & Young, R. (2001). Holins kill without warning. *Proceedings of the National Academy of Sciences, 98*(16), 9348-9352.

Guerra, N. P. (2014). Modeling the batch bacteriocin production system by lactic acid bacteria by using modified three-dimensional Lotka–Volterra equations. *Biochemical Engineering Journal, 88*, 115-130. doi:https://doi.org/10.1016/j.bej.2014.04.010

Gumpert, J., & Taubeneck, U. (1968). Microtubules in *Proteus mirabilis* as a result of defective lysogeny. *Zeitschrift Fur Allgemeine Mikrobiologie, 8*(2), 101-105.

Gury, J., Barthelmebs, L., Tran, N. P., Diviès, C., & Cavin, J. F. (2004). Cloning, deletion, and characterisation of PadR, the transcriptional repressor of the phenolic acid decarboxylase-encoding padA gene of *Lactobacillus plantarum* [Article]. *Applied and Environmental Microbiology, 70*(4), 2146-2153. doi:https://doi.org/10.1128/AEM.70.4.2146-2153.2004

Haas, M., & Yoshikawa, H. (1969). Defective bacteriophage PBSH in *Bacillus subtilis*: I. Induction, purification, and physical properties of the bacteriophage and its deoxyribonucleic acid. *Journal of Virology, 3*(2), 233-247.

Hadfield, M. G. (2011). Biofilms and marine invertebrate larvae: what bacteria produce that larvae use to choose settlement sites. *Annual Review of Marine Science, 3*, 453-470.

Hambly, E., & Suttle, C. A. (2005). The viriosphere, diversity, and genetic exchange within phage communities. *Current Opinion in Microbiology, 8*(4), 444-450.

Hannay, C. L. (1957). The parasporal body of *Bacillus laterosporus* Laubach. *The Journal of Cell Biology, 3*(6), 1001-1010.

Harcourt, D. (1957). Biology of the diamondback moth, *Plutella maculipennis* (Curt.)(Lepidoptera: Plutellidae), in Eastern Ontario. II. Life-history, behaviour, and host relationships. *The Canadian Entomologist, 89*(12), 554-564.

Hardies, S. C., Thomas, J. A., & Serwer, P. (2007). Comparative genomics of *Bacillus thuringiensis* phage 0305ϕ8-36: defining patterns of descent in a novel ancient phage lineage. *Virology Journal, 4*(1), 1-17.

Harrison, E., & Brockhurst, M. A. (2017a). Ecological and evolutionary benefits of temperate phage: what does or doesn't kill you makes you stronger. *BioEssays, 39*(12), 1700112. doi:https://doi.org/10. 1002/bies.201700112

Harrison, E., & Brockhurst, M. A. (2017b). Ecological and evolutionary benefits of temperate phage: What does or doesn't kill you makes you stronger. *BioEssays, 39*(12),1700112. doi:https://doi.org/10. 1002/bies.201700112

Harrison, P. M., & Arosio, P. (1996). The ferritins: molecular properties, iron storage function and cellular regulation. *Biochimica et Biophysica Acta- Bioenergetics, 1275*(3), 161-203. doi:https://doi.org/10.1016/0005-2728(96)00022-9

Hartford, O. M., & Dowds, B. C. (1992). Cloning and characterisation of genes induced by hydrogen peroxide in *Bacillus subtilis*. *Journal of General Microbiology, 138*(10), 2061-2068. doi:https://doi.org/10.1099/00221287-138-10-2061

Hata, T., Tanaka, R., & Ohmomo, S. (2010). Isolation and characterisation of plantaricin ASM1: A new bacteriocin produced by *Lactobacillus plantarum* A-1. *International Journal of Food Microbiology, 137*(1), 94-99. doi:https://doi.org/10.1016/j.ijfoodmicro.2009.10.021

Hatfull, G. F. (2001). The great escape. *Science, 292*(5525), 2263-2264.

Hazan, R., Que, Y. A., Maura, D., & Rahme, L. G. (2012). A method for high throughput determination of viable bacteria cell counts in 96-well plates. *BMC Microbiology, 12*, 259. doi:10.1186/1471-2180-12-259

He, D., Hughes, S., Vanden-Hehir, S., Georgiev, A., Altenbach, K., Tarrant, E., . . . Marles-Wright, J. (2016a). Structural characterisation of encapsulated ferritin provides insight into iron storage in bacterial nanocompartments. *E-Life, 5*, e18972. doi:https://doi.org/10.7554/eLife.18972

He, D., Hughes, S., Vanden-Hehir, S., Georgiev, A., Altenbach, K., Tarrant, E., . . . Marles-Wright, J. (2016b). Structural characterisation of encapsulated ferritin provides insight into iron storage in bacterial nanocompartments. *E-Life, 5*, e18972. doi:https://doi.org/10.7554/eLife.18972

He, D., & Marles-Wright, J. (2015). Ferritin family proteins and their use in bionanotechnology. *New Biotechnology, 32*(6), 651-657. doi:https://doi.org/10.1016/j.nbt.2014.12.006

Hedges, A. J. (2002). Estimating the precision of serial dilutions and viable bacterial counts. *International Journal of Food Microbiology, 76*(3), 207-214. doi:https://doi.org/10.1016/s0168-1605(02)00022-3

Hegarty, J. P., Sangster, W., Ashley, R. E., Myers, R., Hafenstein, S., & Stewart, D. B., Sr. (2016). Induction and purification of *Clostridium difficile* phage tail-like particles. *Methods in Molecular Biology, 1476*, 167-175. doi:https://doi.org/10.1007/978-1-4939-6361-4_12

Heinemann, J., Maaty, W. S., Gauss, G. H., Akkaladevi, N., Brumfield, S. K., Rayaprolu, V., . . . Bothner, B. (2011). Fossil record of an archaeal HK97-like provirus. *Virology, 417*(2), 362-368.

Held, G. A., Bulla, L. A., Ferrari, E., Hoch, J., Aronson, A. I., & Minnich, S. A. (1982). Cloning and localisation of the lepidopteran protoxin gene of *Bacillus thuringiensis* subsp. *kurstaki*. *Proceedings of the National Academy of Sciences, 79*(19), 6065-6069.

Hemphill, H. E., & Whiteley, H. (1975). Bacteriophages of *Bacillus subtilis*. *Bacteriological Reviews, 39*(3), 257-315.

Hendrix, R. W. (1999). Evolution: the long evolutionary reach of viruses. *Current Biology, 9*(24), R914-R917.

Hendrix, R. W. (2002). Bacteriophages: evolution of the majority. *Theoretical Population Biology, 61*(4), 471-480.

Heng, N. C. K., Wescombe, P. A., Burton, J. P., Jack, R. W., & Tagg, J. R. (2007). The diversity of bacteriocins in gram-positive bacteria. In M. A. Riley & M. A. Chavan (Eds.), *Bacteriocins: Ecology and evolution* (pp. 45-92). Berlin, Heidelberg: Springer Berlin Heidelberg.

Henriques, S. T., Melo, M. N., & Castanho, M. A. (2006). Cell penetrating peptides and antimicrobial peptides: How different are they? *Biochemical Journal, 399*(1), 1-7.

Herzner, A. M., Dischinger, J., Szekat, C., Josten, M., Schmitz, S., Yakéléba, A., . . . Bierbaum, G. (2011). Expression of the lantibiotic mersacidin in *Bacillus amyloliquefaciens* FZB42. *Plos One, 6*(7), e22389. doi:https://doi.org/10.1371/journal.pone.0022389

Heymann, J. B., Bartho, J. D., Rybakova, D., Venugopal, H. P., Winkler, D. C., Sen, A., . . . Mitra, A. K. (2013). Three-dimensional structure of the toxin-delivery particle antifeeding prophage of *Serratia entomophila*. *Journal of Biological Chemistry, 288*(35), 25276-25284.

Hibbing, M. E., Fuqua, C., Parsek, M. R., & Peterson, S. B. (2010). Bacterial competition: surviving and thriving in the microbial jungle. *Nature Reviews Microbiology, 8*(1), 15-25. doi:https://doi.org/10.1038/nrmicro2259

Hicks, P. M., Rinker, K. D., Baker, J. R., & Kelly, R. M. (1998). Homomultimeric protease in the hyperthermophilic bacterium *Thermotoga maritima* has structural and amino acid sequence homology to bacteriocins in mesophilic bacteria. *FEBS Letters, 440*(3), 393-398. doi:https://doi.org/10.1016/S0014-5793(98)01451-3

Higerd, T. B., Baechler, C. A., & Berk, R. S. (1967). In vitro and in vivo characterisation of pyocin. *Journal of Bacteriology, 93*(6), 1976-1986.

Ho, B. T., Dong, T. G., & Mekalanos, J. J. (2014). A view to a kill: the bacterial type VI secretion system. *Cell Host and Microbe, 15*(1), 9-21. doi:https://doi.org/10.1016/j.chom.2013.11.008

Hockett, K. L., & Baltrus, D. A. (2017). Use of the soft-agar overlay technique to screen for bacterially produced inhibitory compounds. *Journal of Visualised Experiments: JoVE*(119).

Hockett, K. L., Renner, T., & Baltrus, D. A. (2015). Independent co-option of a tailed bacteriophage into a killing complex in *Pseudomonas*. *ASM Journals mBio, 6*(4), e00452. doi:https://doi.org/10.1128/mBio.00452-15

Höfler, C., Heckmann, J., Fritsch, A., Popp, P., Gebhard, S., Fritz, G., & Mascher, T. (2016). Cannibalism stress response in *Bacillus subtilis*. *Microbiology, 162*(1), 164-176. doi:https://doi.org/10.1099/mic.0.000176

Holtzman, T., Globus, R., Molshanski-Mor, S., Ben-Shem, A., Yosef, I., & Qimron, U. (2020). A continuous evolution system for contracting the host range of bacteriophage T7. *Scientific Reports, 10*(1), 1-8.

Hong, P., Koza, S., & Bouvier, E. S. (2012a). Size exclusion chromatography for the analysis of protein biotherapeutics and their aggregates. *Journal of Liquid Chromatoghy and Related Technologies, 35*(20), 2923-2950. doi:https://doi.org/10.1080/10826076.2012.743724

Hong, S. H., Wang, X., O'Connor, H. F., Benedik, M. J., & Wood, T. K. (2012b). Bacterial persistence increases as environmental fitness decreases. *Microbial Biotechnology, 5*(4), 509-522.

Hood, R. D., Singh, P., Hsu, F., Güvener, T., Carl, M. A., Trinidad, R. R., . . . Plemel, R. L. (2010). A type VI secretion system of *Pseudomonas aeruginosa* targets a toxin to bacteria. *Cell Host and Microbe, 7*(1), 25-37.

Howard-Varona, C., Hargreaves, K. R., Abedon, S. T., & Sullivan, M. B. (2017). Lysogeny in nature: mechanisms, impact and ecology of temperate phages. *The ISME Journal, 11*(7), 1511-1520.

Howard, S. A., & Filloux, A. (2019). Bacterial protein secretion: Looking inside an injection system. *E-Life, 8*, e50815.

Hu, W., Murata, K., & Zhang, D. (2017). Applicability of LIVE/DEAD BacLight stain with glutaraldehyde fixation for the measurement of bacterial abundance and viability in rainwater. *Journal of Environmental Sciences, 51*, 202-213.

Hudson, J. A., & Mott, S. J. (1994). Comparison of lag times obtained from optical density and viable count data for a strain of *Pseudomonas fragi*. *Journal of Food Safety, 14*(4), 329-339.

Hudzicki, J. (2009). *Kirby-Bauer disc diffusion susceptibility test protocol*. Retrieved 15th December, 2018,from https://asm.org/a/ASMScience

Humphrey, S. B., Stanton, T. B., & Jensen, N. S. (1995). Mitomycin C induction of bacteriophages from *Serpulina hyodysenteriae* and *Serpulina innocens*. *FEMS Microbiology Letters, 134*(1), 97-101.

Hurst, M. R., Beattie, A., Jones, S. A., Laugraud, A., van Koten, C., & Harper, L. (2018). *Serratia proteamaculans* strain AGR96X encodes an antifeeding prophage (tailocin) with activity against grass grub (*Costelytra giveni*) and Manuka beetle (*Pyronota species*) larvae. *Applied and Environmental Microbiology, 84*(10), e02739-02717.

Hurst, M. R., Glare, T. R., & Jackson, T. A. (2004). Cloning *Serratia entomophila* antifeeding genes-a putative defective prophage active against the grass grub *Costelytra zealandica*. *Journal of Bacteriology, 186*(15), 5116-5128.

Hurst, M. R. H., Jones, S. A., Beattie, A., van Koten, C., Shelton, A. M., Collins, H. L., & Brownbridge, M. (2019). Assessment of *Yersinia entomophaga* as a control agent of the diamondback moth *Plutella xylostella*. *Journal of Invertebrate Pathology, 162*, 19-25.

Hyman, P., & Abedon, S. T. (2010). Bacteriophage host range and bacterial resistance. *Advances in Applied Microbiology, 70*, 217-248.

Hyman, P., & Abedon, S. T. (2019). Bacteriophage: overview.

Idris, H. A., Labuschagne, N., & Korsten, L. (2008). Suppression of *Pythium ultimum* root rot of sorghum by rhizobacterial isolates from Ethiopia and South Africa. *Biological Control, 45*(1), 72-84.

Imlay, J. A. (2002). How oxygen damages microbes: oxygen tolerance and obligate anaerobiosis. *Advances in Microbial Physiology, 46*, 111-153. doi:https://doi.org/10.1016/s0065-2911(02)46003-1

Imlay, J. A. (2015). Diagnosing oxidative stress in bacteria: not as easy as you might think. *Current Opinion in Microbiology, 24*, 124-131.

Islam, M. Z., Fokine, A., Mahalingam, M., Zhang, Z., Garcia-Doval, C., van Raaij, M. J., . . . Rao, V. B. (2019). Molecular anatomy of the receptor binding module of a bacteriophage long tail fibre. *Plos Pathogens, 15*(12), e1008193.

Ito, S., Nishimune, T., Abe, M., Kimoto, M., & Hayashi, R. (1986). Bacteriocin like killing action of a temperate bacteriophage phiBA1 of *Bacillus aneurinolyticus*. *Journal of Virology, 59*(1), 103-111.

Jabrane, A., Sabri, A., Compere, P., Jacques, P., Vandenberghe, I., Van Beeumen, J., & Thonart, P. (2002a). Characterisation of serracin P, a phage-tail-like bacteriocin, and its activity against *Erwinia amylovora*, the fire blight pathogen. *Applied and Environmental Mcrobiology, 68*(11), 5704-5710. doi:https://doi.org/10.1128/aem.68.11.5704-5710.2002

Jabrane, A., Sabri, A., Compère, P., Jacques, P., Vandenberghe, I., Van Beeumen, J., & Thonart, P. (2002b). Characterization of serracin P, a phage-tail-like bacteriocin, and its activity against *Erwinia amylovora*, the fire blight pathogen. *Appllied and Environmental Microbiology, 68*(11), 5704-5710. doi:10.1128/aem.68.11.5704-5710.2002

Jack, R. W., Tagg, J. R., & Ray, B. (1995). Bacteriocins of gram-positive bacteria. *Microbiological Reviews, 59*(2), 171-200.

Jackson, T. A. (2017). Chapter 8 - Entomopathogenic bacteria: Mass production, formulation, and quality control. In L. A. Lacey (Ed.), *Microbial Control of Insect and Mite Pests* (pp. 125-139):

Academic Press. Retrieved from https://www.sciencedirect.com/science/article/pii/B9780128035276000081. doi:https://doi.org/10.1016/B978-0-12-803527-6.00008-1

Jackson, T. A., Pearson, J., O'callaghan, M., Mahanty, H., & Willocks, M. (1992). Pathogen to product-development of *Serratia entomophila* (Enterobacteriaceae) as a commercial biological control agent for the New Zealand grass grub (*Costelytra zealandica*). *Use of pathogens in scarab pest management/edited by Trevor A. Jackson and Travis R. Glare*.

Jacob, F., & Wollman, E. L. (1953). Induction of phage development in lysogenic bacteria. *Cold Spring Harbor Laboratory Press.* Symposium conducted at the meeting of the Cold Spring Harbor symposia on quantitative biology

Jallouli, W., Driss, F., Fillaudeau, L., & Rouis, S. (2020). Review on biopesticide production by *Bacillus thuringiensis* subsp. *kurstaki* since 1990: Focus on bioprocess parameters. *Process Biochemistry, 98*, 224-232. doi:https://doi.org/10.1016/j.procbio.2020.07.023

Järver, P., & Langel, Ü. (2006). Cell penetrating peptides- a brief introduction. *Biochimica et Biophysica Acta- Biomembranes, 3*(1758), 260-263.

Jatoi, G. H., Lihua, G., Xiufen, Y., Gadhi, M. A., Keerio, A. U., Abdulle, Y. A., & Qiu, D. (2019). A novel protein elicitor PeBL2, from *Brevibacillus laterosporus* A60, induces systemic resistance against *Botrytis cinerea* in tobacco plant. *The Plant Pathology Journal, 35*(3), 208.

Jayaraman, R. (2008). Bacterial persistence: some new insights into an old phenomenon. *Journal of Bioscience, 33*(5), 795-805. doi:https://doi.org/10.1007/s12038-008-0099-3

Jayawardene, A., & Farkas-Himsley, H. (1968). Particulate nature of vibriocin: a bacteriocin from *Vibrio comma*. *Nature, 219*(5149), 79-80. doi:https://doi.org/10.1038/219079a0

Jeong, H., Jeong, D. E., Park, S. H., Kim, S. J., & Choi, S. K. (2018). Complete genome sequence of *Bacillus subtilis* strain WB800N, an extracellular protease-deficient derivative of strain 168. *Microbiology Resource Announcements, 7*(18). doi:https://doi.org/10.1128/mra.01380-18

Jeziorowski, A., & Gordon, D. M. (2007). Evolution of mcrocin V and colicin Ia lasmids in *Escherichia coli*. *Journal of Bacteriology, 189*(19), 7045-7052. doi:https://doi.org/doi:10.1128/JB.00243-07

Jin, T., Zhang, X., Zhang, Y., Hu, Z., Fu, Z., Fan, J., . . . Chen, X. (2014). Biological and genomic analysis of a PBSX-like defective phage induced from *Bacillus pumilus* AB94180. *Archives of Virology, 159*(4), 739-752. doi:https://doi.org/10.1007/s00705-013-1898.x

Joerger, M. C., & Klaenhammer, T. R. (1986). Characterisation and purification of helveticin J and evidence for a chromosomally determined bacteriocin produced by *Lactobacillus helveticus* 481. *Journal of Bacteriology, 167*(2), 439-446.

Johnson, V., Pearson, J., & Jackson, T. (2001). Formulation of *Serratia entomophila* for biological control of grass grub. *New Zealand Plant Protection, 54*, 125-127.

Jones, D. T., Shirley, M., Wu, X., & Keis, S. (2000). Bacteriophage infections in the industrial acetone butanol (AB) fermentation process. *Journal of Molecular Microbiology and Biotechnology, 2*(1), 21-26.

Jones, S. A., & Hurst, M. R. (2016). Purification of the *Yersinia entomophaga* Yen-TC toxin complex using size exclusion chromatography. *Methods in Molecular Biology, 1477*, 39-48. doi:https://doi.org/10.1007/978-1-4939-6367-6_4

Journet, L., & Cascales, E. (2016). The type VI secretion system in *Escherichia coli* and related species. *EcoSal Plus, 7*(1).

Joux, F., & Lebaron, P. (2000). Use of fluorescent probes to assess physiological functions of bacteria at single-cell level. *Microbes and Infection, 2*(12), 1523-1535. doi:https://doi.org/10.1016/s1286-4579(00)01307-1

Juárez-Pérez, V., & Delécluse, A. (2001). The Cry toxins and the putative hemolysins of *Clostridium bifermentans* ser. Malaysia are not involved in mosquitocidal activity. *Journal of Invertebrate Pathology, 1*(78), 57-58.

Jurat-Fuentes, J. L., & Jackson, T. A. (2012). Bacterial entomopathogens. In F. E. Vega & H. K. Kaya (Eds.), *Insect Pathology* (2nd ed., pp. 265-349): Elsevier. Retrieved from https://www.sciencedirect.com/science/article/pii/B9780123849847000087. doi:https://doi.org/10.1016/B978-0-12-384984-7.00008-7

Juturu, V., & Wu, J. C. (2018). Microbial production of bacteriocins: Latest research development and applications. *Biotechnology Advances, 36*(8), 2187-2200. doi:https://doi.org/10.1016/j.biotechadv.2018.10.007

Kabaluk, T., & Gazdik, K., &. (2005). *Directory of microbial pesticides for agricultural crops in OECD countries, Agriculture and Agri-food Canada*.

Kaewklom, S., Lumlert, S., Kraikul, W., & Aunpad, R. (2013). Control of *Listeria monocytogenes* on sliced bologna sausage using a novel bacteriocin, amysin, produced by *Bacillus amyloliquefaciens* isolated from Thai shrimp paste (Kapi). *Food Control, 32*(2), 552-557.

Kageyama, M. (1975). Bacteriocins and bacteriophages in *Pseudomonas aeruginosa*. *Microbial Drug Resistance*, 291-305.

Kageyama, M., & Egami, F. (1962). On the purification and some properties of a pyocin, a bacteriocin produced by *Pseudomonas aeruginosa*. *Life Sciences, 1*(9), 471-476.

Kaji, K., Tomino, S., & Asano, T. (2009). A serine protease in the midgut of the silkworm, *Bombyx mori*: protein sequencing, identification of cDNA, demonstration of its synthesis as zymogen form and activation during midgut remodeling. *Insect Biochemistry and Molecular Biology, 39*(3), 207-217. doi:https://doi.org/10.1016/j.ibmb.2008.12.001

Kakar, K. U., Nawaz, Z., Cui, Z., Almoneafy, A. A., Zhu, B., & Xie, G. L. (2014). Characterising the mode of action of *Brevibacillus laterosporus* B4 for control of bacterial brown strip of rice caused by *A. avenae subsp. avenae* RS-1. *World Journal of Microbiology and Biotechnology, 30*(2), 469-478.

Kallberg, K., Johansson, H. O., & Bulow, L. (2012). Multimodal chromatography: an efficient tool in downstream processing of proteins. *Biotechnology Journal, 7*(12), 1485-1495. doi:https://doi.org/10.1002/biot.201200074

Kamada, K., Hanaoka, F., & Burley, S. K. (2003). Crystal structure of the MazE/MazF complex: molecular bases of antidote-toxin recognition. *Molecular Cell, 11*(4), 875-884.

Kandel, P. P., & Baltrus, D. A. (2020). *Pseudomonas* can survive tailocin killing via persistence-like and heterogenous resistance mechanisms. *202*(13). doi:https://doi.org/10.1128/jb.00142-20

Kang, J. H., & Lee, M. S. (2005). Characterisation of a bacteriocin produced by *Enterococcus faecium* GM-1 isolated from an infant. *Journal of Applied Microbiology, 98*(5), 1169-1176. doi:https://doi.org/10.1111/j.1365-2672.2005.02556.x

Kapitein, N., & Mogk, A. (2013). Deadly syringes: type VI secretion system activities in pathogenicity and interbacterial competition. *Current Opinion in Microbiology, 16*(1), 52-58.

Kawamoto, S., Watanabe, M., Saito, N., Hesketh, A., Vachalova, K., Matsubara, K., & Ochi, K. (2001). Molecular and functional analyses of the gene (eshA) encoding the 52-kilodalton protein of *Streptomyces coelicolor* A3 (2) required for antibiotic production. *Journal of Bacteriology, 183*(20), 6009-6016.

Kearse, M., Moir, R., Wilson, A., Stones-Havas, S., Cheung, M., Sturrock, S., . . . Duran, C. (2012). Geneious Basic: an integrated and extendable desktop software platform for the organisation and analysis of sequence data. *Bioinformatics, 28*(12), 1647-1649.

Kellenberger, E., & Boy de la Tour, E. (1964). On the fine structure of normal and “polymerised” tail sheath of phage T4. *Journal of Ultrastructure Research, 11*(5), 545-563. doi:https://doi.org/10.1016/S0022-5320(64)80081-2

Kelley, L. A., Mezulis, S., Yates, C. M., Wass, M. N., & Sternberg, M. J. (2015). The Phyre2 web portal for protein modeling, prediction and analysis. *Nature Protocols, 10*(6), 845-858.

Keren, I., Shah, D., Spoering, A., Kaldalu, N., & Lewis, K. (2004). Specialised persister cells and the mechanism of multidrug tolerance in *Escherichia coli*. *Journal of Bacteriology, 186*(24), 8172-8180. doi:https://doi.org/10.1128/jb.186.24.8172-8180.2004

Kerfeld, C. A., Heinhorst, S., & Cannon, G. C. (2010). Bacterial microcompartments. *Annual Review of Microbiology, 64*, 391-408.

Khakame, S. K., Wang, X., & Wu, Y. (2013). Baseline toxicity of metaflumizone and lack of cross resistance between indoxacarb and metaflumizone in diamondback moth (Lepidoptera: Plutellidae). *Journal of Economic Entomology, 106*(3), 1423-1429.

Kim, B. O., Kim, E. S., Yoo, Y. J., Bae, H. W., Chung, I. Y., & Cho, Y. H. (2019). Phage-derived antibacterials: Harnessing the simplicity, plasticity, and diversity of phages. *11*(3). doi:https://doi.org/10.3390/v11030268

Kim, Y., & Wood, T. K. (2010). Toxins Hha and CspD and small RNA regulator Hfq are involved in persister cell formation through MqsR in *Escherichia coli*. *Biochemical and Biophysical Research Communications, 391*(1), 209-213. doi:https://doi.org/10.1016/j.bbrc.2009.11.033

Kirby, W. M., Yoshihara, G. M., Sundsted, K. S., & Warren, J. H. (1956). Clinical usefulness of a single disc method for antibiotic sensitivity testing. *Antibiotic Annual*, 892-897.

Kirchhoff, C., & Cypionka, H. (2017). Propidium ion enters viable cells with high membrane potential during live-dead staining. *Journal of Microbiological Methods, 142*, 79-82.

Kjos, M., Borrero, J., Opsata, M., Birri, D. J., Holo, H., Cintas, L. M., . . . Diep, D. B. (2011). Target recognition, resistance, immunity and genome mining of class II bacteriocins from Gram-positive bacteria. *Microbiology (Reading), 157*(Pt 12), 3256-3267. doi:https://doi.org/10.1099/mic.0.052571-0

Kleerebezem, M. (2004). Quorum sensing control of lantibiotic production; nisin and subtilin autoregulate their own biosynthesis. *Peptides, 25*(9), 1405-1414.

Klein, M. G. (1988). Pest management of soil-inhabiting insects with microorganisms. *Agriculture, Ecosystems and Environment, 24*(1-3), 337-349.

Klein, T., Eckhard, U., Dufour, A., Solis, N., & Overall, C. M. (2018). Proteolytic cleavage-mechanisms, function, and "omic" approaches for a near-ubiquitous posttranslational modification. *Chemical Review, 118*(3), 1137-1168. doi:https://doi.org/10.1021/acs.chemrev.7b00120

Klein, T. A., Ahmad, S., & Whitney, J. C. (2020). Contact-dependent interbacterial antagonism mediated by protein secretion machines. *Trends in Microbiology, 28*(5), 387-400.

Klumpp, J., Calendar, R., & Loessner, M. J. (2010). Complete nucleotide sequence and molecular characterisation of *Bacillus* Phage TP21 and its relatedness to other phages with the same name. *Viruses, 2*(4), 961-971. doi:https://doi.org/10.3390/v2040961

Köhler, T., Donner, V., & Van Delden, C. (2010). Lipopolysaccharide as shield and receptor for R-pyocin-mediated killing in *Pseudomonas aeruginosa*. *Journal of Bacteriology, 192*(7), 1921-1928.

Koivunen, M., Chanbusarakum, L., Fernández, L., Asolkar, R., Tan, E., Wallner, D., & Marrone, P. (2009). Development of a new microbial insecticide based on *Chromobacterium subtsugae*. *IOBC/WPRS Bulletin, 45*, 183-186.

Kooliyottil, R., Upadhyay, D., Inman III, F., Mandjiny, S., & Holmes, L. (2013). A comparative analysis of entomoparasitic nematodes *Heterorhabditis bacteriophora* and *Steinernema carpocapsae*. *Open Journal of Animal Sciences, 3*(04), 326.

Koppenhöfer, A. M., Jackson, T. A., & Klein, M. G. (2012). Bacteria for use against soil-inhabiting insects. In L. A. Lacey (Ed.), *Manual of Techniques in Invertebrate Pathology. Academic Press, San Diego* (2nd ed., pp. 129-149): Elsevier.

Koul, O. (2011). Microbial biopesticides: opportunities and challenges. *CAB Review, 6*, 1-26.

Kristensen, D. M., Waller, A. S., Yamada, T., Bork, P., Mushegian, A. R., & Koonin, E. V. (2013). Orthologous gene clusters and taxon signature genes for viruses of prokaryotes. *Journal of Bacteriology, 195*(5), 941-950.

Krogh, S., Jørgensen, S. T., & Devine, K. M. (1998). Lysis genes of the *Bacillus subtilis* defective prophage PBSX. *Journal of Bacteriology, 180*(8), 2110-2117.

Krogh, S., O'Reilly, M., Nolan, N., & Devine, K. M. (1996). The phage-like element PBSX and part of the skin element, which are resident at different locations on the *Bacillus subtilis* chromosome, are highly homologous. *Microbiology, 142*(8), 2031-2040.

Kropinski, A. M., Mazzocco, A., Waddell, T. E., Lingohr, E., & Johnson, R. P. (2009). Enumeration of bacteriophages by double agar overlay plaque assay. In M. R. J. Clokie & A. M. Kropinski (Eds.), *Bacteriophages* (pp. 69-76): Springer. doi:https://doi.org/10.1007/978-1-60327-164-6

Kumar, G. N., Sundarrajan, S., Paul, V. D., Nandini, S., Saravanan, R. S., Hariharan, S., . . . Padmanabhan, S. (2012a). Use of prophage free host for achieving homogenous population of bacteriophages: New findings. *Virus Research, 169*(1), 182-187.

Kumar, J. K. (2008). Lysostaphin: an antistaphylococcal agent. *Applied Microbiology and Biotechnology, 80*(4), 555-561.

Kumar, S. N., Siji, J. V., Ramya, R., Nambisan, B., & Mohandas, C. (2012b). Improvement of antimicrobial activity of compounds produced by *Bacillus* sp. associated with a *Rhabditid* sp. (entomopathogenic nematode) by changing carbon and nitrogen sources in fermentation media. *The Journal of Microbiology, Biotechnology and Food Sciences, 1*, 1424-1438.

Kunst, F., Ogasawara, N., Moszer, I., Albertini, A. M., Alloni, G., Azevedo, V., . . . Danchin, A. (1997). The complete genome sequence of the gram-positive bacterium *Bacillus subtilis*. *Nature, 390*(6657), 249-256. doi:https://doi.org/10.1038/36786

Kurochkina, L. P., Semenyuk, P. I., Sykilinda, N. N., & Miroshnikov, K. A. (2018). The unique two-component tail sheath of giant *Pseudomonas phage* PaBG. *Virology, 515*, 46-51. doi:https://doi.org/10.1016/j.virol.2017.12.010

Kuroda, K., & Kageyama, M. (1979). Biochemical properties of a new flexuous bacteriocin, pyocin F1, produced by *Pseudomonas aeruginosa*. *The Journal of Biochemistry, 85*(1), 7-19.

Kuroda, K., & Kageyama, M. (1981). Comparative study on F-type pyocins of *Pseudomonas aeruginosa*. *The Journal of Biochemistry, 89*(6), 1721-1736.

Kusaoke, H., Hayashi, Y., Kadowaki, Y., & Kimoto, H. (1989). Optimum conditions for electric pulse-mediated gene transfer to *Bacillus subtilis* cells. *Agricultural and Bological Chemistry, 53*(9), 2441-2446.

Kwan, T., Liu, J., DuBow, M., Gros, P., & Pelletier, J. (2006). Comparative genomic analysis of 18 *Pseudomonas aeruginosa* bacteriophages. *Journal of Bacteriology, 188*(3), 1184-1187.

Labrie, S. J., & Moineau, S. (2007). Abortive infection mechanisms and prophage sequences significantly influence the genetic makeup of emerging lytic lactococcal phages. *Journal of Bacteriology, 189*(4), 1482-1487. doi:https://doi.org/10.1128/JB.01111-06

Labrou, N. E. (2014). Protein purification: An overview. In N. E. Labrou (Ed.), *Proteins downstream processing: Design, development, and application of high and low resolution methods* (1st ed., Vol. 1129, pp. 3-10): Springer. doi:https://doi.org/10.1007/978-1-62703-977-2

Lacey, L. A. (2007). *Bacillus thuringiensis* serovariety *israelensis* and *Bacillus sphaericus* for mosquito control. *Journal of the American Mosquito Control Association, 23*(sp2), 133-163.

Lacey, L. A., Frutos, R., Kaya, H., & Vail, P. (2001). Insect pathogens as biological control agents: do they have a future? *Biological Control, 21*(3), 230-248.

Lacey, L. A., Grzywacz, D., Shapiro-Ilan, D. I., Frutos, R., Brownbridge, M., & Goettel, M. S. (2015). Insect pathogens as biological control agents: Back to the future. *Journal of Invertebrate Pathology, 132*, 1-41. doi:https://doi.org/10.1016/j.jip.2015.07.009

Laemmli, U. (1970). SDS-PAGE Laemmli method. *Nature, 227*, 680-685.

Lajis, A. F. B. (2020). Biomanufacturing process for the production of bacteriocins from *Bacillaceae* family. *Bioresources and Bioprocessing, 7*(1), 8. doi:https://doi.org/10.1186/s40643-020-0295-z

Lander, E. S., Linton, L. M., Birren, B., Nusbaum, C., Zody, M. C., Baldwin, J., . . . The Wellcome, T. (2001). Initial sequencing and analysis of the human genome. *Nature, 409*(6822), 860-921. doi:https://doi.org/10.1038/35057062

Lang, A. S., Zhaxybayeva, O., & Beatty, J. T. (2012). Gene transfer agents: phage-like elements of genetic exchange. *Nature Reviews Microbiology, 10*(7), 472-482.

Laubach, A., Rice, J., & Ford, W. (1916). Studies on aerobic, spore bearing, non-pathogenic bacteria. *Journal of Bacteriology, 1*, 505-512.

Lavigne, R., Seto, D., Mahadevan, P., Ackermann, H.-W., & Kropinski, A. M. (2008). Unifying classical and molecular taxonomic classification: analysis of the *Podoviridae* using BLASTp-based tools. *Research in Microbiology, 159*(5), 406-414.

Lawrence, J. E., & Steward, G. F. (2010). Purification of viruses by centrifugation. In S. W. Wilhelm, M.G.Weinbauer & C.A.Suttle (Eds.), *Manual of Aquatic Viral Ecology* (pp. 166-181): American Society of Limnology and Oceanography, Inc.

Lawrence, J. G. (2004). The dynamic bacterial genome. *The Bacterial Chromosome*, 19-37.

Lay, C., Sutren, M., Rochet, V., Saunier, K., Doré, J., & Rigottier-Gois, L. (2005). Design and validation of 16S rRNA probes to enumerate members of the *Clostridium leptum* subgroup in human faecal microbiota. *Environmental Microbiology, 7*(7), 933-946.

Leães, F. L., Velho, R. V., Caldas, D. G., Pinto, J. V., Tsai, S. M., & Brandelli, A. (2013). Influence of pH and temperature on the expression of sboA and ituD genes in *Bacillus* sp. P11. *Antonie Van Leeuwenhoek, 104*(1), 149-154. doi:https://doi.org/10.1007/s10482-013-9935-z

Lee, C., il Kim, M., & Hong, M. (2017). Structural and functional analysis of BF2549, a PadR-like transcription factor from *Bacteroides fragilis*. *Biochemical and Biophysical Research Communications, 483*(1), 264-270.

Lee, F. K., Dudas, K. C., Hanson, J. A., Nelson, M. B., LoVerde, P. T., & Apicella, M. A. (1999). The R-type pyocin of *Pseudomonas aeruginosa* C is a bacteriophage tail-like particle that contains single-stranded DNA. *Infection and Immunity, 67*(2), 717-725.

Lee, G., Chakraborty, U., Gebhart, D., Govoni, G. R., Zhou, Z. H., & Scholl, D. (2016). F-type bacteriocins of *Listeria monocytogenes*: a new class of phage tail-like structures reveals broad parallel coevolution between tailed bacteriophages and high molecular-weight bacteriocins. *Journal of Bacteriology, 198*(20), 2784-2793.

Lee, K. H., Jun, K. D., Kim, W. S., & Paik, H. D. (2001). Partial characterisation of polyfermenticin SCD, a newly identified bacteriocin of *Bacillus polyfermenticus*. *Letters in Applied Microbiology, 32*(3), 146-151. doi:https://doi.org/10.1046/j.1472-765x.2001.00876.x

Legwaila, M. M., Munthali, D. C., Kwerepe, B. C., & Obopile, M. (2015). Efficacy of *Bacillus thuringiensis* (var. *kurstaki*) against diamondback moth (*Plutella xylostella* L.) eggs and larvae on cabbage under semi-controlled greenhouse conditions. *International Journal of Insect Science, 7*, S23637.

Leiman, P. G., Basler, M., Ramagopal, U. A., Bonanno, J. B., Sauder, J. M., Pukatzki, S., . . . Mekalanos, J. J. (2009). Type VI secretion apparatus and phage tail-associated protein complexes share a common evolutionary origin. *Proceedings of the National Academy of Sciences, 106*(11), 4154-4159.

Leiman, P. G., & Shneider, M. M. (2012). Contractile tail machines of bacteriophages. *Viral Molecular Machines*, 93-114.

Léonard, L., Bouarab Chibane, L., Ouled Bouhedda, B., Degraeve, P., & Oulahal, N. (2016). Recent advances on multi-parameter flow cytometry to characterise antimicrobial treatments. *Frontiers in Microbiology, 7*, 1225.

Leuko, S., Legat, A., Fendrihan, S., & Stan-Lotter, H. (2004). Evaluation of the LIVE/DEAD Bac Light kit for detection of extremophilic archaea and visualisation of microorganisms in environmental hypersaline samples. *Applied and Environmental Microbiology, 70*(11), 6884-6886.

Levin, J. C., & Stein, D. C. (1996). Cloning, complementation, and characterisation of an rfaE homolog from *Neisseria gonorrhoeae*. *Journal of Bacteriology, 178*(15), 4571-4575.

Lewis, G. D., & Metcalf, T. G. (1988). Polyethylene glycol precipitation for recovery of pathogenic viruses, including hepatitis A virus and human rotavirus, from oyster, water, and sediment samples. *Applied and Environmental Microbiology, 54*(8), 1983.

Lewis, K. (2008). Multidrug tolerance of biofilms and persister cells. *Current Topics in Microbiology and Immunology, 322*, 107-131. doi:https://doi.org/10.1007/978-3-540-75418-3_6

Lewis, K. (2010). Persister cells. *Annual Review of Microbiology, 64*(1), 357-372. doi:10.1146/annurev.micro.112408.134306

Lewus, C. B., & Montville, T. J. (1991). Detection of bacteriocins produced by lactic acid bacteria. *Journal of Microbiological Methods, 13*(2), 145-150.

Li, G., Xu, J., Wu, L., Ren, D., Ye, W., Dong, G., . . . Guo, L. (2015). Full genome sequence of *Brevibacillus laterosporus* strain B9, a biological control strain isolated from Zhejiang, China. *Journal of Biotechnology, 207*, 77-78.

Liao, W., Song, S., Sun, F., Jia, Y., Zeng, W., & Pang, Y. (2008). Isolation, characterisation and genome sequencing of phage MZTP02 from *Bacillus thuringiensis* MZ1. *Archives of Virology, 153*(10), 1855-1865. doi:https://doi.org/10.1007/s00705-008-0201-z

Liao, W., Sun, F., Song, S., Shi, W., & Pang, Y. (2007). Biology of two lysogenic phages from *Bacillus thuringiensis* MZ1. *Wei sheng wu xue bao= Acta Microbiologica Sinica, 47*(1), 92-97.

Lichens-Park, A., Smith, C., & Syvanen, M. (1990). Integration of bacteriophage lambda into the cryptic lambdoid prophages of *Escherichia coli*. *Journal of Bacteriology, 172*(5), 2201-2208.

Lillehaug, D. (1997). An improved plaque assay for poor plaque-producing temperate *Lactococcal* bacteriophages. *Journal of Applied Microbiology, 83*(1), 85-90.

Lindell, D., Sullivan, M. B., Johnson, Z. I., Tolonen, A. C., Rohwer, F., & Chisholm, S. W. (2004). Transfer of photosynthesis genes to and from *Prochlorococcus* viruses. *Proceedings of the National Academy of Sciences, 101*(30), 11013-11018.

Line, J. E., Svetoch, E. A., Eruslanov, B. V., Perelygin, V. V., Mitsevich, E. V., Mitsevich, I. P., . . . Stern, N. J. (2008). Isolation and purification of enterocin E-760 with broad antimicrobial activity against gram-positive and gram-negative bacteria. *Antimicrobial Agents and Chemotheraphy, 52*(3), 1094-1100. doi:https://doi.org/10.1128/aac.01569-06

Liu, B., Li, S., & Hu, J. (2004). Technological advances in high-throughput screening. *American Journal of Pharmacogenomics, 4*(4), 263-276.

Liu, J., Chen, P., Zheng, C., & Huang, Y.-P. (2013). Characterisation of maltocin P28, a novel phage tail-like bacteriocin from *Stenotrophomonas maltophilia*. *Applied and Environmental Microbiology, 79*(18), 5593-5600.

Loessner, M. J. (2005). Bacteriophage endolysins-current state of research and applications. *Current Opinion in Microbiology, 8*(4), 480-487.

Longchamp, P. F., Mauel, C., & Karamata, D. (1994). Lytic enzymes associated with defective prophages of *Bacillus subtilis*: sequencing and characterisation of the region comprising the N-acetylmuramoyl-L-alanine amidase gene of prophage PBSX. *Microbiology, 140*(8), 1855-1867.

López Martín, M. (2014). The SOS response and the dissemination of antibiotic resistances.

Loś, J. M., Golec, P., Wegrzyn, G., Wegrzyn, A., & Loś, M. (2008). Simple method for plating *Escherichia coli* bacteriophages forming very small plaques or no plaques under standard conditions. *Applied and Environmental Microbiology, 74*(16), 5113-5120. doi:https://doi.org/10.1128/aem.00306-08

Łos, M., Czyz, A., Sell, E., Wegrzyn, A., Neubauer, P., & Wegrzyn, G. (2004). Bacteriophage contamination: is there a simple method to reduce its deleterious effects in laboratory cultures and biotechnological factories? *Journal of Applied Genetics, 45*(1), 111-120.

Lotz, W. (1976). Defective bacteriophages: The phage tail-like particles. In F. E. Halin (Ed.), *Progress in Molecular and Subcellular Biology* (1st ed., pp. 53-102). Berlin, Heidelberg: Springer. doi:https://doi.org/10.1007/978-3-642-66249-2

Lotz, W., & Mayer, F. (1972). Isolation and characterisation of a bacteriophage tail-like bacteriocin from a strain of *Rhizobium*. *Journal of Virology, 9*(1), 160-173.

Louca, S., Mazel, F., Doebeli, M., & Parfrey, L. W. (2019). A census-based estimate of earth's bacterial and archaeal diversity. *Plos Biology, 17*(2), e3000106. doi:https://doi.org/10.1371/journal.pbio.3000106

Lu, J., Turnbull, L., Burke, C. M., Liu, M., Carter, D. A., Schlothauer, R. C., . . . Harry, E. J. (2014). Manuka-type honeys can eradicate biofilms produced by *Staphylococcus aureus* strains with different biofilm-forming abilities. *Peer Journal, 2*, e326.

Lu, Y. P., Zhang, C., Lv, F., Bie, X., & Lu, Z. X. (2012). Study on the electro-transformation conditions of improving transformation efficiency for *Bacillus subtilis*. *Letters in Applied Microbiology, 55*(1), 9-14.

Lubelski, J., De Jong, A., Van Merkerk, R., Agustiandari, H., Kuipers, O. P., Kok, J., & Driessen, A. J. (2006). LmrCD is a major multidrug resistance transporter in *Lactococcus lactis*. *Molecular Microbiology, 61*(3), 771-781.

Lucas, R., Grande, M. A., Abriouel, H., Maqueda, M., Ben Omar, N., Valdivia, E., . . . Gálvez, A. (2006). Application of the broad-spectrum bacteriocin enterocin AS-48 to inhibit *Bacillus coagulans* in canned fruit and vegetable foods. *Food Chemical Toxicology, 44*(10), 1774-1781. doi:https://doi.org/10.1016/j.fct.2006.05.019

Lwoff, A. (1953a). Lysogeny. *Bacteriol Reviews, 17*(4), 269-337.

Lwoff, A. (1953b). Lysogeny. *Bacteriological Reviews, 17*(4), 269-337.

Lwoff, A. (1966). Interaction among virus, cell, and organism. *Science, 152*(3726), 1216-1220.

Lyer, V., & Szybalski, W. (1964). Mitomycins and porfiromycin: chemical mechanism of activation and cross-linking of DNA. *Science, 145*(3627), 55-58.

Ma, A. T., & Mekalanos, J. J. (2010). In vivo actin cross-linking induced by *Vibrio cholerae* type VI secretion system is associated with intestinal inflammation. *Proceedings of the National Academy of Sciences, 107*(9), 4365-4370.

Madani, F., Lindberg, S., Langel, Ü., Futaki, S., & Gräslund, A. (2011). Mechanisms of cellular uptake of cell-penetrating peptides. *Journal of Biophysics, 2011*.

Makino, K., Yokoyama, K., Kubota, Y., Yutsudo, C. H., Kimura, S., Kurokawa, K., . . . Abe, H. (1999). Complete nucleotide sequence of the prophage VT2-Sakai carrying the verotoxin 2 genes of the enterohemorrhagic *Escherichia coli* O157: H7 derived from the Sakai outbreak. *Genes and Genetic Systems, 74*(5), 227-239.

Maldonado-Barragán, A., Caballero-Guerrero, B., Lucena-Padrós, H., & Ruiz-Barba, J. L. (2013). Induction of bacteriocin production by coculture is widespread among plantaricin-producing *Lactobacillus plantarum* strains with different regulatory operons. *Food Microbiology, 33*(1), 40-47. doi:https://doi.org/10.1016/j.fm.2012.08.009

Marche, M. G., Camiolo, S., Porceddu, A., & Ruiu, L. (2018). Survey of *Brevibacillus laterosporu*s insecticidal protein genes and virulence factors. *Journal of Invertebrate Pathology, 155*, 38-43.

Marche, M. G., Mura, M. E., Falchi, G., & Ruiu, L. (2017). Spore surface proteins of *Brevibacillus laterosporus* are involved in insect pathogenesis. *Scientific Reports, 7*(1), 1-10.

Marche, M. G., Satta, A., Floris, I., Lazzeri, A. M., & Ruiu, L. (2019). Inhibition of *Paenibacillu*s larvae by an extracellular protein fraction from a honeybee-borne *Brevibacillus laterosporus* strain. *Microbiological Research, 227*, 126303.

Marcó, M. B., Reinheimer, J. A., & Quiberoni, A. (2010). Phage adsorption to *Lactobacillus plantarum*: Influence of physiological and environmental factors. *International Journal of Food Microbiology, 138*(3), 270-275. doi:https://doi.org/10.1016/j.ijfoodmicro.2010.01.007

Mardanov, A. V., & Ravin, N. V. (2007). The antirepressor needed for induction of linear plasmid-prophage N15 belongs to the SOS regulon. *Journal of bacteriology, 189*(17), 6333-6338.

Marichal-Gallardo, P. A., & Alvarez, M. M. (2012). State-of-the-art in downstream processing of monoclonal antibodies: process trends in design and validation. *Biotechnology Progress, 28*(4), 899-916. doi:https://doi.org/10.1002/btpr.1567

Marshall, S. D., Hares, M. C., Jones, S. A., Harper, L. A., Vernon, J. R., Harland, D. P., . . . Hurst, M. R. (2012). Histopathological effects of the Yen-Tc toxin complex from *Yersinia entomophaga* MH96 (Enterobacteriaceae) on the *Costelytra zealandica* (Coleoptera: Scarabaeidae) larval midgut. *Applied and Environmental Microbiology, 78*(14), 4835-4847.

Martin, P., Shropshire, A., Gundersen-Rindal, D., & Blackburn, M. (2007). Google Patent.

Martínez-Cuesta, M. C., Kok, J., Herranz, E., Peláez, C., Requena, T., & Buist, G. (2000). Requirement of autolytic activity for bacteriocin-induced lysis. *Applied and Environmental Microbiology, 66*(8), 3174-3179.

Mataragas, M., Metaxopoulos, J., & Drosinos, E. H. (2002). Characterisation of two bacteriocins produced by *Leuconostoc mesenteroides* L124 and *Lactobacillus curvatus* L442, isolated from dry fermented sausages. *World Journal of Microbiology and Biotechnology, 18*(9), 847-856. doi:https://doi.org/10.1023/A:1021239008582

Mateos, M., Martinez Montoya, H., Lanzavecchia, S. B., Conte, C., Guillén, K., Morán-Aceves, B. M., . . . Doudoumis, V. (2020). *Wolbachia pipientis* associated with tephritid fruit fly pests: From basic research to applications. *Frontiers in Microbiology, 11*, 1080.

Mauël, C., & Karamata, D. (1984a). Characterisation of proteins induced by Mitomycin C treatment of *Bacillus subtilis*. *Journal of Virology, 49*(3), 806-812.

Mauël, C., & Karamata, D. (1984b). Characterization of proteins induced by mitomycin C treatment of *Bacillus subtilis*. *Journal of virology, 49*(3), 806-812.

McAuliffe, O., Ross, R. P., & Hill, C. (2001). Lantibiotics: structure, biosynthesis and mode of action. *FEMS Microbiology Reviews, 25*(3), 285-308.

McCool, J. D., Long, E., Petrosino, J. F., Sandler, H. A., Rosenberg, S. M., & Sandler, S. J. (2004). Measurement of SOS expression in individual *Escherichia coli* K-12 cells using fluorescence microscopy. *Molecular Microbiology, 53*(5), 1343-1357. doi:https://doi.org/10.1111/j.1365-2958.2004.04225.x

McDonald, I., Riley, P., Sharp, R., & McCarthy, A. (1995). Factors affecting the electroporation of *Bacillus subtilis*. *Journal of Applied Bacteriology, 79*(2), 213-218.

McDonnell, G. E., & McConnell, D. J. (1994). Overproduction, isolation, and DNA-binding characteristics of Xre, the repressor protein from the *Bacillus subtilis* defective prophage PBSX. *Journal of Bacteriology, 176*(18), 5831-5834.

McDonnell, G. E., Wood, H., Devine, K. M., & McConnell, D. J. (1994). Genetic control of bacterial suicide: regulation of the induction of PBSX in *Bacillus subtilis*. *Journal of Bacteriology, 176*(18), 5820-5830. doi:https://doi.org/10.1128/jb.176.18.5820-5830.1994

McHugh, C. A., Fontana, J., Nemecek, D., Cheng, N., Aksyuk, A. A., Heymann, J. B., . . . Hoiczyk, E. (2014). A virus capsid-like nanocompartment that stores iron and protects bacteria from oxidative stress. *The EMBO Journal, 33*(17), 1896-1911. doi:https://doi.org/10.15252/embj.201488566

McKenney, P. T., Driks, A., & Eichenberger, P. (2013). The *Bacillus subtilis* endospore: assembly and functions of the multilayered coat. *Nature Reviews Microbiology, 11*(1), 33-44.

McShan, W. M. (2006). The bacteriophages of group A *streptococci*. *Gram-Positive Pathogens*, 123-142.

Mercy, C., Ize, B., Salcedo, S. P., de Bentzmann, S., & Bigot, S. (2016). Functional characterisation of *Pseudomonas* contact dependent growth inhibition (CDI) systems. *Plos One, 11*(1), e0147435. doi:https://doi.org/10.1371/journal.pone.0147435

Merino, S., Camprubi, S., & Tomás, J. M. (1990). Isolation and characterisation of bacteriophage PM3 from *Aeromonas hydrophila* the bacterial receptor for which is the monopolar flagellum. *FEMS Microbiology Letters, 57*(3), 277-282. doi:https://doi.org/10.1016/0378-1097(90)90080.x

Merrill, B. D., Grose, J. H., Breakwell, D. P., & Burnett, S. H. (2014). Characterisation of *Paenibacillus* larvae bacteriophages and their genomic relationships to Firmicute bacteriophages. *BMC Genomics, 15*(1), 745. doi:https://doi.org/10.1186/1471-2164-15-745

Michel-Briand, Y., & Baysse, C. (2002). The pyocins of *Pseudomonas aeruginosa*. *Biochimie, 84*(5-6), 499-510. doi:https://doi.org/10.1016/s0300-9084(02)01422-0

Michiels, J. E., Van den Bergh, B., Verstraeten, N., & Michiels, J. (2016). Molecular mechanisms and clinical implications of bacterial persistence. *Drug Resistance Updates, 29*, 76-89. doi:https://doi.org/10.1016/j.drup.2016.10.002

Miljkovic, M., Jovanovic, S., O'Connor, P. M., Mirkovic, N., Jovcic, B., Filipic, B., . . . Kojic, M. (2019). *Brevibacillus laterosporus* strains BGSP7, BGSP9 and BGSP11 isolated from silage produce broad spectrum multi-antimicrobials. *Plos One, 14*(5), e0216773. doi:https://doi.org/10.1371/journal.pone.0216773

Milletti, F. (2012). Cell penetrating peptides: classes, origin, and current landscape. *Drug Discovery Today, 17*(15-16), 850-860.

Milner, R. J. (1994). History of *Bacillus thuringiensis*. *Agriculture, Ecosystems, and Environment, 49*(1), 9-13. doi:https://doi.org/10.1016/0167-8809(94)90014-0

Mistry, J., Chuguransky, S., Williams, L., Qureshi, M., Salazar, G. A., Sonnhammer, E. L., . . . Richardson, L. J. (2021). Pfam: The protein families database in 2021. *Nucleic Acids Research, 49*(D1), D412-D419.

Mobberley, J., Authement, R. N., Segall, A. M., Edwards, R. A., Slepecky, R., & Paul, J. (2010). Lysogeny and sporulation in *Bacillus* isolates from the Gulf of Mexico. *Applied and Environmental Microbiology, 76*(3), 829-842.

Morales-Soto, N., Gaudriault, S., Ogier, J. C., Thappeta, K. R., & Forst, S. (2012). Comparative analysis of P2-type remnant prophage loci in *Xenorhabdus bovienii* and *Xenorhabdus nematophila* required for xenorhabdicin production. *FEMS Microbiology Letters, 333*(1), 69-76. doi:https://doi.org/10.1111/j.1574-6968.2012.02600.x

Moreira, A. C., Mesquita, G., & Gomes, M. S. (2020). Ferritin: an inflammatory player keeping iron at the core of pathogen-host interactions. *Microorganisms, 8*(4), 589.

Moretti, R., Yen, P.-S., Houé, V., Lampazzi, E., Desiderio, A., Failloux, A.-B., & Calvitti, M. (2018). Combining *Wolbachia*-induced sterility and virus protection to fight *Aedes albopictus*-borne viruses. *Plos Neglected Tropical Diseases, 12*(7), e0006626.

Morgan, S., Ross, R. P., & Hill, C. (1995). Bacteriolytic activity caused by the presence of a novel lactococcal plasmid encoding lactococcins A, B, and M. *Applied and Environmental Microbiology, 61*(8), 2995-3001. doi:https://doi.org/10.1128/aem.61.8.2995-3001.1995

Morin, N., Lanneluc, I., Connil, N., Cottenceau, M., Pons, A. M., & Sablé, S. (2011). Mechanism of bactericidal activity of microcin L in *Escherichia coli* and *Salmonella enterica*. *Antimicrobial Agents and Chemotherapy, 55*(3), 997-1007. doi:https://doi.org/10.1128/AAC.01217-10

Morona, R., & Henning, U. (1984). Host range mutants of bacteriophage Ox2 can use two different outer membrane proteins of *Escherichia coli* K-12 as receptors. *Journal of Bacteriology, 159*(2), 579-582. doi:https://doi.org/10.1128/jb.159.2.579-582.1984

Morse, S. A., Vaughan, P., Johnson, D., & Iglewski, B. H. (1976). Inhibition of *Neisseria gonorrhoeae* by a bacteriocin from *Pseudomonas aeruginosa*. *Antimicrobial Agents and Chemotherapy, 10*(2), 354-362. doi:https://doi.org/10.1128/aac.10.2.354

Morton, J. T., Freed, S. D., Lee, S. W., & Friedberg, I. (2015). A large scale prediction of bacteriocin gene blocks suggests a wide functional spectrum for bacteriocins. *BMC Bioinformatics, 16*, 381. doi:https://doi.org/10.1186/s12859-015-0792-9

Moszer, I., Jones, L. M., Moreira, S., Fabry, C., & Danchin, A. (2002). SubtiList: the reference database for the *Bacillus subtilis* genome. *Nucleic Acids Research, 30*(1), 62-65.

Mota-Sanchez, D., & Wise, J. (2020). *The arthropod pesticide resistance database*. Retrieved 1st June, 2021,from https://www.pesticideresistance.org

Mougous, J. D., Cuff, M. E., Raunser, S., Shen, A., Zhou, M., Gifford, C. A., . . . Lory, S. (2006). A virulence locus of *Pseudomonas aeruginosa* encodes a protein secretion apparatus. *Science, 312*(5779), 1526-1530.

Moura de Sousa, J. A., Pfeifer, E., Touchon, M., & Rocha, E. P. C. (2021). Causes and consequences of bacteriophage diversification via genetic exchanges across lifestyles and bacterial taxa. *Molecular Biology and Evolution, 38*(6), 2497-2512. doi:https://doi.org/10.1093/molbev/msab044

Munyuki, G., Jackson, G. E., Venter, G. A., Kövér, K. E., Szilágyi, L., Rautenbach, M., . . . Spoel, D. (2013). β-sheet structures and dimer models of the two major tyrocidines, antimicrobial peptides from *Bacillus aneurinolyticus*. *Biochemistry, 52*. doi:https://doi.org/10.1021/bi401363m

Myers, J. A., Curtis, B. S., & Curtis, W. R. (2013). Improving accuracy of cell and chromophore concentration measurements using optical density. *BMC Biophysics, 6*(1), 1-16.

Nagai, T. (2014). A defective bacteriophage produced by *Bacillus subtilis* MAFF 118147 and a mutant producing no normal particles of the defective bacteriophage. *Food Science and Technology Research, 20*(6), 1229-1234. doi:https://doi.org/10.3136/fstr.20.1229

Nakayama, K., Takashima, K., Ishihara, H., Shinomiya, T., Kageyama, M., Kanaya, S., . . . Hayashi, T. (2000). The R-type pyocin of *Pseudomonas aeruginosa* is related to P2 phage, and the F-type is related to lambda phage. *Molecular Microbiology, 38*(2), 213-231.

Nanda, A. M., Heyer, A., Krämer, C., Grünberger, A., Kohlheyer, D., & Frunzke, J. (2014). Analysis of SOS-induced spontaneous prophage induction in *Corynebacterium glutamicum* at the single-cell level. *Journal of Bacteriology, 196*(1), 180-188.

Nanda, A. M., Thormann, K., & Frunzke, J. (2015). Impact of spontaneous prophage induction on the fitness of bacterial populations and host-microbe interactions. *Journal of Bacteriology, 197*(3), 410. doi:https://doi.org/10.1128/JB.02230-14

Neeley, E. T., Phister, T. G., & Mills, D. A. (2005). Differential real-time PCR assay for enumeration of lactic acid bacteria in wine. *Applied and Environmental Microbiology, 71*(12), 8954-8957.

Nelson, D. (2004). Phage taxonomy: we agree to disagree. *Journal of Bacteriology, 186*(21), 7029-7031.

Nguyen, A. H., Tomita, T., Hirota, M., Sato, T., & Kamio, Y. (1999). A simple purification method and morphology and component analyses for carotovoricin Er, a phage-tail-like bacteriocin from the plant pathogen *Erwinia carotovora* Er. *Bioscience, Biotechnology, and Biochemistry, 63*(8), 1360-1369.

Nguyen, H. A., Tomita, T., Hirota, M., Kaneko, J., Hayashi, T., & Kamio, Y. (2001). DNA inversion in the tail fibre gene alters the host range specificity of carotovoricin Er, a phage-tail-like bacteriocin of phytopathogenic *Erwinia carotovora* subsp. carotovora Er. *Journal of Bacteriology, 183*(21), 6274-6281. doi:https://doi.org/10.1128/jb.183.21.6274-6281.2001

Nguyen, T. K. C., Tran, N. P., & Cavin, J.-F. (2011). Genetic and biochemical analysis of PadR-padC promoter interactions during the phenolic acid stress response in *Bacillus subtilis* 168. *Journal of Bacteriology, 193*(16), 4180-4191.

Nobrega, F. L., Vlot, M., de Jonge, P. A., Dreesens, L. L., Beaumont, H. J. E., Lavigne, R., & Dutilh, B. E. (2018). Targeting mechanisms of tailed bacteriophages. *16*(12), 760-773. doi:https://doi.org/10.1038/s41579-018-0070-8

Nocker, A., Cheswick, R., Dutheil de la Rochere, P.-M., Denis, M., Léziart, T., & Jarvis, P. (2017). When are bacteria dead? a step towards interpreting flow cytometry profiles after chlorine disinfection and membrane integrity staining. *Environmental Technology, 38*(7), 891-900.

O'Callaghan, M., Jackson, T., & Mahanty, H. (1992). Selection, development and testing of phage-resistant strains of *Serratia entomophila* for grass grub control. *Biocontrol Science and Technology, 2*(4), 297-305.

O'Toole, G. A. (2016). Classic spotlight: How the gram stain works. *Journl of Bacteriology, 198*(23), 3128. doi:https://doi.org/10.1128/JB.00726-16

Oh, S., Kim, S. H., & Worobo, R. W. (2000). Characterisation and purification of a bacteriocin produced by a potential probiotic culture, *Lactobacillus acidophilus* 30SC. *Journal of Dairy Science, 83*(12), 2747-2752. doi:https://doi.org/10.3168/jds.S0022-0302(00)75169-1

Ohnishi, Y., Ishikawa, J., Hara, H., Suzuki, H., Ikenoya, M., Ikeda, H., . . . Horinouchi, S. (2008). Genome sequence of the streptomycin-producing microorganism *Streptomyces griseus* IFO 13350. *Journal of Bacteriology, 190*(11), 4050-4060.

Oliver, J. D. (2005). The viable but nonculturable state in bacteria. *Journal of Microbiology, 43*(spc1), 93-100.

Oliver, J. D. (2010). Recent findings on the viable but nonculturable state in pathogenic bacteria. *FEMS Microbiology Reviews, 34*(4), 415-425.

Olszak, T., Latka, A., Roszniowski, B., Valvano, M. A., & Drulis-Kawa, Z. (2017). Phage life cycles behind bacterial biodiversity. *Current Medicinal Chemistry, 24*(36), 3987-4001.

Orlova, E., White, H., Sherman, M., Brasilès, S., Tavares, P., Jacquet, E., & Seavers, P. (2012). Capsid structure and its stability at the late stages of bacteriophage SPP1 assembly. *Microscopy and Microanalysis, 18*(S2), 114-115.

Ormskirk, M. M. (2017). *Brevibacillus laterosporus as a potential bio-control agent of the diamondback moth and other insects* (Doctoral Thesis). Lincoln University. Retrieved from https://researcharchive.lincoln.ac.nz

Ormskirk, M. M., Narciso, J., Hampton, J. G., & Glare, T. R. (2019). Endophytic ability of the insecticidal bacterium *Brevibacillus laterosporus* in Brassica. *Plos One, 14*(5), e0216341. doi:https://doi.org/10.1371/journal.pone.0216341

Oscáriz, J. C., & Pisabarro, A. G. (2001). Classification and mode of action of membrane-active bacteriocins produced by gram-positive bacteria. *International Microbiology, 4*(1), 13-19.

Owen, S. V., Canals, R., Wenner, N., Hammarlöf, D. L., Kröger, C., & Hinton, J. C. D. (2020). A window into lysogeny: revealing temperate phage biology with transcriptomics. *Microbial Genomics, 6*(2). doi:https://doi.org/10.1099/mgen.0.000330

Paczesny, J., Richter, Ł., & Hołyst, R. (2020). Recent progress in the detection of bacteria using bacteriophages: A review. *Viruses, 12*(8), 845.

Pandey, D. P., & Gerdes, K. (2005). Toxin–antitoxin loci are highly abundant in free-living but lost from host-associated prokaryotes. *Nucleic Acids Research, 33*(3), 966-976.

Parente, E., & Ricciardi, A. (1999). Production, recovery and purification of bacteriocins from lactic acid bacteria. *Applied Microbiology and Biotechnology, 52*(5), 628-638. doi:https://doi.org/10.1007/s002530051570

Park, S. C., Kwak, Y. M., Song, W. S., Hong, M., & Yoon, S.-i. (2017). Structural basis of effector and operator recognition by the phenolic acid-responsive transcriptional regulator PadR. *Nucleic Acids Research, 45*(22), 13080-13093.

Parker, G. F., Daniel, R. A., & Errington, J. (1996). Timing and genetic regulation of commitment to sporulation in *Bacillus subtilis*. *Microbiology, 142*(12), 3445-3452.

Patz, S., Becker, Y., Richert-Pöggeler, K. R., Berger, B., Ruppel, S., Huson, D. H., & Becker, M. (2019). Phage tail-like particles are versatile bacterial nanomachines -a mini review. *Journal of Advanced Research, 19*, 75-84. doi:https://doi.org/10.1016/j.jare.2019.04.003

Paul, J. H., Sullivan, M. B., Segall, A. M., & Rohwer, F. (2002). Marine phage genomics. *Comparative Biochemistry and Physiology Part B: Biochemistry and Molecular Biology, 133*(4), 463-476.

Paul, P., Sahu, B. R., & Suar, M. (2019). Plausible role of bacterial toxin–antitoxin system in persister cell formation and elimination. *Molecular Oral Microbiology, 34*(3), 97-107.

Pedulla, M. L., Ford, M. E., Houtz, J. M., Karthikeyan, T., Wadsworth, C., Lewis, J. A., . . . Pannunzio, N. R. (2003). Origins of highly mosaic mycobacteriophage genomes. *Cell, 113*(2), 171-182.

Pell, L. G., Cumby, N., Clark, T. E., Tuite, A., Battaile, K. P., Edwards, A. M., . . . Maxwell, K. L. (2013). A conserved spiral structure for highly diverged phage tail assembly chaperones. *Journal of Molecular Biology, 425*(14), 2436-2449. doi:https://doi.org/10.1016/j.jmb.2013.03.035

Pennington, J. M., & Rosenberg, S. M. (2007). Spontaneous DNA breakage in single living *Escherichia coli* cells. *Nature Genetics, 39*(6), 797-802.

Peralta, C., & Palma, L. (2017). Is the insect world overcoming the efficacy of *Bacillus thuringiensis*? *Toxins, 9*(1), 39.

Phillips, N. J., John, C. M., Reinders, L. G., Gibson, B. W., Apicella, M. A., & Griffiss, J. M. (1990). Structural models for the cell surface lipooligosaccharides of *Neisseria gonorrhoeae* and *Haemophilus influenzae*. *Biomedical and Environmental Mass Spectrometry, 19*(11), 731-745.

Pingitore, E. V., Salvucci, E., Sesma, F., & Nader-Macias, M. (2007). Different strategies for purification of antimicrobial peptides from lactic acid bacteria (LAB). *Communicating Current Research and Educational Topics and Trends in Applied Microbiology, 1*, 557-568.

Pinto, S. N., Dias, S. A., Cruz, A. F., Mil-Homens, D., Fernandes, F., Valle, J., . . . Coutinho, A. (2019). The mechanism of action of pepR, a viral-derived peptide, against *Staphylococcus aureus* biofilms. *Journal of Antimicrobial and Chemotherapy, 74*(9), 2617-2625.

Polson, A. (1993). A theory for the displacement of proteins and viruses with polyethylene glycol. 1977. *Preparative Biochemistry, 23*(1-2), 31-50. doi:https://doi.org/10.1080/10826069308544535

Popescu, A., & Doyle, R. (1996). The gram stain after more than a century. *Biotechnic and Histochemistry, 71*(3), 145-151.

Popp, P. F., & Mascher, T. (2019). Coordinated cell death in isogenic bacterial populations: Sacrificing some for the benefit of many? *Journal of Molecular Biology, 431*(23), 4656-4669. doi:https://doi.org/10.1016/j.jmb.2019.04.024

Posey, J. E., & Gherardini, F. C. (2000). Lack of a role for iron in the lyme disease pathogen. *Science, 288*(5471), 1651-1653.

Prasanna, L., Eijsink, V. G., Meadow, R., & Gåseidnes, S. (2013). A novel strain of *Brevibacillus laterosporus* produces chitinases that contribute to its biocontrol potential. *Applied Microbiology and Biotechnology, 97*(4), 1601-1611.

Prenner, E. J., Lewis, R. N. A. H., & McElhaney, R. N. (1999). The interaction of the antimicrobial peptide gramicidin S with lipid bilayer model and biological membranes. *Biochimica et Biophysica Acta-Biomembranes, 1462*(1), 201-221. doi:https://doi.org/10.1016/S0005-2736(99)00207-2

Prozorov, A. A. (1996). Defective phages of bacilli: cell parasites or chromosomal components. *Genetika, 32*(4), 469-481.

Ptashne, M. (1992). A genetic switch: phage k and higher organisms. *Cambridge Massachusetts*.

Pu, X., Yang, Y., Wu, S., & Wu, Y. (2010). Characterisation of abamectin resistance in a field-evolved multiresistant population of *Plutella xylostella*. *Pest Management Science, 66*(4), 371-378.

Qian, Y., Huang, H.-H., Jiménez, J. I., & Del Vecchio, D. (2017). Resource competition shapes the response of genetic circuits. *ACS Synthetic Biology, 6*(7), 1263-1272.

Rajnovic, D., Muñoz-Berbel, X., & Mas, J. (2019). Fast phage detection and quantification: an optical density-based approach. *Plos One, 14*(5), e0216292.

Rakhuba, D., Kolomiets, E., Dey, E. S., & Novik, G. (2010). Bacteriophage receptors, mechanisms of phage adsorption and penetration into host cell. *Polish Journal of Microbiology, 59*(3), 145.

Ramachandran, S., Buntin, G. D., & All, J. N. (2000). Response of canola to simulated diamondback moth (Lepidoptera: Plutellidae) defoliation at different growth stages. *Canadian Journal of Plant Science, 80*(3), 639-646.

Ramisetty, B. C. M., & Sudhakari, P. A. (2019). Bacterial 'grounded'prophages: hotspots for genetic renovation and innovation. *Frontiers in Genetics, 10*, 65.

Rao, V. B., & Feiss, M. (2008). The bacteriophage DNA packaging motor. *Annual Review of Genetics, 42*, 647-681.

Ravantti, J. J., Gaidelyte, A., Bamford, D. H., & Bamford, J. K. (2003). Comparative analysis of bacterial viruses Bam35, infecting a gram-positive host, and PRD1, infecting gram-negative hosts, demonstrates a viral lineage. *Virology, 313*(2), 401-414.

Raymond, B., & Federici, B. A. (2017). In defence of *Bacillus thuringiensis*, the safest and most successful microbial insecticide available to humanity- a response to EFSA. *FEMS Microbiology Ecology, 93*(7). doi:https://doi.org/10.1093/femsec/fix084

Raymond, B., Johnston, P. R., Nielsen-LeRoux, C., Lereclus, D., & Crickmore, N. (2010). *Bacillus thuringiensis*: an impotent pathogen? *Trends in Microbiology, 18*(5), 189-194.

Rea, M. C., Sit, C. S., Clayton, E., O'Connor, P. M., Whittal, R. M., Zheng, J., . . . Hill, C. (2010). Thuricin CD, a posttranslationally modified bacteriocin with a narrow spectrum of activity against *Clostridium difficile*. *Proceedings of the National Academy of Sciences, 107*(20), 9352-9357.

Reddy, P. V., Puri, R. V., Khera, A., & Tyagi, A. K. (2012). Iron storage proteins are essential for the survival and pathogenesis of *Mycobacterium tuberculosis* in THP-1 macrophages and the guinea pig model of infection. *Journal of Bacteriology, 194*(3), 567-575.

Reim, D. F., & Speicher, D. W. (2001). N-terminal sequence analysis of proteins and peptides. *Current Protocol in Protein Science, Chapter 11*, Unit 11.10. doi:https://doi.org/10.1002/0471140864.ps1110s08

Riaz, M. A., Adang, M. J., Hua, G., Rezende, T. M. T., Rezende, A. M., & Shen, G. M. (2020). Identification of *Lysinibacillus sphaericus* binary toxin binding proteins in a malarial mosquito cell line by proteomics: a novel approach towards improving mosquito control. *Journal of Proteomics, 227*, 103918.

Ribatti, D. (2020). François Jacob, lysogeny, and the development of the operon model. *Critical Reviews in Eukaryotic Gene Expression, 30*(5).

Riley, M. A. (2011). Bacteriocin-mediated competitive interactions of bacterial populations and communities. In D. Drider & S. Rebuffat (Eds.), *Prokaryotic antimicrobial peptides from genes to applications* (pp. 13-26). New York: Springer. doi:https://doi.org/10.1007/978-1-4419-7692-5

Riley, M. A., & Chavan, M. A. (2007). *Bacteriocins: Ecology and evolution* (1st ed.). Berlin, Heidelberg: Springer.

Riley, M. A., & Wertz, J. E. (2002a). Bacteriocin diversity: ecological and evolutionary perspectives. *Biochimie, 84*(5-6), 357-364. doi:https://doi.org/10.1016/s0300-9084(02)01421-9

Riley, M. A., & Wertz, J. E. (2002b). Bacteriocins: evolution, ecology, and application. *Annual Reviews in Microbiology, 56*(1), 117-137.

Roberts, J. N., Singh, R., Grigg, J. C., Murphy, M. E., Bugg, T. D., & Eltis, L. D. (2011). Characterisation of dye-decolorising peroxidases from *Rhodococcus jostii* RHA1. *Biochemistry, 50*(23), 5108-5119.

Robertson, J., McGoverin, C., Vanholsbeeck, F., & Swift, S. (2019). Optimisation of the protocol for the LIVE/DEAD® BacLightTM bacterial viability kit for rapid determination of bacterial load. *Frontiers in Microbiology, 10*, 801.

Rocchi, I., Ericson, C. F., Malter, K. E., Zargar, S., Eisenstein, F., Pilhofer, M., . . . Shikuma, N. J. (2019). A bacterial phage tail-like structure kills eukaryotic cells by injecting a nuclease effector. *Cell Reports, 28*(2), 295-301. e294.

Rodriguez, R. A., Bounty, S., Beck, S., Chan, C., McGuire, C., & Linden, K. G. (2014). Photoreactivation of bacteriophages after UV disinfection: Role of genome structure and impacts of UV source. *Water Research, 55*, 143-149.

Roh, J.-Y., Choi, J.-Y., Li, M.-S., Jin, B.-R., & Je, Y.-H. (2007). *Bacillus thuringiensis* as a specific, safe, and effective tool for insect pest control. *Journal of Microbiology and Biotechnology, 17*(4), 547-559.

Rohwer, F. (2003). Global phage diversity. *Cell, 113*(2), 141. doi:https://doi.org/10.1016/S0092-8674(03)00276-9

Rohwer, F., & Edwards, R. (2002). The phage proteomic tree: a genome-based taxonomy for phage. *Journal of Bacteriology, 184*(16), 4529-4535.

Ronneau, S., & Helaine, S. (2019). Clarifying the link between toxin-antitoxin modules and bacterial persistence. *Journal of Molecular Biology, 431*(18), 3462-3471.

Rosenkrands, I., Rasmussen, P. B., Carnio, M., Jacobsen, S., Theisen, M., & Andersen, P. (1998). Identification and characterisation of a 29-kilodalton protein from *Mycobacterium tuberculosis* culture filtrate recognised by mouse memory effector cells. *Infection and Immunity, 66*(6), 2728-2735.

Ross, A., Ward, S., & Hyman, P. (2016). More is better: selecting for broad host range bacteriophages. *Frontiers in Microbiology, 7*, 1352.

Roy, I., Mondal, K., & Gupta, M. N. (2007). Leveraging protein purification strategies in proteomics. *Journal of Chromatography B, 849*(1), 32-42. doi:https://doi.org/10.1016/j.jchromb.2006.11.016

Ruiu, L. (2013). *Brevibacillus laterosporus,* a pathogen of invertebrates and a broad-spectrum antimicrobial species. *Insects, 4*(3), 476-492. doi:https://doi.org/10.3390/insects4030476

Ruiu, L. (2018). Microbial biopesticides in agroecosystems. *Agronomy, 8*(11), 235.

Ruiu, L., Delrio, G., Ellar, D. J., Floris, I., Paglietti, B., Rubino, S., & Satta, A. (2006). Lethal and sublethal effects of *Brevibacillus laterosporus* on the housefly *(Musca domestica*). *Entomologia Experimentalis et Applicata, 118*(2), 137-144.

Ruiu, L., Floris, I., Satta, A., & Ellar, D. (2007). Toxicity of a *Brevibacillus laterosporus* strain lacking parasporal crystals against *Musca domestica* and *Aedes aegypti*. *Biological Control, 43*(1), 136-143.

Ruiu, L., Lazzeri, A. M., Nuvoli, M. T., Floris, I., & Satta, A. (2020). Safety evaluation of the entomopathogenic bacterium *Brevibacillus laterosporus* for the green lacewing *Chrysoperla agilis* (Neuroptera: Chrysopidae). *Journal of Invertebrate Pathology, 169*, 107281.

Ruiu, L., Satta, A., & Floris, I. (2013). Emerging entomopathogenic bacteria for insect pest management. *Bulletin of Insectology, 66*(2), 181-186.

Russell, A. B., Peterson, S. B., & Mougous, J. D. (2014). Type VI secretion system effectors: poisons with a purpose. *Nature Reviews Microbiology, 12*(2), 137-148.

Rybakova, D., Mitra, A. K., & Hurst, M. R. H. (2014). Purification and TEM of Afp and Its variants. *Bio-protocol, 4*(10), e1132. doi:https://doi.org/10.21769/BioProtoc.1132

Rybakova, D., Radjainia, M., Turner, A., Sen, A., Mitra, A. K., & Hurst, M. R. (2013). Role of antifeeding prophage (Afp) protein Afp 16 in terminating the length of the Afp tailocin and stabilising its sheath. *Molecular Microbiology, 89*(4), 702-714.

Saha, S. (2016). *A tale of two tails: Characterisation of R-type and F-type pyocins of Pseudomonas aeruginosa* (Doctoral Thesis). University of Toronto (Canada). Retrieved from https://tspace.library.utoronto.ca

Saha, S., Ojobor, C. D., Mackinnon, E., North, O. I., Bondy-Denomy, J., Lam, J. S., . . . Davidson, A. R. (2021). F-type pyocins are diverse non-contractile phage tail-like weapons for killing *Pseudomonas aeruginosa*. *BioRxiv*, 2021.2002.2016.431561. doi:https://doi.org/10.1101/2021.02.16.431561

Saikia, R., Gogoi, D., Mazumder, S., Yadav, A., Sarma, R., Bora, T., & Gogoi, B. (2011). *Brevibacillus laterosporus* strain BPM3, a potential biocontrol agent isolated from a natural hot water spring of Assam, India. *Microbiological Research, 166*(3), 216-225.

Salama, H., Foda, M., El-Bendary, M., & Abdel-Razek, A. (2004). Infection of red palm weevil, *Rhynchophorus ferrugineus*, by spore-forming bacilli indigenous to its natural habitat in Egypt. *Journal of Pest Science, 77*(1), 27-31.

Sampson, K. S., Tomso, D. J., & Guo, R., &. (2016). *Pesticidal genes from Brevibacillus and methods for their use*. US Patent No. 2013/0167264 A1. Washington DC:US Patent and Trademark Office

Sanchez-Contreras, M., & Vlisidou, I. (2008). The diversity of insect-bacteria interactions and its applications for disease control. *Biotechnology and Genetic Engineering Reviews, 25*(1), 203-244.

Sanchis, V. (2011). From microbial sprays to insect-resistant transgenic plants: History of the biospesticide *Bacillus thuringiensis*. a review. *Agronomy for Sustainable Development, 31*(1), 217-231.

Sanders, E. R. (2012). Aseptic laboratory techniques: plating methods. *Journal of Visualised Experiments (JoVE)* (63), e3064.

Sanderson, J. M. (2005). Peptide-lipid interactions: insights and perspectives [10.1039/B415499A]. *Organic and Biomolecular Chemistry, 3*(2), 201-212. doi:https://doi.org/10.1039/B415499A

Sandiford, S. K. (2015). Perspectives on lantibiotic discovery - where have we failed and what improvements are required? *Expert Opinion Drug Discovery, 10*(4), 315-320. doi:https://doi.org/10.1517/17460441.2015.1016496

Sanjuán, R., Nebot, M. R., Chirico, N., Mansky, L. M., & Belshaw, R. (2010). Viral mutation rates. *Journal of Virology, 84*(19), 9733-9748.

Sano, Y., & Kageyama, M. (1987). The sequence and function of the recA gene and its protein in *Pseudomonas aeruginosa* PAO. *Molecular and General Genetics, 208*(3), 412-419. doi:https://doi.org/10.1007/bf00328132

Saren, A.-M., Ravantti, J. J., Benson, S. D., Burnett, R. M., Paulin, L., Bamford, D. H., & Bamford, J. K. (2005). A snapshot of viral evolution from genome analysis of the *Tectiviridae* family. *Journal of Molecular Biology, 350*(3), 427-440.

Sarfraz, M., Keddie, A. B., & Dosdall, L. M. (2005). Biological control of the diamondback moth, *Plutella xylostella*: a review. *Biocontrol Science and Technology, 15*(8), 763-789.

Sarris, P. F., Ladoukakis, E. D., Panopoulos, N. J., & Scoulica, E. V. (2014). A phage tail-derived element with wide distribution among both prokaryotic domains: a comparative genomic and phylogenetic study. *Genome Biology and Evolution, 6*(7), 1739-1747. doi:https://doi.org/10.1093/gbe/evu136

Sauder, A. B., Quinn, M. R., Brouillette, A., Caruso, S., Cresawn, S., Erill, I., . . . Scott, C. (2016). Genomic characterisation and comparison of seven *Myoviridae* bacteriophage infecting *Bacillus thuringiensis*. *Virology, 489*, 243-251.

Sayyed, A. H., & Wright, D. J. (2006). Genetics and evidence for an esterase-associated mechanism of resistance to indoxacarb in a field population of diamondback moth (Lepidoptera: Plutellidae). *Pest Management Science, 62*(11), 1045-1051.

Schnepf, E., Crickmore, N., Van Rie, J., Lereclus, D., Baum, J., Feitelson, J., . . . Dean, D. H. (1998). *Bacillus thuringiensis* and its pesticidal crystal proteins. *Microbiology and Molecular Biology Reviews : MMBR, 62*(3), 775-806. doi:https://doi.org/10.1128/MMBR.62.3.775-806.1998

Scholl, D. (2017). Phage tail–like bacteriocins. *Annual Review of Virology, 4*(1), 453-467. doi:https://doi.org/10.1146/annurev-virology-101416-041632

Scholl, D., Cooley, M., Williams, S. R., Gebhart, D., Martin, D., Bates, A., & Mandrell, R. (2009). An engineered R-type pyocin is a highly specific and sensitive bactericidal agent for the food-borne pathogen *Escherichia coli* O157: H7. *Antimicrobial Agents and Chemotherapy, 53*(7), 3074-3080.

Scholl, D., Gebhart, D., Williams, S. R., Bates, A., & Mandrell, R. (2012). Genome sequence of *Escherichia coli* O104: H4 leads to rapid development of a targeted antimicrobial agent against this emerging pathogen. *Plos One, 7*(3), e33637.

Scholl, D., & Martin, D. W., Jr. (2008). Antibacterial efficacy of R-type pyocins towards *Pseudomonas aeruginosa* in a murine peritonitis model. *Antimicrobial Agents and Chemotherapy, 52*(5), 1647-1652. doi:https://doi.org/10.1128/aac.01479-07

Schuster, C. F., & Bertram, R. (2013). Toxin-antitoxin systems are ubiquitous and versatile modulators of prokaryotic cell fate. *FEMS Microbiology Letters, 340*(2), 73-85. doi:https://doi.org/10.1111/1574-6968.12074

Schwemmlein, N., Pippel, J., Gazdag, E. M., & Blankenfeldt, W. (2018). Crystal structures of R-type bacteriocin sheath and tube proteins CD1363 and CD1364 from *Clostridium difficile* in the pre-assembled state. *Frontiers Microbiology, 9*, 1750. doi:https://doi.org/10.3389/fmicb.2018.01750

Seaman, E., Tarmy, E., & Marmur, J. (1964). Inducible phages of *Bacillus subtilis*. *Biochemistry, 3*(5), 607-613.

Senior, B. W. (1984). The effect of temperature on the synthesis and assembly of proticine 3 particles by *Proteus mirabilis*. *Journal of General Microbiology, 130*(10), 2699-2708. doi:https://doi.org/10.1099/00221287-130-10-2699

Serwer, P., Hayes, S. J., Zaman, S., Lieman, K., Rolando, M., & Hardies, S. C. (2004). Improved isolation of undersampled bacteriophages: finding of distant terminase genes. *Virology, 329*(2), 412-424.

Shah, D., Zhang, Z., Khodursky, A. B., Kaldalu, N., Kurg, K., & Lewis, K. (2006). Persisters: a distinct physiological state of *Escherichia coli*. *BMC Microbiology, 6*(1), 53. doi:https://doi.org/10.1186/1471-2180-6-53

Sharma, V., Singh, P. K., Midha, S., Ranjan, M., Korpole, S., & Patil, P. B. (2012). Genome sequence of *Brevibacillus laterosporus* strain GI-9. *Journal of Bacteriology, 194*. doi:https://doi.org/10.1128/JB.06659-11

Shelton, A. (2004). Management of the diamondback moth: déjà vu all over again. *The Management of Diamondback Moth and Other Crucifer Pests*, 3-8.

Shendure, J., & Aiden, E. L. (2012). The expanding scope of DNA sequencing. *Nature Biotechnology, 30*(11), 1084-1094.

Shi, Y., Zhang, X., Lou, K., & Adams, M. (2013). Isolation, characterisation, and insecticidal activity of an endophyte of drunken horse grass, *Achnatherum inebrians*. *Journal of Insect Science, 13*(1).

Shida, O., Takagi, H., Kadowaki, K., & Komagata, K. (1996). Proposal for two new genera, *Brevibacillus* gen. nov. and *Aneurinibacillus* gen. nov. *International Journal of Systematic and Evolutionary Microbiology, 46*(4), 939-946.

Shikuma, N. J., Pilhofer, M., Weiss, G. L., Hadfield, M. G., Jensen, G. J., & Newman, D. K. (2014). Marine tubeworm metamorphosis induced by arrays of bacterial phage tail–like structures. *Science, 343*(6170), 529-533.

Shinomiya, T., Shiga, S., Kikuchi, A., & Kageyama, M. (1983). Genetic determinant of pyocin R2 in *Pseudomonas aeruginosa* PAO. *Molecular and General Genetics 189*(3), 382-389.

Shneider, M. M., Buth, S. A., Ho, B. T., Basler, M., Mekalanos, J. J., & Leiman, P. G. (2013). PAAR-repeat proteins sharpen and diversify the type VI secretion system spike. *Nature, 500*(7462), 350-353. doi:https://doi.org/10.1038/nature12453

Shoji, J., & Kato, T. (1976). The structure of brevistin. *Journal of Antibiotics, 29*. doi:https://doi.org/10.7164/antibiotics.29.380

Shopera, T., He, L., Oyetunde, T., Tang, Y. J., & Moon, T. S. (2017). Decoupling resource-coupled gene expression in living cells. *ACS Synthetic Biology, 6*(8), 1596-1604. doi:https://doi.org/10.1021/acssynbio.7b00119

Siegwart, M., Graillot, B., Blachere Lopez, C., Besse, S., Bardin, M., Nicot, P. C., & Lopez-Ferber, M. (2015). Resistance to bio-insecticides or how to enhance their sustainability: a review. *Frontiers in Plant Science, 6*, 381.

Sieuwerts, S., de Bok, F. A., Mols, E., de vos, W. M., & Vlieg, J. E. (2008). A simple and fast method for determining colony forming units. *Letters in Applied Microbiology, 47*(4), 275-278. doi:https://doi.org/10.1111/j.1472-765X.2008.02417.x

Silva Filha, M. H. N. L., Berry, C., & Regis, L. (2014). *Lysinibacillus sphaericus*: Toxins and mode of action, applications for mosquito control and resistance management. In T. S. Dhadialla & S. S. Gill (Eds.), *Advances in Insect Physiology* (Vol. 47, pp. 89-176): Elsevier. Retrieved from https://www.sciencedirect.com/science/article/pii/B9780128001974000038. doi:https://doi.org/10.1016/B978-0-12-800197-4.00003-8

Silva, I., Campos, F., Hogg, T., & Couto, J. (2011). Wine phenolic compounds influence the production of volatile phenols by wine-related lactic acid bacteria. *Journal of Applied Microbiology, 111*(2), 360-370.

Šimoliūnas, E., Truncaitė, L., Rutkienė, R., Povilonienė, S., Goda, K., Kaupinis, A., . . . Meškys, R. (2019). The robust self-assembling tubular nanostructures formed by gp053 from phage vB_EcoM_FV3. *Viruses, 11*(1), 50.

Simpson, D. J., Sacher, J. C., & Szymanski, C. M. (2016). Development of an assay for the identification of receptor binding proteins from bacteriophages. *Viruses, 8*(1), 17.

Sinègre, G., Babinot, M., Quermal, J., & Gaven, B. (1994). First field occurrence of *Culex pipiens* resistance to *Bacillus sphaericus* in southern France. VII Eur. *Meeting Society of Vector Ecology*, 17.

Singer, S. (1996). The utility of strains of morphological group II *Bacillus*. *Advances in Applied Microbiology, 42*, 219-261.

Singer, S., Bair, T. B., Hammill, T. B., Berte, A. M., Correa-Ochoa, M. M., & Stambaugh, A. D. (1994). Fermentation and toxin studies of the molluscicidal strains of *Bacillus brevis*. *Journal of Industrial Microbiology, 13*(2), 112-119.

Singh, P. K., Sharma, V., Patil, P. B., & Korpole, S. (2012). Identification, purification and characterisation of laterosporulin, a novel bacteriocin produced by *Brevibacillus* sp. strain GI-9. *Plos One, 7*(3), e31498.

Singh, P. K., Solanki, V., Sharma, S., Thakur, K. G., Krishnan, B., & Korpole, S. (2015). The intramolecular disulfide-stapled structure of laterosporulin, a class IId bacteriocin, conceals a human defensin-like structural module. *FEBS Journal, 282*. doi:https://doi.org/10.1111/febs.13129

Smarda, J., & Benada, O. (2005). Phage tail-like (high molecular-weight) bacteriocins of *Budvicia aquatica* and *Pragia fontium* (Enterobacteriaceae). *Applied and Environmental Microbiology, 71*(12), 8970-8973. doi:https://doi.org/10.1128/aem.71.12.8970-8973.2005

Smith, J. L. (2004). The physiological role of Ferritin-like compounds in bacteria. *Critical Reviews in Microbiology, 30*(3), 173-185. doi:https://doi.org/10.1080/10408410490435151

Smith, S. G., Mahon, V., Lambert, M. A., & Fagan, R. P. (2007). A molecular swiss army knife: OmpA structure, function and expression. *FEMS Microbiology Letters, 273*(1), 1-11.

Smits, S. H. J., Schmitt, L., & Beis, K. (2020). Self-immunity to antibacterial peptides by ABC transporters. *FEBS Letters, 594*(23), 3920-3942. doi:https://doi.org/10.1002/1873-3468.13953

Somsap, O.-a., Bangrak, P., Bhoopong, P., & Lertcanawanichakul, M. (2016). Antibacterial activity and purification of bacteriocin produced by *Brevibacillus laterosporus* SA14. *Walailak Journal of Science and Technology 13*(1), 55-65. doi:https://doi.org/doi:10.14456/WJST.2016.6

Song, Z., Liu, K., Lu, C., Yu, J., Ju, R., & Liu, X. (2011). Isolation and characterisation of a potential biocontrol *Brevibacillus laterosporus*. *African Journal of Microbiology Research, 5*(18), 2675-2681.

Song, Z., Liu, Q., Guo, H., Ju, R., Zhao, Y., Li, J., & Liu, X. (2012). Tostadin, a novel antibacterial peptide from an antagonistic microorganism *Brevibacillus brevis* XDH. *Bioresource Technology, 111*. doi:https://doi.org/10.1016/j.biortech.2012.02.051

Soumia, P., Krishna, R., Jaiswal, D. K., Verma, J. P., Yadav, J., & Singh, M. (2021). Entomopathogenic microbes for sustainable crop protection: Future perspectives. In A. N. Yadav, J. Singh, C. Singh & N. Yadav (Eds.), *Current trends in microbial biotechnology for sustainable agriculture* (1st ed., pp. 469-497). Singapore: Springer. doi:https://doi.org/10.1007/978-981-15-6949-4

Sparks, T. C., Crouse, G. D., & Durst, G. (2001). Natural products as insecticides: the biology, biochemistry and quantitative structure- activity relationships of spinosyns and spinosoids. *Pest Management Science, 57*(10), 896-905.

Spizizen, J. (1958). Transformation of biochemically deficient strains of *Bacillus subtilis* by deoxyribonucleate. *Proceedings of the National Academy of Sciences USA, 44*(10), 1072.

Splith, K., & Neundorf, I. (2011). Antimicrobial peptides with cell penetrating peptide properties and vice versa. *European Biophysics Journal, 40*(4), 387-397.

Spoering, A. L., & Lewis, K. (2001). Biofilms and planktonic cells of *Pseudomonas aeruginosa* have similar resistance to killing by antimicrobials. *Journal of Bacteriology, 183*(23), 6746-6751. doi:https://doi.org/10.1128/jb.183.23.6746-6751.2001

Srividhya, K., Alaguraj, V., Poornima, G., Kumar, D., Singh, G., Raghavenderan, L., . . . Krishnaswamy, S. (2007). Identification of prophages in bacterial genomes by dinucleotide relative abundance difference. *Plos One, 2*(11), e1193.

Stachelhaus, T., Mootz, H. D., & Marahiel, M. A. (1999). The specificity-conferring code of adenylation domains in nonribosomal peptide synthetases. *Chemistry and Biology, 6*. doi:https://doi.org/10.1016/S1074-5521(99)80082-9

Stahly, D., & Klein, M. (1992). Problems with in vitro production of spores of *Bacillus popilliae* for use in biological control of the Japanese beetle. *Journal of Invertebrate Pathology, 60*(3), 283-291.

Stamm, M., Prochaska, T., Matz, N., & Baxendale, R. (2013). Efficacy of *Chromobacterium subtsugae* for control of southern masked chafers, 2012. *Arthropod Management Tests, 38*(1).

Steensma, H. (1981). Effect of defective phages on the cell membrane of *Bacillus subtilis* and partial characterisation of a phage protein involved in killing. *Journal of General Virology, 56*(2), 275-286.

Stern, N. J., Svetoch, E. A., Eruslanov, B. V., Perelygin, V. V., Mitsevich, E. V., Mitsevich, I. P., . . . Seal, B. S. (2006). Isolation of a *Lactobacillus salivarius* strain and purification of its bacteriocin, which is inhibitory to *Campylobacter jejuni* in the chicken gastrointestinal system. *Antimicrobial Agents and Chemotherapy, 50*(9), 3111-3116. doi:https://doi.org/10.1128/aac.00259-06

Stevenson, K., McVey, A. F., Clark, I. B. N., Swain, P. S., & Pilizota, T. (2016). General calibration of microbial growth in microplate readers. *Scientific Reports, 6*(1), 38828. doi:https://doi.org/10.1038/srep38828

Stiefel, P., Schmidt-Emrich, S., Maniura-Weber, K., & Ren, Q. (2015). Critical aspects of using bacterial cell viability assays with the fluorophores SYTO9 and propidium iodide. *BMC Microbiology, 15*(1), 1-9.

Stockley, P. G., White, S. J., Dykeman, E., Manfield, I., Rolfsson, O., Patel, N., . . . Twarock, R. (2016). Bacteriophage MS2 genomic RNA encodes an assembly instruction manual for its capsid. *Bacteriophage, 6*(1), e1157666-e1157666. doi:https://doi.org/10.1080/21597081.2016.1157666

Strauch, E., Kaspar, H., Schaudinn, C., Dersch, P., Madela, K., Gewinner, C., . . . Appel, B. (2001). Characterisation of enterocoliticin, a phage tail-like bacteriocin, and its effect on pathogenic *Yersinia enterocolitica* strains. *Applied and Environmental Microbiology, 67*(12), 5634-5642. doi:https://doi.org/10.1128/aem.67.12.5634-5642.2001

Stromsten, N. J., Benson, S. D., & Burnett, R. M. (2003). The *Bacillus thuringiensis* linear double-stranded DNA phage Bam35, which is highly similar to the *Bacillus cereus* linear plasmid pBClin15, has a prophage state. *Journal of Bacteriology, 185*. doi:https://doi.org/10.1128/JB.185.23.6985-6989.2003

Su, M. T., Venkatesh, T. V., & Bodmer, R. (1998). Large and small scale preparation of bacteriophage λ lysate and DNA. *BioTechniques, 25*(1), 44-46.

Su, T. (2017). Microbial control of pest and vector mosquitoes in North America north of Mexico. In *Microbial Control of Insect and Mite Pests* (pp. 393-407): Elsevier.

Su, T., Thieme, J., White, G. S., Lura, T., Mayerle, N., Faraji, A., . . . Brown, M. Q. (2019). High resistance to *Bacillus sphaericus* and susceptibility to other common pesticides in *Culex pipiens* (Diptera: Culicidae) from Salt Lake City, UT. *Journal of Medical Entomology, 56*(2), 506-513. doi:https://doi.org/10.1093/jme/tjy193

Su, Y., Liu, C., Fang, H., & Zhang, D. (2020). *Bacillus subtilis*: a universal cell factory for industry, agriculture, biomaterials and medicine. *Microbial Cell Factories, 19*(1), 1-12.

Sullivan, M. B., Waterbury, J. B., & Chisholm, S. W. (2003). Cyanophages infecting the oceanic cyanobacterium *Prochlorococcus*. *Nature, 424*(6952), 1047-1051. doi:https://doi.org /10.1038 /nature01929

Sun, S., Gao, S., Kondabagil, K., Xiang, Y., Rossmann, M. G., & Rao, V. B. (2012). Structure and function of the small terminase component of the DNA packaging machine in T4-like bacteriophages. *Proceedings of the National Academy of Sciences, 109*(3), 817-822.

Sun, S., Rao, V. B., & Rossmann, M. G. (2010). Genome packaging in viruses. *Current Opinion in Structural Biology, 20*(1), 114-120.

Suslova, M. Y., Lipko, I., Mamaeva, E., & Parfenova, V. (2012). Diversity of cultivable bacteria isolated from the water column and bottom sediments of the Kara Sea shelf. *Microbiology, 81*(4), 484-491.

Sutter, M., Boehringer, D., Gutmann, S., Günther, S., Prangishvili, D., Loessner, M. J., . . . Ban, N. (2008). Structural basis of enzyme encapsulation into a bacterial nanocompartment. *Nature Structural and Molecular Biology, 15*(9), 939-947.

Suttle, C. A. (2005). Viruses in the sea. *Nature, 437*(7057), 356-361.

Szermer-Olearnik, B., Sochocka, M., Zwolinska, K., Ciekot, J., Czarny, A., Szydzik, J., . . . Boratynski, J. (2014). Comparison of microbiological and physicochemical methods for enumeration of microorganisms. *Postepy Hig Med Dosw, 68*, 1392-1396.

Tabashnik, B. E. (1994). Evolution of resistance to *Bacillus thuringiensis*. *Annual Review of Entomology, 39*(1), 47-79.

Tagg, J. R., Dajani, A. S., & Wannamaker, L. W. (1976). Bacteriocins of gram-positive bacteria. *Bacteriological Reviews, 40*(3), 722-756. doi:https://doi.org/10.1128/br.40.3.722-756.1976

Takeda, Y., & Kageyama, M. (1975). Subunit arrangement in the extended sheath of pyocin R. *The Journal of Biochemistry, 77*(3), 679-684.

Takeuchi, T., Iinuma, H., Kunimoto, S., Masuda, T., Ishizuka, M., Takeuchi, M., . . . Umezawa, H. (1981). A new antitumor antibiotic, spergualin: isolation and antitumor activity. *Journal of Antibiotics, 34*. doi:https://doi.org/10.7164/antibiotics.34.1619

Takeya, K., Mlnamishima, Y., Amako, K., & Ohnishi, Y. (1967). A small rod-shaped pyocin. *Virology, 31*(1), 166-168.

Tan, Y., Zhang, K., Rao, X., Jin, X., Huang, J., Zhu, J., . . . Wang, L. (2007). Whole genome sequencing of a novel temperate bacteriophage of *P. aeruginosa:* evidence of tRNA gene mediating integration of the phage genome into the host bacterial chromosome. *Cellular Microbiology, 9*(2), 479-491.

Tardieu, A., Bonneté, F., Finet, S., & Vivares, D. (2002). Understanding salt or PEG induced attractive interactions to crystallize biological macromolecules. *Acta Crystallographica Section D: Biological Crystallography, 58*(10), 1549-1553.

Taylor, N. M., Prokhorov, N. S., Guerrero-Ferreira, R. C., Shneider, M. M., Browning, C., Goldie, K. N., . . . Leiman, P. G. (2016). Structure of the T4 baseplate and its function in triggering sheath contraction. *Nature, 533*(7603), 346-352. doi:https://doi.org/10.1038/nature17971

Taylor, N. M., van Raaij, M. J., & Leiman, P. G. (2018). Contractile injection systems of bacteriophages and related systems. *Molecular Microbiology, 108*(1), 6-15.

Taylor, V. L., Fitzpatrick, A. D., Islam, Z., & Maxwell, K. L. (2019). The diverse impacts of phage morons on bacterial fitness and virulence. *Advanced Virus Research, 103*, 1-31. doi:https://doi.org/10.1016/bs.aivir.2018.08.001

Teich, A., Lin, H., Andersson, L., Meyer, S., & Neubauer, P. (1998). Amplification of ColE1 related plasmids in recombinant cultures of *Escherichia col*i after IPTG induction. *Journal of Biotechnology, 64*(2-3), 197-210.

Terzi, M., & Levinthal, C. (1967). Effects of λ-phage infection on bacterial synthesis. *Journal of Molecular Biology, 26*(3), 525-535. doi:https://doi.org/10.1016/0022-2836(67)90320-8

Thaler, J. O., Baghdiguian, S., & Boemare, N. (1995). Purification and characterisation of xenorhabdicin, a phage tail-like bacteriocin, from the lysogenic strain F1 of *Xenorhabdus nematophilus*. *Applied and Environmental Microbiology, 61*(5), 2049-2052.

Theil, E. C., Behera, R. K., & Tosha, T. (2013). Ferritins for chemistry and for life. *Coordination Chemistry Reviews, 257*(2), 579-586.

Theodore, C. M., Stamps, B. W., King, J. B., Price, L. S. L., Powell, D. R., Stevenson, B. S., & Cichewicz, R. H. (2014). Genomic and metabolomic insights into the natural product biosynthetic diversity of a Feral-Hog associated *Brevibacillus laterosporus* strain. *Plos One, 9*(3), e90124. doi:https://doi.org/10.1371/journal.pone.0090124

Thomas, P., Sekhar, A., & Mujawar, M. (2012). Nonrecovery of varying proportions of viable bacteria during spread plating governed by the extent of spreader usage and proposal for an alternate spotting-spreading approach to maximise the CFU. *Journal of Applied Microbiology, 113*(2), 339-350.

Tomasz, M. (1995). Mitomycin C: small, fast and deadly (but very selective). *Chemistry and Biology, 2*(9), 575-579.

Torrent, M., Di Tommaso, P., Pulido, D., Nogués, M. V., Notredame, C., Boix, E., & Andreu, D. (2012). AMPA: an automated web server for prediction of protein antimicrobial regions. *Bioinformatics, 28*(1), 130-131.

Touchon, M., Bernheim, A., & Rocha, E. P. (2016). Genetic and life-history traits associated with the distribution of prophages in bacteria. *The ISME journal, 10*(11), 2744-2754.

Tran, N. P., Gury, J., Dartois, V., Nguyen, T. K. C., Seraut, H., Barthelmebs, L., . . . Cavin, J.-F. (2008). Phenolic acid-mediated regulation of the padC gene, encoding the phenolic acid decarboxylase of *Bacillus subtilis*. *Journal of Bacteriology, 190*(9), 3213-3224.

Trojet, S. N., Caumont-Sarcos, A., Perrody, E., Comeau, A. M., & Krisch, H. (2011). The Gp38 adhesins of the T4 superfamily: a complex modular determinant of the phage's host specificity. *Genome Biology and Evolution, 3*, 674-686.

Tu, J., Park, T., Morado, D. R., Hughes, K. T., Molineux, I. J., & Liu, J. (2017). Dual host specificity of phage SP6 is facilitated by tailspike rotation. *Virology, 507*, 206-215.

Turgis, M., Vu, K. D., Millette, M., Dupont, C., & Lacroix, M. (2016). Influence of environmental factors on bacteriocin production by human isolates of *Lactococcus lactis* MM19 and *Pediococcus acidilactici* MM33. *Probiotics Antimicrobial Proteins, 8*(1), 53-59. doi:https://doi.org/10.1007/s12602-015-9204-8

Turner, D., Kropinski, A. M., & Adriaenssens, E. M. (2021). A roadmap for genome-based phage taxonomy. *Viruses, 13*(3), 506.

Uratani, Y., & Hoshino, T. (1984). Pyocin R1 inhibits active transport in *Pseudomonas aeruginosa* and depolarizes membrane potential. *Journal of Bacteriology, 157*(2), 632-636.

Vacheron, J., Heiman, C. M., & Keel, C. (2021). Live cell dynamics of production, explosive release and killing activity of phage tail-like weapons for *Pseudomonas* kin exclusion. *Communications Biology, 4*(1), 87. doi:https://doi.org/10.1038/s42003-020-01581-1

Valdes-Stauber, N., & Scherer, S. (1996). Nucleotide sequence and taxonomical distribution of the bacteriocin gene lin cloned from *Brevibacterium linens* M18. *Applied and Environmental Microbiology, 62*(4), 1283-1286. doi:https://doi.org/10.1128/AEM.62.4.1283-1286.1996

Valdés-Stauber, N., & Scherer, S. (1994). Isolation and characterisation of Linocin M18, a bacteriocin produced by *Brevibacterium linens*. *Applied and Environmental Microbiology, 60*(10), 3809-3814. doi:https://doi.org/10.1128/aem.60.10.3809-3814.1994

Vallet-Gely, I., Lemaitre, B., & Boccard, F. (2008). Bacterial strategies to overcome insect defences. *Nature Reviews Microbiology, 6*(4), 302-313.

van Heel, A. J., de Jong, A., Song, C., Viel, J. H., Kok, J., & Kuipers, O. P. (2018). BAGEL4: a user-friendly web server to thoroughly mine RiPPs and bacteriocins. *Nucleic acids research, 46*(W1), W278-W281. doi:https://doi.org/10.1093/nar/gky383

Van Melderen, L., & Saavedra De Bast, M. (2009). Bacterial Toxin-Antitoxin systems: more than selfish entities? *Plos Genetics, 5*(3), e1000437. doi:https://doi.org/10.1371/journal.pgen.1000437

van Zijll de Jong, E., Roush, T. L., Glare, T. R., & Hampton, J. G. (2016). Discovery of two *Brevibacillus laterosporus* isolates from brassica with insecticidal properties against diamondback moth. *Biocontrol Science and Technology, 26*(3), 426-431.

Vasu, K., & Nagaraja, V. (2013). Diverse functions of restriction-modification systems in addition to cellular defence. *Microbiology and Molecular Biology Reviews, 77*(1), 53-72.

Vaughan, E. E., Daly, C., & Fitzgerald, G. F. (1992). Identification and characterisation of helveticin V-1829, a bacteriocin produced by *Lactobacillus helveticus* 1829. *Journal of Applied Bacteriology, 73*(4), 299-308.

Veesler, D., & Cambillau, C. (2011). A common evolutionary origin for tailed-bacteriophage functional modules and bacterial machineries. *Microbiology and Molecular Biology Reviews, 75*(3), 423-433.

Venema, K., Chikindas, M. L., Seegers, J., Haandrikman, A. J., Leenhouts, K. J., Venema, G., & Kok, J. (1997). Rapid and efficient purification method for small, hydrophobic, cationic bacteriocins: purification of lactococcin B and pediocin PA-1. *Applied and Environmental Microbiology, 63*(1), 305-309.

Ventura, M., Canchaya, C., Kleerebezem, M., de Vos, W. M., Siezen, R. J., & Brüssow, H. (2003). The prophage sequences of *Lactobacillus plantarum* strain WCFS1. *Virology, 316*(2), 245-255. doi:https://doi.org/10.1016/j.virol.2003.08.019

Verheust, C., Fornelos, N., & Mahillon, J. (2005). GIL16, a new gram-positive tectiviral phage related to the *Bacillus thuringiensis* GIL01 and the *Bacillus cereus* pBClin15 elements. *Journal of Bacteriology, 187*. doi:https://doi.org/10.1128/JB.187.6.1966-1973.2005

Verkerk, R. H., & Wright, D. J. (1996). Multitrophic interactions and management of the diamondback moth: a review. *Bulletin of Entomological Research, 86*(3), 205-216.

Vetsigian, K., Jajoo, R., & Kishony, R. (2011). Structure and evolution of *Streptomyces* interaction networks in soil and in silico. *Plos Biology, 9*(10), e1001184.

Vijayabharathi, R., Kumari, B. R., Sathya, A., Srinivas, V., Abhishek, R., Sharma, H. C., & Gopalakrishnan, S. (2014). Biological activity of entomopathogenic actinomycetes against lepidopteran insects (Noctuidae: Lepidoptera). *Canadian Journal of Plant Science, 94*(4), 759-769.

Vilmos, P., & Kurucz, E. (1998). Insect immunity: evolutionary roots of the mammalian innate immune system. *Immunology Letters, 62*(2), 59-66.

Vlisidou, I., Hapeshi, A., Healey, J. R., Smart, K., Yang, G., & Waterfield, N. R. (2019). Photorhabdus virulence cassettes: extracellular multi-protein needle complexes for delivery of small protein effectors into host cells. *BioRxiv*, 549964.

Wagner, P. L., & Waldor, M. K. (2002). Bacteriophage control of bacterial virulence. *Infection and Immunity, 70*(8), 3985-3993.

Waldor, M. K., & Mekalanos, J. J. (1996). Lysogenic conversion by a filamentous phage encoding cholera toxin. *Science, 272*(5270), 1910-1914. doi:https://doi.org/10.1126/science.272.5270.1910

Walker, J. (2005). Proteins structure, purification, characterisation, and functional analysis. In K. Wilson & J. Walker (Eds.), *Principles & techniques of biochemistry & molecular biology* (6th ed.). UK: Cambridge University Press. doi:https://doi.org/10.1017/CBO9780511813412

Wang, G.-H., Niu, L.-M., Ma, G.-C., Xiao, J.-H., & Huang, D.-W. (2014). Large proportion of genes in one cryptic WO prophage genome are actively and sex-specifically transcribed in a fig wasp species. *BMC Genomics, 15*(1), 1-10.

Wang, I.-N., Smith, D. L., & Young, R. (2000). Holins: the protein clocks of bacteriophage infections. *Annual Reviews in Microbiology, 54*(1), 799-825.

Weinbauer, M. G. (2004). Ecology of prokaryotic viruses. *FEMS Microbiology Reviews, 28*(2), 127-181.

Weinberg, E. D. (1997). The *Lactobacillus* anomaly: total iron abstinence. *Perspectives in Biology and Medicine, 40*(4), 578-583.

Wernegreen, J. J. (2012). Strategies of genomic integration within insect-bacterial mutualisms. *The Biological Bulletin, 223*(1), 112-122. doi:https://doi.org/10.1086/BBLv223n1p112

Westers, H., Dorenbos, R., Van Dijl, J. M., Kabel, J., Flanagan, T., Devine, K. M., . . . Darmon, E. (2003). Genome engineering reveals large dispensable regions in *Bacillus subtilis*. *Molecular Biology and Evolution, 20*(12), 2076-2090.

Westers, L., Westers, H., & Quax, W. J. (2004). *Bacillus subtilis* as cell factory for pharmaceutical proteins: a biotechnological approach to optimise the host organism. *Biochimica et Biophysica Acta- Molecular Cell Research, 1694*(1), 299-310. doi:https://doi.org/10.1016/j.bbamcr.2004.02.011

White, P., & Lotay, H. K. (1980). Minimal nutritional requirements of *Bacillus sphaericus* NCTC9602 and 26 other strains of this species: the majority grow and sporulate with acetate as sole major source of carbon. *Microbiology, 118*(1), 13-19.

White, R., & Dutky, S. (1940). Effect of the Introduction of milky diseases on populations of Japanese beetle larvae. *Journal of Economic Entomology, 33*(2).

Whitman, W. B., Coleman, D. C., & Wiebe, W. J. (1998). Prokaryotes: the unseen majority. *Proceedings of National Academy of Sciences USA, 95*(12), 6578-6583. doi:https://doi.org/10.1073 /pnas.95.12.6578

Wikoff, W. R., Liljas, L., Duda, R. L., Tsuruta, H., Hendrix, R. W., & Johnson, J. E. (2000). Topologically linked protein rings in the bacteriophage HK97 capsid. *Science, 289*(5487), 2129-2133.

Wilkins, M. R., Sanchez, J. C., Gooley, A. A., Appel, R. D., Humphery-Smith, I., Hochstrasser, D. F., & Williams, K. L. (1996). Progress with proteome projects: why all proteins expressed by a genome should be identified and how to do it. *Biotechnology and Genetic Engineering Reviews, 13*(1), 19-50.

Williams, S. R., Gebhart, D., Martin, D. W., & Scholl, D. (2008). Retargeting R-type pyocins to generate novel bactericidal protein complexes. *Applied and Environmental Microbiology, 74*(12), 3868-3876.

Wilmaerts, D., Windels, E. M., Verstraeten, N., & Michiels, J. (2019). General mechanisms leading to persister formation and awakening. *Trends in Genetics, 35*(6), 401-411.

Wilson, C., Jackson, T., & Mahanty, H. (1993). Preliminary characterisation of bacteriophages of *Serratia entomophila*. *Journal of Applied Bacteriology, 74*(4), 484-489.

Winand, R., Bogaerts, B., Hoffman, S., Lefevre, L., Delvoye, M., Van Braekel, J., . . . Vanneste, K. (2020). Targeting the 16s rRNA gene for bacterial identification in complex mixed samples: Comparative evaluation of second (illumina) and third (oxford nanopore technologies) generation sequencing technologies. *International Journal of Molecular Sciences, 21*(1), 298.

Winter, N., Triccas, J. A., Rivoire, B., Pessolani, M. C. V., Eiglmeier, K., Lim, E.-M., . . . Britton, W. J. (1995). Characterisation of the gene encoding the immunodominant 35 kDa protein of *Mycobacterium leprae*. *Molecular Microbiology, 16*(5), 865-876. doi:https://doi.org/10.1111/j.1365-2958.1995.tb02314.x

Wirawan, R. E., Swanson, K. M., Kleffmann, T., Jack, R. W., & Tagg, J. R. (2007). Uberolysin: a novel cyclic bacteriocin produced by *Streptococcus uberis*. *Microbiology, 153*(5), 1619-1630.

Wirth, M. C., Walton, W. E., & Federici, B. A. (2015). Evolution of resistance in *Culex quinquefasciatus* (Say) selected with a recombinant *Bacillus thuringiensis* strain-producing Cyt1Aa and Cry11Ba, and the binary toxin, Bin, from *Lysinibacillus sphaericus*. *Journal of Medical Entomology, 52*(5), 1028-1035. doi:https://doi.org/10.1093/jme/tjv115

Wommack, K. E., & Colwell, R. R. (2000). Virioplankton: viruses in aquatic ecosystems. *Microbiology and Molecular Biology Reviews, 64*(1), 69-114.

Woo, P. C. Y., Lau, S. K. P., Teng, J. L. L., Tse, H., & Yuen, K. Y. (2008). Then and now: use of 16S rDNA gene sequencing for bacterial identification and discovery of novel bacteria in clinical microbiology laboratories. *Clinical Microbiology and Infection, 14*(10), 908-934. doi:https://doi.org/10.1111/j.1469-0691.2008.02070.x

Wood, H. E., Dawson, M., Devine, K. M., & Mcconnell, D. J. (1990). Characterisation of PBSX, a defective prophage of *Bacillus subtilis*. *Journal of Bacteriology, 172*(5), 2667-2674.

Wright, D. J., Iqbal, M., Granero, F., & Ferre, J. (1997). A change in a single midgut receptor in the diamondback moth (*Plutella xylostella)* is only in part responsible for field resistance to *Bacillus thuringiensis* subsp. *kurstaki* and *B. thuringiensis* subsp. *aizawai*. *Applied and Environmental Microbiology, 63*(5), 1814-1819.

Wu, D., Yuan, Y., Liu, P., Wu, Y., & Gao, M. (2014). Cellular responses in *Bacillus thuringiensis* CS33 during bacteriophage BtCS33 infection. *Journal of Proteomics, 101*, 192-204.

Wu, S.-C., Yeung, J. C., Duan, Y., Ye, R., Szarka, S. J., Habibi, H. R., & Wong, S.-L. (2002). Functional production and characterisation of a fibrin-specific single-chain antibody fragment from *Bacillus subtilis*: effects of molecular chaperones and a wall-bound protease on antibody fragment production. *Applied and Environmental Microbiology, 68*(7), 3261-3269.

Wu, X. (1998). Characterisation of a large temperate bacteriophage from *Clostridium beijerinckii*. *Department of Microbiology, University of Otago, Dunedin*.

Wu, X., Ballard, J., & Jiang, Y. W. (2005). Structure and biosynthesis of the BT peptide antibiotic from *Brevibacillus texasporus*. *Applied and Environmental Microbiology, 71*. doi:https://doi.org/10.1128/AEM.71.12.8519-8530.2005

Xu, C., Qin, C., Zhang, R., Niu, W., & Shang, X. (2010). Solid-phase synthesis and antibiotic activities of cyclodecapeptides on the scaffold of naturally occurring laterocidin. *Bioorganic and Medical Chemistry Letter, 20*. doi:https://doi.org/10.1016/j.bmcl.2009.11.009

Yamada, K., Hirota, M., Niimi, Y., Nguyen, H. A., Takahara, Y., Kamio, Y., & Kaneko, J. (2006). Nucleotide sequences and organisation of the genes for carotovoricin (Ctv) from *Erwinia carotovora* indicate that Ctv evolved from the same ancestor as *Salmonella typhi* prophage. *Bioscience, Biotechnology, and Biochemistry, 70*(9), 2236-2247.

Yamaguchi, Y., Park, J. H., & Inouye, M. (2011). Toxin-antitoxin systems in bacteria and archaea. *Annual Review of Genetics, 45*, 61-79.

Yang, G., Dowling, A., Gerike, U., Ffrench-Constant, R., & Waterfield, N. (2006). Photorhabdus virulence cassettes confer injectable insecticidal activity against the wax moth. *Journal of Bacteriology, 188*(6), 2254-2261.

Yang, X., Huang, E., Yuan, C., Zhang, L., & Yousef, A. E. (2016). Isolation and structural elucidation of brevibacillin, an antimicrobial lipopeptide from *Brevibacillus laterosporus* that combats drug-resistant gram-positive bacteria. *Applied and Environmental Microbiology, 82*. doi:https://doi.org/10.1128/AEM.00315-16

Yang, X., & Yousef, A. E. (2018a). Antimicrobial peptides produced by *Brevibacillus* spp.: structure, classification and bioactivity: a mini review. *World Journal of Microbiology and Biotechnology, 34*(4), 57. doi:https://doi.org/10.1007/s11274-018-2437-4

Yang, X., & Yousef, A. E. (2018b). Antimicrobial peptides produced by *Brevibacillus* spp.: structure, classification and bioactivity: a mini review. *World Journal of Microbiology and Biotechnology, 34*(4), 57. doi:10.1007/s11274-018-2437-4

Yang, X. M., & Wang, S. S. (1998). Development of *Bacillus thuringiensis* fermentation and process control from a practical perspective. *Biotechnology and Applied Biochemistry, 28*(2), 95-98.

Yao, G. W., Duarte, I., Le, T. T., Carmody, L., LiPuma, J. J., Young, R., & Gonzalez, C. F. (2017). A broad-host-range tailocin from *Burkholderia cenocepacia*. *Applied and Environmental Microbiology, 83*(10). doi:https://doi.org/10.1128/aem.03414-16

Yarmolinsky, M. B. (1995). Programmed cell death in bacterial populations. *Science, 267*(5199), 836-838.

Yasumitsu, H., Ozeki, Y., Kawsar, S. M., Fujii, Y., Sakagami, M., Matuo, Y., . . . Katsuno, H. (2010). RAMA stain: a fast, sensitive and less protein-modifying CBB R250 stain. *Electrophoresis, 31*(12), 1913-1917.

Yeaman, M. R., & Yount, N. Y. (2003). Mechanisms of antimicrobial peptide action and resistance. *Pharmacological Reviews, 55*(1), 27-55.

Yeates, T. O., Thompson, M. C., & Bobik, T. A. (2011). The protein shells of bacterial microcompartment organelles. *Current Opinion in Structural Biology, 21*(2), 223-231.

Yin, J. (1991). A quantifiable phenotype of viral propagation. *Biochemical and Biophysical Research Communications, 174*(2), 1009-1014.

Yin, J. (1993). Evolution of bacteriophage T7 in a growing plaque. *Journal of Bacteriology, 175*(5), 1272-1277.

Yokoyama, K., Makino, K., Kubota, Y., Watanabe, M., Kimura, S., Yutsudo, C. H., . . . Tatsuno, I. (2000). Complete nucleotide sequence of the prophage VT1-Sakai carrying the Shiga toxin 1 genes of the enterohemorrhagic *Escherichia coli* O157: H7 strain derived from the Sakai outbreak. *Gene, 258*(1-2), 127-139.

Yosef, I., Goren, M. G., Globus, R., Molshanski-Mor, S., & Qimron, U. (2017). Extending the host range of bacteriophage particles for DNA transduction. *Molecular cell, 66*(5), 721-728. e723.

Young, I., Wang, I., & Roof, W. D. (2000). Phages will out: strategies of host cell lysis. *Trends in Microbiology, 8*(3), 120-128. doi:https://doi.org/10.1016/s0966-842x(00)01705-4

Young, R. (2013). Phage lysis: do we have the hole story yet? *Current Opinion in Microbiology, 16*(6), 790-797.

Young, R. (2014). Phage lysis: three steps, three choices, one outcome. *Journal of Microbiology, 52*(3), 243-258.

Young, R., & Bläsi, U. (1995). Holins: form and function in bacteriophage lysis. *FEMS Microbiology Reviews, 17*(1-2), 191-205.

Yuan, Y., Gao, M., Peng, Q., Wu, D., Liu, P., & Wu, Y. (2014). Genomic analysis of a phage and prophage from a *Bacillus thuringiensis* strain. *Journal of General Virology, 95*(Pt 3), 751-761. doi:https://doi.org/10.1099/vir.0.058735-0

Yuan, Y., Gao, M., Wu, D., Liu, P., & Wu, Y. (2012). Genome characteristics of a novel phage from *Bacillus thuringiensis* showing high similarity with phage from *Bacillus cereus*. *Plos One, 7*(5), e37557.

Zalucki, M. P., Shabbir, A., Silva, R., Adamson, D., Shu-Sheng, L., & Furlong, M. J. (2012). Estimating the economic cost of one of the world's major insect pests, *Plutella xylostella* (Lepidoptera: Plutellidae): just how long is a piece of string? *Journal of Economic Entomology, 105*(4), 1115-1129.

Zeidner, G., Bielawski, J. P., Shmoish, M., Scanlan, D. J., Sabehi, G., & Béjà, O. (2005). Potential photosynthesis gene recombination between *Prochlorococcus* and *Synechococcus* via viral intermediates. *Environmental Microbiology, 7*(10), 1505-1513.

Zeigler, D. (2001). The genus *Geobacillus.* Introduction and strain catalog. *Catalog of strains, 3*.

Zhao, J., Guo, L., Zeng, H., Yang, X., Yuan, J., Shi, H., . . . Qiu, D. (2012a). Purification and characterisation of a novel antimicrobial peptide from *Brevibacillus laterosporus* strain A60. *Peptides, 33 (2)*. doi:https://doi.org/10.1016/j.peptides.2012.01.001

Zhao, J., Guo, L., Zeng, H., Yang, X., Yuan, J., Shi, H., . . . Qiu, D. (2012b). Purification and characterisation of a novel antimicrobial peptide from *Brevibacillus laterosporus* strain A60. *Peptides, 33*(2), 206-211. doi:10.1016/j.peptides.2012.01.001

Zhao, J. Z., Li, Y. X., Collins, H., Gusukuma-Minuto, L., Mau, R., Thompson, G., & Shelton, A. (2002). Monitoring and characterisation of diamondback moth (Lepidoptera: Plutellidae) resistance to spinosad. *Journal of Economic Entomology, 95*(2), 430-436.

Zheng, Z., Zheng, J., Zhang, Z., Peng, D., & Sun, M. (2016). Nematicidal spore-forming *Bacilli* share similar virulence factors and mechanisms. *Scientific Reports, 6*(1), 1-9.

Zhou, J., Gu, Y., & Chen, Y. (2006). Development of a formulation against phytopathogens using *Brevibacillus laterosporus* YMF3. 00003 strain. *Journal of Yunnan University Natural Sciences, 28*(5), 456.

Zhou, K., Zeng, Y. T., Han, X. F., & Liu, S. L. (2015). Modelling growth and bacteriocin production by *Lactobacillus plantarum* BC-25 in response to temperature and pH in batch fermentation. *Applied Biochemistry and Biotechnology, 176*(6), 1627-1637. doi:https://doi.org/10.1007/s12010-015-1666-3

Zhou, L., Huang, J., & Xu, H. (2011). Monitoring resistance of field populations of diamondback moth *Plutella xylostella* L.(Lepidoptera: Yponomeutidae) to five insecticides in South China: A ten-year case study. *Crop Protection, 30*(3), 272-278.

Zimina, M., Babich, O., Prosekov, A., Sukhikh, S., Ivanova, S., Shevchenko, M., & Noskova, S. (2020). Overview of global trends in classification, methods of preparation and application of bacteriocins. *Antibiotics, 9*(9), 553.

Zou, J., Jiang, H., Cheng, H., Fang, J., & Huang, G. (2018a). Strategies for screening, purification and characterisation of bacteriocins. *International Journal of Biological Macromolecules, 117*, 781-789. doi:https://doi.org/10.1016/j.ijbiomac.2018.05.233

Zou, J., Jiang, H., Cheng, H., Fang, J., & Huang, G. (2018b). Strategies for screening, purification and characterization of bacteriocins. *International Journal of Biological Macromolecules, 117*, 781-789. doi:10.1016/j.ijbiomac.2018.05.233

Zubasheva, M., Ganushkina, L., Smirnova, T., & Azizbekyan, R. (2010). Larvicidal activity of crystal-forming strains of *Brevibacillus laterosporus*. *Applied Biochemistry and Microbiology, 46*(8), 755-762.

Zvenigorodskii, V. I., Izakson, I. S., & Kapitonova, O. N. (1975). Identification of bacteriophages and study of the properties of phage-resistant mutants of *Bacillus thuringiensis* var. *galleriae*. *Nauchnye Doki Vyss Shkoly Biol Nauki, 5*.

Zweers, J. C., Barák, I., Becher, D., Driessen, A. J., Hecker, M., Kontinen, V. P., . . . van Dijl, J. M. (2008). Towards the development of *Bacillus subtilis* as a cell factory for membrane proteins and protein complexes. *Microbial Cell Factories, 7*(1), 1-20.

Appendices

Appendix A

A.1 Composition of modified LB medium

A		
LB medium		
NaOH (0.0125% V/V)	10% w/v	0.0125% w/v
MQW	994 ml	
Agar (Solid Media)	15 g	15 g/L
B (Filter sterilised)		
Glucose 20% w/v	50 ml	
Nitrilotriacetic acid (1.05 M)	1 ml	1.05 mM
$MgSO_4.7H_2o$ (0.59 M)	1 ml	0.059 mM
$CaCl_2.2H_2O$ (0.91 M)	1 ml	0.91 mM
$FeSO_4.7H_2o$ (0.04M)	1 ml	0.04 mM

A.2 Spectrophotometer reading (OD_{600nm}) of *Bl* 1951 culture after treatment with the mitomycin C at various concentrations

Treatments	**Time intervals (Hours)**					**% Decrease in OD_{600nm}**
	0	**2**	**4**	**6**	**24**	
Mitomycin C (1 µg/ml)	1.28	1.29	1.30	1.12	0.70	45.10
Mitomycin C (3 µg/ml)	1.26	1.25	1.22	1.16	0.20	83.93
Control	1.11	1.24	1.16	1.22	1.74	-57.24
*LSD (5%) (Control vs Treated)	0.17	0.08	0.08	0.09	0.27	32.71
LSD (5%) (MMC1 vs MMC3)	0.15	0.07	0.07	0.08	0.24	29.26

A.3 Spectrophotometer reading (OD_{600nm}) of *Bl* 1821L culture after treatment with the mitomycin C at various concentrations

Treatments	Time intervals (Hours)					% Decrease in OD_{600nm}
	0	2	4	6	24	
Mitomycin C (1 µg/ml)	1.41	1.44	1.46	1.48	0.71	49.65
Mitomycin C (3 µg/ml)	1.56	1.56	1.57	1.58	0.92	41.03
Control	1.30	1.34	1.47	1.49	1.35	-3.85
LSD (5%) (Control vs Treated)	0.18	0.15	0.12	0.12	0.37	24.49
LSD (5%) (MMC1 vs MMC3)	0.16	0.14	0.12	0.11	0.34	22.68

A.4 Spectrophotometer reading (OD_{600}) of *Bl* Rsp culture after treatment with the mitomycin C at various concentrations

Treatments	Time intervals (Hours)					% Decrease in OD_{600nm}
	0	2	4	6	24	
Mitomycin C (1 µg/ml)	1.81	1.54	1.49	1.16	0.78	56.91
Mitomycin C (3 µg/ml)	1.84	1.64	1.60	1.47	0.53	71.20
Control	1.82	1.54	1.51	1.51	1.55	14.84
LSD (5%) (Control vs Treated)	0.09	0.06	0.18	0.21	0.43	24.30
LSD (5%) (MMC1 vs MMC3)	0.08	0.05	0.16	0.18	0.37	21.04

A.5 PHASTER analysis of *Bl* 1821L genomic sequence

***Brevibacillus laterosporus* 1821L putative phage regions**							
Region	**Region length (Kb)**	**Completeness**	**Score**	**#CDS**	**Region position**	**Possible phage**	**GC%**
1	10.6	Incomplete	20	15	348784-359404	PHAGE_Brevib_Abouo_NC_029029	37.42
2	51	Intact	150	75	1076136-1127198	PHAGE_Brevib_Davies_NC_022980	41.05
3	12	Incomplete	30	17	1577874-1589929	PHAGE_Brevib_Abouo_NC_029029	37.14
4	15.4	Incomplete	60	15	2590041-2605538	PHAGE_Paenib_Fern_NC_029029	38.84
5	55.4	Questionable	80	62	2982707-3038154	PHAGE_Paenib_Tripp_NC_028930	47.73
6	8	Incomplete	40	8	3092762-3100813	PHAGE_Bacill_Stahl_NC_028930	41.33
7	12.7	Incomplete	30	17	3198519-3211275	PHAGE_Bacill_G_NC_023719	45.48
8	24.5	Incomplete	30	26	3420150-3444700	PHAGE_Brevib_Jenst_NC_028805	38.84
9	40.8	Incomplete	30	23	4379165-4419991	PHAGE_Bacill_SP_15_NC_031245	33.42
10	21.2	Incomplete	20	24	4435295-4456587	PHAGE_Bacill_SPbeta_15_NC_001884	32.77
11	54.5	Questionable	90	41	4488701-4543274	PHAGE_Brevib_Sundance_NC_028749	34.40
12	9.3	Incomplete	30	16	5121841-5131188	PHAGE_Bacill_G_NC_023719	42.39
13	27.3	Questionable	70	31	5353890-5381235	PHAGE_Bacter_Sitara_NC_028854	40.81
14	7.6	Incomplete	40	7	5420595-5428284	PHAGE_Bacter_Diva_NC_028788	41.57

A.6 PHASTER analysis of *Bl* 1951 genomic sequence

***Brevibacillus laterosporus* 1951 putative phage regions**							
Region	**Region length (Kb)**	**Completeness**	**Score**	**# CDS**	**Region position**	**Possible phage**	**GC%**
1	24.4	Incomplete	40	26	183763-208221	PHAGE_Brevib_Jenst_NC_028805	38.47
2	13.4	Incomplete	30	19	869072-882492	PHAGE_Brevib_Sundance_NC_028749	35.21
3	38.7	Incomplete	50	30	1203410-1242204	PHAGE_Brevib_Sundance_NC_028749	36.93
4	21.8	Incomplete	10	32	1245431-1267281	PHAGE_Bacill_SPbeta_NC_001884	35.07
5	47.7	Intact	100	43	1315240-1363038	PHAGE_Brevib_Sundance_NC_028749	34.28
6	72.4	Intact	110	52	1509413-1581817	PHAGE_Brevib_Sundance_NC_028749	37.26
7	11.4	Incomplete	30	16	1921184-1932589	PHAGE_Bacill_G_NC_023719	43.78
8	23.4	Incomplete	50	45	3847737-3871182	PHAGE_Staphy_SLPW_NC_031008	41.16
9	9.6	Incomplete	40	9	3944371-3954020	PHAGE_Strep_Dp_1_NC_015274	38.45
10	28.8	Intact	130	35	4367288-4396142	PHAGE_Clostr_phiCD481_NC_028951	35.14
11	23	Questionable	80	27	4880737-4903739	PHAGE_Bacer_Diva_NC_028788	38.28
12	12.3	Incomplete	40	15	5424432-5436759	PHAGE_Bacill_G_NC_023719	45.81

A.7 PHASTER analysis of *Bl* Rsp genomic sequence

***Brevibacillus laterosporus* Rsp putative phage regions**							
Region	**Region length (Kb)**	**Completeness**	**Score**	**# CDS**	**Region position**	**Possible phage**	**GC%**
1	21.9	Intact	100	37	365934-387895	PHAGE_Bacter_Diva_NC_028788	37.66
2	24.4	Questionable	70	37	1525405-1549833	PHAGE_Brevib_Jenst_NC_028805	38.74
3	23	Incomplete	60	26	1627951-1650993	PHAGE_Brevib_Jenst_NC_028805	40.23
4	47.3	Intact	150	75	2356533-2403923	PHAGE_Deep_s_D6E_NC_019544	42.44
5	55.5	Intact	150	94	2479215-2534771	PHAGE_Brevib_Jimmer1_NC_029104	38.22
6	10.4	Incomplete	40	18	3228457-3248947	PHAGE_Brevib_Abouo_NC_029029	39.08
7	22.9	Intact	130	41	3249471-3272447	PHAGE_Lister_B054_NC_009813	42.88
8	53.3	Intact	110	66	3774989-3828309	PHAGE_Rhodov_Vb_RhkS_P1_NC_031059	42.08
9	29.9	Incomplete	60	26	38201193850102	PHAGE_Bcill_G_NC_031059	39.367
10	14.1	Incomplete	40	31	4092920-4107070	PHAGE_Bacill_Shhbh1_NC_030925	43.27
11	13.4	Incomplete	50	26	4932074-4945490	PHAGE_Brevib_Sundance_NC_028749	35.22

A.8 PHASTER analysis of *Bl* DSM 25 genomic sequence

***Brevibacillus laterosporus* DSM 25 putative phage regions**							
Region	**Region length (Kb)**	**Completeness**	**Score**	**# CDS**	**Region position**	**Possible phage**	**GC%**
1	97.3	Intact	140	89	1070680-1168033	PHAGE_Brevib_Jenst_NC_028805	45.11
2	13.9	Incomplete	10	24	1187150-1201124	PHAGE_Brevib_Jenst_NC_028805	43.40
3	55.6	Questionable	90	38	2645632-2701303	PHAGE_Bacill_WBeta_NC_007734	37.40
4	48.9	Intact	140	79	2941099-2990036	PHAGE_Brevib_Abouo_NC_029029	39.13
5	7.3	Incomplete	40	7	3153753-3161146	PHAGE_Mycoba_Thibault_NC_023738	43.55
6	8.9	Incomplete	40	9	3627507-3636432	PHAGE_Clostr_c_st_NC_007581	38.07
7	60.4	Intact	130	90	4014505-4074995	PHAGE_Paenib_Tripp_NC_028930	48.40
8.	44.7	Questionable	80	35	4502347-4547140	PHAGE_Brevib_Jenst_NC_028805	38.95

A.9 PHASTER analysis of *Bl* PE 36 genomic sequence

***Brevibacillus laterosporus* PE 36 putative phage regions**							
Region	**Region length (Kb)**	**Completeness**	**Score**	**# CDS**	**Region position**	**Possible phage**	**GC%**
1	31.2	Intact	130	48	459-31753	PHAGE_Brevib_Jimmer1_NC_029104)	38.27
2	7.5	Incomplete	30	16	406951-414470	PHAGE_Bacill_G_NC_023719	43.64
3	43.5	Incomplete	50	27	1489860-1533406	PHAGE_Bacill_BalMu_1_NC_030945	42.84
4	24.3	Incomplete	40	45	1548765-1573104	PHAGE_Brevib_Abouo_NC_029029	38.11
5	44.9	Questionable	80	38	1854453-1899409	PHAGE_Brevib_Jenst_NC_028805	40.11
6	42.2	Intact	110	51	3514438-3556715	PHAGE_Geobac_E2_NC_009552	42.01
7	25.3	Incomplete	20	25	4665645-4690965	PHAGE_Brevib_Abouo_NC_029029	39.20

A.10 PHASTER analysis of *Bl* UNISS 18 genomic sequence

***Brevibacillus laterosporus* UNISS 18 putative phage regions**

Region	Region length (Kb)	Completeness	Score	# CDS	Region position	Possible phage	GC%
1	30.2	Questionable	70	28	301757-331978	PHAGE_Brevib_Jenst_NC_028805	39.75
2	60.1	Intact	120	44	787599-847724	PHAGE_Deep_s_D6E_NC_019544	40.96
3	37.7	Intact	130	49	2000754-2038539	PHAGE_Entero_phiFL4A_NC_013644	41.51
4	19.1	Incomplete	40	17	5035744-5054936	PHAGE_Brevib_Jenst_NC_028805	40.35
5	2.3	Incomplete	20	6	5060196-5062527	PHAGE_Brevib_Abouo_NC_029029	40.57
6	29.4	Incomplete	60	13	5502159-5531646	PHAGE_Bacill_G_NC_023719	42.17

A.11 PHASTER analysis of *Bl* LMG 15441 genomic sequence

***Brevibacillus laterosporus* LMG 15441 putative phage regions**							
Region	**Region length (Kb)**	**Completeness**	**Score**	**# CDS**	**Region position**	**Possible phage**	**GC%**
1	8.4	Incomplete	40	11	494147-502623	PHAGE_Clostr_c_st_NC_007581	41.31
2	11.3	Incomplete	50	12	753408-764725	PHAGE_Clostr_phiSM101_NC_008265	36.27
3	45	Questionable	80	39	2205017-2250064	PHAGE_Brevib_Jenst_NC_028805	40.12
4	42.3	Questionable	90	33	3407363-3449731	PHAGE_Brevib_Abouo_NC_029029	38.03
5.	30.2	Questionable	70	45	3490330-3520588	PHAGE_Strept_phiARI0462_NC_031942	37.73

A.12 PHASTER analysis of *Bl* B9 genomic sequence

***Brevibacillus laterosporus* B9 putative phage regions**							
Region	**Region length (Kb)**	**Completeness**	**Score**	**# CDS**	**Region position**	**Possible phage**	**GC%**
1	59.3	Intact	110	47	538520-597821	PHAGE_Brevib_Abouo_NC_029029	39.01
2	22.9	Questionable	80	30	635805-658770	PHAGE_Lister_B054_NC_009812	42.02
3	29.7	Incomplete	50	27	1417222-1446939	PHAGE_Bacill_BalMu_1_NC_030945	42.46
4	4.7	Incomplete	40	7	1604147-1608926	PHAGE_Bacill_phi105_NC_004167	39.87
5	45.2	Incomplete	40	23	3064465-3109735	PHAGE_Paenib_Fern_NC_028851	37.34

A.13 PHASTER analysis of *Bl* GI9 genomic sequence

***Brevibacillus laterosporus* GI9 putative phage regions**							
Region	**Region length (Kb)**	**Completeness**	**Score**	**# CDS**	**Region position**	**Possible phage**	**GC%**
1	25	Incomplete	60	23	1177018-1202038	PHAGE_Bacill_phi105_NC_004167	37.99
2	23.9	Questionable	90	34	2306331-2330297	PHAGE_Paenib_Tripp_NC_028930	47.64
3	9.7	Incomplete	10	19	3543787-3553575	PHAGE_Brevib_Abouo_NC_029029	36.09
4	24.6	Incomplete	40	26	4665074-4689724	PHAGE_Brevib_Jenst_NC_0298805	38.50

A.14 PHASTER analysis of *Bl* NRS 590 genomic sequence

***Brevibacillus laterosporus* NRS590 putative phage regions**							
Region	**Region length (Kb)**	**Completeness**	**Score**	**# CDS**	**Region position**	**Possible phage**	**GC%**
1	7.5	Incomplete	40	8	2941007-2948555	PHAGE_Bacill_BalMu_1_NC_030945	43.21
2	5	Intact	109	7	3139933-3145027	PHAGE_Entero_lato_NC_001422	44.51
3	25	Incomplete	50	29	3541081-3566175	PHAGE_Bacill_G_NC_023719	42.35
4	47.2	Questionable	90	41	3727968-3775213	PHAGE_Brevib_Jenst_NC_028805	38.94

A.15 PHASTER analysis of *Bl* CCEB 342 genomic sequence

***Brevibacillus laterosporus* CCEB 342 putative phage regions**							
Region	**Region length (Kb)**	**Completeness**	**Score**	**# CDS**	**Region position**	**Possible phage**	**GC%**
1	54.6	Intact	130	49	1973507-2028201	PHAGE_Brevib_Jenst_NC_028805	40.45
2	33.5	Incomplete	20	15	4448591-4482090	PHAGE_Brevib_Abouo_NC_029029	39.06
3	10.8	Incomplete	20	17	4471092-4481982	PHAGE_Bacill_PfEFR_NC_031055	41.57

Appendix B

B.1 BLASTp analysis of N-terminal sequenced protein (tr|A0A328R421|A0A328R421_BRELA) of *Bl* 1821L in GenBank database

Accession	Description & % amino acids similarity to the GenBank accessions	Amino acid sequence
WP_113756845.1	Phage tail sheath subtilisin-like domain containing protein *Brevibacillus laterosporus* (Identity 100%)	MTIQRERPGVNVELKAKAQERVLPKSGVVLVPYLAEWGAPDQVITMKGYEERVAETFGHIGILELAAEGGATVLGYRMTS GNGVAASYTQSDSFTLEARYPGLVGNDLQISIKESTVELGKKELQVKGPIKTEKFSFANVDELVTKAEQSIYIKVKKLGD KVAEETMMISLEGGTSGITSLTANDFTTLFNSISGTDFDAMYLPSADVAIQAAAKQFMSDRELFSKKRSTLVIGGLKDKD NNMNEHVQRSVANNSRRVVNCAIAGQHVNGKTYGSLEWAAWLAGMIAATPAHISLSAQLVPLKKAEKDWGHTDIQAALNS GTLIAVRDGDVYLIESAVNTLTTLKAAEREDFGKIRVSMTLDQIVNDITSVGKKYKGKLDNNDIGGATFVGAVKTYLEVR EAQGAIDQGWIFEDKKNGIGDKRGFRLAAKPLDAIEIFDIEWEVL
WP_158325968.1	Phage tail sheath subtilisin-like domain containing protein *Brevibacillus laterosporus* (Identity 99%)	MTIQRERPGVNVELKAKAQERVLPKSGVVLVPYLAEWGAPDQVITMKGYEERVAETFGHIGILELAAEGGATVLGYRMTS GNGVAASYTQSDSFTLEARYPGLVGNDLQISIKESTAELGKKELQVKGPIKTEKFSFANVDELVTKAEQSIYIKVKKLGD KVAEETMMISLEGGTSGITSLTANDFTTLFNSISGTDFDAMYLPSADVAIQAAAKQFMSDRELFSKKRSTLVIGGLKDKD NNMNEHVQRSVANNSRRVVNCAIAGQHVNGKTYGSLEWAAWLAGMIAATPAHISLSAQLVPLKKAEKDWGHTDIQAALNS GTLIAVRDGDVCLIESAVNTLTTLKAAEREDFGKIRVSMTLDQIVNDITSVGKKYKGKLDNNDIGGATFVGAVKTYLEVR EAQGAIDQGWIFEDKKNGFGDKRGFRLAAKPLDAIEIFDIEWEVL

WP_192547583.1	Phage tail sheath subtilisin-like domain containing protein *Brevibacterium* sp. JNUCC-42 (Identity 98%)	MTIQRERPGVNVELKAKAQERVLPKSGVVLVPYLAEWGAPDQVITMKGYEERVAETFGHIEILELAAEGGATVLGYRMTS GNGVAASYTQSDSFTLEARYPGLVGNDLQISIKESTAELGKKELQVKGPIKTEKFSFANVDELVTKAEQSIYIKVKKLGD EAAEETMMISLEGGISGITSLTANDFTTLFNSISGIDFDAMYLPSADVAIQAAAKQFMSDRELFSKKRSTLVIGGLKDKD NNMNEHVQRSVANNSRRVVNCAIAGQHVNGKTYGSLEWAAWLAGMIAATPAHISLSAQLVPLKKAEKDWGHTDIQVALNS GTLIAVRDGDVYLIESAVNTLTTLKAAEREDFGKIRVSMTLDQIVNDITSVGKKYKGKLDNNDIGGATFVGAVKTYLEVR EAQGAIDQGWIFEDKKNGIGDKRGFRLAAKPLDAIEIFDIEWEVL
WP_104032222.1	Phage tail sheath subtilisin-like domain containing protein *Brevibacillus laterosporus* (Identity 92%)	MTIQRERPGVNVELKAKAQERVLPKSGVVLVPYLAEWGAPDQVITMKGYEERVAETFGQIGILELAAEGGATVVGYRMTN GKGVAATYSQEGSFAIEARYPGLVGNELQISIKDSTAELGKKELQVKGPVKTEKFSFANMDELVTKAEQSIYIKVKKLGD KAAEETTLTSLSGGTSGITTLAANDFTTLFNSIAGIDFDAMYLPSADAGIQAAAKQFMVDRELFSKKRSTLVIGGMPEKD SNMNEHVERSVANNSRRVVNCAIAGQHVNGKTYGSLEWAAWLAGMIAATPAHISLSAQLVPLKKATKDWGHTEIQNALNS GTLIAVRDGDVYLIESAVNTLTTLKAVEREDFGKIRVSMTLDQIVNDITSVGKKYKGKLDNNDIGGATFVGAVKTYLEVR EAQGAIDQGWIFEDKKNGIGDKRGFRLAAKPLDAIELFDIEWEVL
WP_018674075.1	Phage tail sheath subtilisin-like domain containing protein *Brevibacillus laterosporus* (Identity 91%)	MTIQRERPGVNVELKAKAQERVLPKSGVVLVPYLAEWGAPDQVITMKGYEERVAETFGQIGILELAAEGGATVVGYRMTN GKGVAATYSQEGSFAIEARYPGLVGNELQISIKDSTAELGKKELQVKGPVKTEKFSFANMDELVTKAEQSIYIKVKKLGD KAAEETTLTSLSGGTSGITTLAANDFTTLFNSIAGIDFDAMYLPSADAGIQAAAKQFMVDRELFSKKRSTLVIGGMPEKD SNMNEHVERSVANNSRRVVNCAIAGQHVNGKTYGSLEWAAWLAGMIAATPAHISLSAQLVPLKKATKDWGHTEIQNALNS GTLIAVRDGDVYLIESAVNTLTTLKAVEREDFGKIRVSMTLDQIVNDITSVGKKYKGKLDNNDIGGATFVGAVKTYLEVR EAQGAIEQGWIFEDKKNGIGDKRGFRLAAKPLDAIELFDIEWEVL
MBG9772719.1	Phage tail protein *Brevibacillus laterosporus* ((Identity 91%)	MTIQRERPGVNVELKAKAQERVLPKSGVVLVPYLAEWGAPDQVITMKGYEERVAETFGQIGILELAAEGGATVVGYRMTN GKGVAATFSQEGSFAIEARYPGLVGNELQISIKDSTAELGKKELQVKGPVKTEKFSFANMDELVTKAEQSIYIKVKKLGD KAAEETTLTSLSGGTSGITTLAANDFTTLFNSIAGIDFDAMYLPSADAGIQAAAKQFMVDRELFSKKRSTLVIGGMPEKD SNMNEHVERSVANNSRRVVNCAIAGQHVNGKTYGSLEWAAWLAGMIAATPAHISLSAQLVPLKKATKDWGHTEIQNALNS GTLIAVRDGDVYLIESAVNTLTTLKAVEREDFGKIRVSMTLDQIVNDITSVGKKYKGKLDNNDIGGATFVGAVKTYLEVR EAQGAIDQGWIFEDKKNGIGDKRGFRLAAKPLDAIELFDIEWEVL

WP_094700868.1	Multispecies: phage tail sheath subtilisin-like domain containing protein (*Brevibacillus*) (Identity 91%)	MTIQRERPGVNVELKAKAQERVLPKSGVVLVPYLAEWGAPDQVITMKGYEERVAETFGQIGILELAAEGGATVVGYRMTN GKGVAATYSQEGSFAIEARYPGLVGNELQISIKDSTAELGKKELQVKGPVKTEKFSFANMDELVTKAEQSIYIKVKKLGD KAAEETTLTSLSGGTSGITTLAANDFTTLFNSIAGIDFDAMYLPSADAGIQAAAKQFMVDRELFSKKRSTLVIGGMPEKD SNMNEQVERSVANNSRRVVNCAIAGQHVNGKTYGSLEWAAWLAGMIAATPAHISLSAQLVPLKKATKDWGHTEIQNALNS GTLIAVRDGDVYLIESAVNTLTTLKAVEREDFGKIRVSMTLDQIVNDITSVGKKYKGKLDNNDIGGATFVGAVKTYLEVR EAQGAIDQGWIFEDKKNGIGDKRGFRLAAKPLDAIELFDIEWEVL
WP_168420254.1	Phage tail sheath subtilisin-like domain containing protein *Brevibacillus laterosporus* (Identity 91%)	MTIQRERPGVNVELKAKAQERVLPKSGVVLVPYLAEWGAPDQVITMKGYEERVSETFGQIGILELAAEGGATVVGYRMTN GKGVSATYSQEGSFAIEARYPGLVGNELQISIKDSTAELGKKELQVKGPVKTEKFSFANMDELVTKAEQSIYIKVKKLGD KAAEETTLTSLSGGTSGITTLAANDFTTLFNSIAGIDFDAMHLPSADAGIQAAAKQFMVDRELFSKKRSTLVIGGMPEKD SNMNEHVERSVANNSRRVVNCAIAGQHVNGKTYGSLEWAAWLAGMIAATPAHISLSAQLVPLKKATKDWGHTEIQNALNS GTLIAVRDGDVYLIESAVNTLTTLKAVEREDFGKIRVSMTLDQIVNDITSVGKKYKGKLDNNDIGGATFVGAVKTYLEVR EAQGAIDQGWIFEDKKNGIGDKRGFRLAAKPLDAIELFDIEWEVL
WP_197262180.1	Phage tail sheath subtilisin-like domain containing protein *Brevibacillus laterosporus* (Identity 91%)	MTIQRERPGVNVELKAKAQERVLPKSGVVLVPYLAEWGAPDQVITMKGYEERVAETFGQIGILELAAEGGATVVGYRMTN GKGVAATYSQEGSFAIEARYPGLVGNELQISIKDSTAELGKKELQVKGPVKTEKFSFANMDELVTKAEQSIYIKVKKLGD KAAEETTLTSLSGGTSGITTLAANDFTTLFNSIAGIDFDAMYLPSADDGIQAAAKQFMVDRELFSKKRSTLVIGGMPEKD SNMNEQVERSVANNSRRVVNCAIAGQHVNGKTYGSLEWAAWLAGMIAATPAHISLSAQLVPLKKATKDWGHTEIQNALNS GTLIAVRDGDVYLIESAVNTLTTLKAVEREDFGKIRVSMTLDQIVNDITSVGKKYKGKLDNNDIGGATFVGAVKTYLEVR EAQGAIDQGWIFEDKKNGIGDKRGFRLAAKPLDAIELFDIEWEVL
WP_163245513.1	Phage tail sheath subtilisin-like domain containing protein *Brevibacillus* sp. 7WMA2 (Identity 91%)	MTIQRERPGVNVELKAKAQERVLPKSGVVLVPYLAEWGAPDQVITMKGYEERVAETFGQIDILELAAEGGATVVGYRMTN GKSIAASYSQEGSIAIQARYPGLVGNELQISIKDSTAELGKKELQVKGPIKTEKFSFANMDELVTKAEQSIYIKVKKLGD KAVEETAMTALSGGTSGIATLSATDFTTLFNSISGVDFDAMYLPSADAGIQAAAKQFMVDRELFSKKRSTLVIGGLPEKD SNMNEHVDRSVANNSRRVVNCAIAGQHVNGKTYGSLEWAAWLAGMIAATPAHISLSAQLVPMKKAAKDWGHTEIQNALNS GTLIAVRDGDVYLIESAVNTLTTLKAAEREDFGKIRVSMTLDQIVNDITSVGKKYKGKLDNNDIGGATFVGAVKTYLEVR EAQGAIDKGWIFEDKKNGIGDKRGFRLAAKPLDAIELFDIEWEVL

WP_121472689.1	Phage tail sheath subtilisin-like domain containing protein *Brevibacillus laterosporus* (Identity 91%)	MTIQRERPGVNVELKAKAQERVLPKSGVVLVPYLAEWGAPDQVITMKGYEERVAETFGQIDILELAAEGGATVVGYRMTN GKSVAASYSQEGSIAIQARYPGLVGNELQISIKDSTAELGKKELQVKGPIKTEKFSFANMDELVTKAEQSIYIKVKKLGD KAVEETAMTALSGGTSGIATLSATDFTTLFNSISGVDFDAMYLPSADAGIQAAAKQFMVDRELFSKKRSTLVIGGLPEKD SNMNEHVDRSVANNSRRVVNCAIAGQHVNGKTYGSLEWAAWLAGMIAATPAHISLSAQLVPMKKAAKDWGHTEIQNALNS GSLIAVRDGDVYLIESAVNTLTTLKAAEREDFGKIRVSMTLDQIVNDITSVGKKYKGKLDNNDIGGATFVGAVKTYLEVR EAQGAIDKGWIFEDKKNGIGDKRGFRLAAKPLDAIELFDIEWEVL
WP_022584624.1	Phage tail sheath subtilisin-like domain containing protein *Brevibacillus laterosporus* (Identity 91%)	MTIQRERPGVNVELKAKAQERVLPKSGVVLVPYLAEWGAPDQVITMKGYEERVAETFGQIDILELAAEGGATVVGYRMTN GKSIAASYSQEGSIAIQARYPGLVGNELQISIKDSTAELGKKELQVKGPIKTEKFSFANMDELVTKAEQSIYIKVKKLGD KAVEETAMTALSGGTSGIATLSATDFTTLFNSISGVDFDAMYLPLADVGIQAAAKQFMVDRELFSKKRSTLVIGGLPEKD SNMNEHVDRSVANNSRRVVNCAIAGQHVNGKTYGSLEWAAWLAGMIAATPAHISLSAQLVPMKKAAKDWGHTEIQNALNS GTLIAVRDGDVYLIESAVNTLTTLKAAEREDFGKIRVSMTLDQIVNDITSVGKKYKGKLDNNDIGGATFVGAVKTYLEVR EAQGAIDKGWIFEDKKNGIGDKRGFRLAAKPLDAIELFDIEWEVL
WP_064018501.1	Phage tail sheath subtilisin-like domain containing protein *Brevibacillus* sp. SKDU 10 (Identity 90%)	MTIQRERPGVNVELKAKAQERVLPKSGVVLVPYLAEWGAPDQVITMKGYEERVAETFGQIDILELAAEGGATVVGYRMTN GKSVAASYSQEGSIAIQARYPGLVGNELQISIKDSTAELGKKELQVKGPVKTEKFSFANMDELVTKAEQSIYIKVKKLGD KAVEETAMTALSGGTSGIATLSATDFTTLFNSISGVDFDAMYLPSADAGIQAAAKQFMVDRELFSKKRSTLVIGGLPEKD SNMNEHVERSVANNSRRVVNCAIAGQHVNGKTYASLEWAAWLAGMIAATPAHISLSAQLVPMKKAAKDWGHTEIQNALNS GTLIAVRDGDVYLIESAVNTLTTLKAAEREDFGKIRVSMTLDQIVNDITSVGKKYKGKLDNNDIGGATFVGAVKTYLEVR EAQGAIDKGWIFEDKKNGIGDKRGFRLAAKPLDAIELFDIEWEVL
WP_181748616.1	Phage tail sheath subtilisin-like domain containing protein *Brevibacillus laterosporus* (Identity 90%)	MTIQRERPGVNVELKAKAQERVLPKSGVVLVPYLAEWGAPDQVITMKGYEERVAETFGQIDILELAAEGGATVVGYRMTN GKSVAASYSQEGSIAIQARYPGLVGNELQISIKDSTAELGKKELQVKGPVKTEKFSFANMDELVTKAEQSIYIKVKKLGD KAVEETAMTALSGGTSGIATLSATDFTTLFNSISGVDFDAMYLPSADAGIQAAAKQFMVDRELFSKKRSTLVIGGLPEKD SNMNEHVDRSVANNSRRVVNCAIAGQHVNGKTYGSLEWTAWLAGMIAATPAHISLSAQLVPMKKAAKDWGHTEIQNALNS GTLIAVRDGDVYLIESAVNTLTTLKAAEREDFGKIRVSMTLDQIVNDITSVGKKYKGKLDNNDIGGATFVGAVKTYLEVR EAQGAIDKGWIFEDKKNGIGDKRGFRLAAKPLDAIELFDIEWEVL

WP_003336523.1	Phage tail sheath subtilisin-like domain containing protein *Brevibacillus laterosporus* (Identity 90%)	MTIQRERPGVNVELKAKAQERVLPKSGVVLVPYLAEWGAPDQVITMKGYEERVAETFGQIDILELAAEGGATVVGYRMTN GKSVAASYSQEGSIAIQARYPGLVGNELQISIKDSTAELGKKELQVKGPIKTEKFSFANMDELVTKAEQSIYIKVKKLGD KAVEETAMTALSGGTSGIATLSATDFTTLFNSISGVDFDAMYLPSADAGIQAAAKQFMVDRELFSKKRSTLVIGGLPEKD SNMNEHVDRSAANNSRRVVNCAIAGQHVNGKTYGSLEWAAWLAGMIAATPAHISLSAQLVPMKKAAKDWGHTEIQNALNS GSLIAVRDGDVYLIESAVNTLTTLKAAEREDFGKIRVSMTLDQIVNDITSVGKKYKGKLDNNDIGGATFVGAVKTYLEVR EAQGAIDKGWIFEDKKNGIGDKRGFRLAAKPLDAIELFDIEWEVL
WP_101668822.1	Phage tail sheath subtilisin-like domain containing protein *Brevibacillus laterosporus* (Identity 90%)	MTIQRERPGVNVELKAKAQERILPKSGVVLVPYLAEWGAPDQVITMKGYEERVAETFGQIDILELAAEGGATVVGYRMTN GKSVAASYSQEGSIAIQARYPGLVGNELQISIKDSTAELGKKELQVKGPVKTEKFSFANMDELVTKAEQSIYIKVKKLGD KAVEETAMTALSGGTSGIATLSATDFTTLFNSISGVDFDAMYLPSADAGIQAAAKQFMVDRELFSKKRSTLVIGGLPEKD SNMNEHVDRSVANNSRRVVNCAIAGQHVNGKTYGSLEWAAWLAGMIAATPAHISLSAQLVPMKKAAKDWGHTEIQNALNS GSLIAVRDGDVYLIESAVNTLTTLKAAEREDFGKIRVSMTLDQIVNDITSVGKKYKGKLDNNDIGGATFVGAVKTYLEVR EAQGAIDKGWIFEDKKNGIGDKRGFRLAAKPLDAIELFDIEWEVL
WP_096887431.1	Phage tail sheath subtilisin-like domain containing protein *Brevibacillus laterosporus* (Identity 90%)	MTIQRERPGVNVELKAKAQERVLPKSGVVLVPYLAEWGAPDQIITMKGYEERVAETFGQIDILELAAEGGATVVGYRMTN GKSVAASYSQEGSIAIQARYPGLVGNELQISIKDSTAELGKKELQVKGPVKTEKFSFANMDELVTKAEQSIYIKVKKLGD KAVEETAMTALSGGTSGIATLSATDFTTLFNSISGVDFDAMYLPSADAGIQAAAKQFMVDRELFSKKRSTLVIGGLPEKD SNMNEHVDRSVANNSRRVVNCTIAGQHVNGKTYGSLEWAAWLAGMIAATPAHISLSAQLVPMKKAAKDWGHTEIQNALNS GTLIAVRDGDVYLIESAVNTLTTLKAAEREDFGKIRVSMTLDQIVNDITSVGKKYKGKLDNNDIGGATFVGAVKTYLEVR EAQGAIDKGWIFEDKKNGIGDKRGFRLAAKPLDAIELFDIEWEVL
WP_068793304.1	Phage tail sheath subtilisin-like domain containing protein *Brevibacillus laterosporus* (Identity 90%)	MTIQRERPGVNVELKAKAQERVLPKSGVVLVPYLAEWGAPDQVITMKGYEERVAETFGQIDILELAAEGGATVVGYRMTN GKSVAASYSQEGSIAIQARYPGLIGNELQISIKDSTAELGKKELQVKGPVKTEKFSFANMDELVTKAEQSIYIKVKKLGD KAVEETAMAALSGGTSGIATLSATDFTTLFNSISGVDFDAMYLPSADAGIQAAAKQFMVDRELFSKKRSTLVIGGLPEKD SNMNEHVDRSVANNSRRVVNCAIAGQHVNGKTYGSLEWAAWLAGMIAATPAHISLSAQLVPMKKAAKDWGHTEIQNALNS GSLIAVRDGDVYLIESAVNTLTTLKAAEREDFGKIRVSMTLDQIVNDITSVGKKYKGKLDNNDIGGATFVGAVKTYLEVR EAQGAIDKGWIFEDKKNGIGDKRGFRLAAKPLDAIELFDIEWEVL

AIG27948.1	Phage tail sheath protein *Brevibacillus laterosporus* LMG 15441 (Identity 90%)	MKNKYDNTYLHFEEVNSMTIQRERPGVNVELKAKAQERVLPKSGVVLVPYLAEWGAPDQVITMKGYEERVAETFGQIDIL ELAAEGGATVVGYRMTNGKSVAASYSQEGSIAIQARYPGLVGNELQISIKDSTAELGKKELQVKGPIKTEKFSFANMDEL VTKAEQSIYIKVKKLGDKAVEETAMTALSGGTSGIATLSATDFTTLFNSISGVDFDAMYLPSADAGIQAAAKQFMVDREL FSKKRSTLVIGGLPEKDSNMNEHVDRSAANNSRRVVNCAIAGQHVNGKTYGSLEWAAWLAGMIAATPAHISLSAQLVPMK KAAKDWGHTEIQNALNSGSLIAVRDGDVYLIESAVNTLTTLKAAEREDFGKIRVSMTLDQIVNDITSVGKKYKGKLDNND IGGATFVGAVKTYLEVREAQGAIDKGWIFEDKKNGIGDKRGFRLAAKPLDAIELFDIEWEVL
WP_003339729.1	Phage tail sheath subtilisin-like domain containing protein *Brevibacillus laterosporus* (90%)	MTIQRERPGVNVELKAKAQERVLPKSGVVLVPYLAEWGAPDQVITMKGYEERVAETFGQIDILELAAEGGATVVGYRMTN GKSVAASYSQEGSIAIQARYPGLVGNELQISIKDSTAELGKKELQVKGPVKTEKFSFANMDELVTKAEQSIYIKVKKLGD KAVEETAMTALSGGTSGIATLSATDFTTLFNSISGVDFDAMYLPSADAGIQAAAKQFMVDRELFSKKRSTLVIGGLPAKD SNMNEHVDRSVANNSRRVVNCAIAGQHVNGKTYGSLEWTAWLAGMIAATPAHISLSAQLVPMKKAAKDWGHTEIQNALNS GTLIAVRDGDVYLIESAVNTLTTLKAAEREDFGKIRVSMTLDQIVNDITSVGKKYKGKLDNNDIGGATFVGAVKTYLEVR EAQGAIDKGWIFEDKKNGIGDKRGFRLAAKPLDAIELFDIEWEVL
AKF93359.1	Phage tail protein *Brevibacillus laterosporus* (90%)	MTIQRERPGVNVELKAKAQERVLPKSGVVLVPYLAEWGAPDQVITMKGYEERVAETFGQIDILELAAEGGATVVGYRMMN GKSVAASYSQEGSLAIQARYPGLVGNELQISIKDSTAELGKKELQVKGPVKTEKFSFANMDELVTKAEQSIYIKVKKLGE KAVEETAMTALSGGTSGIATLSATDFTTLFNSISGVDFDAMYLPSADAGIQAAAKQFMVDRELFSKKRSTLVIGGLPEKD SNMNEHVERSVANNSRRVVNCAIAGQHVNGKTYSSLEWAAWLAGMIAATPAHISLSAQLVPMKKAAKDWGHTEIQNALNS GTLIAVRDGDVYLIESAVNTLTTLKAAEREDFGKIRVSMTLDQIVNDITSVGKKYKGKLDNNDIGGATFVGAVKTYLEVR EAQGAIDKGWIFEDKKNGIGDKRGFRLAAKPLDAIELFDIEWEVL

B.2 BLASTp analysis of the N-terminal sequenced 48 kD putative antibacterial protein and the identified accessions tr|A0A518VEB0|A0A518VEB0_BRELA & tr|A0A0F7EFA2|A0A0F7EFA2_BRELA of *Bl* 1821L in the Uniprot database

Accession	Description & % amino acids similarity to the Uniprot accessions	Amino acid sequence
tr|A0A075R9L5|A0A075R9L5_BRELA	Phage tai sheath protein *Brevibacillus laterosporus* LMG 15441 90.3% identical to A0A518VEB0 98.2% identical to A0A0F7EFA2	MKNKYDNTYLHFEEVNSMTIQRERPGVNVELKAKAQERVLPKSGVVLVPYLAEWGAPDQV ITMKGYEERVAETFGQIDILELAAEGGATVVGYRMTNGKSVAASYSQEGSIAIQARYPGL VGNELQISIKDSTAELGKKELQVKGPIKTEKFSFANMDELVTKAEQSIYIKVKKLGDKAV EETAMTALSGGTSGIATLSATDFTTLFNSISGVDFDAMYLPSADAGIQAAAKQFMVDREL FSKKRSTLVIGGLPEKDSNMNEHVDRSAANNSRRVVNCAIAGQHVNGKTYGSLEWAAWLA GMIAATPAHISLSAQLVPMKKAAKDWGHTEIQNALNSGSLIAVRDGDVYLIESAVNTLTT LKAAEREDFGKIRVSMTLDQIVNDITSVGKKYKGKLDNNDIGGATFVGAVKTYLEVREAQ GAIDKGWIFEDKKNGIGDKRGFRLAAKPLDAIELFDIEWEVL
tr|M8E4N0|M8E4N0_9BACL	Uncharacterised protein *Brevibacillus borstelensis* AK1 69.9% identical to A0A518VEB0 69.4% identical to A0A0F7EFA2	MAIQRERPGVTVEMIAVAQERVLPKSGVVLVPYQAEWGAPDTMVRMTGYDERVAETFAEN DVIELAAEGGATIIGYRVTNGAAVAASYEQPDAIRIEARYPGLRGNDLKVSISASTAEPG KQELQVVGPISTEKFSFADAAELVMKTKQSIYVRVKKLGDADIADVSLTSLSGGVTGTAP LTSADATKMFTAVSGADFDTMYLPFADPAVQAAAKQFMSDRRGLNKKLSTLVIAGKEADD DNMVSHTERSVAQNVRYVVNNAIAGEHNNGKYYNSLQWAAWVAGMIAATPAHESMTGVVV PLKKAKKDWGHTEILQALSTGTLIAIRDGDVYVIESAVNTLSVLGPKDREDYGKIRVSMT LDQIQNDIQTVGKKYKGKLSNNDIGGATFVGAVKAYLEVREQQGAIDTGWIFEDKKNGVG DRRGFRLSAKPLDAIEYFDVEWEVL

tr|A0A3M8DWU9|A0A3M8DWU9_9BACL	Phage tail protein *Brevibacillus fluminis* 68.0% identical to A0A518VEB0 68.9% identical to A0A0F7EFA2	MTIQRERPGVTVELIAKAQERVLPKSGVVLVPYQAEWGAPDTLIRMAGFEERVAETFGEI DVLELAAASGATVIGFRMTDANTKTASYSQNDAIKIEARYPGTRGNQLRISITASSAEPG KKELQVTGGIKTEKYSFATAEELVGKTAESLHIRVTKLGTTSVTDVAETSLSGGTTGTAA LTAADFTKLFSAIGGADFDTLYLPSADPAIQAAAKQFMLDRRTLNKKMSTLVIGGKVEDD ANMAKHTERSVAQNARYVINCAIAGEHVSGKDYSSLQWAAWVAGMAAATPAHVSLTAQPV PLKKARKDWSHTEILSALYTGTLIATRDGDSYLIESAINTLSVLGTGEREDFGKIRVSMT IDQIQNDALTVGKKYMGKLPNNDLGAAVFVGAYTTYLKIREEQGAIDAGWVFEDTKNGVG DRRSFRLAARPLDAIEYFDLSWEVQ
tr|C0Z5G9|C0Z5G9_BREBN	Uncharacterised protein *Brevibacillus brevis* (strain 47/JCM 6285 /NBRC 100599) 68.1% identical to A0A518VEB0 68.1% identical to A0A0F7EFA2	DTVELAAEGGATILAYRMTNGTATKAAYEQADAIRVEALYPGLVGNELKVTITVSTSEPG KKELQVTGPLQTEKFSFADANELAAKTSQSNYVRVKKLGETAVTIVPETALTGAKSGTVA LASADSTKLFMAVSGADFDAMYLPFDDSAVQAAAKQFMSDRRTQNKKLSTLVIGGKAADD ENMAKHIERSVAQNARFVVNSAIAGQHNNGKVYGSLEWAAWVAGMIAATPAHESLTAVVV PLKKALKDWGHTDILSALGSGTLIATRDGDVYIIESAVNTLAVLGTHEREDYGKIRVSMT LDQIVNDISQVGKKYKGKLGNNDLGGAVFVSAVNAYMTVREQQGAIDTGWTFTDKKNGIG DRRGFLLSAKPLDAIEYFDIDWEVL

B.3 Amino acid alignment of the 48 kD Uniprot predicted proteins of *Bl* 1821L (tr|A0A518VEB0|A0A518VEB0_BRELA & tr|A0A0F7EFA2|A0A0F7EFA2_BRELA), and their identical proteins of the genus *Brevibacillus* along with the PBSX-like region proteins of *Bs* 168 using CLUSTALO

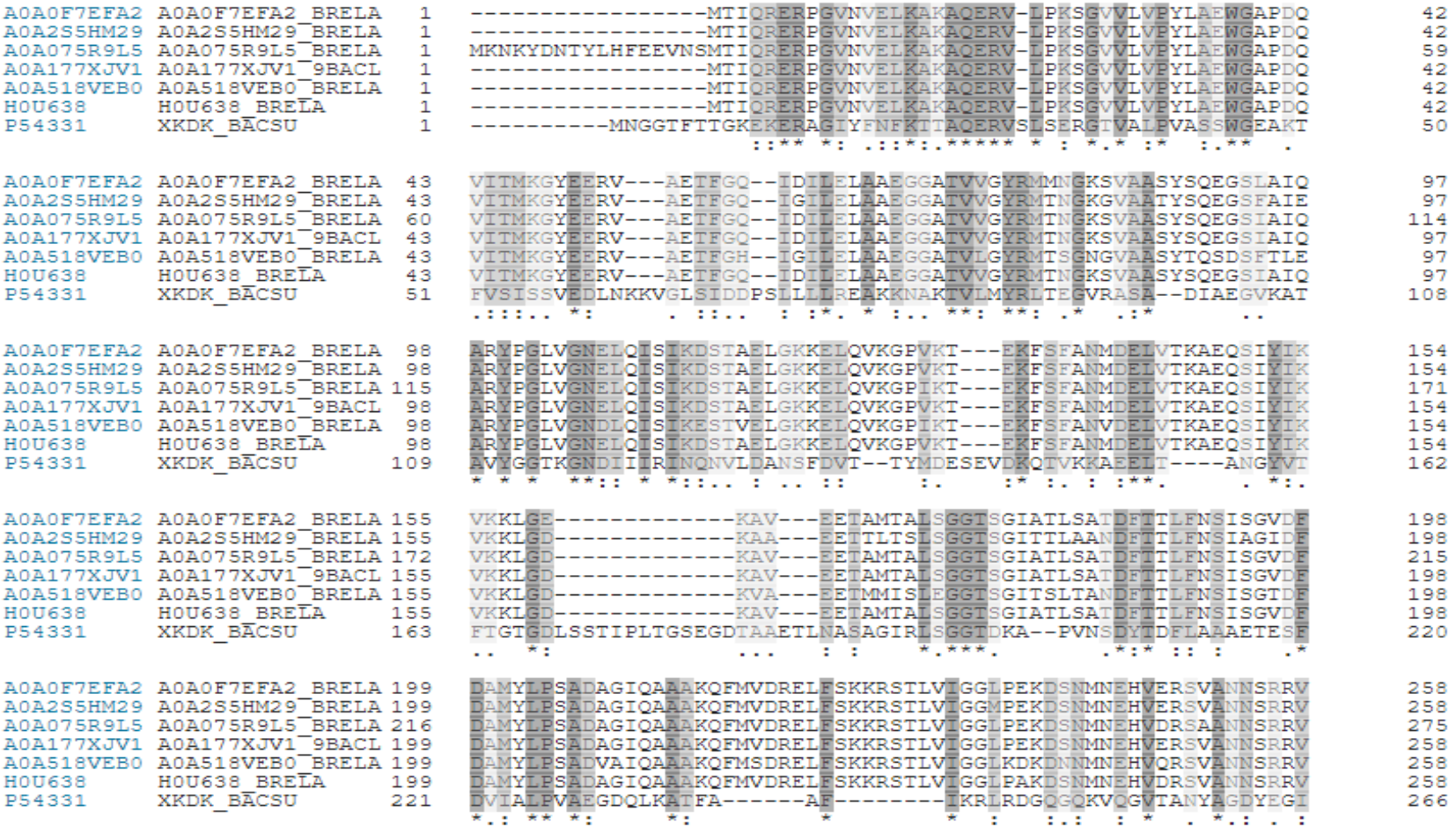

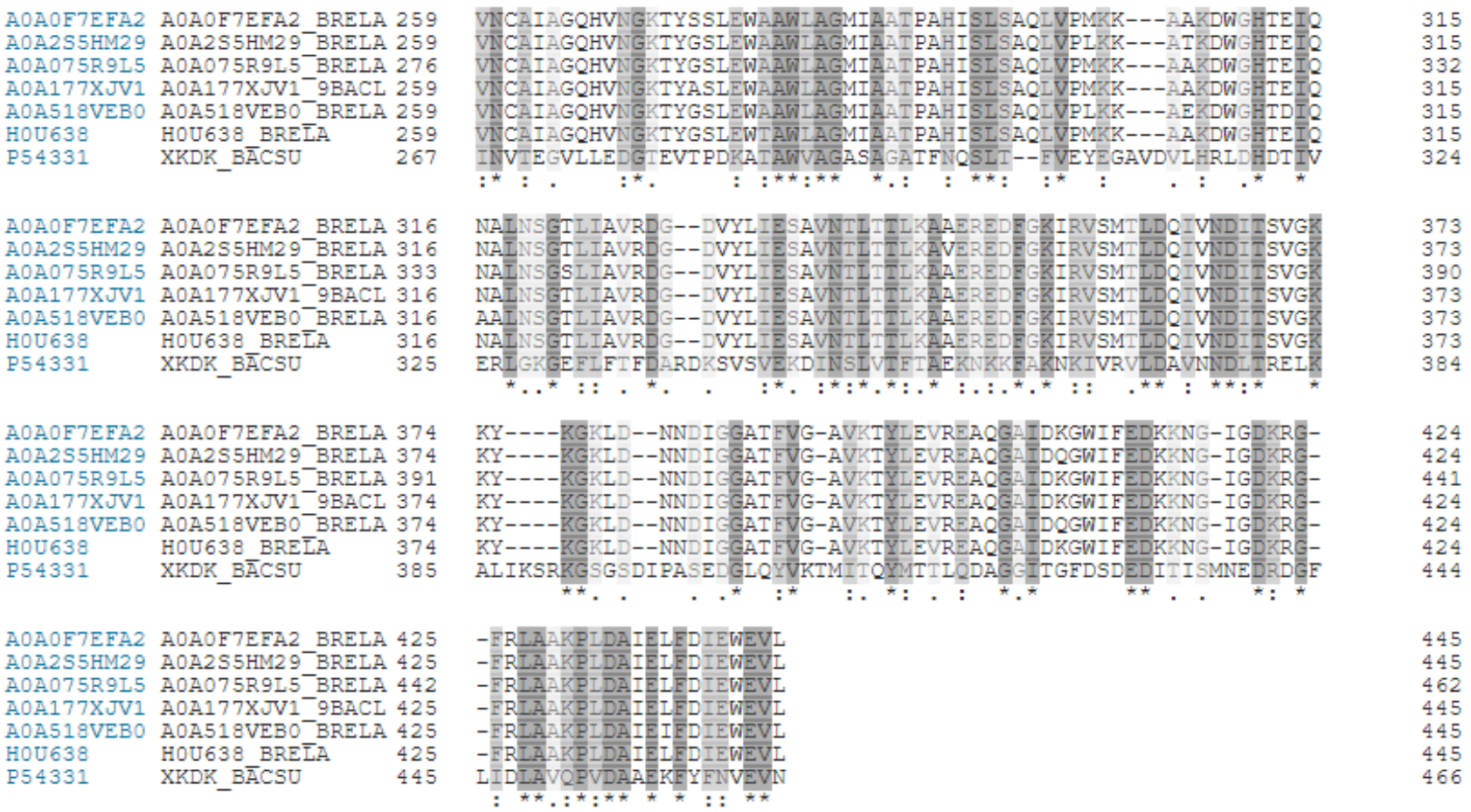

*Highlighted dark grey color amino acids denote similarity among the aligned phage tail-sheath proteins.
(Refer to Appendix B.4 & B.5)

B.4 Distance matrices of 48 kD predicted *Bl* 1821L proteins (tr|A0A0F7EFA2|A0A0F7EFA2_BRELA & tr|A0A518VEB0|A0A518VEB0_BRELA) to the identical proteins of the genus *Brevibacillus* along with the analogous protein of the *Bs* 168 using the programme Geneious basic

Uniprot Accession # (https://www.uniprot.org)	Uniprot Accession # (https://www.uniprot.org)						
	A0A0F7EFA2	**A0A2S5HM29**	**A0A075R9L5**	**A0A177XJV1**	**A0A518VEB0**	**H0U638**	**P54331**
A0A0F7EFA2		0.05	0.02	0.01	0.11	0.02	1.53
A0A2S5HM29	0.05		0.05	0.05	0.09	0.05	1.51
A0A075R9L5	0.02	0.05		0.01	0.1	0.01	1.55
A0A177XJV1	0.01	0.05	0.01		0.1	0.01	1.54
A0A518VEB0	0.11	0.09	0.1	0.1		0.1	1.45
H0U638	0.02	0.05	0.01	0.01	0.1		1.53
P54331	1.53	1.51	1.55	1.54	1.45	1.53	

B.5 Amino acids alignment (%) of 48 kD predicted *Bl* 1821L proteins (tr|A0A0F7EFA2|A0A0F7EFA2_BRELA & tr|A0A518VEB0 |A0A518VEB0_BRELA) to the identical proteins of the genus *Brevibacillus* along with the analogous protein of the *Bs* 168 using the programme Geneious basic

Uniprot Accession # (https://www.uniprot.org)	Uniprot Accession # (https://www.uniprot.org)						
	A0A0F7EFA2	**A0A2S5HM29**	**A0A075R9L5**	**A0A177XJV1**	**A0A518VEB0**	**H0U638**	**P54331**
A0A0F7EFA2		95.1	98.2	99.1	89.9	98.4	22.3
A0A2S5HM29	95.1		94.8	95.5	91.7	95.1	22.1
A0A075R9L5	98.2	94.8		98.8	90.3	98.9	22.4
A0A177XJV1	99.1	95.5	98.8		90.3	99.1	22.7
A0A518VEB0	89.9	91.7	90.3	90.3		90.3	22.7
H0U638	98.4	95.1	98.8	99.1	90.3		22.9
P54331	22.3	22.1	22.4	22.7	22.7	22.9	

B.6 BAGEL4 analysis of *Bl* 1821L and *Bl* 1951 genomes

***Bl* 1821L predicted areas of interest (AOI)**

AOI	start	end	Class
NZ_CP0334641.0.AOI_01	3538373	3558526	131.2;laterosporulin
NZ_CP0334641.0.AOI_02	331652	351652	Sactipeptides
NZ_CP0334641.0.AOI_03	4195511	4216354	Sactipeptides
NZ_CP0334641.0.AOI_04	4700327	4720585	223.2;UviB
NZ_CP0334641.0.AOI_05	1999385	2019385	Lanthipeptide_class_I
NZ_CP0334641.0.AOI_06	5170724	5191426	LAPs
NZ_CP0334641.0.AOI_07	5344331	5365282	LAPs

***Bl* 1951 predicted areas of interest (AOI)**

AOI	start	end	Class
NZ_RHPK010000031.0.AOI_01	315749	335902	131.2;laterosporulin
NZ_RHPK010000031.0.AOI_02	2664911	2684911	Sactipeptides
NZ_RHPK010000031.0.AOI_03	940691	961537	Sactipeptides
NZ_RHPK010000031.0.AOI_04	1914094	1934352	223.2;UviB
NZ_RHPK010000031.0.AOI_05	4272827	4292827	Lanthipeptide_class_I
NZ_RHPK010000031.0.AOI_06	1964561	1985512	LAPs
NZ_RHPK010000031.0.AOI_07	2145044	2165995	LAPs

Note: The red arrows denote the BAGEL4 predicted core peptides laterosporulin and UviB in the *Bl* 1821L and *Bl* 1951 genomes.

B.7 BAGEL4 analysis showing encoded genes of the predicted areas of interest (AOI) in the *Bl* 1821L genome

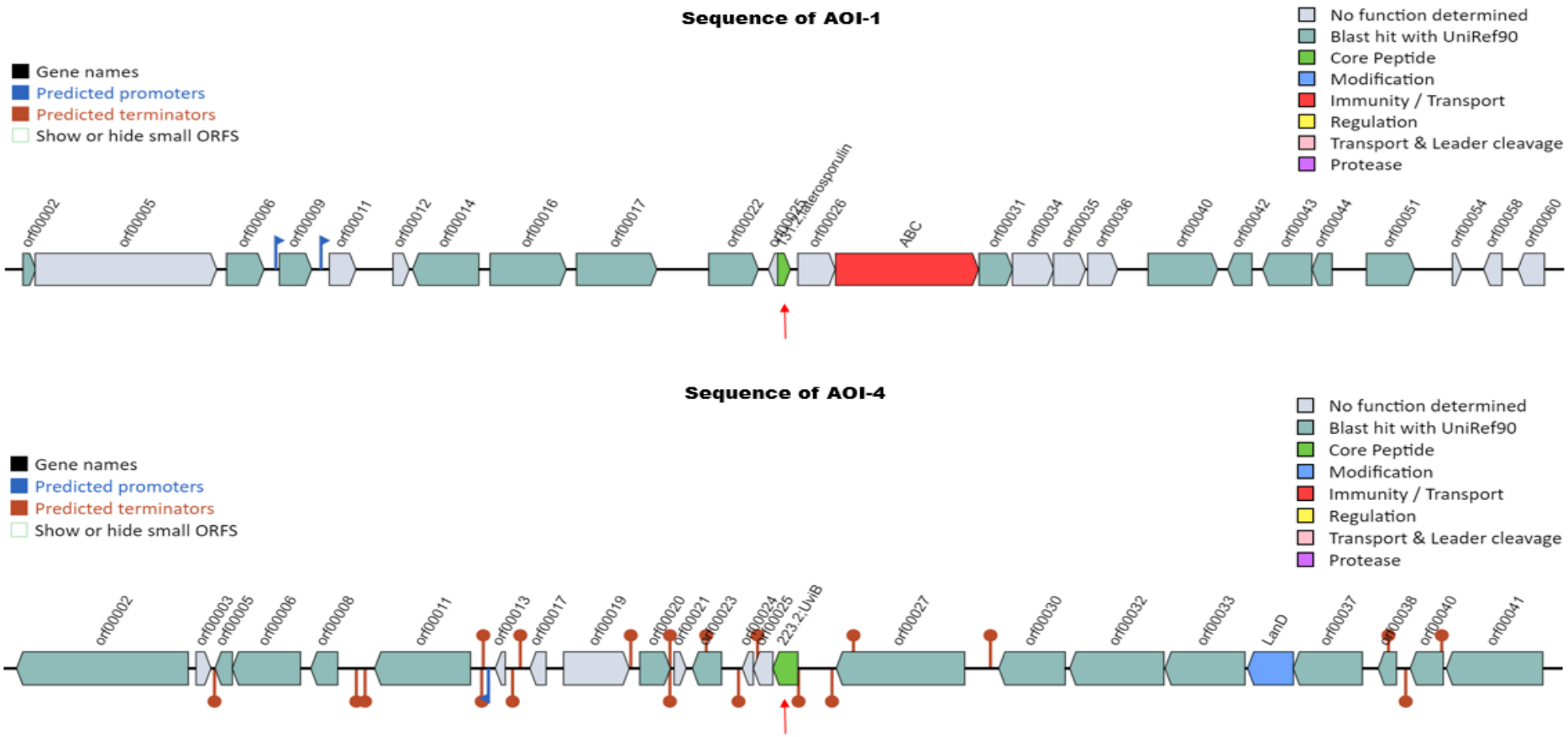

Note: The red arrows denote the location of the encoded core peptide genes in the *Bl* 1821L genome.
(Refer to Appendix B.8 & B.9).

B.8 BAGEL4 analysis describing genes of the area of interest (AOI-1) in the *Bl* 1821L genome

Name	Function	Motifs
orf00002	Protein VanZ OS=Enterococcus faecium OX=1352 GN=vanZ PE=4 SV=2	
orf00005		
orf00006	Protein YtsP OS=Bacillus subtilis (strain 168) OX=224308 GN=ytsP PE=3 SV=2	
orf00009	Uncharacterized HTH-type transcriptional regulator YusO OS=Bacillus subtilis (strain 168) OX=224308 GN=yusO PE=1 SV=1	
orf00011		
orf00012		
orf00014	Uncharacterized HTH-type transcriptional regulator YwbI OS=Bacillus subtilis (strain 168) OX=224308 GN=ywbI PE=3 SV=1	
orf00016	Formimidoylglutamase OS=Lysinibacillus sphaericus (strain C3-41) OX=444177 GN=hutG PE=3 SV=1	
orf00017	Sodium/glutamate symporter OS=Haemophilus influenzae (strain ATCC 51907 / DSM 11121 / KW20 / Rd) OX=71421 GN=gltS PE=3 SV=1	
orf00022	Spore germination protein GerE OS=Bacillus subtilis (strain 168) OX=224308 GN=gerE PE=1 SV=2	
orf00025		
131.2;laterosporulin	131.2;laterosporulin	
orf00026		
ABC	Lantibiotic ABC transporter	PF00005
orf00031	Methylamine utilization protein MauD OS=Paracoccus versutus OX=34007 GN=mauD PE=2 SV=1	
orf00034		
orf00035		
orf00036		
orf00040	CAAX prenyl protease 2 OS=Methanococcus maripaludis (strain S2 / LL) OX=267377 GN=rce1 PE=1 SV=1	
orf00042	NH(3)-dependent NAD(+) synthetase OS=Bacillus halodurans (strain ATCC BAA-125 / DSM 18197 / FERM 7344 / JCM 9153 / C-125) OX=272558 GN=nadE PE=3 SV=1	
orf00043	Probable nicotinate-nucleotide adenylyltransferase OS=Methylacidiphilum infernorum (isolate V4) OX=481448 GN=nadD PE=3 SV=1	
orf00044	Nicotinate phosphoribosyltransferase OS=Bacillus subtilis (strain 168) OX=224308 GN=pncB PE=3 SV=1	
orf00051	Uncharacterized HTH-type transcriptional regulator pXO2-48/BXB0055/GBAA_pXO2_0055 OS=Bacillus anthracis OX=1392 GN=pXO2-48 PE=4 SV=1	
orf00054		
orf00058		
orf00060		

Note: The red arrow denote the predicted core peptide laterosporulin in the *Bl* 1821L genome.

B.9 BAGEL4 analysis describing genes of the of the area of interest (AOI-4) in the *Bl* 1821L genome

Name	Function	Motifs
orf00002	DNA translocase FtsK OS=Oceanobacillus iheyensis (strain DSM 14371 / CIP 107618 / JCM 11309 / KCTC 3954 / HTE831) OX=221109 GN=ftsK PE=3 SV=1	
orf00003		
orf00005	Uncharacterized protein YlzJ OS=Bacillus subtilis (strain 168) OX=224308 GN=ylzJ PE=4 SV=1	
orf00006	Translocation-enhancing protein TepA OS=Bacillus halodurans (strain ATCC BAA-125 / DSM 18197 / FERM 7344 / JCM 9153 / C-125) OX=272558 GN=tepA PE=3 SV=1	
orf00008	Uncharacterized protein YxeA OS=Bacillus subtilis (strain 168) OX=224308 GN=yxeA PE=1 SV=1	
orf00011	Uncharacterized UDP-glucosyltransferase YojK OS=Bacillus subtilis (strain 168) OX=224308 GN=yojK PE=3 SV=2	
orf00013		
orf00017		
orf00019		
orf00020	Putative ankyrin repeat protein RBE_0220 OS=Rickettsia bellii (strain RML369-C) OX=336407 GN=RBE_0220 PE=4 SV=1	
orf00021		
orf00023	Modification methylase DpnIIB OS=Streptococcus pneumoniae OX=1313 GN=dpnA PE=1 SV=1	
orf00024		
orf00025		
223.2;UviB	223.2;UviB	
orf00027	Ribonuclease J1 OS=Bacillus subtilis (strain 168) OX=224308 GN=rnjA PE=1 SV=1	
orf00030	4-hydroxy-tetrahydrodipicolinate synthase 1 OS=Bacillus halodurans (strain ATCC BAA-125 / DSM 18197 / FERM 7344 / JCM 9153 / C-125) OX=272558 GN=dapA1 PE=3 SV=1	
orf00032	Aspartokinase 1 OS=Bacillus subtilis (strain 168) OX=224308 GN=dapG PE=3 SV=3	
orf00033	Aspartate-semialdehyde dehydrogenase OS=Bacillus subtilis (strain 168) OX=224308 GN=asd PE=1 SV=1	
LanD	Dipicolinate synthase subunit B OS=Bacillus subtilis (strain 168) OX=224308 GN=dpaB PE=1 SV=1	PF02441
orf00037	Dipicolinate synthase subunit A OS=Bacillus subtilis (strain 168) OX=224308 GN=dpaA PE=1 SV=1	
orf00038	Uncharacterized protein YmxH OS=Bacillus subtilis (strain 168) OX=224308 GN=ymxH PE=3 SV=1	
orf00040	Deoxyuridine 5'-triphosphate nucleotidohydrolase OS=Shewanella denitrificans (strain OS217 / ATCC BAA-1090 / DSM 15013) OX=318161 GN=dut PE=3 SV=1	
orf00041	Uncharacterized zinc protease YmxG OS=Bacillus subtilis (strain 168) OX=224308 GN=ymxG PE=3 SV=3	

Note: The red arrow denote the predicted core peptide UviB in the *Bl* 1821L genome.

B.10 BAGEL4 analysis showing encoded genes of the predicted areas of interest (AOI) in the *Bl* 1951 genome

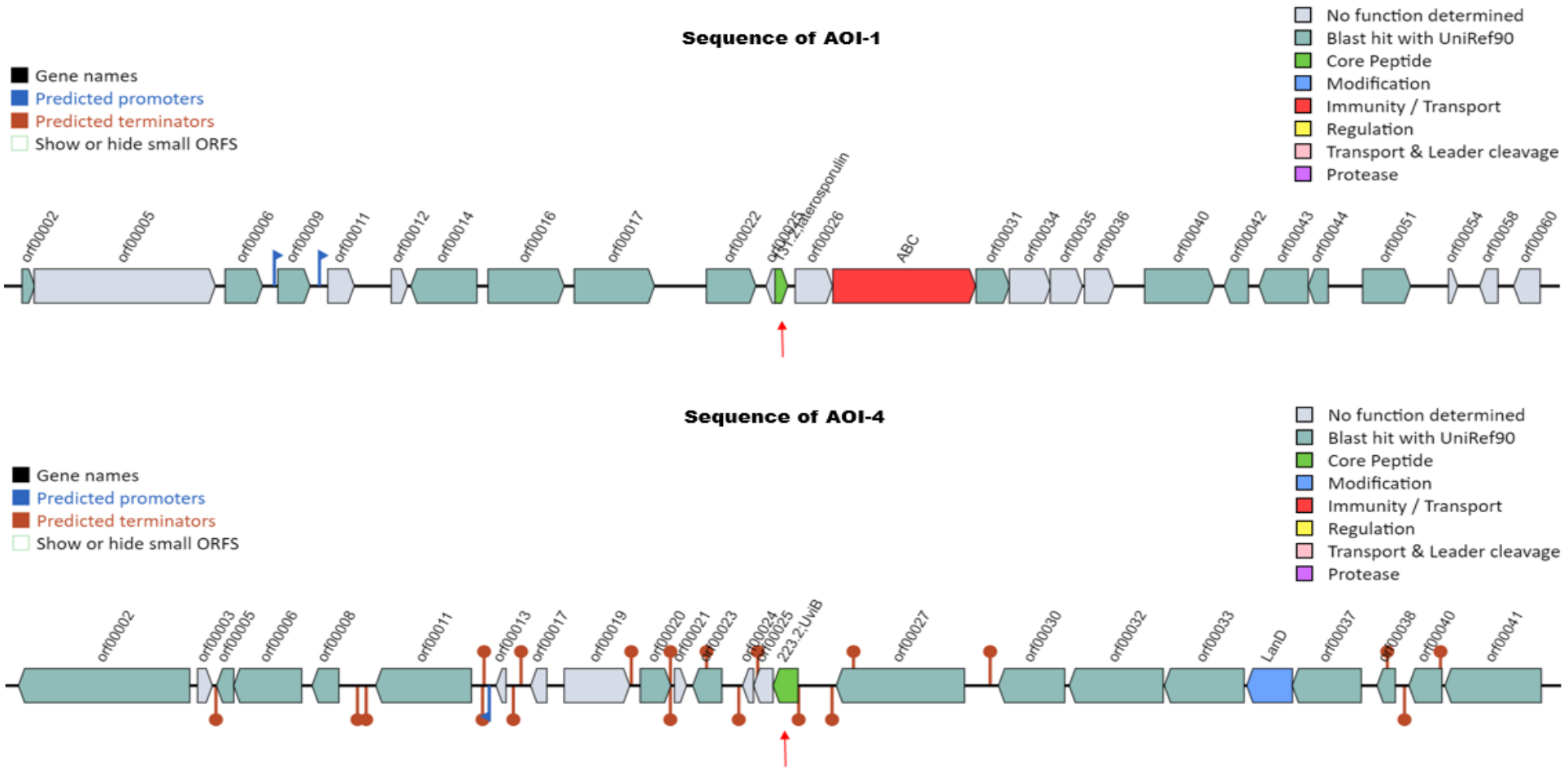

Note: The red arrows denote the location of the encoded core peptide genes in the *Bl* 1951 genome.
(Refer to Appendix B.11 & B.12).

B.11 BAGEL4 analysis describing genes of the of the area of interest (AOI-1) in the *Bl* 1951 genome

Name	Function	Motifs
orf00001	Protein VanZ OS=Enterococcus faecium OX=1352 GN=vanZ PE=4 SV=2	
orf00003		
orf00004	Protein YtsP OS=Bacillus subtilis (strain 168) OX=224308 GN=ytsP PE=3 SV=2	
orf00006	Uncharacterized HTH-type transcriptional regulator YusO OS=Bacillus subtilis (strain 168) OX=224308 GN=yusO PE=1 SV=1	
orf00008		
orf00010		
orf00012	Uncharacterized HTH-type transcriptional regulator YybE OS=Bacillus subtilis (strain 168) OX=224308 GN=yybE PE=3 SV=2	
orf00015	Formimidoylglutamase OS=Lysinibacillus sphaericus (strain C3-41) OX=444177 GN=hutG PE=3 SV=1	
orf00016	Sodium/glutamate symporter OS=Haemophilus influenzae (strain ATCC 51907 / DSM 11121 / KW20 / Rd) OX=71421 GN=gltS PE=3 SV=1	
orf00020	Spore germination protein GerE OS=Bacillus subtilis (strain 168) OX=224308 GN=gerE PE=1 SV=2	
131.2;laterosporulin	131.2;laterosporulin	RBS=TAAACATTTGAATGGAGG
orf00024		
ABC	Lantibiotic ABC transporter	PF00005
orf00028	Methylamine utilization protein MauD OS=Paracoccus versutus OX=34007 GN=mauD PE=2 SV=1	
orf00031		
orf00032		
orf00033		
orf00037	CAAX prenyl protease 2 OS=Methanococcus maripaludis (strain S2 / LL) OX=267377 GN=rce1 PE=1 SV=1	
orf00038	NH(3)-dependent NAD(+) synthetase OS=Exiguobacterium sibiricum (strain DSM 17290 / JCM 13490 / 255-15) OX=262543 GN=nadE PE=3 SV=1	
orf00039	Probable nicotinate-nucleotide adenylyltransferase OS=Methylacidiphilum infernorum (isolate V4) OX=481448 GN=nadD PE=3 SV=1	
orf00043	Nicotinate phosphoribosyltransferase OS=Bacillus subtilis (strain 168) OX=224308 GN=pncB PE=3 SV=1	
orf00049	Uncharacterized HTH-type transcriptional regulator pXO2-48/BXB0055/GBAA_pXO2_0055 OS=Bacillus anthracis OX=1392 GN=pXO2-48 PE=4 SV=1	
orf00055	Epoxyqueuosine reductase OS=Thermosynechococcus elongatus (strain BP-1) OX=197221 GN=queG PE=3 SV=2	

Note: The red arrow denote the predicted core peptide laterosporulin in the *Bl* 1951 genome.

B.12 BAGEL4 analysis describing genes of the of the area of interest (AOI-4) in the *Bl* 1951 genome

Name	Function	Motifs
orf00001	Putative transcriptional regulator protein YobU OS=Bacillus subtilis (strain 168) OX=224308 GN=yobU PE=4 SV=1	
orf00003	3-hydroxybutyryl-CoA dehydratase OS=Methylorubrum extorquens (strain ATCC 14718 / DSM 1338 / JCM 2805 / NCIMB 9133 / AM1) OX=272630 GN=croR PE=4 SV=1	
orf00004	Uncharacterized protein YrhO OS=Bacillus subtilis (strain 168) OX=224308 GN=yrhO PE=4 SV=1	
orf00005	Putative peptidoglycan O-acetyltransferase YrhL OS=Bacillus subtilis (strain 168) OX=224308 GN=yrhL PE=3 SV=1	
orf00006		
orf00008		
orf00012	Hypoxanthine DNA glycosylase OS=Methanosarcina acetivorans (strain ATCC 35395 / DSM 2834 / JCM 12185 / C2A) OX=188937 GN=MA_0462 PE=1 SV=1	
orf00014	Uncharacterized HTH-type transcriptional regulator CPE0189 OS=Clostridium perfringens (strain 13 / Type A) OX=195102 GN=CPE0189 PE=4 SV=1	
orf00015	Aryl-phospho-beta-D-glucosidase BglC OS=Bacillus subtilis (strain 168) OX=224308 GN=bglC PE=1 SV=1	
orf00019		
orf00021		
orf00022	N-acetylmuramoyl-L-alanine amidase CwlM OS=Bacillus licheniformis OX=1402 GN=cwlM PE=3 SV=1	
223.2;UviB	223.2;UviB	
orf00026		
orf00027		
orf00031		
orf00033		
orf00038		
orf00039	Uncharacterized protein YqcC OS=Bacillus subtilis (strain 168) OX=224308 GN=yqcC PE=4 SV=2	
orf00042	Uncharacterized protein XkzA OS=Bacillus subtilis (strain 168) OX=224308 GN=xkzA PE=4 SV=1	
orf00044	Uncharacterized protein YqcA OS=Bacillus subtilis (strain 168) OX=224308 GN=yqcA PE=4 SV=2	
orf00046	Phage-like element PBSX protein XkdT OS=Bacillus subtilis (strain 168) OX=224308 GN=xkdT PE=3 SV=1	
orf00049		
orf00050		
orf00053		
orf00055		
orf00058		

Note: The red arrow denote the predicted core peptide UviB in the *Bl* 1951 genome.

Appendix C

C.1 *Bl* 1821L CFU/ml at various time intervals converted into log_{10} CFU/ml

Time intervals (Hours)	1st Experiment		2nd Experiment		3rd Experiment		Mean value	
	CFU/ml	log_{10} CFU/ml	CFU/ml	log_{10} CFU/ml	CFU/ml	log_{10} CFU/ml	CFU/ml	log_{10} CFU/ml
3	2.00E+05	5.301	4.20E+05	5.623	6.35E+05	5.803	4.18E+05	5.576
6	1.45E+05	5.161	4.30E+05	5.633	5.75E+05	5.760	3.83E+05	5.518
12	3.30E+05	5.519	2.35E+05	5.371	1.05E+05	5.021	2.23E+05	5.304
18	2.60E+05	5.415	6.50E+04	4.813	4.50E+04	4.653	1.23E+05	4.960
24	3.40E+05	5.531	3.70E+05	5.568	5.50E+04	4.740	2.55E+05	5.280
36	4.15E+05	5.618	1.55E+05	5.190	2.20E+05	5.342	2.63E+05	5.384
48	4.15E+05	5.618	4.90E+05	5.690	1.20E+06	6.079	7.02E+05	5.796
60	4.31E+06	6.634	1.65E+05	5.217	1.36E+06	6.132	1.94E+06	5.995
72	3.85E+06	6.585	1.60E+05	5.204	6.15E+05	5.789	1.54E+06	5.859
96	2.40E+05	5.380	1.85E+05	5.267	1.70E+06	6.229	7.07E+05	5.626
120	4.25E+05	5.628	5.40E+05	5.732	2.66E+06	6.425	1.21E+06	5.929
144	1.39E+06	6.143	1.39E+06	6.143	1.63E+06	6.212	1.47E+06	6.166
168	6.05E+05	5.782	2.52E+06	6.401	1.70E+06	6.230	1.61E+06	6.138
192	2.38E+06	6.376	2.30E+06	6.362	3.83E+06	6.583	2.84E+06	6.440
216	1.58E+06	6.197	1.30E+06	6.112	2.62E+06	6.418	1.83E+06	6.243
240	1.86E+06	6.270	2.14E+06	6.330	1.33E+06	6.124	1.78E+06	6.241

C.2 Experiment 1: Production kinetics of putative antibacterial proteins of *Bl* 1821L

Time interval (Hours)	log_{10} CFU/ ml	pH of CFS	Zone of inhibition diameter (mm)	
			***Bl* 1821L as the host bacterium**	***Bl* 1951 as the host bacterium**
3	5.301	7.02	10.33	10.00
6	5.161	7.02	11.00	11.00
12	5.519	8.43	12.00	15.00
18	5.415	8.59	12.33	15.67
24	5.531	8.71	11.67	15.00
36	5.618	8.97	12.67	14.67
48	5.618	9.02	13.33	13.00
60	6.634	9.14	14.00	17.33
72	6.585	8.92	13.33	18.00
96	5.380	9.20	12.00	14.67
120	5.628	9.34	12.67	12.67
144	6.143	9.28	12.67	12.67
168	5.782	9.16	13.00	13.00
192	6.376	9.15	13.00	12.67
216	6.197	9.11	13.00	13.33
240	6.270	9.10	12.00	13.33

Note: Host bacterium (*Bl* 1821L) was grown under laboratory conditions in LB broth on an orbital shaker with 250 rpm at 30^{o}C. The host bacterial samples were drawn at the aforementioned time intervals to determine the effect of produced putative antibacterial proteins on the number of viable cells. CFS of each time interval were obtained to find out the pH and the antibacterial activity of the produced putative antibacterial proteins.

C.3 Experiment 2: Production kinetics of putative antibacterial proteins of *Bl* 1821L

Time interval (Hours)	log_{10} CFU/ ml	pH of CFS	Zone of inhibition diameter (mm)	
			***Bl* 1821L as the host bacterium**	***Bl* 1951 as the host bacterium**
3	5.623	7.10	12.00	10.33
6	5.633	7.14	11.33	11.33
12	5.371	7.84	14.00	12.33
18	4.813	8.19	12.33	14.67
24	5.568	8.62	12.33	16.00
36	5.190	9.13	12.33	16.67
48	5.690	9.27	10.67	13.33
60	5.217	9.43	11.00	14.33
72	5.204	9.44	11.33	14.00
96	5.267	9.41	12.33	14.00
120	5.732	9.40	12.00	14.00
144	6.143	9.25	12.33	12.00
168	6.401	9.21	13.00	11.67
192	6.362	9.32	13.67	12.33
216	6.112	9.54	13.33	10.33
240	6.330	9.51	13.67	12.33

Note: Host bacterium (*Bl* 1821L) was grown under laboratory conditions in LB broth on an orbital shaker with 250 rpm at 30^{o}C. The host bacterial samples were drawn at the aforementioned time intervals to determine the effect of produced putative antibacterial proteins on the number of viable cells. CFS of each time interval were obtained to find out the pH and the antibacterial activity of the produced putative antibacterial proteins.

C.4 Experiment 3: Production kinetics of putative antibacterial proteins of *Bl* 1821L

Time interval (Hours)	log_{10} CFU/ ml	pH of CFS	Zone of inhibition diameter (mm)	
			***Bl* 1821L as the host bacterium**	***Bl* 1951 as the host bacterium**
3	5.803	7.07	11.67	12.00
6	5.760	6.97	12.67	12.67
12	5.021	7.77	14.00	15.67
18	4.653	8.27	15.00	15.33
24	4.740	8.75	15.33	14.67
36	5.342	9.27	16.00	14.67
48	6.079	9.48	13.00	15.00
60	6.132	9.55	14.00	15.33
72	5.789	9.58	13.67	14.33
96	6.229	9.65	10.67	13.00
120	6.425	9.68	11.67	13.67
144	6.212	9.45	12.67	13.67
168	6.230	9.59	13.33	13.00
192	6.583	9.48	11.00	11.67
216	6.418	9.54	12.33	10.67
240	6.124	9.56	9.33	11.00

Note: Host bacterium (*Bl* 1821L) was grown under laboratory conditions in LB broth on an orbital shaker with 250 rpm at 30^{o}C. The host bacterial samples were drawn at the aforementioned time intervals to determine the effect of produced putative antibacterial proteins on the number of viable cells. CFS of each time interval were obtained to find out the pH and the antibacterial activity of the produced putative antibacterial proteins.

C.5 *BI* 1951 CFU/ml at various time intervals converted into log_{10} CFU/ml

Time intervals (Hours)	1st Experiment		2nd Experiment		3rd Experiment		Mean values	
	CFU/ml	log_{10} CFU/ml	CFU/ml	log_{10} CFU/ml	CFU/ml	log_{10} CFU/ml	CFU/ml	log_{10} CFU/ml
3	1.30E+06	6.114	1.10E+06	6.041	2.80E+06	6.447	1.73E+06	6.239
6	1.90E+06	6.279	2.25E+06	6.352	2.05E+06	6.312	2.07E+06	6.315
12	1.38E+07	7.138	3.05E+06	6.484	5.35E+06	6.728	7.38E+06	6.868
18	1.40E+06	6.146	2.20E+06	6.342	7.00E+05	5.845	1.43E+06	6.156
24	2.50E+05	5.398	1.45E+06	6.161	1.30E+06	6.114	1.00E+06	6.000
36	4.00E+06	6.602	2.25E+06	6.352	5.00E+06	6.699	3.75E+06	6.574
48	1.21E+07	7.083	2.80E+06	6.447	2.11E+07	7.323	1.20E+07	7.079
60	8.25E+06	6.916	5.25E+06	6.720	5.20E+06	6.716	6.23E+06	6.795
72	6.40E+06	6.806	7.80E+06	6.892	5.25E+06	6.720	6.48E+06	6.812
96	9.95E+06	6.998	1.14E+07	7.055	6.55E+06	6.816	9.28E+06	6.968
120	8.15E+06	6.911	2.67E+07	7.426	7.65E+06	6.884	1.42E+07	7.151
144	1.57E+07	7.195	1.57E+07	7.195	6.70E+06	6.826	1.27E+07	7.103
168	7.10E+06	6.851	1.44E+07	7.158	1.17E+07	7.068	1.11E+07	7.044
192	9.80E+06	6.991	9.00E+06	6.954	1.04E+07	7.017	9.73E+06	6.988
216	1.11E+07	7.043	1.06E+07	7.025	1.49E+07	7.173	1.22E+07	7.086
240	2.52E+07	7.401	2.48E+07	7.394	3.75E+06	6.574	1.79E+07	7.253

C.6 Experiment 1: Production kinetics of putative antibacterial proteins of *Bl* 1951

Time interval (Hours)	log_{10} CFU/ ml	pH of CFS	Zone of inhibition diameter (mm)	
			Bl 1951 as the host bacterium	*Bl* 1821L as the host bacterium
3	6.114	6.55	0.00	14.33
6	6.279	6.93	0.00	13.33
12	7.138	7.55	10.00	13.67
18	6.146	8.17	14.00	16.00
24	5.398	8.47	12.67	13.67
36	6.602	9.00	13.33	13.00
48	7.083	8.93	13.33	12.67
60	6.916	8.89	13.33	12.67
72	6.806	8.96	13.33	12.00
96	6.998	9.07	13.67	12.33
120	6.911	9.03	13.00	12.67
144	7.195	9.19	11.33	13.00
168	6.851	9.13	13.00	13.67
192	6.991	9.13	12.33	13.00
216	7.043	9.11	12.67	13.33
240	7.401	8.88	12.00	13.33

Note: Host bacterium (*Bl* 1951) was grown under laboratory conditions in LB broth on an orbital shaker with 250 rpm at 30^{o}C. The host bacterial samples were drawn at the aforementioned time intervals to determine the effect of produced putative antibacterial proteins on the number of viable cells. CFS of each time interval were obtained to find out the pH and the antibacterial activity of the produced putative antibacterial proteins.

C.7 Experiment 2: Production kinetics of putative antibacterial proteins of *Bl* 1951

Time interval (Hours)	log_{10} CFU/ ml	pH of CFS	Zone of inhibition diameter (mm)	
			***Bl* 1951 as the host bacterium**	***Bl* 1821L as the host bacterium**
3	6.041	7.12	0.00	12.67
6	6.352	7.15	0.00	11.00
12	6.484	7.63	12.00	14.00
18	6.342	8.15	13.33	14.33
24	6.161	8.60	12.33	11.33
36	6.352	9.12	11.00	12.67
48	6.447	9.07	12.67	11.33
60	6.720	9.10	11.67	11.00
72	6.892	9.17	12.33	14.00
96	7.055	9.22	14.00	15.33
120	7.426	9.29	13.33	13.67
144	7.195	9.18	13.33	13.33
168	7.158	9.28	11.67	16.33
192	6.954	9.22	14.00	14.33
216	7.025	9.29	12.33	14.33
240	7.394	9.33	13.00	16.00

Note: Host bacterium (*Bl* 1951) was grown under laboratory conditions in LB broth on an orbital shaker with 250 rpm at 30^{o}C. The host bacterial samples were drawn at the aforementioned time intervals to determine the effect of produced putative antibacterial proteins on the number of viable cells. CFS of each time interval were obtained to find out the pH and the antibacterial activity of the produced putative antibacterial proteins.

C.8 Experiment 3: Production kinetics of putative antibacterial proteins of *Bl* 1951

Time interval (Hours)	log_{10} CFU/ ml	pH of CFS	Zone of inhibition diameter (mm)	
			***Bl* 1951 as the host bacterium**	***Bl* 1821L as the host bacterium**
3	6.447	7.17	0.00	10.00
6	6.312	7.17	0.00	12.33
12	6.728	7.85	10.00	13.00
18	5.845	8.22	12.67	14.67
24	6.114	8.77	10.67	14.33
36	6.699	9.04	10.67	13.67
48	7.323	9.24	12.00	13.00
60	6.716	9.37	11.67	11.00
72	6.720	9.42	11.67	12.00
96	6.816	9.42	13.67	11.67
120	6.884	9.37	12.00	12.33
144	6.826	9.36	12.00	12.00
168	7.068	9.42	11.33	14.00
192	7.017	9.53	13.00	13.67
216	7.173	9.56	10.67	13.33
240	6.574	9.39	13.33	11.33

Note: Host bacterium (*Bl* 1951) was grown under laboratory conditions in LB broth on an orbital shaker with 250 rpm at 30^{o}C. The host bacterial samples were drawn at the aforementioned time intervals to determine the effect of produced putative antibacterial proteins on the number of viable cells. CFS of each time interval were obtained to find out the pH and the antibacterial activity of the produced putative antibacterial proteins.

Appendix D

D.1 N-terminal sequenced short amino acid match hits to the gene of 25 kD putative hypothetical protein encoded in *Bl* 1821 and *Bl* 1951 genomes

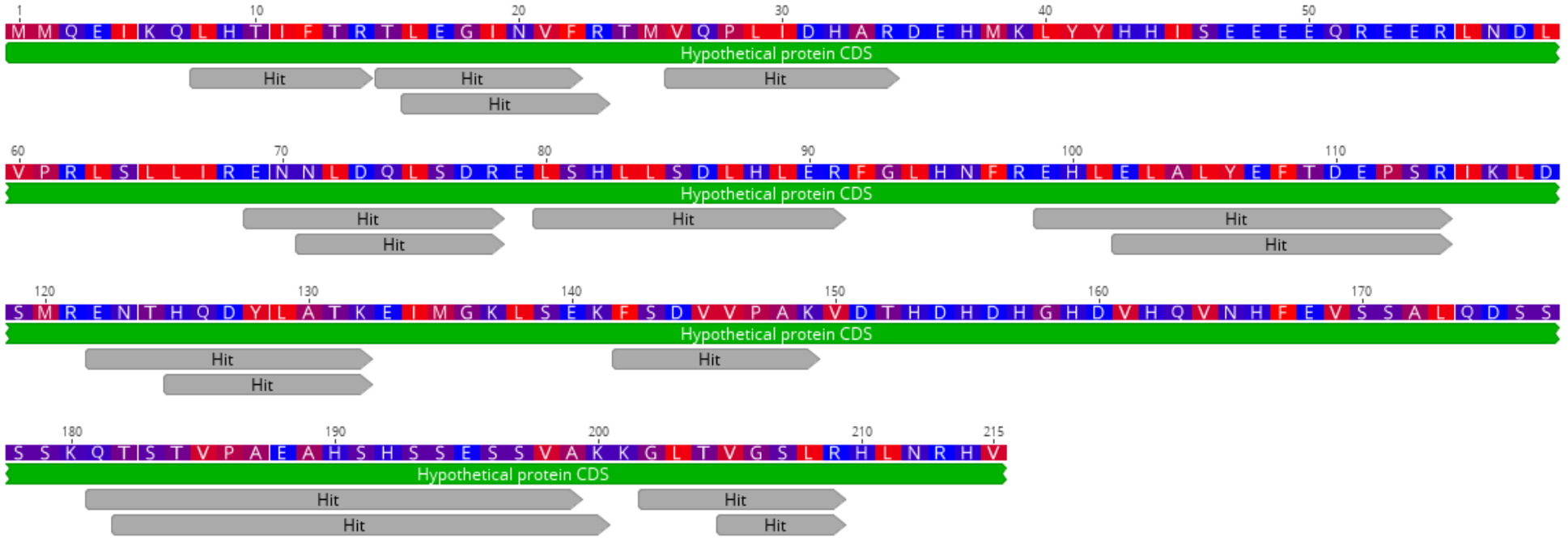

Note: Refer to supplementary material for N-terminal sequence data of purified ~30 kD excised bands of *Bl* 1821L & *Bl* 1951.

https://doi.org/10.25400/lincolnuninz.16713442

D.2 N-terminal sequenced short amino acid match hits to the 30 kD putative bacteriocin family protein/encapsulating protein for a DyP-type peroxidase or ferritin-like protein oligomer gene encoded in *Bl* 1821 and *Bl* 1951 genomes

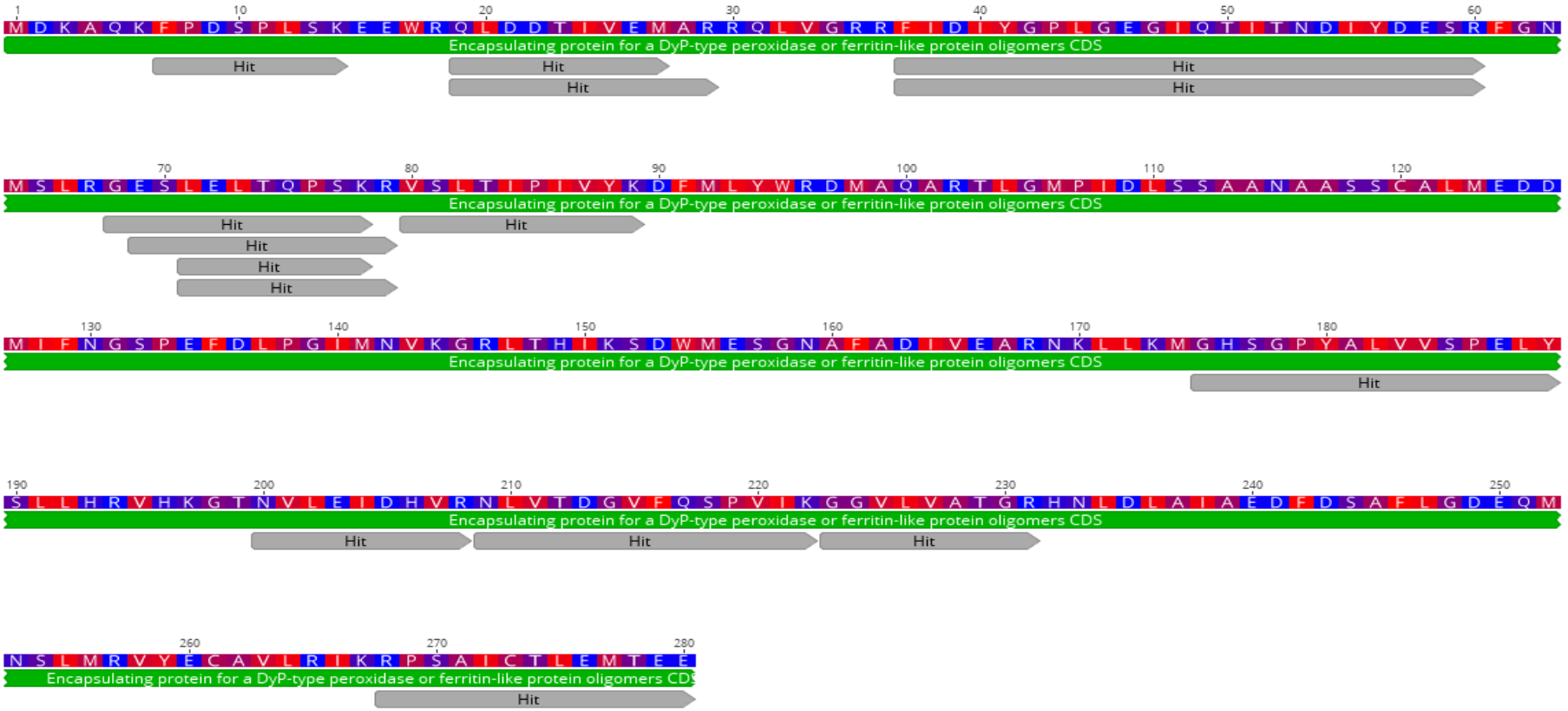

Note: Refer to supplementary material for N-terminal sequence data of purified ~30 kD excised bands of *Bl* 1821L & *Bl* 1951.

https://doi.org/10.25400/lincolnuninz.16713442

D.3 Amino acids alignment of 25 kD putative hypothetical protein of *Bl* 1821L and *Bl* 1951 using BLASTp analysis

Score	Expect	Method	Identities	Positives	Gaps
433 bits(1114)	5e-162	Compositional matrix adjust.	215/215(100%)	215/215(100%)	0/215(0%)

```
Query  1    MMQEIKQLHTIFTRTLEGINVFRTMVQPLIDHARDEHMKLYYHHISEEEEQREERLNDLV  60
            MMQEIKQLHTIFTRTLEGINVFRTMVQPLIDHARDEHMKLYYHHISEEEEQREERLNDLV
Sbjct  1    MMQEIKQLHTIFTRTLEGINVFRTMVQPLIDHARDEHMKLYYHHISEEEEQREERLNDLV  60

Query  61   PRLSLLIRENNLDQLSDRELSHLLSDLHLERFGLHNFREHLELALYEFTDEPSRIKLDSM  120
            PRLSLLIRENNLDQLSDRELSHLLSDLHLERFGLHNFREHLELALYEFTDEPSRIKLDSM
Sbjct  61   PRLSLLIRENNLDQLSDRELSHLLSDLHLERFGLHNFREHLELALYEFTDEPSRIKLDSM  120

Query  121  RENTHQDYLATKEIMGKLSEKFSDVVPAKVDTHDHDHGHDVHQVNHFEVSSALQDSSSSK  180
            RENTHQDYLATKEIMGKLSEKFSDVVPAKVDTHDHDHGHDVHQVNHFEVSSALQDSSSSK
Sbjct  121  RENTHQDYLATKEIMGKLSEKFSDVVPAKVDTHDHDHGHDVHQVNHFEVSSALQDSSSSK  180

Query  181  QTSTVPAEAHSHSSESSVAKKGLTVGSLRHLNRHV  215
            QTSTVPAEAHSHSSESSVAKKGLTVGSLRHLNRHV
Sbjct  181  QTSTVPAEAHSHSSESSVAKKGLTVGSLRHLNRHV  215
```

D.4 Amino acid alignment of putative bacteriocin family protein (30 kD) of *Bl* 1821L and putative encapsulating protein for a DyP-type peroxidase or ferritin-like protein (30 kD) of *Bl* 1951 using BLASTp analysis

Score	Expect	Method	Identities	Positives	Gaps
582 bits(1500)	0.0	Compositional matrix adjust.	280/280(100%)	280/280(100%)	0/280(0%)

```
Query  1    MDKAQKFPDSPLSKEEWRQLDDTIVEMARRQLVGRRFIDIYGPLGEGIQTITNDIYDESR  60
            MDKAQKFPDSPLSKEEWRQLDDTIVEMARRQLVGRRFIDIYGPLGEGIQTITNDIYDESR
Sbjct  1    MDKAQKFPDSPLSKEEWRQLDDTIVEMARRQLVGRRFIDIYGPLGEGIQTITNDIYDESR  60

Query  61   FGNMSLRGESLELTQPSKRVSLTIPIVYKDFMLYWRDMAQARTLGMPIDLSSAANAASSC  120
            FGNMSLRGESLELTQPSKRVSLTIPIVYKDFMLYWRDMAQARTLGMPIDLSSAANAASSC
Sbjct  61   FGNMSLRGESLELTQPSKRVSLTIPIVYKDFMLYWRDMAQARTLGMPIDLSSAANAASSC  120

Query  121  ALMEDDMIFNGSPEFDLPGIMNVKGRLTHIKSDWMESGNAFADIVEARNKLLKMGHSGPY  180
            ALMEDDMIFNGSPEFDLPGIMNVKGRLTHIKSDWMESGNAFADIVEARNKLLKMGHSGPY
Sbjct  121  ALMEDDMIFNGSPEFDLPGIMNVKGRLTHIKSDWMESGNAFADIVEARNKLLKMGHSGPY  180

Query  181  ALVVSPELYSLLHRVHKGTNVLEIDHVRNLVTDGVFQSPVIKGGVLVATGRHNLDLAIAE  240
            ALVVSPELYSLLHRVHKGTNVLEIDHVRNLVTDGVFQSPVIKGGVLVATGRHNLDLAIAE
Sbjct  181  ALVVSPELYSLLHRVHKGTNVLEIDHVRNLVTDGVFQSPVIKGGVLVATGRHNLDLAIAE  240

Query  241  DFDSAFLGDEQMNSLMRVYECAVLRIKRPSAICTLEMTEE  280
            DFDSAFLGDEQMNSLMRVYECAVLRIKRPSAICTLEMTEE
Sbjct  241  DFDSAFLGDEQMNSLMRVYECAVLRIKRPSAICTLEMTEE  280
```

D.5 BLASTp analysis of 30 kD putative encapsulating protein of *Bl* 1821L and *Bl* 1951 identified accessions tr|A0A502IA18|A0A502IA18_BRELA and tr|A0A2S5H3X5|A0A2S5H3X5_BRELA after N-terminal sequencing

Accession	Description & % amino acid similarity to the Uniprot identified accessions	Amino acid sequence
tr|A0A075R6D8|A0A075R6D8_BRELA	Linocin M18 bacteriocin family protein *Brevibacillus laterosporus* LMG 15441 (97.1% identity to A0A502IA18) (99.3% identity to A0A2S5H3X5)	MDKSQKFPDSPLSKEEWRQLDETIVDMARRQLVGRRFIDIYGPLGEGIQTITNDIYDESR FGNMSLRGESLELTQPSKRVSLTIPIVYKDFMLYWRDMAQARTLGMPIDLSPAANAASSC ALMEDDLIFNGNPEFDLPGIMNVKGRLTHIKSDWMESGNAFADIVEARNKLLKMGHSGPY ALVVSPELYSLLHRVHKGTNVLEIDHIRNLVTDGVFQSPVIKGGALVATGRHNLDLAIAE DFDSAFLGDEQMNSLMRVYECAVLRIKRPSAICTLEMTEE
tr|A0A1A5XQ92|A0A1A5XQ92_BRELA	Bacteriocin *Brevibacillus sp.* WF146 (87.9% identity to A0A502IA18) (87.9% identity to A0A2S5H3X5)	MDKLRKFPDSPLTNDEWRQLDQTVVEMARRQLVGRRFIDIYGPLGEGIQTITNDIYEESR FGGLSLRGESLELTQPSRRVSLTIPILYKDFVLYWRDVAQARTLGMPLDMSAAANAAAGC ALMEDDLIFNGSAEFDLPGLMNVKGRLTHLKSDWMESGNAFADIVEARNKLLKMGHSGPY ALVVSPELYSLLHRVHKGTNVLEIEHIRNLVTDGVYQSPTIKGRTGVLVATGRHNLDLAI AEDFDTAFLGDEQMNSFFRVYECVVLRIKRPSAICTLEETEE

tr|M8DYN1|M8DYN1_9BACL	Uncharacterised protein *Brevibacillus borstelensis* AK1 (87.2% identity to A0A502IA18) (86.9% identity to A0A2S5H3X5)	MDKLRKYPDSPLTHDEWKQLDETVVDMARRQLVGRRFLDIYGPLGEGIQTITNDIYDESR FGGLNLRGESLEMTQPSKRVSLTIPILYKDFMLYWRDVAQARTLGMPLDMSAAANAAAGC ALMEDDLIFNGSPGLDLPGLMNVKGRLTHLKSDWMESGNAFADIVEARNKLLKMGHSGPY ALVVSPELYSLLHRVHKGTNVLEIEHVRNLVTDGVFQSPTIKGRSGVLVATGRHNLDLAI AEDFDTSFLGDEQMNSLFRVYECVVLRIKRPSAICTLEETEE
tr|C0ZHN4|C0ZHN4_BREBN	Uncharacterised protein *Brevibacillus brevis* (strain 47/ JCM 6285/ NBRC 100599) (87.2% identity to A0A502IA18) (86.9% identity to A0A2S5H3X5)	MDKLRKYPDSPLTTEEWNQLDATVVDMARRQLVGRRFIDIYGPLGEGIQTITNDVYEESR FGGLSLRGESLEMTQPSRRVSMTIPILYKDFMLYWRDVAQARTLGMPLDMSAAANAAAGG ALMEDDLIFNGAAEFDLPGLMNVKGRLTHLKSDWMESGNAFADIVEARNKLLKMGHSGPY ALVVSPELYSLLHRVHKGTNVLEIEHVRNLVTDGVFQSPTIKGRSGVLVATGRHNLDLAI AEDFDSAFLGDEQMNSLFRVYECVVLRIKRPSAICTLEETEE

tr|A0A1I3VYI9|A0A1I3VYI9_9BACL	Uncharacterised protein Lincocin/CFP29 family *Brevibacillus centrosporus* (86.5% identity to A0A502IA18) (86.2% identity to A0A2S5H3X5)	MDKLRKYPDSPLTNEEWNQLDATVIDMARRQLVGRRFIDIYGPLGEGIQTITNDVYDESR FGGLSLRGESLEMTQPSRRVSMTIPILYKDFMLYWRDVAQARTLGMPLDMSAAANAAAGG ALMEDDLIFNGAAEFDLPGLMNVKGRLTHLKSDWMESGNAFADIVEARNKLLKMGHSGPY ALVVSPELYALLHRVHKGTNVLEIEHVRNLVTDGVFQSPTIKGRSGVLIATGRHNLDLAI AEDFDSAFLGDEQMNSLFRVYECVVLRIKRPSAICTLEETEE
tr|V6M3H3|V6M3H3_9BACL	Bacteriocin *Brevibacillus panacihumi* W25 (85.5 % identity to A0A502IA18) (85.5 % identity to A0A2S5H3X5)	MDKLRKYPDSPLTHDEWKQLDETVVDMARRQLVGRRFIDIYGPLGEGIQTITNDVYEESR FGGLSLRGESLEMTQPSKRVSMTIPILYKDFMLYWRDVAQARTLGMPLDMSAAANAAAGG ALMEDDLIFNGAAEFDLPGLMNVKGRLTHLKSDWMESGNAFADVVEARNKLLKMGHSGPY ALVVSPELYALLHRVHKGTNVLEIEHVRNLVTDGVYQSPTIKGRSGVLVATGRHNLDLAI AEDFDTSFLGDEQMNSLFRVYECVVLRIKRPSAICTLEDTEE

tr|A0A3M8DJY3|A0A3M8DJY3_9BACL	Bacteriocin *Brevibacillus fluminis* (85.4% identity to A0A502IA18) (85.1% identity to A0A2S5H3X5)	MDKLSRYPDSPLSRDEWKQLDDTVIDMARRQLVGRRFLDIYGPLGEGVQTITNDIYDESR FGGLNLRGESLELTQPSRRVSLTIPILYKDFMLYRRDISQARTLGMPLDLSASANAAASC ALMEDDLIFNGSSEFDLPGLMNVKGRLTHLKSDWMESGNAFADVVEARNKLLKMGHSGPY AMVVSPELYTLLHRVHKGTTVLEIEHIRNLVTDGVYQSPVIKGRSGVIVATGRHNLDLAI AEDFDSAFLGDEQMNSLLRVYECAALRIKRPSAICTLEETE
tr|A0A6M1UFS1|A0A6M1UFS1_9BACL	Bacteriocin family protein *Brevibacillus sp*. SYP-B805 (68.8% identity to A0A502IA18) (79.1% identity to A0A2S5H3X5)	MEKHHKFPDAPLSPDEWRQLDETVVEMARRQLVGRRFIDIYGPLGEGIQAISNDLYEESR VGALNLRGEGLELTQPSRRVSLTIPILYNDFVLYWRDISQARTLGIPLDFSGAANAAAGC ALLEDDLIFNGSPAFELPGLMNVTGRLTHLKSDWMESGNAFADIVEARNKLLKMGHSGPY ALAVSPELYSLLHRVHQGTNVLEIEHIRSLVTEGVYQTPAIQGRAGVLVSCGRHNLDLAI AEDFNTAFMEDEQMNSVFRVYECVVLRIKRPSAICTLEEAEK

tr|A0A4Q1T7Q9|A0A4Q1T7Q9_9BACL	Bacteriocin *Ammoniphilus* sp. CFH 90114 (71.9% identity to A0A502IA18) (75.8% identity to A0A2S5H3X5)	MTKISRFPDSPLSSAEWQQLDETIVNVARKQLVGRRFIDVYGPLGQGVQSVSNDIYTESQ SGGMSLRGDTLSLSTSIKRVNLTIPILYKDFMLYWRDIQQAKTLDMPIDMGPAANASIQC ARLEDDLIFNGSEEMDLPGLMNVKGRLTHIRSDWMESGKAFSDIVEAINKLLQMGHTGPY ALAVSPQLYALLHRVHPGTNVLEIEHIRELVTDGVYQTPVIKGNAGVLVATGQHNLDLAI AEDFDSAFLGDEQMNHLFRVYECVALRIKRPSAICTLEDHE
tr|A0A366XWJ9|A0A366XWJ9_9BACI	Bacteriocin *Bacillus taeanensis* (68.8% identity to A0A502IA18) (72.3 % identity to A0A2S5H3X5)	MDKLTRYADSPLNETDWHQLDETVIENARRNLVGRRFIDIYGPLGQGVQSVINDIYEQSE LGVVSIHGNSLELTEPTRRVHLTIPMLYKDFQLYWRDIEQAKTLNLPIDFSAAANAAAQC ALLEDDLIFNGSNQFDFPGLMNVKGRLTHIRSDWMKSGNAFSDIVEARNKLLQMGNTGPY ALVVSPSLYALLHRVHQGTNVLEIEHIRELVTDGVYQSPVIKGEAGVVVATGRHHLDLAI SEDFDTAYMDSEHMNHFFRVYECAVLRIKRPSAICTLEDPKGGK

D.6 BLASTp analysis of 25 kD putative hypothetical protein of *Bl* 1821L and *Bl* 1951 identified accession tr|A0A502I846|A0A502I846_BRELA after N-terminal sequencing

Accession	Description & % amino acid similarity to the Uniprot identified accessions	Amino acid sequence
tr|A0A075R9Z9|A0A075R9Z9_BRELA	Uncharacterised protein *Brevibacillus laterosporus* LMG 15441 (90.7% identity to A0A502I846)	MLQEIKQLHTIFTRTLEGINVFRTMVQPLIDHARDEHMKLYYHHISEEEEQREERLHDLV PRLSQIIQEKNLDQLSDRELSHLLSDLNLERFGLHNFREHLELALYEFTDEPSRLKLDSM RENTHQDYLATKEIMVKLSEKFSDVVPAKMDTHDHDHGHDIHQVNHFEASSALQDSSSSK QPATVHADTHSHSAETSVMKKGLTVGSLRHLNRHV
tr|A0A1I3VYL5|A0A1I3VYL5_9BACL	Encapsulated protein *Brevibacillus centrosporus* (57.8% identity to A0A502I846)	MQDFTQLHTIFDRTRGYINRFMGIIQPIIDAAQDEHTRLYYHHILEEEEQRMGRLQQLVP HLESLSAEKKSDQLSDRELSQLLSDINLERFGLHNFREHLELSLYEFRDDETRMELDGMR EKTHADYLQVKDIMSKLSERFSDVYTTDLTDHDEGHDVHQVDHLKASASAPLGVASVITH PQTPVSGKKGLTVGSLKGLH

tr|A0A1A5XPH2|A0A1A5XPH2_9BACL	Uncharacterised *Brevibacillus sp.*WF 146 (57.6% identity to A0A502I846)	MQEMSQLHAIFTRTSGFIERFMGIIQPIIDAAQDEHTRLYYHHILEEEEQRLGRLNELIP YLGSLIDGNKAEQLSDRELSRLLSDINLERFGLHNFREHLELSLYEFQDEETRSALNSMR EATQEDYLRVKEIIAALSERFSDGDRRPDLTDHDEGHDIHQVDHLKASAAQTGAAHAGKA PGAAQTVSAPAAKKGLTVGSLKGL
tr|V6MCN7|V6MCN7_9BACL	Uncharacterised protein *Brevibacillus panacihumi* W25 (57.4% identity to A0A502I846)	MQELSQLHAIFDRTQGYIHRFMSLIQPIIDAAQDEHTRLYYHHILEEEEQREDRLKELIP YLQSLSAEKAEQLSDRELSRLLSDINLERFGLHNFREHLELALYEFRDEETRLDLDGMRA TTHEDYLRVKDIMASLSERFSDVSHPALTDHDEGHDIHAVDHLKASAALPKGVASVIKHE TSPAPAKKGLTVGSLKGK

tr|C0ZHN3|C0ZHN3_BREBN	Uncharacterised protein *Brevibacillus borstelensis* AK1 (56.2% identity to A0A502I846)	MDKLRKYPDSPLTHDEWKQLDETVVDMARRQLVGRRFLDIYGPLGEGIQTITNDIYDESR FGGLNLRGESLEMTQPSKRVSLTIPILYKDFMLYWRDVAQARTLGMPLDMSAAANAAAGC ALMEDDLIFNGSPGLDLPGLMNVKGRLTHLKSDWMESGNAFADIVEARNKLLKMGHSGPY ALVVSPELYSLLHRVHKGTNVLEIEHVRNLVTDGVFQSPTIKGRSGVLVATGRHNLDLAI AEDFDTSFLGDEQMNSLFRVYECVVLRIKRPSAICTLEETEE
tr|M8DFC9|M8DFC9_9BACL	Uncharacterised protein *Brevibacillus borstelensis* AK1 (55.3% identity to A0A502I846)	MQEMSQLHAIFSRTRGYIDRFAEIIQPIIDAAQDEHTRLYYHHILEEEEQRLGRLQELIP YIGSLDEAKKAEQLSDRELSRLLSDINLERFGLHNFREHLELSLYEFKDEETRQLLNSMR ESTQEDYLRVKEIMAALSERFSDVHRPDLTDHDEGYDIHQVDHLKASSSPAVANTGKTAA APAAKTGRKGLTVGSLKGMF

tr|A0A3M8DHE0|A0A3M8DHE0_9BACL	Uncharacterised protein *Brevibacillus fluminis* (54.8% identity to A0A502I846)	MQTIVEAHAIFERTKAAIGKFMSIIQPVIDNAQDEHTRLYYHHILEEEEQRLGRLEELIP YLKEISSAPVENLSDRELSHMLSDLNLERFGLHNFREHLELSLYEFSDEERRSLLNTMRE STQNDYLRMKDIMTELASRFSDVKLSSIEDHDHGHDIHQVDHLKASSKTATPAATAPAVA IPAKKGLTVGSLRGK

D.7 (A). Amino acids alignment of *Bl* 1821L hypothetical protein located at the 5' end of putative bacteriocin family protein (30 kD) with the corresponding protein residing in the analogous position in the *Bl* 1951 genome. (B). Amino acids alignment of hypothetical protein encoded immediate position to the (A) with the corresponding protein of *Bl* 1951

A

Score	Expect	Method	Identities	Positives	Gaps
326 bits(835)	1e-121	Compositional matrix adjust.	157/157(100%)	157/157(100%)	0/157(0%)

```
Query  1    MTRYQINGYTDMYTVVSNERKIGGAVEADTIKLRSGEEYKHAVITRLEMSDSQFCSLGFV  60
            MTRYQINGYTDMYTVVSNERKIGGAVEADTIKLRSGEEYKHAVITRLEMSDSQFCSLGFV
Sbjct  1    MTRYQINGYTDMYTVVSNERKIGGAVEADTIKLRSGEEYKHAVITRLEMSDSQFCSLGFV  60

Query  61   TEEGKRLIVHIQDISMIVDARHLNVCELVNNYMRQQKVAERLKHLKRLCELNEGSCTLPF  120
            TEEGKRLIVHIQDISMIVDARHLNVCELVNNYMRQQKVAERLKHLKRLCELNEGSCTLPF
Sbjct  61   TEEGKRLIVHIQDISMIVDARHLNVCELVNNYMRQQKVAERLKHLKRLCELNEGSCTLPF  120

Query  121  CEEVDVLVCDIGYETAISHVDMPFLHTADTQKIVRIA  157
            CEEVDVLVCDIGYETAISHVDMPFLHTADTQKIVRIA
Sbjct  121  CEEVDVLVCDIGYETAISHVDMPFLHTADTQKIVRIA  157
```

B

Score	Expect	Method	Identities	Positives	Gaps
186 bits(472)	2e-68	Compositional matrix adjust.	96/97(99%)	97/97(100%)	0/97(0%)

```
Query  1    MLEVLFILLVITYTISVSYTVAFTRSEGKDERGKQILTNGYTLGYSIAVIGILLSFLTAK  60
            MLEVLFILLVITYTISVSYTVAFTRSEGKDERGKQILTNGYTLGYSIAVIGILLSFLTAK
Sbjct  1    MLEVLFILLVITYTISVSYTVAFTRSEGKDERGKQILTNGYTLGYSIAVIGILLSFLTAK  60

Query  61   LSFISVGYKIAFDFALMSIWISGIFIAVYIFYKNKTV  97
            LSFISVGYK+AFDFALMSIWISGIFIAVYIFYKNKTV
Sbjct  61   LSFISVGYKVAFDFALMSIWISGIFIAVYIFYKNKTV  97
```

D.8 N-terminal sequenced short amino acid match hits to the gene of putative phage tail protein (48 kD) encoded in *Bl* 1821L genome

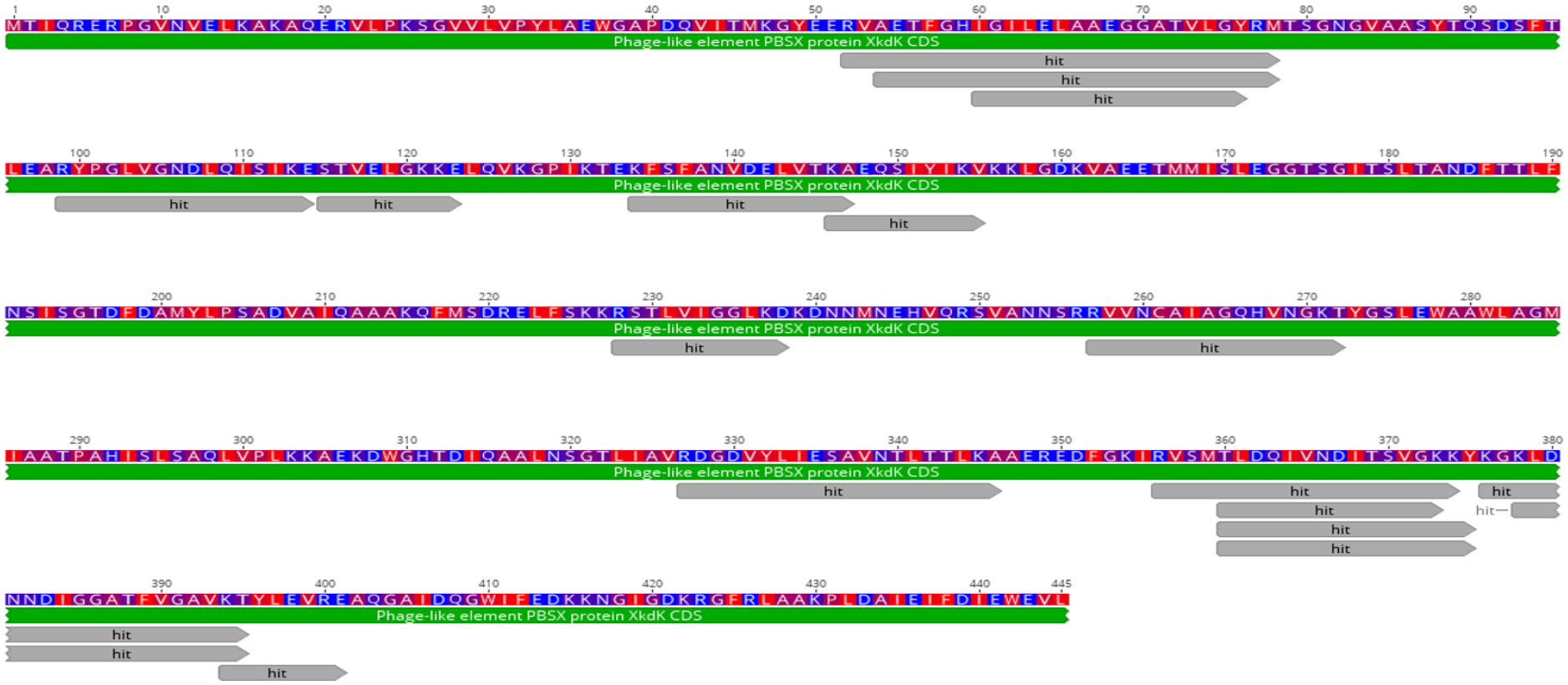

Note: Refer to supplementary material for N-terminal sequence data of purified ~48 kD excised band of *Bl* 1821L

https://doi.org/10.25400/lincolnuninz.16713727

D.9 BLASTp analysis of 48 kD identified putative phage tail protein of *Bl* 1821L with accessions tr|A0A518VEB0|A0A518VEB0_BRELA and tr|A0A0F7EER1|A0A0F7EER1_BRELA after N-terminal sequencing

Accession	Description & % amino acid similarity to the Uniprot identified accessions	Amino acid sequence
tr|A0A075R9L5|A0A075R9L5_BRELA	Phage tail sheath protein *Brevibacillus laterosporus* LMG 15441 (90.3% Homology to A0A518VEB0) (73.5% Homology to A0A0F7EER1)	MKNKYDNTYLHFEEVNSMTIQRERPGVNVELKAKAQERVLPKSGVVLVPYLAEWGAPDQV ITMKGYEERVAETFGQIDILELAAEGGATVVGYRMTNGKSVAASYSQEGSIAIQARYPGL VGNELQISIKDSTAELGKKELQVKGPIKTEKFSFANMDELVTKAEQSIYIKVKKLGDKAV EETAMTALSGGTSGIATLSATDFTTLFNSISGVDFDAMYLPSADAGIQAAAKQFMVDREL FSKKRSTLVIGGLPEKDSNMNEHVDRSAANNSRRVVNCAIAGQHVNGKTYGSLEWAAWLA GMIAATPAHISLSAQLVPMKKAAKDWGHTEIQNALNSGSLIAVRDGDVYLIESAVNTLTT LKAAEREDFGKIRVSMTLDQIVNDITSVGKKYKGKLDNNDIGGATFVGAVKTYLEVREAQ GAIDKGWIFEDKKNGIGDKRGFRLAAKPLDAIELFDIEWEVL
tr|M8E4N0|M8E4N0_9BACL	Uncharacterised protein *Brevibacillus borstelensis* AK1 (69.9% Homology to A0A518VEB0) (66.5% Homology to A0A0F7EER1)	MAIQRERPGVTVEMIAVAQERVLPKSGVVLVPYQAEWGAPDTMVRMTGYDERVAETFAEN DVIELAAEGGATIIGYRVTNGAAVAASYEQPDAIRIEARYPGLRGNDLKVSISASTAEPG KQELQVVGPISTEKFSFADAAELVMKTKQSIYVRVKKLGDADIADVSLTSLSGGVTGTAP LTSADATKMFTAVSGADFDTMYLPFADPAVQAAAKQFMSDRRGLNKKLSTLVIAGKEADD DNMVSHTERSVAQNVRYVVNNAIAGEHNNGKYYNSLQWAAWVAGMIAATPAHESMTGVVV PLKKAKKDWGHTEILQALSTGTLIAIRDGDVYVIESAVNTLSVLGPKDREDYGKIRVSMT LDQIQNDIQTVGKKYKGKLSNNDIGGATFVGAVKAYLEVREQQGAIDTGWIFEDKKNGVG DRRGFRLSAKPLDAIEYFDVEWEVL

tr|A0A3M8DWU9|A0A3M8DWU9_9BACL	Phage tail protein *Brevibacillus fluminis* (68.0% Homology to A0A518VEB0) (65.1% Homology to A0A0F7EER1)	MTIQRERPGVTVELIAKAQERVLPKSGVVLVPYQAEWGAPDTLIRMAGFEERVAETFGEI DVLELAAASGATVIGFRMTDANTKTASYSQNDAIKIEARYPGTRGNQLRISITASSAEPG KKELQVTGGIKTEKYSFATAEELVGKTAESLHIRVTKLGTTSVTDVAETSLSGGTTGTAA LTAADFTKLFSAIGGADFDTLYLPSADPAIQAAAKQFMLDRRTLNKKMSTLVIGGKVEDD ANMAKHTERSVAQNARYVINCAIAGEHVSGKDYSSLQWAAWVAGMAAATPAHVSLTAQPV PLKKARKDWSHTEILSALYTGTLIATRDGDSYLIESAINTLSVLGTGEREDFGKIRVSMT IDQIQNDALTVGKKYMGKLPNNDLGAAVFVGAYTTYLKIREEQGAIDAGWVFEDTKNGVG DRRSFRLAARPLDAIEYFDLSWEVQ
tr|C0Z5G9|C0Z5G9_BREBN	Uncharacterised protein *Brevibacillus brevis* (strain 47/JCM 6285/ NBRC 100599) (68.1% Homology to A0A518VEB0) (66.3% Homology to A0A0F7EER1)	MTIQRERPGVTVELIAKAKERVVPKSGVVLVPYQAEWGAPDELVKLGSFEERIAQTFGKV DTVELAAEGGATILAYRMTNGTATKAAYEQADAIRVEALYPGLVGNELKVTITVSTSEPG KKELQVTGPLQTEKFSFADANELAAKTSQSNYVRVKKLGETAVTIVPETALTGAKSGTVA LASADSTKLFMAVSGADFDAMYLPFDDSAVQAAAKQFMSDRRTQNKKLSTLVIGGKAADD ENMAKHIERSVAQNARFVVNSAIAGQHNNGKVYGSLEWAAWVAGMIAATPAHESLTAVVV PLKKALKDWGHTDILSALGSGTLIATRDGDVYIIESAVNTLAVLGTHEREDYGKIRVSMT LDQIVNDISQVGKKYKGKLGNNDLGGAVFVSAVNAYMTVREQQGAIDTGWTFTDKKNGIG DRRGFLLSAKPLDAIEYFDIDWEVL

tr|A0A6M1UCS4|A0A6M1UCS4_9BACL	Phage tail protein *Brevibacillus* sp. SYP-B805 (66.6% Homology to A0A518VEB0) (66.1% Homology to A0A0F7EER1)	MTIQRDRPGLTLEMIAKAKERVLTKTGVALVPYVAEWGAPDTLVKMTGYDERIAETFGEV DVIELAAEGGATILGYRITNGSAVAAYYSQADAIKIEARYPGLRGNDLKVSIAPSTAEPG KKELQVKGPIKTEKFSFADADELVSKTSQSIYVRVSKLGDAAITDLAETNLQNGTSGTPA TLSSADAIKLFTAVSGADFDSMYLPFDDPAIQAAFRQFVYDRRKLSKKMSTGVIGGKAEE DEIMEKHTERSVAMNARYMVNCAIAGTHNNGKEYDSLQWAAWAAGIIAATPAHESLTAVV VPMKKAKKDWGHTEILNALSTGTLIATRDGDVYTIESAVNTLSTLGPGEREDFGKIRVSM TLDQIYNDIAAPVKKYKGKLDNNDIGGGVFVGAVKAYMEIREEQGAIASGWTFTDKKNGV GDRRGFKLSAQPLDAIEYFDVEWEVL
tr|A0A0X8D434|A0A0X8D434_9BACL	Phage tail sheath protein *Aneurinibacillus sp*. XH2 (49.1% Homology to A0A0F7EER1) (50.7% Homology to A0A0F7EER1)	MSIQRIRGGVYIDLMAVAKERILPRSGRVLVPYQGDWGRPNFPVDMANTAERTAETCLLV DEVELAAENGATVVGFNITNGTEKKAAIEVATNYVIEAKYPGARGNDFGRLIRKSIGDPS KKEMVVKDTKGIFEDEVFVFESRKDLENRLKKSKMVRFVDKSTDEALDIPETTFEQLSGG VSGIGTITPTDWTRIFNQINGVQFDAMYLPTFDPAVQAAAKQWMTDRRKQERRLSQLVVA GDPNKDDDMEAHNARSRAMNARFIINNTIAGRHINGKEYNSLQWAAWLAGLVAGTPANVS MTNMKVPLEEALIDWGHSDVMKGLSEGTLMATRDGYDYVIESAVNTLTTLGPGEREDFGK IRVSMTIDQIMNDIYTAGKKYKAKLDNDSDGRAIFIGAVLEYLKIRAEQKAIDKQFSFTE HPTKKSDFDFAYFKLFAKPLDAVEAFFVDWEVA

tr|A0A2Z2KS77|A0A2Z2KS77_9BACL	Phage tail sheath protein *Paenibacillus donghaensis* (48.3% Homology to A0A0F7EER1) (49.7% Homology to A0A0F7EER1)	MSIQRNRPGAYVELQAIAKSRVQSVSGRVLIPCQAEWGAPNKAVDMADRSERLKETGLQV DELELAAESGATVIGYRVTNGNEKAAAVAVEDSYTIEARYPGTRGNDFEYMVRAALVDAA KKEIVIRDSKGIYDTETFLVTDKAEAVETLKKSNMVRLKDTGATALADVAYTKLIGGTTG TAAITAANWSSVFNRIDGLMFDVVYLPSPDAAVQAAAKQWLLDRRNKARKLAQLVIAGAA ASDSDIEAHNARSRAANARFIINCSLAGEHTNGKIYTSLQWAAWVAGLAAGTPANKSFTG VKVPMTEAKVDWSHSEVLKGLSEGTLMATRDGYDYIIESAVNTLTTLGAGEREDFGKIRV SMTIDQVLNDIYAAGKKNKAKLDNDPEGRGLFIAAVVGYLKIRAEQKAIGSEFTFTEHPT KTSDMDYAYFSLSAKPLDAIEIFNIDWEVA

D.10 Amino acid alignment of the *Bl* 1821L PBSX-like region tail fibre protein (A0A518VE83) with the tail fibre protein (S5M627) and putative tail fibre protein (S5MNY5) of *Brevibacillus* phage Abouo using the Geneious basic (A) and CLUSTALO (B)

D.11 Amino acid alignment % of the *Bl* 1821L PBSX-like region tail fibre protein (tr|A0A518VE83|A0A518VE83_BRELA) with the tail fibre protein tr|S5M627|S5M627_9CAUD and putative tail fibre protein tr|S5MNY5|S5MNY5_9CAUD of *Brevibacillus* phage Abouo using Geneious basic

Uniprot Accession # (https://www.uniprot.org)	Uniprot Accession # (https://www.uniprot.org)		
	A0A518VE83	**S5M627**	**S5MNY5**
A0A518VE83		3.51	30.0
S5M627	3.51		50.0
S5MNY5	30.0	50.0	

D.12 Amino acids alignment of 48 kD identified *Bl* 1821L and *Bl* 1951 phage like-element PBSX protein XkdK (tr|A0A518VEB0|A0A518VEB0) with the similar proteins of other gram-positive bacteria (See Table 6.10) using the programme CLUSTALO

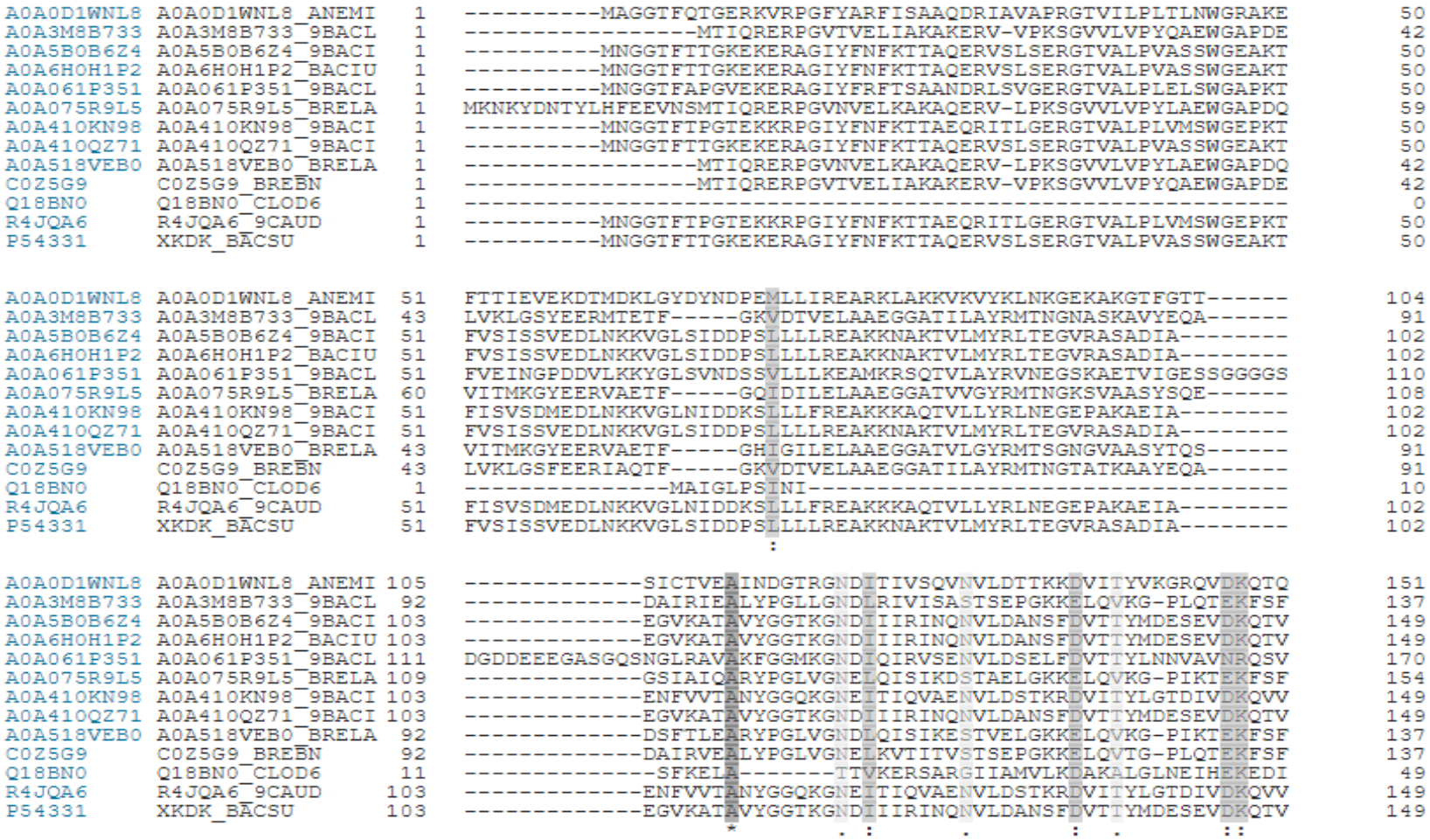

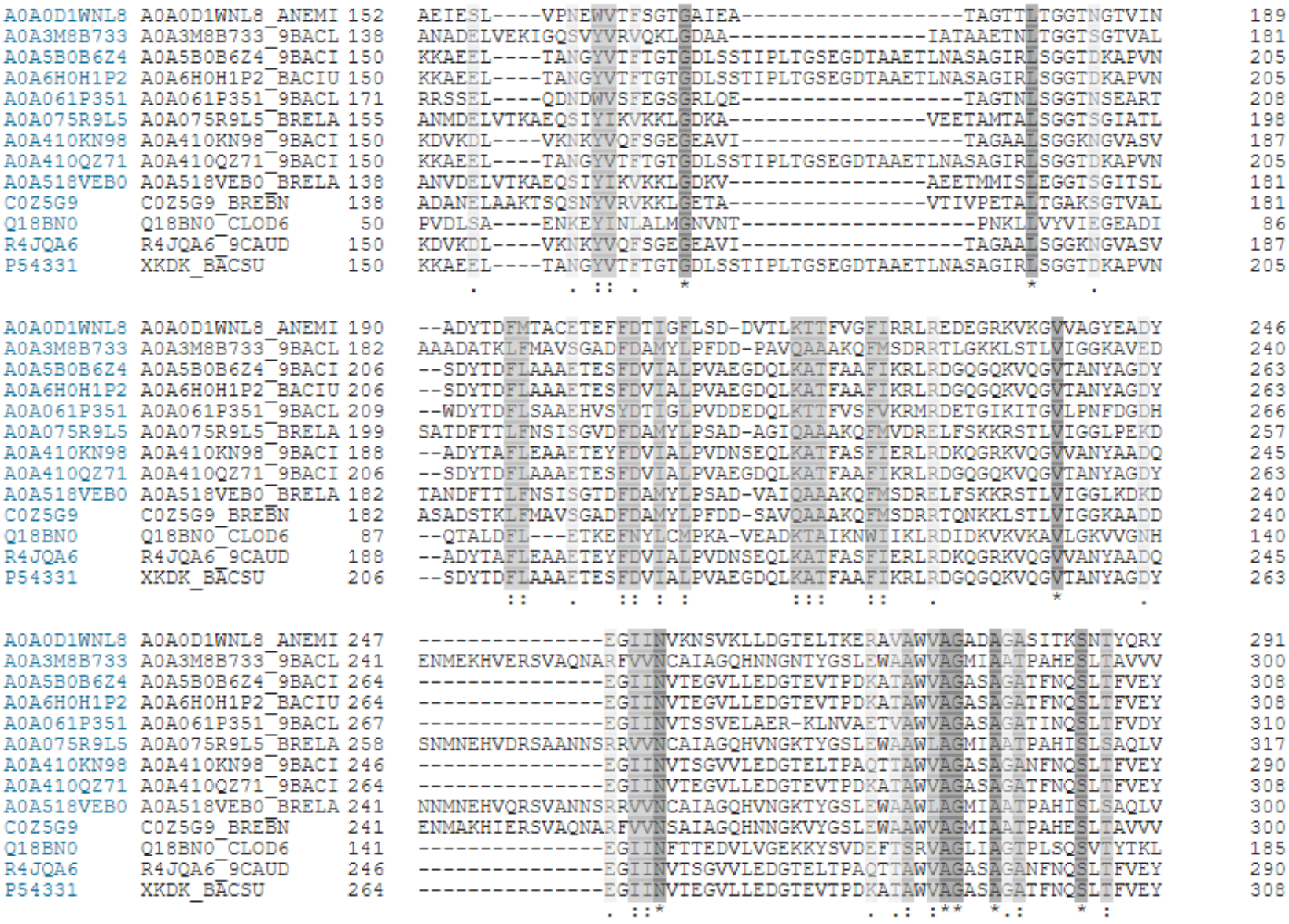
A0A0D1WNL8 A0A0D1WNL8_ANEMI 152 AEIESL----VPNEWVTFSGTGAIEA----------TAGTTLTGGTNGTVIN 189
A0A3M8B733 A0A3M8B733_9BACL 138 ANADELVEKIGQSVYVRVQKLGDAA----------IATAAETNLTGGTSGTVAL 181
A0A5B0B6Z4 A0A5B0B6Z4_9BACI 150 KKAEEL----TANGYVTFTGTGDLSSTIPLTGSEGDTAAETLNASAGIRLSGGTDKAPVN 205
A0A6H0H1P2 A0A6H0H1P2_BACIU 150 KKAEEL----TANGYVTFTGTGDLSSTIPLTGSEGDTAAETLNASAGIRLSGGTDKAPVN 205
A0A061P351 A0A061P351_9BACL 171 RRSSEL----QDNDWVSFEGSGRLQE----------TAGTNLSGGTNSEART 208
A0A075R9L5 A0A075R9L5_BRELA 155 ANMDELVTKAEQSIYIKVKKLGDKA----------VEETAMTALSGGTSGIATL 198
A0A410KN98 A0A410KN98_9BACI 150 KDVKDL----VKNKYVQFSGEGEAVI----------TAGAALSGGKNGVASV 187
A0A410QZ71 A0A410QZ71_9BACI 150 KKAEEL----TANGYVTFTGTGDLSSTIPLTGSEGDTAAETLNASAGIRLSGGTDKAPVN 205
A0A518VEB0 A0A518VEB0_BRELA 138 ANVDELVTKAEQSIYIKVKKLGDKV----------AEETMMISLEGGTSGITSL 181
C0Z5G9 C0Z5G9_BREBN 138 ADANELAAKTSQSNYVRVKKLGETA----------VTIVPETALTGAKSGTVAL 181
Q18BN0 Q18BN0_CLOD6 50 PVDLSA----ENKEYINLALMGNVNT----------PNKLLVYVIEGEADI 86
R4JQA6 R4JQA6_9CAUD 150 KDVKDL----VKNKYVQFSGEGEAVI----------TAGAALSGGKNGVASV 187
P54331 XKDK_BACSU 150 KKAEEL----TANGYVTFTGTGDLSSTIPLTGSEGDTAAETLNASAGIRLSGGTDKAPVN 205
A0A0D1WNL8 A0A0D1WNL8_ANEMI 190 --ADYTDFMTACETEFFDTIGFLSD-DVTLKTTFVGFIRRLREDEGRKVKGVVAGYEADY 246
A0A3M8B733 A0A3M8B733_9BACL 182 AAADATKLFMAVSGADFDAMYLPFDD-PAVQAAAKQFMSDRRTLGKKLSTLVIGGKAVED 240
A0A5B0B6Z4 A0A5B0B6Z4_9BACI 206 --SDYTDFLAAAETESFDVIALPVAEGDQLKATFAAFIKRLRDGQGQKVQGVTANYAGDY 263
A0A6H0H1P2 A0A6H0H1P2_BACIU 206 --SDYTDFLAAAETESFDVIALPVAEGDQLKATFAAFIKRLRDGQGQKVQGVTANYAGDY 263
A0A061P351 A0A061P351_9BACL 209 --WDYTDFLSAAEHVSYDTIGLPVDDEDQLKTTFVSFVKRMRDETGIKITGVLPNFDGDH 266
A0A075R9L5 A0A075R9L5_BRELA 199 SATDFTTLFNSISGVDFDAMYLPSAD-AGIQAAAKQFMVDRELFSKKRSTLVIGGLPEKD 257
A0A410KN98 A0A410KN98_9BACI 188 --ADYTAFLEAAETEYFDVIALPVDNSEQLKATFASFIERLRDKQGRKVQGVVANYAADQ 245
A0A410QZ71 A0A410QZ71_9BACI 206 --SDYTDFLAAAETESFDVIALPVAEGDQLKATFAAFIKRLRDGQGQKVQGVTANYAGDY 263
A0A518VEB0 A0A518VEB0_BRELA 182 TANDFTTLFNSISGTDFDAMYLPSAD-VAIQAAAKQFMSDRELFSKKRSTLVIGGLKDKD 240
C0Z5G9 C0Z5G9_BREBN 182 ASADSTKLFMAVSGADFDAMYLPFDD-SAVQAAAKQFMSDRRTQNKKLSTLVIGGKAADD 240
Q18BN0 Q18BN0_CLOD6 87 --QTALDFL---ETKEFNYLCMPKA-VEADKTAIKNWIIKLRDIDKVKVKAVLGKVVGNH 140
R4JQA6 R4JQA6_9CAUD 188 --ADYTAFLEAAETEYFDVIALPVDNSEQLKATFASFIERLRDKQGRKVQGVVANYAADQ 245
P54331 XKDK_BACSU 206 --SDYTDFLAAAETESFDVIALPVAEGDQLKATFAAFIKRLRDGQGQKVQGVTANYAGDY 263
A0A0D1WNL8 A0A0D1WNL8_ANEMI 247 ----------EGIINVKNSVKLLDGTELTKERAVAWVAGADAGASITKSNTYQRY 291
A0A3M8B733 A0A3M8B733_9BACL 241 ENMEKHVERSVAQNARFVVNCAIAGQHNNGNTYGSLEWAAWVAGMIAATPAHESLTAVVV 300
A0A5B0B6Z4 A0A5B0B6Z4_9BACI 264 ----------EGIINVTEGVLLEDGTEVTPDKATAWVAGASAGATFNQSLTFVEY 308
A0A6H0H1P2 A0A6H0H1P2_BACIU 264 ----------EGIINVTEGVLLEDGTEVTPDKATAWVAGASAGATFNQSLTFVEY 308
A0A061P351 A0A061P351_9BACL 267 ----------EGIINVTSSVELAER-KLNVAETVAWVAGASAGATINQSLTFVDY 310
A0A075R9L5 A0A075R9L5_BRELA 258 SNMNEHVDRSAANNSRRVVNCAIAGQHVNGKTYGSLEWAAWLAGMIAATPAHISLSAQLV 317
A0A410KN98 A0A410KN98_9BACI 246 ----------EGIINVTSGVVLEDGTELTPAQTTAWVAGASAGANFNQSLTFVEY 290
A0A410QZ71 A0A410QZ71_9BACI 264 ----------EGIINVTEGVLLEDGTEVTPDKATAWVAGASAGATFNQSLTFVEY 308
A0A518VEB0 A0A518VEB0_BRELA 241 NNMNEHVQRSVANNSRRVVNCAIAGQHVNGKTYGSLEWAAWLAGMIAATPAHISLSAQLV 300
C0Z5G9 C0Z5G9_BREBN 241 ENMAKHIERSVAQNARFVVNSAIAGQHNNGKVYGSLEWAAWVAGMIAATPAHESLTAVVV 300
Q18BN0 Q18BN0_CLOD6 141 ----------EGIINFTTEDVLVGEKKYSVDEFTSRVAGLIAGTPLSQSVTYTKL 185
R4JQA6 R4JQA6_9CAUD 246 ----------EGIINVTSGVVLEDGTELTPAQTTAWVAGASAGANFNQSLTFVEY 290
P54331 XKDK_BACSU 264 ----------EGIINVTEGVLLEDGTEVTPDKATAWVAGASAGATFNQSLTFVEY 308

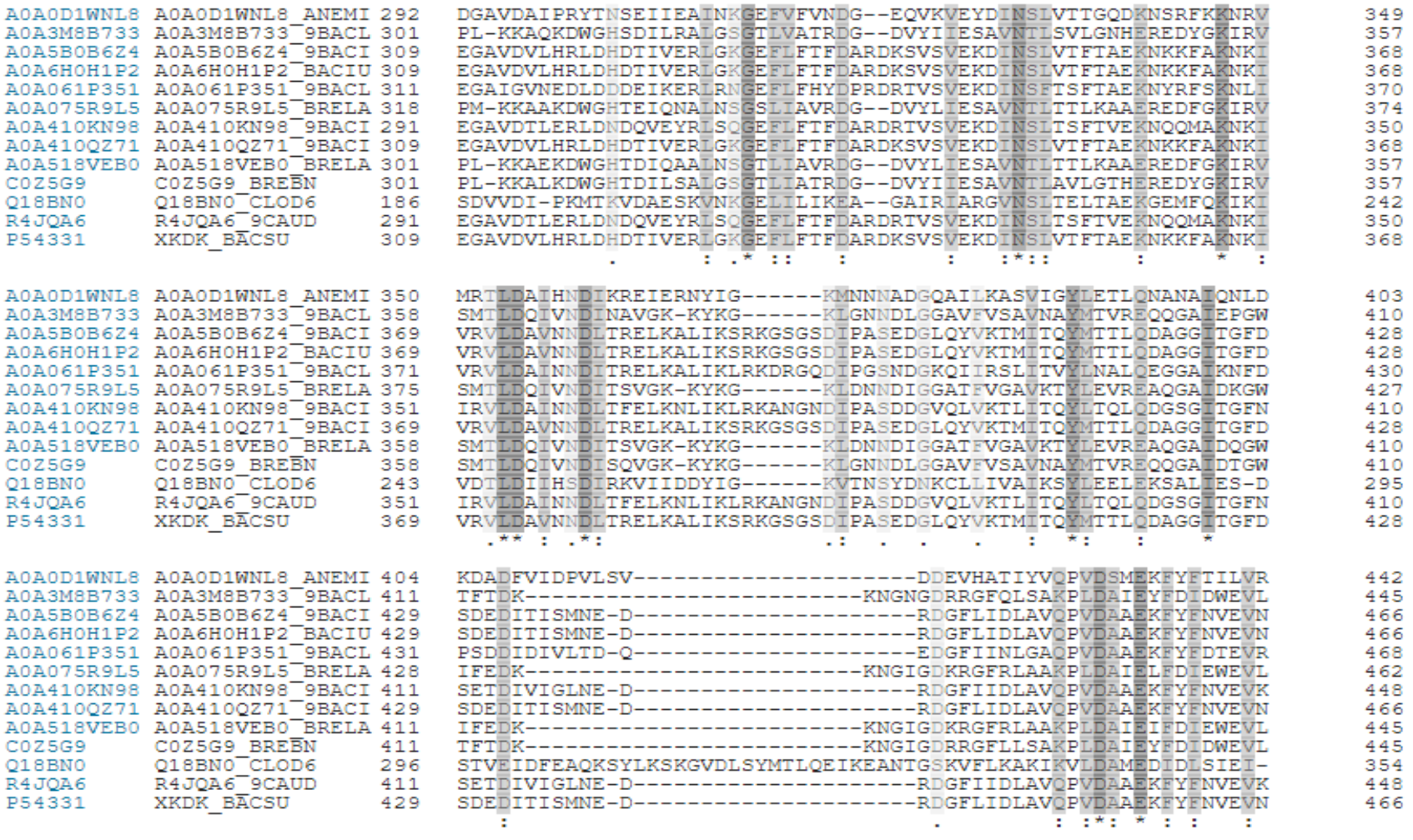

*Highlighted dark grey colour amino acids denote similarity among the aligned phage-like element PBSX protein XkdK.
(Refer to Appendix D.13 & D.14).

D.13 Distance matrices of 48 kD identified *Bl* 1821L and *Bl* 1951 phage-like element PBSX protein XkdK (tr|A0A518VEB0|A0A518VEB0_BRELA) with the similar proteins of other gram-positive bacteria

Uniprot Accession # (www.uniprot.org)	Uniprot Accession # (https://www.uniprot.org)												
	A0A0D1WNL8	A0A3M8B733	A0A5B0B6Z4	A0A6H0H1P2	A0A061P351	A0A075R9L5	A0A410KN98	A0A410QZ71	A0A518VEB0	C0Z5G9	Q18BN0	R4JQA6	P54331
A0A0D1WNL8		1.34	0.8	0.8	0.84	1.4	0.8	0.8	1.33	1.46	1.51	0.8	0.8
A0A3M8B733	1.34		1.44	1.44	1.43	0.38	1.4	1.44	0.36	0.14	1.64	1.4	1.44
A0A5B0B6Z4	0.8	1.44		0	0.56	1.52	0.37	0	1.45	1.45	1.49	0.37	0
A0A6H0H1P2	0.8	1.44	0		0.56	1.52	0.37	0	1.45	1.45	1.49	0.37	0
A0A061P351	0.84	1.43	0.56	0.56		1.42	0.57	0.56	1.45	1.38	1.54	0.57	0.56
A0A075R9L5	1.4	0.38	1.52	1.52	1.42		1.44	1.55	0.1	0.39	1.49	1.44	1.55
A0A410KN98	0.8	1.4	0.37	0.37	0.57	1.44		0.37	1.4	1.37	1.66	0	0.37
A0A410QZ71	0.8	1.44	0	0	0.56	1.55	0.37		1.45	1.45	1.49	0.37	0
A0A518VEB0	1.33	0.36	1.45	1.45	1.45	0.1	1.4	1.45		0.39	1.52	1.4	1.45
C0Z5G9	1.46	0.14	1.45	1.45	1.38	0.39	1.37	1.45	0.39		1.66	1.37	1.45
Q18BN0	1.51	1.64	1.49	1.49	1.54	1.49	1.66	1.49	1.52	1.66		1.66	1.49
R4JQA6	0.8	1.4	0.37	0.37	0.57	1.44	0	0.37	1.4	1.37	1.66		0.37
P54331	0.8	1.44	0	0	0.56	1.55	0.37	0	1.45	1.45	1.49	0.37	

D.14 Amino acids alignment % of 48 kD identified *Bl* 1821L and *Bl* 1951 phage-like element PBSX protein XkdK (tr|A0A518VEB0|A0A518VEB0_BRELA) with the similar proteins of other gram-positive bacteria

Uniprot Accession # (www.uniprot.org)	Uniprot Accession # (https://www.uniprot.org)												
	A0A0D1WNL8	A0A3M8B733	A0A5B0B6Z4	A0A6H0H1P2	A0A061P351	A0A075R9L5	A0A410KN98	A0A410QZ71	A0A518VEB0	C0Z5G9	Q18BN0	R4JQA6	P54331
A0A0D1WNL8		23.9	41.5	41.5	39.8	22.0	42.6	41.5	22.7	23.2	22.0	42.6	41.5
A0A3M8B733	23.9		21.2	21.2	20.7	68.2	20.6	21.2	69.0	86.0	18.4	20.6	21.2
A0A5B0B6Z4	41.5	21.2		100.0	51.8	20.3	64.8	100.0	21.2	20.5	22.4	64.8	100.0
A0A6H0H1P2	41.5	21.2	100.0		51.8	20.3	64.8	100.0	21.2	20.5	22.4	64.8	100.0
A0A061P351	39.8	20.7	51.8	51.8		19.0	53.4	51.8	18.8	19.4	20.5	53.4	51.8
A0A075R9L5	22.0	68.2	20.3	20.3	19.0		19.8	20.3	89.1	67.4	19.3	19.8	20.3
A0A410KN98	42.6	20.6	64.8	64.8	53.4	19.8		64.8	20.3	22.0	20.1	100.0	64.8
A0A410QZ71	41.5	21.2	100.0	100.0	51.8	20.3	64.8		21.2	20.5	22.4	64.8	100.0
A0A518VEB0	22.7	69.0	21.2	21.2	18.8	89.1	20.3	21.2		68.1	19.9	20.3	21.2
C0Z5G9	23.2	86.0	20.5	20.5	19.4	67.4	22.0	20.5	68.1		20.2	22.0	20.5
Q18BN0	22.0	18.4	22.4	22.4	20.5	19.3	20.1	22.4	19.9	20.2		20.1	22.4
R4JQA6	42.6	20.6	64.8	64.8	53.4	19.8	100.0	64.8	20.3	22.0	20.1		64.8
P54331	41.5	21.2	100.0	100.0	51.8	20.3	64.8	100.0	21.2	20.5	22.4	64.8	

D.15 Amino acids alignment of 48 kD identified *Bl* 1821L and *Bl* 1951 putative phage tail-sheath protein accession tr|A0A0F7EER1|A0A0F7EER1_BRELA with the phage tail-sheath protein of different *Bl* phages

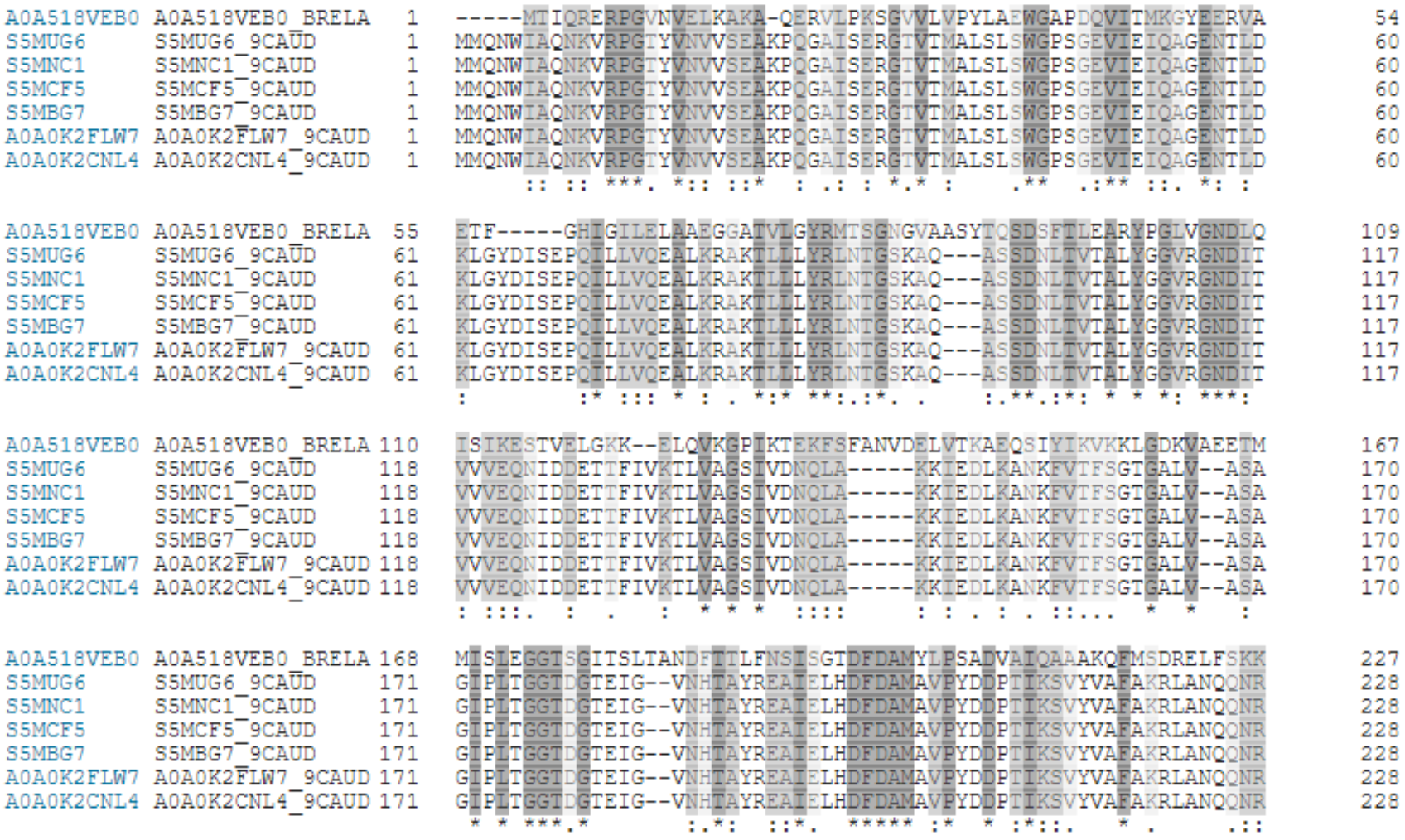

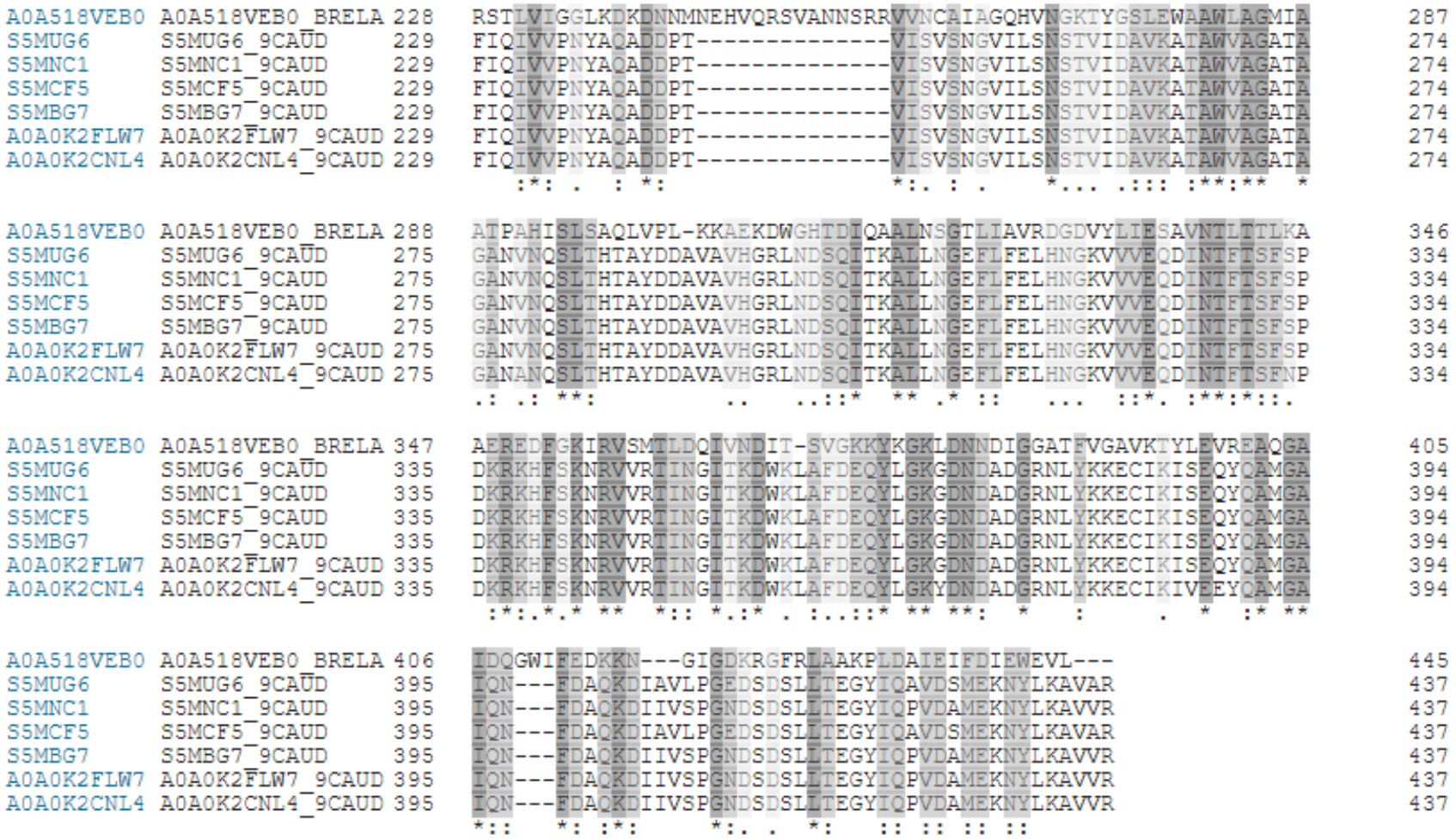

*Highlighted dark grey colour amino acids denote similarity among the aligned phage tail-sheath like proteins.
(Refer to Appendix D.16 & D.17).

D.16 Distance matrices of 48 kD identified *Bl* 1821L and *Bl* 1951 putative phage tail-sheath protein accession tr|A0A0F7EER1|A0A0F7EER1_BRELA with the phage tail-sheath proteins of different *Bl* phages

Uniprot Accession # (https://www.uniprot.org)	Uniprot Accession # (https://www.uniprot.org)						
	S5MUG6	S5MNC1	S5MCF5	S5MBG7	A0A518VEB0	A0A0K2FLW7	A0A0K2CNL4
S5MUG6		0.01	0	0.01	1.56	0.01	0.03
S5MNC1	0.01		0.01	0	1.51	0	0.01
S5MCF5	0	0.01		0.01	1.56	0.01	0.03
S5MBG7	0.01	0	0.01		1.51	0	0.01
A0A518VEB0	1.56	1.51	1.56	1.51		1.51	1.52
A0A0K2FLW7	0.01	0	0.01	0	1.51		0.01
A0A0K2CNL4	0.03	0.01	0.03	0.01	1.52	0.01	

D.17 Amino acids alignment (%) of 48 kD identified *Bl* 1821L and *Bl* 1951 putative phage tail-sheath protein accession tr|A0A0F7EER1|A0A0F7EER1_BRELA with the phage tail-sheath proteins of different *Bl* phages

Uniprot Accession # (https://www.uniprot.org)	Uniprot Accession # (https://www.uniprot.org)						
	S5MUG6	S5MNC1	S5MCF5	S5MBG7	A0A518VEB0	A0A0K2FLW7	A0A0K2CNL4
S5MUG6		98.6	100	98.6	21.9	98.6	97.5
S5MNC1	98.6		98.6	100	21.7	100	98.9
S5MCF5	100	98.6		98.6	21.9	98.6	97.5
S5MBG7	98.6	100	98.6		21.7	100	98.9
A0A518VEB0	21.9	21.7	21.9	21.8		21.7	21.7
A0A0K2FLW7	98.6	100	98.6	100	21.7		98.7
A0A0K2CNL4	97.5	98.9	97.5	98.9	21.7	98.9	

D.18 Amino acids alignment of 48 kD identified *Bl* 1821L and *Bl* 1951 phage-like element PBSX protein XkdK accession tr|A0A518VEB0|A0A518VEB0_BRELA with the similar proteins of the defective prophages PBSZ, PBSX, and PBP180 using programme CLUSTALO

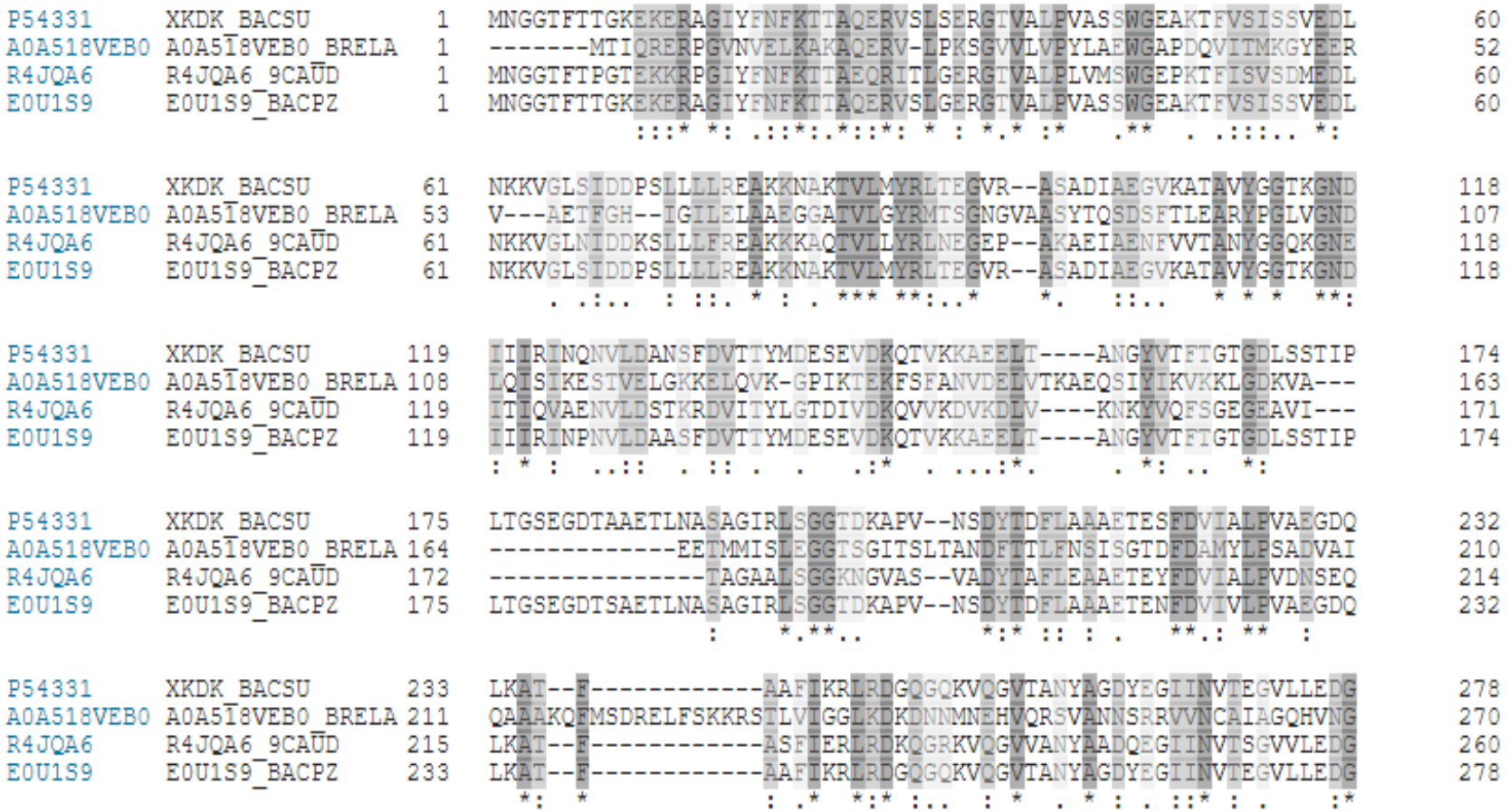

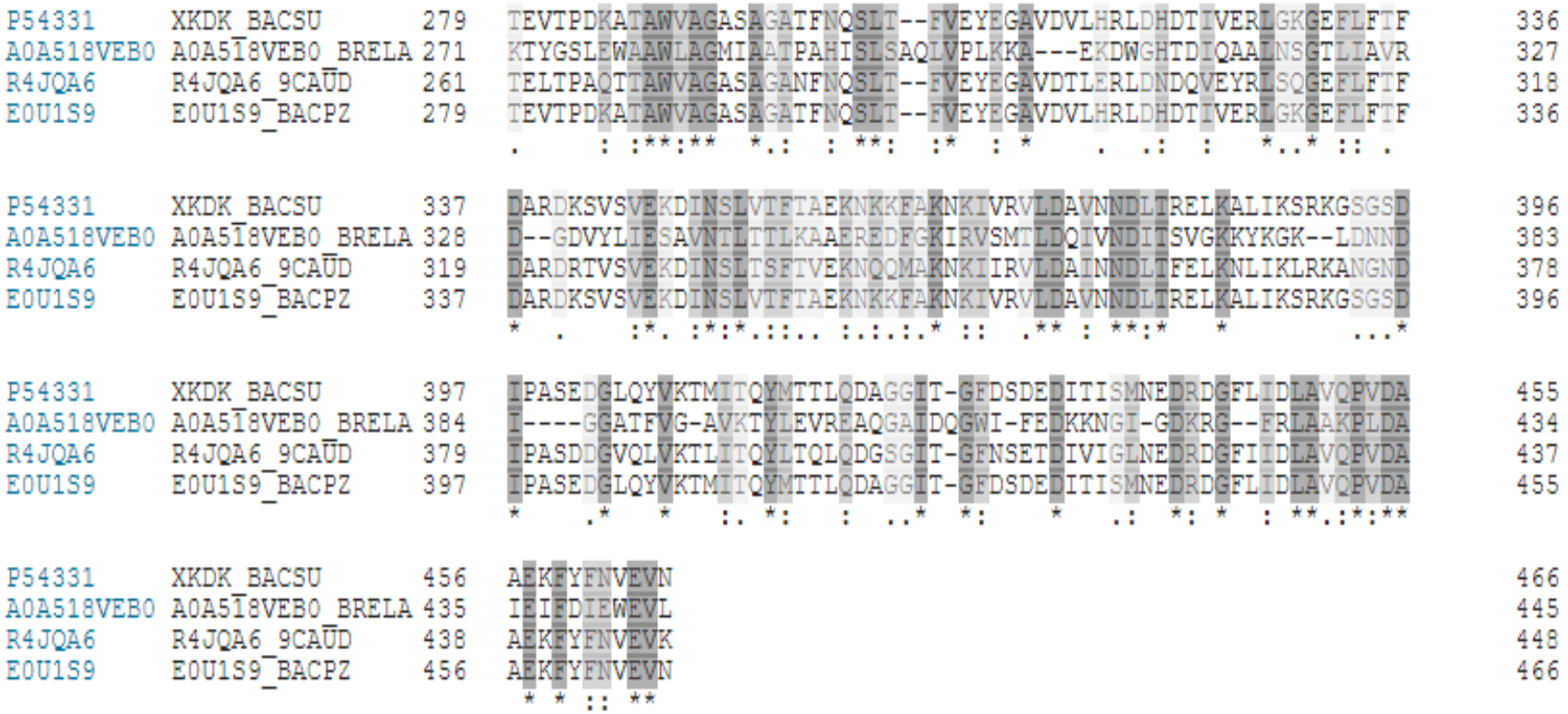

*Highlighted dark grey colour amino acids denote similarity among the aligned phage-like element PBSX protein XkdK.
(Refer to Appendix D.19 & D.20)

D.19 Distance matrices of 48 kD identified *Bl* 1821L and *Bl* 1951 phage-like element PBSX protein XkdK accession tr|A0A518VEB0|A0A518VEB0_BRELA with the similar proteins of the defective prophages PBSZ, PBSX, and PBP180

Uniprot Accession # (https://www.uniprot.org)	Uniprot Accession # (https://www.uniprot.org)			
	P54331	**A0A518VEB0**	**R4JQA6**	**E0U1S9**
P54331		1.45	0.37	0.01
A0A518VEB0	1.45		1.40	1.47
R4JQA6	0.37	1.40		0.37
E0U1S9	0.01	1.47	0.37	

D.20 Amino acids alignment (%) of 48 kD identified *Bl* 1821L and *Bl* 1951 phage-like element PBSX protein XkdK accession tr|A0A518VEB0|A0A518VEB0_BRELA with the similar proteins of the defective prophages PBSZ, PBSX, and PBP180

Uniprot Accession # (https://www.uniprot.org)	Uniprot Accession # (https://www.uniprot.org)			
	P54331	**A0A518VEB0**	**R4JQA6**	**E0U1S9**
P54331		22.9	66.5	98.7
A0A518VEB0	22.9		21.6	22.9
R4JQA6	66.5	21.6		66.5
E0U1S9	98.7	22.9	66.5	

D.21 Amino acids alignment of tail protein (tr|A0A518VEA0|A0A518VEA0_BRELA) of PBSX-like region of *Bl* 1821L and *Bl* 1951 with the similar proteins of the defective prophages PBSZ, PBSX, and PBP180 using programme CLUSTALO

```
A0A518VEA0 A0A518VEA0_BRELA    1 ---------MNNDMVVELLSVQKEMYKVRQGMMEWKRDA--VSL--QVAWGQMGRDFLRE        47
E0U1T3     E0U1T3_BACPZ        1 MAKLTARFDMEDRVS-------KKLRKVQNGFRALEKYRKMVQRKSAIDIRKDSKTILRT        53
R4JJ03     R4JJ03_9CAUD        1 ------------------------------------------------------------          0
P54334     XKDO_BACSU          1 MAKLTARFDLEDKVS-------KKLKRIHKGFQEVEKKVKTINRQIKISIRAEDQAFY--        51

A0A518VEA0 A0A518VEA0_BRELA   48 TDKMERRIK--------------------ELHSQLKRLGT-------------------        67
E0U1T3     E0U1T3_BACPZ       54 IDRIQKSLKKKLGSQMISISAEDNASAVIQQVQTQLQGLPASVSINIGASDQATERFERL       113
R4JJ03     R4JJ03_9CAUD        1 ------------------------------------------------------------          0
P54334     XKDO_BACSU         52 ------------------------------------------------------------         51

A0A518VEA0 A0A518VEA0_BRELA   68 ------------------------------------------------------------         67
E0U1T3     E0U1T3_BACPZ      114 RELVAGFKGFTIVLSAEDQVSPAVQKIQRYMETALKNGYSVTIRVIDHVMKTVGRISAGI       173
R4JJ03     R4JJ03_9CAUD        1 ------------------------------------------------------------          0
P54334     XKDO_BACSU         52 ------------------------------------------------------------         51

A0A518VEA0 A0A518VEA0_BRELA   68 ----SVQAKLRVTIDDQATQKISQ-------MRSQISQSLVISGGGSSGGSKASVMDPMG       116
E0U1T3     E0U1T3_BACPZ      174 DALTGKDNKLELAINDKVSDKLDSLQKRIDSMRSSGSPDKAAPSAGGNTGDIASMFDPET       233
R4JJ03     R4JJ03_9CAUD        1 ------------------------------------------------------------          0
P54334     XKDO_BACSU         52 ------------------------------------------------------------         51

A0A518VEA0 A0A518VEA0_BRELA  117 DY-----LINSYNDAIPDSQAAAKE----------RGLFMARGKT---ELEGQ----ELD       154
E0U1T3     E0U1T3_BACPZ      234 ILTALDKFASSFMEKVDEIATKFSPETILTELDKFTTSFMNKVDAIATKFSPETILTQLD       293
R4JJ03     R4JJ03_9CAUD        1 ------------------------------------------------------------          0
P54334     XKDO_BACSU         52 ------------------------------------------------------------         51

A0A518VEA0 A0A518VEA0_BRELA  155 ---------------------------------------------RSVGRMTQINPEM       167
E0U1T3     E0U1T3_BACPZ      294 KFTTSFMSKVDAIATKFSPETILTQLDKFTTSFMSKVDAIATKFSPETILGQLDKFTTSF       353
R4JJ03     R4JJ03_9CAUD        1 ------------------------------------------------------------          0
P54334     XKDO_BACSU         52 ------------------------------------------------------------         51
```

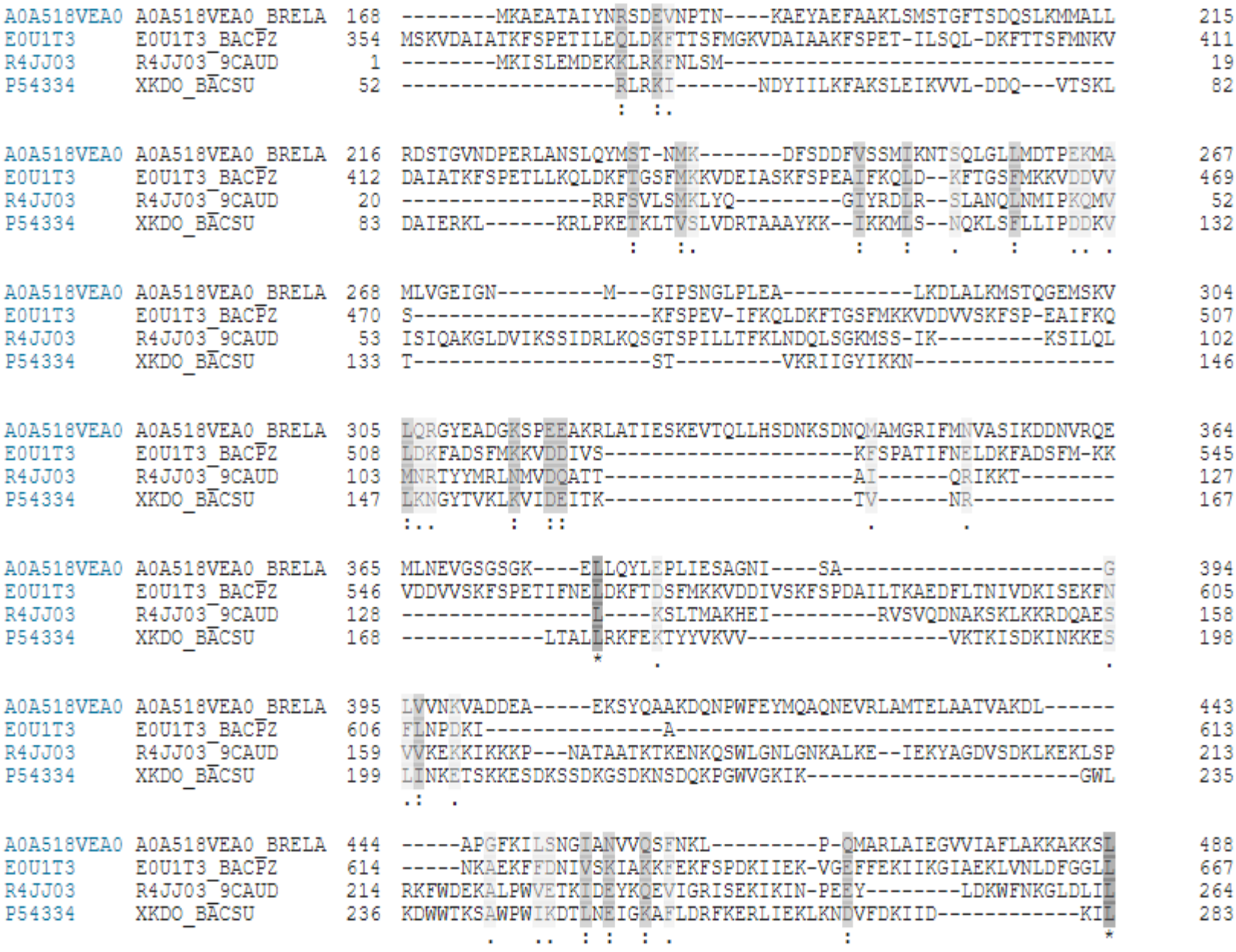
A0A518VEA0 A0A518VEA0_BRELA 168 --------MKAEATAIYNRSDEVNPTN----KAEYAEFAAKLSMSTGFTSDQSLKMMALL 215
E0U1T3 E0U1T3_BACPZ 354 MSKVDAIATKFSPETILEQLDKFTTSFMGKVDAIAAKFSPET-ILSQL-DKFTTSFMNKV 411
R4JJ03 R4JJ03_9CAUD 1 --------MKISLEMDEKKLRKFNLSM---------- 19
P54334 XKDO_BACSU 52 ----------RLRKI-------NDYIILKFAKSLEIKVVL-DDQ---VTSKL 82
A0A518VEA0 A0A518VEA0_BRELA 216 RDSTGVNDPERLANSLQYMST-NMK-------DFSDDFVSSMIKNTSQLGLLMDTPEKMA 267
E0U1T3 E0U1T3_BACPZ 412 DAIATKFSPETLLKQLDKFTGSFMKKVDEIASKFSPEAIFKQLD--KFTGSFMKKVDDVV 469
R4JJ03 R4JJ03_9CAUD 20 ----------RRFSVLSMKLYQ---------GIYRDLR--SLANQLNMIPKQMV 52
P54334 XKDO_BACSU 83 DAIERKL------KRLPKETKLTVSLVDRTAAAYKK--IKKMLS--NQKLSFLLIPDDKV 132
A0A518VEA0 A0A518VEA0_BRELA 268 MLVGEIGN---------M---GIPSNGLPLEA----------LKDLALKMSTQGEMSKV 304
E0U1T3 E0U1T3_BACPZ 470 S----------KFSPEV-IFKQLDKFTGSFMKKVDDVVSKFSP-EAIFKQ 507
R4JJ03 R4JJ03_9CAUD 53 ISIQAKGLDVIKSSIDRLKQSGTSPILLTFKLNDQLSGKMSS-IK---------KSILQL 102
P54334 XKDO_BACSU 133 T----------ST---------VKRIIGYIKKN---------- 146
A0A518VEA0 A0A518VEA0_BRELA 305 LQRGYEADGKSPEEAKRLATIESKEVTQLLHSDNKSDNQMAMGRIFMNVASIKDDNVRQE 364
E0U1T3 E0U1T3_BACPZ 508 LDKFADSFMKKVDDIVS----------KFSPATIFNELDKFADSFM-KK 545
R4JJ03 R4JJ03_9CAUD 103 MNRTYYMRLNMVDQATT----------AI------QRIKKT-------- 127
P54334 XKDO_BACSU 147 LKNGYTVKLKVIDEITK----------TV------NR---------- 167
A0A518VEA0 A0A518VEA0_BRELA 365 MLNEVGSGSGK----ELLQYLEPLIESAGNI----SA----------G 394
E0U1T3 E0U1T3_BACPZ 546 VDDVVSKFSPETIFNELDKFTDSFMKKVDDIVSKFSPDAILTKAEDFLTNIVDKISEKFN 605
R4JJ03 R4JJ03_9CAUD 128 ----------L----KSLTMAKHEI---------RVSVQDNAKSKLKKRDQAES 158
P54334 XKDO_BACSU 168 ----------LTALLRKFEKTYYVKVV----------VKTKISDKINKKES 198
A0A518VEA0 A0A518VEA0_BRELA 395 LVVNKVADDEA-----EKSYQAAKDQNPWFEYMQAQNEVRLAMTELAATVAKDL------ 443
E0U1T3 E0U1T3_BACPZ 606 FLNPDKI----------A---------- 613
R4JJ03 R4JJ03_9CAUD 159 VVKEKKIKKKP---NATAATKTKENKQSWLGNLGNKALKE--IEKYAGDVSDKLKEKLSP 213
P54334 XKDO_BACSU 199 LINKETSKKESDKSSDKGSDKNSDQKPGWVGKIK----------GWL 235
A0A518VEA0 A0A518VEA0_BRELA 444 -----APGFKILSNGIANVVQSFNKL---------P-QMARLAIEGVVIAFLAKKAKKSL 488
E0U1T3 E0U1T3_BACPZ 614 -----NKAEKFFDNIVSKIAKKFEKFSPDKIIEK-VGEFFEKIIKGIAEKLVNLDFGGLL 667
R4JJ03 R4JJ03_9CAUD 214 RKFWDEKALPWVETKIDEYKQEVIGRISEKIKIN-PEEY--------LDKWFNKGLDLIL 264
P54334 XKDO_BACSU 236 KDWWTKSAWPWIKDTLNEIGKAFLDRFKERLIEKLKNDVFDKIID----------KIL 283

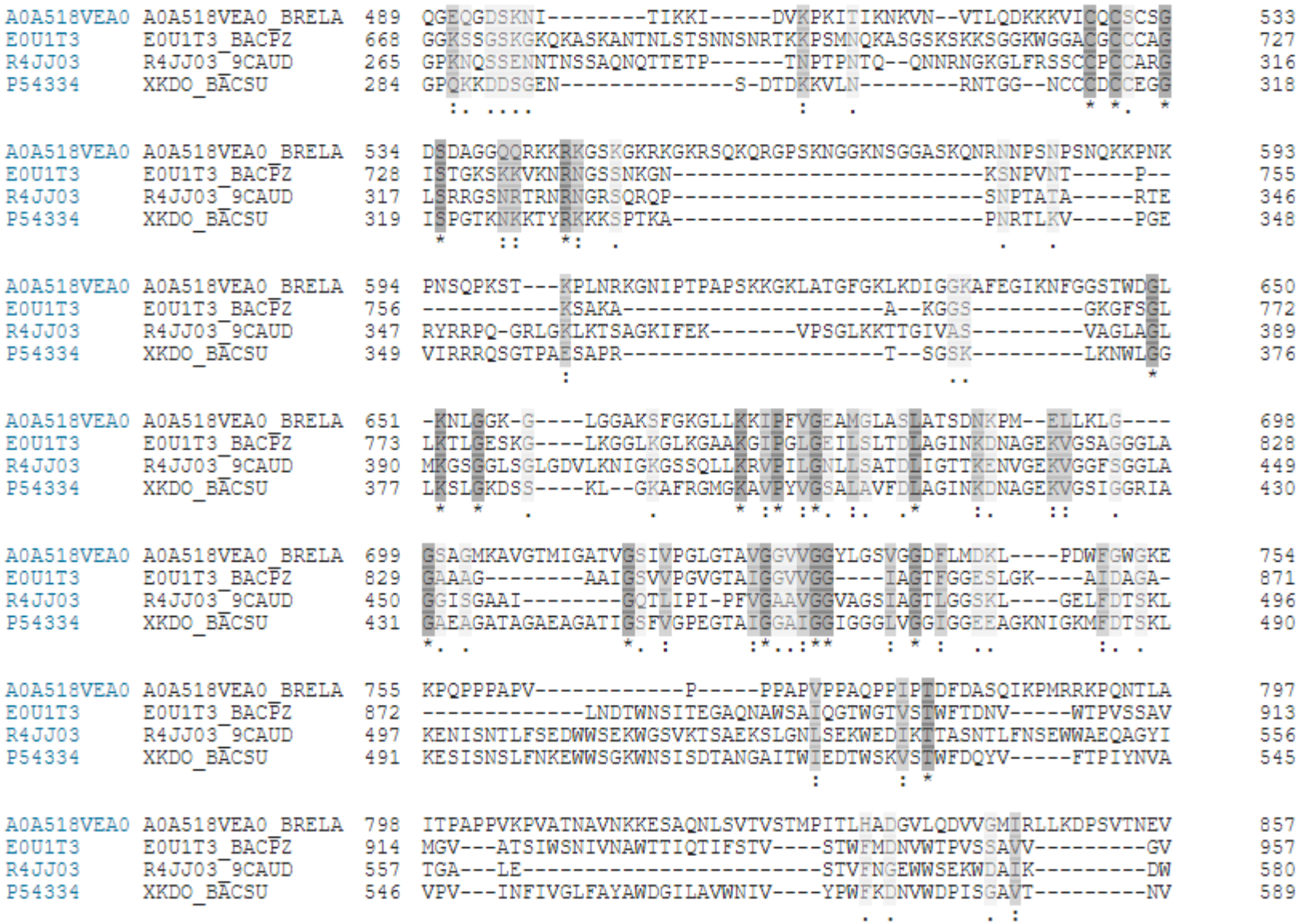
A0A518VEA0 A0A518VEA0_BRELA 489 QGEQGDSKNI--------TIKKI-----DVKPKITIKNKVN--VTLQDKKKVICQCSCSG 533
E0U1T3 E0U1T3_BACPZ 668 GGKSSGSKGKQKASKANTNLSTSNNSNRTKKPSMNQKASGSKSKKSGGKWGGACGCCCAG 727
R4JJ03 R4JJ03_9CAUD 265 GPKNQSSENNTNSSAQNQTTETP------TNPTPNTQ--QNNRNGKGLFRSSCCPCCARG 316
P54334 XKDO_BACSU 284 GPQKKDDSGEN--------------S-DTDKKVLN--------RNTGG--NCCCDCCEGG 318
A0A518VEA0 A0A518VEA0_BRELA 534 DSDAGGQQRKKRKGSKGKRKGKRSQKQRGPSKNGGKNSGGASKQNRNNPSNPSNQKKPNK 593
E0U1T3 E0U1T3_BACPZ 728 ISTGKSKKVKNRNGSSNKGN-------------------------KSNPVNT-----P-- 755
R4JJ03 R4JJ03_9CAUD 317 LSRRGSNRTRNRNGRSQRQP-------------------------SNPTATA-----RTE 346
P54334 XKDO_BACSU 319 ISPGTKNKKTYRKKKSPTKA-------------------------PNRTLKV-----PGE 348
A0A518VEA0 A0A518VEA0_BRELA 594 PNSQPKST---KPLNRKGNIPTPAPSKKGKLATGFGKLKDIGGKAFEGIKNFGGSTWDGL 650
E0U1T3 E0U1T3_BACPZ 756 ----------KSAKA--------------------A--KGGS---------GKGFSGL 772
R4JJ03 R4JJ03_9CAUD 347 RYRRPQ-GRLGKLKTSAGKIFEK-------VPSGLKKTTGIVAS---------VAGLAGL 389
P54334 XKDO_BACSU 349 VIRRRQSGTPAESAPR---------------------T--SGSK---------LKNWLGG 376
A0A518VEA0 A0A518VEA0_BRELA 651 -KNLGGK-G----LGGAKSFGKGLLKKIPFVGEAMGLASLATSDNKPM--ELLKLG---- 698
E0U1T3 E0U1T3_BACPZ 773 LKTLGESKG----LKGGLKGLKGAAKGIPGLGEILSLTDLAGINKDNAGEKVGSAGGGLA 828
R4JJ03 R4JJ03_9CAUD 390 MKGSGGLSGLGDVLKNIGKGSSQLLKRVPILGNLLSATDLIGTTKENVGEKVGGFSGGLA 449
P54334 XKDO_BACSU 377 LKSLGKDSS----KL--GKAFRGMGKAVPYVGSALAVFDLAGINKDNAGEKVGSIGGRIA 430
A0A518VEA0 A0A518VEA0_BRELA 699 GSAGMKAVGTMIGATVGSIVPGLGTAVGGVVGGYLGSVGGDFLMDKL----PDWFGWGKE 754
E0U1T3 E0U1T3_BACPZ 829 GAAAG--------AAIGSVVPGVGTAIGGVVGG----IAGTFGGESLGK----AIDAGA- 871
R4JJ03 R4JJ03_9CAUD 450 GGISGAAI--------GQTLIPI-PFVGAAVGGVAGSIAGTLGGSKL----GELFDTSKL 496
P54334 XKDO_BACSU 431 GAEAGATAGAEAGATIGSFVGPEGTAIGGAIGGIGGGLVGGIGGEEAGKNIGKMFDTSKL 490
A0A518VEA0 A0A518VEA0_BRELA 755 KPQPPPAPV------------P-----PPAPVPPAQPPIPIDFDASQIKPMRRKPQNTLA 797
E0U1T3 E0U1T3_BACPZ 872 -------------LNDTWNSITEGAQNAWSAIQGTWGTVSIWFTDNV-----WTPVSSAV 913
R4JJ03 R4JJ03_9CAUD 497 KENISNTLFSEDWWSEKWGSVKTSAEKSLGNLSEKWEDIKITASNTLFNSEWWAEQAGYI 556
P54334 XKDO_BACSU 491 KESISNSLFNKEWWSGKWNSISDTANGAITWIEDTWSKVSIWFDQYV-----FTPIYNVA 545
A0A518VEA0 A0A518VEA0_BRELA 798 ITPAPPVKPVATNAVNKKESAQNLSVTVSTMPITLHADGVLQDVVGMIRLLKDPSVTNEV 857
E0U1T3 E0U1T3_BACPZ 914 MGV---ATSIWSNIVNAWTTIQTIFSTV----STWFMDNVWTPVSSAVV---------GV 957
R4JJ03 R4JJ03_9CAUD 557 TGA---LE-----------------------STVFNGEWWSEKWDAIK---------DW 580
P54334 XKDO_BACSU 546 VPV---INFIVGLFAYAWDGILAVWNIV----YPWFKDNVWDPISGAVT---------NV 589

```
A0A518VEA0 A0A518VEA0_BRELA  858  KRIIETAFVNALETRGGKA----------------------------------------  876
E0U1T3     E0U1T3_BACPZ      958  ATAIWSKIVNAWTTIKNVFSTVASWFMSNVWGPVKSAVIGAATTIWDKMTGAWTKIKSV-  1016
R4JJ03     R4JJ03_9CAUD      581  TQEKWDGAVEIWNSITKKLGE--TVFNGEWWGEKWDSVKKWTKEKWDGAVNIWNSIKGKI  638
P54334     XKDO_BACSU        590  ATTIWTGLCNAWTVISGIWSTVSTWFMDNVWNPVSEAVTTAATWIWSKINDAWTIISNI-  648
                                                :

A0A518VEA0 A0A518VEA0_BRELA  877  ----------------------------------------------------------  876
E0U1T3     E0U1T3_BACPZ     1017  ------------FSTVSGWFMDIVWNPVKNTVLDVGKGISDAFKKAIDTVKNIWKGLSG  1063
R4JJ03     R4JJ03_9CAUD      639  RETVFNKDWWGEKWDDVKNWSE-NKWEQSKTIWS-AAKATASSTLFNKNWWTNKWNDVKS  696
P54334     XKDO_BACSU        649  ------------WTGVSNWFYDNVWNPIVKKVEDIKTSIKEKFDDARKFFEDAWDGIET  695

A0A518VEA0 A0A518VEA0_BRELA  877  ----------------------------------------------------------  876
E0U1T3     E0U1T3_BACPZ     1064  WFKKNIQEPLTKVGEAISDAFSKAFGWVKQIWDKAGGVASKVINFVTGGGD---------  1114
R4JJ03     R4JJ03_9CAUD      697  WGKNILG----------------------DTWDLIKSKGAEVIGRH----------IV--  722
P54334     XKDO_BACSU        696  WFNEHVKDPLVKVSEKIAEK----FQWLFDLKDSVGGFVAKVIHRGEEVTHLKKKPIKKD  751

A0A518VEA0 A0A518VEA0_BRELA  877  ----------------------------------------------------------  876
E0U1T3     E0U1T3_BACPZ     1115  -------------------------PNKGKDPDKKATGGYITKPTISWIGEAGKEFVIPV  1149
R4JJ03     R4JJ03_9CAUD      723  -----------------KFEKGREKGRKDFKPDQKATGGYITQPTLSWIGEAGNEFVIPT  765
P54334     XKDO_BACSU        752  SKEKKTSSKPTTNNIFAQSPSNNNMTVFQQALDQNATGGYITKPTISWIGEAGKEFVIPV  811

A0A518VEA0 A0A518VEA0_BRELA  877  ----------------------------------------------------------  876
E0U1T3     E0U1T3_BACPZ     1150  DNNRGRGKMLLSQAASKLGMQVVDDMG-AASSSSGNPVSVSGGAASSPLSGSASP-SMDT  1207
R4JJ03     R4JJ03_9CAUD      766  QNNRGRGKMLLAQAASHLGMSVVPSSSGAASPVSSSPAPITPNAPAAPTASAGSIGGTVS  825
P54334     XKDO_BACSU        812  DNNRGRGKMLLSQAASKLGMQVVDDMG-AASSSGGSPASVSGGAAVSPLSGTASP-VMNT  869

A0A518VEA0 A0A518VEA0_BRELA  877  ----------------------------------------------------------  876
E0U1T3     E0U1T3_BACPZ     1208  ANLTGQASTLGQQFSEGFGKGISNQPVKMEDWKKKNINTPFTQMISSSQNYGKQMVSGYA  1267
R4JJ03     R4JJ03_9CAUD      826  MNGNIQSASIGEQFNHDFEQGLNQKVVSLDQWKQKNIQQPFNQMTSDSGKYGQQTVSAFA  885
P54334     XKDO_BACSU        870  ANLTGQASTLGQQFSEGFGKGISDQPVKMEDWKKKNINTPFTQMISASPNYGKQMVSGYA  929

A0A518VEA0 A0A518VEA0_BRELA  877  ----------------------------------------------------------  876
E0U1T3     E0U1T3_BACPZ     1268  KGQNGTATGTDGFLQSKVKTPFQATVNKSSSWGTETVKGFAQGQNSTQTGTAQYVSTHVD  1327
R4JJ03     R4JJ03_9CAUD      886  TGQQMTPTGTDSFLQSRVKAPYQQVMTASPTWGSGTVSGFATGQNATSIGTSQYVDQHVK  945
P54334     XKDO_BACSU        930  KGQSGTATGTDGFLQSKVKTPFQATVSKSSSWGTGTVKGFAQGQNSTQTGTAQYVSTHVD  989
```

```
A0A518VEA0 A0A518VEA0_BRELA  877  ------------------------------------------------------------  876
E0U1T3     E0U1T3_BACPZ     1268  KGQNGTATGTDGFLQSKVKTPFQATVNKSSSWGTETVKGFAQGQNSTQTGTAQYVSTHVD  1327
R4JJ03     R4JJ03_9CAUD      886  TGQQMTPTGTDSFLQSRVKAPYQQVMTASPTWGSGTVSGFATGQNATSIGTSQYVDQHVK   945
P54334     XKDO_BACSU        930  KGQSGTATGTDGFLQSKVKTPFQATVSKSSSWGTGTVKGFAQGQNSTQTGTAQYVSTHVD   989

A0A518VEA0 A0A518VEA0_BRELA  877  ------------------------------------------------------------  876
E0U1T3     E0U1T3_BACPZ     1328  KPFLRSKDTSNSWGSGMVGNFVTGMNSKSSEVKQAAKDMAKRVEQAFREELDIHSPSRVM  1387
R4JJ03     R4JJ03_9CAUD      946  QPFLQAKQESPGWGSGMIDAFNSGMRSKASEVTQAAKEMAKKVEQAFREELDIHSPSRVM  1005
P54334     XKDO_BACSU        990  KPFLRSKDTSNSWGSGLIGNFVTGMNSKSSEVKQAAKDMAKRVEQAFREELDIHSPSRVM  1049

A0A518VEA0 A0A518VEA0_BRELA  877  ------------------------------------------------------------  876
E0U1T3     E0U1T3_BACPZ     1388  MSLGRFASIGVVKGLGSVDVKKYAEKQAGSLAAAYSGMGAMSGNVKQWIMAALMATKTPM  1447
R4JJ03     R4JJ03_9CAUD     1006  MSLGKFASIGVVKGLDSVDVKKFAENQAGSLIGAFSGMGASGLSVQQWLMAALMATGTSM  1065
P54334     XKDO_BACSU       1050  MSLGRFASVGVVKGLDSVDVKKYAEKQAGSLAAAYSGMGAVGGNVKQWLMAAIMATKTPL  1109

A0A518VEA0 A0A518VEA0_BRELA  877  ------------------------------------------------------------  876
E0U1T3     E0U1T3_BACPZ     1448  SWLPGLMTIAQHESGGNPNAINLWDSNAKAGHPSQGLMQTIPSTFNDHKAPSMGNIKNPI  1507
R4JJ03     R4JJ03_9CAUD     1066  SWLPGLMTIAQHESNGNPKAINLWDSNAKKGTPSKGLMQTIGPTFHSNKGKGMNDIWNPI  1125
P54334     XKDO_BACSU       1110  SWLSGLMTIAQYESGGNPNSINLWDSNAKAGNPSQGLMQTVPTTFNAHKAPGMGNIRNPI  1169

A0A518VEA0 A0A518VEA0_BRELA  877  ------------------------------------------------------------  876
E0U1T3     E0U1T3_BACPZ     1508  HNAAAAIGYIKSRYGSINNVPGIKSLNHGGPYVGYANGGLITKEQIARVGEGNKREWIIP  1567
R4JJ03     R4JJ03_9CAUD     1126  HNAVAAINYIKGRYGTVFNTPGLRSMRRGGPYKGYANGGLITQEQVARVGEGNKREWIIP  1185
P54334     XKDO_BACSU       1170  HNAAAAIGYIKSRYGSIDNVPGIKSLKRGGPYVGYANGGLITKEQIARVGEGNKREWIIP  1229

A0A518VEA0 A0A518VEA0_BRELA  877  ------------------------------------------------------------  876
E0U1T3     E0U1T3_BACPZ     1568  EERGIRGRYLLQKAAQALGMEVTDPSQSQ-SDLSSGQVSAI-TAGTRQTIHTAGTKEIKI  1625
R4JJ03     R4JJ03_9CAUD     1186  EERGIRGRYLLTQAAKALGMQVYDPSNASAPL-PESQMQQVTSAQSAGNTTTSGNKQITI  1244
P54334     XKDO_BACSU       1230  EERGIRGRYLLQRAAQALGMEVTDPSQSQQSELSSGQVSAV-TSASRPTAAVSGSKEIYI  1288

A0A518VEA0 A0A518VEA0_BRELA  877  ---------------------------------------------  876
E0U1T3     E0U1T3_BACPZ     1626  EFNGDQHFHNEQDADSLVAKIKQALLDELQKDINTGTKGVVAFD  1669
R4JJ03     R4JJ03_9CAUD     1245  QFNGDQHFHNGQDQQSLVEKIRQMLVDELEVELQTGTKGVVIDG  1288
P54334     XKDO_BACSU       1289  QFNGDQHFHNGQDAESLAAKIKQALIDELQKDINIGTKGVVAFD  1332
```

*Highlighted dark grey colour amino acids denote similarity among the aligned phage-like element PBSX protein XkdK.
(Refer to Appendix D.22 & D.23)

D.22 Distance matrices of tail protein (tr|A0A518VEA0|A0A518VEA0_BRELA) of PBSX-like region of *Bl* 1821L and *Bl* 1951 with the similar proteins of the defective prophages PBSZ, PBSX, and PBP180

Uniprot Accession # (https://www.uniprot.org)	Uniprot Accession # (https://www.uniprot.org)			
	P54334	**E0U1T3**	**R4JJ03**	**A0A518VEA0**
P54334		0.56	0.85	0.71
E0U1T3	0.56		0.84	1.73
R4JJ03	0.85	0.84		1.79
A0A518VEA0	0.71	1.73	1.79	

D.23 Amino acids alignment (%) of tail protein (tr|A0A518VEA0|A0A518VEA0_BRELA) of PBSX-like region of *Bl* 1821L and *Bl* 1951 with the similar proteins of the defective prophages PBSZ, PBSX, and PBP180

Uniprot Accession # (https://www.uniprot.org)	Uniprot Accession # (https://www.uniprot.org)			
	P54334	**E0U1T3**	**R4JJ03**	**A0A518VEA0**
P54334		51	37	0
E0U1T3	51.9		37.1	50
R4JJ03	37	37.1		0
A0A518VEA0	0	50	0	

D.24 Amino acids alignment of holin protein (tr|A0A075R9K7|A0A075R9K7_BRELA) of PBSX-like region of *Bl* 1821L and *Bl* 1951 with the similar protein of the defective prophages PBSZ, PBSX, and PBP180 using programme CLUSTALO

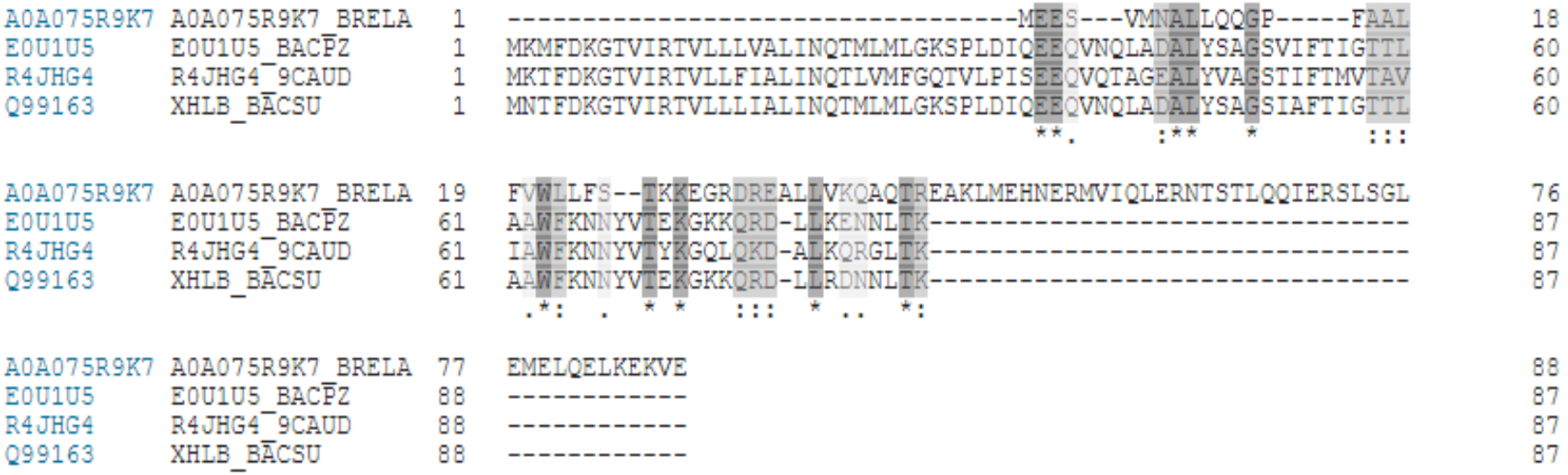

*Highlighted dark grey colour amino acids denote similarity among the aligned holin proteins.
(Refer to Appendix D.25 & D.26)

D.25 Distance matrices of holin protein (tr|A0A075R9K7|A0A075R9K7_BRELA) of PBSX-like region of *Bl* 1821L and *Bl* 1951 with the similar proteins of the defective prophages PBSZ, PBSX, and PBP180

Uniprot Accession # (https://www.uniprot.org)	Uniprot Accession # (https://www.uniprot.org)			
	A0A075R9K77	**E0U1U5**	**R4JHG4**	**Q99163**
A0A075R9K77		2.41	1.48	1.89
E0U1U5	2.41		0.45	0.08
R4JHG4	1.48	0.45		0.47
Q99163	1.89	0.08	0.47	

D.26 Amino acids alignment (%) of holin protein (tr|A0A075R9K7|A0A075R9K7_BRELA) of PBSX-like region of *Bl* 1821L and *Bl* 1951 with the similar proteins of the defective prophages PBSZ, PBSX, and PBP180

Uniprot Accession # (https://www.uniprot.org)	Uniprot Accession # (https://www.uniprot.org)			
	A0A075R9K77	**E0U1U5**	**R4JHG4**	**Q99163**
A0A075R9K77		13.6	11.4	13.6
E0U1U5	13.6		64.4	89.8
R4JHG4	11.4	64.4		61.4
Q99163	13.6	89.8	61.6	

D.27 Schematic presentation of amino acids alignment of holin protein tr|A0A075R9K7|A0A075R9K7_BRELA of PBSX-like region of *Bl* 1821L and *Bl* 1951 with the similar proteins of the defective prophages PBSZ, PBSX, and PBP180 using programme Geneious basic (A) and CLUSTALO (B)

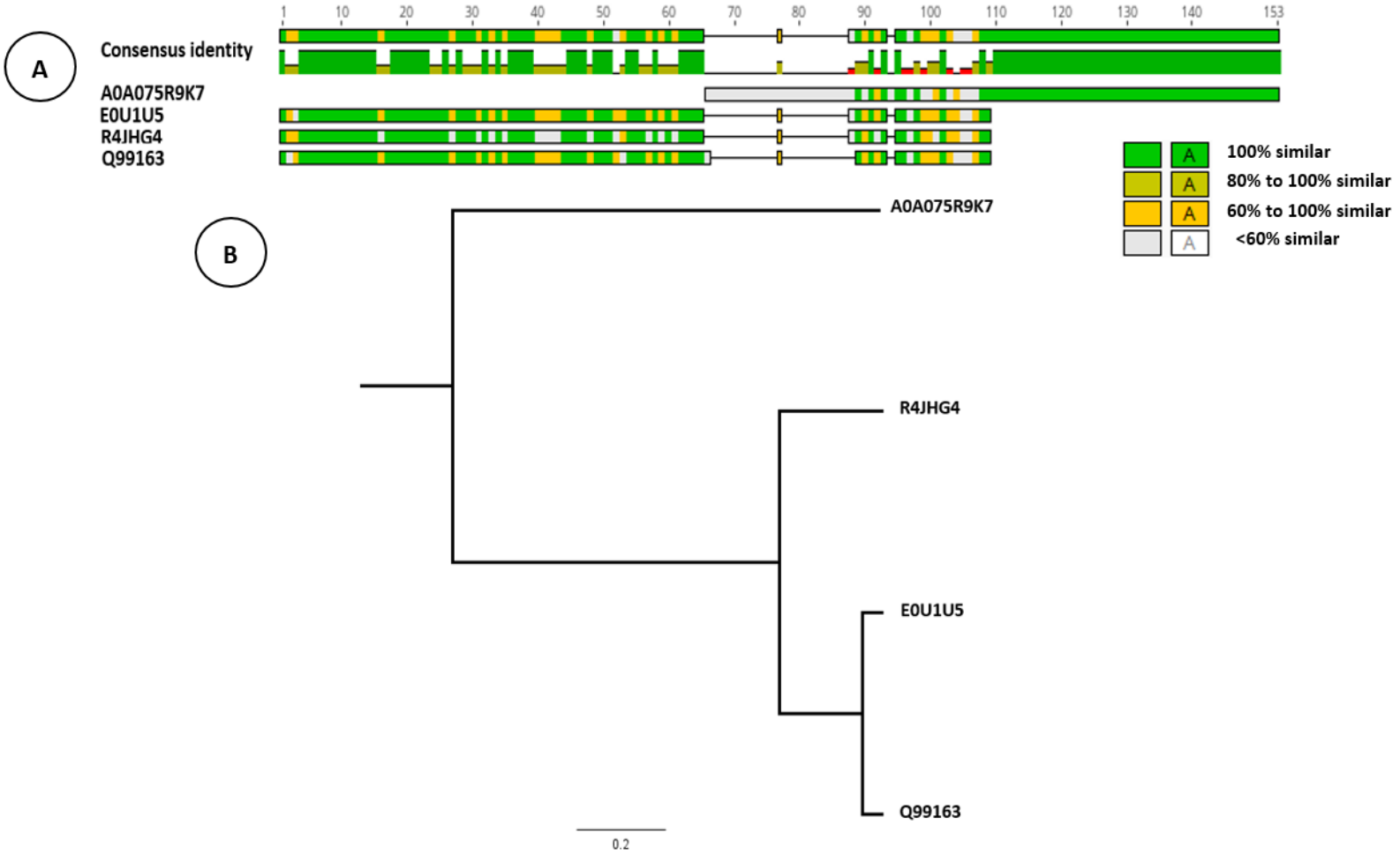

D.28 Amino acids alignment of N-acetylmuramoyl-L-alanine amidase protein (tr|A0A518VEA4|A0A518VEA4_BRELA) of PBSX-like region of *Bl* 1821L and *Bl* 1951 genome with the similar proteins of the defective prophages PBSZ, PBSX, and PBP180 using the programme CLUSTALO

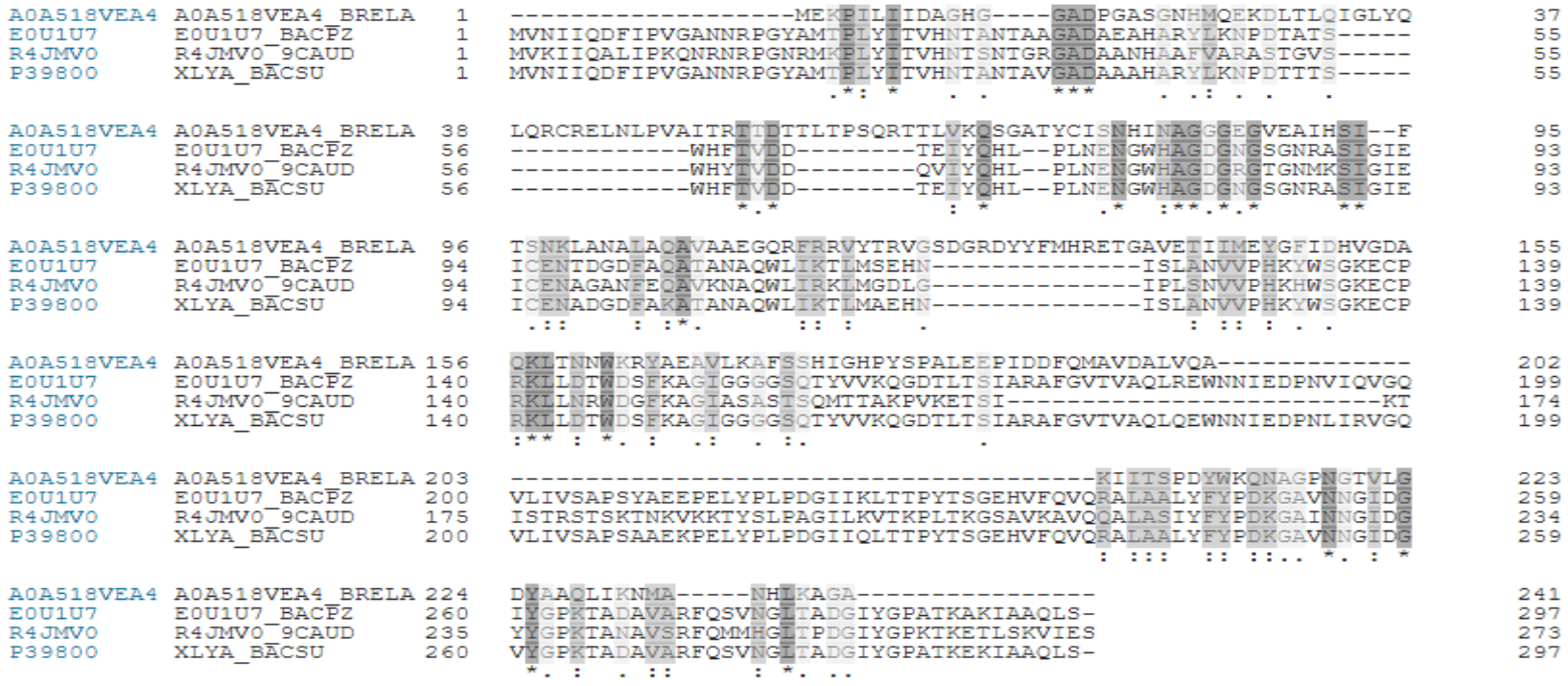

*Highlighted dark grey colour amino acids denote similarity among the aligned N-acetylmuramoyl-L-alanine amidase proteins. (Refer to Appendix D.29 & D.30).

D.29 Distance matrices of N-acetylmuramoyl-L-alanine amidase protein (tr|A0A518VEA4|A0A518VEA4_BRELA) of PBSX-like region of *Bl* 1821L and *Bl* 1951 with the similar proteins of the defective prophages PBSZ, PBSX, and PBP180

Uniprot Accession # (https://www.uniprot.org)	Uniprot Accession # (https://www.uniprot.org)			
	A0A518VEA4	**E0U1U7**	**R4JMV0**	**P39800**
A0A518VEA4		0.22	1.75	1.40
E0U1U7	0.22		0.55	0.05
R4JMV0	1.75	0.55		0.54
P39800	1.40	0.05	0.54	

D.30 Alignment (%) of N-acetylmuramoyl-L-alanine amidase protein (tr|A0A518VEA4|A0A518VEA4_BRELA) of PBSX-like region of *Bl* 1821L and *Bl* 1951 with the similar proteins of the defective prophages PBSZ, PBSX, and PBP180

Uniprot Accession # (https://www.uniprot.org)	Uniprot Accession # (https://www.uniprot.org)			
	A0A518VEA4	**E0U1U7**	**R4JMV0**	**P39800**
A0A518VEA4		15.4	7.7	15.4
E0U1U7	15.4		53.5	95.3
R4JMV0	7.7	53.5		53.9
P39800	15.4	95.3	53.9	

D.31 Schematic presentation of amino acids alignment of N-acetylmuramoyl-L-alanine amidase protein tr|A0A518VEA4|A0A518VEA4_BRELA of PBSX-like region of *Bl* 1821L and *Bl* 1951 with the similar proteins of the defective prophages PBSZ, PBSX, and PBP180 using programme Geneious basic (A) and CLUSTALO (B)

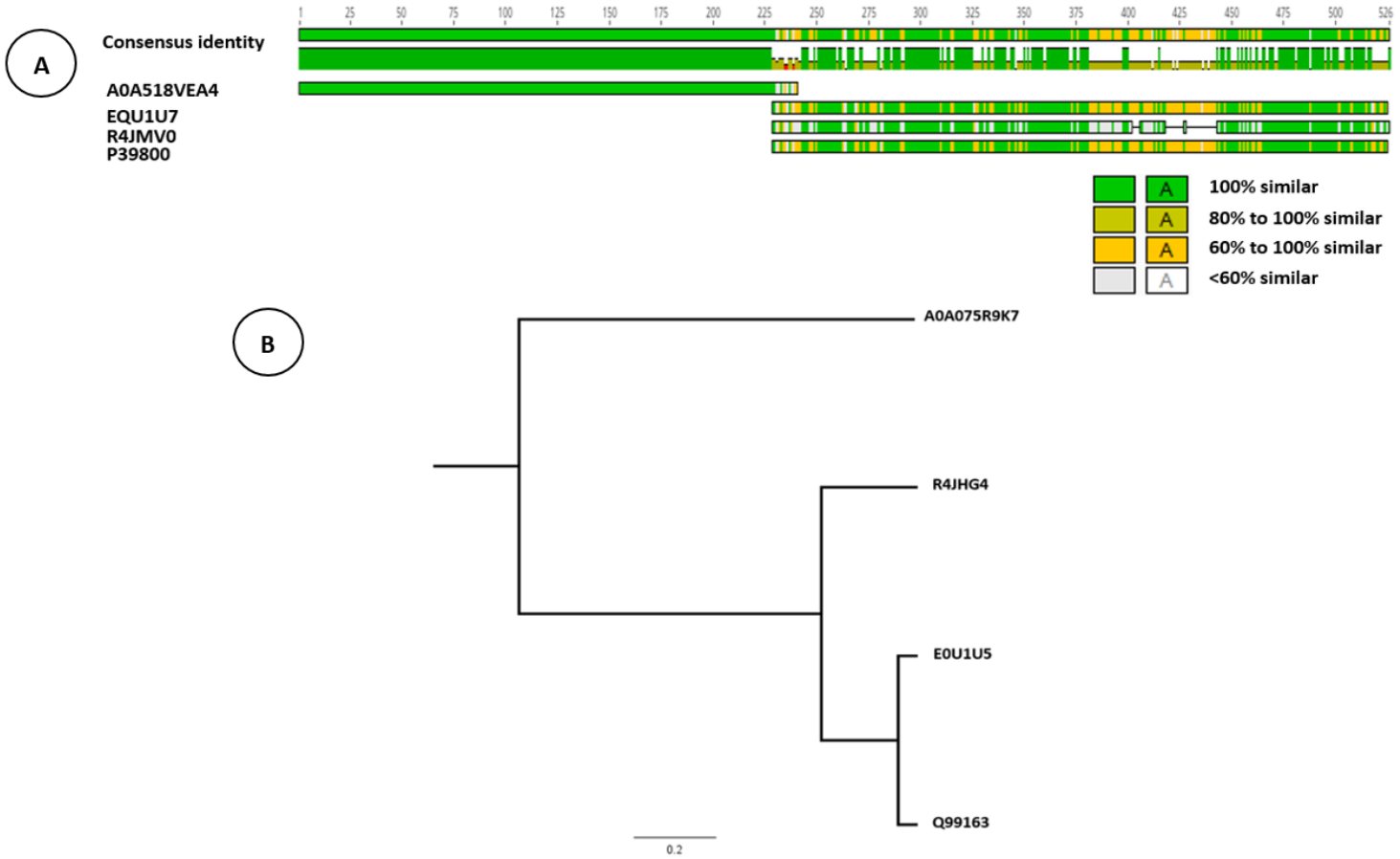

Appendix E

E.1 Interaction table showing the effect of crude *Bl* 1821L putative antibacterial proteins (ABPs) on the number of viable cells (log_{10} CFU/ml) of the host bacteria (*Bl* 1821L & *Bl* 1951)

Time intervals (Hours)	Host	Treatments		*LSD (5%)
		Control (LB broth)	Crude *Bl* 1821L ABPs	
1	*Bl* 1821L	6.633	6.645	0.350
	Bl 1951	6.501	6.616	
3	*Bl* 1821L	6.529	6.529	0.281
	Bl 1951	6.552	6.686	
6	*Bl* 1821L	6.432	6.330	0.377
	Bl 1951	6.556	6.703	
12	*Bl* 1821L	7.034	6.937	0.312
	Bl 1951	6.912	7.093	
18	*Bl* 1821L	7.100	7.199	0.228
	Bl 1951	7.019	7.067	
24	*Bl* 1821L	7.199	7.130	0.317
	Bl 1951	6.727	6.882	

*=Least significant difference

E.2 Effect of crude *Bl* 1821L putative antibacterial proteins (ABPs) on the number of viable cells of host bacterium *Bl* 1821L and *Bl* 1951 (Experiment no. 1). Values of % decrease/increase in the number of viable cells are calculated from CFUs values of corresponding time intervals

Time intervals (Hours)	Treatments					
	***Bl* 1821L**	***Bl* 1821L + *Bl* 1821L ABPs**	**% Decrease/increase in CFU/ml**	***Bl* 1951**	***Bl* 1951 + *Bl* 1821L ABPs**	**% Decrease/increase in CFU/ml**
1	4.20E+06 (6.623)*	1.55E+06 (6.190)	63.10	3.40E+06 (6.531)	5.30E+06 (6.724)	-55.88
3	1.55E+06 (6.190)	1.65E+06 (6.217)	-6.45	3.70E+06 (6.568)	5.30E+06 (6.724)	-43.24
6	8.20E+06 (6.914)	5.10E+06 (6.708)	37.80	3.30E+06 (6.519)	7.50E+06 (6.875)	-127.27
12	1.60E+07 (7.203)	1.33E+07 (7.122)	16.93	1.04E+07 (7.015)	2.23E+07 (7.347)	-114.98
18	1.87E+07 (7.272)	1.22E+07 (7.085)	35.03	1.20E+07 (7.079)	1.20E+07 (7.079)	0.00
24	2.59E+07 (7.412)	2.46E+07 (7.390)	5.03	3.80E+06 (6.580)	9.10E+06 (6.959)	-139.47

* The values in parenthesis indicate the converted value of number of viable cells (CFU/ml) into $\log_{10}$ CFU/ml.

E.3 Effect of crude *Bl* 1821L putative antibacterial proteins (ABPs) on the number of viable cells of host bacterium *Bl* 1821L and *Bl* 1951 (Experiment no. 2). Values of % decrease/increase in the number of viable cells are calculated from CFUs values of corresponding time intervals

Time intervals (Hours)	Treatments					
	***Bl* 1821L**	***Bl* 1821L + *Bl* 1821L ABPs**	**% Decrease/increase in CFU/ml**	***Bl* 1951**	***Bl* 1951 + *Bl* 1821L ABPs**	**% Decrease/increase in CFU/ml**
1	5.45E+06 (6.736)*	3.90E+06 (6.591)	28.44	2.90E+06 (6.462)	4.30E+06 (6.633)	-48.28
3	4.60E+06 (6.663)	6.25E+06 (6.796)	-35.87	3.65E+06 (6.562)	5.75E+06 (6.760)	-57.53
6	1.00E+06 (6.000)	1.45E+06 (6.161)	-45.00	3.05E+06 (6.484)	8.10E+06 (6.908)	-165.57
12	1.58E+07 (7.197)	1.89E+07 (7.275)	-19.68	1.12E+07 (7.047)	8.40E+06 (6.924)	24.66
18	1.74E+07 (7.241)	2.18E+07 (7.338)	-25.29	8.50E+06 (6.929)	1.27E+07 (7.102)	-48.82
24	1.28E+07 (7.107)	8.15E+06 (6.911)	36.33	4.85E+06 (6.686)	8.55E+06 (6.932)	-76.29

* The values in parenthesis indicate the converted value of number of viable cells (CFU/ml) into $\log_{10}$ CFU/ml.

E.4 Effect of crude *Bl* 1821L putative antibacterial proteins (ABPs) on the number of viable cells of host bacterium *Bl* 1821L and *Bl* 1951 (Experiment no. 3). Values of % decrease/increase in the number of viable cells are calculated from CFUs values of corresponding time intervals

Time intervals (Hours)	Treatments					
	***Bl* 1821L**	***Bl* 1821L + *Bl* 1821L ABPs**	**% Decrease/increase in CFU/ml**	***Bl* 1951**	***Bl* 1951 + *Bl* 1821L ABPs**	**% Decrease/increase in CFU/ml**
1	2.70E+06 (6.431)*	1.12E+07 (7.047)	-312.96	3.00E+06 (6.477)	3.45E+06 (6.538)	-15.00
3	4.95E+06 (6.695)	4.95E+06 (6.695)	0.00	2.60E+06 (6.415)	3.65E+06 (6.562)	-40.38
6	2.60E+06 (6.415)	1.35E+06 (6.130)	48.08	2.95E+06 (6.470)	1.85E+06 (6.267)	37.29
12	5.40E+06 (6.732)	2.30E+06 (6.362)	57.41	3.25E+06 (6.512)	1.20E+07 (7.079)	-269.23
18	7.00E+06 (6.845)	2.23E+07 (7.348)	-218.57	1.10E+07 (7.041)	1.10E+07 (7.039)	0.45
24	2.14E+07 (7.330)	1.85E+07 (7.266)	13.79	5.25E+06 (6.720)	4.70E+06 (6.672)	10.48

* The values in parenthesis indicate the converted value of number of viable cells (CFU/ml) into $\log_{10}$ CFU/ml.

E.5 Effect of crude *Bl* 1821L putative antibacterial proteins (ABPs) on the number of viable cells of host bacterium *Bl* 1821L and *Bl* 1951 (Experiment no. 4). Values of % decrease/increase in the number of viable cells are calculated from CFUs values of corresponding time intervals

Time intervals (Hours)	Treatments					
	***Bl* 1821L**	***Bl* 1821L + *Bl* 1821L ABPs**	**% Decrease/increase in CFU/ml**	***Bl* 1951**	***Bl* 1951 + *Bl* 1821L ABPs**	**% Decrease/increase in CFU/ml**
1	5.50E+06 (6.740)*	5.65E+06 (6.752)	-2.73	3.40E+06 (6.531)	3.70E+06 (6.568)	-8.82
3	3.70E+06 (6.568)	2.55E+06 (6.407)	31.08	4.60E+06 (6.663)	5.00E+06 (6.699)	-8.70
6	2.50E+06 (6.398)	2.10E+06 (6.322)	16.00	5.65E+06 (6.752)	5.75E+06 (6.760)	-1.77
12	1.01E+07 (7.002)	9.75E+06 (6.989)	2.99	1.19E+07 (7.074)	1.05E+07 (7.021)	11.39
18	1.10E+07 (7.041)	1.06E+07 (7.025)	3.64	1.07E+07 (7.027)	1.12E+07 (7.049)	-5.16
24	8.80E+06 (6.944)	8.95E+06 (6.652)	-1.70	8.40E+06 (6.924)	9.20E+06 (6.964)	-9.52

* The values in parenthesis indicate the converted value of number of viable cells (CFU/ml) into $\log_{10}$ CFU/ml.

E.6 Effect of crude *Bl* 1821L putative antibacterial proteins (ABPs) on the OD_{600nm} reading of the host bacterium *Bl* 1821L and *Bl* 1951 (Experiment no. 1)

Time intervals (Hours)	Treatments					
	***Bl* 1821L**	***Bl* 1821L + *Bl* 1821L ABPs**	**% Decrease/increase in OD_{600nm} reading**	***Bl* 1951**	***Bl* 1951 + *Bl* 1821L ABPs**	**% Decrease/increase in OD_{600nm} reading**
1	1.98	1.98	0.00	1.99	1.97	1.01
3	1.86	1.84	0.81	1.91	1.80	6.02
6	1.69	1.69	0.00	1.75	1.71	2.29
12	1.35	1.30	4.07	1.69	1.51	10.39
18	1.29	1.19	7.78	1.66	1.49	10.27
24	1.30	1.13	13.13	1.72	1.28	25.58

E.7 Effect of crude *Bl* 1821L putative antibacterial proteins (ABPs) on the OD_{600nm} reading of the host bacterium *Bl* 1821L and *Bl* 1951 (Experiment no. 2)

Time intervals (Hours)	Treatments					
	Bl 1821L	*Bl* 1821L + *Bl* 1821L ABPs	% Decrease/increase in OD_{600nm} reading	*Bl* 1951	*Bl* 1951 + *Bl* 1821L ABPs	% Decrease/increase in OD_{600nm} reading
1	1.98	1.99	-0.25	1.93	1.91	1.04
3	1.86	1.83	1.35	1.75	1.77	-1.43
6	1.66	1.56	6.02	1.52	1.63	-6.91
12	1.32	1.25	5.32	1.35	1.44	-6.67
18	1.23	1.25	-1.63	1.25	1.32	-5.62
24	1.29	1.21	6.23	1.30	1.26	3.46

E.8 Effect of crude *Bl* 1821L putative antibacterial proteins (ABPs) on the OD_{600nm} reading of the host bacterium *Bl* 1821L and *Bl* 1951 (Experiment no. 3)

Time intervals (Hours)	Treatments					
	***Bl* 1821L**	***Bl* 1821L + *Bl* 1821L ABPs**	**% Decrease/increase in OD_{600nm} reading**	***Bl* 1951**	***Bl* 1951 + *Bl* 1821L ABPs**	**% Decrease/increase in OD_{600nm} reading**
1	1.99	1.99	0.00	1.84	1.82	1.09
3	1.82	1.86	-0.03	1.71	1.70	0.29
6	1.51	1.59	-0.08	1.50	1.50	0.00
12	1.28	1.26	0.02	1.35	1.25	7.43
18	1.19	1.20	-0.01	1.11	1.16	-4.52
24	1.19	1.18	0.01	1.10	1.06	3.64

E.9 Effect of crude Bl 1821L putative antibacterial proteins (ABPs) on the OD_{600nm} reading of the host bacterium *Bl* 1821L and *Bl* 1951 (Experiment no. 4)

Time intervals (Hours)	Treatments					
	***Bl* 1821L**	***Bl* 1821L + *Bl* 1821L ABPs**	**% Decrease/increase in OD_{600nm} reading**	***Bl* 1951**	***Bl* 1951 + *Bl* 1821L ABPs**	**% Decrease/increase in OD_{600nm} reading**
1	2.00	1.99	0.25	1.95	1.92	1.44
3	1.93	1.89	2.33	1.60	1.67	-4.06
6	1.75	1.69	3.44	1.54	1.38	10.39
12	1.24	1.26	-2.02	1.43	1.35	5.61
18	1.21	1.20	0.83	0.97	1.03	-5.67
24	1.22	1.21	1.64	1.03	1.12	-8.74

E.10 Interaction table showing the effect of crude *Bl* 1951 putative antibacterial proteins (ABPs) on the number of viable cells (log_{10} CFU/ml) of the host bacterium (*Bl* 1951 & *Bl* 1821L)

Time intervals (Hours)	Host	Treatments		LSD* (5%)
		Control (LB broth)	Crude *Bl* 1951 ABPs	
1	*Bl* 1951	6.70	6.83	0.377
	Bl 1821L	7.13	7.14	
3	*Bl* 1951	6.639	6.590	0.150
	Bl 1821L	6.762	6.894	
6	*Bl* 1951	6.444	6.317	0.268
	Bl 1821L	6.943	6.193	
12	*Bl* 1951	6.902	6.659	0.243
	Bl 1821L	6.867	6.851	
18	*Bl* 1951	6.865	6.827	0.159
	Bl 1821L	6.807	6.877	
24	*Bl* 1951	6.985	6.743	0.311
	Bl 1821L	7.003	7.083	

*=Least significant difference

E.11 Effect of crude *Bl* 1951 putative antibacterial proteins (ABPs) on the number of viable cells of host bacterium *Bl* 1951 and *Bl* 1821L (Experiment no. 1). Values of % decrease/increase in the number of viable cells are calculated from CFUs values of corresponding time intervals

Time intervals (Hours)	Treatments					
	***Bl* 1951**	***Bl* 1951 + *Bl* 1951 ABPs**	**% Decrease/increase in CFU/ml**	***Bl* 1821L**	***Bl* 1821L + *Bl* 1951 ABPs**	**% Decrease/increase in CFU/ml**
1	1.25E+06 (6.097)*	1.65E+06 (6.217)	-32.00	5.16E+07 (7.713)	3.63E+07 (7.559)	29.75
3	6.95E+06 (6.842)	5.75E+06 (6.760)	17.27	1.12E+07 (7.047)	1.33E+07 (7.122)	-18.83
6	9.50E+05 (5.978)	8.00E+05 (5.903)	15.79	1.84E+07 (7.265)	1.72E+07 (7.234)	6.79
12	3.25E+06 (6.512)	2.50E+06 (6.398)	23.08	2.47E+07 (7.392)	1.84E+07 (7.265)	25.35
18	3.60E+06 (6.556)	6.40E+06 (6.806)	-77.78	1.21E+07 (7.083)	1.58E+07 (7.199)	-30.58
24	5.80E+06 (6.763)	4.00E+06 (6.602)	31.03	1.37E+07 (7.137)	1.33E+07 (7.122)	3.28

* The values in parenthesis indicate the converted value of number of viable cells (CFU/ml) into $\log_{10}$ CFU/ml.

E.12 Effect of crude *Bl* 1951 putative antibacterial proteins (ABPs) on the number of viable cells of host bacterium *Bl* 1951 and *Bl* 1821L (Experiment no. 2). Values of % decrease/increase in the number of viable cells are calculated from CFUs values of corresponding time intervals

Time intervals (Hours)	Treatments					
	***Bl* 1951**	***Bl* 1951 + *Bl* 1951 ABPs**	**% Decrease/increase in CFU/ml**	***Bl* 1821L**	***Bl* 1821L + *Bl* 1951 ABPs**	**% Decrease/increase in CFU/ml**
1	3.15E+06 (6.498)*	6.50E+06 (6.813)	-106.35	2.05E+07 (7.331)	2.87E+07 (7.458)	-40.34
3	2.05E+06 (6.312)	4.00E+06 (6.602)	-95.12	7.80E+06 (6.892)	1.77E+07 (7.248)	-126.92
6	2.90E+06 (6.462)	1.90E+06 (6.279)	34.48	1.95E+07 (7.289)	1.49E+07 (7.173)	23.39
12	1.68E+07 (7.224)	5.90E+06 (6.771)	64.78	1.14E+07 (7.055)	1.01E+07 (7.002)	11.45
18	1.23E+07 (7.090)	1.52E+07 (7.180)	-23.17	3.85E+06 (6.585)	3.65E+06 (6.562)	5.19
24	4.50E+06 (6.653)	3.55E+06 (6.550)	21.11	1.49E+07 (7.173)	1.80E+07 (7.255)	-20.81

* The values in parenthesis indicate the converted value of number of viable cells (CFU/ml) into $\log_{10}$ CFU/ml.

E.13 Effect of crude *Bl* 1951 putative antibacterial proteins (ABPs) on the number of viable cells of host bacterium *Bl* 1951 and *Bl* 1821 (Experiment no. 3). Values of % decrease/increase in the number of viable cells are calculated from CFUs values of corresponding time intervals

Time intervals (Hours)	Treatments					
	***Bl* 1951**	***Bl* 1951 + *Bl* 1951 PTLBs**	**% Decrease/increase in CFU/ml**	***Bl* 1821L**	***Bl* 1821L + *Bl* 1951 PTLBs**	**% Decrease/increase in CFU/ml**
1	2.28E+07 (7.357)*	2.42E+07 (7.384)	-6.37	5.95E+06 (6.775)	6.70E+06 (6.826)	-12.61
3	6.15E+06 (6.789)	3.55E+06 (6.550)	42.28	4.50E+06 (6.653)	5.85E+06 (6.767)	-30.00
6	4.80E+06 (6.681)	4.20E+06 (6.623)	12.50	4.80E+06 (6.681)	6.40E+06 (6.806)	-33.33
12	9.40E+06 (6.973)	5.25E+06 (6.720)	44.15	2.05E+06 (6.312)	2.20E+06 (6.342)	-7.32
18	8.05E+06 (6.906)	9.20E+06 (6.964)	-14.29	6.85E+06 (6.836)	9.15E+06 (6.961)	-33.58
24	1.00E+07 (7.000)	7.10E+06 (6.851)	29.00	8.90E+06 (6.949)	1.17E+07 (7.066)	-30.90

* The values in parenthesis indicate the converted value of number of viable cells (CFU/ml) into $\log_{10}$ CFU/ml.

E.14 Effect of crude *Bl* 1951 putative antibacterial proteins (ABPs) on the number of viable cells of host bacterium *Bl* 1951 and *Bl* 1821L (Experiment no. 4). Values of % decrease/increase in the number of viable cells are calculated from CFUs values of corresponding time intervals

Time intervals (Hours)	Treatments					
	***Bl* 1951**	***Bl* 1951 + *Bl* 1951 PTLBs**	**% Decrease/increase in CFU/ml**	***Bl* 1821L**	***Bl* 1821L + *Bl* 1951 PTLBs**	**% Decrease/increase in CFU/ml**
1	7.00E+06 (6.845)*	7.70E+06 (6.886)	-10.00	5.20E+06 (6.716)	5.30E+06 (6.724)	-1.92
3	4.10E+06 (6.613)	2.80E+06 (6.447)	31.71	2.85E+06 (6.445)	2.75E+06 (6.439)	3.51
6	4.50E+06 (6.653)	2.90E+06 (6.462)	35.56	3.45E+06 (6.538)	2.75E+06 (6.439)	20.29
12	7.90E+06 (6.898)	5.60E+06 (6.748)	29.11	5.10E+06 (6.708)	6.25E+06 (6.796)	-22.55
18	8.10E+06 (6.908)	7.65E+06 (6.884)	5.56	5.30E+06 (6.724)	6.10E+06 (6.785)	-15.09
24	9.95E+06 (6.998)	9.30E+06 (6.968)	6.53	5.65E+06 (6.752)	7.70E+06 (6.886)	-36.28

* The values in parenthesis indicate the converted value of number of viable cells (CFU/ml) into $\log_{10}$ CFU/ml.

E.15 Effect of crude *Bl* 1951 putative antibacterial proteins (ABPs) on the OD_{600nm} reading of the host bacterium *Bl* 1951 and *Bl* 1821L (Experiment no. 1)

Time intervals (Hours)	Treatments					
	***Bl* 1951**	***Bl* 1951 + *Bl* 1951 ABPs**	**% Decrease/increase in OD_{600nm} reading**	***Bl* 1821L**	***Bl* 1821L + *Bl* 1951 ABPs**	**% Decrease/increase in OD_{600nm} reading**
1	1.50	1.41	6.00	3.61	3.13	13.30
3	1.26	1.27	-0.79	1.90	1.71	10.00
6	1.19	1.23	-3.36	1.72	1.46	15.12
12	0.96	0.76	20.83	1.48	1.27	14.19
18	0.79	0.73	7.59	1.37	1.19	13.14
24	0.75	0.75	0.00	0.90	0.85	5.56

E.16 Effect of crude *Bl* 1951 putative antibacterial proteins (ABPs) on the OD_{600nm} reading of the host bacterium *Bl* 1951 and *Bl* 1821L (Experiment no. 2)

Time intervals (Hours)	Treatments					
	***Bl* 1951**	***Bl* 1951 + *Bl* 1951 ABPs**	**% Decrease/increase in OD_{600nm} reading**	***Bl* 1821L**	***Bl* 1821L + *Bl* 1951 ABPs**	**% Decrease/increase in OD_{600nm} reading**
1	1.93	1.95	-1.04	3.14	3.04	3.18
3	1.64	1.84	-12.20	1.96	1.92	2.30
6	1.32	1.69	-28.03	1.73	1.69	2.60
12	1.78	1.56	12.36	1.40	1.44	-2.86
18	1.01	1.39	-37.62	1.37	1.33	3.28
24	1.05	1.28	-21.90	1.31	1.26	4.20

E.17 Effect of crude *Bl* 1951 putative antibacterial proteins (ABPs) on the OD_{600nm} reading of the host bacterium *Bl* 1951 and *Bl* 1821L (Experiment no. 3)

Time intervals (Hours)	Treatments					
	***Bl* 1951**	***Bl* 1951 + *Bl* 1951 ABPs**	**% Decrease/increase in OD_{600nm} reading**	***Bl* 1821L**	***Bl* 1821L + *Bl* 1951 ABPs**	**% Decrease/increase in OD_{600nm} reading**
1	1.85	1.86	-0.54	1.66	1.68	-1.20
3	1.71	1.78	-4.09	1.58	1.56	1.27
6	1.61	1.63	-1.24	1.58	1.52	3.80
12	1.50	1.64	-9.33	1.49	1.44	3.36
18	1.38	1.49	-7.97	1.38	1.41	-2.17
24	1.02	1.37	-34.31	1.24	1.28	-3.23

E.18 Effect of crude *Bl* 1951 putative antibacterial proteins (ABPs) on the OD_{600nm} reading of the host bacterium *Bl* 1951 and *Bl* 1821L (Experiment no. 4)

Time intervals (Hours)	Treatments					
	***Bl* 1951**	***Bl* 1951 + *Bl* 1951 ABPs**	**% Decrease/increase in OD_{600nm} reading**	***Bl* 1821L**	***Bl* 1821L + *Bl* 1951 ABPs**	**% Decrease/increase in OD_{600nm} reading**
1	1.96	1.96	0.26	2.90	2.85	1.72
3	1.78	1.77	0.56	1.86	1.88	-1.08
6	1.66	1.63	1.51	1.73	1.72	0.87
12	1.60	1.58	1.56	1.22	1.29	-5.33
18	1.09	1.17	-6.88	1.01	1.01	0.50
24	1.09	1.08	0.92	1.03	1.04	-0.97